QUORUM NETWORK (SENSING/QUENCHING) IN MULTIDRUG-RESISTANT PATHOGENS

EDITED BY: Rodolfo Garcia-Conteras, Thomas K. Wood and Maria Tomás
PUBLISHED IN: Frontiers in Cellular and Infection Microbiology

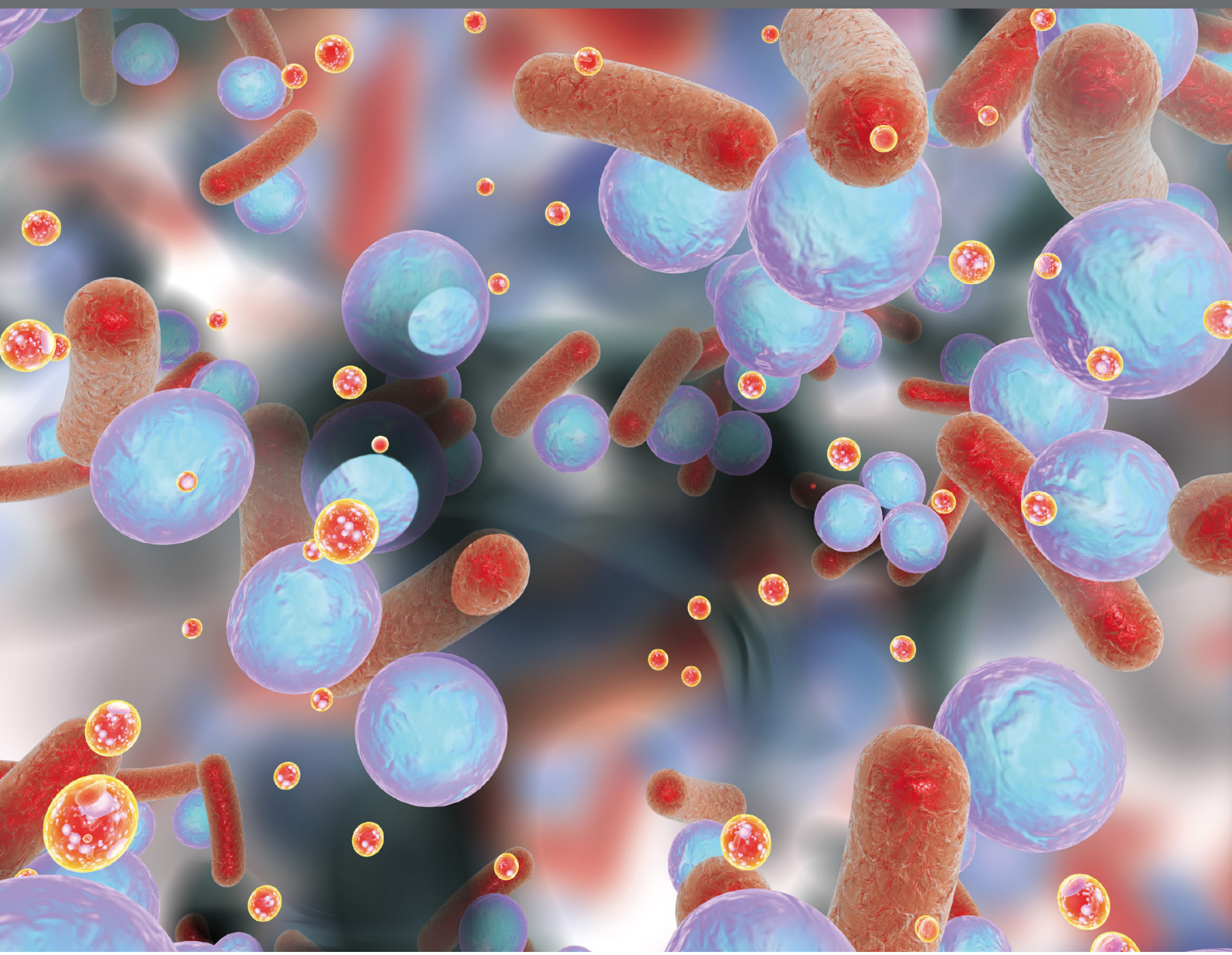

frontiers Research Topics

frontiers

ISSN 1664-8714
ISBN 978-2-88945-882-0
DOI 10.3389/978-2-88945-882-0

About Frontiers

Frontiers is more than just an open-access publisher of scholarly articles: it is a pioneering approach to the world of academia, radically improving the way scholarly research is managed. The grand vision of Frontiers is a world where all people have an equal opportunity to seek, share and generate knowledge. Frontiers provides immediate and permanent online open access to all its publications, but this alone is not enough to realize our grand goals.

Frontiers Journal Series

The Frontiers Journal Series is a multi-tier and interdisciplinary set of open-access, online journals, promising a paradigm shift from the current review, selection and dissemination processes in academic publishing. All Frontiers journals are driven by researchers for researchers; therefore, they constitute a service to the scholarly community. At the same time, the Frontiers Journal Series operates on a revolutionary invention, the tiered publishing system, initially addressing specific communities of scholars, and gradually climbing up to broader public understanding, thus serving the interests of the lay society, too.

Dedication to Quality

Each Frontiers article is a landmark of the highest quality, thanks to genuinely collaborative interactions between authors and review editors, who include some of the world's best academicians. Research must be certified by peers before entering a stream of knowledge that may eventually reach the public - and shape society; therefore, Frontiers only applies the most rigorous and unbiased reviews.
Frontiers revolutionizes research publishing by freely delivering the most outstanding research, evaluated with no bias from both the academic and social point of view. By applying the most advanced information technologies, Frontiers is catapulting scholarly publishing into a new generation.

What are Frontiers Research Topics?

Frontiers Research Topics are very popular trademarks of the Frontiers Journals Series: they are collections of at least ten articles, all centered on a particular subject. With their unique mix of varied contributions from Original Research to Review Articles, Frontiers Research Topics unify the most influential researchers, the latest key findings and historical advances in a hot research area! Find out more on how to host your own Frontiers Research Topic or contribute to one as an author by contacting the Frontiers Editorial Office: researchtopics@frontiersin.org

QUORUM NETWORK (SENSING/QUENCHING) IN MULTIDRUG-RESISTANT PATHOGENS

Topic Editors:
Rodolfo Garcia-Conteras, National Autonomous University of Mexico, Mexico
Thomas K. Wood, Pennsylvania State University, United States
Maria Tomás, Hospital A Coruña (CHUAC-INIBIC), Spain

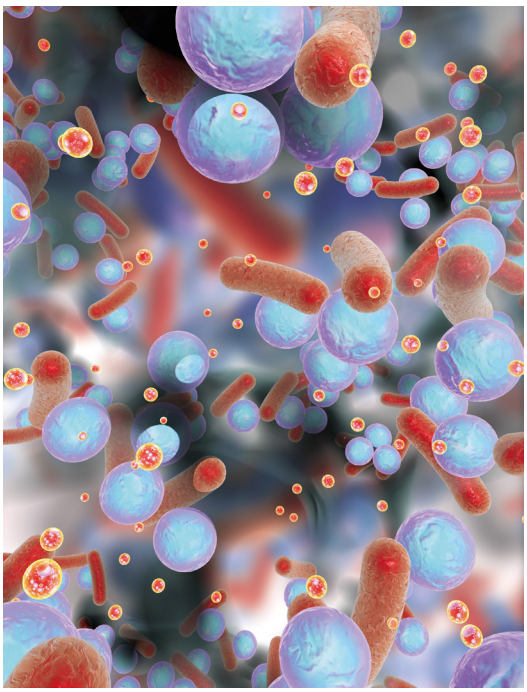

Image: Kateryna Kon/Shutterstock.com

The findings of the contributed studies from this Research Topic reflect important aspects (hot topics) of Quorum network (Sensing/Quenching) in multidrug-resistant pathogens, which including: (i) novel mechanisms of QS and detection techniques, (ii) QS/QQ in clinical multidrug resistant strains, (iii) the relationship between QS/QQ as well as multidrug resistance, and (iv) the application of new QQ therapies.

Citation: Garcia-Conteras, R., Wood, T. K., Tomás, M., eds. (2019). Quorum Network (Sensing/Quenching) in Multidrug-Resistant Pathogens. Lausanne: Frontiers Media. doi: 10.3389/978-2-88945-882-0

Table of Contents

frontiers in Cellular and Infection Microbiology

EDITORIAL
published: 03 April 2019
doi: 10.3389/fcimb.2019.00080

Editorial: Quorum Network (Sensing/Quenching) in Multidrug-Resistant Pathogens

Rodolfo García-Contreras[1]*, *Thomas K. Wood*[2]* and *Maria Tomás*[3]*

[1] Department of Microbiology and Parasitology, Faculty of Medicine, National Autonomous University of Mexico, Mexico City, Mexico, [2] Department of Chemical Engineering, Pennsylvania State University, University Park, PA, United States, [3] Microbiology Department, Complejo Hospitalario Universitario A Coruña, Instituto de Investigación Biomédica (INIBIC-CHUAC), Universidad de A Coruña, A Coruña, Spain

Keywords: quorum sensing (QS), quorum quenching (QQ), multi-resistant bacteria, enzymes, inhibitors

Editorial on the Research Topic

Quorum Network (Sensing/Quenching) in Multidrug-Resistant Pathogens

In relation to the basic aspects of quorum sensing (QS) research, three works were published in this Research Topic. In the first one, Higgins et al. developed a new approach with the *Pseudomona aeruginosa* PAO1-N strain QS regulatory network to study the contribution of the two phenazine-1-carboxylic acid (PCA) operons involved in pyocyanin production. The data of this manuscript show the complexity of the QS cascade in *P. aeruginosa* controlling the production of phenazine secondary metabolites. In the second work, the authors improved the state of the art for surface-enhanced Raman scattering (SERS) spectroscopy for the detection of bioactive extracellular compounds that are involved in interspecies microbial interactions as well as involved in the relationship between the microbes and their hosts (Bodelón et al.); their approach is suitable for *P. aeruginosa* and other multi-resistant pathogens. Highlighting advances in nanotechnology and photonics have increased the possibility of SERS being a more robust analytical tool in the microbiology field. There are several applications of this methodology, including the detection of pathogenic bacteria, and culturing bacterial cells. Moreover, in this review, Bodelón et al. concluded this technology reveals the "hidden" chemistry of microbes which allows the early detection and diagnosis of infectious diseases (Bodelón et al.). Finally, in the third work, Pawar et al. described a theoretical network model using access to a set of small protein interactions (SPINs) together with the whole genome (GPIN) to identify *in silico* proteins involved in the QS in *Proteus mirabilis*. The authors identified new proteins involved in the QS of this pathogen PMI1345, GltB, PMI3678, and RcsC, which could be used as new targets to develop of new treatments for *Proteus mirabilis*.

Current efforts in quorum quenching (QQ) research are dedicated to expanding the existent repertoire of extracts and molecules with anti-virulence properties, useful against important Gram negative multidrug resistant (MDR) bacterial pathogens. Among the newest agents is 1,2-benzenedicarboxylic acid, isolated from an extract of the bacterium *Delftia tsuruhatensis* SJ01, which was obtained from the rhizosphere and is able to inhibit biofilm formation, swarming, and the production of rhamnolipids, pyocyanin, and exoproteases of the reference strain *P. aeruginosa* PAO1 and a clinical isolate, probably by binding and inactivating the LasR receptor (Singh et al.). In addition, bakuchiol isolated from a methanolic seed extract of *Psoralea corylifolia* showed remarkable anti-virulence activity and is also effective for inhibiting the biofilm formation of *P. aeruginosa*, *Chromobacterium violaceum*, *Listeria monocytogenes*, and *Serratia marcescens*. Computational analysis demonstrated that this meroterpene binds and disturbs LasR and RhlR

OPEN ACCESS

Edited and reviewed by:
John S. Gunn,
The Research Institute at Nationwide Children's Hospital, United States

***Correspondence:**
Rodolfo García-Contreras
rgarc@bq.unam.mx
Thomas K. Wood
tuw14@psu.edu
Maria Tomás
ma.del.mar.tomas.carmona@sergas.es

Specialty section:
This article was submitted to Molecular Bacterial Pathogenesis, a section of the journal Frontiers in Cellular and Infection Microbiology

Received: *26 February 2019*
Accepted: *08 March 2019*
Published: *03 April 2019*

Citation:
García-Contreras R, Wood TK and Tomás M (2019) Editorial: Quorum Network (Sensing/Quenching) in Multidrug-Resistant Pathogens. Front. Cell. Infect. Microbiol. 9:80. doi: 10.3389/fcimb.2019.00080

structures (Husain et al.) leading to the inhibition of QS-mediated biofilm maturation. Recently, virtual screening 4,687 phytochemicals based docking analysis to detect different potential interactions with the QS receptor of *C. violaceum* the protein CviR. As a consequence, four new inhibitors were identified: sappanol, butein, bavachin, and catechin 7-xyloside. Further, studies using microscale thermophoresis confirmed the predicted interactions, and accordingly, all the compounds were able to able to reduce biofilm formation and the production of violacein (Ravichandran et al.). Also, recently it was discovered that the diterpene alcohol phytol has remarkable anti-QS and anti-virulence properties against *S. marcescens* including *in vitro* inhibition of biofilm formation and swarming motility as well as inhibition of lipase, hemolysin, and exopolysccharide production. In addition, phytol caused an *in vivo* reduction of the bacterial load in kidneys, bladder and urine of Wistar rats inoculated with *S. marcescens* that developed acute pyelonephritis, and the administration of phytol decreased several inflammatory markers and the production of bacterial lipase and protease in the tissues. Since phytol has low toxicity and is widely used in the cosmetic industry, it is possible to envision its application for the treatment of *S. marcescens* in human infections (Srinivasan et al.).

Another way to interfere with QS is the degradation of QS signals like acyl-homoserine lactones (AHL) by acylases and lactonases. This approach has demonstrated better virulence factor attenuation *in vitro* than classical chemical inhibitors, such as the brominated furanone C-30 and 5-fluorouracyl in clinical isolates (Guendouze et al., 2017). Moreover, recently it was demonstrated that such inhibition is more effective under oxidative stress, such as that exerted by the addition of nicotine, since QS is also linked to stress response in *P. aeruginosa* (García-Contreras et al., 2015), particularly in the expression of antioxidant enzymes, such as catalase (Tang et al.). Besides its remarkable effects *in vitro* and in simple infection models, such as in the nematode *C. elegans*, enzymatic QQ by the acylase PvdQ intranasally administrated is also effective in attenuating virulence in murine pulmonary infections caused by *P. aeruginosa*, increasing life expectancy in lethal infections and decreasing damage and inflammation in sub lethal ones (Utari et al.). In addition, lactonases have been used in engineering to reduce biofouling in reverse osmosis systems (Oh et al., 2017); however, this approach is less effective than reducing biofouling by controlling the secondary messenger cyclic diguanylate (Wood et al., 2016). Finally, we highlight new QQ enzymes in isolates of the *Acinetobacter baumannii* (López et al., 2017; Mayer et al.). The first one was described in clinical isolates of *A. baumannii*, the AidA protein (AHL lactonase) described in isolates clinical of the *A. baumannii* (López et al., 2017). This protein showed activity hydrolyzing the 3-oxo-C12-HSL signal which reduced the QS of this bacteria, and also degraded signals from other bacteria. The second QQ enzyme was the A1_2662 protein (AHL lactonase) (Mayer et al.).

Other QS/QQ reference models use *Vibrio* species, which are responsible for severe infections in humans like gastroenteritis, wound infections and septicemia. *Vibrio* spp. is also important pathogens of fish and crustaceans (Liu et al.). The best known is *V. cholerae* due to pandemics. QS in this bacterium is controlled by the global regulator LuxO, which allows the production of virulence factors, such as the cholera toxin and toxin co-regulated pilus formation at low cell densities while downregulating them at high cell densities and promoting detachment from the intestinal epithelial cells via the HapA protease. Due to the central role of LuxO in QS and virulence, it is an adequate target for QS inhibitors. Among the ones discovered so far are 2,3 pyrazine dicarboxylic acid and their derivatives, such as $PDCA^{py}$ that incorporates a pyrrolidine moiety and that is able to downregulate the expression of the toxin and pilus genes and reduce the adhesion of vibrios onto and invasion into (Hema et al.).

Another important *Vibrio* species is *V. campbellii* which is a major problem for aquaculture, since is responsible for "luminescent vibriosis" that causes mass mortality in farmed shrimp. Compound screening based on the inhibition of bioluminisnece, a QS-controlled phenotype, has been useful for the identification of QS inhibitors, and also direct inhibitors of luciferase enzymes, such as SAM461, a 9H-fluroen-9yl vinyl ether derivative that likely binds to the active site of the enzyme and that has no effect on the QS systems. Remarkably, the administration of this compound at low micromolar concentrations protected *Artemia franciscana* against *V. campbellii* infection, suggesting a role of luciferase in virulence and revealing a novel target for anti-virulence therapies (Martín-Rodríguez et al.).

Besides the inhibition of QS receptors and the degradation of the signals, another strategy to interfere with QS and virulence is to inhibit their production by targeting important enzymes participating in their biosynthesis. These are good targets since they only exist in bacteria and are absent in animal hosts. Exploiting this kind of inhibition is in its infancy but already has produced some remarkable results for the inhibition of homoserine lactone synthesis as well as other important signals, such as autoinducer 2, the quinolone PQS and peptide autoinducers of Gram positive bacterial pathogens (Fleitas Martínez et al.).

As another approach, Ma et al. found that 15% of marine bacteria from coral microbial consortia have QQ activity (resulting in the inhibition of biofilm formation and virulence production). A representative of this approach is an isolate of *Staphylococcus hominis* D11 that has genes predicted to be involved in the production of homocysteine thiolactone. The authors purified and analyzed this QS analog and demonstrated that it competes with the auto-inducers producers by *P. aeruginosa*.

Moreover, new approaches in QQ research were described for Gram positive MDR bacterial pathogens like *S. mutans* (Kaur et al.). A new inhibitor of QS, the aromatic 1,3-di-m-tolylurea (DMTU) was identified that acts on the ComDE pathway associated with biofilm formation, and has been studied *in vivo* by Kaur et al. through *S. mutans* infections in Wistar rats. Interestingly, the authors analyzed the incidence of the caries due to the synergistic activity of this QQ compound mixed with fluoride in this animal model. The results show that DMTU decreases the incidence of caries by inhibiting ComA that is an

ABC transporter that belongs to the ComDE QS circuit in *S. mutans*. This study also shows that the combination of DMTU with fluoride at lower concentrations can be used as a potential substitute to the current chemotherapeutic approaches to prevent the incidence of dental caries.

Finally, Huedo et al. analyzed in a review article interesting advances in the understanding of the QS/QQ of *S. maltophilia* highlighting those works related with diffusible signal factor (DSF), AHL signaling (acyl homoserine lactones) and the factor Ax21. *S. maltophilia* naturally interacts with the organisms present in its environment. An interesting example of cooperation via DSF is the increment of biofilm formation and antibiotic resistance of *P. aeruginosa* in the lungs. However, in most known cases, *S. maltophilia* inhibits its competitors' QS systems. This is because *S. maltophilia* strains have an extraordinary array of QQ mechanisms including production of virulence factors with quenching activities as well as degradation of AHL and palmitic acid methyl ester activity.

In conclusion, important topics in relation to quorum network (sensing/quenching) in multi-drug resistant pathogens are described in this special issue of Frontiers in Cellular and Infection Microbiology.

AUTHOR CONTRIBUTIONS

RG-C and MT wrote the manuscript using papers revised as editors in this Research Topic. TKW participated in the supervision of the writing of the manuscript.

ACKNOWLEDGMENTS

This study was funded by grant PI16/01163 awarded to MT within the State Plan for R + D + I 2013–2016 (National Plan for Scientific Research, Technological Development and Innovation 2008–2011) and co-financed by the ISCIII-Deputy General Directorate for Evaluation and Promotion of Research—European Regional Development Fund A way of Making Europe and Instituto de Salud Carlos III FEDER, Spanish Network for the Research in Infectious Diseases (REIPI, RD16/0016/0006) and by the Study Group on Mechanisms of Action and Resistance to Antimicrobials, GEMARA (SEIMC, http://www.seimc.org/).

REFERENCES

García-Contreras, R., Nuñez-López, L., Jasso-Chávez, R., Kwan, B. W., Belmont, J. A., Rangel-Vega, A., et al. (2015). Quorum sensing enhancement of the stress response promotes resistance to quorum quenching and prevents social cheating. *ISME J.* 9, 115–125. doi: 10.1038/ismej.2014.98

Guendouze, A., Plener, L., Bzdrenga, J., Jacquet, P., Rémy, B., Elias, M., et al. (2017). Effect of quorum quenching lactonase in clinical isolates of Pseudomonas aeruginosa and comparison with quorum sensing inhibitors.*Front. Microbiol.* 8:227. doi: 10.3389/fmicb.2017.00227

López, M., Mayer, C., Fernández-García, L., Blasco, L., Muras, A., Ruiz, F. M., et al., GEIH-GEMARA (SEIMC). (2017). Quorum sensing network in clinical strains of *A. baumannii*: AidA is a new quorum quenching enzyme. *PLoS ONE* 12:e0174454. doi: 10.1371/journal.pone.0174454

Oh, H.-S., Tan, C. H., Low, J. H., Rzechowicz, M., Siddiqui, M. F., Winters, H., et al. (2017). Quorum quenching bacteria can be used to inhibit the biofouling of reverse osmosis membranes. *Water Res.* 112, 29–37. doi: 10.1016/j.watres.2017.01.028

Wood, T. L., Guha, R., Tang, L., Geitner, M., Kumar, M., and Wood, T. K. (2016). Living biofouling-resistant membranes as a model for the beneficial use of engineered biofilms. *Proc. Natl. Acad. Sci. U.S.A.* 113, E2802–E2811. doi: 10.1073/pnas.1521731113

Conflict of Interest Statement: The authors declare that the research was conducted in the absence of any commercial or financial relationships that could be construed as a potential conflict of interest.

frontiers in Cellular and Infection Microbiology

ORIGINAL RESEARCH
published: 23 July 2018
doi: 10.3389/fcimb.2018.00252

Differential Regulation of the Phenazine Biosynthetic Operons by Quorum Sensing in *Pseudomonas aeruginosa* PAO1-N

Steven Higgins[1,2], *Stephan Heeb*[1], *Giordano Rampioni*[1,3], *Mathew P. Fletcher*[1], *Paul Williams*[1] *and Miguel Cámara*[1]*

[1] Centre for Biomolecular Science, School of Life Science, University of Nottingham, Nottingham, United Kingdom, [2] Department of Plant and Microbial Biology, University of Zürich, Zurich, Switzerland, [3] Department of Science, University Roma Tre, Rome, Italy

The *Pseudomonas aeruginosa* quorum sensing (QS) network plays a key role in the adaptation to environmental changes and the control of virulence factor production in this opportunistic human pathogen. Three interlinked QS systems, namely *las*, *rhl,* and *pqs*, are central to the production of pyocyanin, a phenazine virulence factor which is typically used as phenotypic marker for analysing QS. Pyocyanin production in *P. aeruginosa* is a complex process involving two almost identical operons termed $phzA_1B_1C_1D_1E_1F_1G_1$ (*phz1*) and $phzA_2B_2C_2D_2E_2F_2G_2$ (*phz2*), which drive the production of phenazine-1-carboxylic acid (PCA) which is further converted to pyocyanin by two modifying enzymes PhzM and PhzS. Due to the high sequence conservation between the *phz1* and *phz2* operons (nucleotide identity > 98%), analysis of their individual expression by RNA hybridization, qRT-PCR or transcriptomics is challenging. To overcome this difficulty, we utilized luminescence based promoter fusions of each phenazine operon to measure in planktonic cultures their transcriptional activity in *P. aeruginosa* PAO1-N genetic backgrounds impaired in different components of the *las*, *rhl,* and *pqs* QS systems, in the presence or absence of different QS signal molecules. Using this approach, we found that all three QS systems play a role in differentially regulating the *phz1* and *phz2* phenazine operons, thus uncovering a higher level of complexity to the QS regulation of PCA biosynthesis in *P. aeruginosa* than previously appreciated.

IMPORTANCE

The way the *P. aeruginosa* QS regulatory networks are intertwined creates a challenge when analysing the mechanisms governing specific QS-regulated traits. Multiple QS regulators and signals have been associated with the production of phenazine virulence factors. In this work we designed experiments where we dissected the contribution of specific QS switches using individual mutations and complementation strategies to gain further understanding of the specific roles of these QS elements in controlling expression of the two *P. aeruginosa* phenazine operons. Using this approach we have teased out which QS regulators have either indirect or

OPEN ACCESS

Edited by:
Maria Tomas,
Complexo Hospitalario Universitario A Coruña, Spain

Reviewed by:
Rodolfo García-Contreras,
Universidad Nacional Autónoma de México, Mexico
Eric Déziel,
Institut National de la Recherche Scientifique (INRS), Canada
Thibault Géry Sana,
Stanford University, United States

***Correspondence:**
Miguel Cámara
miguel.camara@nottingham.ac.uk

Received: *10 April 2018*
Accepted: *03 July 2018*
Published: *23 July 2018*

Citation:
Higgins S, Heeb S, Rampioni G, Fletcher MP, Williams P and Cámara M (2018) Differential Regulation of the Phenazine Biosynthetic Operons by Quorum Sensing in Pseudomonas aeruginosa PAO1-N. Front. Cell. Infect. Microbiol. 8:252. doi: 10.3389/fcimb.2018.00252

direct effects on the regulation of the two phenazine biosynthetic operons. The data obtained highlight the sophistication of the QS cascade in *P. aeruginosa* and the challenges in analysing the control of phenazine secondary metabolites.

Keywords: *Pseudomonas aeruginosa*, phenazines, pyocyanin, quorum sensing, LasR, RhlR, RsaL, PqsE

INTRODUCTION

Pseudomonas aeruginosa is a highly adaptable bacterium, which can be found in a range of challenging environments, including the human host. This is achieved in great part by the ability of this opportunistic pathogen to finely control the expression of a wide range of genes, including those involved in the production of virulence determinants, in response to environmental and metabolic stimuli (Lee et al., 2006; Balasubramanian et al., 2013; Sun et al., 2016). The expression of many virulence genes in *P. aeruginosa* is also controlled in a cell density dependent manner by quorum sensing (QS) (Smith and Iglewski, 2003; Bjarnsholt and Givskov, 2007).

P. aeruginosa has a sophisticated QS network consisting of three separate but interwoven systems, namely *las*, *rhl,* and *pqs* and their cognate QS signal molecules (QSMs). The QSMs *N*-3-oxo-dodecanoyl-homoserine lactone ($3OC_{12}$-HSL) produced by LasI, and *N*-butanoyl-homoserine lactone (C_4-HSL) produced by RhlI interact with their cognate transcriptional regulators LasR and RhlR respectively, leading to the activation or repression of multiple genes including the genes coding for their cognate signal synthases (Schuster et al., 2013). The LasR/$3OC_{12}$-HSL complex also induces the transcription of *rsaL*, a gene integrated in the *las* QS system coding for the global transcriptional regulator RsaL (de Kievit et al., 1999). This protein directly represses the transcription of multiple genes, including *lasI*, hence exerting a homeostatic effect on $3OC_{12}$-HSL production, and conferring robustness to the expression of a sub-set of genes of the *las* regulon with respect to fluctuations in LasR levels (Rampioni et al., 2006, 2007; Bertani et al., 2007).

The *pqs* QS system is more complex than the *las* and *rhl* systems, since multiple enzymes encoded by the *pqsABCDE* operon are required for the synthesis of 2-alkyl-4(1*H*)-quinolones (AQs) including the QSMs 2-heptyl-4-hydroxyquinoline (HHQ), which in turn is converted to 2-heptyl-3-hydroxy-4-quinolone (PQS) by the monooxygenase PqsH. Both HHQ and PQS can bind to and activate the transcriptional regulator PqsR (also known as MvfR). The PqsR/HHQ and PqsR/PQS complexes bind the P*pqsA* promoter region and increase the transcription of the *pqsABCDE* operon, thus generating a feedback loop that accelerates AQ biosynthesis and increasing production of PqsE, coded by the last gene of the *pqsABCDE* operon (Heeb et al., 2011; Dulcey et al., 2013). PqsE is a thioesterase involved in AQ biosynthesis (Drees and Fetzner, 2015) but this protein also controls indirectly the expression of multiple virulence factors even in the absence of AQs. The molecular mechanism by which PqsE impacts on QS target gene expression remains unknown (Hazan et al., 2010; Rampioni et al., 2010, 2016).

The QS circuit of *P. aeruginosa* has been widely reported to have a hierarchal structure. Under growth conditions using rich media, it is generally accepted that the *las* QS system is the first to become active leading to the activation of the *rhl* and *pqs* systems (Pesci et al., 1997; de Kievit et al., 2002; Gallagher et al., 2002; Xiao et al., 2006). However it has been reported that RhlR can in part overcome the absence of the *las* system in late stationary phase (Dekimpe and Deziel, 2009). RhlR is required for production of certain virulence factors but has a negative impact on the *pqs* system by repressing PQS signal production through interference with the expression of *pqsR* and *pqsABCDE* (McKnight et al., 2000; Wade et al., 2005; Xiao et al., 2006; Brouwer et al., 2014). In turn the *pqs* system has a positive effect upon the *rhl* system, as addition of PQS to a *P. aeruginosa* culture has been shown to increase the levels of RhlR and the *rhl* QS signal C_4-HSL (McKnight et al., 2000; Diggle et al., 2003). The interactions of the QS systems are detailed in Figure S1.

QS has been shown to affect the transcription of hundreds of downstream genes (Schuster et al., 2003; Wagner et al., 2003; Rampioni et al., 2007, 2010) with some of these specifically controlled by distinct QS systems, while others are induced or repressed by multiple QS regulators (Schuster and Greenberg, 2007; Farrow et al., 2008; Cornforth et al., 2014; Rampioni et al., 2016).

The production of pyocyanin (PYO), a key virulence factor produced by *P. aeruginosa*, has been linked to multiple QS systems. This particular phenazine is often used as a marker to assess QS behavior as it is easily measurable and contributes significantly toward the green color of *P. aeruginosa* cultures (Frank and Demoss, 1959). Although PYO is the most studied phenazine in *P. aeruginosa*, this organism is capable of producing up to 5 different phenazine derivatives (Mavrodi et al., 2001, 2010). Phenazine biosynthesis begins with the conversion of chorismic acid to phenazine-1-carboxylic acid (PCA) by the action of the enzymes encoded by the biosynthetic operon *phzABCDEFG*, which is conserved across the fluorescent Pseudomonad species (Mavrodi et al., 2006, 2010). Interestingly *P. aeruginosa* has 2 functional copies of this operon designated *phz1* and *phz2*. Both operons produce PCA, which can be further converted to phenazine-1-carboxamide by the action of PhzH and to 1-hydroxyphenazine by PhzS. The action of PhzM is to convert PCA to 5-methylphenazine-1-carboxylic acid betaine, which can be further converted to PYO by PhzS (Mavrodi et al., 2001, 2006, 2010).

PYO production has been linked to QS in many reported studies and to date LasR, RhlR, RsaL, PqsE, PqsR and both AQ signal molecules HHQ and PQS have been found to play a role in the control of its production (Whiteley and Greenberg, 2001; Gallagher et al., 2002; Diggle et al., 2003; Schuster et al., 2003; Wagner et al., 2003; Rampioni et al., 2007, 2010; Farrow

et al., 2008; Lu et al., 2009; Liang et al., 2011; Recinos et al., 2012; Cabeen, 2014; Sun et al., 2017). Although QS controls PYO production, the high sequence conservation between the two phenazine producing operons *phz1* and *phz2* have made analysing their individual expression by DNA hybridization techniques challenging (Schuster et al., 2003; Wagner et al., 2003; Rampioni et al., 2007, 2010).

It is unlikely that both phenazine biosynthesis operons are controlled in the same manner as they are located some distance apart on the PAO1 chromosome and have very different promoter regions (Mavrodi et al., 2001; Whiteley and Greenberg, 2001; Rampioni et al., 2007; Winsor et al., 2011). The *phz1* operon (from PA4210 to PA4216) is flanked by *phzM* upstream (PA4209) and *phzS* downstream (PA4217), both of which are required to produce PYO. The *phz2* operon (from PA1899 to PA1905) is flanked upstream by the *qscR* gene (PA1898), coding for the orphan QS receptor QscR, and downstream by the PA1906 gene, coding for a hypothetical protein of unknown function. The *phzH* gene (PA0051) is unlinked to the other phenazine biosynthetic genes (Figure S2). It would appear by looking at the positions of the operons on the chromosome of *P. aeruginosa* PAO1 that the *phz1* operon is clustered with the genes required to produce PYO, and hence could be more closely associated with PYO production than *phz2*. That said, the *phz2* operon has been shown to contribute significantly to the production of PYO, especially under non-planktonic growth conditions (Recinos et al., 2012; Dietrich et al., 2013).

There is a greater quantity of available information about the control of *phz1* than *phz2*, and a *lux* box, for LasR or RhlR binding, has been predicted upstream of the −10 region of the *phz1* promoter (P*phzA1*) (Whiteley and Greenberg, 2001). The QS repressor RsaL has also been shown to bind to this promoter in an electrophoretic mobility shift assay (EMSA) at the downstream end of the −10 promoter region, thus acting as a repressor of *phz1* transcription (Rampioni et al., 2007). Moreover, RsaL exerts an indirect negative effect on *phz1* transcription by increasing the production of the *phz1* repressor protein CdpR (Sun et al., 2017).

Less is known about the regulation of the *phz2* promoter (P*phzA2*). The intergenic region between *qscR* and *phz2* was probed for RsaL binding by different groups with negative results (Rampioni et al., 2007; Sun et al., 2017), hence RsaL appears to control P*phzA1* but not P*phzA2*. Recinos and colleagues found that *phz2* transcription is induced by HHQ under anaerobic conditions (Recinos et al., 2012). Identification of a predicted ANR/DNR binding site within the P*phzA2* promoter supports the notion that *phz2* transcription is increased in anaerobic environments (Trunk et al., 2010). The orphan *luxR* QS regulator, QscR, which is encoded directly upstream of *phzA2* has been reported to be a repressor of *phzA2* (Ledgham et al., 2003; Lequette et al., 2006). The *qscR* and *phz2* intergenic region was probed for QscR binding with a negative result (Lee et al., 2006) suggesting the effect of QscR on *phzA2* is indirect due to the ability of QscR to form inactive heterodimers with LasR and RhlR (Chugani et al., 2001).

To gain a further understanding of the control of each phenazine biosynthesis operon by QS, *lux*-based promoter fusions for each operon were created and tested in a range of QS mutants. We identified an RsaL dependent switch, which can move PCA production from one operon to the other, and *vice versa*. This switching mechanism was confirmed by modification of the QS network activity in selected mutants with the addition of QS signal molecules and specific QS regulator genes expressed from plasmids. This allowed us to confirm the hierarchal structure of QS in rich media under planktonic conditions and to develop a more in depth model of how QS controls *phz1* and *phz2* transcription in *P. aeruginosa*.

MATERIALS AND METHODS

Bacterial Strains and Growth Conditions

The bacterial strains and plasmids used in this study are detailed in Table S1. They were routinely grown in Lysogeny Broth (LB) at 37°C with shaking at 200 rpm, with the exception of *P. aeruginosa* conjugation recipient strains, which were incubated at 42°C. When required, LB was supplemented with the following antibiotics: for *E. coli*, 10 μg ml^{-1} tetracycline (Tc), 30 μg ml^{-1} chloramphenicol (Cm), or 100 μg ml^{-1} ampicillin (Ap); for *P. aeruginosa*, 150 μg ml^{-1} Tc, 375 μg ml^{-1} Cm or 800 μg ml^{-1} streptomycin (Sm). Media were supplemented with 1 mM (final concentration) isopropyl β-D-1-thiogalactopyranoside (IPTG) for inducible strains where required, unless otherwise stated. Synthetic signal molecules PQS and 2-methyl-3-hydroxy-4-quinolone (mPQS) were added to cultures at a final concentration of 100 μM where required. To select for *P. aeruginosa* after mating experiments LB agar plates were supplemented with 15 μg ml^{-1} nalidixic acid (Nal).

DNA Manipulations

All plasmids generated and/or used in this study are listed in Table S1. Routine DNA manipulations including extraction, restriction, ligation, electroporation, conjugation and agarose gel electrophoresis were performed using standard molecular methods (Sambrook and Russell, 2001). Plasmid extraction was completed using a Qiagen™ QiaQuick miniprep kit following the manufacturer's instructions. The Tc^R marker of pMINI-CTX1 derived constructs integrated into the chromosome of *P. aeruginosa* was removed using the Flp recombinase system as previously described (Hoang et al., 1998, 2000). All primers used for DNA amplification by PCR are detailed in Table S2. DNA sequencing was conducted at the University of Nottingham's DNA sequencing facility.

Generation of pP*phzA1*-lux, pP*phzA2*-lux, and pRsaI Plasmids

pMINI-lux was generated by cloning the *Bam*HI-*Eco*RI fragment of pBluelux (Atkinson et al., 2008), containing the *luxCDABE* operon, into similarly digested mini-CTX1, using standard molecular methods (Sambrook and Russell, 2001). The P*phzA1* and P*phzA2* promoter regions were PCR amplified from *P. aeruginosa* PAO1 chromosomal DNA using primer pairs FWP*phzA1*-RVP*phzA1*, and FWP*phzA2*-RVP*phzA2*, respectively (Table S2). The PCR products were independently cloned into the pMINI-lux construct between the *Eco*RI and

*Xho*I restriction sites, resulting in the plasmids pP*phzA1*-lux and pP*phzA1*-lux, respectively.

The *rsaL* coding region was amplified by PCR from *P. aeruginosa* PAO1 chromosomal DNA using primers FW*rsaL* and RV*rsaL* (Table S2). The resulting PCR product was cloned into pME6032 between the *Eco*RI and *Xho*I restriction sites using standard molecular techniques. This plasmid was introduced to *P. aeruginosa* strains by electroporation (Choi et al., 2006).

All cloned fragments obtained by PCR were verified by DNA sequencing to match the reference sequences (Winsor et al., 2011).

Generation of *P. aeruginosa* Mutant Strains

To generate the double mutant strain *P. aeruginosa pqsE*ind Δ*lasR*, the *lasR* gene was deleted from the chromosome of the PAO1 *pqsE*ind strain (Rampioni et al., 2010) by using the pME3087-Δ*lasR* plasmid (Harrison et al., 2014).

Briefly, the pME3087-Δ*lasR* plasmid was mobilized by conjugation into the *P. aeruginosa pqsE*ind recipient strain using *E. coli* S17.1 λ*pir* as a donor. Exconjugants were selected on LB plates supplemented with 150 μg ml^{-1} Tc and 15 μg ml^{-1} Nal. Strains were re-streaked twice on LB lacking antibiotic and then subjected to 1 round of Tc sensitivity enrichment to select for double cross-over events (Voisard et al., 1994). Five colonies which were Tc^{S} were then tested by PCR for loss of the *lasR* coding region.

To generate a *P. aeruginosa* PAO1 mutant strain with an *rsaL* deletion (Δ*rsaL*), allelic exchange was obtained by using the pDM4-Δ*rsaL* plasmid, derived from the suicide vector pDM4 (Milton et al., 1996). The upstream and the downstream DNA regions of *rsaL* were PCR amplified from *P. aeruginosa* PAO1 chromosomal DNA using primer pairs FW*rsaL*UP + RV*rsaL*UP and FW*rsaL*DOWN + RV*rsaL*DOWN, respectively (Table S2). The upstream and downstream PCR fragments were subsequently cloned in pDM4 by XhoI-BamHI and BamHI-XbaI restriction, respectively. The resulting pDM4-Δ*rsaL* plasmid was verified by restriction analysis and sequencing. Allelic exchange in *P. aeruginosa* PAO1 following conjugal mating with the *E. coli* S17.1 λ*pir* (pDM4-Δ*rsaL*) donor strain and sucrose counter selection was performed as previously described (Westfall et al., 2004). The resulting PAO1 Δ*rsaL* mutant strain was confirmed by PCR.

Gene Expression Assays

Three independent single colonies of *P. aeruginosa* strains carrying reporter constructs were grown overnight in LB (separate tubes) at 37°C with shaking at 200 rpm. One-milliliter of overnight culture was washed in 1 ml of fresh LB to remove secreted bacterial products and QS signal molecules. Twenty-microliters aliquots were inoculated into 1 ml of fresh LB, and 300 μl of the resulting cultures were dispensed into wells of a 96-well black flat-transparent-bottom microtiter plate. When needed, strains with inducible genes were grown with or without 1 mM IPTG unless otherwise stated. Microtiter plates were incubated at 37°C in a TECAN GENios automated luminometer-spectrophotometer with which luminescence and turbidity were recorded every 30 min. Promoter activity per cell is given as relative light units divided by absorbance at 600 nm wavelength (A_{600}).

Statistical Tests

Standard deviation of the mean of the three biological replicates is reported. A paired *t*-test was used to compare each mutant with the relevant control for reach experiment. A *P*-value of ≤ 0.05 was considered significant.

RESULTS

QS Control of *phz1* and *phz2* Expression

To ascertain how the phenazine operons *phz1* and *phz2* are regulated by the different elements of the QS circuit in *P. aeruginosa* PAO1-N, the pP*phzA1*-lux and pP*phzA2*-lux reporter plasmids, containing transcriptional fusions between the P*phzA1* and P*phzA2* promoter regions and the *luxCDABE* operon for bioluminescence, respectively, were generated and inserted in the chromosome of strain PAO1-N and different mutants derived from it. In detail, in the pP*phzA1*-lux plasmid a 727-bp DNA fragment comprising the entire intergenic region between *phzM* and *phzA1* was cloned upstream of the *luxCDABE* operon, while in pP*phzA2*-lux a 497-bp DNA fragment including the entire intergenic region between *qscR* and *phzA2* was cloned instead. By including these relatively large promoter regions the likelihood of missing any key regulatory element upstream of the known unique transcription start sites of P*phzA1* and P*phzA2* (Dötsch et al., 2012) was minimized. Cloned promoter regions include the first two codons of *phzA1* and *phzA2*, respectively. Since the vast majority of studies on the QS circuit of *P. aeruginosa* have been undertaken in rich media, LB was used in this work so that predictions about the behavior of the QS network in specific QS mutants could be made and the results obtained compared with previous studies.

Firstly, the impact of QS elements, previously identified as key players in the regulation of PYO production, on P*phzA1* and P*phzA2* activity was investigated in PAO1-N, since there have been some strain-specific differences shown in the regulation of these operons by QS (Sun et al., 2016). **Figure 1**, shows that under the planktonic conditions studied the activity of P*phzA1* is several fold higher than that of P*phzA2* which is in line with what has been detected in *P. aeruginosa* PA14 (Recinos et al., 2012). LasR, RhlR, and PqsE showed a positive effect on the activation of the P*phzA1* and P*phzA2* promoters. P*phzA1* activity was completely abrogated in the Δ*lasR* and Δ*rhlR* mutants, and strongly decreased (90% reduction) in the non-induced *pqsE* conditional mutant strain, *pqsE*ind ($P < 0.01$). The effect of LasR, RhlR, and PqsE on P*phzA2* appear to be milder although still significant ($P < 0.05$), with reporter activities reduced by 78, 71, and 52% in the Δ*lasR*, Δ*rhlR* and non-induced *pqsE*ind strains, respectively. When PqsE was fully induced with 1 mM IPTG in the *pqsE*ind strain, a 3.5-fold increase in promoter activity of both P*phzA1* and P*phzA2* was observed relative to the PAO1-N wild type ($P < 0.01$). Conversely, RsaL had an opposite effect on the two promoters, since P*phzA1* activity is significantly increased (298% increase) and P*phzA2* activity decreased (80%

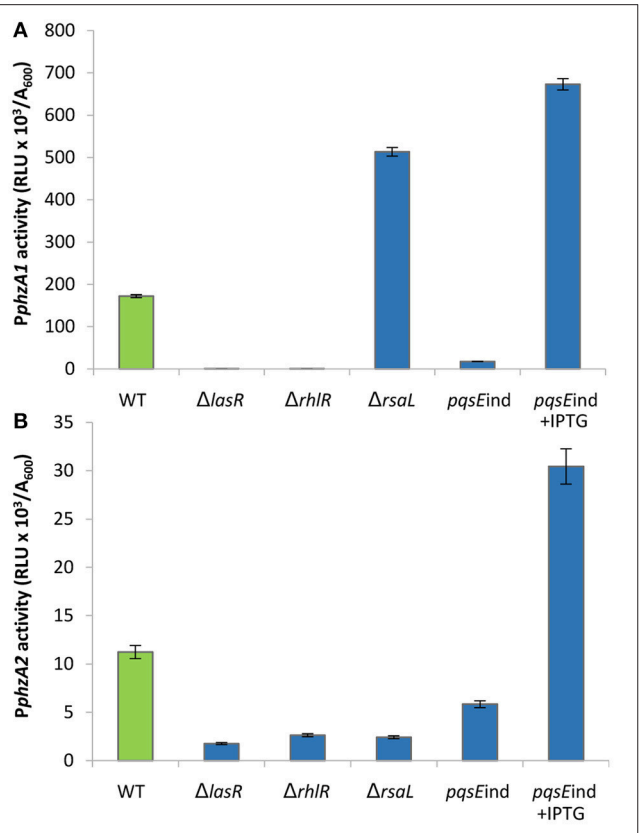

FIGURE 1 | Effect of QS elements on P*phzA1* and P*phzA2* activity. Maximal promoter activity per cell measured in the indicated strains derived from *P. aeruginosa* PAO1-N carrying the transcriptional fusions P*phzA1-lux* **(A)** or P*phzA2-lux* **(B)**. Bioluminescence (relative light units, RLU) and cell density (A_{600}) were recorded after 6 h incubation at 37°C. Mean of three independent experiments is shown with standard deviation.

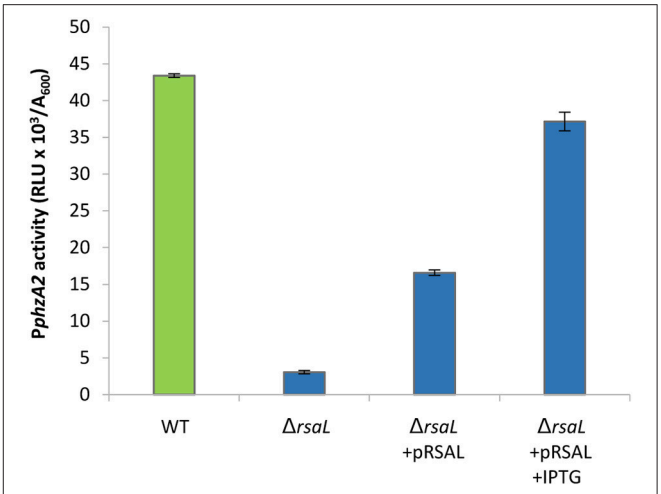

FIGURE 2 | Effect of pRsaL on P*phzA2* activity. Maximal promoter activity of P*phzA2-lux* in the wild type PAO1-N and the *rsaL* mutant background, with and without complementation. Promoter activities are normalized by cell density (A_{600}).

reduction) ($P < 0.01$), in the Δ*rsaL* mutant compared to PAO1-N wild type. These results are in accordance with published data for other *P. aeruginosa* strains, showing a positive effect of LasR, RhlR and PqsE on PCA biosynthesis in the human pathogen *P. aeruginosa* PA14 and in the rhizosphere bacterium *P. aeruginosa* PA1201 (Recinos et al., 2012; Sun et al., 2016, 2017). Also the dual effect of RsaL on P*phzA1* and P*phzA2* is in line with what was previously observed in *P. aeruginosa* PA1201 (Sun et al., 2017). The growth data for this experiment is shown in Figure S3.

To further validate the regulation of P*phzA2* by RsaL, the *rsaL* deletion was complemented *via* the IPTG inducible pRsaL plasmid. Some partial restoration of P*phzA2* activity was observed in the Δ*rsaL* strain in the presence of pRsaL, likely as a consequence of basal *rsaL* transcription from the *tac* promoter (Guzman et al., 1995), while in the presence of 0.1 mM IPTG P*phzA2* activity was restored to wild type levels ($P < 0.05$) (**Figure 2**). Overall, these data confirm that in PAO1-N RsaL is a repressor of *phz1* transcription and has a positive effect upon P*phzA2,* the latter likely mediated by an ancillary P*phzA2*-regulator under the control of RsaL, since purified RsaL has not been shown to directly bind to P*phzA2* in EMSA studies (Rampioni et al., 2007; Sun et al., 2017). The growth data for this experiment is shown in Figure S4.

Detailed Analysis of the Impact of the QS Cascade on P*phzA1* Activity

High levels of PqsE resulted in an increase in promoter activity for both phenazine biosynthesis operons (**Figure 1**). Since a *lux*-box is present in the P*phzA1* promoter region and PqsE does not act as a transcriptional regulator, it can be hypothesized that PqsE exerts a positive effect on P*phzA1* activity *via* the LasR and/or RhlR transcriptional regulators. This hypothesis was tested by analysing P*phzA1* activity in the double mutants *pqsE*ind Δ*lasR* and *pqsE*ind Δ*rhlR* respectively in which *pqsE* expression can be restored in the presence of IPTG. **Figure 3** reveals that while PqsE induction with IPTG resulted in high P*phzA1* activity in the *pqsE*ind strain, the activity of this promoter under induced conditions was reduced by 80% in the *pqsE*ind Δ*lasR* mutant and a 2 h delay in activation of P*phzA1* relative to the *pqsE*ind strain induced with IPTG was observed. P*phzA1* activity was completely abrogated in the *pqsE*ind Δ*rhlR* background. The growth data for this experiment is shown in Figure S5.

The *las* QS system has a positive effect on the activity of both the *rhl* and *pqs* QS systems (Pesci et al., 1997; Medina et al., 2003; Xiao et al., 2006). Moreover, a study by McKnight et al. (2000) showed that addition of exogenous PQS positively regulates the *rhl* system, and Diggle et al. (2003) showed that addition of exogenous PQS advances and enhances pyocyanin production and increases RhlR levels. We therefore hypothesized that the reduction of transcriptional activity of P*phzA1* in the *pqsE*ind Δ*lasR* mutant could be caused by reduced activity of the *rhl* and *pqs* systems in this mutant background, and hence exogenous provision of PQS should compensate for a *las* mutation. To test this, P*phzA1* activity was analyzed in the Δ*lasR* and Δ*rhlR* strains

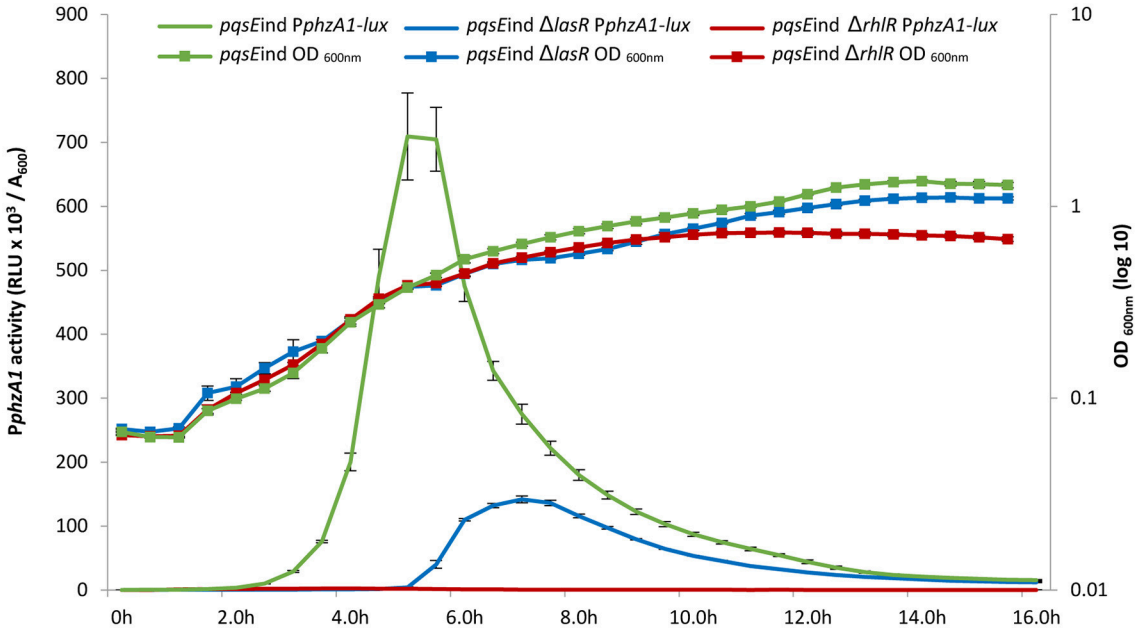

FIGURE 3 | A delay in the timing of P*phzA1* activation was observed when *lasR* was mutated in the *pqsE*ind strain. The *pqsE*ind strain increased the activity of P*phzA1-lux* (green line) but when *lasR* is mutated a 2 h delay in promoter activation is observed (blue line) compared with the *pqsE*ind. When *rhlR* is deleted from the *pqsE*ind strain P*phzA1-lux* activity is abolished (red line). The growth curves of the 3 mutants are also shown and this data is plotted on the *Z* axis. All strains were induced with 1 mM IPTG and promoter activities are normalized by cell density (A_{600}).

in the presence of 100 μM exogenous PQS. To discard any effects related to the iron chelating properties of PQS, the non-signaling quinolone molecule methyl PQS (mPQS) was used as a control, since this molecule is capable of binding iron like PQS, but is unable to trigger gene expression *via* PqsR (Diggle et al., 2007). Addition of PQS was found to compensate for a *lasR* deletion ($P < 0.05$), while an *rhlR* deletion resulted in no activation of the P*phzA1* promoter, irrespective of the absence or presence of PQS (**Figure 4**). The addition of PQS also impacted on the timing of P*phzA1* gene expression in both wild type and *lasR* deletion strains with the activation of this promoter triggered 1 h earlier than in the absence of this signal molecule (data not shown). The growth data for this experiment is shown in Figure S6.

These data suggest that RhlR is a direct positive regulator of the *phz1* operon, as loss of this element abolishes P*phzA1* activity, while LasR acts as an indirect P*phzA1* regulator.

Addition of PQS in the previous experiment would be expected to increase the expression of the *pqsABCDE* operon and hence PqsE production through the activation of PqsR. The data presented here suggests that PqsE is required to activate P*phzA1* and PqsE would be present in high levels after the addition of exogenous PQS to the culture. To further investigate the importance of RhlR and LasR in the PqsE-mediated activation of P*phzA1* the above experiments were repeated using the *pqsE*ind conditional mutant with additional *lasR* and *rhlR* mutations.

Addition of PQS to the un-induced *pqsE*ind strain resulted in no significant increase in P*phzA1* activity, compared to the un-induced *pqsE*ind strain ($P < 0.05$). This result confirms that PqsE rather than PQS on its own or through PqsR activation is required to reach high levels of P*phzA1* transcription (**Figure 5**). Since PqsR has been reported to directly bind to *rhlI/R* resulting in some increased expression of these genes (Maura et al., 2016) this result suggests that activated RhlR in combination with PqsR are unable to activate P*phzA1* transcription. In the *pqsE*ind strain the expression of *pqsE* is decoupled from that of *pqsABCD*, due to a transcriptional terminator introduced downstream of *pqsD*, hence PqsE production is not under the control of PqsR (Rampioni et al., 2010). Addition of PQS when *pqsE*ind was induced by IPTG slightly increased P*phzA1* activity compared with the non-induced *pqsE*ind without PQS, this may be due to some PqsR direct activation of *rhlI/R*. Again PQS was unable to trigger reporter gene expression in the *pqsE*ind Δ*lasR* strain when *pqsE* was not induced. Interestingly, when *pqsE* was fully induced and PQS was added to the *pqsE*ind Δ*lasR* mutant, a significant increase in P*phzA1* activity ($P < 0.05$) of approximately 50% was observed compared with the fully induced *pqsE*ind mutant. No P*phzA1* expression was detected in the *pqsE*ind Δ*rhlR* strain under any of the conditions tested confirming the importance of RhlR in activating *phz1* transcription (**Figure 5**). The growth data for this experiment is shown in Figure S6.

The high levels of P*phzA1* activity observed when both, PQS is added and PqsE expression is induced with IPTG in the *pqsE*ind Δ*lasR* strain, could be due to low levels of RsaL, which is a repressor of P*phzA1* (**Figure 1**). Since LasR activates the *rsaL* promoter (P*rsaL*), the Δ*lasR* mutant is expected to express low

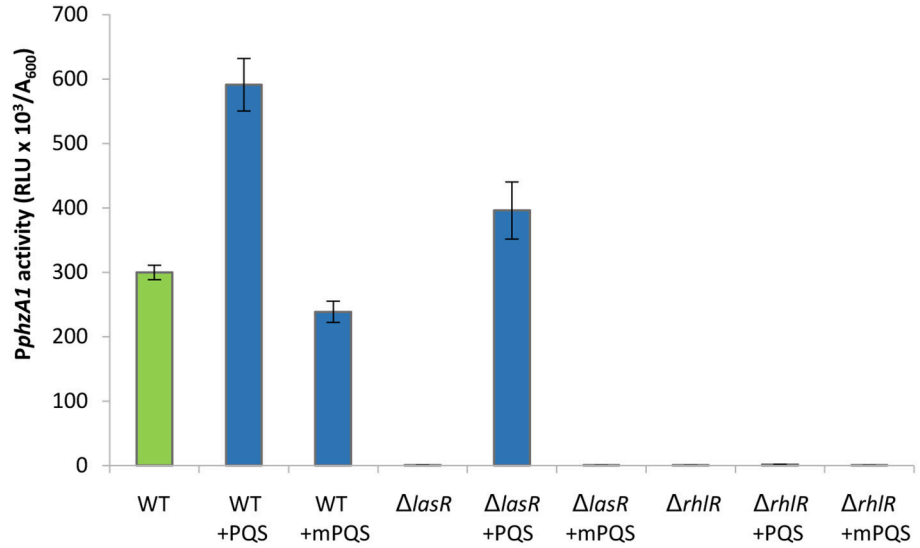

FIGURE 4 | The addition of exogenous PQS compensates for a mutation in *lasR* by increasing activity of P*phzA1*. Maximal promoter activity of P*phzA1-lux* in the wild type PAO1-N, *lasR* and *rhlR* deletion backgrounds in the presence of PQS or methyl PQS (mPQS). Promoter activities are normalized by cell density (A_{600}).

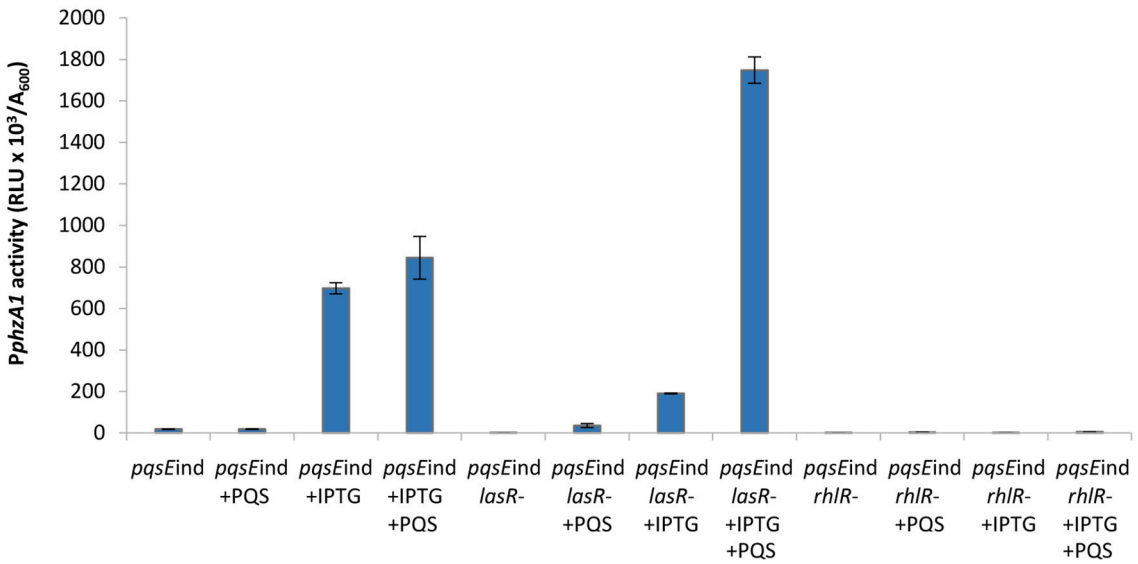

FIGURE 5 | PQS is unable to induce high levels of P*phzA1* transcription in the absence of PqsE or RhlR. Maximal promoter activity of P*phzA1-lux* in the *pqsE*ind strain and *pqsE*ind strain carrying additional *lasR* or *rhlR* mutations in the presence or absence of IPTG and PQS. Promoter activities are normalized by cell density (A_{600}).

levels of RsaL. Overall, these data are consistent with PqsE and RhlR as the key activators of the *phz1* operon with RsaL acting as a repressor.

Detailed Analysis of the Impact of the QS Cascade on P*phzA2* Activity

In **Figure 1** we show that both PqsE and RsaL exert positive control over the expression of P*phzA2* but the influence the *las* and *rhl* systems may have on this regulation is not clear. To investigate this further, the expression of P*phzA2* was studied in *pqsE*ind and *pqsE*ind with a *lasR* or a *rhlR* deletion. When *pqsE* was induced in either strain, P*phzA2* activity could only achieve 5% and 10% of the *pqsE*ind strain (**Figure 6**), growth data Figure S7. This differed from the result obtained for P*phzA1*, as a *lasR* deletion in the *pqsE*ind induced strain decreased but did not abrogate P*phzA1* activity (**Figure 5**). To ascertain whether addition of exogenous PQS could compensate for *lasR* and *rhlR* deletions, P*phzA2* activity was evaluated in the Δ*lasR* and Δ*rhlR* mutants supplemented with exogenous PQS or mPQS, the latter molecule used as an iron-binding negative control as before.

Unlike P*phzA1*, where PQS restored promoter activity in the Δ*lasR* mutant, no significant increase ($P < 0.05$) in P*phzA2* activity was observed when PQS was added to the Δ*lasR* and Δ*rhlR* strains (**Figure 7**), growth data Figure S8.

These results suggests that both LasR and RhlR are required to activate P*phzA2*. Since addition of exogenous PQS increases the levels of PqsE (Heeb et al., 2011) we next investigated whether PqsE or PqsR were responsible for the increase in P*phzA2* activity. The same experimental strategy as for P*phzA1* analysis was used and activity of P*phzA2* was assayed in the *pqsE*ind mutant strain and the *pqsE*ind strains with additional *lasR* and *rhlR* deletions, in the presence of exogenously added PQS and IPTG.

The result of this experiment showed that addition of PQS to the un-induced *pqsE*ind strain resulted in no significant increase in P*phzA2* activity, compared to the un-induced *pqsE*ind strain ($P < 0.05$). When *pqsE* was induced with IPTG, P*phzA2* activity was triggered and further increased by addition of exogenous PQS ($P < 0.05$) (**Figure 6**). These data suggest that PqsE rather than PqsR is required to positively regulate P*phzA2*, as it was for P*phzA1*. Hardly any increase in the expression of the P*phzA2* promoter was observed in the *pqsE*ind strains carrying additional *lasR* and

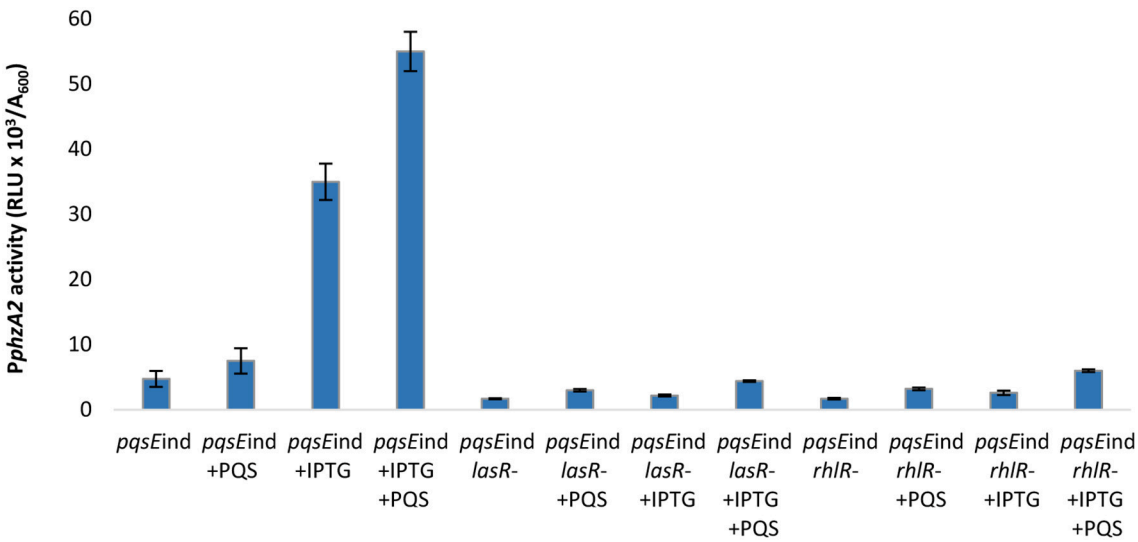

FIGURE 6 | PQS is unable to induce P*phzA2* transcription in the absence of PqsE, LasR, and RhlR. Maximal promoter activity of P*phzA1-lux* in the *pqsE*ind strain and *pqsE*ind strain carrying additional *lasR* or *rhlR* mutations in the presence or absence of IPTG and PQS. Promoter activities are normalized by cell density (A_{600}).

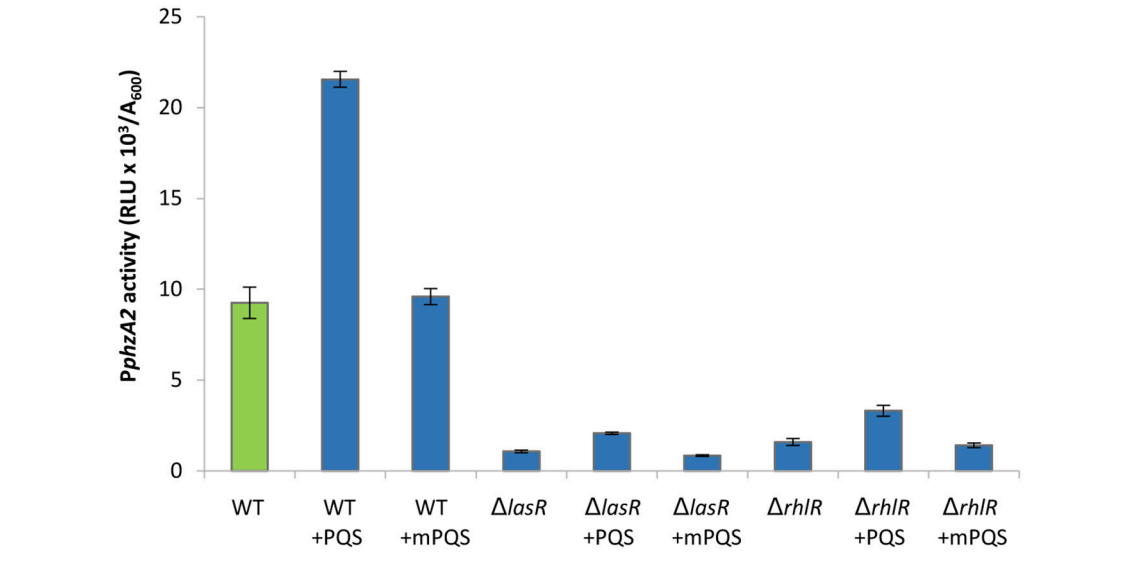

FIGURE 7 | P*phzA2* activity cannot be restored by exogenous PQS in *lasR* or *rhlR* mutants. Maximal promoter activity of P*phzA2-lux* in the wild type PAO1-N, *lasR* and *rhlR* deletion backgrounds in the presence of PQS or methyl PQS (mPQS). Promoter activities are normalized by cell density (A_{600}).

rhlR deletions, either in the absence or presence of IPTG and/or PQS, suggesting that LasR, RhlR and PqsE are all key for P*phzA2* transcription.

We have shown that RsaL has a positive effect on P*phzA2* (**Figures 1**, **2**). The *rsaL* promoter is positively regulated by LasR, hence in the *lasR* deletion mutant low levels of RsaL would be expected, which in turn should have a negative impact on P*phzA2* activity. Therefore, we hypothesized that LasR is an indirect activator of P*phzA2* acting *via* RsaL, and to test this we transformed the *lasR* mutant strain with the inducible pRsaL plasmid. As LasR affects the activity of the *rhl* and *pqs* QS systems, exogenous PQS was also added to increase the activity of the *rhl* and *pqs* QS systems.

The result of these experiments suggest that LasR is an indirect activator of P*phzA2*, since an increase in P*phzA2* activity in the *lasR* mutant carrying pRsaL was observed, compared with the *lasR* mutant. Addition of exogenous PQS further increased P*phzA2* activity to the level of the wild type PAO1-N level when pRsaL was induced with IPTG ($P < 0.05$) (**Figure 8**), growth data Figure S9.

These data suggest that RsaL alone is unable to induce the P*phzA2* promoter to wild type levels and must be working in conjunction with other regulatory elements. To gain further evidence that LasR is an indirect activator of P*phzA2* and investigate the requirement of PqsE and RhlR to activate P*phzA2*, we introduced pRsaL in the *pqsE*ind and *pqsE*ind strains with additional *lasR* and *rhlR* deletions. When RsaL and PqsE expression was induced in these strains with IPTG, P*phzA2* activity of the *pqsE*ind Δ*lasR* strain carrying pRsaL was significantly increased ($P < 0.05$) compared to the *pqsE*ind Δ*lasR* strain and P*phzA2* activity was comparable to the induced *pqsE*ind strain. No P*phzA2* activity was observed in the *pqsE*ind strain carrying an additional *rhlR* deletion, confirming that RsaL, RhlR, and PqsE are all required to trigger transcription of the *phz2* operon (**Figure 9**). The growth data for this experiment is shown in Figure S10.

DISCUSSION

New Model of Phenazine Production Control by QS

Here it has been demonstrated that the QS regulators LasR, RhlR, RsaL and the enzyme PqsE are all involved in controlling the expression of both phenazine operons *phz1* and *phz2* in *P. aeruginosa* with some differences. Initially it was unclear which regulators played a direct role in activating each operon and which were indirect because of the hierarchal structure of the QS network in rich media (**Figure 1**). A combination of the deletion of specific genes, the inducible expression of specific QS regulators and/or exogenous provision of QS signal molecules has allowed us to tease out which regulators are direct activators and which can be considered indirect because of their effect upon the QS network (**Figures 3–9**). Although rich media is not representative of the natural environment in which *P. aeruginosa* is found our experiments have closed an unanswered question of which QS regulators directly control each *phz* operon.

The results obtained allow us to postulate a model by which the QS cascade interacts and controls phenazine production in planktonic cultures (**Figure 10**).

Evidence has been presented showing that RhlR is a positive regulator for both operons and also that PqsE must be present to induce each operon. This is not surprising as it has been previously reported that PqsE and RhlR are both required for pyocyanin production (Farrow et al., 2008). It could be the case that all genes in the *rhl* regulon may be co-dependent upon PqsE as the production of the RhlR controlled genes *lasB* and *rhlA* are

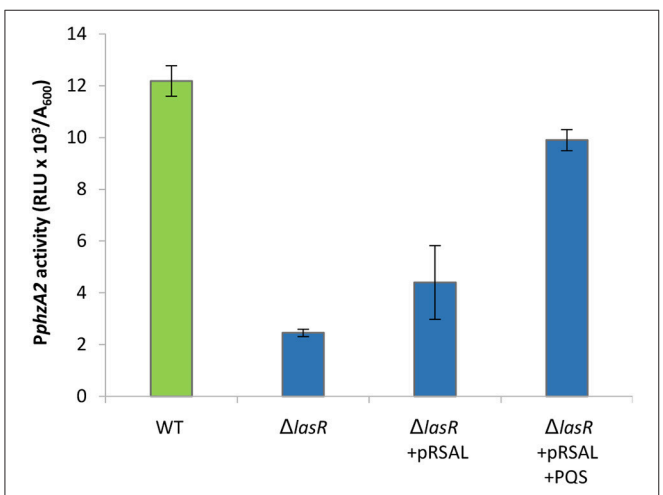

FIGURE 8 | P*phzA2* activity in a *lasR* mutant is restored by overexpressing RsaL and supplementing with exogenous PQS. Maximal promoter activity of P*phzA2-lux* in the wild type PAO1-N, *lasR* and *lasR* deletion carrying pRsaL in the presence of PQS. Promoter activities are normalized by cell density (A_{600}).

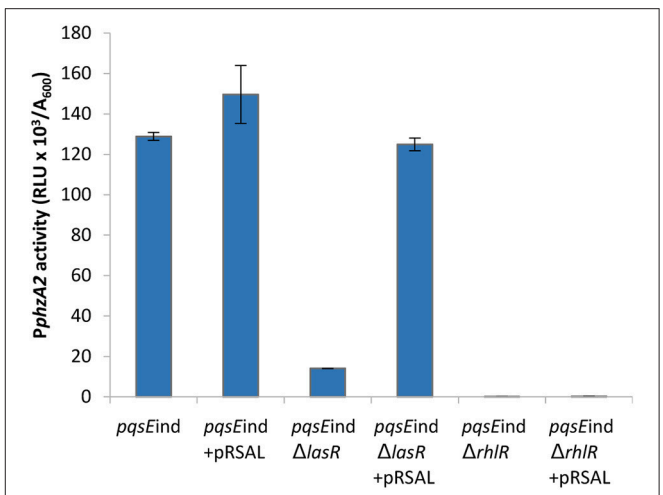

FIGURE 9 | RsaL can activate P*phzA2* in the absence of LasR when *pqsE* is induced and RhlR is present. Maximal promoter activity of P*phzA2-lux* in the *pqsE*ind strain and *pqsE*ind strain with additional *lasR* or *rhlR* mutations and in the presence or absence of pRsaL. All strains were induced with 0.1 mM IPTG. Promoter activities are normalized by cell density (A_{600}).

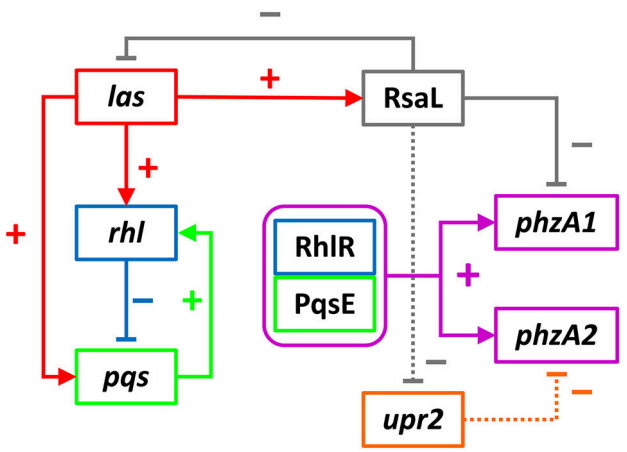

FIGURE 10 | Interactions of the QS cascade to control P*phzA1* and P*phzA2* activity. The auto-inducing *las* system positively regulates the *rhl* and *pqs* system via its regulator LasR, as well as the QS repressor RsaL. The *rhl* system represses the *pqs* system, which in turn has a positive effect on the *rhl* system. These two systems interact via RhlR and PqsE (purple box) which are both required to induce P*phzA1* and P*phzA2*. The QS repressor RsaL is a repressor of P*phzA1* but an indirect activator of P*phzA2*. We hypothesize that this is achieved by its ability to repress the promoter of an Unknown Phenazine Regulator of *phzA2* (orange box), that remains to be identified. Through this mechanism production of PCA from *phz1* can be switched to *phz2* and vice versa. Positive interactions are indicated by arrows whereas negative interactions are indicated by T-bars.

enhanced in the presence of PqsE (Farrow et al., 2008; Rampioni et al., 2010). The data presented show that PqsE rather than PqsR is required to activate the transcription of both phenazine biosynthesis operons. It was demonstrated by Recinos et al. (2012) that HHQ plays a role in activation of P*phzA2* under anaerobic conditions. HHQ would inevitably increase the levels of PqsE as *pqsABCDE* is a direct target for PqsR when bound to either HHQ or PQS (Fletcher et al., 2007; Rampioni et al., 2016). As molecular oxygen is required to convert HHQ to PQS (Schertzer et al., 2010) it would appear that under anaerobic conditions PqsE can still be produced when the signal HHQ binds PqsR, emphasizing that PqsE is important for activating the phenazine operons under both aerobic and anaerobic conditions.

In rich media, LasR drives expressions of the *rhl* and *pqs* systems, which then interact through RhlR and PqsE to activate the phenazine operon promoters. A deletion of *lasR* caused a reduction in P*phzA1* activity, which further demonstrates that in rich media the QS cascade has a hierarchal structure. This is in accordance with the work of others who have demonstrated that the loss of LasR results in a delay in production of pyocyanin (Dekimpe and Deziel, 2009; Cabeen, 2014). LasR also drives expression from P*rsaL* and in turn RsaL represses P*phzA1*, P*lasI* and its own production. *In vitro* protein-DNA interaction experiments revealed that RsaL binds to the P*phzA1* promoter at a region encompassing the −10 sequence (Rampioni et al., 2007; Sun et al., 2017), hence RsaL directly exerts a repressive effect on *phz1* expression. Moreover, RsaL was shown to exert an indirect repressive effect on P*phzA1* by increasing the expression of the P*phzA1*-repressor CdpR (Sun et al., 2017). It has been hypothesized by Rampioni et al. (2007) that RsaL maintains signal homeostasis by repressing P*lasI* and in the context of phenazine production could provide a similar feature (Bondi et al., 2017). RsaL could act to keep P*phzA1* inactive until the *rhl* and *pqs* systems are interacting before commencing transcription, thereby creating a checkpoint in the system. The QS signal molecule PQS has multiple functions as it can bind iron and also act as an anti-oxidant (Diggle et al., 2007; Häussler and Becker, 2008). In the presence of oxygen, pyocyanin generates reactive oxygen species (ROS) (Rada and Leto, 2013). Hence this checkpoint could function to allow adequate PQS to be produced and reduce deleterious effects of ROS produced by pyocyanin before triggering transcription of *phz1*.

It is thought that RsaL has a secondary function and strong evidence that RsaL can repress P*phzA1* but indirectly induce P*phzA2* has been presented. Previous studies have failed to demonstrate an interaction between RsaL and a DNA probe encompassing the P*phzA2* promoter region (Rampioni et al., 2007; Sun et al., 2017), suggesting that the positive effect exerted by RsaL on *phz2* expression is not direct. RsaL increases the expression of the P*phzA1*-repressor CdpR, but a ChIP-seq assay did not show any interaction between CdpR and the P*phzA2* promoter region in strain PA1201 (Zhao et al., 2016), suggesting that CdpR is not involved in the RsaL-mediated activation of P*phzA2*. The positive effect of RsaL on P*phzA2* is probably achieved *via* an unidentified phenazine biosynthesis gene regulator, which we termed Unidentified Phenazine Regulator of *phzA2* (Upr2). Although this regulator has not been identified, data presented thus far strongly imply the existence of this additional regulator, which in turn is controlled by the QS repressor RsaL.

We hypothesize that Upr2 is a P*phzA2* repressor and its expression could be repressed by RsaL. If Upr2 had a positive effect upon P*phzA2* we would expect that in an *rhlR* mutant some P*phzA2* activity would be observed. We show that when RsaL and PqsE are present but *rhlR* is mutated, no P*phzA2* activity was observed (**Figure 9**) making it unlikely that Upr2 is a positive regulator. It is likely that when the QS network is activated by LasR, that RsaL represses the promoter of *upr2* and as Upr2 is turned over and diluted through cell division that P*phzA2* can be triggered by RhlR in conjunction with PqsE, since both the *rhl* and *pqs* systems are positively regulated by LasR. In these experiments we observed significantly less activity from P*phzA2* compared with P*phzA1*, further suggesting that the P*phzA2* promoter is tightly controlled by a repressor. Upr2 could have its own regulon which may have significant overlap with that of the *las* regulon. We found that *phz2* transcription can be triggered in a *lasR* mutant when the *rsaL* deletion is complemented and PQS added exogenously to stimulate RhlR and PqsE production (**Figure 8**). Hence it is likely that some of the genes identified as *lasR*- or *rsaL*- specific in comparative transcriptome studies could belong to the *upr2* regulon.

We hypothesize that *P. aeruginosa* can switch PCA production from *phz1* to *phz2* when RsaL levels are elevated and from *phz2* to *phz1* when RsaL is absent. This switch could be related to a reduction in oxygen availability and an increase in oxidative

stress as the population size increases, however, this remains to be investigated.

PCA is converted to PYO *via* the action of PhzM and PhzS. The *phzM* gene is located directly upstream of *phzA1* and the intergenic region between these has two predicted *lux* boxes (Whiteley and Greenberg, 2001). The *lux* boxes are flanked by two *rsaL* binding sites (Rampioni et al., 2007) which suggests that *phz1* and *phzM* are controlled in a similar manner. In the study by Rampioni et al. (2007) a microarray assay was used to identify the *rsaL* regulon. In that work it was discovered that both *phzM* and *phzS* were up regulated in the *rsaL* mutant compared with the wild type, suggesting that RsaL represses both genes. Here we present evidence that RsaL also represses P*phzA1*. As *phzM*, *phzS,* and *phz1* are all required to produce PYO, which in turn contributes toward oxidative stress. It is conceivable that when oxidative stress is high, RsaL can repress *phz1*, *phzM* and *phzS* but maintain PCA production by indirectly activating *phz2*. Evidence to support this hypothesis was provided when the oxidative stress response regulator OxyR was shown to bind the promoter of *rsaL* (Wei et al., 2012). A previous study of the OxyR regulon showed that when this regulator is mutated, pyocyanin levels increase, suggesting that OxyR can repress pyocyanin production and this could be achieved through RsaL (Vinckx et al., 2010).

One of the proposed main functions of phenazines is to cycle electrons which allows *P. aeruginosa* to continue respiration in microaerophilic environments by controlling the intracellular redox state (Dietrich et al., 2013). Switching off PYO production would therefore cause a problem under these conditions. Unlike PYO, PCA can donate electrons to iron (III) rather than oxygen, hence maintaining redox homeostasis without producing ROS (Wang and Newman, 2008; Wang et al., 2011). PYO may be used in addition to PCA to cycle electrons as O_2 is a better electron accepter than iron. Through this switch, phenazine production may continue while lowering oxidative stress on the bacterium and maintaining redox balance.

AUTHOR CONTRIBUTIONS

SHi, SHe, GR, MF, PW, and MC designed the study and analyzed the data. SHi, GR, and MF conducted the experiments. SHi, SHe, GR, and MC wrote the manuscript. All authors reviewed the manuscript.

FUNDING

This work was supported by the Biotechnology and Biological Sciences Research Council [grant number BB/F014392/1] and the Engineering and Physical Sciences Research Council [grant number 977836].

SUPPLEMENTARY MATERIAL

The Supplementary Material for this article can be found online at: https://www.frontiersin.org/articles/10.3389/fcimb.2018.00252/full#supplementary-material

REFERENCES

Atkinson, S., Chang, C. Y., Patrick, H. L., Buckley, C. M., Wang, Y., Sockett, R. E., et al. (2008). Functional interplay between the *Yersinia pseudotuberculosis* YpsRI and YtbRI quorum sensing systems modulates swimming motility by controlling expression of *flhDC* and *fliA*. *Mol. Microbiol.* 69, 137–151. doi: 10.1111/j.1365-2958.2008.06268.x

Balasubramanian, D., Schneper, L., Kumari, H., and Mathee, K. (2013). A dynamic and intricate regulatory network determines *Pseudomonas aeruginosa* virulence. *Nucleic Acids Res.* 41, 1–20. doi: 10.1093/nar/gks1039

Bertani, I., Rampioni, G., Leoni, L., and Venturi, V. (2007). The *Pseudomonas putida* Lon protease is involved in *N*-acyl homoserine lactone quorum sensing regulation. *BMC Microbiol.* 7:71. doi: 10.1186/1471-2180-7-71

Bjarnsholt, T., and Givskov, M. (2007). The role of quorum sensing in the pathogenicity of the cunning aggressor *Pseudomonas aeruginosa*. *Anal. Bioanal. Chem.* 387, 409–414. doi: 10.1007/s00216-006-0774-x

Bondí, R., Longo, F., Messina, M., D'Angelo, F., Visca, P., Leoni, L., et al. (2017). The multi-output incoherent feedforward loop constituted by the transcriptional regulators LasR and RsaL confers robustness to a subset of quorum sensing genes in *Pseudomonas aeruginosa*. *Mol. Biosyst.* 13, 1080–1089. doi: 10.1039/c7mb00040e

Brouwer, S., Pustelny, C., Ritter, C., Klinkert, B., Narberhaus, F., and Häussler, S. (2014). The PqsR and RhlR transcriptional regulators determine the level of Pseudomonas quinolone signal synthesis in *Pseudomonas aeruginosa* by producing two different pqsABCDE mRNA isoforms. *J. Bacteriol.* 196, 4163–4171. doi: 10.1128/jb.02000-14

Cabeen, M. T. (2014). Stationary phase-specific virulence factor overproduction by a *lasR* mutant of *Pseudomonas aeruginosa*. *PLoS ONE* 9:e88743. doi: 10.1371/journal.pone.0088743

Choi, K. H., Kumar, A., and Schweizer, H. P. (2006). A 10-min method for preparation of highly electrocompetent *Pseudomonas aeruginosa* cells: application for DNA fragment transfer between chromosomes and plasmid transformation. *J. Microbiol. Methods* 64, 391–397. doi: 10.1016/j.mimet.2005.06.001

Chugani, S. A., Whiteley, M., Lee, K. M., D'Argenio, D., Manoil, C., and Greenberg, E. P. (2001). QscR, a modulator of quorum-sensing signal synthesis and virulence in *Pseudomonas aeruginosa*. *Proc. Natl. Acad. Sci U.S.A.* 98, 2752–2757. doi: 10.1073/pnas.051624298.

Cornforth, D. M., Popat, R., McNally, L., Gurney, J., Scott-Phillips, T. C., Ivens, A., et al. (2014). Combinatorial quorum sensing allows bacteria to resolve their social and physical environment. *Proc. Nat. Acad. Sci. U.S.A.* 111, 4280–4284. doi: 10.1073/pnas.1319175111.

de Kievit, T., Kakai, Y., Register, J. K., Pesci, E. C., and Iglewski, B. H. (2002). Role of the *Pseudomonas aeruginosa* las and rhl quorum-sensing systems in *rhlI* regulation. *Fems Microbiol. Lett.* 212, 101–106. doi: 10.1016/S0378-1097(02)00735-8

de Kievit, T., Seed, P. C., Nezezon, J., Passador, L., and Iglewski, B. H. (1999). RsaL, a novel repressor of virulence gene expression in *Pseudomonas aeruginosa*. *J. Bacteriol.* 181, 2175–2184

Dekimpe, V., and Déziel, E. (2009). Revisiting the quorum-sensing hierarchy in *Pseudomonas aeruginosa*: the transcriptional regulator RhlR regulates LasR-specific factors. *Microbiology* 155, 712–723. doi: 10.1099/mic.0.022764-0

Dietrich, L. E., Okegbe, C., Price-Whelan, A., Sakhtah, H., Hunter, R. C., and Newman, D. K. (2013). Bacterial community morphogenesis is intimately linked to the intracellular redox state. *J. Bacteriol.* 195, 1371–1380. doi: 10.1128/jb.02273-12

Diggle, S. P., Matthijs, S., Wright, V. J., Fletcher, M. P., Chhabra, S. R., Lamont, I. L., et al. (2007). The *Pseudomonas aeruginosa* 4-quinolone signal molecules HHQ and PQS play multifunctional roles in quorum sensing and iron entrapment. *Chem. Biol.* 14, 87–96. doi: 10.1016/j.chembiol.2006.11.014

Diggle, S. P., Winzer, K., Chhabra, S. R., Worrall, K. E., Cámara, M., and Williams, P. (2003). The *Pseudomonas aeruginosa* quinolone signal

molecule overcomes the cell density-dependency of the quorum sensing hierarchy, regulates rhl-dependent genes at the onset of stationary phase and can be produced in the absence of LasR. *Mol. Microbiol.* 50, 29–43. doi: 10.1046/j.1365-2958.2003.03672.x

Dötsch, A., Eckweiler, D., Schniederjans, M., Zimmermann, A., Jensen, V., Scharfe, M., et al. (2012). The *Pseudomonas aeruginosa* transcriptome in planktonic cultures and static biofilms using RNA sequencing. *PLoS ONE* 7:e31092. doi: 10.1371/journal.pone.0031092

Drees, S. L., and Fetzner, S. (2015). PqsE of *Pseudomonas aeruginosa* acts as pathway-specific thioesterase in the biosynthesis of alkylquinolone signaling molecules. *Chem. Biol.* 22, 611–618. doi: 10.1016/j.chembiol.2015.04.012

Dulcey, C. E., Dekimpe, V., Fauvelle, D. A., Milot, S., Groleau, M. C., Doucet, N., et al. (2013). The end of an old hypothesis: the *pseudomonas* signaling molecules 4-hydroxy-2-alkylquinolines derive from fatty acids, not 3-ketofatty acids. *Chem. Biol.* 20, 1481–1491. doi: 10.1016/j.chembiol.2013.09.021

Farrow, J. M., Sund, Z. M., Ellison, M. L., Wade, D. S., Coleman, J. P., and Pesci, E. C. (2008). PqsE functions independently of PqsR-pseudomonas quinolone signal and enhances the rhl quorum-sensing system. *J. Bacteriol.* 190, 7043–7051. doi: 10.1128/jb.00753-08

Fletcher, M. P., Diggle, S. P., Crusz, S. A., Chhabra, S. R., Cámara, M., and Williams, P. (2007). A dual biosensor for 2-alkyl-4-quinolone quorum-sensing signal molecules. *Environ. Microbiol.* 9, 2683–2693. doi: 10.1111/j.1462-2920.2007.01380.x

FRANK, L. H., and DEMOSS, R. D. (1959). On the biosynthesis of pyocyanine. *J. Bacteriol.* 77, 776–782.

Gallagher, L. A., McKnight, S. L., Kuznetsova, M. S., Pesci, E. C., and Manoil, C. (2002). Functions required for extracellular quinolone signaling by *Pseudomonas aeruginosa*. *J. Bacteriol.* 184, 6472–6480. doi: 10.1128/jb.184.23.6472-6480.2002

Guzman, L. M., Belin, D., Carson, M. J., and Beckwith, J. (1995). Tight regulation, modulation, and high-level expression by vectors containing the arabinose P-bad promoter. *J. Bacteriol.* 177, 4121–4130.

Harrison, F., Muruli, A., Higgins, S., and Diggle, S. P. (2014). Development of an *ex vivo* porcine lung model for studying growth, virulence, and signaling of *Pseudomonas aeruginosa*. *Infect. Immun.* 82, 3312–3323. doi: 10.1128/iai.01554-14

Häussler, S., and Becker, T. (2008). The Pseudomonas quinolone signal (PQS) balances life and death in *Pseudomonas aeruginosa* populations. *PLoS Pathog.* 4:e1000166. doi: 10.1371/journal.ppat.1000166

Hazan, R., He, J., Xiao, G., Dekimpe, V., Apidianakis, Y., Lesic, B., et al. (2010). Homeostatic interplay between bacterial cell-cell signaling and iron in virulence. *PLoS Pathog.* 6:e1000810. doi: 10.1371/journal.ppat.1000810

Heeb, S., Fletcher, M. P., Chhabra, S. R., Diggle, S. P., Williams, P., and Cámara, M. (2011). Quinolones: from antibiotics to autoinducers. *FEMS Microbiol. Rev.* 35, 247–274. doi: 10.1111/j.1574-6976.2010.00247.x

Hoang, T. T., Karkhoff-Schweizer, R. R., Kutchma, A. J., and Schweizer, H. P. (1998). A broad-host-range Flp-FRT recombination system for site-specific excision of chromosomally-located DNA sequences: application for isolation of unmarked *Pseudomonas aeruginosa* mutants. *Gene* 212, 77–86. doi: 10.1016/s0378-1119(98)00130-9

Hoang, T. T., Kutchma, A. J., Becher, A., and Schweizer, H. P. (2000). Integration-proficient plasmids for *Pseudomonas aeruginosa*: site-specific integration and use for engineering of reporter and expression strains. *Plasmid* 43, 59–72 doi: 10.1006/plas.1999.1441

Ledgham, F., Ventre, I., Soscia, C., Foglino, M., Sturgis, J. N., and Lazdunski, A. (2003). Interactions of the quorum sensing regulator QscR: interaction with itself and the other regulators of *Pseudomonas aeruginosa* LasR and RhlR. *Mol. Microbiol.* 48, 199–210 doi: 10.1046/j.1365-2958.2003.03423.x

Lee, J. H., Lequette, Y., and Greenberg, E. P. (2006). Activity of purified QscR, a *Pseudomonas aeruginosa* orphan quorum-sensing transcription factor. *Mole. Microbiol.* 59, 602–609. doi: 10.1111/j.1365-2958.2005.04960.x

Lequette, Y., Lee, J. H., Ledgham, F., Lazdunski, A., and Greenberg, E. P. (2006). A distinct QscR regulon in the *Pseudomonas aeruginosa* quorum-sensing circuit. *J. Bacteriol.* 188, 3365–3370. doi: 10.1128/jb.188.9.3365-3370.2006

Liang, H., Duan, J., Sibley, C. D., Surette, M. G., and Duan, K. (2011). Identification of mutants with altered phenazine production in *Pseudomonas aeruginosa*. *J. Med. Microbiol.* 60, 22–34. doi: 10.1099/jmm.0.022350-0

Lu, J., Huang, X., Li, K., Li, S., Zhang, M. Y., Wang, Y., et al. (2009). LysR family transcriptional regulator PqsR as repressor of pyoluteorin biosynthesis and activator of phenazine-1-carboxylic acid biosynthesis in *Pseudomonas* sp M18. *J. Biotechnol.* 143, 1–9. doi: 10.1016/j.jbiotec.2009.06.008

Maura, D., Hazan, R., Kitao, T., Ballok, A. E., and Rahme, L. G. (2016). Evidence for direct control of virulence and defense gene circuits by the *Pseudomonas aeruginosa* Quorum Sensing Regulator, MvfR. *Sci. Rep.* 6:34083. doi: 10.1038/srep34083

Mavrodi, D. V., Blankenfeldt, W., and Thomashow, L. S. (2006). Phenazine compounds in fluorescent *Pseudomonas* spp. biosynthesis and regulation. *Ann. Rev. Phytopathol.* 44, 417–445. doi: 10.1146/annurev.phyto.44.013106.145710

Mavrodi, D. V., Bonsall, R. F., Delaney, S. M., Soule, M. J., Phillips, G., and Thomashow, L. S. (2001). Functional analysis of genes for biosynthesis of pyocyanin and phenazine-1-carboxamide from *Pseudomonas aeruginosa* PAO1. *J. Bacteriol.* 183, 6454–6465. doi: 10.1128/jb.183.21.6454-6465.2001

Mavrodi, D. V., Peever, T. L., Mavrodi, O. V., Parejko, J. A., Raaijmakers, J. M., Lemanceau, P., et al. (2010). Diversity and evolution of the phenazine biosynthesis pathway. *Appl. Environ. Microbiol.* 76, 866–879. doi: 10.1128/aem.02009-09

McKnight, S. L., Iglewski, B. H., and Pesci, E. C. (2000). The Pseudomonas quinolone signal regulates rhl quorum sensing in *Pseudomonas aeruginosa*. *J. Bacteriol.* 182, 2702–2708. doi: 10.1128/jb.182.10.2702-2708.2000

Medina, G., Juárez, K., Díaz, R., and Sóberon-Chaávez, G. (2003). Transcriptional regulation of *Pseudomonas aeruginosa rhlR*, encoding a quorum-sensing regulatory protein. *Microbiology* 149, 3073–3081. doi: 10.1099/mic.0.26282-0

Milton, D. L., O'Toole, R., Horstedt, P., and Wolf-Watz, H. (1996). Flagellin A is essential for the virulence of *Vibrio anguillarum*. *J. Bacteriol.* 178, 1310–1319.

Pesci, E. C., Pearson, J. P., Seed, P. C., and Iglewski, B. H. (1997). Regulation of las and rhl quorum sensing in *Pseudomonas aeruginosa*. *J. Bacteriol.* 179, 3127–3132.

Rada, B., and Leto, T. L. (2013). Pyocyanin effects on respiratory epithelium: relevance in *Pseudomonas aeruginosa* airway infections. *Trends Microbiol.* 21, 73–81. doi: 10.1016/j.tim.2012.10.004

Rampioni, G., Bertani, I., Zennaro, E., Polticelli, F., Venturi, V., and Leoni, L. (2006). The quorum-sensing negative regulator RsaL of *Pseudomonas aeruginosa* binds to the lasI promoter. *J. Bacteriol.* 188, 815–819. doi: 10.1128/jb.188.2.815-819.2006

Rampioni, G., Falcone, M., Heeb, S., Frangipani, E., Fletcher, M. P., Dubern, J. F., et al. (2016). Unravelling the genome-wide contributions of specific 2-Alkyl-4-quinolones and PqsE to quorum sensing in *Pseudomonas aeruginosa*. *PLOS Pathog.* 12:e1006029. doi: 10.1371/journal.ppat.1006029

Rampioni, G., Pustelny, C., Fletcher, M. P., Wright, V. J., Bruce, M., Rumbaugh, K. P., et al. (2010). Transcriptomic analysis reveals a global alkyl-quinolone-independent regulatory role for PqsE in facilitating the environmental adaptation of *Pseudomonas aeruginosa* to plant and animal hosts. *Environ. Microbiol.* 12, 1659–1673. doi: 10.1111/j.1462-2920.2010.02214.x

Rampioni, G., Schuster, M., Greenberg, E. P., Bertani, I., Grasso, M., Venturi, V., et al. (2007). RsaL provides quorum sensing homeostasis and functions as a global regulator of gene expression in *Pseudomonas aeruginosa*. *Mol. Microbiol.* 66, 1557–1565. doi: 10.1111/j.1365-2958.2007.06029.x

Recinos, D. A., Sekedat, M. D., Hernandez, A., Cohen, T. S., Sakhtah, H., Prince, A. S., et al. (2012). Redundant phenazine operons in *Pseudomonas aeruginosa* exhibit environment-dependent expression and differential roles in pathogenicity. *Proc. Nat. Acad. Sci. U.S.A.* 109, 19420–19425. doi: 10.1073/pnas.1213901109

Sambrook, J., and Russell, D. W. (2001). *Molecular Cloning: A Laboratory Manual.* Cold Spring Harbor, NY: Cold Spring Harbor Laboratory Press.

Schertzer, J. W., Brown, S. A., and Whiteley, M. (2010). Oxygen levels rapidly modulate *Pseudomonas aeruginosa* social behaviours via substrate limitation of PqsH. *Mol. Microbiol.* 77, 1527–1538. doi: 10.1111/j.1365-2958.2010.07303.x

Schuster, M., and Greenberg, E. P. (2007). Early activation of quorum sensing in *Pseudomonas aeruginosa* reveals the architecture of a complex regulon. *BMC Genomics* 8:287. doi: 10.1186/1471-2164-8-287

Schuster, M., Lostroh, C. P., Ogi, T., and Greenberg, E. P. (2003). Identification, timing, and signal specificity of *Pseudomonas aeruginosa* quorum-controlled genes: a transcriptome analysis. *J. Bacteriol.* 185, 2066–2079. doi: 10.1128/jb.185.7.2066-2079.2003

Schuster, M., Sexton, D. J., Diggle, S. P., and Greenberg, E. P. (2013). Acyl-homoserine lactone quorum sensing: from evolution to application. *Annu. Rev. Microbiol.* 67, 43–63. doi: 10.1146/annurev-micro-092412-155635

Smith, R. S., and Iglewski, B. H. (2003). *Pseudomonas aeruginosa* quorum sensing as a potential antimicrobial target. *J. Clin. Invest.* 112, 1460–1465. doi: 10.1172/jci20364

Sun, S., Chen, B., Jin, Z. J., Zhou, L., Fang, Y. L., Thawai, C., et al. (2017). Characterization of the multiple molecular mechanisms underlying RsaL control of phenazine-1-carboxylic acid biosynthesis in the rhizosphere bacterium *Pseudomonas aeruginosa* PA1201. *Mol. Microbiol.* 104, 931–947. doi: 10.1111/mmi.13671

Sun, S., Zhou, L., Jin, K., Jiang, H., and He, Y. W. (2016). Quorum sensing systems differentially regulate the production of phenazine-1-carboxylic acid in the rhizobacterium *Pseudomonas aeruginosa* PA1201. *Sci. Rep.* 6:30352. doi: 10.1038/srep30352

Trunk, K., Benkert, B., Quäck, N., Münch, R., Scheer, M., Garbe, J., et al. (2010). Anaerobic adaptation in *Pseudomonas aeruginosa*: definition of the Anr and Dnr regulons. *Environ. Microbiol.* 12, 1719–1733. doi: 10.1111/j.1462-2920.2010.02252.x

Vinckx, T., Wei, Q., Matthijs, S., and Cornelis, P. (2010). The *Pseudomonas aeruginosa* oxidative stress regulator OxyR influences production of pyocyanin and rhamnolipids: protective role of pyocyanin. *Microbiology* 156, 678–686. doi: 10.1099/mic.0.031971-0

Voisard, C., Bull, C., Keel, C., Laville, J., Maurhofer, M., Schnider, U., et al. (1994). "Biocontrol of root diseases by *Pseudomonas fluorescens* CHA0: current concepts and experimental approaches," in *Molecular Ecology of Rhizosphere Microorganisms*, eds F. O'Gara, D. N. Dowling, and B. Boesten (Weinheim: VCH Publishers), 67–89. doi: 10.1002/9783527615810.ch6

Wade, D. S., Calfee, M. W., Rocha, E. R., Ling, E. A., Engstrom, E., Coleman, J. P., et al. (2005). Regulation of Pseudomonas quinolone signal synthesis in *Pseudomonas aeruginosa*. *J. Bacteriol.* 187, 4372–4380. doi: 10.1128/JB.187.13.4372-4380.2005

Wagner, V. E., Bushnell, D., Passador, L., Brooks, A. I., and Iglewski, B. H. (2003). Microarray analysis of *Pseudomonas aeruginosa* quorum-sensing regulons: effects of growth phase and environment. *J. Bacteriol.* 185, 2080–2095. doi: 10.1128/jb.185.7.2080-2095.2003

Wang, Y., and Newman, D. K. (2008). Redox reactions of phenazine antibiotics with ferric (hydr)oxides and molecular oxygen. *Environ. Sci. Tech.* 42, 2380–2386. doi: 10.1021/es702290a

Wang, Y., Wilks, J. C., Danhorn, T., Ramos, I., Croal, L., and Newman, D. K. (2011). Phenazine-1-Carboxylic acid promotes bacterial biofilm development via ferrous iron acquisition. *J. Bacteriol.* 193, 3606–3617. doi: 10.1128/jb.00396-11

Wei, Q., Minh, P. N., Dötsch, A., Hildebrand, F., Panmanee, W., Elfarash, A., et al. (2012). Global regulation of gene expression by OxyR in an important human opportunistic pathogen. *Nucleic Acids Res.* 40, 4320–4333. doi: 10.1093/nar/gks017

Westfall, L. W., Luna, A. M., San Francisco, M., Diggle, S. P., Worrall, K. E., Williams, P., et al. (2004). The *Pseudomonas aeruginosa* global regulator MvaT specifically binds to the *ptxS* upstream region and enhances *ptxS* expression. *Microbiology* 150(Pt 11), 3797–3806. doi: 10.1099/mic.0.27270-0

Whiteley, M., and Greenberg, E. P. (2001). Promoter specificity elements in *Pseudomonas aeruginosa* quorum-sensing-controlled genes. *J. Bacteriol.* 183, 5529–5534. doi: 10.1128/jb.183.19.5529-5534.2001

Winsor, G. L., Lam, D. K., Fleming, L., Lo, R., Whiteside, M. D., Yu, N. Y., et al. (2011). Pseudomonas genome database: improved comparative analysis and population genomics capability for Pseudomonas genomes. *Nucl. Acids Res.* 39(Suppl 1), D596–D600. doi: 10.1093/nar/gkq869

Xiao, G., He, J., and Rahme, L. G. (2006). Mutation analysis of the *Pseudomonas aeruginosa mvfR* and *pqsABCDE* gene promoters demonstrates complex quorum-sensing circuitry. *Microbiology* 152, 1679–1686. doi: 10.1099/mic.0.28605-0

Zhao, J., Yu, X., Zhu, M., Kang, H., Ma, J., Wu, M., et al. (2016). Structural and molecular mechanism of CdpR involved in quorum-sensing and bacterial virulence in *Pseudomonas aeruginosa*. *PLoS Biol.* 14:e1002449. doi: 10.1371/journal.pbio.1002449

Conflict of Interest Statement: The authors declare that the research was conducted in the absence of any commercial or financial relationships that could be construed as a potential conflict of interest.

frontiers in Cellular and Infection Microbiology

REVIEW
published: 11 May 2018
doi: 10.3389/fcimb.2018.00143

Surface-Enhanced Raman Scattering Spectroscopy for Label-Free Analysis of *P. aeruginosa* Quorum Sensing

Gustavo Bodelón, Verónica Montes-García, Jorge Pérez-Juste and Isabel Pastoriza-Santos**

Departamento de Química Física y Centro Singular de Investigaciones Biomédicas (CINBIO), Universidad de Vigo, Vigo, Spain

Bacterial quorum sensing systems regulate the production of an ample variety of bioactive extracellular compounds that are involved in interspecies microbial interactions and in the interplay between the microbes and their hosts. The development of new approaches for enabling chemical detection of such cellular activities is important in order to gain new insight into their function and biological significance. In recent years, surface-enhanced Raman scattering (SERS) spectroscopy has emerged as an ultrasensitive analytical tool employing rationally designed plasmonic nanostructured substrates. This review highlights recent advances of SERS spectroscopy for label-free detection and imaging of quorum sensing-regulated processes in the human opportunistic pathogen *Pseudomonas aeruginosa*. We also briefly describe the challenges and limitations of the technique and conclude with a summary of future prospects for the field.

Keywords: quorum sensing, bacteria, imaging, metabolites, *Pseudomonas aeruginosa*, SERS, raman scattering

OPEN ACCESS

Edited by:
Maria Tomas, Complexo Hospitalario Universitario A Coruña, Spain

Reviewed by:
Maria Alejandra Mussi, Consejo Nacional de Investigaciones Científicas y Técnicas (CONICET), Argentina
Tamara Manso Gómez, Universidade de Santiago de Compostela, Spain

****Correspondence:***
Gustavo Bodelón
gbodelon@uvigo.es
Isabel Pastoriza-Santos
pastoriza@uvigo.es

Received: *27 February 2018*
Accepted: *20 April 2018*
Published: *11 May 2018*

Citation:
Bodelón G, Montes-García V, Pérez-Juste J and Pastoriza-Santos I (2018) Surface-Enhanced Raman Scattering Spectroscopy for Label-Free Analysis of P. aeruginosa Quorum Sensing. Front. Cell. Infect. Microbiol. 8:143. doi: 10.3389/fcimb.2018.00143

INTRODUCTION

During their growth, bacteria secrete a large repertoire of chemical compounds that can function in the environment as signaling molecules, cues, virulence factors and agents of microbial warfare (Phelan et al., 2011; Ratcliff and Denison, 2011; Davies and Ryan, 2012; Davies, 2013). These bioactive compounds are involved in competitive strategies, and other community behaviors, such as biofilm formation and syntrophy, and they are believed to play a major role on the survival of the producing organisms in the natural environment (O'Brien and Wright, 2011; Stubbendieck and Straight, 2016; van der Meij et al., 2017). Besides their influence in the ecology of microbial communities, bacterial extracellular compounds have a direct impact in human health and disease, as they have been associated with infection, inflammation, cancer, as well as neurological disorders, and their expression has been correlated to changes in the composition of the human microbiota (Peters et al., 2012; Garg et al., 2017). Many of these biomolecules display a remarkable range of drug-like bioactivities, and thereby they have been used as a source of antibiotics, chemotherapeutic drugs, immune suppressants and crop protection agents for biomedicine and agricultural applications (Newman and Cragg, 2007; Harvey et al., 2015). However, despite the myriad of compounds with pharmaceutical interest identified so far, their true biological role and the ecological significance remain poorly characterized (Davies, 2013). In this respect, recent studies have shown that at sub-inhibitory concentrations, molecules released by bacterial cells bearing antibiotic capacity can modulate gene expression, acting in the natural

environment as molecules for signaling, cueing and chemical manipulation (Bernier and Surette, 2013). Indeed, the general term "antibiotic," commonly used to describe antibacterial drugs, overlooks its suspected range of biological activities. In this context, it has been proposed that whether a microbial compound acts as an antimicrobial agent, signal, cue, or coercion, depends on the fitness consequences of the interaction (Diggle et al., 2007).

The production of an ample array of extracellular bioactive compounds is often regulated under quorum sensing (QS) systems (Antunes et al., 2010; Popat et al., 2015). In general, the QS systems of Gram-negative bacteria include an enzyme that synthesizes the signaling molecule and a transcription factor that binds to the signal modulating the expression of QS regulons, including upregulation of the synthase. This "autoinduction" positive feedback loop promotes synchronous gene expression in the population (Papenfort and Bassler, 2016). It is firmly established that QS plays global regulatory roles in bacterial metabolism, virulence, and contributes to the modulation of bacterial antibiotic tolerance and host defense mechanisms. The early observation that QS mutants of clinically-relevant pathogens have greatly reduced virulence has spurred an explosion of research aimed at targeting QS as a potential therapeutic avenue to treat bacterial infections (LaSarre and Federle, 2013; Whiteley et al., 2017).

Gram-negative *P. aeruginosa* is a ubiquitous and highly versatile opportunistic human pathogen that can cause acute and severe biofilm-related chronic infections, which can readily develop multi-drug resistance leading to high morbidity and mortality rates, especially in immunocompromised and cystic fibrosis (CF) patients. Significantly, the number of multi-drug and pan-drug resistant strains of this pathogen is increasing worldwide, complicating therapeutics (Poole, 2011). The ubiquitous presence of this organism, as well as its prevalence and persistence in clinical settings is attributed to its extraordinary capability of adaptation and survival, in which QS has a central regulatory role (Moradali et al., 2017). The QS network of *P. aeruginosa* is comprised by at least four QS systems that are highly interconnected and function in a hierarchical way (Lee and Zhang, 2014; Papenfort and Bassler, 2016). The sophisticated QS regulatory mechanisms present in *P. aeruginosa* are mainly involved in signaling, virulence determinant production, motility, biofilm development, antibiotic resistance mechanisms, as well as the adjustment of metabolic pathways and physiological processes in response to environmental cues and stresses, endowing this organism with the capacity to colonize different ecological niches and thrive in multispecies communities.

Several lines of evidence indicate that QS is implicated in the virulence of *P. aeruginosa* in human infections. Most isolates of this microorganism preserve functional QS systems, and QS signals are detected in biofluids of infected patients, which correlates with active QS expression during infection (Castillo-Juárez et al., 2015). In the context of polymicrobial infections, it is recognized the potential impact of interspecies interactions in disease severity and antibiotic efficacy (Peters et al., 2012). Studies investigating interactions between *P. aerigunosa* and *Staphylococcus aureus*, frequently isolated from the lungs of CF patients and chronic wounds, have shown that QS-regulated extracellular compounds produced by these microorganisms strongly influence the interaction between the coexisting bacterial species leading to phenotypes with decreased susceptibility to antibiotic treatment (i.e., persister cells, small colony variants) and worse disease outcomes (Hotterbeekx et al., 2017). A recent study has shown that alginate overproduction by *P. aeruginosa* during the conversion to mucoid phenotypes promotes coexistence with *S. aureus* in the CF lung (Limoli et al., 2017). *P. aeruginosa* and strains of *Burkholderia cepacia* can also co-exist in CF airways. It has been shown that *P. aeruginosa* can activate the QS system of *B. cepacia* (Riedel et al., 2001), and *P. aeruginosa*-derived rhamnolipids can modulate biological responses in *Burkholderia* spp. at low concentrations (Bernier et al., 2017). Similarly, it has been reported QS-based interactions between *P. aeruginosa* and *Candida albicans* in polymicrobial communities of these typical pneumonia pathogens (Fourie et al., 2016). The nature of the different bacterial processes controlled by QS in infections is currently an active area of research. It is believed that a clearer understanding of how QS-regulated extracellular compounds are used by *P. aeruginosa* to interact with other organisms and influence their local environment, as well as the conditions under which these molecules are expressed, could yield valuable information to assist the rational development of novel therapeutic drugs and improved therapeutics to treat microbial infections. In this framework, the ability to detect these chemical compounds with high sensitivity, and to non-invasively visualize their spatiotemporal distributions in live multispecies microbial communities is fundamental to provide new insights into their function, as well as the spatial dependencies required for chemical crosstalk.

Surface-enhanced Raman scattering (SERS) spectroscopy is an analytical tool that combines the molecular specific information provided by Raman scattering with the signal-enhancing power of plasmonic nanostructures. Through SERS it is possible to harness chemical information of biomolecules without the need of any external labeling (i.e., label-free), as well as non-invasive analysis of biological samples and imaging of cells (Cialla-May et al., 2017; Kahraman et al., 2017; Laing et al., 2017). Based on its high sensitivity and spectral resolution, SERS has been applied successfully to trace analysis, reaching single-molecule detection level under favorable conditions (Nie, 1997). Owing to significant key advantages, SERS has emerged in microbiology research for chemical profiling of microbial cells (Liu et al., 2017; Lorenz et al., 2017), detection and identification of bacteria at different taxonomic levels (Pahlow et al., 2015; Rebrošová et al., 2017), single cell analysis (Kuku et al., 2017), or *in vivo* diagnostics and multimodal imaging (Henry et al., 2016; Cialla-May et al., 2017; Krafft et al., 2017).

In this review we aim to highlight recent applications of SERS spectroscopy for label-free detection and imaging of *P. aeruginosa* extracellular compounds in the context of QS communication. Since in this specific topic there are still few examples in the literature, our objective is to introduce this technology to interested readers, as well as to pinpoint current challenges and limitations of SERS as an analytical tool for the

detection of microbial extracellular biomolecules, as well as other classes of SERS-active cellular compounds.

RAMAN SCATTERING AND SERS SPECTROSCOPY

Raman scattering may be defined as the inelastic scattering of photons by molecular bond vibrations. The detection of scattered photons from a molecule yields a spectrum of Raman peaks, each of which is characteristic of a specific molecular bond, thereby allowing molecular identification on the basis of specific vibrational fingerprints (**Figure 1**). As compared with fluorescence and infrared spectroscopy, the higher spectral resolution and narrower bandwidths that characterize the Raman spectra facilitate the simultaneous detection of different analytes in multiplex analysis. In addition, the linear dependence of the Raman signal intensity on the analyte concentration offers the possibility for quantitative analysis (Schlücker, 2014). However, the Raman scattering signal is very weak, as only a very small fraction of the incident photons are scattered inelastically (about 1 out of 10 millions), whereby only high concentration of molecules can be detected, seriously limiting the application of this technique. SERS is a surface phenomenon that can amplify the inherently weak Raman scattering signal of molecules adsorbed, or in close vicinity, on a plasmonic metal nanoparticle when it is excited with an appropriate laser wavelength (Schlücker, 2014). Under such conditions single molecule detection levels can be reached, while retaining the structural information provided by Raman scattering (**Figure 1**). In SERS, average enhancement factors range between 10^4 and 10^8, and even values about 10^{11} can be achieved in some cases (Prochazka, 2016). This has rendered SERS spectroscopy a powerful analytical technique for ultrasensitive chemical or biochemical analysis.

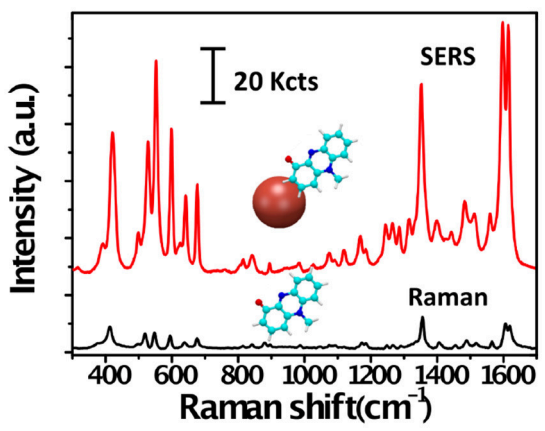

FIGURE 1 | Raman and SERS spectra of pyocyanin. Raman (black) and SERS (red) spectra of pyocyanin bound to a plasmonic gold nanoparticle (red sphere). The peaks in the Raman spectrum correspond to vibrational modes of the molecule. Note the difference in intensity between the Raman and SERS signals of pyocyanin.

In general terms, the SERS effect can be explained in terms of two enhancement mechanisms; electromagnetic and chemical. The former relies on the generation of high local electromagnetic fields at the surface of metal nanoparticles due to localized surface plasmon resonance (LSPR) excitation, which occurs when conduction electrons collectively oscillate in resonance with the frequency of incident light (**Figure 2A**). This in turn promotes large enhancements (by many orders of magnitude) of the Raman scattering by adsorbed molecules. Nanoparticle aggregates can provide a significantly larger enhancement due to coupling between LSPRs of the different particles within the aggregate, resulting in higher electromagnetic fields at interparticle gaps within the interacting nanostructures, which are called "hot spots" (Halas et al., 2011). The intense localized fields can interact with molecules in contact with or near the metal surface, typically at distances below 10 nm, so that SERS can be measured (Schlücker, 2014). The chemical mechanism is based on charge transfer processes occurring between the metal nanoparticle and the molecule, but this mechanism has proved to have much lower contribution than the electromagnetic enhancement (Schlücker, 2014; Prochazka, 2016). In addition, the intensity of the Raman scattering signal can be further increased by several orders of magnitude when the frequency of the excitation laser is in resonance with an electronic transition of the molecule, which is known as surface-enhanced resonance Raman scattering (SERRS) (McNay et al., 2011).

Nanoparticles of noble metals, su ch as gold and silver, are optical enhancers of choice in SERS because they resonantly scatter and absorb light in the visible and near-infrared spectral region upon excitation (**Figure 2B**). The plasmonic properties of these noble metal nanoparticles, namely LSPR and the magnitude of the electromagnetic field generated at the surface, are mainly determined by the nanoparticle size, shape and composition (**Figure 2C**), and dielectric properties of surrounding medium (Kelly et al., 2003; Yu et al., 2017).

In general, silver is a much more efficient optical transducer than gold, and therefore higher SERS enhancement is to be expected. However, silver displays toxic effects to living organisms, which limits its use for *in vivo* applications. Gold is more chemically inert and robust, and offers better control of its particle size and shape, thereby enabling a wider range of synthetic possibilities, as well as its significantly higher biocompatibility. This is fundamental, since size, shape, composition and stability should be carefully controlled in order to achieve sensitive and reproducible SERS detection. It has been known for a long time that nanoparticle aggregates exhibit larger Raman signal enhancements than individual nanoparticles. This is due to the generation of hot spots within the interparticle gaps. Remarkably, the electromagnetic field enhancement in hot spots is highly sensitive to the detailed local structure and nature of nanoparticle assemblies (Halas et al., 2011), thus top-down lithographic approaches and bottom-up self-assembly methods have been developed to assemble plasmonic nanostructures with precisely controlled geometry and hot spots (Gwo et al., 2016; Mosier-Boss, 2017; Hamon and Liz-Marzán, 2018).

Broadly, two strategies may be followed for direct, label-free, SERS measurements of a biological system (i.e., biomolecule, protein, bacterial cell, biofilm, etc.). The first one involves

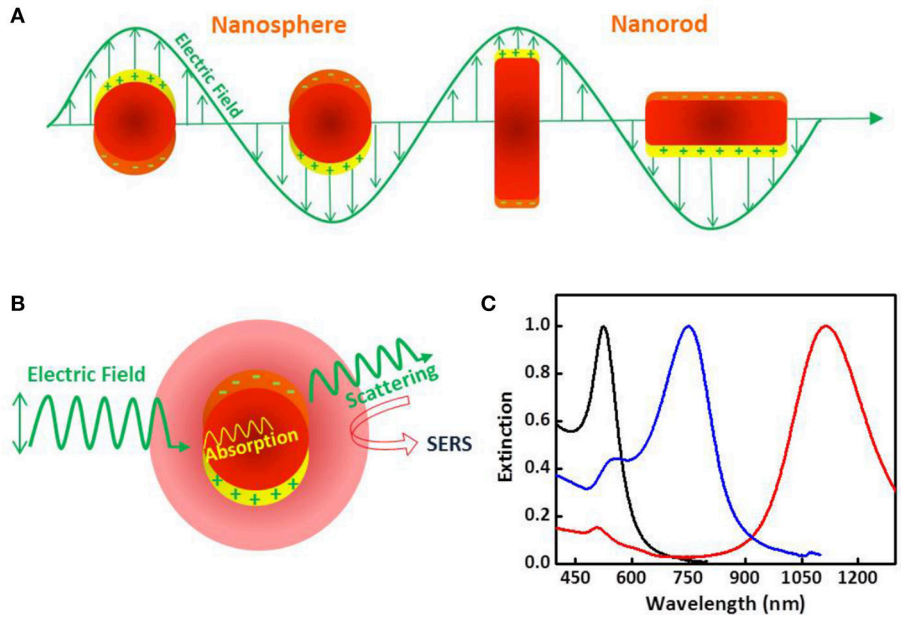

FIGURE 2 | Plasmonic and optical properties of metallic nanoparticles. **(A)** Schematic drawing of the interaction of an electromagnetic radiation with a nanosphere (left) and a nanorod (right). It generates a dipole that oscillates in resonance with the electric field of the incident light as well as a strong confined electric field at the nanoparticle surface. In the case of the metal nanorod two different oscillation modes are observed due to the electron oscillation along the long and short axes. **(B)** Schematic drawing of the two processes, light scattering and absorption, occurring when a metal nanoparticle interacts with light. **(C)** Extinction (scattering + absorption) spectra of gold nanospheres (blak), nanostars (blue) and nanorods (red) in water.

plasmonic colloids, which are mixed with the sample and the SERS spectra are recorded upon aggregation of nanoparticles. The second approach entails the use of plasmonic platforms based on assemblies of plasmonic nanoparticles and plasmonic patterns over a surface (i.e., nanostructured plasmonic substrates), which offers the possibility to control nanoparticle clustering and the topological parameters of hot spots, leading to improved sensitivity and reproducibility of the SERS measurements. In **Figure 3** it is shown different nanostructured platforms bearing increased complexity, from clusters of gold nanoparticles randomly formed on a glass surface, to self-assembled gold octahedral nanoparticles, and gold nanorods supercrystals embedded in a silica layer (**Figures 3A–C**). This figure also illustrates two measuring modalities for direct SERS detection of metabolites excreted by a bacterial colony grown on the nanostructured plasmonic substrate. In one of them, SERS measurements can be recorded on the plasmonic platform at different points and an average spectrum may be generated (**Figure 3D).** In the SERS mapping modality (i.e., SERS imaging), a two-dimensional SERS intensity map can be generated in order to visualize the spatial distribution of the detected metabolite on the plasmonic sensor (**Figure 3E)**. For SERS mapping, an area over the substrate is divided into a grid where each square represents a pixel. A series of SERS spectra are acquired at each pixel, and the SERS intensity image (false color) is generated by representing a specific spectral peak of the molecule of interest measured at a fixed wavenumber.

Different parameters such as the excitation laser wavelength and the microscope objective are important aspects that may be considered during SERS. The choice of the excitation laser line depends on the analyte and the optical properties of the plasmonic material. Regarding the analyte, an excitation laser wavelength overlapping or being very close to an electronic transition of the molecule is preferred so as to measure under SERRS conditions. Regarding the plasmonic material, it is important to consider an appropriate wavelength source to enable efficient excitation of the surface plasmons. For nanoparticle suspensions it is predicted that maximum SERS signal can be obtained when the plasmon frequency is tuned to be slightly red-shifted from the laser wavelength. For hot-spot containing plasmonic materials it has been demonstrated that depending on symmetry effects and differences in plasmonic coupling strength the highest SERS intensity could be independent of the excitation source (Sharma et al., 2012). The choice of the microscope objective will determine the spatial resolution of the measurements. The spatial resolution is dependent on the spot size of the illuminating beam, which is dependent on the optics and the wavelength of the laser, leading the higher magnification objectives to the highest spatial resolution. Detailed information regarding the experimental setup of SERS can be found elsewhere (Palonpon et al., 2013; Butler et al., 2016). A typical SERS analysis can accumulate highly complex spectral data sets, by which extraction of chemical and structural information underpinning the biological system is often challenging. For this reason, chemometric analysis such as principal component analysis (PCA), hierarchical cluster analysis (HCA) or partial least squares discriminant analysis (PLS-DA), among others, have become routine in SERS studies. These

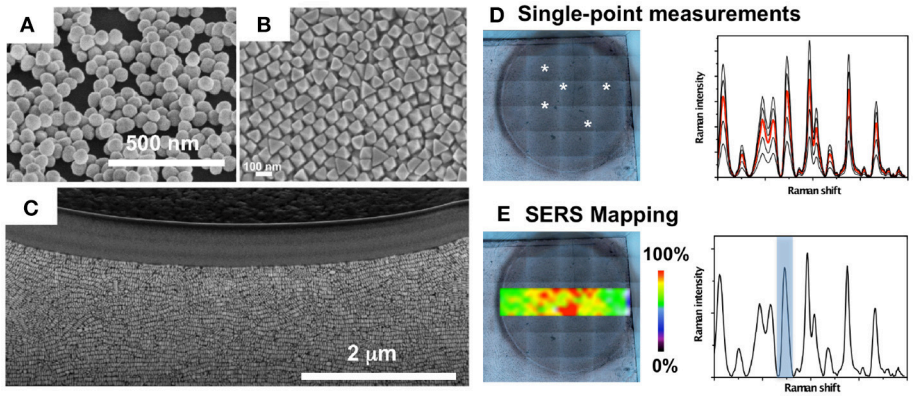

FIGURE 3 | Nanostructured plasmonic substrates for SERS spectroscopy. **(A–C)** Nanostructured plasmonic platforms: Clusters of gold nanoparticles **(A)**, self-assembled gold octahedral nanoparticles **(B)**, and gold nanorods supercrystals embedded in a silica layer **(C)**. **(D)** Single-point SERS measurements on a bacterial colony (white asterisks) grown on a plasmonic nanostructured substrate, and recorded SERS spectra highlighting in red the mean spectrum. **(E)** SERS intensity mapping performed with the spectral peak indicated in the SERS spectrum with a blue bar. **(A,D,E)** Images reproduced with permission from Bodelón et al. (2017). **(B)** Image reproduced with permission from Gómez-Graña et al. (2015). **(C)** Image reproduced with permission from Hamon et al. (2016).

statistical methods enable to properly evaluate extensive Raman spectroscopic data, and to facilitate reliable identification and potential quantification of the SERS detected chemical features (Cooper, 1999).

SERS APPLICATIONS IN RESEARCH ON QUORUM SENSING IN *P. AERUGINOSA*

Bacteria possess an extraordinary chemical repertoire for intercellular communication and social behavior. Among them, N-acyl homoserine lactones (AHLs) are employed as signaling molecules for many Gram-negative bacteria and have become a paradigm for bacteria intercellular signaling (Papenfort and Bassler, 2016). Different types of AHLs have been identified and characterized in the last decades. In general, they are composed of a homoserine lactone ring with an acyl chain that varies from C4 to C18, which can be slightly modified in some cases by substitution at the C3 position and unsaturation at the C1 position. Once produced they diffuse in and out of the cell and, at a given threshold cell number, they bind to a cognate DNA-binding transcription factor that regulates the expression of QS regulons. The structure and concentration of these molecules play significant roles in the intercellular signaling process (Papenfort and Bassler, 2016). The detection of AHL signal molecules is important not only for gaining new understanding of cell-to-cell communication in live microbial populations, but also because these signaling molecules are involved in the regulation of virulence phenotypes and they have been identified in patients infected with *P. aeruginosa* (Singh et al., 2000). Thus, numerous analytical procedures have been developed for the detection and structural determination of these chemical compounds (Steindler and Venturi, 2007; Wang et al., 2011).

Several approaches employing colloidal suspensions of silver nanoparticles have been applied to determine the viability of SERS to detect AHL signaling molecules. Aggregation of silver nanoparticles is a very common means of achieving strong SERS signals owing to the hot-spots formation and facile preparation. However, this method has traditionally strived with inconsistent measuring and low reproducibility. Following this strategy, Pearman and collaborators detected seven types of commercial AHLs in water. In this study it was shown that the Raman spectra of the different AHLs were highly similar, which hinders the differentiation of signaling molecules by SERS. Among the different AHLs, only 3-oxo-C6-AHL was detected at the relevant biological concentration of 10^{-6} M (Pearman et al., 2016). Likewise, Claussen and collaborators employed silver nanoparticles to detected N-Dodecanoyl-DL-homoserine lactones (C12-AHLs) in spiked culture medium, achieving a detection limit of 0.2 nM (Claussen et al., 2013). This study demonstrated the possibility of SERS for label-free detection of AHLs in bacterial cultures. However, despite these efforts, the SERS detection of natural AHLs produced by bacterial cultures *in situ* has not been achieved yet, most likely due to their low Raman activity. Interestingly, non-enhanced confocal Raman spectroscopy, combined with secondary ion mass spectrometry (SIMS), has been successfully applied in a multimodal chemical imaging approach to evaluate the spatial distribution of quinolone QS molecules across *P. aeruginosa* biofilms throughout various states of organization (Lanni et al., 2014; Baig et al., 2015). The use of SERS for the detection of these signaling molecules remains to be shown.

Due to the inherent limitations of SERS, direct detection of target analytes (i.e., microbial metabolites) in complex biological environments still represents a significant challenge. One of these limitations is related to the intrinsic complexity of the biological matrix that may prevent the interaction of the target analyte with the metallic surface. In turn, this would hinder analysis by SERS, as other molecular species interacting with the metal would increase background signal

(see limitations and challenges section). In a recent work Bodelón and coworkers developed an approach for label-free SERS detection and imaging of pyocyanin, as a proxy of QS in live biofilm communities of *P. aeruginosa* grown on rationally designed plasmonic substrates (Bodelón et al., 2016). The nanostructured hybrid materials comprised a plasmonic component (i.e., gold nanoparticles) embedded in a porous matrix acting as a molecular sieve for allowing diffusion of small molecules into the underlying optical sensor. The porous nature of the substrates was devised so as to restrict the contact of the plasmonic component with high-molecular weight biomolecules that could otherwise contaminate the SERS spectrum and hinder the sensitivity of the detection. With this in mind and aiming at providing different analytical tools to investigate this form of bacterial communication in live biofilm communities of *P. aeruginosa*, three different cell-compatible plasmonic substrates were fabricated: (1) poly N-isopropylacrylamide (pNIPAM) hydrogel doped with gold nanorods (Au@pNIPAM), (2) mesoestructured Au@TiO_2 thin film over a layer of gold nanospheres, and (3) micropatterned Au@SiO_2 supercrystal arrays comprising gold nanorods assembled in micrometer-sized pedestal-like structures coated with a mesoporous silica thin layer. In their study, the authors focused on pyocyanin, a heterocyclic nitrogen containing metabolite that is regulated by QS. Pyocyanin functions as an intercellular signaling molecule in the QS network of *P. aeruginosa* (Dietrich et al., 2006), acts as a virulence factor in infected hosts (Hall et al., 2016), and displays antimicrobial properties against a number of bacterial species (Baron and Rowe, 1981). Taking advantage that pyocyanin exhibits an absorption band in the visible (550–900 nm) the authors employed a 785 nm excitation laser line to increase the Raman scattering signal of the molecule by SERRS (**Figures 4A,B**). SERRS analysis of cell-free stationary-phase cultures obtained from wild-type PA14 bacteria (WT) grown with constant agitation, showed a SERRS fingerprint almost identical to that of commercial pyocyanin (PYO), whereas no pyocyanin signal was detected in a sample from a phenazine-null mutant strain (Δ*phz*) (Mavrodi et al., 2001; **Figure 4C**). The SERRS fingerprint is pyocyanin-specific since it is not detected in stationary-phase cultures of PA14 mutant strains Δ*phzM* and Δ*phzS* (Mavrodi et al., 2001), which are deficient in the biosynthesis of this phenazine (**Figure 4D**). The measurement under resonance Raman conditions facilitates the selective detection of pyocyanin over the rest of the phenazines produced by PA14 bacteria because they lack the 550–900 nm absorption band (**Figures 4E,F**; Bodelón et al., 2016).

The authors demonstrated quantitative SERRS detection of pyocyanin in a concentration range between 0.1 μM down to 1 nM in aqueous samples obtained from chloroform extracted *P. aeruginosa* culture supernatants, achieving limits of detection (LOD) ranging from 10^{-10} M for Au@pNIPAM hydrogel, 10^{-9} M for mesoporous Au@TiO_2 thin film and 10^{-14} M for the micropatterned mesoporous Au@SiO_2 substrate. Interestingly, the hybrid plasmonic substrates were shown to facilitate *in situ* SERRS detection of pyocyanin produced by biofilms and small cellular aggregates of *P. aeruginosa* grown in droplets, and yielded spatially resolved 2D maps of the QS molecule with high spatial resolution. The Au@pNIPAM hydrogel, devised as a highly porous platform with enhanced diffusivity, led to plasmonic detection of pyocyanin throughout the growth of the colony-biofilm (**Figures 5A,B**) with a homogeneous distribution in both colonized and non-colonized regions of the substrate. Interestingly, the 785 nm near-infrared laser enabled to detect this metabolite at biologically relevant concentrations (i.e., as low as 0.1 μM) in spiked Au@pNIPAM hydrogels implanted subcutaneously in mice (**Figures 5C,D**), indicating that pyocyanin could be used as a reporter for non-invasive monitoring of QS and screening potential antimicrobial drugs in animal models of infections using SERRS (Bodelón et al., 2016). Indeed, the expression of pyocyanin is a common phenotypic assay widely used in quorum quenching studies as an indicator of the efficacy of the treatment. In view of these results, the authors suggested that plasmonic hydrogels could be used as implantable materials in experimental animal models, to investigate QS triggered by natural populations of *P. aeruginosa* and to assess anti-virulence therapies by SERS (Bodelón et al., 2016). Imaging QS in live biofilms with spatiotemporal resolution is important toward gaining new understanding of this form of bacterial communication. In this work, it was demonstrated spatial imaging of pyocyanin produced by biofilms of *P. aeruginosa* PA14 grown on mesostructured Au@TiO_2 thin films with a resolution of about 20 μm, as well as variation of the QS signal up to millimeter-scale areas (**Figures 5E,F**).

Owing to its extremely high enhancement factor toward pyocyanin detection (LOD 10^{-14} M), the Au@SiO_2 supercrystal platform enabled ultrasensitive SERRS detection of pyocyanin in low-density bacterial cultures at early stages of biofilm development, and imaging of bacterial communication triggered by small clusters of cells colonizing the micrometer-sized plasmonic features (**Figure 6**). The high performance of this substrate was most likely due to a high density of efficient hot-spots and collective plasmon modes in the supercrystal, as well as a contribution of the mesoporous silica coating, which infiltrates within the highly ordered structure of nanorods, thereby increasing the "plasmonically active space" and leading to an extremely high electromagnetic enhancement factor (Hamon et al., 2014, 2016). The SERS-based approach employed by Bodelón and collaborators, focusing on the detection of pyocyanin released from bacterial biofilms and small clusters of cells, demonstrated the potential of plasmonics as an alternative method for non-invasive detection and imaging SERS-active metabolites released from undisturbed microbial populations. For diagnostic purposes, ultrasensitive SERRS detection of pyocyanin at trace levels could aid in early detection and effective treatment of *P. aeruginosa* infectious disease.

Multidrug resistance is an increasing threat to the successful treatment of bacterial infections. In particular, *P. aeruginosa* has the ability to rapidly develop resistance to multiple classes of antibiotics leading to high morbidity and mortality rates (Rossolini and Mantengoli, 2005). Early detection and timely administration of antimicrobial therapy is critical in optimizing patient outcomes, including hospital length of stay, mortality, and healthcare costs. Therefore, sensitive and reliable methods

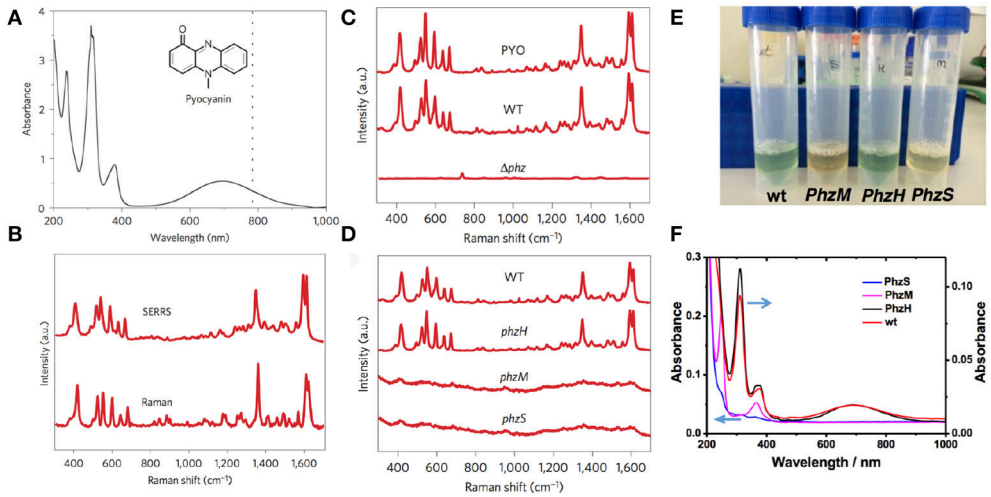

FIGURE 4 | SERRS detection of pyocyanin produced by *P. aeruginosa* PA14 strains grown in planktonic culture. **(A)** UV–visible–near-infrared spectrum of aqueous pyocyanin solution (10^{-4} M) and molecular structure of pyocyanin (inset). The dotted line indicates 785 nm, corresponding to the excitation wavelength used for SERRS. **(B)** Resonance Raman and SERRS spectra of pyocyanin measured in solid state and in aqueous solution (1 μM, Au@pNIPAM hydrogel), respectively. Raman measurement was carried out with a 50× objective, a maximum power of 54.22 kW cm^{-2} and an acquisition time of 10 s. SERRS measurement was carried out with a 20× objective, a maximum power of 4.24 kW cm^{-2} and an acquisition time of 10 s. **(C)** SERRS spectra of commercial pyocyanin (PYO) and of pyocyanin produced by the wild-type (WT) and the phenazine-null *phz1/2* (Δ*phz*) strains. **(D)** SERRS spectra of pyocyanin produced by wild-type and the indicated phenazine mutant strains. **(E)** Photographs of the phenazine-containing samples obtained from the wild type PA14 (wt) and the different mutants (PhzH, PhzS and PhzM), as labeled, under visible light illumination. **(F)** UV-Vis-NIR spectra of the samples containing different phenazines; pyocyanin (wt and PhzH), 1-hydroxyphenazine (1-HO-PHZ, wt, PhzM, and PhzH) and phenazine-1-carboxamide (PCN, wt, PhzS, and PhzM). All SERRS measurements were performed with a 785 nm laser line employing a 20× objective, maximum power between 1.72 kW cm^{-2} and an acquisition time of 10 s (intensity at 418 cm^{-1}) employing Au@pNIPAM hydrogels. Images reproduced with permission from Bodelón et al. (2016).

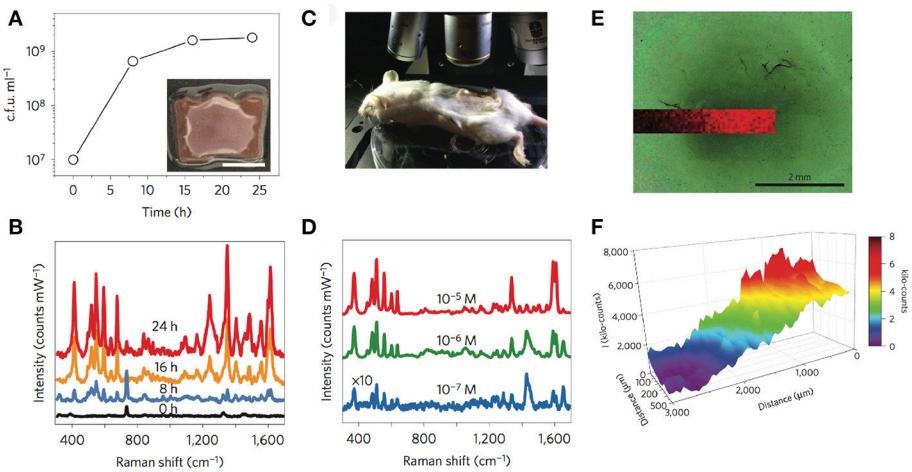

FIGURE 5 | *In situ* detection and imaging of pyocyanin secreted by *P. aeruginosa* PA14 colonies and biofilms grown on Au@pNIPAM hydrogels and mesoestructured Au@TiO_2 thin films. **(A)** Graphical representation of viable bacteria (c.f.u. ml^{-1}) quantified over time. The inset shows an image of the colony-biofilm grown on Au@pNIPAM (scale bar, 0.5 cm). **(B)** SERRS spectra recorded at the indicated times. Measurements of colony-biofilms were done using a 785 nm laser line for 10 s and using a maximum power of 0.91 kW cm^{-2} employing a 20× objective. **(C)** Photograph showing the Raman experimental set-up for detection of pyocyanin in subcutaneous implants in mice. **(D)** Under-skin SERRS spectra of pyocyanin spiked at the indicated concentrations on Au@pNIPAM hydrogel. SERRS measurements of pyocyanin-spiked hydrogels were performed using a 785 nm laser line for 10 s using a maximum power of 24.45 kW cm^{-2} employing a 10× objective. For clarity, the spectra noted with ×10 have been multiplied by a factor of 10. **(E)** Optical image of bacterial biofilm (dark central region) grown on Au@TiO_2 substrate captured with the Raman microscope and superimposed pyocyanin SERRS mapping (418 cm^{-1}) acquired with excitation laser wavelength of 785 nm, 5× objective and a laser power of 0.94 mW for 10 s. **(F)** Graphical representation of the SERRS intensity mapping shown in **(E)**. Images reproduced with permission from Bodelón et al. (2016). Copyright © 2016, Springer Nature.

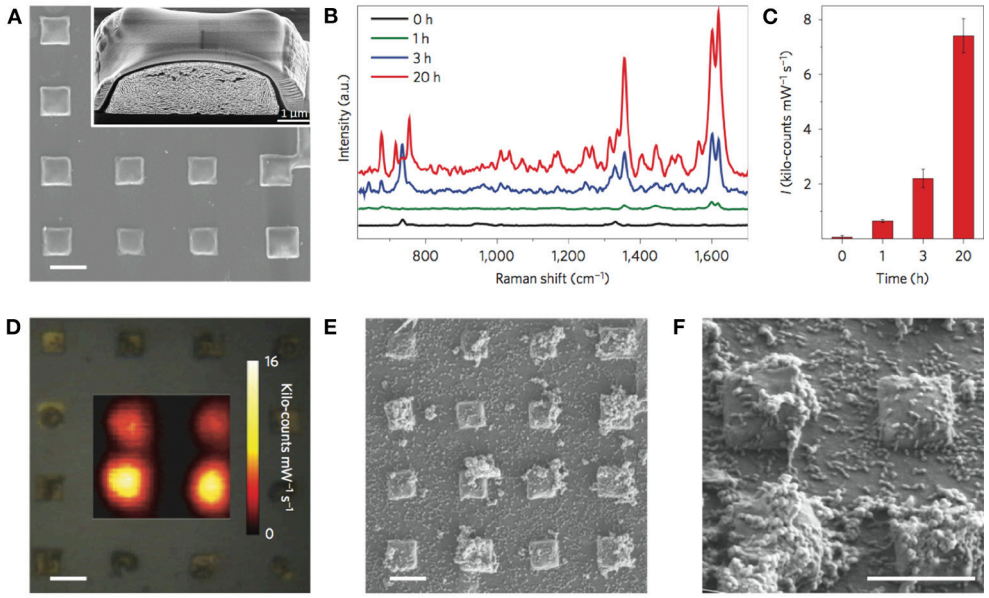

FIGURE 6 | *In situ* detection and imaging of pyocyanin secreted by *P. aeruginosa* PA14 biofilms grown on micropatterned Au@SiO_2 supercrystals. **(A)** SEM images of micropatterned Au@SiO_2 supercrystals. Scale bar, 5 µm. The inset shows a cross-section SEM image of a Au@SiO_2 supercrystal. **(B)** Representative SERRS spectra measured at 0, 1, 3, and 20 h. **(C)** Relative SERRS intensities (1,600 cm^{-1}) recorded at 0, 1, 3, and 20 h. Error bars indicate standard deviation. **(D)** Optical image of the substrate and SERRS mapping of pyocyanin (1,600 cm^{-1}) recorded at 20 h of growth. Scale bar, 5 µm. **(E,F)** SEM images of Au@SiO_2 supercrystals colonized by *P. aeruginosa* (20 h) at different magnifications. Scale bars, 5 µm. All SERS measurements were carried out with a 785 nm laser line, 50× objective and a maximum power of 0.98 kW cm^{-2}. The acquisition time was 0.1 s. Images reproduced with permission from Bodelón et al. (2016).

for rapid microbial identification are essential in modern healthcare (Bauer et al., 2014; Cookson et al., 2017). An alternative approach relies in the identification of the infectious agent based on the detection of pathogen-specific biomarkers. In this context, Hunter and collaborators demonstrated a correlation between pyocyanin concentration in sputum and rates of pulmonary decline in adult patients with CF chronically infected with *P. aeruginosa*, indicating that this metabolite can serve as an important diagnostic indicator (Hunter et al., 2012). The detection and quantification of pyocyanin in sputum was determined by high performance liquid chromatography, an analytical technique with limited throughput that requires substantial expertise and know-how. As an alternative diagnostic analytical method, Wu and collaborators implemented a SERS-based approach employing silver nanorod arrays for detecting pyocyanin in processed (i.e., chloroform-extracted) clinical sputum samples. The system allowed the detection of the metabolite at clinically relevant concentrations with the advantage to process multiple samples rapidly (Wu et al., 2014).

Recent advances in microfabrication technologies have made it possible to obtain microscale devices for culturing microbial cells (Weibel et al., 2007), which have the capability not only to transform the study of microbial physiology and cellular communication, including QS, but also hold great potential for many practical applications including drug discovery and diagnosis (Srinivasan et al., 2015; Nai and Meyer, 2017). The success of this emerging field requires the adaptation of sensitive analytical tools able to detect trace amounts of target biomolecules, an application for which SERS has great potential. In this respect, Žukovskaja and collaborators developed a lab-on-a-chip SERS (LoC-SERS)-based microfluidic system (**Figure 7**), which was applied to detect pyocyanin spiked in saliva at the clinical micromolar range employing silver colloids without the need of sample processing (Žukovskaja et al., 2017).

In an effort to extend the use of SERS as a imaging tool to study interspecies QS communication, Bodelón and collaborators demonstrated the simultaneous detection of pyocyanin and violacein produced by interacting colonies of *P. aeruginosa* PA14 and *Chromobacterium violaceum* CV026, respectively, grown as a co-culture on agar-based hybrid nanostructured plasmonic (Au@agar) substrates (Bodelón et al., 2017). This platform comprises a multilayer thin film of gold nanospheres on glass covered by a thin layer of nutrient LB agar. The motivation behind the use of a solid culture medium (e.g., agar-based) is that it enables co-culturing of microbial colonies at predefined locations with controlled separation. By confronting microbial populations on agar, the microorganisms can be readily identified as discrete colonies, as well as the region of chemical interaction between them. In the study, *P. aeruginosa* PA14 and *C. violaceum* CV026 were selected as a dual species co-culture model because the QS systems of these soil saprophytic bacteria are known to regulate the biosynthesis of pyocyanin and violacein, respectively, molecules amenable to Raman spectroscopy detection most likely due to their high Raman cross-section. *P. aeruginosa* produces two types of AHL QS signaling molecules: C12-AHL and N-butyryl-L-homoserine lactones (C4-AHLs) that are involved in

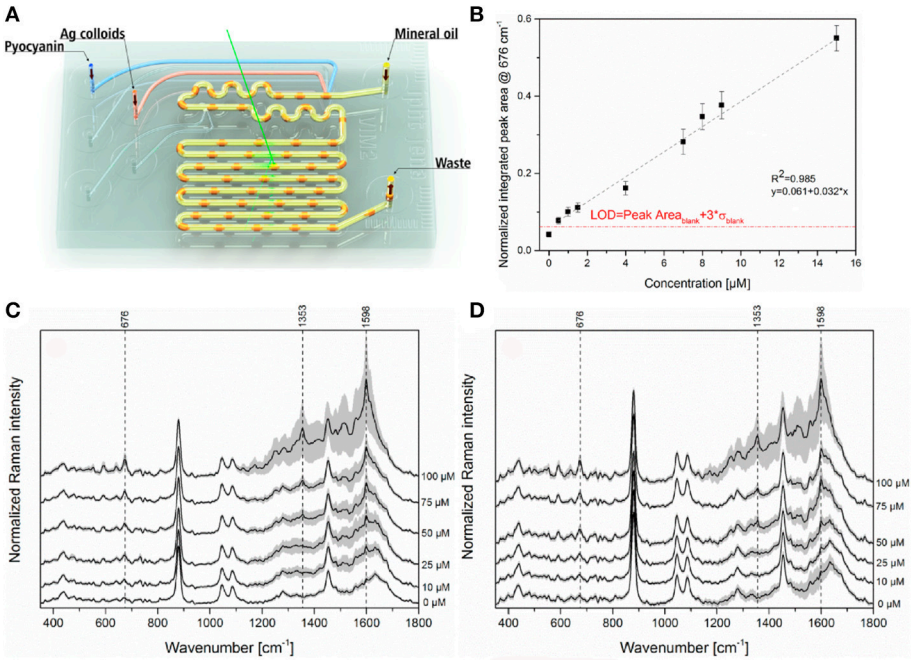

FIGURE 7 | LoC-SERS approach for detection of pyocyanin in saliva. **(A)** Schematic representation of the droplet based microfluidic chip used for LoC-SERS measurements. **(B)** Calibration curve for the determination of pyocyanin relative concentration in aqueous solution. The peak area ratio of the 676 cm^{-1} and 240 cm^{-1} Raman modes as a function of pyocyanin concentration in aqueous solution in the range between 0.5 and 15 μM with linear fitting. The red line indicates the calculated LOD. **(C,D)** Average SERS spectra and their double standard deviation of the different concentrations of pyocyanin in the saliva sample from volunteer number one **(C)**, two **(D)**. Images reproduced with permission from Žukovskaja et al. (2017).

the production of pyocyanin (Lee and Zhang, 2014). CV026 is a mutant strain of *C. violaceum* that cannot generate its own AHL signals, but can respond to compatible AHLs bearing short C4 to C8 acyl chains, such as *P. aeruginosa* C4-AHLs, thereby resulting in the expression of QS-regulated phenotypes, including the synthesis of violacein (McClean et al., 1997). The precise biological function of this pigmented metabolite still remains to be elucidated, but it has been shown to display toxic activities against certain bacterial species and predator organisms (Durán et al., 2016). As violacein and pyocyanin possess absorption bands centered at 580 and 695 nm, respectively, the use of a 785 nm excitation laser line enabled SERS detection of violacein and SERRS detection of pyocyanin (**Figure 8**).

Initially, the detection of violacein expression was demonstrated by SERS in CV026 bacterial cells grown as a colony on Au@agar upon treatment with commercial C4-AHL. The high sensitivity of the plasmonic approach was demonstrated by the detection of violacein spectral features in non-pigmented CV026 colonies stimulated with a low concentration of commercial C4-AHL. Interestingly, the levels of pyocyanin expression observed by SERRS in co-culture were significantly lower than those in monoculture. Moreover, in co-culture (**Figures 9A,B**), the amount of pyocyanin and violacein detected were inversely proportional in the confrontation zone (**Figures 9C,D**), suggesting a possible role of violacein in the down-regulation of the phenazine. To confirm the above data, the phenazine concentration was measured by UV–vis spectroscopy at 691 nm (λmax of pyocyanin) following chloroform extraction from the agar on which the PA14 colonies were grown. Significantly, whereas the amount of pyocyanin released by PA14 cells in monoculture averaged 2.3 μM, its concentration could not be determined in co-culture, as it was below the detection limits of this method (**Figure 9E**). Since the growth of PA14 bacteria in monoculture and co-culture was very similar (**Figure 9F**), the differential expression of pyocyanin was not attributed to growth defects.

Notably, quantitative PCR analysis of gene expression indicated that the decreased levels of pyocyanin were, at least in part, due to the repression of the *P. aeruginosa phzS* gene responsible for the last step of pyocyanin biosynthesis. Treatment of PA14 bacteria with commercial violacein reduced pyocyanin expression, as well as and transcription of the *phzS* gene, which indicated a potential role of violacein in the down-regulation of the phenazine. Interestingly, violacein is a bis-indole compound, and it has been reported that indole and its derivatives have been shown to repress QS-regulated phenotypes in *P. aeruginosa* (Lee et al., 2015), including the production of pyocyanin (Chu et al., 2012). Remarkably, PA14 strains expressing pyocyanin (i.e., wild type and Δ*phzH*), as opposed to strains deficient in the biosynthesis of this phenazine (i.e., Δ*phz1/2*, Δ*phzM*, and Δ*phzS*), compromised the growth of CV026. Therefore, this experimental evidence indicated that pyocyanin exerted a toxic effect to *C. violaceum*. As stated by the authors, although PA14 and CV026 bacteria can initially coexist, *P. aeruginosa* eventually

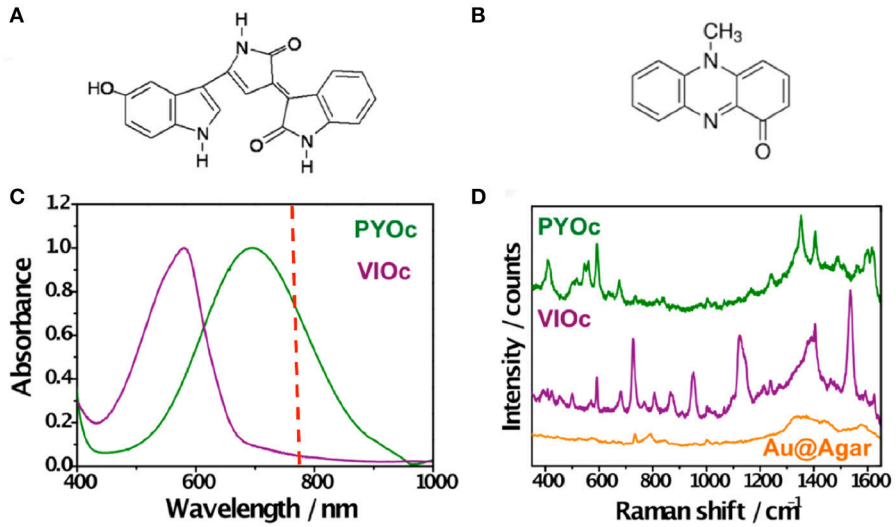

FIGURE 8 | Detection of violacein and pyocyanin on Au@agar by SERS/SERRS. **(A,B)** Chemical structures of violacein and pyocyanin, respectively. **(C)** Normalized visible–NIR spectra of commercial pyocyanin (PYOc) and violacein (VIOc). The dashed red line indicates the laser wavelength used (785 nm). **(D)** SERRS spectrum of PYOc, SERS spectrum of VIOc, and SERS spectrum of Au@agar. All spectra were measured with a 50× objective, a maximum power of 0.64 kWcm^{-2}, and an acquisition time of 10 s. Excitation laser line was 785 nm. Images reproduced with permission from Bodelón et al. (2017).

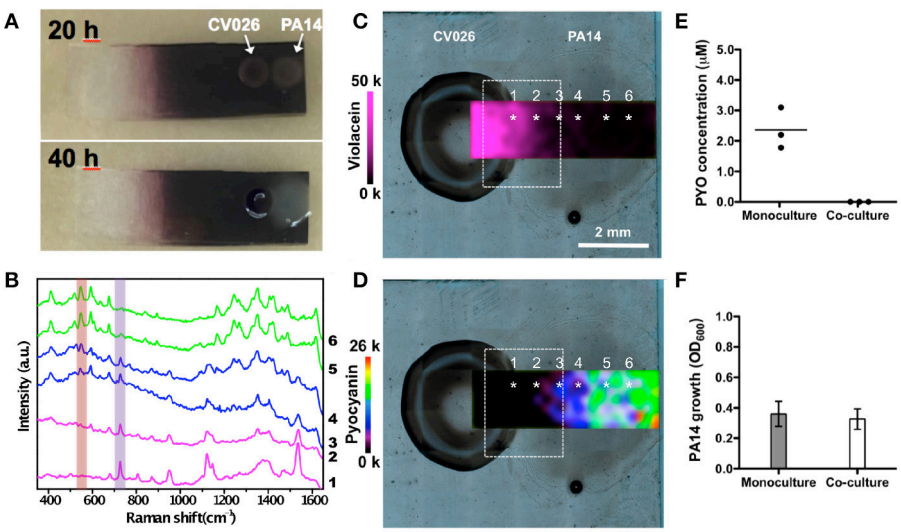

FIGURE 9 | Detection and imaging of interspecies QS on Au@agar by SERS/SERRS. **(A)** Photographs of *C. violaceum* CV026 and *P. aeruginosa* PA14 colonies co-cultured on Au@agar taken at 20 and 40 h. **(B)** SERS/SERRS spectra recorded at the points indicated with asterisks in **(C,D)**. The purple and orange bars indicate violacein (727 cm^{-1}) and pyocyanin (544 cm^{-1}) specific bands. **(C,D)** SERS mapping of violacein (727 cm^{-1}) **(C)** and SERRS mapping of pyocyanin (544 cm^{-1}) **(D)** in co-culture at 20 h. The dashed squares indicate the confrontation zone. **(E)** Quantification of pyocyanin (PYO) produced by PA14 colonies grown in monoculture or in co-culture by UV-Vis spectroscopy. Dark circles indicate the value obtained from biological triplicates ($n = 6$, for each group). Straight line within the data points indicates average. **(F)** Growth of PA14 bacterial cells in monoculture and in co-culture. Error bars indicate the standard deviation of biological triplicates. Images reproduced with permission from Bodelón et al. (2017).

overgrows *C. violaceum*, reducing the viability of its partner in extended co-cultures. In view of these results, it was suggested that the promiscuous CviR transcriptional receptor of CV026 can sense C4-AHLs produced by PA14 bacteria producing violacein, which in turn may contribute to pyocyanin down-regulation. This hypothesis points toward a potential defensive mechanism of *C. violaceum* CV026 in the chemical interplay between the bacterial species. This study illustrates the potential of SERS for non-invasive chemical analysis of microbial interactions on agar, which is the standard support matrix for culturing microbial cells, enabling to visualize the expression of two microbial metabolites in the co-culture taking place as a result of QS interspecies

communication. In the context of polymicrobial diseases, similar SERS-based approaches could be applied for studying clinically relevant interactions between *P. aeruginosa* and other microbial species such as *S. aureus*, *Burkholderia* spp, *C. albicans*, etc.

P. aeruginosa is a versatile bacterium that has evolved a set of regulatory mechanisms to adapt to nutritional changes and thrive in hostile environments. Recent studies have shown that carbon source has a high impact on bacterial QS signaling, virulence, biofilm formation and pyocyanin production (Shrout et al., 2006; Huang et al., 2012). In this context, Polisetti and collaborators used SERS to image the production of pyoacyanin in pellicle biofilms of a CF clinical strain (FRD1) or a laboratory strain (PAO1C) of *P. aeruginosa* grown in the presence of glutamate or glucose as carbon sources (Polisetti et al., 2016). In this study, silver nanoparticles (12–14 nm) were incubated with biofilms and used as SERS optical enhancers to spatially map pyocyanin by confocal Raman microespectroscopy. For conducting SERS mapping, biofilm samples were deposited onto silicon wafers and dried. A PCA multivariate statistical approach was implemented in the analysis so as to accurately integrate the SERS spectral data acquired from the highly heterogeneous biological matrix. The analysis showed a relatively homogeneous distribution of pyocyanin in biofilms of the CF clinical strain when grown with glucose and glutamate, while the laboratory strain only produced detectable levels of pyocyanin when glutamate was used as the carbon source, thereby demonstrating strain-level differences in carbon metabolism. In addition to pyocyanin, SERS analysis of biofilms from CF clinical strain showed a spectral feature that may correspond to vibrational bands of alginate carbohydrates, associated by the authors to the mucoid phenotype specific of this strain. Mucoid isolates of *P. aeruginosa* are highly prevalent in the CF lung, and their emergence during the course of infection is associated with increased inflammation, respiratory decline, and poor prognosis for CF patients (Koch, 1993).

It has long been known that QS-regulated factors influence different stages of biofilm formation, including cell attachment, growth and dispersal (Passos da Silva et al., 2017). Moreover, the densely populated environment within the biofilm facilitates intercellular chemical interactions and QS communication (Parsek and Greenberg, 2005; Flemming et al., 2016). SERS has been applied for *in-situ* chemical analysis of biofilms, as well as to evaluate the spatial biodistribution of biofilm matrix components and their relative abundance, which has been recently reviewed. (Ivleva et al., 2017) Ivleva and collaborators employed silver nanoparticles as SERS optical enhancers to investigate the matrix components in multispecies biofilms (Ivleva et al., 2008, 2010). Their plasmonic approach led to a significant enhancement of the Raman signals that enabled them to chemically image biofilm matrix constituents. SERS, in contrast to non-enhanced (i.e., conventional) Raman spectroscopy, can help to harness chemical information of the biofilm matrix in more detail, especially at low cell densities (Ivleva et al., 2010). It should be noted that the biotoxicity associated to silver nanoparticles and silver ions may give rise to potential artifacts that could hamper the analysis of the biofilm under *in vivo* conditions (Ivleva et al., 2017). Chao and Zhang also employed silver nanoparticles to investigate chemical variations in the matrix of biofilms of various Gram-negative and Gram-positive bacteria including *Escherichia coli*, *Pseudomonas putida,* and *Bacillus subtilis*. In this study, biofilms cultivated for 4, 8, 24, and 72 h were incubated with the silver nanoparticles and dried before SERS analysis. By assigning peaks of averaged SERS spectra into the different components of the biofilm matrix, the authors showed that the lipid, nucleic acid, and protein content increased significantly in growing biofilms (Chao and Zhang, 2012). Interestingly, the authors hypothesized that the significant increase during biofilm growth of a predominant Raman band at 730 cm^{-1} assigned to nucleic acids, could be attributed to the accumulation of extracellular DNA. In certain bacterial species such as *P. aeruginosa*, the release of this major structural component of the biofilm matrix is induced by lysis of a bacterial subpopulation in response to QS (Ibáñez de Aldecoa et al., 2017). These studies illustrate the potential of SERS to chemically monitor biofilm microbial communities and provide new insights regarding their structural and spatial organization.

Biochemical and functional analysis have shown that most QS LuxR family members require appropriate AHL molecules to properly fold into their active conformations, which is mostly based on the production of soluble and stable protein upon supplementing the bacterial growth medium with cognate signaling molecules. This strategy has been applied toward the structural characterization of several LuxR homologs (Papenfort and Bassler, 2016), including the ligand-binding domain (LBD) of LasR from *P. aeruginosa* (Bottomley et al., 2007). Resolution of their crystal structures have enabled researchers to design and identify chemical compounds capable of binding to the ligand-binding pockets of LuxR-type receptors so as to develop potent QS inhibitors (LaSarre and Federle, 2013). However, the failure to express LuxR homologs in the apoprotein form (i.e., ligand-free) at the high concentrations required for structural characterization has limited the understanding of the mechanisms by which QS receptors are modulated by native and non-native ligands. Taking advantage that certain LuxR homologs, such as LasR from *P. aeruginosa,* can fold into an active conformation in the absence of their cognate AHL ligands (Sappington et al., 2011), Costas and collaborators implemented a SERS-based approach to detect interactions between the LBD of LasR and QS agonists and antagonists (Costas et al., 2015). To this end the LBD of LasR ($LasR_{LBD}$) bearing a hexa-histidine tag and a cysteine in its carboxyl-terminus was expressed and affinity-purified in a soluble, ligand-free active form. By chemical crosslinking of purified $LasR_{LBD}$ with disuccinimidyl suberate (DSS) authors demonstrated the presence of dimeric complexes of $LasR_{LBD}$ at similar levels regardless of the presence or absence of its cognate C12-AHL ligand. This indicates that the polypeptide can exist in the form of homodimers even when it is expressed in the absence of cognate signal molecules (**Figures 10A,B**). Costas and collaborators showed that apo $LasR_{LBD}$ can bind C12-AHLs, which acted as quorum quencher in a QS reporter system, demonstrating that the apoprotein is competent for ligand-binding. For SERS analysis, $LasR_{LBD}$ was attached to the plasmonic sensor via the thiol group of the carboxy-terminal cysteine and incubated with cognate C12-AHL ligands, C4-AHL agonists and Furanone C30 or acetylsalicylic acid antagonists. Label-free SERS allowed the authors to detect conformational

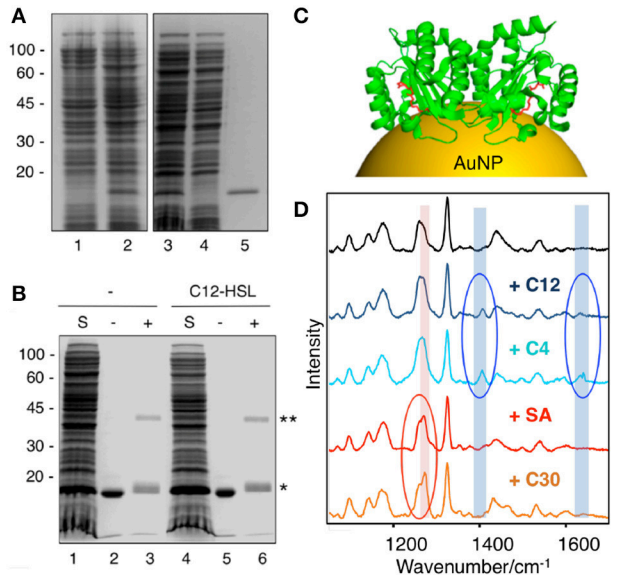

FIGURE 10 | Application of SERS for detection of QS protein-ligand interactions. **(A)** SDS-PAGE and Coomassie blue staining of $LasR_{LBD}$ expression and purification. Lane 1, uninduced total fraction; lane 2, IPTG-induced total fraction; lane 3, IPTG-induced soluble fraction; lane 4, affinity chromatography flow-through; lane 5, eluted protein. **(B)** Cross-linking assay of $LasR_{LBD}$. The polypeptide expressed in bacteria in the absence (lanes 1-3) or in the presence (lanes 4–6) of C12-HSL was solubilized (S), affinity purified and subjected to crosslinking (+) with 0.5 mM DSS (lanes 3,6) or not (lanes 2,5). Bands corresponding to dimeric (**) and monomeric (*) forms are indicated on the right. **(C)** Schematic illustration of dimeric $LasR_{LBD}$ bound to C12-AHL (in red) (PDB:2UV0) attached to a gold nanoparticle (AuNP). **(D)** SERS spectra (after baseline correction) of $LasR_{LBD}$ polypeptide (black spectrum), incubated with C12-AHL (+C12), C4-AHL, salicylic acid (+SA) or furanone C30 (+C30). The red and blue ovals indicate inhibitor-specific and activator-specific SERS fingerprints, respectively. Illumination with a 785 nm laser line was used to avoid protein damage. Images reproduced with permission from Costas et al. (2015).

changes of $LasR_{LBD}$ as a result of its interaction with the different QS ligands. The highly sensitive and reproducible SERS spectra allowed the discrimination between activators and inhibitors of QS, through their distinctive vibrational signatures (**Figure 10C**). This study features SERS as a fast and cost-effective tool to analyze ligand-induced conformational changes in proteins, confirming the applicability of SERS for *in vitro* screening of QS modulators. In this framework, this SERS strategy has great potential to be implemented in structure-activity relationship studies for pharmacophore generation of inhibitors targeting bacterial virulence and antibiotic resistance mechanisms linked with QS.

LIMITATIONS AND CHALLENGES

Our understanding of SERS mechanisms and the ability to engineer plasmonic nanostructures has increased enormously during the last decade. Researchers have mastered the fabrication of rationally designed plasmonic transducers with tunable optical properties, large SERS enhancement factors, and appropriate surface functionalization (Hamon and Liz-Marzán, 2018), which has allowed to apply this technique with great success in the analytical field to detect a wide range of chemical species at ultralow (i.e., attomolar) concentrations (Wang and Kong, 2015; Mosier-Boss, 2017). However, the implementation of plasmonic transducers for label-free sensing and imaging applications in complex biological environments is still a challenging task.

One of the main hurdles that must be overcome is that the target analyte must be in contact with the plasmonic surface and often has to compete with metal surface ligands and biomolecules, which are usually present in biological media at much higher concentrations. Detecting target molecules with no or low affinity for the metal surface may also represent a significant problem. Different strategies can be applied in order to overcome these potential issues. In general terms, the surface chemistry of nanoparticles may be tailored to improve binding selectivity and facilitate detection. Materials with selective porosity (López-Puente et al., 2013; Bodelón et al., 2016), non-fouling surfaces (Sun et al., 2015), and tunable charge (Jia et al., 2016), offer attractive alternatives by providing chemical or physical filtering of interfering molecules. Due to the fact that SERS is influenced by the nature of the interactions between molecules and nanostructured surfaces, the charge properties and functional groups of molecules and components of the plasmonic substrate play an important role in SERS analysis. SERS performance can be significantly improved upon minimizing electrostatic repulsion forces, as well as by tuning the dielectric (hydrophilic/hydrophobic) properties of the surface, which can be a suitable strategy to trap non-polar molecules (Abalde-Cela et al., 2010). These strategies reduce the need for sample pretreatment, improve selectivity, and can be applied for *in-situ* analysis.

As discussed above, SERS measurements are greatly influenced by the affinity between biomolecules and the metal surface, thereby label-free SERS analysis of target analytes in biological samples (i.e., cells, biofilms) may be dominated by vibrational bands originating from other "contaminating" biomolecular species, which may lead to complex SERS spectra. In this context, the Raman spectrum of the cell and the extracellular medium is characterized by many different vibrational modes of biomolecules, including nucleic acids, proteins, lipids, and carbohydrates, representing a complete biomolecular profile, making the interpretation of the SERS spectrum a challenge for most adsorbates. In order to maximally exploit the capabilities of SERS in microbiology for *in situ* identification, it is essential to understand the molecular and corresponding biochemical origins of SERS vibrational signatures. Researchers have identified the spectral fingerprints of numerous types of biomolecules and molecular constituents, such as lipids, proteins, nucleobases, pigments and certain metabolites. However, despite some efforts (De Gelder et al., 2007), comprehensive databases of SERS and Raman spectra of biomolecules are still needed, and band assignment for the acquired spectra requires the analysis of already published data. Interpretation of the Raman spectra demands data processing as well as statistical treatments such as multivariate data analysis,

which is favored by the high resolution of the SERS spectra. In this framework, chemometric pattern recognition algorithms are widely applied in SERS studies so as to improve the accuracy and reproducibility of the technique facilitating, for instance, the monitoring of different extracellular metabolites in the culture medium (Mishra et al., 2017), the discrimination of five types of penicillin G antibiotics despite their high similarities (Clarke et al., 2005), or the identification of 16 staphylococcal species (Rebrošová et al., 2017). One strategy to avoid the spectral complexity of biological systems consists in enhancing the contribution of the target molecules (i.e., microbial metabolite) employing a laser line with an excitation frequency that is in resonance with an absorption band of the analyte as in SERRS (Bodelón et al., 2016, 2017). On the downside, SERRS analysis of resonant-active metabolites may preclude the detection of non-resonant molecules also present in the sample. The Raman cross-section of the analyte is an important feature to be considered. In general, heterocyclic molecules containing aromatic rings are characterized by high Raman scattering activities. In addition, π-conjugated biomolecules tend to have strong Raman scattering cross-sections, owing to their distributed electron clouds that can be easily polarized in the presence of an electric field (Laing et al., 2017). Remarkably, many antibiotics, chromophore-containing molecules, and other metabolites that may be regulated by QS are characterized by having potential Raman-active features. Obviously, the *a priori* knowledge of the spectral fingerprint of the target biomolecule is essential in SERS studies. However, when aiming at the identification/detection of a target biomolecule produced by microbial cells (i.e., pyocyanin), the origin of the SERS signal must be unequivocally ascertained by the use of mutant strains deficient in the production of the biological compound.

The main challenge to obtain reliable SERS measurements is represented by the performance of the plasmonic substrates. For analytical applications, the preparation of these structures has to be straightforward and reproducible, while at the same time the signal enhancement has to be homogenous. SERS may suffer from issues related to substrate degradation that results in signal decrease over time. For instance, *in situ* measurements of living organisms (i.e., biofims) by SERS requires plasmonic devices that will have to withstand high ionic strength conditions, which may produce detrimental outcomes. Other significant issues are related with homogeneity and reproducibility of the SERS signal within the plasmonic substrate. They consist in the difficulty to generate uniform distributed enhancement factors, occurring only at localized positions (i.e., hot-spots) and the polydispersity of SERS-active colloidal clusters, which may hamper quantitative analysis. Although SERS often requires optimization of the plasmonic sensing system for each target analyte, new approaches have been developed to overcome these limitations and produce SERS-active substrates with high sensitivity, stability and reproducibility. The engineering of hot-spots and plasmonic supercrystals may circumvent some of the aforementioned problems (Shiohara et al., 2014; Scarabelli et al., 2016). Hamon and Liz-Marzán recently reviewed the most important parameters that should be considered in order to address the major issues associated to SERS when using conventional colloidal chemical synthesis, namely reproducibility, simplicity, selectivity, high throughput and sensitivity (Hamon and Liz-Marzán, 2018). In this framework, Cardinal and collaborators have also recently suggested practical considerations to facilitate SERS spectra reproducibility across different laboratories (Cardinal et al., 2017). Although commercial SERS-active substrates are available (Mosier-Boss, 2017), they are in general prepared by physical deposition methods, and not from wet chemistry approaches, which would provide well-defined surfaces, tailored nanoscale features, thereby improving the reproducibility of the measurements (Hamon and Liz-Marzán, 2018). Current high-performance SERS substrates are synthesized in academic laboratories under highly optimized conditions, thus large-scale production of such sophisticated devices with high reproducibility can be challenging. In general terms, in order to broaden the use of SERS and translate its application into the real world (e.g., clinical settings), it would be necessary the standardization and automatization of the procedures for the synthesis and functionalization of plasmonic transducers. Continuous development and improvement in Raman instrumentation, analytical workflow, and software are also crucial.

CONCLUSIONS AND OUTLOOK

Herein we have presented some recent applications of SERS spectroscopy for assessing QS in *P. aeruginosa*, such as detection and quantification of QS signaling molecules, chemical analysis of biofilm formation, *in situ* imaging of QS-regulated metabolites, as well as the use of SERS as a potential tool for screening protein-ligand interactions. In spite some limitations and challenges that still must be overcome, this highly versatile technique offers great potential for the study of extracellular metabolites and other secreted factors produced by microbial populations. The ability to visualize these chemical substances is fundamental to provide new knowledge into their function, as well as the spatiotemporal dependencies required for the chemical interactions shaping microbial communities. In this context, revealing the extensive intercellular signaling potential of bacteria, and other microbial species, can prove breeding ground to yield valuable ecological insight and drug prospecting.

With the prevalence of multidrug resistant bacteria, new antibiotics and therapeutic approaches are urgently needed. Specifically, the capacity of SERS to non-invasively study microbial populations may open new avenues for understanding QS and for the development of new therapies targeting this form of bacterial communication. Microorganisms represent a depository for natural-product discovery, many of which have been shown to be under QS regulation. Holistic approaches for the cultivation of microorganisms are being actively investigated in the search for new antimicrobials and for the development of bioactive substances that can function as antitumor agents, immunosuppressants or cholesterol lowering agents to name just a few (Nai and Meyer, 2017). Importantly, many of these bioactive molecules, some of which contain aromatic compounds, or have been shown to be pigments

and chromophores, are amenable to SERS detection. In this context, recent technological advances in microscale cultivation devices provide a window of opportunity to transform the study of microbial communication, as well as to facilitate the discovery of new bioactive substances (Srinivasan et al., 2015). The success of these methodologies for studying bacterial populations would benefit from the adaptation of analytical tools able to detect trace amounts of the secreted metabolites, as well as their *in situ* characterization, applications for which SERS excels. In this framework, SERS is already being implemented in lab-on-a-chip and nano/microfluidics technologies for sensing in nanoliter volumes (Jahn et al., 2017).

The advancements in nanotechnology and photonics have dramatically incremented the capabilities of SERS, by which this analytical tool is increasingly being adopted in microbiology studies for very diverse applications, including the sensitive detection of pathogenic bacteria (Liu et al., 2017), and culture-free investigation of bacterial cells (Lorenz et al., 2017). As shown herein, SERS spectroscopy has great potential to be incorporated to the set of label-free methodologies already in use for revealing the "hidden" chemistry of microbes such as imaging mass spectrometry and conventional Raman spectroscopy. The advent of portable Raman spectrometer systems makes real-time, on-site, SERS monitoring of analytes an exciting possibility. Additionally, the extraordinary capability of SERS for the detection of analytes in trace amounts could prove to be a great asset for the early detection and diagnosis of infectious diseases.

AUTHOR CONTRIBUTIONS

GB and IP-S conceived and wrote most of the work. VM-G and JP-J participated in the writing of the Raman scattering and SERS spectroscopy section. All listed authors actively contributed in the revision of the manuscript.

ACKNOWLEDGMENTS

This work was supported by the Ministry of Economy and competitiveness of Spain (MINECO) and FEDER (grant MAT2016-77809-R), Xunta de Galicia (GRC ED431C 2016-048 and CINBIO ED431G/02), Fundación Ramón Areces (SERSforSAFETY) and Interreg V-A Spain-Portugal (POCTEP) 2014-2020 and FEDER (0245_IBEROS_1_E).

REFERENCES

Abalde-Cela, S., Aldeanueva-Potel, P., Mateo-Mateo, C., Rodríguez-Lorenzo, L., Alvarez-Puebla, R. A., and Liz-Marzan, L. M. (2010). Surface-enhanced Raman scattering biomedical applications of plasmonic colloidal particles. *J. R. Soc. Interface* 7(Suppl. 4), S435–S450. doi: 10.1098/rsif.2010.0125.focus

Antunes, L. C., Ferreira, R. B., Buckner, M. M., and Finlay, B. B. (2010). Quorum sensing in bacterial virulence. *Microbiol.* 156(Pt 8), 2271–2282. doi: 10.1099/mic.0.038794-0

Baig, N. F., Dunham, S. J., Morales-Soto, N., Shrout, J. D., Sweedler, J. V., and Bohn, P. W. (2015). Multimodal chemical imaging of molecular messengers in emerging *Pseudomonas aeruginosa* bacterial communities. *Analyst* 140, 6544–6552. doi: 10.1039/C5AN01149C

Baron, S. S., and Rowe, J. J. (1981). Antibiotic action of pyocyanin. *Antimicrob. Agents Chemo.* 20, 814–820. doi: 10.1128/AAC.20.6.814

Bauer, K. A., Perez, K. K., Forrest, G. N., and Goff, D. A. (2014). Review of rapid diagnostic tests used by antimicrobial stewardship programs. *Clin. Infect. Dis.* 59(Suppl. 3), S134–S145. doi: 10.1093/cid/ciu547

Bernier, S. P., Hum, C., Li, X., O'Toole, G. A., Magarvey, N. A., Surette, M. G., et al. (2017). *Pseudomonas aeruginosa*-derived rhamnolipids and other detergents modulate colony morphotype and motility in the *Burkholderia cepacia* complex. *J. Bacteriol.* 199, e00171–e00117. doi: 10.1128/JB.00171-17

Bernier, S. P., and Surette, M. G. (2013). Concentration-dependent activity of antibiotics in natural environments. *Front. Microbiol.* 4:20. doi: 10.3389/fmicb.2013.00020

Bodelón, G., Montes-García, V., Costas, C., Pérez-Juste, I., Pérez-Juste, J., Pastoriza-Santos, I., et al. (2017). Imaging bacterial interspecies chemical interactions by surface-enhanced raman scattering. *ACS Nano* 11, 4631–4640. doi: 10.1021/acsnano.7b00258

Bodelón, G., Montes-García, V., López-Puente, V., Hill, E. H., Hamon, C., Sanz-Ortiz, M. N., et al. (2016). Detection and imaging of quorum sensing in *Pseudomonas aeruginosa* biofilm communities by surface-enhanced resonance Raman scattering. *Nat. Mater.* 15, 1203–1211. doi: 10.1038/nmat4720

Bottomley, M. J., Muraglia, E., Bazzo, R., and Carfi, A. (2007). Molecular insights into quorum sensing in the human pathogen *Pseudomonas aeruginosa* from the structure of the virulence regulator LasR bound to its autoinducer. *J. Biol. Chem.* 282, 13592–13600. doi: 10.1074/jbc.M700556200

Butler, H. J., Ashton, L., Bird, B., Cinque, G., Curtis, K., Dorney, J., et al. (2016). Using Raman spectroscopy to characterize biological materials. *Nat. Protoc.* 11, 664–687. doi: 10.1038/nprot.2016.036

Cardinal, M. F., Vander Ende, E., Hackler, R. A., McAnally, M. O., Stair, P. C., Schatz, G. C., et al. (2017). Expanding applications of SERS through versatile nanomaterials engineering. *Chem. Soc. Rev.* 46, 3886–3903. doi: 10.1039/C7CS00207F

Castillo-Juárez, I., Maeda, T., Mandujano-Tinoco, E. A., Tomás, M., Pérez-Eretza, B., García-Contreras, S. J., et al. (2015). Role of quorum sensing in bacterial infections. *World J. Clin. Cases* 3:575. doi: 10.12998/wjcc.v3.i7.575

Chao, Y., and Zhang, T. (2012). Surface-enhanced Raman scattering (SERS) revealing chemical variation during biofilm formation: from initial attachment to mature biofilm. *Anal. Bioanal. Chem.* 404, 1465–1475. doi: 10.1007/s00216-012-6225-y

Chu, W., Zere, T. R., Weber, M. M., Wood, T. K., Whiteley, M., Hidalgo-Romano, B., et al. (2012). Indole production promotes *Escherichia coli* mixed-culture growth with *Pseudomonas aeruginosa* by inhibiting quorum signaling. *Appl. Environ. Microbiol.* 78, 411–419. doi: 10.1128/AEM.06396-11

Cialla-May, D., Zheng, X. S., Weber, K., and Popp, J. (2017). Recent progress in surface-enhanced Raman spectroscopy for biological and biomedical applications: from cells to clinics. *Chem. Soc. Rev.* 46, 3945–3961. doi: 10.1039/C7CS00172J

Clarke, S. J., Littleford, R. E., Smith, W. E., and Goodacre, R. (2005). Rapid monitoring of antibiotics using Raman and surface enhanced Raman spectroscopy. *Analyst* 130, 1019–1026. doi: 10.1039/b502540k

Claussen, A., Abdali, S. W., Berg, R., Givskov, M., and Sams, T. (2013). Detection of the quorum sensing signal molecule N-Dodecanoyl-DLHomoserine lactone below 1 nanomolar concentrations using surface enhanced raman spectroscopy. *Curr. Phys. Chem.* 3, 199–210. doi: 10.2174/1877946811303020010

Cookson, W. O. C. M., Cox, M. J., and Moffatt, M. F. (2017). New opportunities for managing acute and chronic lung infections. *Nat. Rev. Microbiol.* 16, 111–120. doi: 10.1038/nrmicro.2017.122

Cooper, J. B. (1999). Chemometric analysis of Raman spectroscopic data for process control applications. *Chemom. Intell. Lab. Syst.* 46, 231–247. doi: 10.1016/S0169-7439(98)00174-9

Costas, C., López-Puente, V., Bodelón, G., González-Bello, C., Pérez-Juste, J., Pastoriza-Santos, I., et al. (2015). Using surface enhanced raman scattering to analyze the interactions of protein receptors with bacterial quorum sensing modulators. *ACS Nano* 9, 5567–5576. doi: 10.1021/acsnano.5b01800

Davies, J. (2013). Specialized microbial metabolites: functions and origins. *J. Antibiot.* 66, 361–364. doi: 10.1038/ja.2013.61

Davies, J., and Ryan, K. S. (2012). Introducing the parvome: bioactive compounds in the microbial world. *ACS Chem. Biol.* 7, 252–259. doi: 10.1021/cb200337h

De Gelder, J., De Gussem, K., Vandenabeele, P., and Moens, L. (2007). Reference database of Raman spectra of biological molecules. *J. Raman Spectrosc.* 38, 1133–1147. doi: 10.1002/jrs.1734

Dietrich, L. E., Price-Whelan, A., Petersen, A., Whiteley, M., and Newman, D. K. (2006). The phenazine pyocyanin is a terminal signalling factor in the quorum sensing network of *Pseudomonas aeruginosa*. *Mol. Microbiol.* 61, 1308–1321. doi: 10.1111/j.1365-2958.2006.05306.x

Diggle, S. P., Gardner, A., West, S. A., and Griffin, A. S. (2007). Evolutionary theory of bacterial quorum sensing: when is a signal not a signal? *Philos. Trans. Royal Soc. B* 362, 1241–1249. doi: 10.1098/rstb.2007.2049

Durán, N., Justo, G. Z., Durán, M., Brocchi, M., Cordi, L., Tasic, L., et al. (2016). Advances in *Chromobacterium violaceum* and properties of violacein-Its main secondary metabolite: a review. *Biotechnol. Adv.* 34, 1030–1045. doi: 10.1016/j.biotechadv.2016.06.003

Flemming, H. C., Wingender, J., Szewzyk, U., Steinberg, P., Rice, S. A., and Kjelleberg, S. (2016). Biofilms: an emergent form of bacterial life. *Nat. Rev. Microbiol.* 14, 563–575. doi: 10.1038/nrmicro.2016.94

Fourie, R., Ells, R., Swart, C. W., Sebolai, O. M., Albertyn, J., and Pohl, C. H. (2016). *Candida albicans* and *Pseudomonas aeruginosa* Interaction, with Focus on the Role of Eicosanoids. *Front. Physiol.* 7:64. doi: 10.3389/fphys.2016.00064

Garg, N., Luzzatto-Knaan, T., Melnik, A. V., Caraballo-Rodríguez, A. M., Floros, D. J., Petras, D., et al. (2017). Natural products as mediators of disease. *Nat. Prod. Rep.* 34, 194–219. doi: 10.1039/C6NP00063K

Gómez-Graña, S., Fernández-López, C., Polavarapu, L., Salmon, J.-B., Leng, J., Pastoriza-Santos, I., et al. (2015). Gold nanooctahedra with tunable size and microfluidic-induced 3D assembly for highly uniform SERS-active supercrystals. *Chem. Mater.* 27, 8310–8317. doi: 10.1021/acs.chemmater.5b03620

Gwo, S., Chen, H. Y., Lin, M. H., Sun, L., and Li, X. (2016). Nanomanipulation and controlled self-assembly of metal nanoparticles and nanocrystals for plasmonics. *Chem. Soc. Rev.* 45, 5672–5716. doi: 10.1039/C6CS00450D

Halas, N. J., Lal, S., Chang, W. S., Link, S., and Nordlander, P. (2011). Plasmons in strongly coupled metallic nanostructures. *Chem. Rev.* 111, 3913–3961. doi: 10.1021/cr200061k

Hall, S., McDermott, C., Anoopkumar-Dukie, S., McFarland, A., Forbes, A., Perkins, A., et al. (2016). Cellular effects of pyocyanin, a secreted virulence factor of *Pseudomonas aeruginosa*. *Toxins* 8:236. doi: 10.3390/toxins8080236

Hamon, C., and Liz-Marzán, L. M. (2018). Colloidal design of plasmonic sensors based on surface enhanced Raman scattering. *J. Colloid Interface Sci.* 512, 834–843. doi: 10.1016/j.jcis.2017.10.117

Hamon, C., Novikov, S., Scarabelli, L., Basabe-Desmonts, L., and Liz-Marzán, L. M. (2014). Hierarchical self-assembly of gold nanoparticles into patterned plasmonic nanostructures. *ACS Nano* 8, 10694–10703. doi: 10.1021/nn504407z

Hamon, C., Sanz-Ortiz, M. N., Modin, E., Hill, E. H., Scarabelli, L., Chuvilin, A., et al. (2016). Hierarchical organization and molecular diffusion in gold nanorod/silica supercrystal nanocomposites. *Nanoscale* 8, 7914–7922. doi: 10.1039/C6NR00712K

Harvey, A. L., Edrada-Ebel, R., and Quinn, R. J. (2015). The re-emergence of natural products for drug discovery in the genomics era. *Nat. Rev. Drug Discov.* 14, 111–129. doi: 10.1038/nrd4510

Henry, A. I., Sharma, B., Cardinal, M. F., Kurouski, D., and Van Duyne, R. P. (2016). Surface-enhanced raman spectroscopy biosensing: *in vivo* diagnostics and multimodal imaging. *Anal. Chem.* 88, 6638–6647. doi: 10.1021/acs.analchem.6b01597

Hotterbeekx, A., Kumar-Singh, S., Goossens, H., and Malhotra-Kumar, S. (2017). *In vivo* and *in vitro* interactions between *Pseudomonas aeruginosa* and staphylococcus spp. *Front. Cell. Infect. Microbiol.* 7:106. doi: 10.3389/fcimb.2017.00106

Huang, J., Sonnleitner, E., Ren, B., Xu, Y., and Haas, D. (2012). Catabolite repression control of pyocyanin biosynthesis at an intersection of primary and secondary metabolism in *Pseudomonas aeruginosa*. *Appl. Environ. Microbiol.* 78, 5016–5020. doi: 10.1128/AEM.00026-12

Hunter, R. C., Klepac-Ceraj, V., Lorenzi, M. M., Grotzinger, H., Martin, T. R., and Newman, D. K. (2012). Phenazine content in the cystic fibrosis respiratory tract negatively correlates with lung function and microbial complexity. *Am. J. Respir. Cell Mol. Biol.* 47, 738–745. doi: 10.1165/rcmb.2012-0088OC

Ibáñez de Aldecoa, A. L., Zafra, O., and González-Pastor, J. E. (2017). Mechanisms and regulation of extracellular DNA release and its biological roles in microbial communities. *Front. Microbiol.* 8:1390. doi: 10.3389/fmicb.2017.01390

Ivleva, N. P., Kubryk, P., and Niessner, R. (2017). Raman microspectroscopy, surface-enhanced Raman scattering microspectroscopy, and stable-isotope Raman microspectroscopy for biofilm characterization. *Anal. Bioanal. Chem.* 409, 4353–4375. doi: 10.1007/s00216-017-0303-0

Ivleva, N. P., Wagner, M., Horn, H., Niessner, R., and Haisch, C. (2008). *In situ* surface-enhanced raman scattering analysis of biofilm. *Anal. Chem.* 80, 8538–8544. doi: 10.1021/ac801426m

Ivleva, N. P., Wagner, M., Horn, H., Niessner, R., and Haisch, C. (2010). Raman microscopy and surface-enhanced Raman scattering (SERS) for *in situ* analysis of biofilms. *J. Biophotonics* 3, 548–556. doi: 10.1002/jbio.201000025

Jahn, I. J., Žukovskaja, O., Zheng, X. S., Weber, K., Bocklitz, T. W., Cialla-May, D., et al. (2017). Surface-enhanced Raman spectroscopy and microfluidic platforms: challenges, solutions and potential applications. *Analyst* 142, 1022–1047. doi: 10.1039/C7AN00118E

Jia, Y., Shmakov, S. N., and Pinkhassik, E. (2016). Controlled permeability in porous polymer nanocapsules enabling size- and charge-selective SERS nanoprobes. *ACS Appl. Mater. Interfaces* 8, 19755–19763. doi: 10.1021/acsami.6b05522

Kahraman, M., Mullen, E. R., Korkmaz, A., and Wachsmann-Hogiu, S. (2017). Fundamentals and applications of SERS-based bioanalytical sensing. *Nanophotonics* 6, 831–852. doi: 10.1515/nanoph-2016-0174

Kelly, K. L., Coronado, E., Zhao, L. L., and Schatz, G. C. (2003). The optical properties of metal nanoparticles: the influence of size, shape, and dielectric environment. *J. Phys. Chem. B* 107, 668–677. doi: 10.1021/jp026731y

Koch, C. (1993). Pathogenesis of cystic fibrosis. *Lancet* 341, 1065–1069.

Krafft, C., Schmitt, M., Schie, I. W., Cialla-May, D., Matthäus, C., Bocklitz, T., et al. (2017). Label-free molecular imaging of biological cells and tissues by linear and nonlinear raman spectroscopic approaches. *Angew. Chem. Int. Ed.* 56, 4392–4430. doi: 10.1002/anie.201607604

Kuku, G., Altunbek, M., and Culha, M. (2017). Surface-enhanced raman scattering for label-free living single cell analysis. *Anal. Chem.* 89, 11160–11166. doi: 10.1021/acs.analchem.7b03211

Laing, S., Jamieson, L. E., Faulds, K., and Graham, D. (2017). Surface-enhanced Raman spectroscopy for *in vivo* biosensing. *Nat. Rev. Chem.* 1:0060. doi: 10.1038/s41570-017-0060

Lanni, E. J., Masyuko, R. N., Driscoll, C. M., Dunham, S. J. B., Shrout, J. D., Bohn, P. W., et al. (2014). Correlated imaging with C60-SIMS and confocal raman microscopy: visualization of cell-scale molecular distributions in bacterial biofilms. *Anal. Chem.* 86, 10885–10891. doi: 10.1021/ac5030914

LaSarre, B., and Federle, M. J. (2013). Exploiting quorum sensing to confuse bacterial pathogens. *Microbiol. Mol. Biol. Rev.* 77, 73–111. doi: 10.1128/MMBR.00046-12

Lee, J. H., Wood, T. K., and Lee, J. (2015). Roles of indole as an interspecies and interkingdom signaling molecule. *Trends Microbiol.* 23, 707–718. doi: 10.1016/j.tim.2015.08.001

Lee, J., and Zhang, L. (2014). The hierarchy quorum sensing network in *Pseudomonas aeruginosa*. *Protein Cell* 6, 26–41. doi: 10.1007/s13238-014-0100-x

Limoli, D. H., Whitfield, G. B., Kitao, T., Ivey, M. L., Davis, M. R., Grahl, N., et al. (2017). *Pseudomonas aeruginosa* alginate overproduction promotes coexistence with *Staphylococcus aureus* in a model of cystic fibrosis respiratory infection. *MBio* 8:e00186-17. doi: 10.1128/mBio.00186-17

Liu, Y., Zhou, H., Hu, Z., Yu, G., Yang, D., and Zhao, J. (2017). Label and label-free based surface-enhanced Raman scattering for pathogen bacteria detection: a review. *Biosens. Bioelectron.* 94, 131–140. doi: 10.1016/j.bios.2017.02.032

López-Puente, V., Abalde-Cela, S., Angelomé, P. C., Alvarez-Puebla, R. A., and Liz-Marzán, L. M. (2013). Plasmonic mesoporous composites as molecular sieves for SERS detection. *J. Phys. Chem. Lett.* 4, 2715–2720. doi: 10.1021/jz4014085

Lorenz, B., Wichmann, C., Stöckel, S., Rösch, P., and Popp, J. (2017). Cultivation-free raman spectroscopic investigations of bacteria. *Trends Microbiol.* 25, 413–424. doi: 10.1016/j.tim.2017.01.002

Mavrodi, D. V., Bonsall, R. F., Delaney, S. M., Soule, M. J., Phillips, G., and Thomashow, L. S. (2001). Functional analysis of genes for biosynthesis of pyocyanin and phenazine-1-Carboxamide from *Pseudomonas aeruginosa* PAO1. *J. Bacteriol.* 183, 6454–6465. doi: 10.1128/JB.183.21.6454-6465.2001

McClean, K. H., Winson, M. K., Fish, L., Taylor, A., Chhabra, S. R., Camara, M., et al. (1997). Quorum sensing and *Chromobacterium violaceum:* exploitation of violacein production and inhibition for the detection of N-acylhomoserine lactones. *Microbiololgy* 143, 3703–3711. doi: 10.1099/00221287-143-12-3703

McNay, G., Eustace, D., Smith, W. E., Faulds, K., and Graham, D. (2011). Surface-enhanced raman scattering (SERS) and surface-enhanced resonance raman scattering (SERRS): a review of applications. *Appl. Spectrosc.* 65, 825–837. doi: 10.1366/11-06365

Mishra, Y. K., Shalabaeva, V., Lovato, L., La Rocca, R., Messina, G. C., Dipalo, M., et al. (2017). Time resolved and label free monitoring of extracellular metabolites by surface enhanced Raman spectroscopy. *PLoS ONE* 12:e0175581. doi: 10.1371/journal.pone.0175581

Moradali, M. F., Ghods, S., and Rehm, B. H. (2017). *Pseudomonas aeruginosa* lifestyle: a paradigm for adaptation, survival, and persistence. *Front. Cell. Infect. Microbiol.* 7:39. doi: 10.3389/fcimb.2017.00039

Mosier-Boss, P. (2017). Review of SERS substrates for chemical sensing. *Nanomaterials* 7:142. doi: 10.3390/nano7060142

Nai, C., and Meyer, V. (2017). From axenic to mixed cultures: technological advances accelerating a paradigm shift in microbiology. *Trends Microbiol.* doi: 10.1016/j.tim.2017.11.004. [Epub ahead of print].

Newman, D. J., and Cragg, G. M. (2007). Natural products as sources of new drugs over the last 25 years. *J. Nat. Prod.* 70, 461–477. doi: 10.1021/np068054v

Nie, S. (1997). Probing single molecules and single nanoparticles by surface-enhanced raman scattering. *Science* 275, 1102–1106.

O'Brien, J., and Wright, G. D. (2011). An ecological perspective of microbial secondary metabolism. *Curr. Opin. Biotechnol.* 22, 552–558. doi: 10.1016/j.copbio.2011.03.010

Pahlow, S., Meisel, S., Cialla-May, D., Weber, K., Rösch, P., and Popp, J. (2015). Isolation and identification of bacteria by means of Raman spectroscopy. *Adv. Drug Deliv. Rev.* 89, 105–120. doi: 10.1016/j.addr.2015.04.006

Palonpon, A. F., Ando, J., Yamakoshi, H., Dodo, K., Sodeoka, M., Kawata, S., et al. (2013). Raman and SERS microscopy for molecular imaging of live cells. *Nat. Protoc.* 8, 677–692. doi: 10.1038/nprot.2013.030

Papenfort, K., and Bassler, B. L. (2016). Quorum sensing signal–response systems in Gram-negative bacteria. *Nat. Rev. Microbiol.* 14, 576–588. doi: 10.1038/nrmicro.2016.89

Parsek, M. R., and Greenberg, E. P. (2005). Sociomicrobiology: the connections between quorum sensing and biofilms. *Trends Microbiol.* 13, 27–33. doi: 10.1016/j.tim.2004.11.007

Passos da Silva, D., Schofield, M., Parsek, M., and Tseng, B. (2017). An Update on the sociomicrobiology of quorum sensing in gram-negative biofilm development. *Pathogens* 6:51. doi: 10.3390/pathogens6040051

Pearman, W. F., Lawrence-Snyder, M., Angel, S. M., and Decho, A. W. (2016). Surface-enhanced raman spectroscopy for *in situ* measurements of signaling molecules (Autoinducers) relevant to bacteria quorum sensing. *Appl. Spectrosc.* 61, 1295–1300. doi: 10.1366/000370207783292244

Peters, B. M., Jabra-Rizk, M. A., O'May, G. A., Costerton, J. W., and Shirtliff, M. E. (2012). Polymicrobial interactions: impact on pathogenesis and human disease. *Clin. Microbiol. Rev.* 25, 193–213. doi: 10.1128/CMR.00013-11

Phelan, V. V., Liu, W. T., Pogliano, K., and Dorrestein, P. C. (2011). Microbial metabolic exchange–the chemotype-to-phenotype link. *Nat. Chem. Biol.* 8, 26–35. doi: 10.1038/nchembio.739

Polisetti, S., Baig, N. F., Morales-Soto, N., Shrout, J. D., and Bohn, P. W. (2016). Spatial mapping of pyocyanin in *Pseudomonas Aeruginosa* bacterial communities using surface enhanced raman scattering. *Appl. Spectrosc.* 71, 215–223. doi: 10.1177/0003702816654167

Poole, K. (2011). *Pseudomonas Aeruginosa*: resistance to the max. *Front. Microbiol.* 2:65. doi: 10.3389/fmicb.2011.00065

Popat, R., Cornforth, D. M., McNally, L., and Brown, S. P. (2015). Collective sensing and collective responses in quorum-sensing bacteria. *J. R. Soc. Interface* 12:20140882. doi: 10.1098/rsif.2014.0882

Prochazka, M. (2016). "Basics of surface-enhanced raman scattering (SERS)," in *Surface-Enhanced Raman Spectroscopy. Biological and Medical Physics, Biomedical Engineering.* (Cham: Springer), 21–59.

Ratcliff, W. C., and Denison, R. F. (2011). Alternative actions for antibiotics. *Science* 332, 547–548. doi: 10.1126/science.1205970

Rebrošová, K., Šiler, M., Samek, O., RuŽička, F., Bernatová, S., Holá, V., et al. (2017). Rapid identification of staphylococci by Raman spectroscopy. *Sci. Rep.* 7:14846. doi: 10.1038/s41598-017-13940-w

Riedel, K., Steidle, A., Eberl, L., Wu, H., Geisenberger, O., Molin, S., et al. (2001). N-Acylhomoserine-lactone-mediated communication between *Pseudomonas aeruginosa* and *Burkholderia cepacia* in mixed biofilms. *Microbiology* 147, 3249–3262. doi: 10.1099/00221287-147-12-3249

Rossolini, G. M., and Mantengoli, E. (2005). Treatment and control of severe infections caused by multiresistant *Pseudomonas aeruginosa*. *Clin. Microbiol. Infect.* 11, 17–32. doi: 10.1111/j.1469-0691.2005.01161.x

Sappington, K. J., Dandekar, A. A., Oinuma, K. I., and Greenberg, E. P. (2011). Reversible signal binding by the *Pseudomonas aeruginosa* quorum-sensing signal receptor LasR. *MBio* 2:e00011-11. doi: 10.1128/mBio.00011-11

Scarabelli, L., Hamon, C., and Liz-Marzán, L. M. (2016). Design and fabrication of plasmonic nanomaterials based on gold nanorod supercrystals. *Chem. Mater.* 29, 15–25. doi: 10.1021/acs.chemmater.6b02439

Schlücker, S. (2014). Surface-enhanced Raman spectroscopy: concepts and chemical applications. *Angew. Chem. Int. Ed.* 53, 4756–4795. doi: 10.1002/anie.201205748

Sharma, B., Frontiera, R. R., Henry, A.-I., Ringe, E., and Van Duyne, R. P. (2012). SERS: Materials, applications, and the future. *Mater. Today* 15, 16–25. doi: 10.1016/S1369-7021(12)70017-2

Shiohara, A., Wang, Y., and Liz-Marzán, L. M. (2014). Recent approaches toward creation of hot spots for SERS detection. *J. Photochem. Photobiol. C* 21, 2–25. doi: 10.1016/j.jphotochemrev.2014.09.001

Shrout, J. D., Chopp, D. L., Just, C. L., Hentzer, M., Givskov, M., and Parsek, M. R. (2006). The impact of quorum sensing and swarming motility on *Pseudomonas aeruginosa* biofilm formation is nutritionally conditional. *Mol. Microbiol.* 62, 1264–1277. doi: 10.1111/j.1365-2958.2006.05421.x

Singh, P. K., Schaefer, A. L., Parsek, M. R., Moninger, T. O., Welsh, M. J., and Greenberg, E. P. (2000). Quorum-sensing signals indicate that cystic fibrosis lungs are infected with bacterial biofilms. *Nature* 407, 762–764. doi: 10.1038/35037627

Srinivasan, A., Lopez-Ribot, J. L., and Ramasubramanian, A. K. (2015). Microscale microbial culture. *Future Microbiol.* 10, 143–146. doi: 10.2217/fmb.14.129

Steindler, L., and Venturi, V. (2007). Detection of quorum-sensingN-acyl homoserine lactone signal molecules by bacterial biosensors. *FEMS Microbiol. Lett.* 266, 1–9. doi: 10.1111/j.1574-6968.2006.00501.x

Stubbendieck, R. M., and Straight, P. D. (2016). Multifaceted interfaces of bacterial competition. *J. Bacteriol.* 198, 2145–2155. doi: 10.1128/JB.00275-16

Sun, F., Ella-Menye, J.-R., Galvan, D. D., Bai, T., Hung, H.-C., Chou, Y.-N., et al. (2015). Stealth surface modification of surface-enhanced raman scattering substrates for sensitive and accurate detection in protein solutions. *ACS Nano* 9, 2668–2676. doi: 10.1021/nn506447k

van der Meij, A., Worsley, S. F., Hutchings, M. I., and van Wezel, G. P. (2017). Chemical ecology of antibiotic production by actinomycetes. *FEMS Microbiol. Rev.* 41, 392–416. doi: 10.1093/femsre/fux005

Wang, A. X., and Kong, X. (2015). Review of recent progress of plasmonic materials and nano-structures for surface-enhanced raman scattering. *Materials* 8, 3024–3052. doi: 10.3390/ma8063024

Wang, J., Quan, C., Wang, X., Zhao, P., and Fan, S. (2011). Extraction, purification and identification of bacterial signal molecules based on N-acyl homoserine lactones. *Microb. Biotechnol.* 4, 479–490. doi: 10.1111/j.1751-7915.2010.00197.x

Weibel, D. B., Diluzio, W. R., and Whitesides, G. M. (2007). Microfabrication meets microbiology. *Nat. Rev. Microbiol.* 5, 209–218. doi: 10.1038/nrmicro1616

Whiteley, M., Diggle, S. P., and Greenberg, E. P. (2017). Progress in and promise of bacterial quorum sensing research. *Nature* 551, 313–320. doi: 10.1038/nature24624

Wu, X., Chen, J., Li, X., Zhao, Y., and Zughaier, S. M. (2014). Culture-free diagnostics of *Pseudomonas aeruginosa* infection by silver nanorod array based SERS from clinical sputum samples. *Nanomedicine* 10, 1863–1870. doi: 10.1016/j.nano.2014.04.010

Yu, R., Liz-Marzán, L. M., and García de Abajo, F. J. (2017). Universal analytical modeling of plasmonic nanoparticles. *Chem. Soc. Rev.* 46, 6710–6724. doi: 10.1039/C6CS00919K

Žukovskaja, O., Jahn, I. J., Weber, K., Cialla-May, D., and Popp, J. (2017). Detection of *Pseudomonas aeruginosa* metabolite pyocyanin in water and saliva by employing the SERS technique. *Sensors* 17:1704. doi: 10.3390/s17081704

Conflict of Interest Statement: The authors declare that the research was conducted in the absence of any commercial or financial relationships that could be construed as a potential conflict of interest.

frontiers in Cellular and Infection Microbiology

ORIGINAL RESEARCH
published: 07 August 2018
doi: 10.3389/fcimb.2018.00269

In silico Identification of the Indispensable Quorum Sensing Proteins of Multidrug Resistant *Proteus mirabilis*

Shrikant Pawar[1,2‡], *Md. Izhar Ashraf*[3,4†‡], *Shama Mujawar*[5], *Rohit Mishra*[6] *and Chandrajit Lahiri*[5*]

[1] Department of Computer Science, Georgia State University, Atlanta, GA, United States, [2] Department of Biology, Georgia State University, Atlanta, GA, United States, [3] Department of Computer Applications, B.S. Abdur Rahman Crescent Institute of Science and Technology, Chennai, India, [4] Theoretical Physics, The Institute of Mathematical Sciences, Chennai, India, [5] Department of Biological Sciences, Sunway University, Petaling Jaya, Malaysia, [6] Department of Bioinformatics, G.N. Khalsa College, University of Mumbai, Mumbai, India

OPEN ACCESS

Edited by:
Maria Tomas,
Complexo Hospitalario Universitario A Coruña, Spain

Reviewed by:
Adrián Cazares Lopez,
University of Liverpool, United Kingdom
Sara Gertrudis Horna Quintana,
Instituto Salud Global Barcelona (ISGlobal), Spain

***Correspondence:**
Chandrajit Lahiri
chandrajitl@sunway.edu.my

†Present Address:
Md. Izhar Ashraf,
The Institute of Mathematical Sciences, Chennai, India

‡These authors have contributed equally to this work.

Received: 01 March 2018
Accepted: 17 July 2018
Published: 07 August 2018

Citation:
Pawar S, Ashraf MI, Mujawar S, Mishra R and Lahiri C (2018) In silico Identification of the Indispensable Quorum Sensing Proteins of Multidrug Resistant Proteus mirabilis. Front. Cell. Infect. Microbiol. 8:269. doi: 10.3389/fcimb.2018.00269

Catheter-associated urinary tract infections (CAUTI) is an alarming hospital based disease with the increase of multidrug resistance (MDR) strains of *Proteus mirabilis*. Cases of long term hospitalized patients with multiple episodes of antibiotic treatments along with urinary tract obstruction and/or undergoing catheterization have been reported to be associated with CAUTI. The cases are complicated due to the opportunist approach of the pathogen having robust swimming and swarming capability. The latter giving rise to biofilms and probably inducible through autoinducers make the scenario quite complex. High prevalence of long-term hospital based CAUTI for patients along with moderate percentage of morbidity, cropping from ignorance about drug usage and failure to cure due to MDR, necessitates an immediate intervention strategy effective enough to combat the deadly disease. Several reports and reviews focus on revealing the important genes and proteins, essential to tackle CAUTI caused by *P. mirabilis*. Despite longitudinal countrywide studies and methodical strategies to circumvent the issues, effective means of unearthing the most indispensable proteins to target for therapeutic uses have been meager. Here, we report a strategic approach for identifying the most indispensable proteins from the genome of *P. mirabilis* strain HI4320, besides comparing the interactomes comprising the autoinducer-2 (AI-2) biosynthetic pathway along with other proteins involved in biofilm formation and responsible for virulence. Essentially, we have adopted a theoretical network model based approach to construct a set of small protein interaction networks (SPINs) along with the whole genome (GPIN) to computationally identify the crucial proteins involved in the phenomenon of quorum sensing (QS) and biofilm formation and thus, could be therapeutically targeted to fight out the MDR threats to antibiotics of *P. mirabilis*. Our approach utilizes the functional modularity coupled with k-core analysis and centrality scores of eigenvector as a measure to address the pressing issues.

Keywords: *Proteus mirabilis*, urinary tract infection, quorum sensing, eigenvector centrality, k-core analysis

INTRODUCTION

Urinary tract infections (UTI) are the second most common infection prevalent amongst long-term hospital patients, second only to pneumonia. Failure to treat or a delay in treatment can result in systemic inflammatory response syndrome (SIRS), which carries a mortality rate of 20–50% (Jacobsen and Shirtliff, 2011; Schaffer and Pearson, 2015)[1] While *Escherichia coli* remains the most often implicated cause of UTI in previously healthy outpatients, *Proteus mirabilis* take the lead for catheter-associated UTI (CAUTI), causing 10–44% of long-term CAUTIs (Jacobsen and Shirtliff, 2011; Schaffer and Pearson, 2015)[1]. In comparison to normal cases, CAUTI is quite complicated and encountered by patients with multiple prior episodes of UTI, multiple antibiotic treatments, urinary tract obstruction and/or undergoing catheterization as also for those with spinal cord injury or anatomical abnormality (Jacobsen and Shirtliff, 2011; Schaffer and Pearson, 2015)[1]. Such complications of CAUTI caused by *P. mirabilis* arise from the usage of a diverse set of virulence factors by the organism to access and colonize the host urinary tract. These include, but are not limited to, urease and stone formation, fimbriae and other adhesins, iron and zinc acquisition, proteases and toxins and biofilm formation (Schaffer and Pearson, 2015). Despite significant advances made for studying *P. mirabilis* pathogenesis, a meager knowledge of its regulatory mechanism poses an urgent and pressing need to come up with unique health intervention processes for such patients.

In attempts to provide such health interventions, longitudinal, and epidemiological studies on *P. mirabilis* have been reported for extended-spectrum β-lactamase (ESBL) and AmpC β-lactamase (CBL) producers (Luzzaro et al., 2009; Wang J. T. et al., 2014) According to these studies, limited therapeutic options are available for management of such CAUTI which in turn reflects the imminent threats of multi-drug resistance (MDR) *P. mirabilis*. Such MDR phenomenon, exhibited by the gram-negative pathogens like *P. mirabilis*, can be attributed, besides other factors, to the blockade provided by the efflux pumps at the extra-cytoplasmic outer membrane for existing antibiotics entries and remainder drugs expulsion (Eliopoulos et al., 2008; Czerwonka et al., 2016). Besides providing MDR, the cases of CAUTI have been complicated by biofilms formed by the pathogenic *P. mirabilis* (Czerwonka et al., 2016). In fact, different lipopolysaccharide structures of the membrane have been implicated to the adherence of the pathogen on to the surfaces causing CAUTI. Furthermore, along with various other components of the membrane, several cytoplasmic factors interplay among themselves to regulate the cell-density dependent gene regulation. This enables the bacteria for cell-to-cell communication, a phenomenon known as quorum sensing (QS) (Rutherford and Bassler, 2012). Besides other phenotypic traits, QS controls the expression of the virulence factors responsible for pathogenesis of *P. mirabilis* (Stankowska et al., 2012). Again, as per other reports, despite producing two cyclic dipeptides and encoding LuxS-dependent quorum sensing molecule, AI-2, during swarming, *P. mirabilis* has been reported to have no strong evidence of QS (Holden et al., 1999; Schneider et al., 2002; Campbell et al., 2009; Schaffer and Pearson, 2015). However, a highly ordered swarm cycle suggests an existing mechanism for multicellular coordination (Rauprich et al., 1996). Thus, the fact that *P. mirabilis* are engaged in biofilm formation which is managed, albeit in parts, through quorum sensing brings out the complexity of CAUTI. To deal with such complexity, analyses of the proteins involved in such phenomenon, known as the protein interaction networks (PINs), can reveal important information about key role players of the phenomenon (Lahiri et al., 2014; Pan et al., 2015).

The indispensable role players of phenomenon like QS can be determined by analyzing the PIN involving the proteins in the pathway to produce the QS inducer. The essentiality of such small protein interactome (SPIN) can be brought about by an analysis for the most biologically relevant protein to target for inhibiting that phenomenon, also known as quorum quenching. Ideally, a determination of the number of interacting partners of a particular protein identifies its *degree* centrality (DC) which correlates with its essential nature in the biological scenario (Jeong et al., 2001). However, a much deeper understanding of the essential nature of a particular protein comes upon analyzing its interaction with other partners in the global network of all proteins. In this study, we have discussed the relevance of other centrality measures like *Betweenness centrality* (BC), *Closeness centrality* (CC), and *Eigenvector centrality* (EC) (Jeong et al., 2001) parameters for SPIN having the genes and proteins involved in quorum sensing. Again, analyses of a stipulated sets of QS proteins for a valuable knowledge about the most indispensable virulence proteins to render as drug targets for the QS phenomenon could be uninformative. This led us to conduct a deep probing of the whole genome of *P. mirabilis* (WGPM) for a global analysis of the encoding proteins. This comprises the k-core analysis approach of whole genome protein interactome (GPIN) decomposition to a core of highly interacting proteins (Seidman, 1983). Furthermore, to identify the functional modules in the global network (Guimerà and Nunes Amaral, 2005a), we have performed cartographic analyses and predicted the importance of few proteins sharing similar functional modules. To sum up, the sole objective of this study is to utilize several network based models to analyze and identify crucial role players of QS in *P. mirabilis* and thus, propose their importance as potential drug targets.

MATERIALS AND METHODS

Dataset Collection

The *P. mirabilis* QS pathways for autoinducer-2 (AI-2) biosynthesis were collected from curated reference databases of genomes and metabolic pathways like KEGG, MetaCyc and BioCyc (Caspi et al., 2015; Kanehisa et al., 2015, 2016). The proteins involved in these pathways were extracted with their annotated names and identification as per UniProt database and submitted as entries for the STRING 10.5 biological meta-database (Szklarczyk et al., 2016) to retrieve protein interaction datasets with at least 10 or 50 interactors having the default medium (0.4) level confidence about the interaction, where the

[1]https://emedicine.medscape.com/article/226434-overview#a6.

interactor numbers relate to the interacting proteins present in the vicinity of the query [period of access: January to February, 2018]. The interactions of the whole genome proteins of the fully annotated *P. mirabilis* strain HI4320 were retrieved from the detailed protein links file under the accession number 529507 in STRING. The sequenced whole genome of the *P. mirabilis* strain HI4320 contains the profile for the same through its full annotation (Pearson et al., 2008). All proteins data, collected and used for interactome construction hereafter, have been reported in **Supplementary Data 1**.

Interactome Construction

We have taken a stepwise approach to integrate and build the interactomes of the proteins, represented by different sections of **Figure 1**. These are the small protein interactomes (SPIN) comprised of (a) those involved in AI-2 biosynthetic pathway in the organism with small (Holden et al., 1999) and large (Kang et al., 2017) number of interactors retrieved from STRING database (AIPS, AIPL, respectively) (**Figures 1A,B**), (b) only QS genes found (QSPO) (**Figure 1C**), (c) all QS genes reported as homologs (QSPH) present in *P. mirabilis* (**Figure 1D**), (d) all virulence genes reported (QSPV) (**Figure 1E**) and (e) the WGPM (**Figure 1F**). Whereas QSPO contains genes reported to be involved in QS in *P. mirabilis*, QSPH contains additional genes reported to be involved in QS in other organisms and present as homologs in *P. mirabilis*. The virulence genes have been taken from the set reported by Schaffer and Pearson (Schaffer and Pearson, 2015). The number of *P. mirabilis* proteins from the SPIN class of interactomes were 31 for AIPS, 42 for AIPL, 24 for QSPO, 42 for QSPH, 58 for QSPV, and 3548 for GPIN (**Supplementary Data 1**). The medium confidence default values of 0.4 for the individual protein interaction data were obtained from String 10.5. Interactions were 1151 for AIPS, 1571 for AIPL, 30 for QSPO, 129 for QSPH, 2376 for QSPV, and 33462 for GPIN, respectively. These interactions are presented in separate sheets of **Supplementary Data 2**.

All individual interaction data obtained above were imported into Cytoscape version 3.6.0 (Cline et al., 2007) and Gephi 0.9.2 (Bastian et al., 2009) to integrate, build and analyze five SPIN namely AIPS, AIPL, QSPO, QSPH and QSPV and the GPIN (**Figure 1**). Interactomes were considered as undirected graphs represented by $G = (V, E)$ comprising a finite set of V vertices and E edges where an edge $e = (u,v)$ connects two vertices u and v (nodes). In the biological PIN context, a vertex/node represents a protein. The number of physical and functional interactions a protein has with other proteins comprises its degree $d(v)$ (Diestel, 2000).

Network Analyses

SPIN

The constructed five SPIN were subsequently analyzed individually through the common four measures of centrality applied to biological networks, namely, eigenvector centrality (EC), betweenness centrality (BC), degree centrality (DC) and closeness centrality (CC) (Koschützki and Schreiber, 2004; Özgür et al., 2008; Pavlopoulos et al., 2011; **Supplementary Data 3**). This was done either via Gephi or the Cytoscape integrated java plugin CytoNCA (Tang et al., 2015). For computing CytoNCA scores, the combined scores obtained from different parameters in STRING were taken as edge weights. The combined scores ranging from 0 to 1, considered in STRING for reporting interactions, generally indicate the confidence of the interaction among the proteins with the level of evidence from the parameters like gene neighborhood, gene fusion, gene co-occurrence, gene co-expression, experiments, annotated pathways and text mining. To find common proteins from each centrality measures, the top 5 proteins were taken for drawing Venn diagrams through online tool Venny 2.1 (Oliveros, 2007–2015) to (**Figure 2**).

GPIN

MATLAB version 7.11, a programming language developed by MathWorks (MATLAB Statistics Toolbox Release, 2010), was used for further analyses of the GPIN. To gain an overview of the technical aspects of the GPIN, the distributions of network degree (k) was plotted against the Complementary Cumulative Distribution Function (CCDF) (**Figure 3A**). Further concepts about the core group, comprising very specific proteins, was obtained from a k-core analysis of the proteins in the whole genome context. This essentially prunes the network to a k-core with proteins having degree at least equal to k and classifying in K-shell based on their classes of interacting partners (**Figures 3B,C**). A network decomposition (pruning) technique was adopted to produce gradually increasing cohesive sequence of subgraphs (Seidman, 1983). Further, a significant knowledge of the functional connectivity and participation of each protein was obtained from the network topological representation of the within-module degree z-score of the protein vs. its participation coefficient, P, cartographically represented first by Guimerà and Nunes Amaral (2005b) (**Figure 4**). The intra-connectivity of a node "i" to other nodes in the same module is measured by the z-score while the positioning of the node "i" in its own module with respect to other modules measures the participation coefficient, P. Participation of each protein reflected its intra- and inter-modular positioning, where functional modules were calculated based on Rosvall method (Rosvall and Bergstrom, 2011). A modular network has high intra-connectivity and sparse inter-connectivity due to which each module has relatively high density and high separability. Each group of nodes in these type of networks share a common biological function as mentioned by Vella et al. (2018). This analysis divided the proteins into mainly two major categories namely the non-hub nodes and hub nodes, where the latter is the connecting point of many nodes. The category of the former has been assigned the roles of ultra-peripheral nodes (R1), peripheral nodes (R2), non-hub connector nodes (R3), and the non-hub kinless nodes (R4). Likewise, the hub nodes have been designated as provincial hubs (R5), connector hubs (R6), and kinless hubs (R7) (Guimerà and Nunes Amaral, 2005b) (**Figure 4**, **Supplementary Data 4**).

RESULTS

To have an understanding of the important protein(s) of QS in *P. mirabilis*, we have taken a stepwise approach of

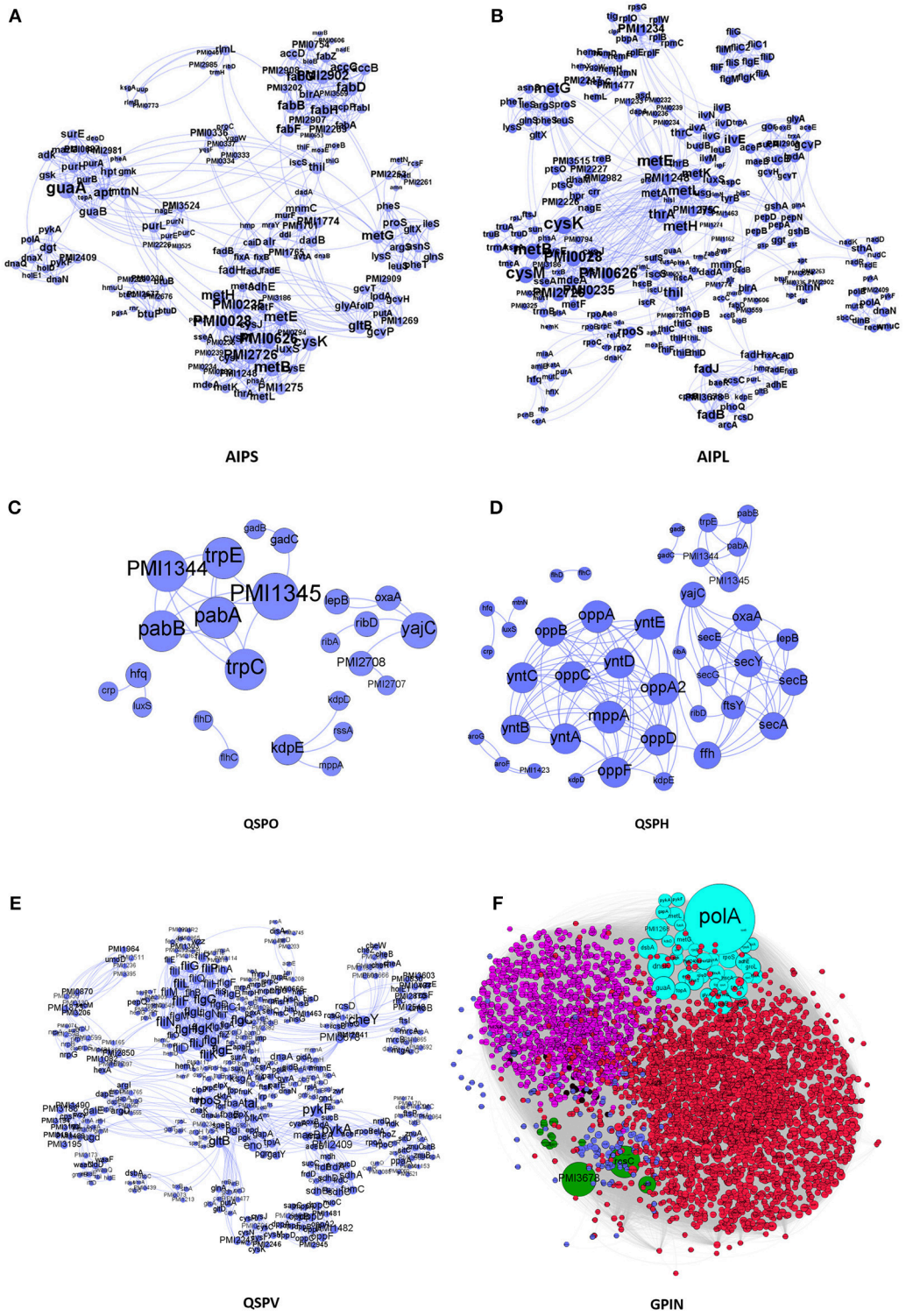

FIGURE 1 | The interactomes of *P. mirabilis* reflecting the degree of connectivity. These comprise the SPIN having proteins coded in light blue colored circles connected to each other through light blue curved lines as in **(A)** AIPS, with 10 interactors from STRING, **(B)** AIPL, with 50 STRING interactors, **(C)** QSPO, having QS genes from *P. mirabilis*, **(D)** QSPH, having *P. mirabilis* homologs reported to be involved in QS of other related species, and **(E)** QSPV, having genes reported to be involved in virulence of *P. mirabilis* (Schaffer and Pearson, 2015). **(F)** GPIN reflecting the 6 different classes (R1–R6) (see **Figure 4**) of connected proteins in topological space of the network. The six different color codes denote the classes.

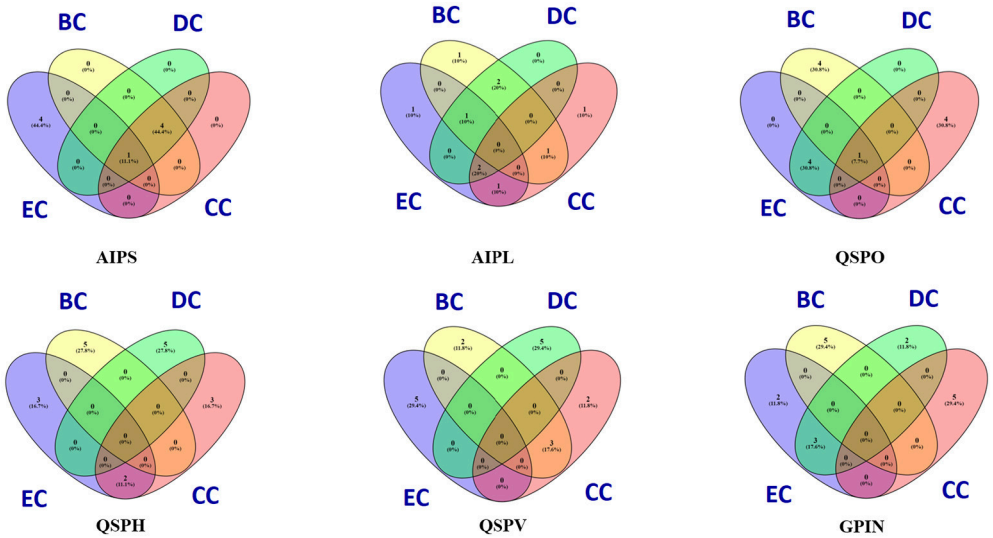

FIGURE 2 | Venn diagram representation for the top five top rankers of BC, CC, DC, and EC parametric analyses of five individual SPIN and GPIN of *P. mirabilis*. BC, CC, DC, and EC stands for betweenness centrality, closeness centrality, degree centrality and eigenvector centrality, degree centrality and closeness centrality, respectively.

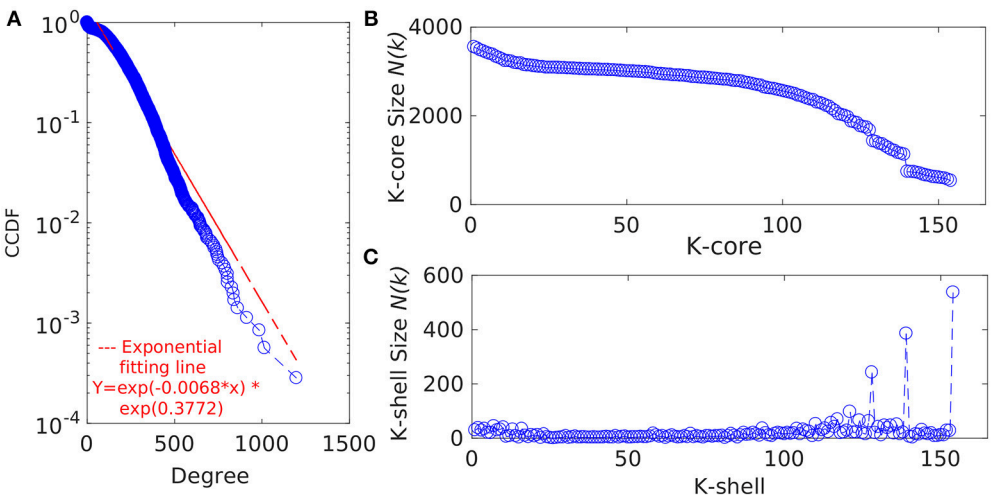

FIGURE 3 | (A) The degree distribution of the proteins from the GPIN of *P. mirabilis*. CCDF stands for Complementary Cumulative Distribution Function. Distribution of the **(B)** *k*-core and **(C)** K-shell sizes for the set of proteins from the GPIN of *P. mirabilis*.

building five SPIN, with an ultimate goal to identify the key role playing proteins in the phenomenon of QS to serve as potential candidates for therapeutic targets. **Table 1** represents the comparative picture of the most common topmost proteins, as per centrality measures, in their descending order. In most of the cases, at least three or two of the centrality measures brought out the same protein. These proteins are the ones reflected to be important through each SPIN analysis. For instance, AIPS has MetG and MtnN as the top rankers while LuxS, MnmC, and PMI3678 turns out to be important for AIPL (**Table 1**). Others like QSPO, QSPH, and QSPV have YajC, PMI1345, OppA, RpoS, flagellar proteins of the *flh and fli* operon and some other two-component systems proteins like CheY and KdpE as important rankers. The functions of these proteins are mentioned in **Table 2**. The top ranking proteins for each of these five SPINs have been reflected in **Figure 2** with Venn diagrams. The common topmost rankers across all the five SPINs are reflected in **Supplementary Figure 1**.

An overview of the important proteins, from individual SPIN as well as across all SPIN, is obtained upon such aforementioned analyses. However, to tackle the MDR *P. mirabilis*, in a global perspective for a drug to be effective, the proteins need to be essentially indispensable. Thus, the whole genome proteins interactome (GPIN) of *P. mirabilis* was then analyzed to understand the global scenario.

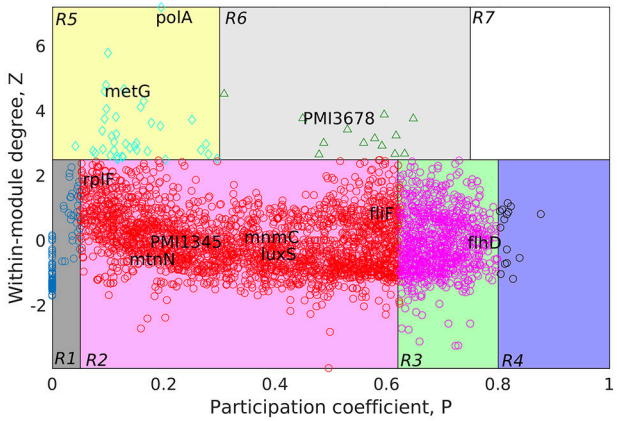

FIGURE 4 | Cartographic representation for classification of proteins from the GPIN of *P. mirabilis* based on its role and region in network space. Quadrants are designated as R1 till R7 with the nodes in each representing different classes of proteins. Colors of quadrants, however, have no significance. Selected topmost proteins, with relevance in QS, biofilm and virulence, analyzed from SPIN are mapped onto different quadrants, as deemed fit as per GPIN analysis.

TABLE 1 | The most common topmost proteins of *P. mirabilis* SPIN and GPIN.

Network	EC	BC	DC	CC
AIPS	**MetG**, LuxS, GcvP, **Hpt**, PMI3524	MtnN, **CysK**, LuxS, MetB, MnmC	MtnN, MnmC, **CysK**, LuxS, MetB	MtnN, **CysK**, LuxS, MetB, MnmC
AIPL	LuxS, **ThrA**, MetH, **MetL**, PMI0028	MnmC, MtnN, LuxS, **PMI3678**, **TrmA**	MnmC, LuxS, MtnN, **ThrA**, MetH	**PMI3678**, **ThrA**, MetH, PMI0028, PMI0626
QSPO	PMI1345, PMI1344, **TrpE**, PabA, **PabB**	YajC, PMI1345, GadC, **RibD**, PMI2708	PMI1345, PMI1344, **TrpE**, PabA, **PabB**	KdpE, **Hfq**, FlhD, FlhC, PMI1345
QSPH	PMI1345, GadC, **TrpE**, FlhD, FlhC	KdpE, **Ffh**, KdpD, **LepB**, **FtsY**	OppA, MppA, OppA2, OppD, OppC	FlhD, FlhC, PMI1423, AroF, AroG
QSPV	FliF, FliK, FlgG, FlgC, FlgI	**RpoS**, **Eno**, Irp, Pgm, **PMI3678**	CheY, PykA, **PykF**, **Tal**, FliN	**RpoS**, **Eno**, **PMI3678**, FliC, CsrA
GPIN	**PolA**, **GuaA**, **DnaK**, **MetG**, **RecA**	**RplP**, PMI1727, PMI1033, PMI2007, **RpoS**	**PolA,** **PMI3678**, **RcsC**, **DnaK**, **GuaA**	PMI2375, PMI2723, PMI0739, PMI3495, PMI2629

The bold cased proteins are present in the innermost 154th k- core. EC, BC, DC, and CC stands for eigenvector centrality, betweenness centrality, degree centrality, and closeness centrality, respectively.

The Complete GPIN

In an attempt to analyze the type of network being built from the functional and physical interactions empirically found and theoretically predicted among the whole genome proteins retrieved from STRING, we have observed the degree distribution of GPIN to be exponential showing a non-linear preferential attachment nature (**Figure 3A**; Vázquez, 2003). Hereafter, we have framed an idea of the important proteins from an array of proteins involved in the five individual SPIN, upon performing a k-core analysis for them (**Figures 3B,C**). Notably, the innermost core was 154th shell and had genes like *thrA, cysK, metG, metL, trpE, rpoS, eno*, etc. which have already been reflected from the four network centrality analyses of the SPINs (**Table 1**, **Supplementary Data 3**: **Sheet 1–5**). Additionally, it is to be noted that top 5 EC and DC measures of the GPIN also had their position in the innermost 154th core, thereby indicating their importance in the global scenario. Other important genes e.g., *luxS, PMI1345* from the k-core analyses were found in the 139th shell. The latter category was found to have direct involvement in QS.

Furthermore, to classify the proteins based on their regional positioning and functional role in the network topological space of *P. mirabilis*, we have analyzed the GPIN represented

TABLE 2 | Functions of centrality based topmost proteins of individual *P. mirabilis* networks.

Protein name	Description of function
MetG	Is required not only for elongation of protein synthesis but also for the initiation of all mRNA translation through initiator tRNA(fMet) aminoacylation
MtnN	Catalyzes the irreversible cleavage of the glycosidic bond in both 5′-methylthioadenosine (MTA) and S-adenosylhomocysteine (SAH/AdoHcy) to adenine and the corresponding thioribose, 5′-methylthioribose and S-ribosylhomocysteine, respectively
LuxS	Involved in the synthesis of autoinducer 2 (AI-2) which is secreted by bacteria and is used to communicate both the cell density and the metabolic potential of the environment. The regulation of gene expression in response to changes in cell density is called quorum sensing. Catalyzes the transformation of S-ribosylhomocysteine (RHC) to homocysteine (HC) and 4,5-dihydroxy-2,3-pentadione (DPD)
MnmC	Catalyzes the last two steps in the biosynthesis of 5-methylaminomethyl-2-thiouridine (mnm_5s_2U) at the wobble position (U34) in tRNA. Catalyzes the FAD-dependent demodification of $cmnm_5s_2U34$ to nm_5s_2U34, followed by the transfer of a methyl group from S-adenosyl-L-methionine to nm_5s_2U34, to form mnm_5s_2U34
PMI3678	Catalyzes the Phosphorelay through sensor kinase activity of two-component Regulatory system
PMI1345	Catalyzes the transfer of the phosphoribosyl group of 5-phosphorylribose-1-pyrophosphate (PRPP) to anthranilate to yield N-(5′-phosphoribosyl)-anthranilate (PRA)
FlhD	Functions in complex with FlhC as a master transcriptional regulator that regulates transcription of several flagellar and non-flagellar operons by binding to their promoter region. Activates expression of class 2 flagellar genes, including fliA, which is a flagellum-specific sigma factor that turns on the class 3 genes. Also regulates genes whose products function in a variety of physiological pathways
FliF	Flagellar protein whose M ring may be actively involved in energy transduction
PolA	In addition to polymerase activity, this DNA polymerase exhibits 5′-3′ exonuclease activity
RplP	Binds 23S rRNA and is also seen to make contacts with the A and possibly P site tRNAs

The functions of the selected proteins are derived from UniProt database.

cartographically (**Figure 4**, **Supplementary Data 4**). Essentially, such representation would classify the complete set of proteins in the genome with respect to their connectivity within similar classes of proteins performing similar biological function (functional module) along with their participation with other related and/or non-related functional module (also see materials and methods and discussion section). Noticeably, the R6 quadrant had the top 5 proteins belonging to either the innermost 154th core or almost close to the 139th core containing most of the proteins related to QS (**Supplementary Data 4**). These are GltB and PMI3678 for the former and PMI3348, PMI0587, and PMI3517 for the latter. Moreover, upon looking deep into EC classification of R6 quadrants, all top 5 proteins, namely PolA, GuaA, DnaK, MetG, and RecA were from the innermost 154th core. Furthermore, analysis after sorting of module followed by R quadrant, k-core followed by either module or EC measures, all revealed the proteins to be mostly belonging to the R6 or R5 categories, besides their 154th or 139th core classification (**Supplementary Data 4**). It is worthwhile to mention here that a similar sorting analyses of BC with respect to Quadrant and k-core had revealed proteins mostly from R2 or R3, none of them occupying the innermost 154th core, except RplP, and RpoS.

DISCUSSION

We have started with the proteins involved in *P. mirabilis* AI-2 biosynthesis pathway (**Supplementary Figure 2**) and derived the AIPS besides AIPL (**Figures 1A,B**). While the former connects the proteins of the pathway as reported by default in STRING with only 10 interactors, supposedly directly involved in the phenomenon of AI biosynthesis, the latter has been formed upon extending those to 50 interactors per protein query. The idea was to incorporate other related proteins having connectivity to the AI-2 whose analysis might give more insight about QS in *P. mirabilis*. Moreover, it was necessary to have an idea of the robustness of the proteins involved in QS pathways and thus, QSPO was constructed to have an idea of the proteins directly involved in the phenomenon of QS in *P. mirabilis* only (**Figure 1C**). Again, with the homologous proteins reported to be involved in QS in other species from KEGG database, it was necessary to look into their association with acknowledged QS proteins of *P. mirabilis* (**Supplementary Figure 3**). Thus, QSPH was constructed to take into consideration of this fact and analyze further (**Figure 1D**). Furthermore, with multiple genes and proteins reviewed for the virulence of *P. mirabilis* (Schaffer and Pearson, 2015), including those involved for QS phenomenon, it was necessary to have an interactome QSPV constructed to analyse their interactions and involvement (**Figure 1E**). All these SPIN were constructed to have an understanding of the indispensable proteins responsible for QS in *P. mirabilis*. Finally, a complete whole genome analyses for other plausible indispensable proteins connecting biofilm formation, AI-2 biosynthesis, quorum sensing and even MDR was necessary to have a bird's eye view of the global scenario. This was done with the construction and analyses of the GPIN (**Figure 1F**).

The five SPIN were then analyzed individually by utilizing the four important centrality measures of DC, CC, BC, and EC. Of these, DC is the most basic, informing the connectivity of any protein in the network. CC might reflect the proximity of a protein in terms of its communication with others to render a functionally virulent phenotype. Being a comparatively better measure in terms of bridging different functionally important groups of virulent proteins, BC might bring out the importance of a protein to be targeted for therapeutic purposes. However, EC might show the most important proteins having their impact on other important proteins in a virulent network and thus, turn out to be indispensable protein to target. We have found a varying range of proteins ranging from the locomotive flagellar proteins of the *flh* and *flg* operon (Claret and Hughes, 2000), LuxS (Schneider et al., 2002) and MtnN directly involved in AI-2 biosynthetic pathway, MetG and MnmC involved in the protein translation machinery along with the proteins PMI1345 (Wang M. C. et al., 2014) and PMI3678 with catalytic activities/domains, chaperone protein, Hfq (Wang M. C. et al., 2014), signal transduction protein, KdpE (Rhoads et al., 1978), and a pre-protein translocase subunit, YajC (Pearson et al., 2008). Among the proteins PMI1345 and PMI3678, as per UniProt database, the former is having an activity as anthranilate phosphoribosyltransferase catalyzing the transfer of the phosphoribosyl group of 5-phosphorylribose-1-pyrophosphate (PRPP) to anthranilate to yield N-(5′-phosphoribosyl)-anthranilate (PRA). Essentially, PMI1345 is involved in the 2nd step of the subpathway synthesizing L-tryptophan from chorismate. Again, PMI3678 has the histidine kinase domain and displays activities of kinase through ATP binding and in-turn regulates transcription via a two-component regulatory system. Thus, as analyzed above, with the different proteins, pertaining to the biofilm formation, flagellar locomotion, translation and signal transduction, a level of complexity of the *P. mirabilis* QS machinery could be perceived.

To gain more insight into the global scenario of the whole genome, we have constructed the GPIN (**Figure 1F**) and analyzed it through several network topological and centrality parametric measures (**Supplementary Datas 3, 4**). For this GPIN, we have observed that the connectivity distribution, P(k), of a particular node gets connected to k other nodes, for large values of k. This confirms that the GPIN is indeed a large network and neither a random, Erdos and Renyi type (Erdos and Rényi, 1960) nor a small-world, Watts and Strogatz type (Watts and Strogatz, 1998). Our GPIN is free of a characteristic scale and roughly followed the power-law (Albert et al., 2000) with an exponential decay of the degree distribution (**Figure 3A**). Initially, we have analyzed the constructed GPIN with *k*-core/K-shell topological parameters (**Figures 3B,C**). Technically speaking, a k-core is a subnetwork with a minimum number of k-links. A K-shell is a set of nodes having exactly k-links. In another words, K-shell is the part of k-core but not of (k+1)-core. Thus, proteins belonging to the outer shell have lower k value thereby reflecting the limited number of interacting partner proteins. On the contrary, proteins from the inner *k*-core/K-shell are very specific ones having high interaction with each other and are considered to be the most

important ones. It has been observed that the inner core member proteins are highly interactive due their robust and central character (Alvarez-Hamelin et al., 2006). In this light, a complete decomposition of the network, achieved by decomposing the core, would reveal the innermost important part of the network. We have found the 154th core as the innermost one for our GPIN having many proteins involved in the biosynthesis of amino acids, including cysteine and methionine, the amino acid precursor of the components of AI-2 biosynthetic pathway. These proteins rank top for most of the EC measures across the other five SPIN as well. Furthermore, the 139th core was on focus due to its nearby proximity to the innermost core and comprising most of the proteins directly involved in QS. Our analyses till this far revealed LuxS and PMI1345 to be the prominent EC proteins in the 139th core of the genome. Interestingly, only PolA and RplP, top rankers of BC measures, made it to the innermost 154th core compared to the other topmost EC proteins in that core. This probably reflects the importance of EC measure to reveal the prominent stakeholders of the machinery responsible for the very survival and probably virulence of the organism. Any effective drug target should, thus, be selected from this core group with high EC rank.

A further delving deep into the functional connectivity of the modules formed in network topological space reinforced our findings this far. The topological orientation of the nodes in space are being represented cartographically where *P*-values have been put in the x-axis and z-score values in the y-axis. In this context, R1 has low *P*-values and low z-scores while R7 has the highest for both of them. Following this representation, the non-hubs and the hubs are classified into the protein groups of R1-4 and R5-7, respectively. Among them, the kinless hubs proteins (R7), having high connection within module (z) as well as between modules (P) scores, becomes important in terms of functionality. Similarly, the ultra-peripheral proteins (R1), with least P and z measures, are the least connected across the network followed by the peripheral proteins (R2). Such proteins can be detached easily and thus, are perceived, not much to affect the whole network when attempted to reach the core upon decomposition. This is nothing but the outermost shells of the k-core measures (refer previous section) which has proteins not grossly affecting the survival of the organism. Likewise, proteins belonging to the non-hub connectors (R3) group might be involved in only a small but fundamental sets of interactions. On the contrary, proteins of the provincial hubs class (R5) have many connections which are within-module. Again, the non-hub kinless proteins (R4) link other proteins which are evenly distributed across all the modules. However, the connector hub proteins (R6) link most of the other modules and are expected to be the most conserved in terms of decomposition as well as evolution. This could be the very set of proteins which the organism would maintain as the essential ones for their very survival. We have observed mostly R5 and R6 classes of proteins occupying the innermost 154th and the QS-involved 139th cores. Furthermore, the EC measures brings out the importance when compared to other measures of centralities.

In order to bring out the biological implication of the cartographic analyses, we now discuss the relevance of the proteins identified as essential in the context of virulence, biofilm formation and QS phenomenon. In this context, it is important to note that, we have observed many of the already known genes and proteins, viz LuxS, FlhDC to be reflected from our *in silico* cartographic analyses as well. For example, with the highest number (17) of fimbrial operons reported in any sequenced bacterial species, four *P. mirabilis* fimbriae, namely, MR/P, UCA, ATF, and PMF have shown prominent roles in biofilm formation (Scavone et al., 2016). The thickness, structure, and the amount of exopolysaccharides produced by some biofilms formed by *P. mirabilis* are influenced by important acylated homoserine lactones (Stankowska et al., 2012). Moreover, some virulence factors are regulated by QS molecules like acylated homoserine lactones (acyl-HSLs) (Henke and Bassler, 2004). Of the two QS types, LuxS is an essential enzyme for AI-2 type which is coded by luxS gene having S-ribosylhomocysteine lyase activity (Schneider et al., 2002). Acetylated homoserine lactone derivatives modifies the expression of virulence factors of *P. mirabilis* strains (Stankowska et al., 2008). The flhDC master operon is a key regulator in swarmer cell differentiation in *P. mirabilis*, it is known to cause an increased viscosity and intracellular signals (Fraser and Hughes, 1999). Furthermore, the extracellular signals can be sensed by two-component regulators such as RcsC–RcsB (Fraser and Hughes, 1999).

Having said the above, we observe that, many such genes and proteins, not reported to have connections with QS and virulence, have also been unearthed from our study. Thus, it is imperative to have an in-depth analysis to bring out the importance of the proteins unearthed through the process. In order to achieve the same, we rely on the fact that the innermost 154th core could harbor the genes/proteins essential for the very survival of the organism. Moreover, our cartographic analysis shows that R6 classes of proteins having high intra- and inter-connectivity, within and between the functional modules might play a crucial role in the maintenance of the organismal structure. This adds up to another level of indispensable nature. Furthermore, the very concept of Eigenvector centrality, which reflects the important proteins' connectivity with other such important proteins in terms of their function, finalize the indispensable factor. This method of utilizing the *k*-core, functional module and centrality measure, like that of Eigenvector, has been used to analyze large networks to reveal the important proteins, albeit, in a complete different scenario (Ashraf et al., 2018). Utilizing this method, referred to as KFC, we found the three topmost indispensable factors for *P. mirabilis* are *gltB, PMI3678,* and *rcsC* (**Supplementary Data 5**). It is important to note that the glutamate synthase encoding gene *gltB*, has been shown to be involved in a quorum sensing-dependent glutamate metabolism which affects the homeostatic osmolality and outer membrane vesiculation in *Burkholderia glumae* (Kang et al., 2017). Expression level of *gltB* has been shown to affected in *E. coli* by the stationary phase QS signals (Ren et al., 2004). Again, *rcsC* encodes an sensor histidine kinase protein which is known to be involved in swarming migration and capsular polysaccharide synthesis along with *yojN* (Belas et al., 1998; Fraser and Hughes, 1999). The sensor kinase activity for *PMI3678* encoding an aerobic respiration control protein, however, has not

been reported earlier for *P. mirabilis*, and thereby could serve as one of the important therapeutic targets. All these proteins are quite different to those reported to be quite important in a recent study to unearth the fitness factors in a single-species and polymicrobial CAUTI setting, performed with a genome wide transposon mutagenesis of *P. mirabilis* (Armbruster et al., 2017). In this study, Armbuster *et al*. has observed the polyamine uptake and biosynthesis to the fitness factor for single species CAUTI while branched chain amino acid (BCAA) synthesis turned out to be important for polymicrobial infection along with *Providencia stuartii* (Armbruster et al., 2017). None of these fitness factors, found to be helpful in colonizing either the catheterized bladder (referred to as *F*actors for *B*ladder *C*olonization, FBC) or the kidney (*F*actors for *K*idney *C*olonization, FKC), were observed in our analysis to be belonging to the R6 quadrant despite some falling within the innermost 154th core (**Supplementary Data 5**). While the reports by Armbuster et al. is in a live and dynamic setting, ours is, a static and theoretical network analysis. However, given the fact that this theoretical analysis reflects only a few indispensable ones, they might have some relevance in therapeutic intervention strategies to tackle CAUTI caused by MDR *P. mirabilis*.

CONCLUSION

This study takes a stepwise approach to identify the crucial role players from different sets of interacting proteins of *P. mirabilis* involved primarily in QS phenomenon. Essentially, this delineates the building of theoretical interactomes comprising the five individual SPIN which are analyzed through network parametric measures to reveal the most important proteins for such phenotype of QS and biofilm formation. All these lead to the identification of LuxS and PMI1345 to be important proteins of this organism. Furthermore, the results are supplemented through a decomposition of the *P. mirabilis* genome interactome, GPIN, followed by analysis of centrality measurements to reach the innermost core of the proteins essential for virulence and survival. Such in-depth analysis of the GPIN revealed other classes of important conserved proteins like GltB, PMI3678, and RcsC having the potential for being the most important ones and thus, indispensable among the set of whole genome proteins of *P. mirabilis*.

AUTHOR CONTRIBUTIONS

The analyses and the study were conceptualized, planned and designed by CL. Data generated by SP, MA, SM, and RM were analyzed by CL supported by SM and RM with tabulation. Additional scripts for QC were written by RM. Artwork was done by MA, SM, and SP. CL primarily wrote and edited the manuscript aided by inputs from SP, MA, and SM.

ACKNOWLEDGMENTS

The authors acknowledge the support of IMSc, Chennai, India and Sunway University, Selangor, Malaysia for providing the computational facilities. We thank Shweta Singh, Eric Wafula and Frank Roberts for their valuable contribution to an earlier form of the work which metamorphosed to the current state.

SUPPLEMENTARY MATERIAL

The Supplementary Material for this article can be found online at: https://www.frontiersin.org/articles/10.3389/fcimb.2018.00269/full#supplementary-material

REFERENCES

Albert, R., Jeong, H., and Barabási, A. L. (2000). Error and attack tolerance of complex networks. *Nature* 406, 378–382. doi: 10.1038/35019019

Alvarez-Hamelin, I., DallAsta, L., Barrat, A., and Vespignani, A. (2006). *Advances in Neural Information Processing Systems 18*. Cambridge, MA: MIT press.

Armbruster, C. E., Forsyth-DeOrnellas, V., Johnson, A. O., Smith, S. N., Zhao, L., Wu, W., et al. (2017). Genome-wide transposon mutagenesis of *Proteus mirabilis*: essential genes, fitness factors for catheter-associated urinary tract infection, and the impact of polymicrobial infection on fitness requirements. *PLoS Pathog.* 13:e1006434. doi: 10.1371/journal.ppat.1006434

Ashraf, M. I., Ong, S. K., Mujawar, S., Pawar, S., More, P., Paul, S., et al. (2018). A side-effect free method for identifying cancer drug targets. *Sci. Rep.* 8:6669. doi: 10.1038/s41598-018-25042-2

Bastian, M., Heymann, S., and Jacomy, M. (2009). Gephi: an open source software for exploring and manipulating networks. *Icwsm* 8, 361–362.

Belas, R., Schneider, R., and Melch, M. (1998). Characterization of *Proteus mirabilis* precocious swarming mutants: identification of rsbA, encoding a regulator of swarming behavior. *J. Bacteriol.* 180, 6126–6139.

Campbell, J., Lin, Q., Geske, G. D., and Blackwell, H. E. (2009). New and unexpected insights into the modulation of LuxR-type quorum sensing by cyclic dipeptides. *ACS Chem. Biol.* 4, 1051–1059. doi: 10.1021/cb900165y

Caspi, R., Billington, R., Ferrer, L., Foerster, H., Fulcher, C. A., Keseler, I. M., et al. (2015). The MetaCyc database of metabolic pathways and enzymes and the BioCyc collection of pathway/genome databases. *Nucleic Acids Res.* 44, D471–D480. doi: 10.1093/nar/gkv1164

Claret, L., and Hughes, C. (2000). Rapid turnover of FlhD and FlhC, the flagellar regulon transcriptional activator proteins, during proteus swarming. *J. Bacteriol.* 182, 833–836. doi: 10.1128/JB.182.3.833-836.2000

Cline, M. S., Smoot, M., Cerami, E., Kuchinsky, A., Landys, N., Workman, C., et al. (2007). Integration of biological networks and gene expression data using Cytoscape. *Nat. Protoc.* 2, 2366– 2382. doi: 10.1038/nprot.2007.324

Czerwonka, G., Guzy, A., Kałuza, K., Grosicka, M., Danczuk, M., Lechowicz, Ł., et al. (2016). The role of *Proteus mirabilis* cell wall features in biofilm formation. *Arch. Microbiol.* 198, 877–884. doi: 10.1007/s00203-016-1249-x

Diestel, R. (2000). *Graph Theory*. Berlin; Heidelberg: Springer-Verlag.

Eliopoulos, G. M., Maragakis, L. L., and Perl, T. M. (2008). *Acinetobacter baumannii*: epidemiology, antimicrobial resistance, and treatment options. *Clin. Infect. Dis.* 46, 1254–1263. doi: 10.1086/529198

Erdos, P., and Rényi, A. (1960). On the evolution of random graphs. *Publ. Math. Inst. Hung. Acad. Sci.* 5, 17–61.

Fraser, G. M., and Hughes, C. (1999). Swarming motility. *Curr. Opin. Microbiol.* 2, 630–635. doi: 10.1016/S1369-5274(99)00033-8

Guimerà, R., and Nunes Amaral, L. A. (2005a). Cartography of complex networks: modules and universal roles. *J. Statist. Mech.* 2005:P02001. doi: 10.1088/1742-5468/2005/02/P02001

Guimerà, R., and Nunes Amaral, L. A. (2005b). Functional cartography of complex metabolic networks. *Nature* 433, 895–900. doi: 10.1038/nature03288

Henke, J. M., and Bassler, B. L. (2004). Bacterial social engagements. *Trends Cell Biol.* 14, 648–656. doi: 10.1016/j.tcb.2004.09.012

Holden, M. T., Ram Chhabra, S., De Nys, R., Stead, P., Bainton, N. J., Hill, P. J., et al. (1999). Quorum-sensing crosstalk: isolation and chemical characterization of cyclic dipeptides from *Pseudomonas aeruginosa* and other gram-negative bacteria. *Mol. Microbiol.* 33, 1254–1266. doi: 10.1046/j.1365-2958.1999.01577.x

Jacobsen, S. M., and Shirtliff, M. E. (2011). *Proteus mirabilis* biofilms and catheter-associated urinary tract infections. *Virulence* 2, 460–465. doi: 10.4161/viru.2.5.17783

Jeong, H., Mason, S. P., Barabási, A. L., and Oltvai, Z. N. (2001). Lethality and centrality in protein networks. *Nature* 411, 41–42. doi: 10.1038/35075138

Kanehisa, M., Furumichi, M., Tanabe, M., Sato, Y., and Morishima, K. (2016). KEGG: new perspectives on genomes, pathways, diseases and drugs. *Nucleic Acids Res.* 45, D353–D361. doi: 10.1093/nar/gkw1092

Kanehisa, M., Sato, Y., Kawashima, M., Furumichi, M., and Tanabe, M. (2015). KEGG as a reference resource for gene and protein annotation. *Nucleic Acids Res.* 44, D457–D462. doi: 10.1093/nar/gkv1070

Kang, Y., Goo, E., Kim, J., and Hwang, I. (2017). Critical role of quorum sensing-dependent glutamate metabolism in homeostatic osmolality and outer membrane vesiculation in Burkholderia glumae. *Sci. Rep.* 7:44195. doi: 10.1038/srep44195

Koschützki, D., and Schreiber, F. (2004). "Comparison of centralities for biological networks," in *German Conference on Bioinformatics* (Bielefield), 199–206.

Lahiri, C., Pawar, S., Sabarinathan, R., Ashraf, M. I., Chand, Y., and Chakravortty, D. (2014). Interactome analyses of Salmonella pathogenicity islands reveal SicA indispensable for virulence. *J. Theor. Biol.* 363, 188–197. doi: 10.1016/j.jtbi.2014.08.013

Luzzaro, F., Brigante, G., D'Andrea, M. M., Pini, B., Giani, T., Mantengoli, E., et al. (2009). Spread of multidrug-resistant *Proteus mirabilis* isolates producing an AmpC-type β-lactamase: epidemiology and clinical management. *Int. J. Antimicrob. Agents* 33, 328–333. doi: 10.1016/j.ijantimicag.2008.09.007

MATLAB and Statistics Toolbox Release (2010). Natick, MA: The MathWorks, Inc.

Oliveros, J. C. (2007–2015). *Venny. An Interactive Tool for Comparing Lists with Venn's Diagrams*. Available online at: http://bioinfogp.cnb.csic.es/tools/venny/index.html

Özgür, A., Vu, T., Erkan, G., and Radev, D. R. (2008). Identifying gene-disease associations using centrality on a literature mined gene-interaction network. *Bioinformatics* 24, i277–i285. doi: 10.1093/bioinformatics/btn182

Pan, A., Lahiri, C., Rajendiran, A., and Shanmugham, B. (2015). Computational analysis of protein interaction networks for infectious diseases. *Brief. Bioinform.* 17, 517–526. doi: 10.1093/bib/bbv059

Pavlopoulos, G. A., Secrier, M., Moschopoulos, C. N., Soldatos, T. G., Kossida, S., Aerts, J., et al. (2011). Using graph theory to analyze biological networks. *BioData Min.* 4:10. doi: 10.1186/1756-0381-4-10

Pearson, M. M., Sebaihia, M., Churcher, C., Quail, M. A., Seshasayee, A. S., Luscombe, N. M., et al. (2008). Complete genome sequence of uropathogenic *Proteus mirabilis*, a master of both adherence and motility. *J. Bacteriol.* 190, 4027–4037. doi: 10.1128/JB.01981-07

Rauprich, O., Matsushita, M., Weijer, C. J., Siegert, F., Esipov, S. E., and Shapiro, J. A. (1996). Periodic phenomena in *Proteus mirabilis* swarm colony development. *J. Bacteriol.* 178, 6525–6538. doi: 10.1128/jb.178.22.6525-6538.1996

Ren, D., Bedzyk, L. A., Ye, R. W., Thomas, S. M., and Wood, T. K. (2004). Stationary-phase quorum-sensing signals affect autoinducer-2 and gene expression in *Escherichia coli*. *Appl. Environ. Microbiol.* 70, 2038–2043. doi: 10.1128/AEM.70.4.2038-2043.2004

Rhoads, D. B., Laimins, L., and Epstein, W. (1978). Functional organization of the kdp genes of *Escherichia coli* K-12. *J. Bacteriol.* 135, 445–452.

Rosvall, M., and Bergstrom, C. T. (2011). Multilevel compression of random walks on networks reveals hierarchical organization in large integrated systems. *PLoS ONE* 6:e18209. doi: 10.1371/journal.pone.0018209

Rutherford, S. T., and Bassler, B. L. (2012). Bacterial quorum sensing: its role in virulence and possibilities for its control. *Cold Spring Harb. Perspect. Med.* 2:a012427. doi: 10.1101/cshperspect.a012427

Scavone, P., Iribarnegaray, V., Caetano, A. L., Schlapp, G., Härtel, S., and Zunino, P. (2016). Fimbriae have distinguishable roles in *Proteus mirabilis* biofilm formation. *FEMS Pathog. Dis.* 74:ftw033. doi: 10.1093/femspd/ftw033

Schaffer, J. N., and Pearson, M. M. (2015). *Proteus mirabilis* and urinary tract infections. *Microbiol. Spectrum* 3:UTI-0017-2013. doi: 10.1128/microbiolspec.UTI-0017-2013

Schneider, R., Lockatell, C. V., Johnson, D., and Belas, R. (2002). Detection and mutation of a luxS-encoded autoinducer in *Proteus mirabilis*. *Microbiology* 148, 773–782. doi: 10.1099/00221287-148-3-773

Seidman, S. B. (1983). Network structure and minimum degree. *Soc. Netw.* 5, 269–287. doi: 10.1016/0378-8733(83)90028-X

Stankowska, D., Czerwonka, G., Rozalska, S., Grosicka, M., Dziadek, J., and Kaca, W. (2012). Influence of quorum sensing signal molecules on biofilm formation in *Proteus mirabilis* O18. *Folia Microbiol.* 57, 53–60. doi: 10.1007/s12223-011-0091-4

Stankowska, D., Kwinkowski, M., and Kaca, W. (2008). Quantification of *Proteus mirabilis* virulence factors and modulation by acylated homoserine lactones. *J. Microbiol. Immunol. Infect.* 41, 243–253.

Szklarczyk, D., Morris, J. H., Cook, H., Kuhn, M., Wyder, S., Simonovic, M., et al. (2016). The STRING database in 2017: quality-controlled protein–protein association networks, made broadly accessible. *Nucleic Acids Res.* 45, D362–D368. doi: 10.1093/nar/gkw937

Tang, Y., Li, M., Wang, J., Pan, Y., and Wu, F. X. (2015). CytoNCA: a cytoscape plugin for centrality analysis and evaluation of protein interaction networks. *BioSystems* 127, 67–72. doi: 10.1016/j.biosystems.2014.11.005

Vázquez, A. (2003). Growing network with local rules: preferential attachment, clustering hierarchy, and degree correlations. *Phys. Rev. E* 67:056104. doi: 10.1103/PhysRevE.67.056104

Vella, D., Marini, S., Vitali, F., Di Silvestre, D., Mauri, G., and Bellazzi, R. (2018). MTGO: PPI network analysis via topological and functional module identification. *Sci. Rep.* 8:5499. doi: 10.1038/s41598-018-23672-0

Wang, J. T., Chen, P. C., Chang, S. C., Shiau, Y. R., Wang, H. Y., Lai, J. F., et al. (2014). Antimicrobial susceptibilities of *Proteus mirabilis*: a longitudinal nationwide study from the Taiwan surveillance of antimicrobial resistance (TSAR) program. *BMC Infect. Dis.* 14:486. doi: 10.1186/1471-2334-14-486

Wang, M. C., Chien, H. F., Tsai, Y. L., Liu, M. C., and Liaw, S. J. (2014). The RNA chaperone Hfq is involved in stress tolerance and virulence in uropathogenic *Proteus mirabilis*. *PLoS ONE* 9:e85626. doi: 10.1371/journal.pone.0085626

Watts, D. J., and Strogatz, S. H. (1998). Collective dynamics of 'small-world' networks. *Nature* 393, 440–442.

Conflict of Interest Statement: The authors declare that the research was conducted in the absence of any commercial or financial relationships that could be construed as a potential conflict of interest.

frontiers in Cellular and Infection Microbiology

ORIGINAL RESEARCH
published: 26 July 2017
doi: 10.3389/fcimb.2017.00337

Anti-quorum Sensing and Anti-biofilm Activity of *Delftia tsuruhatensis* Extract by Attenuating the Quorum Sensing-Controlled Virulence Factor Production in *Pseudomonas aeruginosa*

Vijay K. Singh, Avinash Mishra * and Bhavanath Jha *

Marine Biotechnology and Ecology Division, CSIR-Central Salt and Marine Chemicals Research Institute, Bhavnagar, India

OPEN ACCESS

Edited by:
Rodolfo García-Contreras, National Autonomous University of Mexico, Mexico

Reviewed by:
Anil Kumar Singh, Indian Institute of Agricultural Biotechnology (ICAR), India
Ananda Mustafiz, South Asian University, India
Thibault Géry Sana, Stanford University, United States
Israeñ Castillo Juárez, College of Postgraduates Montecillo, Mexico

****Correspondence:***
Avinash Mishra
avinash@csmcri.org;
avinash@csmcri.res.in;
avinashmishra11@rediffmail.com
Bhavanath Jha
bjha@csmcri.res.in

Received: *11 May 2017*
Accepted: *10 July 2017*
Published: *26 July 2017*

Citation:
Singh VK, Mishra A and Jha B (2017) Anti-quorum Sensing and Anti-biofilm Activity of Delftia tsuruhatensis Extract by Attenuating the Quorum Sensing-Controlled Virulence Factor Production in Pseudomonas aeruginosa. Front. Cell. Infect. Microbiol. 7:337. doi: 10.3389/fcimb.2017.00337

Multidrug-resistance bacteria commonly use cell-to-cell communication that leads to biofilm formation as one of the mechanisms for developing resistance. Quorum sensing inhibition (QSI) is an effective approach for the prevention of biofilm formation. A Gram-negative bacterium, *Delftia tsuruhatensis* SJ01, was isolated from the rhizosphere of a species of sedge (*Cyperus laevigatus*) grown along the coastal-saline area. The isolate SJ01 culture and bacterial crude extract showed QSI activity in the biosensor plate containing the reference strain *Chromobacterium violaceum* CV026. A decrease in the violacein production of approximately 98% was detected with the reference strain *C. violaceum* CV026. The bacterial extract (strain SJ01) exhibited anti-quorum sensing activity and inhibited the biofilm formation of clinical isolates wild-type *Pseudomonas aeruginosa* PAO1 and *P. aeruginosa* PAH. A non-toxic effect of the bacterial extract (SJ01) was detected on the cell growth of the reference strains as *P. aeruginosa* viable cells were present within the biofilm. It is hypothesized that the extract (SJ01) may change the topography of the biofilm and thus prevent bacterial adherence on the biofilm surface. The extract also inhibits the motility, virulence factors (pyocyanin and rhamnolipid) and activity (elastase and protease) in *P. aeruginosa* treated with SJ01 extract. The potential active compound present was identified as 1,2-benzenedicarboxylic acid, diisooctyl ester. Microarray and transcript expression analysis unveiled differential expression of quorum sensing regulatory genes. The key regulatory genes, *LasI*, *LasR*, *RhlI,* and *RhlR* were down-regulated in the *P. aeruginosa* analyzed by quantitative RT-PCR. A hypothetical model was generated of the transcriptional regulatory mechanism inferred in *P. aeruginosa* for quorum sensing, which will provide useful insight to develop preventive strategies against the biofilm formation. The potential active compound identified, 1,2-benzenedicarboxylic acid, diisooctyl ester, has the potential to be used as an anti-pathogenic drug for the treatment of biofilm-forming pathogenic bacteria. For that, a detailed study is needed to investigate the possible applications.

Keywords: anti-biofilm, anti-quorum, microarray, quorum network, quorum quenching, quorum sensing, virulence factors

INTRODUCTION

The biggest challenge for the healthcare sector is drug resistance in pathogenic bacteria. The efficiency of antibiotics against pathogenic bacteria is currently decreasing because of the emergence of multidrug-resistance (Adonizio et al., 2008). Biofilm formation is one of the mechanisms, used by bacteria for developing such resistance (Fuqua and Greenberg, 1998). It is well-established that curing of diseases caused by biofilm-forming bacteria requires prolonged treatment, which may also lead to antibiotic resistance due to high evolutionary pressure. The biofilm formation is controlled by cell-to-cell communication, which is widely known as quorum sensing. The inhibition of quorum sensing is one of the methods among the different strategies deployed to control biofilm forming microorganisms without causing drug resistance (Singh et al., 2013, 2016b). In recent years, several anti-quorum sensing compounds were reported in plants and microbes (Choo et al., 2006; Adonizio et al., 2008; Ni et al., 2009; Kalia and Purohit, 2011; Kalia, 2012).

The ubiquitous gram-negative bacterium *Pseudomonas aeruginosa* is an opportunistic pathogen, having a wide range of hosts such as insects, plants, animals, and humans (Rahme et al., 2000; Vandeputte et al., 2010). The bacterium *P. aeruginosa* causes very severe infection in immunocompromised patients (Driscoll et al., 2007; Vandeputte et al., 2010; Sarabhai et al., 2013) and is responsible for about 57% of all nosocomial infections (Oncul et al., 2009; Sarabhai et al., 2013).

It was observed that *P. aeruginosa* uses a range of virulence factors and multiple mechanisms, including biofilm formation, to successfully infect a diverse range of hosts and to protect itself from environmental stress and antibiotics (Driscoll et al., 2007; Vandeputte et al., 2010; Lee and Zhang, 2015). Quorum sensing controls the virulence factors and biofilm formation of *P. aeruginosa*. Therefore, anti-quorum sensing strategies could be a potential target to prevent *P. aeruginosa* infection.

The rhizosphere, a region of soil that surrounds the plant roots, possess a diverse bacterial community that containing molecules with both quorum sensing and quorum quenching activities (Christiaen et al., 2011), including anti-biofilm activity against *P. aeruginosa* (Christiaen et al., 2014). The anti-quorum sensing activity of *Acinetobacter* sp. strain C1010 (isolated from cucumber rhizosphere) was evaluated and found to degrade the acyl-homoserine lactones (AHLs) produced by *P. chlororaphis* O6 (Kang et al., 2004). A large number of AHL-degrading bacteria, including *Sphingomonas* sp. and *Bosea* sp., were isolated from the tobacco rhizosphere (D'Angelo-Picard et al., 2005). The bacteria *Acinetobacter* (GG2), *Burkholderia* (GG4), and *Klebsiella* (Se14) isolated from the ginger rhizosphere also showed AHL-degrading activity (Chan et al., 2011). Bacterial consortia isolated from the rhizosphere of potato contained anti-quorum sensing and plant growth promoting potential (Cirou et al., 2007). To date, however, there is no report on rhizospheric bacteria with anti-quorum sensing and anti-biofilm activity from the saline ecosystem.

In the present study, the rhizosphere of a monocot *Cyperus laevigatus*, a species of sedge from the coastal saline area, was explored and the bacterium *Delftia tsuruhatensis* SJ01 was isolated. Members of the *Delftia* genus are Gram-negative, aerobic, rod-shaped and motile bacteria comprised of five species: *Delftia acidovorans* (Wen et al., 1999), *D. tsuruhatensis* (Shigematsu et al., 2003), *Delftia lacustris* (Jørgensen et al., 2009), *Delftia litopenaei* (Chen et al., 2012), and *Delftia deserti* (Li et al., 2015). The coral-associated bacterial strain *D. tsuruhatensis* from the Gulf of Mannar was reported for its anti-quorum sensing activity. However, a detailed study and the identification of compounds has still not been performed (Bakkiyaraj et al., 2012, 2013). The isolated bacterium was explored for anti-quorum sensing and anti-biofilm potential. The active fraction was identified, regulatory key genes were studied, and a possible mechanism was inferred.

MATERIALS AND METHODS

Isolation and Screening of Bacteria

A monocot, *C. laevigatus*, growing luxuriantly in the wet coastal areas of New-port, Bhavnagar, India (Latitude N 21° 45.124″, Longitude E 72° 13.579″), was collected. Bacteria were isolated from rhizosphere using a standard method, and axenic cultures were made for each isolate. Isolated axenic cultures were subjected to the screening of anti-quorum sensing activity using the reference strain *Chromobacterium violaceum* (CV026), cinnamaldehyde (Sigma-Aldrich, USA) as a positive control and methanol as a negative control in a plate-based bioassay (Singh et al., 2013). Bacterial isolates showing quorum sensing inhibition (QSI) activity were selected and checked further for antibacterial activity on Mueller-Hinton agar (MHA), along with tobramycin, which used as a positive control (Choo et al., 2006). A bacterial isolate showing promising positive QSI and negative anti-bacterial activities was selected further. The QSI and anti-bacterial activities of the selected isolate were repeated five times independently.

Identification of Bacteria and Fatty Acid Methyl Ester Profiling

Genomic DNA of selected bacteria was isolated, and the 16S rRNA gene amplified with universal primers fD1-5′-AGA GTT TGA TCC TGG CTC AG-3′ and rP2-5′-ACG GCT ACC TTG TTA CGA CTT-3′ (Weisburg et al., 1991) and optimized PCR conditions (Keshri et al., 2013, 2015). The PCR product was purified, sequenced (M/s Macrogen Inc., South Korea) and subjected to BLAST analysis. Phylogenetic analysis was performed using MEGA (Molecular Evolutionary Genetics Analysis) version 6.0 software (Tamura et al., 2013). The phylogenetic tree was reconstructed using neighbor-joining methods (Saitou and Nei, 1987), bootstrap analysis was performed (Felsenstein, 1985), and evolutionary distances were determined using maximum composite likelihood algorithms (Tamura et al., 2004). The bacterial isolate was identified as *D. tsuruhatensis* strain SJ01, and the 16S rRNA gene sequence was deposited in the NCBI GenBank (KX130769).

Fatty acid methyl ester (FAME) profiling of identified bacteria was performed using Microbial Identification System (MIDI;

Microbial ID) coupled with gas chromatography (GC system-6850, Agilent Technologies, USA). For whole cell fatty acid methyl ester profiling, the bacteria were grown on tryptic soy yeast agar for 24 h at 30°C, and fatty acid methyl esters were prepared according to the instruction manual of the Microbial Identification System (MIDI; Microbial ID). Peaks were identified and matched with RTSBA6 6.10 database (Jha et al., 2015).

Preparation of Bacterial Extract

Bacterial culture (*D. tsuruhatensis* strain SJ01, 500 ml in nutrient broth, NB), grown for 48 h, 180 rpm at 30°C was centrifuged for 15 min. at 10,000 × g, 4°C, and the supernatant was collected in a flask. The supernatant was filtered through 0.45 and 0.22 μm vacuum filters for the complete removal of bacterial cells. The filtrate was extracted twice with an equal volume of ethyl acetate. Ethyl acetate extract was evaporated to dryness under vacuum in a rotary evaporator (Büchi, Switzerland) and dissolved in methanol for further studies (Nithya et al., 2010).

Anti-quorum Sensing Activity

The anti-quorum sensing activity of a methanolic extract of bacteria was tested by quantifying violacein (Choo et al., 2006). In brief, 1 ml of the freshly grown (OD_{600nm} 0.7) reference strain *C. violaceum* (CV026) was added to 20 ml NB Hi-veg media (Hi-media, India) containing hexonyl homoserine lactone (0.0625 μg/ml) and different concentrations of bacterial extract (0.01, 0.02, 0.03, 0.04, 0.05, 0.075, or 0.1 mg/ml). Cultures without extract and with methanol were considered the control and negative control, respectively. All cultures (controls and experimental) were incubated for 24 h at 30°C and 180 rpm (Choo et al., 2006). One milliliter of overnight grown culture from each flask was centrifuged 16,000 × g for 10 min, and the pellet containing violacein (produced by CV026) was suspended in 1 ml of dimethylsulfoxide (DMSO). The solution was centrifuged at 16,000 × g for 10 min to remove cell debris and absorbance was read at 585 nm in a microplate reader (Spectra Max Plus, USA).

Biofilm Formation Assay

A measure of 200 μl of overnight grown cultures (OD_{600nm} 0.1) of clinical isolates *P. aeruginosa* PAO1 (ATCC 15692) or *P. aeruginosa* PAH (by courtesy from Govt. Medical College, Bhavnagar; Goswami et al., 2011) was added to a 96-well microtiter plate with different concentrations of bacterial (strain SJ01) extracts (0.01, 0.02, 0.03, 0.04, 0.05, 0.075, and 0.1 mg/ml). The plate was incubated at 37°C, 100 rpm for 24 h, after which the growth of bacteria was measured at 600 nm and colony forming units (CFU) were also determined. Wells were washed after removing planktonic bacterial cells, dried and stained with 1% crystal violet. Excess dye was taken out after 20 min, wells were washed (with sterile distilled water), 200 μl ethanol (aqueous 96%) was added, and absorbance was measured at 590 nm (Andersson et al., 2009; Singh et al., 2013; Kavita et al., 2014). The experiments were performed thrice with five replicates each.

Fluorescence Microscopy

Cell viability within the biofilm was examined at different time points (24, 48, and 72 h) and compared with the control (Singh et al., 2013). Cells inhabiting the biofilm were stained with a fluorescent dye using the FilmTracer™Live/Dead® Biofilm Viability Kit (Invitrogen, USA) following manufacturer's instructions and visualized under an epi-fluorescence microscope (Axio Imager, Carl Zeiss AG, Germany).

Scanning Electron Microscopy

The effect of bacterial extract (SJ01) on biofilm formation was visualized by scanning electron microscopy (SEM; Andersson et al., 2009; Singh et al., 2013). Biofilms of *P. aeruginosa* PAO1 and *P. aeruginosa* PAH, grown on glass coverslips (11 mm) submerged in nutrient broth with (0.1 mg/ml) or without bacterial extract were gently washed with 0.9% NaCl to remove planktonic cells. Samples were kept in 2.5% glutaraldehyde for 20 min followed by 4% OsO_4 in 0.1 M phosphate buffer for 30 min. Samples were dehydrated with a gradient ethanol series (10–95%) for 10 min. The dried biofilms were coated with gold and visualized under a scanning electron microscope (SEM, LEO series VP1430, Germany).

Atomic Force Microscopy

For atomic force microscopy (AFM), biofilms developed on glass coverslips were rinsed gently with phosphate buffer saline (pH 7.4) and kept in a desiccator for drying completely. The biofilm was scanned under AFM (NT-MDT, Russia) in a semi-contact mode at the speed of 1 Hz (Oh et al., 2009; Nithya et al., 2010). The surface bearing index (Sbi), core fluid retention index (Sci), valley fluid retention index (Svi), kernel roughness depth (Sk), reduced peak height (Spk), reduced valley depth (Svk), average roughness (Sa), root mean square (Sq), surface skewness (Ssk), coefficient of kurtosis (Ska), and surface area ratio (Sdr) were calculated.

Bacterial Motility Assay

Bacterial extract (SJ01) was tested on the swarming and swimming motility of *P. aeruginosa*. For the swarming motility assay, *P. aeruginosa* strains were spotted on a plate containing BM2 swarming medium (62 mM PBS at pH 7, 2 mM $MgSO_4$, 10 μM $FeSO_4$, 0.4% glucose, 0.1% casamino acids, and 0.5% agar) supplemented with (0.1 mg/ml) or without extract (Overhage et al., 2007). For the swimming motility assay, *P. aeruginosa* strains were spotted on a plate containing tryptone broth (10 g/l tryptone, 5 g/l NaCl, and 0.3% agar) supplemented with (0.1 mg/ml) or without extract (Rashid and Kornberg, 2000). Plates were analyzed after incubation of 24 h at 37°C.

Virulence Factor Analysis

The effect of bacterial extracts (SJ01; 0.1 mg/ml) was studied on the production of virulence factors of reference *P. aeruginosa* strains by quantifying pyocyanin and rhamnolipid, and analyzing elastase and protease activities. Briefly, *P. aeruginosa* PAO1 and *P. aeruginosa* PAH were grown overnight in 5 ml of PB medium (20 g/l peptone, 1.4 g/l $MgCl_2$ and 10 g/l K_2SO_4) supplemented with extract of strain SJ16 (1.0 mg/ml) and without extract

(control) at 37°C (180 rpm). The culture was centrifuged at 10,000 × g for 10 min, and pyocyanin was extracted first from the supernatant in 3 ml of chloroform, followed by 1 ml of 0.2 N HCl. The absorbance was measured spectrophotometrically at 520 nm (Essar et al., 1990).

For rhamnolipid, reference strains (*P. aeruginosa*) were grown in nutrient broth supplemented with bacterial extract (SJ01; 0.1 mg/ml) or without extract (control). The culture was centrifuged at 10,000 × g for 10 min, supernatants were collected, acidified with HCl (to pH 2) and absorbance was measured at 570 nm (McClure and Schiller, 1992). Supernatants (750 µl) of overnight grown (with 0.1 mg/ml or without extract of strain SJ01) *P. aeruginosa* were incubated with 250 µl elastin Congo-red solution (5 mg/ml in 0.1 M tris-HCl pH 8; 1 mM $CaCl_2$) at 37°C, 180 rpm for 16 h. After incubation, the mixture was centrifuged at 30,000 × g for 10 min, and absorbance was measured at 490 nm for elastase activity (Zhu et al., 2002). For protease activity, supernatant (400 µl) was incubated with an equal volume of 2% azocasein solution (prepared in 50 mM phosphate buffer saline, pH 7) at 37°C for 1 h. The reaction was stopped by adding 500 µl of 10% trichloroacetic acid (TCA), and reaction mix was centrifuged at 8,000 g for 5 min to remove residual azocasein. The absorbance of the supernatant was read at 400 nm (Adonizio et al., 2008).

Fractionation and Identification of Active Compound

Bacterial extract (*D. tsuruhatensis* SJ01) was fractionated by the solid phase extraction (SPE) method using different cartridges (non-polar C18, polar SI, anion exchanger DAE and cation mixed Plexa PCX) and each fraction was screened for anti-quorum sensing activity. The positive fraction was further analyzed, and an active compound was identified by GC-MS. Briefly, crude bacterial extract (1 ml) was loaded to the preconditioned (by 5 ml methanol, 10 ml water and 5 ml acidified water pH 2.0) SPE cartridges (Agilent, USA). The elution was performed with a different concentration of 1 ml methanol (20, 40, 60, 80, and 100% v/v in water) and different fractions were collected (Singh et al., 2013). Each fraction was screened for plate based anti-quorum sensing activity (as described above) using the reference strain *C. violaceum* (CV026). The positive fraction was subjected to GC-MS (GC-2010, Shimadzu, Japan) and the identification of compounds was done by comparing the mass spectra with the reference mass spectra library. The mass of the fractionated compound identified was further confirmed by electrospray ionization mass spectrometry (ESI-MS; Q-Tof micro TM, Micromass, UK), performed in a positive mode.

Microarray and Expression Analysis

Differential expression of regulatory genes of reference strain *P. aeruginosa* PAO1, involved in the quorum sensing was analyzed using microarray. Total RNA was isolated from reference strain *P. aeruginosa* PAO1, grown with or without bacterial extracts (0.1 mg/ml) using TRI reagent (Sigma, USA). Total RNA was quantified, and 10 µg RNA was converted to cDNA, befor being fragmented and labeled by following the GeneChip® *P. aeruginosa* PAO1 genome array user manual (Affymetrix, USA). Labeled cDNAs were hybridized with the *P. aeruginosa* genome array gene chip (containing total 5,886 gene probes), and then washed and stained (Singh et al., 2016a). Hybridized chips were scanned (Scanner 3000 7G, Affymetrix, USA), processed and analyzed using the expression console and the transcriptome analysis console (Affymetrix, USA). Microarray analysis was performed in duplicate ($n = 2$) and genes exhibiting significant fold expression (ANOVA $p < 0.05$) were considered for the study. All microarray data are available with Array-Express accession number E-MTAB-5693. For expression profiling, key regulatory genes (*LasI*, *LasR*, *RhlI,* and *RhlR*) were selected. Total RNA was extracted from control and treated *P. aeruginosa* (PAO1 and PAH strains) converted to cDNA and then quantitative real-time PCR was performed (Wang et al., 2005). A melt curve analysis was also done for the validation of specificity of the qRT-PCR reaction, and the relative fold expression change was calculated using the CT method (Livak and Schmittgen, 2001). The 16S rRNA gene was used as a reference gene (Wang et al., 2005).

RESULTS

Isolation and Screening of Bacteria for Anti-quorum Sensing Activity

A total of 56 bacterial axenic cultures were obtained from the rhizosphere of *C. laevigatus* L., of which two axenic cultures showed anti-quorum sensing activity in a plate-based bioassay. The isolate SJ01 showed promising anti-quorum sensing activity and a clear white opaque zone of inhibition was observed in the biosensor plate containing reference strain *C. violaceum* CV026 (**Figure 1**). Furthermore, the bacterial crude extract also showed QSI, whereas the zone of inhibition was not detected with the negative control (methanol). The disc diffusion antibacterial assay confirmed that selected bacterial isolates did not show antibacterial activity against the reference strain *C. violaceum* CV026 (**Figure S1**).

Identification of Bacteria, Fatty Acid Methyl Ester Profiling, and Phylogenetic Analysis

The 16S rRNA gene sequence (accession no. KX130769) of the selected bacterial isolate showed 99% similarity to *D. tsuruhatensis*, with 100% query coverage; therefore, this was designated *D. tsuruhatensis* SJ01. The phylogenetic tree reconstructed using the neighbor-joining algorithm shows the taxonomic position of identified bacterium with other species (**Figure S2**). The whole cell fatty acid profiling of the bacterium *D. tsuruhatensis* SJ01 revealed the abundance of $C_{16:0}$ fatty acids (**Figure S3**).

Delftia tsuruhatensis SJ01 Extract Shows Anti-quorum Sensing Activity by Inhibiting Violacein Production

The bacterium *D. tsuruhatensis* SJ01 and its methanolic extract showed anti-quorum sensing activity with the reference strain on a biosensor plate. Different concentrations of bacterial extract were used to quantify the inhibition of violacein, an indicator

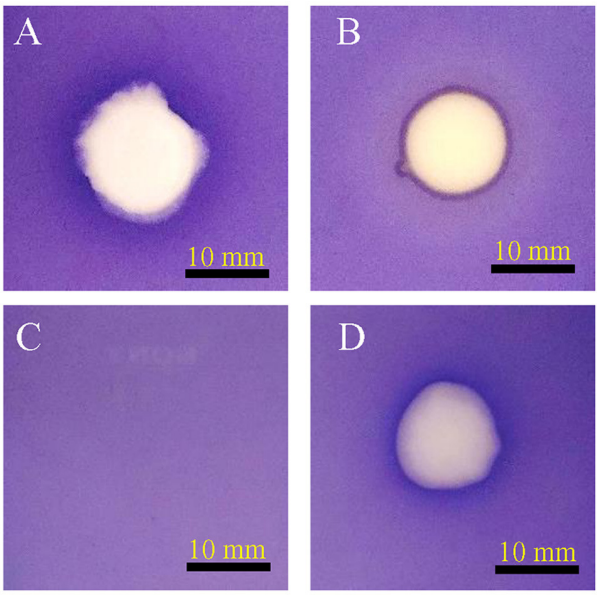

FIGURE 1 | Anti-quorum sensing activity of isolate SJ01. The biosensor plates containing reference strain *C. violaceum* CV026 were spotted with **(A)** cinnamaldehyde, **(B)** SJ01 axenic culture, **(C)** methanol, and **(D)** crude bacterial (SJ01) extract. Cinnamaldehyde was used as a positive control. The isolate SJ01 and its extract showed the anti-quorum sensing activity and a clear white opaque zone of inhibition.

of quorum sensing activity (**Figure 2**). The violacein production decreased concomitantly with the increasing concentration of the extract, and about 98% inhibition was observed with 0.1 mg/ml extract.

Delftia tsuruhatensis SJ01 Extract Inhibits Biofilm Formation

The anti-biofilm activity of the extract (*D. tsuruhatensis* SJ01) was tested against the wild-type, widely used biofilm forming clinical isolate *P. aeruginosa* PAO1 and a local clinical isolate *P. aeruginosa* PAH. The biofilm formation decreased concurrently in both reference strains with increasing concentration of bacterial extracts (**Figure 3**). About 60–64% inhibition of the biofilm formation was observed with 0.1 mg/ml extract. The possibility of an inhibitory effect of *D. tsuruhatensis* SJ01 extract on the growth of reference strains (*P. aeruginosa*) was also analyzed (**Figures S4**, **S5**). No significant effect was observed on the planktonic growth of *P. aeruginosa* in the presence of different concentration of bacterial extracts (0.01–0.1 mg/ml). Further, the disc diffusion antibacterial assay performed with SJ01 extract confirmed that bacterial extract did not show antibacterial activity against the clinical isolates *P. aeruginosa* (**Figure S6**).

Fluorescence Microscopy Analysis Confirms That Biofilm Inhabiting Viable Cells

The effect of the bacterial extract on the viability of the reference strain in the biofilm (24–72 h) was studied with an epi-fluorescence microscope (**Figure 4**). The dead *P. aeruginosa* cells were labeled with propidium iodide whereas live cells stained with SYTO 9, which produced red and green fluorescence, respectively. Less attachment of *P. aeruginosa* cells to the surface was observed even up to 72 h in the treated biofilm compared to control, and an insignificant number of dead cells was detected in the biofilms.

Delftia tsuruhatensis SJ01 Extract Disrupts the Architecture of the Biofilm

The topology of the biofilm developed by *P. aeruginosa* and the effect of *D. tsuruhatensis* SJ01 extract on it was analyzed by SEM and AFM. A well-grown biofilm along with adhering bacterial cells was observed in controls (normal biofilm developed by *P. aeruginosa*) in the SEM analysis, whereas dispersed bacterial cells were observed in treated samples (**Figure 5**). Similarly, AFM clearly showed the disrupted surface topology and height distribution profile of the biofilm developed in the presence of *D. tsuruhatensis* SJ01 extract compared to the control biofilm (**Figure 6**). The surface bearing indices, roughness analysis, and functional parameters based on the linear material ratio curve showed alterations of the biofilm developed in treated samples (**Table 1**).

Delftia tsuruhatensis SJ01 Extract Shows Inhibitory Effect on the Motility of *P. aeruginosa*

Bacterial invasion is a prerequisite for biofilm formation. Therefore, the effect of bacterial extract (*D. tsuruhatensis* SJ01) was studied on the motility of biofilm forming *P. aeruginosa* bacterial cells. It was observed that bacterial extract (0.1 mg/ml) inhibits the swarming and swimming motility of *P. aeruginosa* strains in the plate assay (**Figure 7**). The extract reduced flagellum driven motility of *P. aeruginosa* in the treated sample compared to the control.

Delftia tsuruhatensis SJ01 Extract Relegates the Virulence Activities

It was observed that bacterial extract (*D. tsuruhatensis* SJ01) reduced the production of virulence factors; pyocyanin and rhamnolipid (**Figure 8**). Pyocyanin production decreased about 70 and 55% in PAO1 and PAH strains, respectively with the treatment of 0.1 mg/ml bacterial extract. Similarly, rhamnolipid production was also decreased by 85 and 67% in PAO1 and PAH strains, respectively, in the presence of bacterial extract (0.1 mg/ml). The effect *D. tsuruhatensis* SJ01 extract on the elastase and protease activities of cell-free *P. aeruginosa* bacterial culture supernatant were also assessed (**Figure 8**). About 32–35% decrease in elastase activities was detected for both strains compared to the control. However, about 23–24% inhibition in the protease activity was found in both strains with 0.1 mg/ml bacterial extract compared to untreated samples.

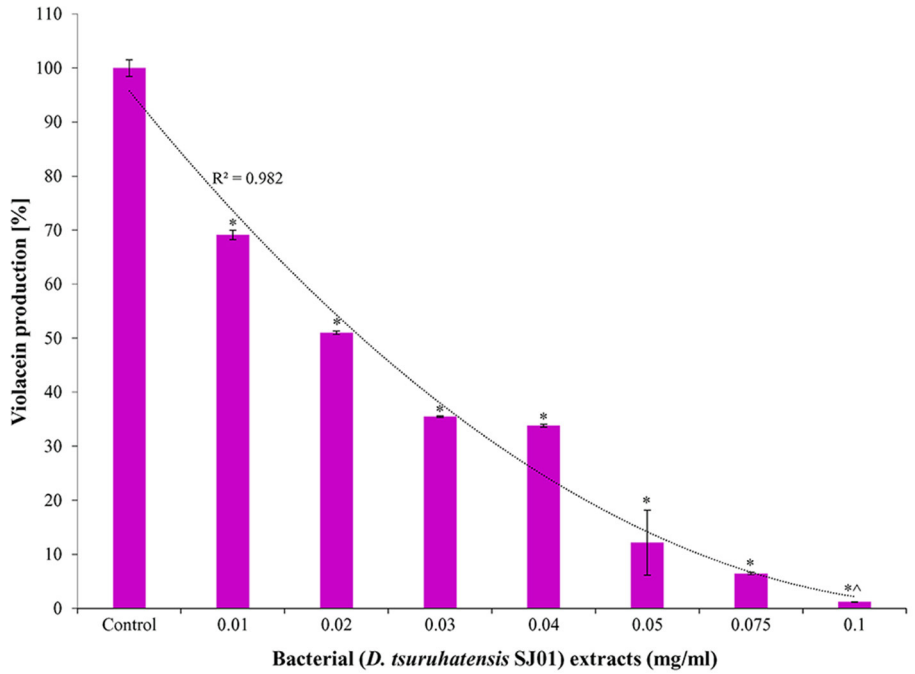

FIGURE 2 | Effect of different concentration of *D. tsuruhatensis* SJ01 extract on violacein production. Different concentration of bacterial extract (0.01−0.1 mg/ml) was used to quantify the inhibition of violacein, an indicator of quorum sensing activity. Cultures without extract were considered as a control. *Indicates significant differences from the control at $P < 0.05$ and ^ indicates maximum significant differences from the control at $P < 0.05$.

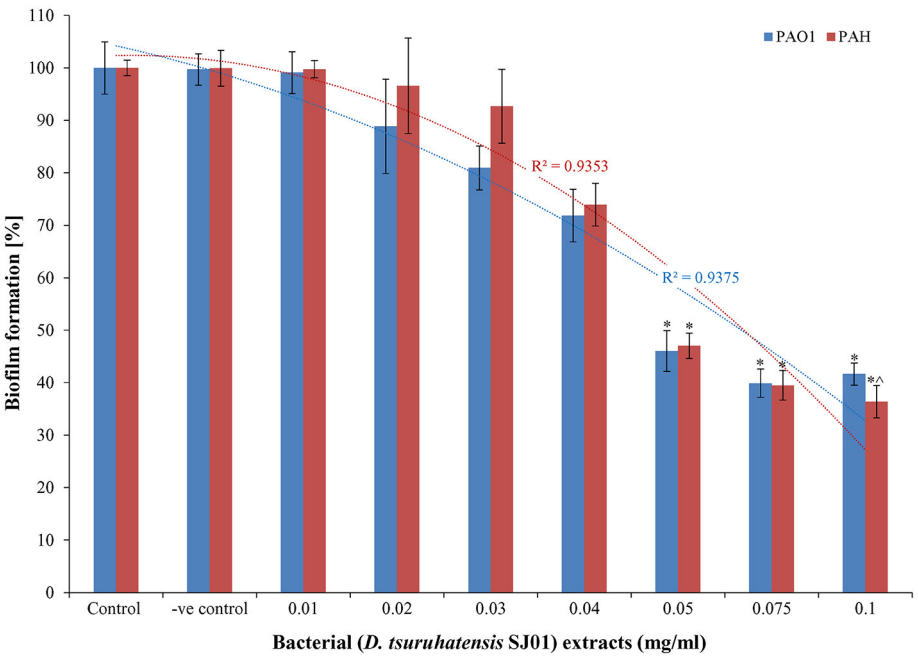

FIGURE 3 | The antibiofilm activity of *D. tsuruhatensis* SJ01 extract. Different concentration of bacterial extracts (0.01−0.1 mg/ml) was tested against wild-type, widely used biofilm forming reference strain *P. aeruginosa* strains. Tests without extract and with methanol were considered as control and negative control, respectively. *Indicates significant differences from the control at $P < 0.05$ and ^ indicates maximum significant differences from the control at $P < 0.05$.

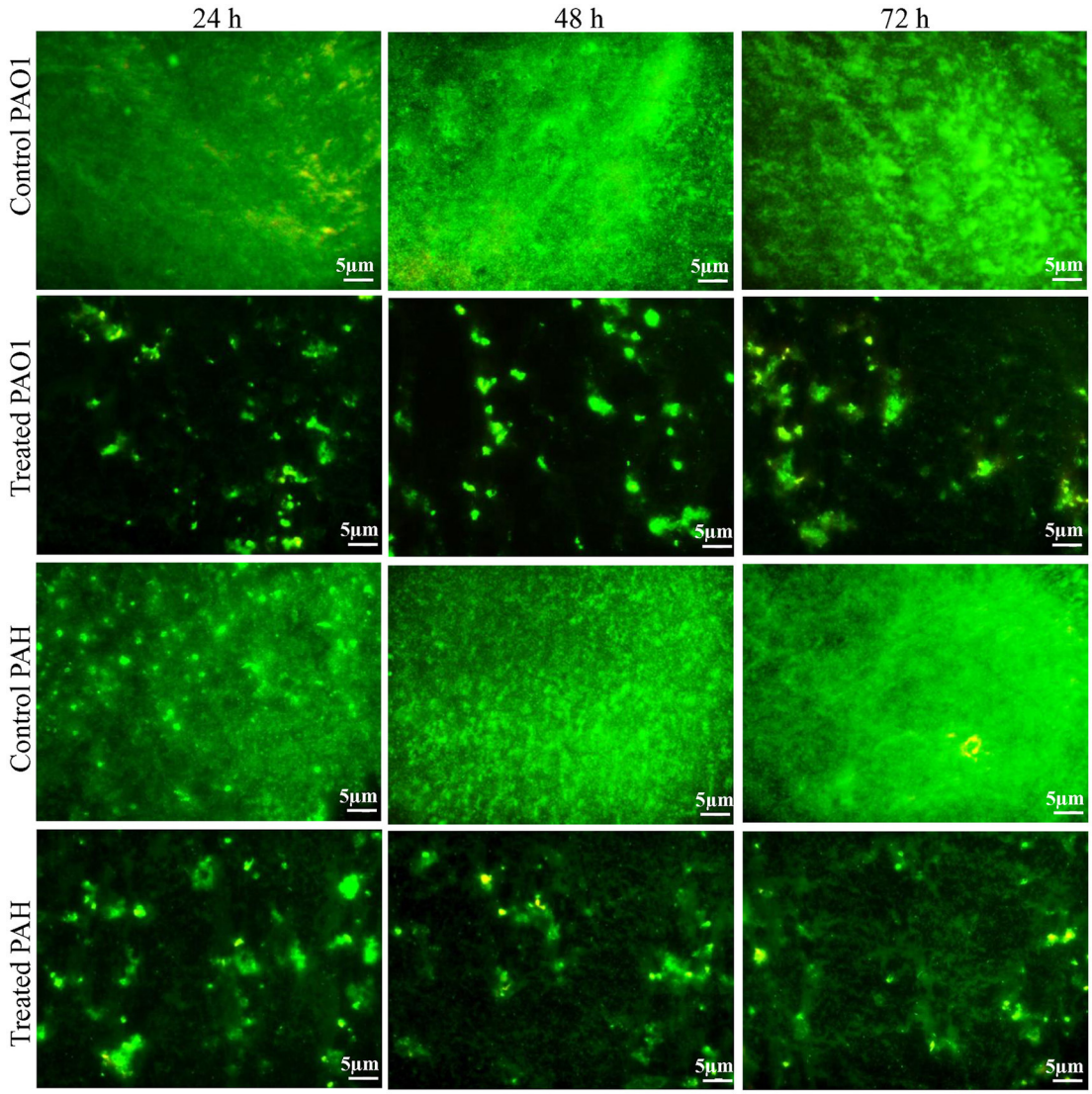

FIGURE 4 | Epi-fluorescence micrographs of biofilms developed by *P. aeruginosa*. The effect of the bacterial extract (0.1 mg/ml) on the viability of reference *P. aeruginosa* strains in the biofilm was examined at different time points (24, 48, and 72 h) and compared with control. The dead bacterial cells were labeled with propidium iodide whereas live cells stained with SYTO 9, which produced red and green fluorescence, respectively.

Identification of Quorum Sensing Inhibitor Compound

In total, five fractions (in 20, 40, 60, 80, and 100% methanol) were collected through each SPE cartridge (non-polar C18, polar SI, anion exchanger DAE, and cation mixed Plexa PCX); all were screened individually for QSI using a biosensor plate containing *C. violaceum* CV026. Fraction (C18-100), collected through the C18 cartridge with 100% methanol, showed a maximum zone of QSI; therefore, this was selected for further characterization. Fraction C18-100 was subjected to GC-MS analysis, and the chromatogram showed a single peak at the retention time 16.518 min (**Figure 9**). The detected mass spectra showed some resemblance to 1,2-benzenedicarboxylic acid, diisooctyl ester, in the GC-MS library (NIST 27. LB). The calculated (theoretical) or expected molecular mass of compound 1,2-benzenedicarboxylic acid, diisooctyl ester ($C_{24}H_{38}O_4$) is 390.55. The molecular mass of the active fraction (C18-100) was further confirmed by ESI-MS. A mass spectral peak, detected at *m/z* 397.1852, was considered the corresponding experimental mass of the active fraction (**Figure 9**).

Microarray and Transcript Expression Analyses Exhibit Differential Expression of QS Regulatory Genes

Differential expression of quorum sensing regulatory genes of reference strain *P. aeruginosa* PAO1 treated with a bacterial fraction (C18-100) containing 1,2-benzenedicarboxylic acid, diisooctyl ester as a probable bioactive compound was analyzed

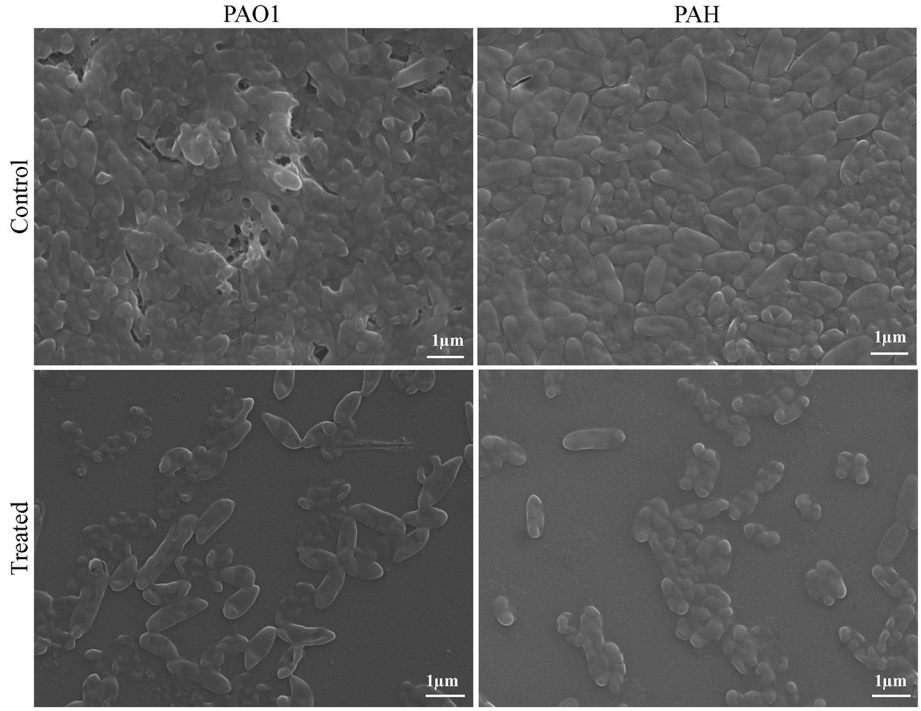

FIGURE 5 | SEM images of biofilms developed by *P. aeruginosa*. SEM images illustrating the effect of bacterial extract (0.1 mg/ml) on biofilm formation. A well-grown biofilm along with adhering bacterial cells was observed in control (normal biofilm developed by *P. aeruginosa*), whereas dispersed bacterial cells were observed in treated samples.

using *P. aeruginosa* PAO1 genome array gene chip. Out of the 5,886 gene probe sets, 1,434 genes were differentially expressed (**Table S1**; Array-Express accession E-MTAB-5693) and showed at least 2-fold up- (>2) or down-(< -2) expression at $p < 0.05$ (**Figure 10**). Of these, 734 genes were up-regulated, whereas 700 genes were down-regulated. Some differentially expressed important genes (as observed in microarray analysis) involved in the quorum sensing and general metabolic pathways are listed in **Table 2**. The microarray scattered plot showed the differential expression of genes; up-regulation of genes was indicated by blue marks whereas green-colored dots represented down-regulation (**Figure S7**). The quantitative RT-PCR revealed that the genes *LasI*, *LasR*, *RhlI,* and *RhlR* were down-regulated in the treated *P. aeruginosa* compared to the control (**Figure 10**). About, 9.7-, 3.9-, 3-, and 5.9-fold down-regulation of the genes *LasI*, *LasR*, *RhlI* and *RhlR*, respectively, was observed in *P. aeruginosa* PAO1 strain. Similarly, 5.7-, 3.1-, 5.2-, and 4-fold decrease in gene expression was found in *P. aeruginosa* PAH strain.

DISCUSSION

Natural products are an imperative source for the discovery of novel therapeutics, and microbes are therefore considered a primary source for drug discovery (Gillespie et al., 2002; Courtois et al., 2003). Biofilm forming bacteria are shown to be resistant toward a broad spectrum of antibiotics and make it difficult to cure biofilm-related infections (Høiby et al., 2010). It has been demonstrated that the social behavior of bacterial life depends on two interrelated phenomena: quorum sensing and biofilm formation (Nadell et al., 2008). Biofilm formation of pathogenic *P. aeruginosa* is controlled by the quorum sensing (QS) regulatory genes, and anti-quorum sensing compounds are explored to inhibit the biofilm formation. These compounds intervene in the QS mechanism and inhibit the expression of virulence factors. Recently, it has been shown that commercially available anti-QS compounds could increase the susceptibility of bacterial biofilm to antibiotics, both *in vitro* and *in vivo* (Brackman et al., 2008). Anti-QS properties have been reported from several rhizospheric bacteria, and *Stenotrophomona rhizosphila* reduced the AHL level (Christiaen et al., 2011). The rhizosphere of different plants (cucumber, tobacco, and ginger) was also exploited to isolate bacteria with anti-quorum sensing activity (Kang et al., 2004; D'Angelo-Picard et al., 2005; Chan et al., 2011). In this study, *D. tsuruhatensis* SJ01 was isolated from the rhizosphere of *C. laevigatus* L. collected from the coastal saline area. Previously, we have demonstrated that *Stenotrophomonas maltophilia*, isolated from *C. laevigatus* rhizosphere, showed quorum quenching and anti-biofilm forming activity (Singh et al., 2013).

Violacein production is a prerequisite for quorum sensing that leads to biofilm formation. A reference strain *C. violaceum* CV026 is well known for the production of violacein in the presence of external AHL and is widely used for quorum sensing studies. Extracts of *D. tsuruhatensis* SJ01 showed anti-QS activity

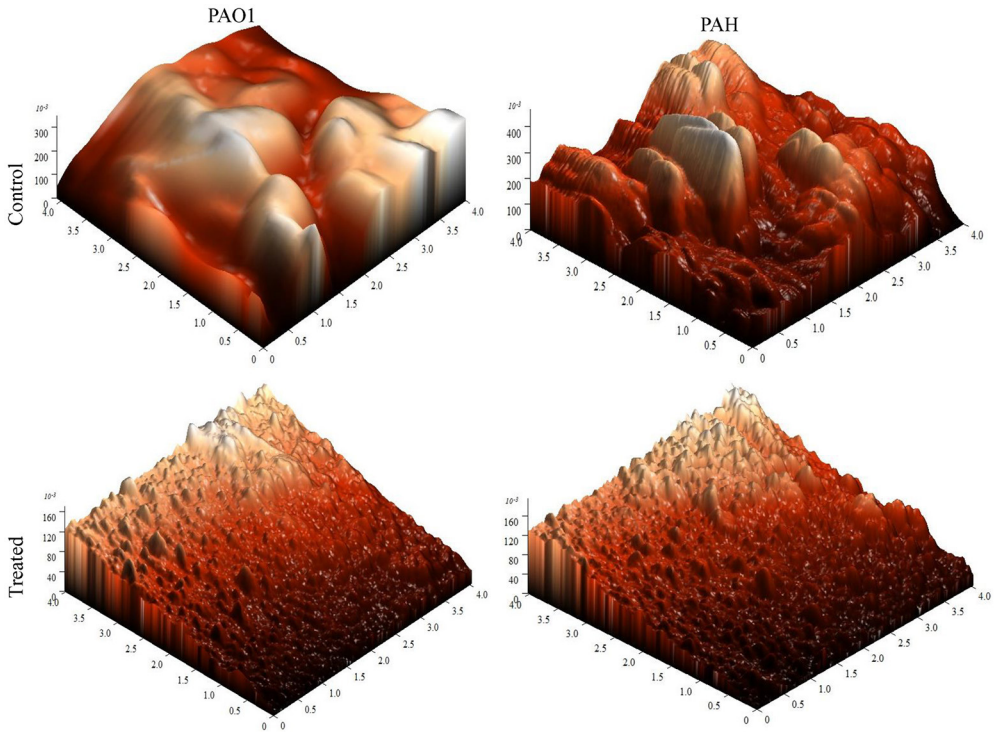

FIGURE 6 | AFM images illustrating the effect of *D. tsuruhatensis* SJ01 extract on *P. aeruginosa* biofilms. AFM showed a disrupt surface topology and height distribution profile of the biofilm developed by reference *P. aeruginosa* strains in the presence of bacterial extract (0.1 mg/ml) compared to the control biofilm.

TABLE 1 | Statistical analysis of biofilm analyzed by atomic force microscopy (AFM).

Statistical parameters	Control PAO1	Treated PAO1	Control PAH	Treated PAH
Root Mean Square (Sq)	0.06	0.04	0.08	0.04
Surface Bearing Index (Sbi)	2.22	1.06	0.74	0.94
Core Fluid Retention Index (Sci)	1.44	1.49	1.76	1.68
Valley Fluid Retention Index (Svi)	0.09	0.07	0.08	0.07
Kernel roughness depth (Sk)	0.20	0.12	0.20	0.12
Reduced peak height (Spk)	0.02	0.02	0.10	0.03
Reduced valley depth (Svk)	0.06	0.01	0.05	0.01
Roughness Average (Sa)	0.05	0.03	0.06	0.03
Surface skewness (Ssk)	0.22	0.09	0.41	0.26
Coefficient of kurtosis (Ska)	2.47	2.02	3.07	2.16
Surface Area Ratio (Sdr), %	0.03	0.01	0.09	0.03

against *C. violaceum* CV026 on biosensor plates (**Figure 1**) and inhibited violacein production in a concentration-dependent manner (**Figure 2**). About 98% inhibition of violacein production was detected with 0.1 mg/ml *D. tsuruhatensis* extract. However, it is difficult to compare the results with previous reports because of variation in the extraction methods and other parameters. About 90–94% reduction in the violacein production was reported with 3–4 mg/ml extract of *S. maltophilia* and *Melicope lunu-ankenda* extracts (Tan et al., 2012; Singh et al., 2013). Furthermore, the zone of inhibition was not observed when *D. tsuruhatensis* was spotted onto a plate containing *C. violaceum* culture (**Figure S1**). This rules out the possibility of antibacterial (*C. violaceum*) activity of *D. tsuruhatensis*. Inhibition of the AHL-dependent quorum sensing mechanism of CV026 (**Figure 2**) revealed the anti-quorum sensing potential of the extract at very low concentration (0.1 mg/ml).

The extract of *D. tsuruhatensis* SJ01 inhibits the biofilm formation of clinical isolates *P. aeruginosa* PAO1 as well as *P. aeruginosa* PAH (**Figure 3**) without affecting planktonic growth (**Figures S4**, **S5**). Strain PAO1 showed about 15% increase in planktonic cell growth (with a higher concentration of extracts), possibly because of the inability of strains to attach to

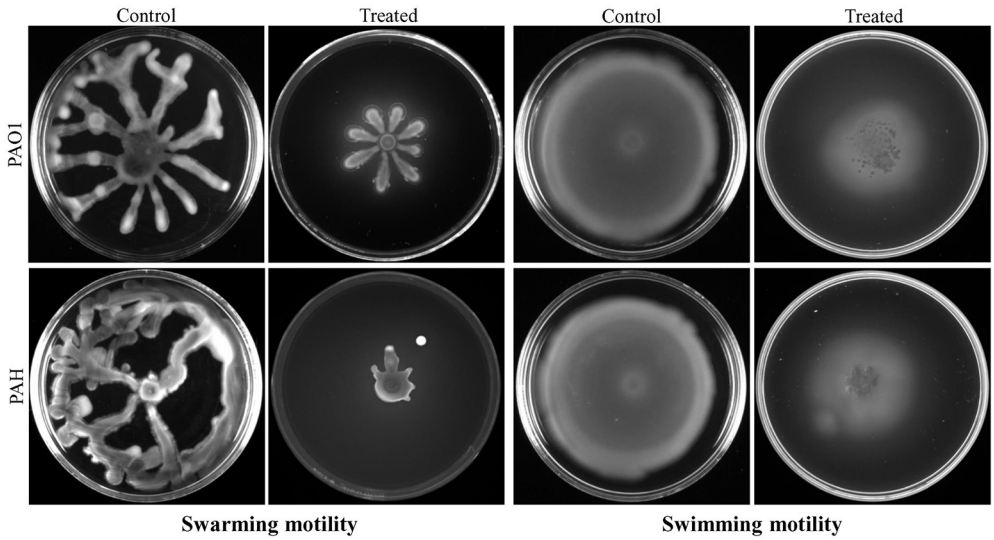

FIGURE 7 | Study of cell motility of *P. aeruginosa*. The effect of bacterial extract (*D. tsuruhatensis* SJ01) on the swarming and swimming motility of reference *P. aeruginosa* strains was studied. *P. aeruginosa* was spotted on a plate supplemented with (0.1 mg/ml) or without extract. Plates were analyzed after incubation of 24 h at 37 °C.

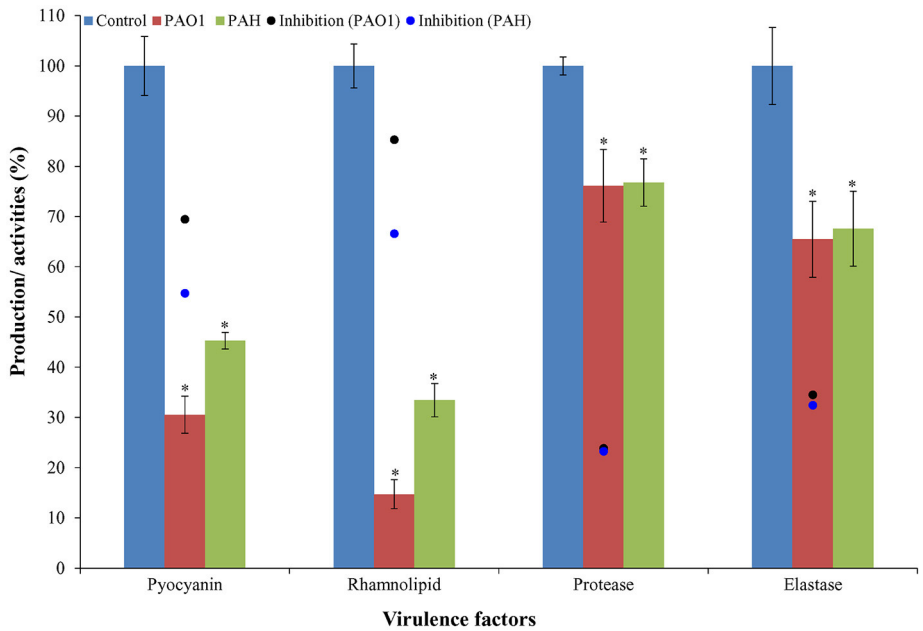

FIGURE 8 | Effect of *D. tsuruhatensis* SJ01 extract on the virulence factors of *P. aeruginosa*. The effect of bacterial extracts (SJ01; 0.1 mg/ml) was studied on the production of virulence factors of reference *P. aeruginosa* strains by quantifying pyocyanin and rhamnolipid, and analyzing elastase and protease activities. *Indicates significant differences from the control at $P < 0.05$.

the surface and subsequently to form a biofilm. This may lead to an increase of planktonic cell growth. However, a detailed study is required to ascertain the exact reason behind it. The viable *P. aeruginosa* cells were observed under epi-fluorescence microscopy (**Figure 4**) which confirmed that extract (SJ01) does not have a toxic effect on cells within the biofilm (**Figure 4**). The functional indices of biofilm exhibited physical characteristics (Ţălu, 2013). The AFM-based statistical analysis indicated a decrease in the bearing property, fluid retention and roughness of the biofilm (**Table 1**). The AFM topographs suggest full grown biofilm in control compared to treated conditions (**Figure 6**). Alterations in the physical property under treated conditions led

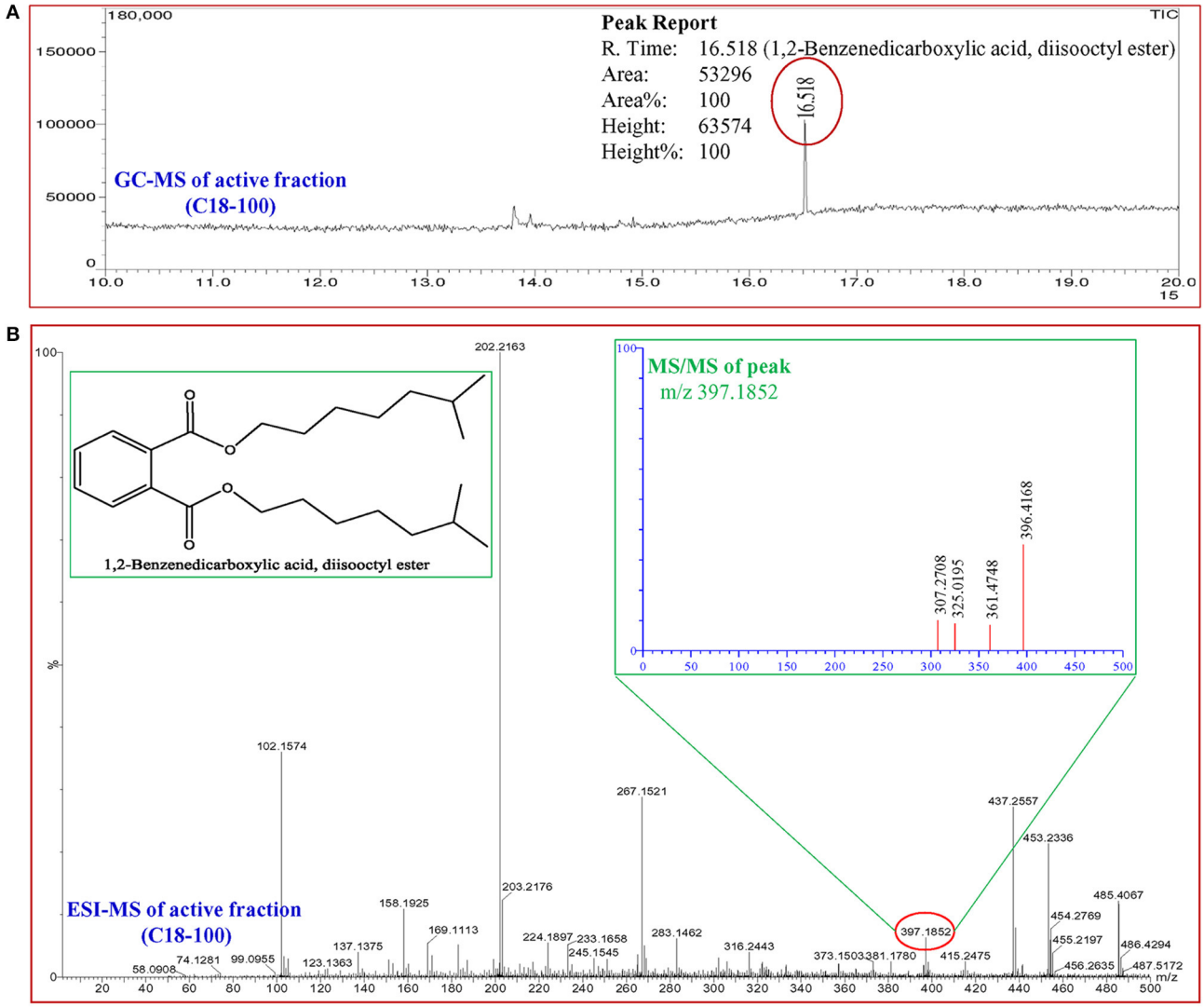

FIGURE 9 | Analysis of active fraction showing quorum sensing inhibition. **(A)** GC chromatograms and **(B)** ESI-MS/MS of the C18-100 active fraction of *D. tsuruhatensis* SJ01 extract and structure of 1,2-benzenedicarboxylic acid, diisooctyl ester (redrawn by ChemBioDraw Ultra 12.0).

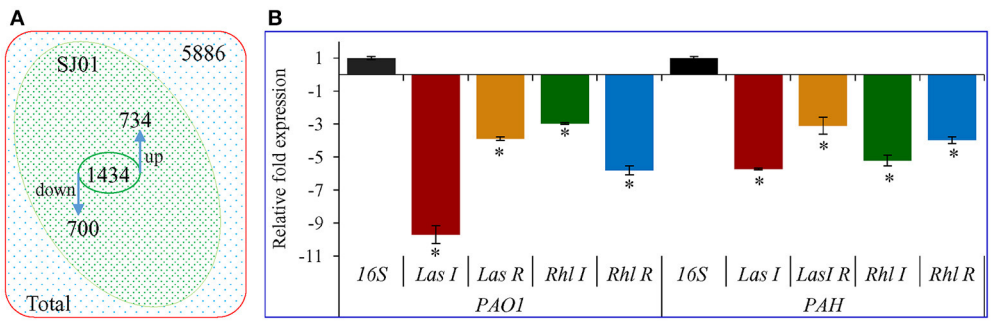

FIGURE 10 | Transcript expression analysis of *P. aeruginosa* treated with *D. tsuruhatensis* SJ01 extract. **(A)** Venn diagram showing genes differentially expressed in *P. aeruginosa* PAO1 as studied by microarray and **(B)** expression profiling of some QSI regulatory genes from *P. aeruginosa* (strains PAO1 and PAH). *Indicates significant differences from the control at $P < 0.05$.

TABLE 2 | Selected transcripts that differentially expressed (up- or down- regulated) in *P. aeruginosa* PAO1, treated with bacterial (*D. tsuruhatensis* SJ01) active fraction (C18-100; containing 1,2-benzenedicarboxylic acid, diisooctyl ester) compared with control (untreated PAO1 strain).

Transcript ID	Gene symbol	Description	Swiss Prot	Fold-change
PA1985	*pqqA*	Pyrroloquinoline quinone biosynthesis protein A	Q9ZAA0	−27.72
PA0998	*pqsC*	Homologous to beta-keto-acyl-acyl-carrier protein synthase	Q9I4X1	−8.94
PA2238	*pslH*	Hypothetical protein	Q9I1N1	−7.13
PA5368	*pstC*	Membrane protein component of ABC phosphate transporter	Q51544	−5.65
PA2236	*pslF*	Hypothetical protein	Q9I1N3	−5.41
PA1988	*pqqD*	Pyrroloquinoline quinone biosynthesis protein D	Q9I2C1	−3.9
PA5070	*tatC*	Transport protein TatC	Q9HUB3	−3.47
PA4225	*pchF*	Pyochelin synthetase	Q9HWG4	−2.79
PA3061	*pelD*	Hypothetical protein	Q9HZE7	−2.46
PA1989	*pqqE*	Pyrroloquinoline quinone biosynthesis protein E	Q9I2C0	−2.31
PA3477	*rhlR*	Transcriptional regulator RhlR	P54292	−2.22
PA2424	*pvdL*	Adaptation/ protection	Q9I157	2.76
PA5373	*betB*	Betaine aldehyde dehydrogenase	Q9HTJ1	2.79
PA1000	*pqsE*	Quinolone signal response protein	–	2.83
PA1003	*mvfR*	Transcriptional regulator	Q9I4X0	3.6
PA3103	*xcpR*	General secretion pathway protein	Q00512	4.14
PA1719	*pscF*	Type III export protein PscF	P95434	4.45
PA2245	*pslO*	Hypothetical protein	–	5.31
PA4205	*mexG*	Hypothetical protein	Q9HWH6	6.49
PA3058	*pelG*	Hypothetical protein	Q9HZF0	7.82
PA4085	*cupB2*	Chaperone protein	Q9HWU3	8.29

"–" sign means down-regulation.

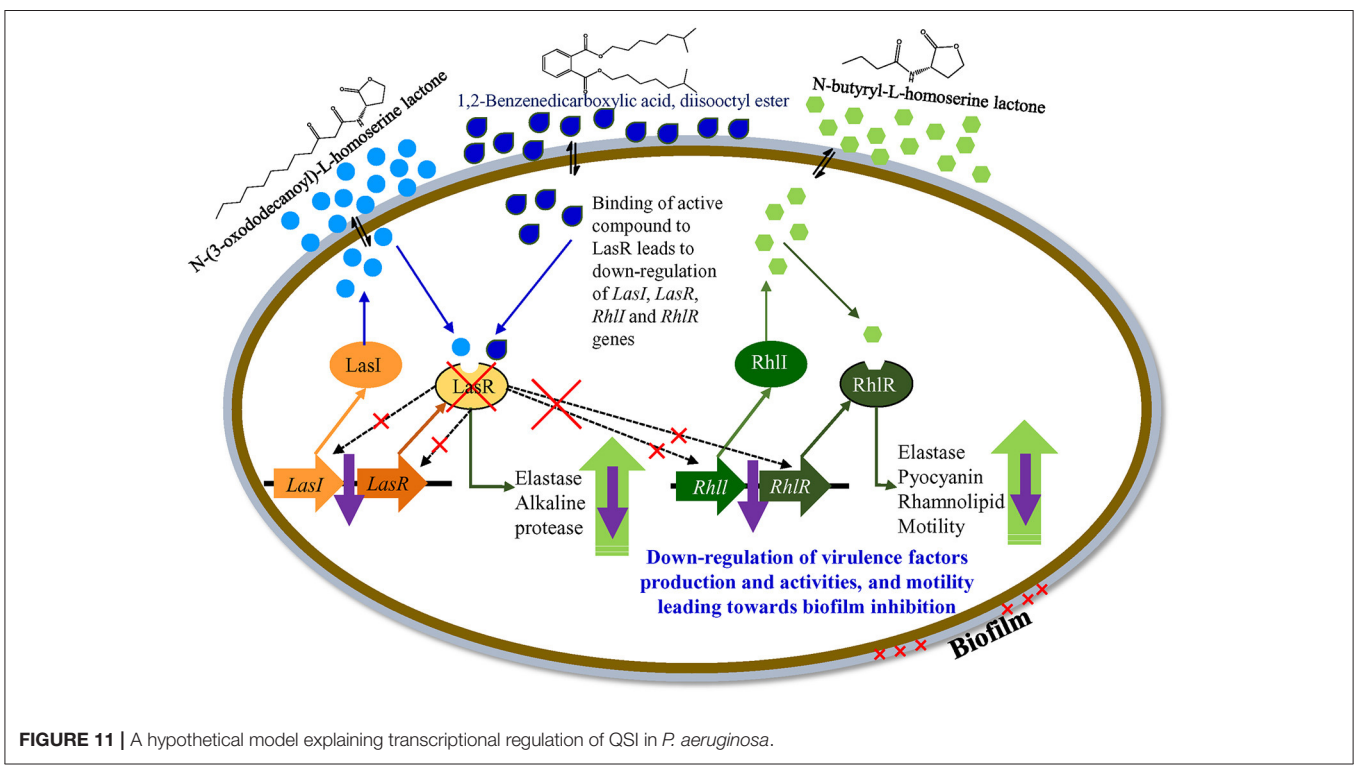

FIGURE 11 | A hypothetical model explaining transcriptional regulation of QSI in *P. aeruginosa*.

to loosely packed polymers which are not supportive for bacterial adherence; as a result, delicate biofilms are formed. Similarly, a discreet biofilm was visualized under a scanning electron microscopy (**Figure 5**). The steady decrease of biofilm formation was associated with an increase of extract concentration and about 60% biofilm inhibition was observed with 0.1 mg/ml SJ01

extract. The motility of bacteria plays a vital role in biofilm formation, for which bacteria need to attach to the surface or substratum. They utilize their flagellum driven motility to reach substratum; once attached to the surface, they were spared all around via swimming and swarming, which led to the biofilm formation (O'May and Tufenkji, 2011). The extract of SJ01 inhibits the motility of the *P. aeruginosa* (**Figure 7**) and thus decreases the possibility of biofilm formation.

A compound 1,2-benzenedicarboxylic acid, diisooctyl ester was identified in the active fraction of the SJ01 extract by GC-MS and ESI (**Figure 9**). A similar compound, 1,2-benzenedicarboxylic acid bis (2α-methylheptyl) ester, was isolated from *Alcaligenes faecalis* YMF 3.175 and reported to have antibacterial activity against *Escherichia coli* and *Staphylococcus aureus* (Zhu et al., 2011). The antibacterial activity was also reported for 1,2-benzenedicarboxylic acid, mono (2-ethylhexyl) ester isolated from the endophytic fungus *Muscodor tigerii* (Saxena et al., 2015). However, in this study, antibacterial activity was not detected for 1,2-benzenedicarboxylic acid, diisooctyl ester (**Figure 4** and **Figure S4**). Secondary infections caused by *P. aeruginosa* are difficult to eradicate due to their high levels of resistance to most conventional antibiotics. The challenge of combatting the infection becomes more complex due to the ability of the pathogen to form a biofilm matrix which protects bacterial cells from environmental stress as well as antibiotics (Driscoll et al., 2007; Lee and Zhang, 2015). It is the first report of anti-quorum sensing and anti-biofilm activity of 1,2-benzenedicarboxylic acid, diisooctyl ester on *P. aeruginosa* however, a detailed study is required to develop this compound as an anti-pathogenic drug for the treatment of the biofilm forming pathogenic bacteria.

Early colonization on host tissues is initiated by elastase and protease, whereas pyocyanin interferes with multiple cellular functions, chelates iron uptake, and promotes virulence expression (Lau et al., 2004; Stehling et al., 2008). The rhamnolipids facilitate surface motility of *P. aeruginosa* for biofilm formation and are also involved in the dispersal of mature biofilm (O'May and Tufenkji, 2011). Thus, the pathogenicity of *P. aeruginosa* depends on the virulence factor, and pyocyanin plays a key role in this infection (Lau et al., 2004). It was observed that pyocyanin production decreased by about 70 and 55% in strain PAO1 and PAH, respectively, by SJ01 extract (**Figure 8**). Furthermore, rhamnolipid, protease, and elastase are also regarded as important indicators for quorum sensing (Sarabhai et al., 2013). About 85 and 67% reduction of rhamnolipid production was noticed for *P. aeruginosa* PAO1 and PAH, respectively; however, a significant decrease (24–35%) was observed for protease and elastase activity by SJ01 extract (**Figure 8**). The production and activity of virulence factors is controlled by the *las* and *rhl* regulatory system in *P. aeruginosa* (De Kievit and Iglewski, 2000; Kohler et al., 2000).

The GeneChip probe array is a powerful tool for monitoring transcriptional regulation of any organism. The array used in this study represents the annotated genome of *P. aeruginosa* strain PAO1 and includes 5,549 protein-coding sequences, 18 tRNA genes, a representative of the ribosomal RNA cluster and 117 genes present in strains other than PAO1. The microarray analysis showed the differential expression of 1,434 genes and revealed that a large number of genes are directly or indirectly involved in biofilm formation (**Figure 10**, **Table 2**, and **Table S1**). Most of these genes are involved in quorum sensing, virulence, motility, and transport. Transcriptional regulators and hypothetical proteins were also differentially expressed and thus may play an important role in biofilm formation. The key genes, *LasI*, *LasR*, *RhlI,* and *RhlR,* were down-regulated in *P. aeruginosa* compared to the control (**Figure 10**).

The *las* regulatory system of *P. aeruginosa* consists of the LasI synthase protein and LasR transcriptional regulator. LasI is essential for the production of the AHL signal molecule N-(3-oxododecanoyl)-l-homoserine lactone (3O-C_{12}-HSL), and LasR requires 3O-C_{12}-HSL to become an active transcription factor (Gambello and Iglewski, 1991; Pearson et al., 1994; Kiratisin et al., 2002). A second QS system (of *P. aeruginosa*), *rhl*, is also comprised of the RhlI and RhlR proteins. RhlI synthase produces the AHL *N*-butyryl-L-homoserine lactone (C_4-HSL) and the transcriptional regulator RhlR becomes activated when complexed with C_4-HSL (Ochsner et al., 1994; Pearson et al., 1995). Both *lasR* and *rhlR* regulate the expression of several genes and activity including, pyocyanin, rhamnolipid, elastase, protease, and motility.

Based on the differential gene expression (microarray and qRT-PCR) of quorum sensing key regulatory gene(s) a theoretical model for the transcriptional regulatory mechanism in *P. aeruginosa* was inferred (**Figure 11**). The proposed model is just a schematic representation (based on available literature) in the form of a hypothetical model explaining transcriptional regulation of QSI in *P. aeruginosa*. However, a detailed study is needed to confirm the exact role of the identified compound in the QSI regulation mechanism. It was hypothesized that the identified compound 1,2-benzenedicarboxylic acid, diisooctyl ester (showing structural similarity with AHL) may compete with AHL and bind to LasR. Binding with LasR down-regulates the protease and elastase activity, along with expression of the *rhl* regulatory system. Down-regulation of the *rhl* QS system leads to the lower activity of pyocyanin and rhamnolipid production along with elastase, protease, and motility. Results indicate that the active compound may decrease the production of virulence factors through transcriptional regulation of the expression of *las* and *rhl* QS systems.

CONCLUSION

A bacterium, *D. tsuruhatensis* SJ01, isolated from the rhizosphere of *C. laevigatus* showed anti-quorum sensing and anti-biofilm activities. Furthermore, SJ01 extract does not possess anti-bacterial properties. A compound 1,2-benzenedicarboxylic acid, diisooctyl ester was identified as a probable active compound in the bacterial fraction. The compound inhibits the biofilm formation of clinical isolate *P. aeruginosa* PAO1 and human pathogenic strain *P. aeruginosa* PAH by decreasing the swimming and swarming motility and regulating virulence factors such as pyocyanin, rhamnolipid, elastase, and protease. The compound

may intervene in the QS system of *P. aeruginosa* and down-regulate the gene(s) responsible for the quorum sensing mechanism. Our results demonstrate that the active compound may target the QS systems. Targeting a QS system is important for therapeutics, and this may be used for the effective treatment of biofilm-related infection. The inhibitor may be a potent drug for the eradication of *P. aeruginosa* infections, and the active compound has the potential to be developed as an anti-pathogenic drug; however, a detailed study is still needed to investigate potential pharmaceutical applications.

AUTHOR CONTRIBUTIONS

Conceived and designed the experiments: AM and BJ; Performed the experiments: VS; Analyzed the data: VS and AM; Wrote the manuscript: AM and VS.

ACKNOWLEDGMENTS

CSIR-CSMCRI Communication No.: PRIS-15/2017. This study was supported by the Ministry of Earth Sciences (MoES), Government of India, New Delhi (Sanction No. MoES/16/06/2013-RDEAS). The funders had no role in study design, data collection, and analysis, decision to publish, or preparation of the manuscript. Authors are duly acknowledged Prof. Anton Hartmann (Helmholtz Zentrum, München, Germany) for providing reference strain *Chromobacterium violaceum* CV026. Authors are also thankful to Govt. Medical College, Bhavnagar (India) for giving clinical isolate *P. aeruginosa* PAH. Analytical Discipline and Centralized Instrument Facility of the Institute is duly acknowledged for running the samples.

SUPPLEMENTARY MATERIAL

The Supplementary Material for this article can be found online at: http://journal.frontiersin.org/article/10.3389/fcimb.2017.00337/full#supplementary-material

Figure S1 | Antibacterial disc diffusion assay of *D. tsuruhatensis* SJ01 against *C. violaceum* CV026. The Mueller-Hinton agar (MHA) plate containing reference strain *C. violaceum* CV026 were tested for antibacterial activity of *D. tsuruhatensis* SJ01. Strain SJ01 represents the culture (5 μl) and the antibiotic tobramycin (5 μl) was used as a positive control.

Figure S2 | Phylogenetic position of *D. tsuruhatensis* SJ01 (KX130769) with taxonomic neighbors. Numbers at nodes are percentage bootstrap values. The phylogenetic tress was computed using the maximum composite likelihood method and are in the units of the number of base substitutions per site. All positions containing gaps and missing data were eliminated by the complete deletion option. Phylogenetic analysis was conducted in MEGA (ver 6). Bar indicates 0.005 substitutions per nucleotide position.

Figure S3 | Whole cell fatty acid profiling of the bacterium *D. tsuruhatensis* SJ01. The whole cell fatty acid profile of strain SJ01 was performed by GC coupled with MIDI. The name of the fatty acids was assigned on the basis of corresponding fatty acids of RTSBA6 6.10 library match.

Figure S4 | Effect of extract of *D. tsuruhatensis* SJ01 extract on planktonic cell growth of *P. aeruginosa*. Different concentration of bacterial extracts (SJ01; 0.01−0.1 mg/ml) was tested against biofilm forming reference strain *P. aeruginosa* PAO1 and pathogenic strain *P. aeruginosa* PAH. Tests without extract and with methanol were considered as control and negative control, respectively.

Figure S5 | Effect of extract (0.1 mg/ml) of *D. tsuruhatensis* SJ01 extract on the growth curve of *P. aeruginosa*. Bacterial extracts (SJ01; 0.1 mg/ml) was tested for effect on growth of biofilm forming reference strain *P. aeruginosa* PAO1 and pathogenic strain *P. aeruginosa* PAH. The OD was taken up to 24 h at 600 nm using spectrophotometer. Growth of bacteria without treatment of extract (SJ01) was considered control.

Figure S6 | Antibacterial disc diffusion assay of *D. tsuruhatensis* SJ01 against *P. aeruginosa*. Clinical isolates of *P. aeruginosa* PAO1 and PAH were tested for antibacterial activity of *D. tsuruhatensis* SJ01 extract. The bacterial extract did not show any antibacterial activity against the clinical isolates *P. aeruginosa*.

Figure S7 | A microarray scattered plot showing differential expression of genes. Up- and down- regulation of genes are indicated by blue and green colored marks, respectively. The analysis was performed in expression console and transcriptome analysis console, and genes exhibiting significant fold expression (ANOVA $p < 0.05$) were considered for the study.

Table S1 | Total transcripts that differentially expressed (up- or down- regulated) in *P. aeruginosa* PAO1, treated with bacterial (*D. tsuruhatensis* SJ01) active fraction (C18-100; containing 1,2-benzenedicarboxylic acid, diisooctyl ester) compared with control (untreated PAO1 strain). Array-Express accession E-MTAB-5693.

REFERENCES

Adonizio, A., Kong, K. F., and Mathee, K. (2008). Inhibition of quorum sensing controlled virulence factor production in *Pseudomonas aeruginosa* by south florida plant extracts. *Antimicrob. Agents Chemother.* 52, 198–203. doi: 10.1128/AAC.00612-07

Andersson, S., Dalhammar, G., Land, C., and Rajarao, G. (2009). Characterization of extracellular polymeric substances from denitrifying organism *Comamonas denitrificans*. *Appl. Microbiol. Biotechnol.* 82, 535–543. doi: 10.1007/s00253-008-1817-3

Bakkiyaraj, D., Sivasankar, C., and Pandian, S. K. (2012). Inhibition of quorum sensing regulated biofilm formation in *Serratia marcescens* causing nosocomial infections. *Bioorg. Med. Chem. Lett.* 22, 3089–3094. doi: 10.1016/j.bmcl.2012.03.063

Bakkiyaraj, D., Sivasankar, C., and Pandian, S. K. (2013). Anti-pathogenic potential of coral associated bacteria isolated from Gulf of Mannar against *Pseudomonas aeruginosa*. *Indian J. Microbiol.* 53, 111–113. doi: 10.1007/s12088-012-0342-3

Brackman, G., Defoirdt, T., Miyamoto, C., Bossier, P., Calenbergh, S. V., Nelis, H., et al. (2008). Cinnamaldehyde and cinnamaldehyde derivatives reduce virulence in *Vibrio* spp. by decreasing the DNA-binding activity of the quorum sensing response regulator LuxR. *BMC Microbiol.* 8:149. doi: 10.1186/1471-2180-8-149

Chan, K., Atkinson, S., Mathee, K., Sam, C., Chhabra, S., Camara, M., et al. (2011). Characterization of N-acylho- moserine lactone-degrading bacteria associated with the *Zingiber officinale* (ginger) rhizosphere: co-existence of quorum quenching and quorum sensing Acinetobacter and Burkholderia. *BMC Microbiol.* 11:51. doi: 10.1186/1471-2180-11-51

Chen, W.-M., Lin, Y.-S., Sheu, D.-S., and Sheu, S.-Y. (2012). *Delftia litopenaei* sp. nov., a poly-β-hydroxybutyrate-accumulating bacterium isolated from a freshwater shrimp culture pond. *Int. J. Syst. Evol. Microbiol.* 62, 2315–2321. doi: 10.1099/ijs.0.037507-0

Choo, J., Rukayadi, Y., and Hwang, J. (2006). Inhibition of bacterial quorum sensing by vanilla extract. *Lett. Appl. Microbiol.* 42, 637–641. doi: 10.1111/j.1472-765x.2006.01928.x

Christiaen, S. E., Brackman, G., Nelis, H. J., and Coenye, T. (2011). Isolation and identification of quorum quenching bacteria from environmental samples. *J. Microbiol. Meth.* 87, 213–219. doi: 10.1016/j.mimet.2011.08.002

Christiaen, S. E., Matthijs, N., Zhang, X. H., Nelis, H. J., Bossier, P., and Coenye, T. (2014). Bacteria that inhibit quorum sensing decrease biofilm formation

and virulence in *Pseudomonas aeruginosa* PAO1. *Pathog. Dis.* 70, 271–279. doi: 10.1111/2049-632X.12124

Cirou, A., Diallo, S., Kurt, C., Latour, X., and Faure, D. (2007). Growth promotion of quorum-quenching bacteria in the rhizosphere of *Solanum tuberosum*. *Environ. Microbiol.* 9, 1511–1522. doi: 10.1111/j.1462-2920.2007.01270.x

Courtois, S., Cappellano, C. M., Ball, M., et al. (2003). Recombinant environmental libraries provide access to microbial diversity for drug discovery from natural products. *Appl. Environ. Microbiol.* 69, 49–55. doi: 10.1128/AEM.69.1.49-55.2003

D'Angelo-Picard, C., Faure, D., Penot, I., and Dessaux, Y. (2005). Diversity of N-acyl homoserine lactone-producing and degrading bacteria in soil and tobacco rhizosphere. *Environ. Microbiol.* 7, 1796–1808. doi: 10.1111/j.1462-2920.2005.00886.x

De Kievit, T. R., and Iglewski, B. H. (2000). Bacterial quorum sensing in pathogenic relationships. *Infect. Immun.* 68, 4839–4849. doi: 10.1128/IAI.68.9.4839-4849.2000

Driscoll, J. A., Brody, S. L., and Kollef, M. H. (2007). The epidemiology, pathogenesis, and treatment of *Pseudomonas aeruginosa* infections. *Drugs* 67, 351–368. doi: 10.2165/00003495-200767030-00003

Essar, D. W., Eberly, L., Hadero, A., and Crawford, I. P. (1990). Identification and characterization of genes for a second anthranilate synthase in *Pseudomonas aeruginosa*: interchangeability of the two anthranilate synthases and evolutionary implications. *J. Bacteriol.* 172, 884–900. doi: 10.1128/jb.172.2.884-900.1990

Felsenstein, J. (1985). Confidence limits on phylogenesis: an approach using the bootstrap. *Evolution* 39, 783–791. doi: 10.1111/j.1558-5646.1985.tb00420.x

Fuqua, C., and Greenberg, E. P. (1998). Self perception in bacteria: quorum sensing with acylated homoserine lactones. *Curr. Opin. Microbiol.* 2, 183–189. doi: 10.1016/S1369-5274(98)80009-X

Gambello, M. J., and Iglewski, B. H. (1991). Cloning and characterization of the *Pseudomonas aeruginosa* lasR gene, a transcriptional activator of elastase expression. *J. Bacteriol.* 173, 3000–3009. doi: 10.1128/jb.173.9.3000-3009.1991

Gillespie, D. E., Brady, S. F., Bettermann, A. D., et al. (2002). Isolation of antibiotics turbomycin A and B fromametagenomic library of soil microbial DNA. *Appl. Environ. Microb.* 68, 4301–4306. doi: 10.1128/AEM.68.9.4301-4306.2002

Goswami, N. N., Trivedi, H. R., Goswami, A. P. P., Patel, T. K., and Tripathi, C. B. (2011). Antibiotic sensitivity profile of bacterial pathogens in postoperative wound infections at a tertiary care hospital in Gujarat, India. *J. Pharmacol. Pharmacother.* 2, 158. doi: 10.4103/0976-500X.83279

Høiby, N., Bjarnsholt, T., Givskov, M., Molin, S., and Ciofu, O. (2010). Antibiotic resistance of bacterial biofilms. *Int. J. Antimicrob.* 35, 322–332. doi: 10.1016/j.ijantimicag.2009.12.011

Jha, B., Singh, V. K., Weiss, A., Hartmann, A., and Schmid, M. (2015). *Zhihengliuella somnathii* sp. nov., a halotolerant actinobacterium from the rhizosphere of a halophyte *Salicornia brachiata*. *Int. J. Syst. Evol. Microbiol.* 65, 3137–3142. doi: 10.1099/ijsem.0.000391

Jørgensen, N. O., Brandt, K. K., Nybroe, O., and Hansen, M. (2009). *Delftia lacustris* sp. nov., a peptidoglycan-degrading bacterium from fresh water, and emended description of *Delftia tsuruhatensis* as a peptidoglycan-degrading bacterium. *Int. J. Syst. Evol. Microbiol.* 59, 2195–2199. doi: 10.1099/ijs.0.008375-0

Kalia, V. C. (2012). Quorum sensing inhibitors: an overview. *Biotechnol. Adv.* 31, 224–245. doi: 10.1016/j.biotechadv.2012.10.004

Kalia, V. C., and Purohit, H. J. (2011). Quenching the quorum sensing system: potential antibacterial drug targets. *Crit. Rev. Microbiol.* 37, 121–140. doi: 10.3109/1040841X.2010.532479

Kang, B. R., Lee, J. H., Ko, S. J., Lee, Y. H., Cha, J. S., Cho, B. H., et al. (2004). Degradation of acyl-homoserine lactone molecules by *Acinetobacter* sp. strain C1010. *Can. J. Microbiol.* 50, 935–941. doi: 10.1139/w04-083

Kavita, K., Singh, V. K., Mishra, A., and Jha, B. (2014). Characterisation and anti-biofilm activity of extracellular polymeric substances from *Oceanobacillus iheyensis*. *Carbohydr. Polym.* 101, 39–35. doi: 10.1016/j.carbpol.2013.08.099

Keshri, J., Mishra, A., and Jha, B. (2013). Microbial population index and community structure in saline-alkaline soil using gene targeted metagenomics. *Microbiol. Res.* 168, 165–173. doi: 10.1016/j.micres.2012.09.005

Keshri, J., Yousuf, B., Mishra, A., and Jha, B. (2015). The abundance of functional genes, cbbL, nifH, amoA and apsA, and bacterial community structure of intertidal soil from Arabian Sea. *Microbiol. Res.* 175, 57–66. doi: 10.1016/j.micres.2015.02.007

Kiratisin, P., Tucker, K. D., and Passador, L. (2002). LasR, a transcriptional activator of *Pseudomonas aeruginosa* virulence genes, functions as a multimer. *J. Bacteriol.* 184, 4912–4919. doi: 10.1128/JB.184.17.4912-4919.2002

Kohler, T., Curty, L. K., Barja, F., Delden, C. V., and Pechere, J. C. (2000). Swarming of *Pseudomonas aeruginosa* is dependent on cell to cell signalling and requires flagella and pili. *J. Bacteriol.* 182, 5990–5996. doi: 10.1128/JB.182.21.5990-5996.2000

Lau, G. W., Hassett, D. J., Ran, H., and Kong, F. (2004). The role of pyocyanin in *Pseudomonas aeruginosa* infection. *Trends Mol. Med.* 10, 599–606. doi: 10.1016/j.molmed.2004.10.002

Lee, J., and Zhang, L. (2015). The hierarchy quorum sensing network in *Pseudomonas aeruginosa*. *Protein Cell* 6, 26–41. doi: 10.1007/s13238-014-0100-x

Li, C. T., Yan, Z. F., Chu, X., Hussain, F., Xian, W. D., Yunus, Z., et al. (2015). *Delftia deserti* sp. nov., isolated from a desert soil sample. *Antonie Van Leeuwenhoek* 107, 1445–1450. doi: 10.1007/s10482-015-0440-4

Livak, K. J., and Schmittgen, T. D. (2001). Analyses of relative gene expression data using real time quantitative PCR and the 2(-Delta Delta C (T) method. *Methods* 25, 402–408. doi: 10.1006/meth.2001.1262

McClure, C. D., and Schiller, N. L. (1992). Effects of *Pseudomonas aeruginosa* rhamnolipids on human monocyte-derived macrophages. *J. Leukocyte Biol.* 51, 97–102.

Nadell, C., Xavier, J., Levin, S., and Foster, K. (2008). The evolution of quorum sensing in bacterial biofilms. *PLoS Biol.* 6:e14. doi: 10.1371/journal.pbio.0060014

Ni, N., Li, M., Wang, J., and Wang, B. (2009). Inhibitors and antagonists of bacterial quorum sensing. *Med. Res. Rev.* 29, 65–124. doi: 10.1002/med.20145

Nithya, C., Begum, M. F., and Pandian, S. K. (2010). Marine bacterial isolates inhibit biofilm formation and disrupt mature biofilms of *Pseudomonas aeruginosa* PAO1. *Appl. Microbiol. Biotechnol.* 88, 341–358. doi: 10.1007/s00253-010-2777-y

Ochsner, U. A., Koch, A. K., Fiechter, A., and Reiser, J. (1994). Isolation and characterization of a regulatory gene affecting rhamnolipid biosurfactant synthesis in *Pseudomonas aeruginosa*. *J. Bacteriol.* 176, 2044–2054. doi: 10.1128/jb.176.7.2044-2054.1994

Oh, Y., Lee, N., Jo, W., Jung, W., and Lim, J. (2009). Effects of substrates on biofilm formation observed by atomic force microscopy. *Ultramicroscopy* 109, 874–880. doi: 10.1016/j.ultramic.2009.03.042

O'May, C., and Tufenkji, N. (2011). The swarming motility of *Pseudomonas aeruginosa* is blocked by cranberry proanthocyanidins and other tannin-containing materials. *Appl. Environ. Microbiol.* 77, 3061–3067. doi: 10.1128/AEM.02677-10

Oncul, O., Ulkur, E., Acar, A., Turhan, V., Yeniz, E., Karacaer, Z., et al. (2009). Prospective analysis of nosocomial infections in a burn care unit, Turkey. *Indian J. Med. Res.* 130, 758–764. Available online at: http://icmr.nic.in/ijmr/2009/december/1214.pdf

Overhage, J., Lewenza, S., Marr, A. K., and Hancock, R. E. (2007). Identification of genes involved in swarming motility using a *Pseudomonas aeruginosa* PAO1 Mini-Tn5-lux mutant library. *J. Bacteriol.* 189, 2164–2169. doi: 10.1128/JB.01623-06

Pearson, J. P., Gray, K. M., Passador, L., Tucker, K. D., Eberhard, A., Iglewski, B. H., et al. (1994). Structure of the autoinducer required for expression of *Pseudomonas aeruginosa* virulence genes. *Proc. Natl. Acad. Sci. U.S.A.* 91, 197–201. doi: 10.1073/pnas.91.1.197

Pearson, J. P., Passador, L., Iglewski, B. H., and Greenberg, E. P. (1995). A second N-acylhomoserine lactone signal produced by *Pseudomonas aeruginosa*. *Proc. Natl. Acad. Sci. U.S.A.* 92, 1490–1494. doi: 10.1073/pnas.92.5.1490

Rahme, L. G., Ausubel, F. M., Cao, H., Drenkard, E., Goumnerov, B. C., Lau, G. W., et al. (2000). Plants and animals share functionally common bacterial virulence factors. *Proc. Natl. Acad. Sci. U.S.A.* 97, 8815–8821. doi: 10.1073/pnas.97.16.8815

Rashid, M. H., and Kornberg, A. (2000). Inorganic polyphosphate is needed for swimming, swarming, and twitching motilities of *Pseudomonas aeruginosa*. *Proc. Natl. Acad. Sci. U.S.A.* 97, 4885–4890. doi: 10.1073/pnas.060030097

Saitou, N., and Nei, M. (1987). The neighbor-joining method: a new method for reconstructing phylogenetic trees. *Mol. Biol. Evol.* 4, 406–425.

Sarabhai, S., Sharma, P., and Capalash, N. (2013). Ellagic acid derivatives from terminalia chebula retz. Downregulate the expression of quorum sensing genes to attenuate *Pseudomonas aeruginosa* PAO1 virulence. *PLoS ONE* 8:e53441. doi: 10.1371/journal.pone.0053441

Saxena, S., Meshram, V., and Kapoor, N. (2015). *Muscodor tigerii* sp. nov.-Volatile antibiotic producing endophytic fungus from the Northeastern Himalayas. *Ann. Microbiol.* 65, 47–57. doi: 10.1007/s13213-014-0834-y

Shigematsu, T., Yumihara, K., Ueda, Y., Numaguchi, M., Morimura, S., and Kida, K. (2003). *Delftia tsuruhatensis* sp. nov., a terephthalate-assimilating bacterium isolated from activated sludge. *Int. J. Syst. Evol. Microbiol.* 53, 1479–1483. doi: 10.1099/ijs.0.02285-0

Singh, V. K., Kavita, K., Prabhakaran, R., and Jha, B. (2013). Cis-9-octadecenoic acid from the rhizospheric bacterium *Stenotrophomonas maltophilia* BJ01 shows quorum quenching and anti-biofilm activities. *Biofouling* 29, 855–867. doi: 10.1080/08927014.2013.807914

Singh, V. K., Mishra, A., Haque, I., and Jha, B. (2016a). A novel transcription factor-like gene SbSDR1 acts as a molecular switch and confers salt and osmotic endurance to transgenic tobacco. *Sci. Rep.* 6:31686. doi: 10.1038/srep31686

Singh, V. K., Mishra, A., and Jha, B. (2016b). "Marine bacterial extracellular polymeric substances: characteristics and applications," in *Marine Glycobiology: Principles and Applications,* ed S. Kim (Boca Raton, FL: Taylor and Francis Group; CRC Press), 369–377. doi: 10.1201/9781315371399-27

Stehling, E. G., da Silveira, W. D., and da Silva Leite, D. (2008). Study of biological characteristics of *Pseudomonas aeruginosa* strains isolated from patients with cystic fibrosis and from patients with extra-pulmonary infections. *Braz. J. Infect. Dis.* 12, 86–88. doi: 10.1590/S1413-86702008000100018

Ţălu, Ş. (2013). Characterization of surface roughness of unworn hydrogel contact lenses at a nanometric scale using methods of modern metrology. *Polym. Eng. Sci.* 53, 2141–2150. doi: 10.1002/pen.23481

Tamura, K., Nei, M., and Kumar, S. (2004). Prospects for inferring very large phylogenies by using the neighbor-joining method. *Proc. Natl. Acad. Sci. U.S.A.* 101, 11030–11035. doi: 10.1073/pnas.0404206101

Tamura, K., Stecher, G., Peterson, D., Filipski, A., and Kumar, S. (2013). MEGA6: molecular evolutionary genetics analysis version 6.0. *Mol. Biol. Evol.* 30, 2725–2729. doi: 10.1093/molbev/mst197

Tan, L. Y., Yin, W. F., and Chan, K. G. (2012). Silencing quorum sensing through extracts of *Melicope lunu-ankenda*. *Sensors* 12, 4339–4351. doi: 10.3390/s120404339

Vandeputte, O. M., Kiendrebeogo, M., Rajaonson, S., Diallo, B., Mol, A., El Jaziri, M., et al. (2010). Identification of catechin as one of the flavonoids from Combretum albiflorum bark extract that reduces the production of quorum-sensing-controlled virulence factors in *Pseudomonas aeruginosa* PAO1. *Appl. Environ. Microbiol.* 76, 243–253. doi: 10.1128/AEM.01059-09

Wang, E. W., Jung, J. Y., Pashia, M. E., Nason, R., Scholnick, S., and Chole, R. A. (2005). Otopathogenic *Pseudomonas aeruginosa* strains as competent biofilm formers. *Arch. Otolaryngol. Head Neck Surg.* 131, 983–989. doi: 10.1001/archotol.131.11.983

Weisburg, W. G., Barns, S. M., Pelletier, D. A., and Lane, D. J. (1991). 16S ribosomal DNA amplification for phylogenetic study. *J. Bacteriol.* 173, 697–703. doi: 10.1128/jb.173.2.697-703.1991

Wen, A., Fegan, M., Hayward, C., Chakraborty, S., and Sly, L. I. (1999). Phylogenetic relationships among members of the Comamonadaceae, and description of *Delftia acidovorans* (den Dooren de Jong 1926 and Tamaoka et al. 1987) gen. nov., comb. nov. *Int. J. Syst. Evol. Microbiol.* 49, 567–576. doi: 10.1099/00207713-49-2-567

Zhu, H., He, C.-C., and Chu, Q.-H. (2011). Inhibition of quorum sensing in *Chromobacterium violaceum* by pigments extracted from *Auricularia auricular*. *Lett. Appl. Microbiol.* 52, 269–274. doi: 10.1111/j.1472-765X.2010.02993.x

Zhu, H., Thuruthyl, S. J., and Willcoxd, M. D. P. (2002). Determination of quorum-sensing signal molecules and virulence factors of *Pseudomonas aeruginosa* isolates from contact lens-induced microbial keratitis. *J. Med. Microbiol.* 51, 1063–1070. doi: 10.1099/0022-1317-51-12-1063

Conflict of Interest Statement: The authors declare that the research was conducted in the absence of any commercial or financial relationships that could be construed as a potential conflict of interest.

frontiers in Cellular and Infection Microbiology

ORIGINAL RESEARCH
published: 25 October 2018
doi: 10.3389/fcimb.2018.00351

Seed Extract of *Psoralea corylifolia* and Its Constituent Bakuchiol Impairs AHL-Based Quorum Sensing and Biofilm Formation in Food- and Human-Related Pathogens

Fohad Mabood Husain[1,2], Iqbal Ahmad[1]*, Faez Iqbal Khan[3], Nasser A. Al-Shabib[1], Mohammad Hassan Baig[4], Afzal Hussain[5], Md Tabish Rehman[5], Mohamed F. Alajmi[5] and Kevin A. Lobb[3]*

[1] Department of Food Science and Nutrition, College of Food and Agriculture Sciences, King Saud University, Riyadh, Saudi Arabia, [2] Department of Agricultural Microbiology, Aligarh Muslim University, Aligarh, India, [3] Department of Chemistry, Rhodes University, Grahamstown, South Africa, [4] School of Biotechnology, Yeungnam University, Gyeongsan, South Korea, [5] Department of Pharmacognosy, College of Pharmacy, King Saud University, Riyadh, Saudi Arabia

OPEN ACCESS

Edited by:
Rodolfo García-Contreras, Universidad Nacional Autónoma de México, Mexico

Reviewed by:
Marcos Soto Hernandez, Colegio de Postgraduados (COLPOS), Mexico
Hafizah Yousuf Chenia, University of KwaZulu-Natal, South Africa

***Correspondence:**
Iqbal Ahmad
ahmadiqbal8@yahoo.co.in
Fohad Mabood Husain
fhussain@ksu.edu.sa; fahadamu@gmail.com

Specialty section:
This article was submitted to Molecular Bacterial Pathogenesis, a section of the journal Frontiers in Cellular and Infection Microbiology

Received: *03 March 2018*
Accepted: *14 September 2018*
Published: *25 October 2018*

Citation:
Husain FM, Ahmad I, Khan FI, Al-Shabib NA, Baig MH, Hussain A, Rehman MT, Alajmi MF and Lobb KA (2018) Seed Extract of Psoralea corylifolia and Its Constituent Bakuchiol Impairs AHL-Based Quorum Sensing and Biofilm Formation in Food- and Human-Related Pathogens. Front. Cell. Infect. Microbiol. 8:351. doi: 10.3389/fcimb.2018.00351

The emergence of multi-drug resistance in pathogenic bacteria in clinical settings as well as food-borne infections has become a serious health concern. The problem of drug resistance necessitates the need for alternative novel therapeutic strategies to combat this menace. One such approach is targeting the quorum-sensing (QS) controlled virulence and biofilm formation. In this study, we first screened different fractions of *Psoralea corylifolia* (seed) for their anti-QS property in the *Chromobacterium violaceum* 12472 strain. The methanol fraction was found to be the most active fraction and was selected for further bioassays. At sub-inhibitory concentrations, the *P. corylifolia* methanol fraction (PCMF) reduced QS-regulated virulence functions in *C. violaceum* CVO26 (violacein); *Pseudomonas aeruginosa* (elastase, protease, pyocyanin, chitinase, exopolysaccharides (EPS), and swarming motility), *A. hydrophila* (protease, EPS), and *Serratia marcescens* (prodigiosin). Biofilm formation in all the test pathogens was reduced significantly ($p \leq 0.005$) in a concentration-dependent manner. The β-galactosidase assay showed that the PCMF at 1,000 μg/ml downregulated *las*-controlled transcription in PAO1. *In vivo* studies with *C. elegans* demonstrated increased survival of the nematodes after treatment with the PCMF. Bakuchiol, a phytoconstituent of the extract, demonstrated significant inhibition of QS-regulated violacein production in *C. violaceum* and impaired biofilm formation in the test pathogens. The molecular docking results suggested that bakuchiol efficiently binds to the active pockets of LasR and RhlR, and the complexes were stabilized by several hydrophobic interactions. Additionally, the molecular dynamics simulation of LasR, LasR–bakuchiol, RhlR, and RhlR–bakuchiol complexes for 50 ns revealed that the binding of bakuchiol to LasR and RhlR was fairly stable. The study highlights the anti-infective potential of the PCMF and bakuchiol instead of bactericidal or bacteriostatic action, as the extract targets QS-controlled virulence and the biofilm.

Keywords: ***Psoralea corylifolia*, bakuchiol, quorum sensing, biofilm, molecular dynamics simulation**

INTRODUCTION

Quorum sensing (QS) is a density-dependent phenomenon facilitating the coordinated regulation of gene expression in bacteria (Winans and Bassler, 2002). N-acyl homoserine lactone (AHL) based QS systems in gram-negative bacteria are the most studied (Wu et al., 2004). With increasing population densities, AHL levels increase and reach threshold concentrations that allow binding to specific regulators, and the resulting complexes then regulate the expression of various genes (Papenfort and Bassler, 2016). Various food- and human-related pathogens employ QS to regulate genes that code for virulence, production of secondary metabolites, plasmid transfer, motility, and biofilm formation (Williams, 2007; Whiteley et al., 2017). Since QS controls virulence, pathogenicity, and biofilm formation, interfering with QS offers an alternative therapeutic strategy that targets the functions that are not essential for the survival of the bacteria and therefore are subject to less selective pressures as observed for conventional drugs (Bjarnsholt and Givskov, 2008; Lowery et al., 2010). Interfering with the bacterial communication forces the bacteria to reside as individuals fending for themselves, whereas the bacteria residing and functioning as a group build strong defense that an individual bacterium finds impossible to achieve (Rasmussen and Givskov, 2006). This strategy of targeting the functions of bacteria that are responsible for pathogenesis rather than growth have been termed as "antivirulence" or "antipathogenesis" therapies (LaSarre and Federle, 2013; de la Fuente-Núñez et al., 2014).

The first QS inhibitory activity was determined in furanones isolated from *Delisea pulchra*, a seaweed (Rasmussen et al., 2000). Numerous QS inhibitors (QSIs) have been reported since the discovery of furanones, and few have been tested in animal models with great success. Unfortunately, studies showed that these compounds are unstable and toxic, and hence, unsuitable for human use (Rasmussen and Givskov, 2006). Therefore, there is an urgent need to search for other safe and stable anti-QS agents.

The use of medicinal plants has increased considerably in the last decade or so, with an estimated 80% of the populations mostly from developing countries relying on traditional medicines for their primary health care (Ahmad et al., 2006; WHO, 2011, 2012). Recently, an increased interest has been shown by the scientific community to screen and search anti-QS activity from natural products (Husain and Ahmad, 2013; Kalia, 2013; Reen et al., 2018). QS inhibitors have also been reported in various natural products including extracts of medicinal plants (Adonizio et al., 2006, 2008a; Omwenga et al., 2017), fruits and spices (Huerta et al., 2008; Abraham et al., 2012; Husain et al., 2015a, 2017), and phytocompounds (Vandeputte et al., 2010, 2011; Husain et al., 2015b; Al-Yousef et al., 2017; Musthafa et al., 2017).

Psoralea corylifolia (Fabaceae) is an annual herb that is widely used both in Ayurvedic as well as in Chinese traditional medicine as a cardiac tonic, vasodilator, and pigment and has antitumor, antibacterial, cytotoxic, and anthelminthic effects. The seeds of *P. corylifolia* are used for its laxative, aphrodisiac, anthelminthic, diuretic, and diaphoretic effects for febrile patients in the traditional system of medicine (Chopra et al., 2013).

Keeping in mind the medicinal properties of *P. corylifolia*, in the present investigation, we screened different fractions of *P. corylifolia* (seed) for their QS inhibition in *Chromobacterium violaceum*. The most active fraction and its major phytoconstituent were selected for further studies on QS-controlled virulence and biofilm formation in various food- and human-related pathogens.

MATERIALS AND METHODS

Bacterial Strains

The bacterial strains under study were *Pseudomonas aeruginosa* PAO1, *P. aeruginosa* PAF79, *C. violaceum* ATCC 12472, *C. violaceum* CVO26, Aeromonas hydrophila WAF38, *Serratia marcescens*, and Listeria monocytogenes (laboratory strains). All strains were maintained on the Luria Bertani (LB) broth solidified with 1.5% agar (Oxoid).

Collection of Plant Material and Extraction

Psoralea corylifolia (PC) seeds were obtained from The Himalaya Drug Company, Dehradun (Uttarakhand). Seeds of PC were ground to powder and extracted sequentially by the method described by Husain et al. (2015a). First, the petroleum ether fraction was dried using a rotary evaporator at 40°C followed by successive sequential extraction with other solvents (benzene, ethyl acetate, acetone, and methanol). Each of the dried fraction was collected and stored at 4°C and reconstituted in DMSO (0.1%) for experimental use.

Screening of Fractions for Quorum Sensing Inhibition

The standard method of McLean et al. (2004) was adopted to screen *P. corylifolia* for anti-QS activity. LB agar plates were overlaid with 5 ml LB soft agar containing 10^6 CFU/ml of *C. violaceum* ATCC 12472. Wells of 8 mm size were punched and sealed with 1–2 drops of molten agar (0.8% agar). The wells were loaded with different concentrations of 100 μl of plant extract. A solvent blank was used as the negative control. The inhibition of purple pigmentation in *C. violaceum* ATCC 12472 around the disk impregnated with the extract was considered as positive anti-QS.

Determination of Minimum Inhibitory Concentration (MIC)

The minimum inhibitory concentration (MIC) of the PC seed extract against test bacteria was determined by using the micro broth dilution method, described by Eloff (1998).

Effect of Sub-MICS of Methanol Fraction on Violacein Production in *Chromobacterium violaceum* CVO26

Overnight-grown *C. violaceum* CV026 (OD_{600nm} = 0.1) was inoculated to Erlenmeyer flasks containing LB, LB supplemented with C6-HSL (10 μM/l), and LB supplemented with C6-HSL and sub-MICs of the extract. The flasks containing treated and untreated CVO26 were incubated at 27°C with 150 rev/min agitation for 24 h (Choo et al., 2006). The effect of the seed extract on violacein production in *C. violaceum*

(CVO26) was determined using the method of Blosser and Gray (2000).

Effect of Sub-MICS of Methanol Fraction on QS-Regulated Virulence

The sub-MICs of the methanol fraction of *P. corylifolia* (seed) were used to study the QS-regulated virulence functions in *P. aeruginosa* [LasB, pyocyanin, protease, chitinase, swarming motility, and exopolysaccharide (EPS) production], *A. hydrophila* (protease and EPS production), and *S. marcescens* (prodigiosin). The method of Husain et al. (2015a) was adopted to study the virulence functions in *P. aeruginosa* and *A. hydrophila*, while the determination of prodigiosin was performed by adopting the protocol described by Morohoshi et al. (2007).

Assay for Biofilm Inhibition

The effect of the sub-MICs of the PCMF on biofilm formation was studied using the microtiter plate (MTP) assay (O'Toole and Kolter, 1998). Briefly, overnight-grown test bacteria were resuspended in a fresh LB medium in the presence and the absence of sub-MICs of the PCMF and incubated at 30°C for 24 h. The biofilm inhibition in the MTP was determined by crystal violet staining and measuring the absorbance at OD_{470nm}.

β-Galactosidase Assay

The β-galactosidase reporter activity was assayed as described by Husain et al. (2015b). Briefly, a supernatant of overnight cultures of PAO1 grown in the presence and absence of the sub-MICs of the PCMF was extracted with ethyl acetate for AHLs. Then, 0.5 ml of the extracted supernatant and 2 ml of the *E. coli* MG4 (pKDT17) (Zhou et al., 2013) strain were incubated at 30°C in a water bath rotating at 100 rpm for 5 h. The cells were centrifuged (3,200 g for 15 min) and the resultant cell pellet was suspended in an equal volume of the Z-buffer ($Na_2HPO_4.7H_2O$, 0.06 M; $NaH_2PO_4.H_2O$, 0.04 M; KCl, 0.01 M; $MgSO_4.7H_2O$, 0.001 M; β-mercaptoethanol, 0.05 M; pH 7.0). To lyse the cells, 1 ml of cell suspension, 1ml of the Z-buffer, 200 μl of chloroform, and 100 μl of 0.1% sodium dodecyl sulfate were added; further, 0.4 ml of O-nitrophenol-β-D-galactopyranoside was also added. To stop the reaction after the development of yellow color, 1 ml of 1 M Na_2CO_3 was used. Optical density (OD) was measured at 420 and 550 nm. The units of β-galactosidase were calculated as $1{,}000 \times OD_{420nm}-(1.75 \times OD_{550nm})/\text{time} \times \text{volume} \times OD_{600nm}$.

Caenorhabditis Elegans Survival Assay

The method described by Musthafa et al. (2012) was adopted to study the antipathogenic potential of the PCMF *in vivo* in the *C. elegans* nematode model. Briefly, PAO1-infected nematodes were incubated at 25°C for 12 h. Incubated *C. elegans* were washed thrice with the M9 buffer to remove surface-bound bacteria. Approximately ten PAO1-infected worms were transferred to the wells of the MTP containing the PCMF treatment/untreated 10% LB broth in the M9 buffer and incubated at 25°C. Every 12 h, the plate was scored for live and dead worms. *C. elegans* with the PCMF was maintained to assess the toxicity, if any.

Total Phenolic Content of PCMF

The total phenolic content of the PCMF was determined by the method of Spanos and Wrolstad (1990), as modified by Lister and Wilson (2001).

Gas Chromatography–Mass Spectrometry (GC–MS) Analysis of PCMF

The compositions of the PCMF were analyzed by using the Perkin Elmer GC AutoSystem XL and TurboMass software as described previously by Husain et al. (2015a). The components were identified by the method described by Masada (1976). Quantitative data were obtained by the peak normalization technique using the integrated flame ionization detector (FID) response.

Molecular Docking Analysis

The knowledge of protein three-dimensional (3D) structures are vital for rational drug design (Stephens et al., 2014; Khan et al., 2017a; Lan et al., 2017; Zhao et al., 2017). The 3D structure of RhlR was predicted using homology. Molecular docking studies were carried out to understand the proper positioning of drugs into the active pocket of a receptor to understand the mechanism of substrate binding and selectivity (Khan et al., 2015, 2016a). The molecular docking of bakuchiol was performed using LasR (PDB: 2UV0) and the homology-modeled structure of Rh1R as receptors. The 3D structure of bakuchiol was obtained from PubChem with compound identifier 5468522. The docking studies were performed to understand the bound confirmations and the binding affinity of bakuchiol with LasR and Rh1R. Bakuchiol was docked by describing the grid box with a spacing of 1 Å and size of 20 × 20 × 20, pointing in x, y, and z directions around the active pocket of protein following the standard docking protocol (Cosconati et al., 2010; Khan et al., 2017b) by using AutoDockTools and AutoDockVina (Trott and Olson, 2010) with default docking parameters. The Lamarckian genetic algorithm was selected as the search algorithm. The most apposite docked conformation was selected for the analysis. PyMol (Rigsby and Parker, 2016), Discovery Studio Visualizer (Biovia, 2015), and LigPlot$^+$ (Laskowski and Swindells, 2011) were used for visualizing the docked complex. Further, the selected docked complex was subjected to molecular dynamics (MD) simulations to validate the stability of the docked complex.

MD Simulations

MD simulations were performed on the LasR, LasR–bakuchiol, Rh1R, and Rh1R–bakuchiol complexes using the GROMOS96 43a1 force-field at 300 *K* using GROMACS 5.1.2 (Van Der Spoel et al., 2005). Bakuchiol was extracted from the docked complexes such as LasR–bakuchiol and Rh1R–bakuchiol using the *gmx grep* command. The force-field parameter and the topology files of bakuchiol were generated using the PRODRG server (Schüttelkopf and van Aalten, 2004). The charges in the topology file were properly corrected. The topologies of LasR and Rh1R using the *pdb2gmx* modules of GROMACS, and that of bakuchiol using the PRODRG server were combined and a further 24 atoms of bakuchiol were included. The bakuchiol parameter

was incorporated in the system topology file. The individual protein atoms and complexes were soaked with water molecules in a cubic box having a dimension of 10 Å, i.e., box edge of 10 Å from the molecule periphery. The modules *gmx editconf* and *gmx solvate* modules were used for creating the boundary conditions and for solvation, respectively. The simple point-charge (spc216) water model was used to solvate the protein and the complex.

The *gmx genion* module was used to counterbalance the charges on LasR and LasR–bakuchiol. The Rh1R and Rh1R–bakuchiol complexes were counterbalanced by the addition of Na^+ and Cl^- ions to maintain neutrality and preserve a physiological concentration of 0.15 M. For the LasR–bakuchiol and Rh1R–bakuchiol complexes, bakuchiol was added to the energy groups of the molecular dynamics parameters (mdp) file, to inspect the interactions of bakuchiol with LasR and Rh1R, respectively. The final system was minimized using the steepest descent method, and the temperature was then elevated from 0 to 300 K during the equilibration period of 100 ps at a constant volume under periodic boundary conditions.

The restraints to the bakuchiol were applied during the NVT equilibration period using the *genrestr* module, and then the treatment of the temperature coupling groups. Two-phase equilibrations were achieved: the NVT ensemble with a constant number of particles, volume, and temperature at 100 ps, and the NPT ensemble with a constant number of particles, pressure, and temperature at 100 ps. The C^{α} backbone atoms of the structure were restrained, and all other atoms were allowed to move freely during equilibration steps. The particle-mesh Ewald method (Norberto de Souza and Ornstein, 1999) was applied after the equilibration steps, and the 100 ns production phases were carried out at 300 *K*. The results were analyzed using the *gmx energy*, *gmx rms*, *gmx confirms*, *gmx rmsf*, *gmx gyrate*, *make_ndx*, *gmx hbond*, *gmx do_dssp*, and *gmx sasa* utilities of GROMACS. The graphical presentations of the 3D models were prepared using Discovery Studio and Visual Molecular Dynamics (VMD) (Humphrey et al., 1996).

Statistical Analysis

All studies were performed in triplicate and the data obtained from experiments were presented as mean values and the differences between the control and the test were analyzed using a Student's *t*-test.

RESULTS AND DISCUSSION

Fraction-Based Screening for Violacein Inhibition in *C. violaceum*

Different fractions of *P. corylifolia* (seed) obtained in petroleum ether, benzene, ethyl acetate, acetone, and methanol were tested for their QS modulatory activity at varying concentrations against the *C. violaceum* ATCC 12472 (CV12472) strain. Fraction-based anti-QS activity against *C. violaceum* ATCC 12472 was demonstrated by the *P. corylifolia* methanol extract at 400 and 800 μg/ml concentrations, while at 1,600 μg/ml, pigment inhibition was accompanied by the inhibition of growth.

TABLE 1 | Pigment inhibitory activity of different fractions of *Psoralea corylifolia* (seed) extract.

Name of the fraction	Concentration of extract (μg/ml)	Zone of inhibition against *C. violaceum* ATCC 12472 (CV12472) in mm		
		Total inhibition (r_1)	Growth inhibition (r_2)	Pigment inhibition (r_1-r_2)
Petroleum ether	200	-	-	-
	400	-	-	-
	800	-	-	-
	1,600	-	-	-
Benzene	100	-	-	-
	200	-	-	-
	400	-	-	-
	800	-	-	-
Ethyl acetate	150	-	-	-
	300	-	-	-
	600	13	13	-
	1,200	13	9	4
Acetone	100	-	-	-
	200	19	17	2
	400	25	21	4
	800	27	25	2
Methanol	200	-	-	-
	400	15	-	15
	800	16	-	16
	1,600	18	3	15

Data are the mean value of three experiments.
- Shows no activity
Total inhibition = total zone of pigment inhibition including growth inhibition, if any.

Similarly, acetone and ethyl acetate extracts also demonstrated comparatively less pigment inhibition accompanied by growth inhibition. However, no activity was detected in petroleum ether and benzene fraction at all tested concentrations (**Table 1**).

The MIC of the *P. corylifolia* methanol fraction was determined against all test pathogens. An MIC of 750 μg/ml was observed against *C. violaceum* CVO26, *S. marcescens*, and *L. monocytogenes*, while a concentration of 1,250 μg/ml was recorded for *P. aeruginosa* PAF79 and *A. hydrophila* WAF38. The highest MIC of 1,500 μg/ml was observed against PAO1. Concentrations below the MICs i.e., sub-MICs were considered for all assays on the QS-regulated virulence functions and the biofilm.

The QS inhibitory activity of the methanol fraction of *P. corylifolia* (seed) was confirmed by determining the extent of violacein production in *C. violaceum* CV026, a mutant strain of wild-type CV12472 as depicted in **Figure 1**. The extract exhibited a significant reduction in violacein production and this reduction increased with the increasing concentration of the PCMF. A maximum reduction of 63.3% over control was observed at a concentration of 600 μg/ml of the extract. An insignificant difference in the number of colony-forming units (CFU) was recorded. Violacein production in *C. violaceum* is regulated by

the CviIR-dependent QS system. Therefore, any inhibition of the pigment in CVO26 is indicative of the fact that the extract is acting on the CviIR QS system and is a direct evidence of QS interference. Similar dose-dependent inhibition of violacein in CVO26 has been demonstrated in the extracts of *Terminalia chebula* (Sarabhai et al., 2013), *T. foenum-graceum* (Husain et al., 2015a), *Centella asiatica* (Vasavi et al., 2016), and *M. indica* (Husain et al., 2017).

Effect on QS-Regulated Functions in *P. aeruginosa*

QS interference by the methanol extract of *P. corylifolia* (seed) against *P. aeruginosa* strains is presented in **Tables 2**, **3**. The data showed a statistically significant reduction in the LasB elastolytic activity of PAO1 and PAF79 by 49.7 and 46.1%, respectively.

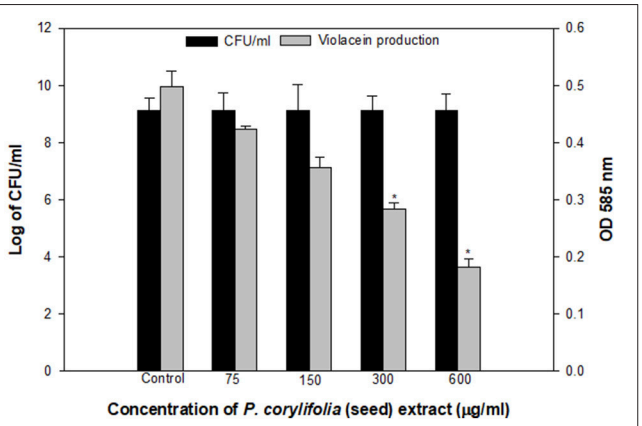

FIGURE 1 | Quantitative assessment of violacein inhibition in CVO26 by sub-MICs of *P. corylifolia* (seed) extract. All the data are presented as mean ± SD. * significance at $p \leq 0.05$.

Similarly, the total proteolytic activity was reduced by 50.5% in PAF79 and 43.5% in PAO1 at the respective sub-MICs. Proteases and LasB play a major role in the pathogenesis of *P. aeruginosa* by degrading the host tissues (Kessler et al., 1993). The virulence factor LasB (elastase) is controlled both by the *lasI–lasR* and *rhlI–rhlR* systems (Brint and Ohman, 1995; Pearson et al., 1997; Hentzer and Givskov, 2003). Our findings are in agreement with previous reports on the extracts of *Ananas comosus*, *Musa paradiciaca*, *Manilkara zapota*, *Ocimum santum*, *Lagerstroemia speciosa*, and *Allium cepa* (Musthafa et al., 2010; Singh et al., 2012; Vasavi et al., 2016; Al-Yousef et al., 2017).

Pyocyanin production is regulated by QS and causes severe toxic effects in humans by inducing the apoptosis of neutrophils and damaging the neutrophil-mediated host defense (Fothergill et al., 2007). Pyocyanin production was reduced significantly at all concentrations in PAO1. However, in PAF79, pyocyanin production was reduced maximally to 57.8% over untreated control at a concentration of 800 µg/ml. The inhibition of pyocyanin by sub-MICs of the PCMF is an important finding, considering the role of pyocyanin in the pathogenesis of *P. aeruginosa*. Similar concentration-dependent results were observed with the *T. foenum-graceum* seed extract, leaf extracts of *Piper betle* and *M. indica*, and *Forsythia suspensa* extract (Husain et al., 2015a, 2017; Datta et al., 2016; Zhang and Chu, 2017).

Chitinase activity in both the strains of *P. aeruginosa* was impaired significantly upon treatment with sub-MICs of the PCMF. In PAO1, 31.6–75.8% reduction in chitinase was observed while in PAF79, the decrease in chitinase production ranged from 17.9 to 63.3% over untreated control (**Tables 2**, **3**). This significant reduction in chitinase produced by the *P. aeruginosa* strains after treatment with sub-MICs of the PCMF corroborates well with the findings on *T. foenum-graceum* (21–48% reduction) and *M. indica* (21–55%) (Husain et al., 2015a, 2017).

EPS and swarming motility are vital at various stages of biofilm formation. EPS protects the biofilm from antimicrobial

TABLE 2 | Effect of sub-MICs of methanolic extract of *Psoralea corylifolia* (seed) on inhibition of quorum sensing-regulated virulence factors in *P. aeruginosa* PAO1.

Extract concentration (µg/ml)	Elastase activity [a]	Total protease[b]	Pyocyanin production[c]	Chitinase activity[d]	EPS production[e]	Swarming motility[f]
Control	0.181 ± 0.044	1.420 ± 0.038	5.2 ± 0.6	0.120 ± 0.009	0.991 ± 0.045	72 ± 1.5
125	0.156 ± 0.021 (13.8)	1.075 ± 0.036 (24.2)	2.45 ± 0.19 (52.8)*	0.082 ± 0.011 (31.6)	0.754 ± 0.049 (23.9)	46 ± 1.45 (36.1)
250	0.115 ± 0.013 (36.4)	1.01 ± 0.025 (28.8)	1.72 ± 0.33 (66.9)**	0.048 ± 0.017 (60)**	0.700 ± 0.018 (29.3)	37 ± 2.0 (48.6)*
500	0.101 ± 0.006 (44.1)	0.938 ± 0.019 (33.9)	1.5 ± 0.22 (71.1)**	0.040 ± 0.005 (66.6)**	0.515 ± 0.027 (48.0)*	29 ± 0.80 (59.7)*
1,000	0.091 ± 0.009 (49.7)*	0.801 ± 0.007 (43.5)*	0.69 ± 0.10 (86.7)***	0.029 ± 0.005 (75.8)***	0.429 ± 0.025 (56.7)*	26 ± 1.2 (63.8)*

[a] *Elastase activity is expressed as the absorbance at OD_{495}.*
[b] *Total protease activity is expressed as the absorbance at OD_{600}.*
[c] *Pyocyanin concentrations were expressed as micrograms of pyocyanin produced per microgram of total protein.*
[d] *Chitinase activity is expressed as the absorbance at OD_{570}.*
[e] *EPS production is expressed as absorbance at OD_{480}.*
[f] *Swarming motility is expressed as diameter of swarm in mm.*
*All the data are presented as mean ± SD. * significance at $p \leq 0.05$.*
Values in the parentheses indicate percent reduction over control.

TABLE 3 | Effect of sub-MICs of methanolic extract of *Psoralea corylifolia* (seed) on inhibition of quorum sensing-regulated virulence factors in *P. aeruginosa* PAF-79.

Extract concentration (μg/ml)	Elastase activity[a]	Total protease[b]	Pyocyanin production[c]	Chitinase activity [d]	EPS production[e]	Swarming motility[f]
Control	0.167 ± 0.025	1.039 ± 0.041	3.8 ± 0.25	0.139 ± 0.005	0.886 ± 0.036	48 ± 1.5
100	0.148 ± 0.004 (11.3)	0.938 ± 0.021 (9.7)	3 ± 0.2 (21)	0.114 ± 0.008 (17.9)	0.661 ± 0.015 (25.3)	40 ± 0.5 (16.6)
200	0.140 ± 0.015 (16.1)	0.891 ± 0.030 (14.2)	2.4 ± 0.13 (36.8)	0.07 ± 0.005 (49.6)*	0.525 ± 0.018 (40.6)	33 ± 2 (31.2)*
400	0.115 ± 0.007 (31.1)	0.748 ± 0.014 (28)	2.1 ± 0.082 (44.7)*	0.063 ± 0.007 (54.6)*	0.373 ± 0.012 (57.9)*	24 ± 1.5 (50)*
800	0.090 ± 0.003 (46.1)*	0.515 ± 0.012 (50.5)*	1.6 ± 0.054 (57.8)*	0.051 ± 0.008 (63.3)*	0.292 ± 0.014 (67)*	22 ± 2.5 (54.1)*

[a] *Elastase activity is expressed as the absorbance at OD_{495}.*
[b] *Total protease activity is expressed as the absorbance at OD_{600}.*
[c] *Pyocyanin concentrations were expressed as micrograms of pyocyanin produced per microgram of total protein.*
[d] *Chitinase activity is expressed as the absorbance at OD_{570}.*
[e] *EPS production is expressed as absorbance at OD_{480}.*
[f] *Swarming motility is expressed as diameter of swarm in mm.*
*All the data are presented as mean ± SD. * significance at $p \leq 0.05$.*
Values in the parentheses indicate percent reduction over control.

agents and is important during the maturation of the biofilm. Motility is essential during the initial attachment of the cells to the surface (Rabin et al., 2015). Sub-MICs of the PCMF effectively interfered with the production of EPS in PAO1 and PAF79. Swarming motility was also reduced substantially in both the test strains at the respective sub-MICs as depicted in **Tables 2**, **3** and **Figure 2**. Since EPS and swarming motility are crucial to biofilm formation, it is envisaged that the PCMF at sub-inhibitory concentrations will decrease the biofilm-forming capabilities of the test pathogens.

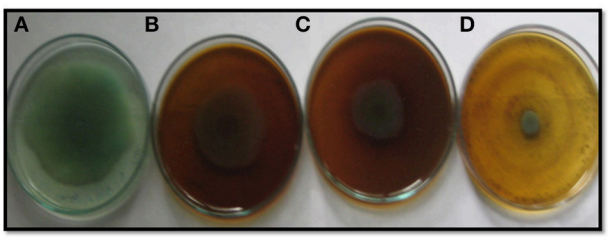

FIGURE 2 | Inhibition of swarming motility in *P. aeruginosa* PAF79 by sub-MICs of methanol extract of *P. corylifolia* (seed), **(A)** Untreated control; **(B)** 200 μg/ml; **(C)** 400 μg/ml; **(D)** 800 μg/ml.

Effect on QS-Regulated Functions in *A. hydrophila*

The extract of *P. corylifolia* (100–800 μg/ml) effectively interfered with the QS-regulated traits of *A. hydrophila* WAF38 and showed a significant reduction in the total protease activity to the level of 39.5–65.5% ($p \leq 0.005$) without affecting the growth significantly (**Figure S1A**). Similar concentration-dependent decrease (29.1–69.9%) in EPS production was also recorded at the tested sub-MICs of the PCMF (**Table 4**). The production of EPS and proteases in *A. hydrophila* is regulated by the *ahyRI* QS system. The decrease in the production of total proteases and EPS indicates that the PCMF interferes with the *ahyRI* QS system of *A. hydrophila* and consequently impairs C4-HSL production.

Effect on Prodigiosin Production in *Serratia marcescens*

A dose-dependent decrease in the production of prodigiosin by *S. marcescens* was recorded at the sub-MICs ranging from 75 to 600 μg/ml. The reduction was statistically significant ($p \leq 0.005$) at all the sub-inhibitory concentrations tested (**Figure 3**). The maximum inhibition of 71% and the lowest of 43% were recorded at concentrations of 600 and 75 μg/ml of the PCMF, respectively. The growth of the pathogen was not inhibited significantly (**Figure S1B**). Prodigiosin is considered as a major virulence factor of *S. marcescens* and is QS-regulated (Morohoshi et al., 2007). Hence, it is envisaged that the inhibition of prodigiosin will reduce the pathogenicity of *S. marcescens*. Methanol extracts of *Anethum graveolens* and three marine sponges have been previously reported for similar concentration-dependent reduction of prodigiosin (Annapoorani et al., 2012; Salini and Pandian, 2015).

Effect on PCMF on Biofilm Formation

Biofilms are cells growing in a self-produced matrix of EPS, which protects the encapsulated bacteria from the external environment and increases their resistance against antimicrobial agents many folds (Aitken et al., 2011). Reports have suggested that the negative charge on the polymers of the biofilm matrix interacts with positively charged antibiotics such as the aminoglycoside group of antibiotics and hampers the entry of such antibacterial drugs (Stewart and Costerton, 2001). In the present study, the PCMF significantly reduced biofilm formation in all the selected human- and food-related pathogens at the respective sub-MICs. Maximum reductions of 79, 71, 50, 64, 77, and 80% in the

TABLE 4 | Effect of sub-MICs of methanolic extract of *Psoralea corylifolia* (seed) on inhibition of quorum sensing-regulated virulence factors in *Aeromonas hydrophila* WAF-38.

Concentration (μg/ml)	Total protease[a]	EPS production[b]
Control	0.589 ± 0.051	0.748 ± 0.021
100	0.356 ± 0.016 (39.5)	0.530 ± 0.039 (29.1)
200	0.298 ± 0.029 (49.4)*	0.364 ± 0.026(51.3)*
400	0.278 ± 0.010 (52.8)*	0.29 ± 0.013 (61.2)**
800	0.203 ± 0.004 (65.5)**	0.255 ± 0.013 (69.9)**

[a] *Total protease activity is expressed as the absorbance at OD_{600}.*
[b] *EPS production is expressed as absorbance at OD_{480}.*
*All the data are presented as mean ± SD. * significance at $p \leq 0.05$, **, significance at $p \leq 0.005$.*
Values in the parentheses indicate percent reduction over control.

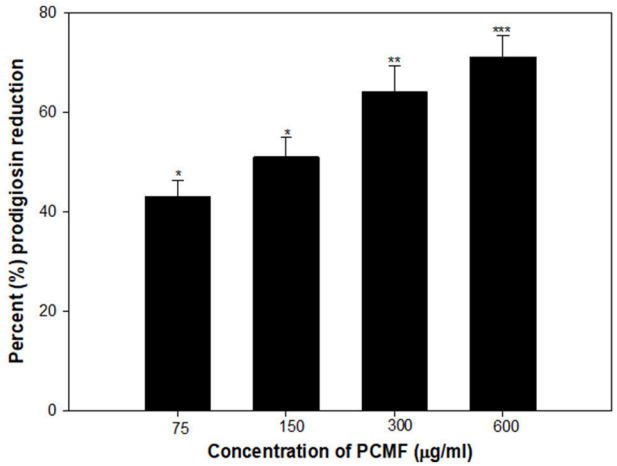

FIGURE 3 | Quantitative assessment of Prodigiosin inhibition in *S. marcescens* by sub-MICs of PCMF. All the data are presented as mean ± SD. * significance at $p \leq 0.05$, ** significance at $p \leq 0.005$, *** significance at $p \leq 0.001$.

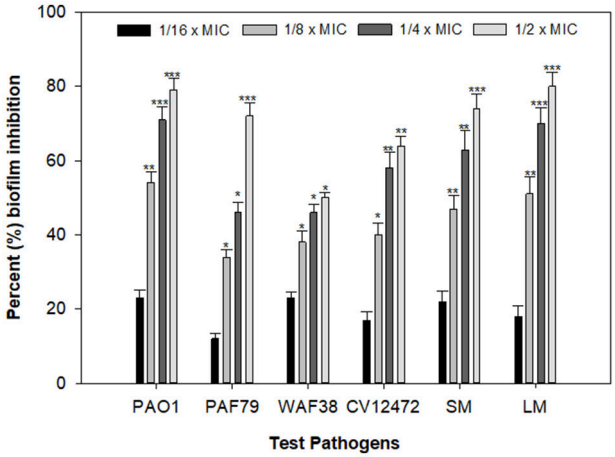

FIGURE 4 | Effect of PCMF on biofilm formation of test bacterial pathogens as quantified by crystal violet staining. Data are represented as the percentage inhibition of biofilm formation. All the data are presented as mean ± SD. * significance at $p \leq 0.05$, ** significance at $p \leq 0.005$, *** significance at $p \leq 0.001$.

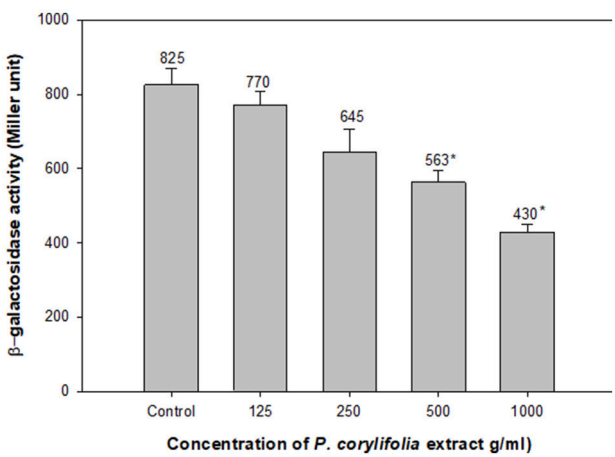

FIGURE 5 | Effect of PCMF on β-galactosidase activity in *E. coli* MG4/pKDT17. All the data are presented as mean ± SD. * significance at $p \leq 0.05$.

biofilm-forming capability of *P. aeruginosa* PAO1, *P. aeruginosa* PAF79, *A. hydrophila* WAF38, *C. violaceum* 12472, *S. marcescens*, and *L. monocytogenes* were observed over untreated control, respectively (**Figure 4**). Similar observations have been recorded with *Capparis spinosa* (Issac Abraham et al., 2011), *Rosa rugosa* (Zhang et al., 2014), leaf extract of *Kalanchoe blossfeldina* (Sarkar et al., 2015), and onion peel extract (Al-Yousef et al., 2017), which are known to reduce biofilm formation in pathogenic bacteria.

Effect on β-Galactosidase Activity

The effect of the *P. corylifolia* (seed) extract (125–1,000 μg/ml) was also assessed on the levels of the AHL produced by PAO1 using the β-galactosidase activity of *E. coli* MG4/pKDT17. A dose-dependent decrease was recorded for all the sub-MICs tested and a significant reduction of 47.8% was observed at 1,000 μg/ml as shown in **Figure 5**. The results of the β-galactosidase assay suggest that the quorum-sensing and biofilm-inhibitory activities of the PCMF were initiated by the downregulation of *las*-controlled transcription by sublethal concentrations of the PCMF.

Assessment of Anti-infective Potential of PCMF in *C. elegans* Nematode Model

The findings of the *in vitro* assays were also investigated *in vivo* using the liquid killing assay in the *C. elegans* nematode model. Potent pathogenicity of PAO1 toward the *C. elegans* nematode was observed as all the preinfected nematodes died within 72 h of the infection. However, preinfected *C. elegans* treated with *P. corylifolia* (1,000 μg/ml) displayed an enhanced survival rate of 58% (**Figure 6**). Methanol alone did not cause any significant mortality of the nematodes. *P. aeruginosa*

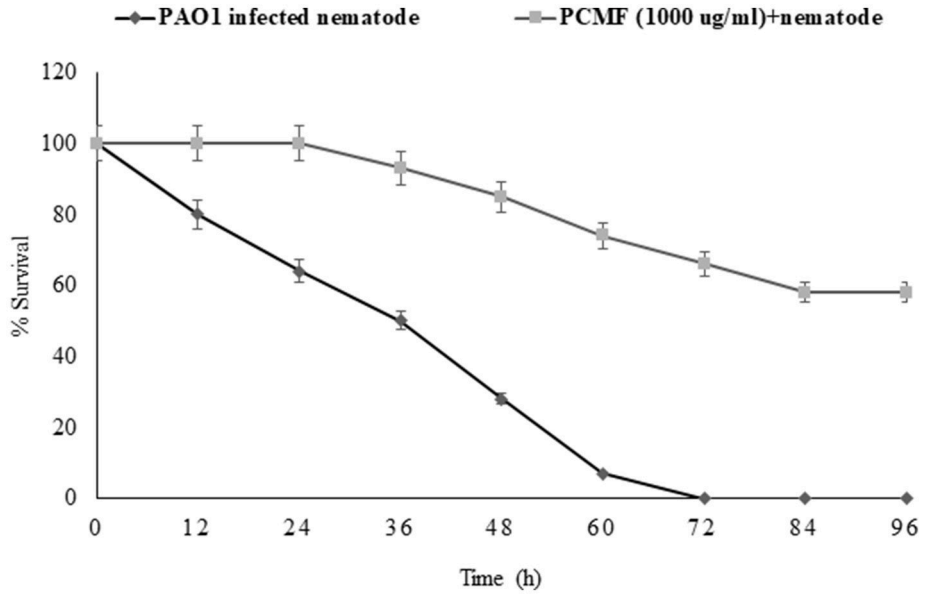

FIGURE 6 | Anti-infection potential of sub-MIC (1,000 μg/ml) of methanol fraction of *P. corylifolia* (seed) against PAO1-preinfected *C. elegans* nematode model. Means values and SDs are shown.

PAO1 kills the nematodes by causing cyanide asphyxiation and paralysis (Gallagher and Manoil, 2001). The increased survival of preinfected nematodes treated with 1,000 μg/ml of the PCMF suggests that the extract interferes with the QS system of PAO1, leading to reduction in deaths of the nematodes. The outcome of the *in vivo* studies are in accordance with the reports on South Florida plants, *Murraya koengii* essential oil, and *M. indica* (Adonizio et al., 2008b; Ganesh and Rai, 2016; Husain et al., 2017).

Total Phenolic Content

The total phenolic content of various fractions (mg/g of dry extract) was determined as the gallic acid equivalent (GAE) by the Folin–Ciocalteu method. The methanol fraction of seed contained 367.6 ± 1.5 mg GAE/g of dry extracts followed by acetone (337.6 ± 1.4), ethyl acetate (292 ± 2.3), benzene (43.3 ± 1.1), and petroleum ether (43.1 ± 1.0) fractions.

GC–MS Analysis

A total of 21 chemical components were identified in the seed extract by GC–MS analysis. These numbers may be extended with the help of chemometric techniques. The major compounds identified were 9,12-Octadecadienoic acid (35.72%), followed by bakuchiol (27.73%), palmitic acid (23.12%), and myristic acid (1.050%). The percentages of the remaining compounds ranged from 0.1 to 0.5 as presented in **Table 5**.

TABLE 5 | Components of *Psoralea corylifolia* (seed) extract as identified by GC–MS analysis.

Peak no.	Components	Retention time	Area (%)
1.	Trans(β)-caryophyllene	8.58	0.22
2.	1-Heptatriacotanol	10.69	0.29
3.	Caryophyllene oxide	11.32	0.48
4.	3-Methyl-5-(2,6,6-trimethyl-1-cyclohexen-1-yl)-1-pentyn-3-ol	11.60	0.64
5.	3-Ethyl-3-hydroxyandrostan-17-one	11.75	0.25
6.	Myristic acid	12.64	1.05
7.	3,7,11,15-Tetramethyl-2-hexadecen-1-ol	13.40	0.35
8.	Palmitic acid, methyl ester	14.29	0.57
9.	Palmitic acid	14.87	23.12
10.	Bakuchiol	16.37	27.73
11.	9,12-Octadecadienoic acid	16.66	35.72
12.	Linalol oxide, trimethylsilyl ether	21.67	0.20
13.	Squalene	24.80	0.11
14.	Hexacosane	25.71	0.20
15.	(+)-cis-Longipinane	25.84	0.42
16.	γ-Tocopherol	27.34	0.34
17.	Thunbergol	27.62	0.37
18.	Cholesteryl myristate	27.87	0.24
19.	Stigmasterol	29.00	0.57
20.	γ –Sitosterol	29.49	0.19
21.	trans-Longipinocarveol	29.60	0.22

Evaluation of Quorum Sensing Inhibitory Activity of Bakuchiol

Since bakuchiol was found to be the chief phytoconstituent present in the PCMF, it was assessed for anti-QS and anti-biofilm potential *in vitro* using *C. violaceum* CVO26, *P. aeruginosa* PAO1, *S. marcescens*, and *L. monocytogenes*. The MIC of bakuchiol was found to be 64, 128, 32, and 64 μg/ml against *C. violaceum* CVO26, *P. aeruginosa* PAO1, *S. marcescens*,

and *L. monocytogenes*, respectively. At the tested sub-MICs (4–32 μg/ml), bakuchiol demonstrated statistically significant inhibition of the violacein pigment ranging from 8 to 61% over untreated control (**Figure 7A**). The biofilm formation by PAO1 was also impaired by 22, 39, 55, and 69% at 8, 16, 32, and 64 μg/ml concentrations, respectively (**Figure 7B**). Further, bakuchiol significantly reduced the biofilm-forming capabilities of *C. violaceum* CV12472, *S. marcescens*, and *L. monocytogenes* at the respective sub-MICs. Biofilm formation in *C. violaceum* ATCC 12472 was reduced by 27–71% at concentrations ranging from 4 to 32 μg/ml (**Figure 7B**), while the biofilm formed by *S. marcescens* and *L. monocytogenes* decreased by 13–55% and 25–74%, respectively (**Figure 7B**). Scanning electron microscopic images demonstrated significant reduction in the number of microcolonies of *P. aeruginosa* and *L. monocytogenes* after treatment with ½× MIC of bakuchiol (**Figures 8A–D**). In a similar study, quercetin 4′-O-β-D glucopyranoside, without impacting the growth of pathogens such as *C. violaceum* 12472, *P. aeruginosa* PAO1, *S. marcescens*, and *L. monocytogenes*, significantly inhibited ($P < 0{\cdot}05$) the biofilm formation and production of virulence factors including pyocyanin, protease, and elastase at sublethal doses (Al-Yousef et al., 2017). Further, our findings are in accordance with other results published on methyl eugenol (Abraham et al., 2012), eugenol (Zhou et al., 2013), carvacrol (Burt et al., 2014), caffeine (Husain et al., 2015a), menthol (Husain et al., 2015b), and coumarins (D'Almeida et al., 2017). Owing to the previous report on QS inhibition by palmitic acid and linoleic acid (Widmer et al., 2007), it is envisaged that the QS inhibitory property of the PCMF is due to the presence of palmitic acid, linoleic acid, and bakuchiol.

Molecular Docking Studies

Molecular docking studies revealed the preferred positioning of bakuchiol in the active site of LasR and Rh1R. Bakuchiol binds in the active site cavity of LasR and Rh1R with a reasonable binding energy of −8.6 and −8.6 kcal/mol, respectively. The docked conformations indicate that bakuchiol binds into the cavity, and possibly inhibits LasR and Rh1R, and this may account for the modulation of its biological functions. The orientation of bakuchiol and a detailed interaction with the active site residues of LasR and Rh1R are shown in **Figure 9**. Bakuchiol was further examined on the basis of Lipinski's rule and the parameters calculated are listed in **Table 6**, demonstrating the drug-likeness of bakuchiol that can be implicated in LasR and Rh1R after further validation and optimization. The docked complexes were subjected to MD simulations to check the stability and the validity of the complexes. Four systems were prepared for each 100 ns MD simulation.

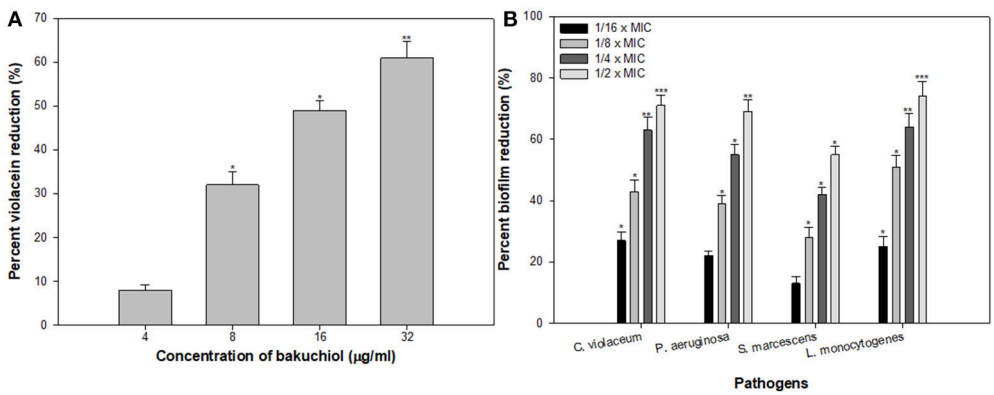

FIGURE 7 | (A) Inhibition of violacein in *C. violaceum* by sub-MICs of bakuchiol. **(B)** Effect of bakuchiol on biofilm formation by the test pathogens. All the data are presented as mean ± SD. * significance at $p \leq 0.05$, ** significance at $p \leq 0.005$, *** significance at $p \leq 0.001$.

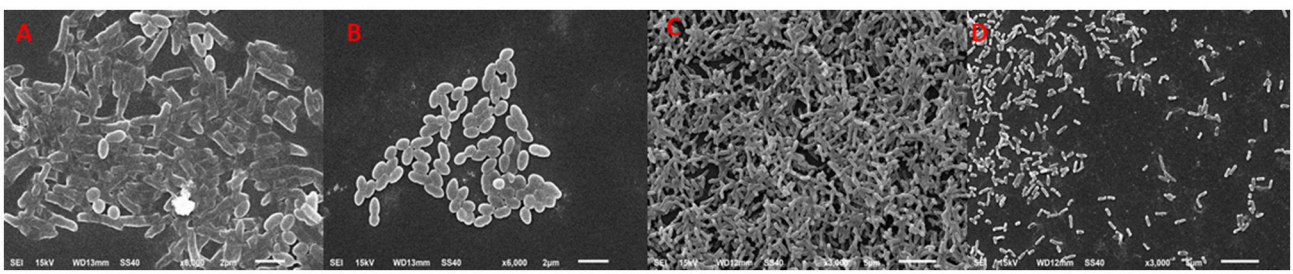

FIGURE 8 | Scanning electron microscopic images demonstrating biofilm inhibition by sub-MICs of bakuchiol. **(A,C)** untreated control of *L. monocytogenes* and *P. aeruginosa*, respectively; **(B,D)** inhibition of biofilm formed by *L. monocytogenes* and *P. aeruginosa*, respectively by ½ × MIC of bakuchiol.

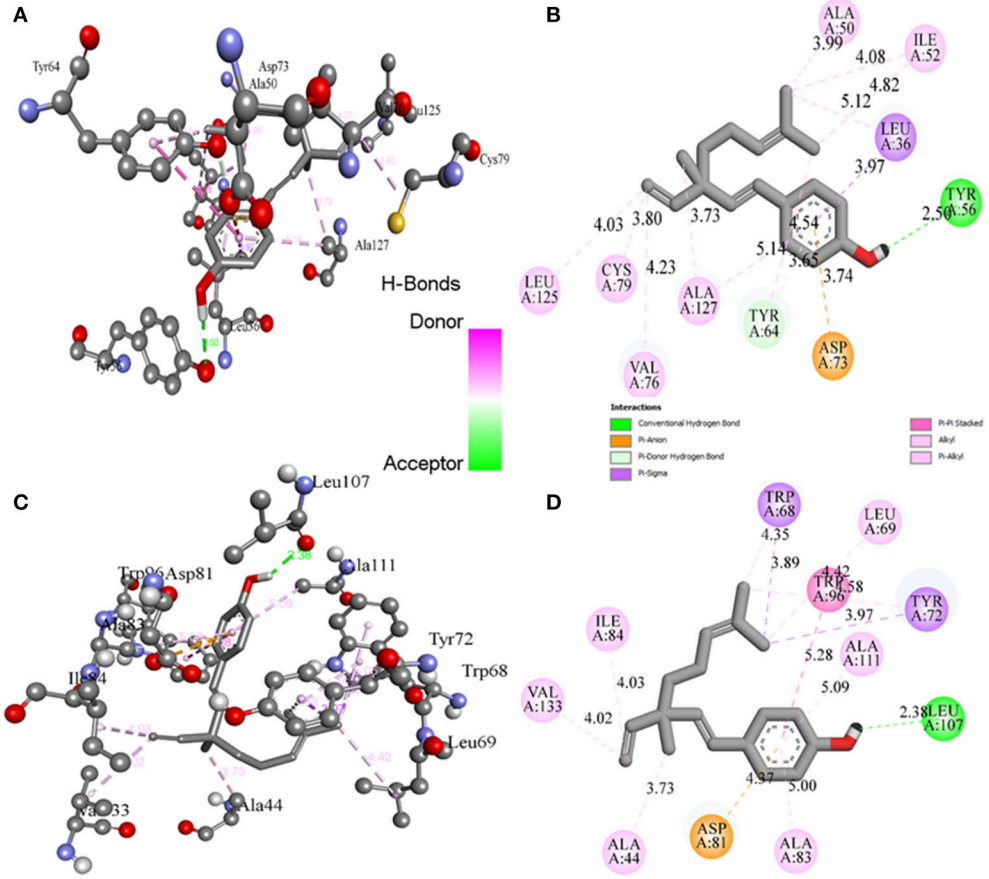

FIGURE 9 | Binding of bakuchiol to the LasR and Rh1R estimated by molecular docking. **(A,B)** 3D and 2D representation of LasR showing the interaction with bakuchiol. **(C,D)** 3D and 2D representation of Rh1R showing the interaction with bakuchiol. Residues of LasR and Rh1R interact with bakuchiol were shown by ball and stick.

TABLE 6 | Physiochemical properties of bakuchiol based on Lipinski's rule of 5 and showing drug likeliness*.

Ligand	Molecular weight	iLOGP	H bond donor	H bond acceptor	Rotatable bond	Bioavailability score	Drug likeness
Bakuchiol	256.38 (g/mol)	3.54	1	1	6	0.55	Yes

**http://www.swissadme.ch/.*

MD Analysis

Potential Energy

The MD simulation trajectories of LasR, LasR–bakuchiol, Rh1R, and Rh1R–bakuchiol were examined. To establish the equilibrium between systems tested earlier and MD data analysis, the average potential energy and the average fluctuation of temperature were checked. A constant continual temperature fluctuation at 300 *K* for each system was found to produce stable and accurate MD simulation results. The average potential energy for the LasR, LasR–bakuchiol, Rh1R, and Rh1R–bakuchiol complexes were found to be −586038.00, −585598.00, −1145220.00, and −1144500.00 kJ/mol, respectively.

Conformational Changes in LasR and RhlR

The structural comparison between protein molecules is an important tool for the analysis of protein structures and folding (Gramany et al., 2016; Khan et al., 2016b, 2018; Naz et al., 2018; Syed et al., 2018). The average root-mean-square deviation (RMSD) values were 0.20–0.30 nm for the LasR and LasR–bakuchiol complexes, respectively. The RMSD value of LasR decreased upon the binding of bakuchiol to the active pocket (**Figure 10A**). The RMSD trajectories suggested that LasR deviated from its native conformation upon binding to bakuchiol. Accordingly, the binding of bakuchiol to RhlR led to random fluctuations in

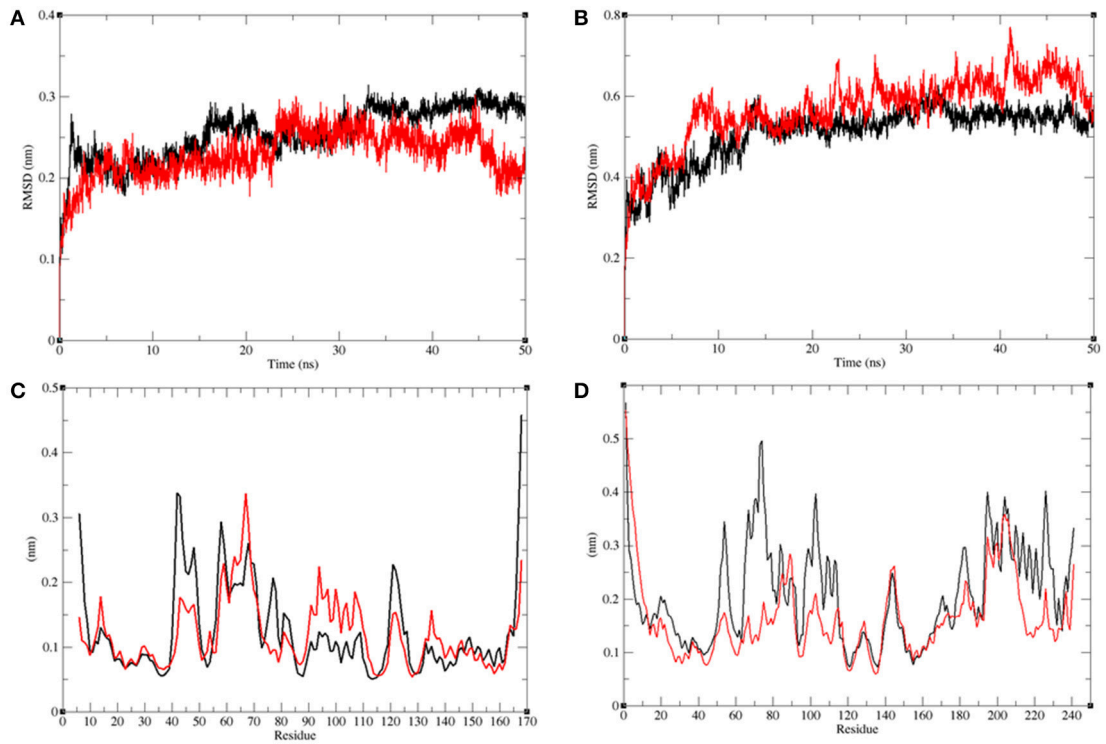

FIGURE 10 | Analysis of conformational changes in the LasR and RhlR after binding of bakuchiol. **(A)** Plot of RMSD as a function of time obtained for unbound LasR (black), LasR–bakuchiol (red), respectively. **(B)** Plot of RMSD as a function of time obtained for unbound RhlR (black), RhlR–bakuchiol (red), respectively. **(C)** Plot of RMSF as a function of residues number obtained for unbound LasR (black), LasR–bakuchiol (red), respectively. **(D)** Plot of RMSF as a function of residues number obtained for unbound RhlR (black), RhlR–bakuchiol (red), respectively.

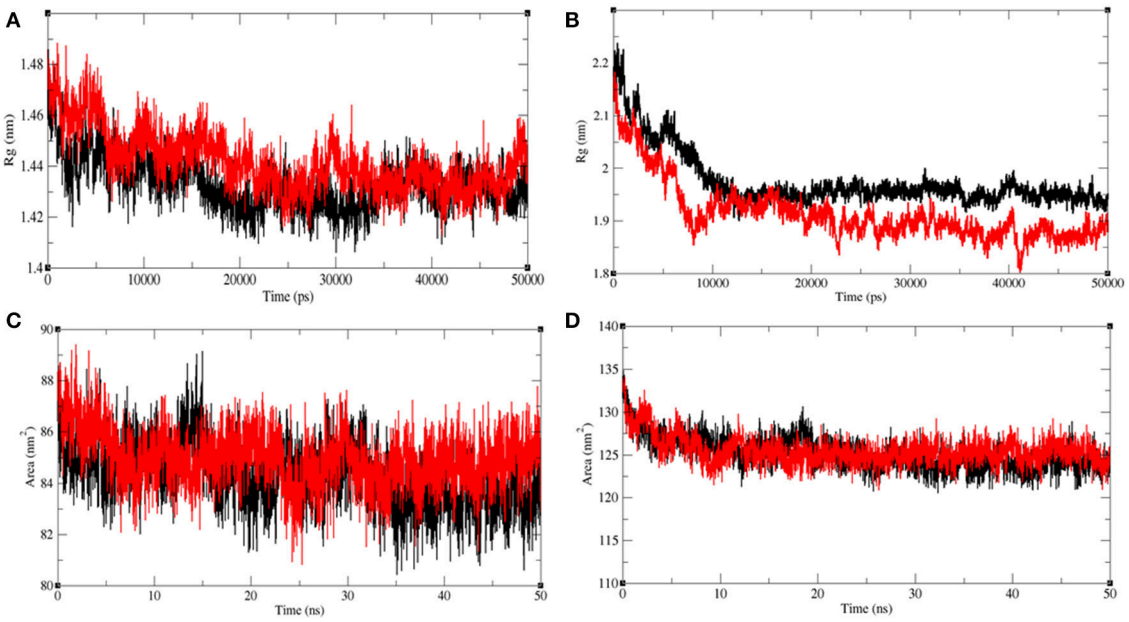

FIGURE 11 | Analysis of compactness in the LasR and RhlR after binding of bakuchiol. Radius of gyration obtained for **(A)** unbound LasR (black), LasR–bakuchiol (red), and **(B)** unbound RhlR (black), RhlR–bakuchiol (red), respectively. Solvent accessible surface area as a function of time obtained **(A)** unbound LasR (black), LasR–bakuchiol (red), and **(B)** unbound RhlR (black), RhlR–bakuchiol (red), respectively.

the RMSD trajectories that arise due to structural deviations (**Figure 10B**).

The residual vibrations around the equilibrium are not accidental but governed by local structure flexibility. To determine the average fluctuation of all residues during the MD simulation, the root-mean-square fluctuation (RMSF) of the LasR, LasR–bakuchiol, Rh1R, and Rh1R–bakuchiol complexes were plotted as a function of residue number. The RMSF plot of LasR showed the least fluctuations at 40–60 amino acid (*aa*) residues; thereafter, it showed comparatively large fluctuations at 60–70 *aa* and 90–110 *aa* residues upon binding with bakuchiol. These fluctuations arose due to the binding of bakuchiol, thus leading to the structural deviations of LasR (**Figure 10C**). The binding of bakuchiol to RhlR minimized the residual fluctuations, and this may be attributed to the strong binding of bakuchiol to the active pocket of RhlR (**Figure 10D**).

Structural Compactness

The radius of gyration (R_g) is related to the tertiary structure of a protein molecule. Rg is calculated to determine the protein stability in a biological system. Higher values of Rg suggest loose packing in the protein structure and vice versa. The average R_g value for LasR was found to be higher upon bakuchiol binding (**Figure 11A**). We observed that the structure of LasR is relatively compact in the free state, but the binding of bakuchiol leads to slight deviations from its native conformations. Additionally, the average compactness of Rh1R changes slightly upon bakuchiol binding (**Figure 11B**).

Solvent-accessible surface area (SASA) is the surface area of a molecule that interacts with the solvent molecules (Mazola et al., 2015). The average SASA values for the LasR, LasR–bakuchiol, Rh1R, and Rh1R–bakuchiol complexes were calculated using the *gmx sasa* module of GROMACS. It was found that the

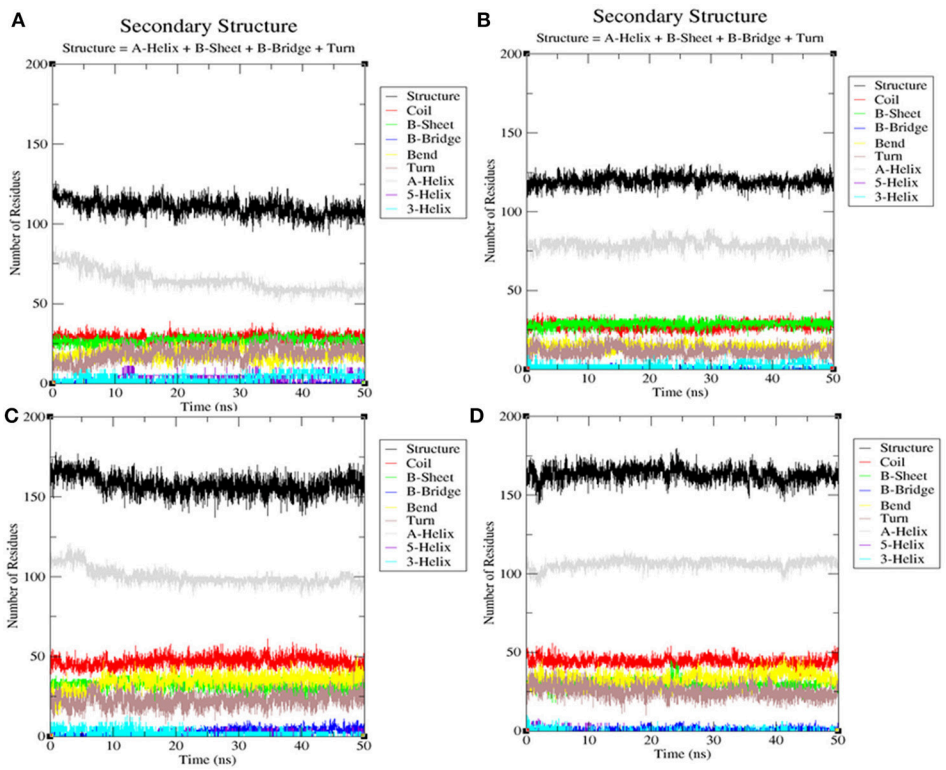

FIGURE 12 | Secondary structure analysis indicating the structural elements of **(A)** LasR, **(B)** LasR–bakuchiol, **(C)** RhlR, and **(D)** RhlR–bakuchiol, respectively.

TABLE 7 | Percentage of residues in LasR, LasR–bakuchiol, RhlR, and RhlR–bakuchiol that participated in average structure formation during 100 ns MD simulations*.

	Percentage of protein secondary structure (SS %)							
Protein type	**Structure***	**Coil**	**β-sheet**	**β -bridge**	**Bend**	**Turn**	**α-helix**	**3_{10}-helix**
LasR	67	18	16	0	13	11	39	2
LasR-bakuchiol	73	16	18	0	9	7	49	1
RhlR	66	19	14	1	14	9	42	1
Rh1R-bakuchiol	68	18	13	1	14	11	44	0

**Structure* = α-*helix* + β-*sheet* + β-*bridge* + *Turn*.*

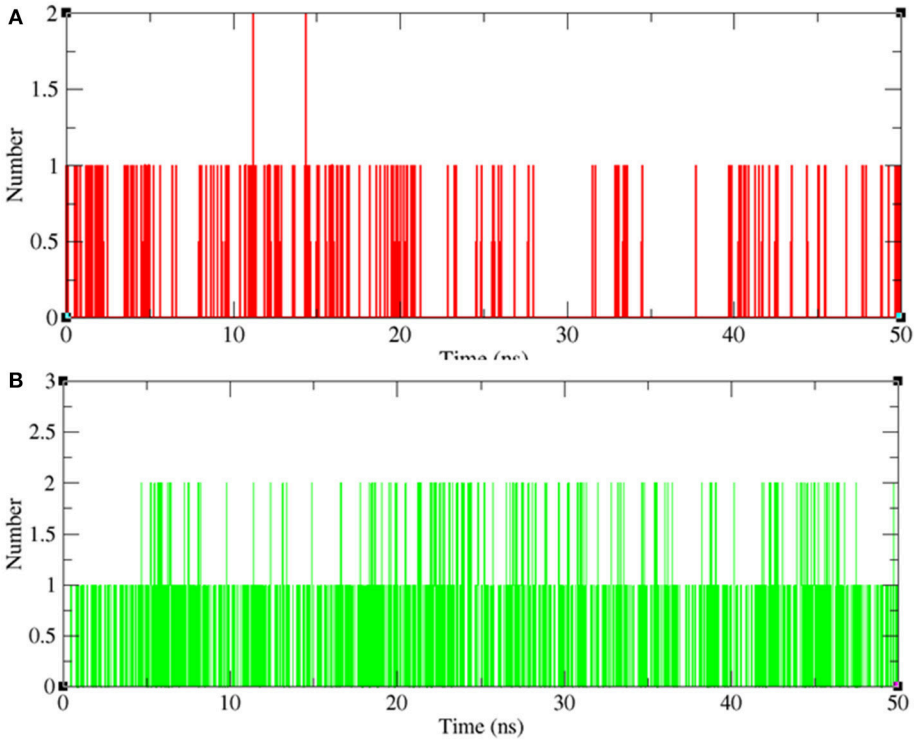

FIGURE 13 | Hydrogen bond analysis between bakuchiol and **(A)** LasR (red) and **(B)** RhlR (green), respectively.

average SASA values for LasR and RhlR when bound to bakuchiol were slightly higher than that in the unbound state. This is possibly due to the exposure of the internal residues in LasR and RhlR to the solvent due to the denaturation or conformational changes in the protein, arising due to the inhibition by bakuchiol (**Figures 11C,D**).

Secondary Structure Analysis

The secondary structures obtained during the MD simulation analysis are depicted in **Figure 12**. This analysis was aimed to measure the changes in the secondary structure of LasR and RhlR when bound with bakuchiol as a function of time. During the MD simulations, the secondary structure assignments such as α-helix, β-strand, and turns were broken into separate residues to measure the data in meaningful ways. The average number of residues contributing in the secondary structure formation was found to be more in the case of LasR–bakuchiol and RhlR–bakuchiol complexes than in LasR and RhlR, respectively (**Table 7**). This is due to the increase in α-helices in the protein structure. This analysis suggests that bakuchiol binding with LasR and RhlR leads to a considerable change in the secondary structure.

Hydrogen Bond Analysis

Hydrogen bonding between a receptor and ligands offers directionality and demonstrates the specificity of molecular interactions that are important aspects of molecular recognition (Hubbard and Kamran Haider, 2001). To validate the stability of docked complexes, the hydrogen bonds were paired within 0.35 nm between the protein and the ligands. During the 50 ns MD simulation studies for LasR-bakuchiol and RhlR-bakuchiol complexes, all calculations were performed in the solvent environment. Analysis revealed that bakuchiol binds to active pockets of LasR and RhlR with 1–2 hydrogen bonds (**Figure 13**).

CONCLUSION

In conclusion, it is envisaged that the PCMF and bakuchiol obtained from *P. corylifolia* seeds may provide a possible substitute for the management of drug-resistant strains that cause infections/contamination, predominantly pathogens that form biofilms. The study highlights the anti-infective potential of the PCMF and bakuchiol instead of their bactericidal or bacteriostatic action, because the extract targets QS-controlled virulence and the biofilm. Computational analysis revealed that bakuchiol binds to the active pockets of LasR and RhlR during MD simulations. The binding of bakuchiol leads to structural deviations of LasR and Rh1R. This approach forms the basis of effective antimicrobial therapy in modern phytomedicine.

AUTHOR CONTRIBUTIONS

IA, FH, MB, and FK designed and conceived experiments. FH, FK, MB, NA-S, AH, MR, MA, KL performed experiments. FH,

FK, NA-S, AH, MR, MA, and KL analyzed and interpreted data. FH, IA, FK, MB, NA-S, AH, MR, MA, and KL wrote the manuscript and all the authors approved it.

ACKNOWLEDGMENTS

We would like to extend their sincere appreciation to the Deanship of Scientific Research at King Saud University for its funding of this research through the Research Group Project No. RGP-150. FK and KL would like to express their gratitude to the Centre for High Performance Computing (CHPC), South Africa.

SUPPLEMENTARY MATERIAL

The Supplementary Material for this article can be found online at: https://www.frontiersin.org/articles/10.3389/fcimb.2018.00351/full#supplementary-material

REFERENCES

Abraham, I. S. V. P., Agilandeswari, P., Musthafa, K. S., Pandian, S. K., and Ravi, A. V. (2012). Antibiofilm and quorum sensing inhibitory potential of *Cuminum cyminum* and its secondary metabolite methyl eugenol against gram negative bacterial pathogens. *Food Res. Int.* 45, 85–92. doi: 10.1016/j.foodres.2011.10.022

Adonizio, A., Kong, K. F., and Mathee, K. (2008a). Inhibition of quorum sensing-controlled virulence factor production in *Pseudomonas aeruginosa* by south Florida plant extracts. *Antimicrob. Agents Chemother.* 52, 198–203. doi: 10.1128/AAC.00612-07

Adonizio, A., Leal, S. M., Ausubel, F. M., and Mathee, K. (2008b). Attenuation of *Pseudomonas aeruginosa* virulence by medicinal plants in a *Caenorhabditis elegans* model system. *J. Med. Microbiol.* 57, 809–813. doi: 10.1099/jmm.0.47802-0

Adonizio, A. L., Downum, K., Bennett, B. C., and Mathee, K. (2006). Anti-quorum sensing activity of medicinal plants in southern Florida. *J. Ethnopharmacol.* 105, 427–435. doi: 10.1016/j.jep.2005.11.025

Ahmad, I., Aqil, F., Ahmad, F., and Owais, M. (2006). "Herbal medicines: prospects and constraints," in *Modern Phytomedicine: Turning Medicinal Plants Into Drugs*, eds I. Ahmad, F. Aqil and M. Owais (Weinheim: Wiley-VCH), 59–76.

Aitken, E., Cheema, A., Elliot, S., and Khan, S. (2011). Different composition of biofilm extracellular polymeric substances reveals contrasting antibiotic resistance profiling in *Pseudomonas aeruginosa*. *J. Exp. Microbiol. Immunol.* 15, 79–83.

Al-Yousef, H. M., Ahmed, A. F., Al-Shabib, N. A., Laeeq, S., Khan, R. A., Rehman, M. T., et al. (2017). Onion peel ethylacetate fraction and its derived constituent Quercetin 4′-*O*-β-D Glucopyranoside attenuates quorum sensing regulated virulence and biofilm formation. *Front. Microbiol.* 8:1675. doi: 10.3389/fmicb.2017.01675

Annapoorani, A., Jabbar, A. K. K. A., Musthafa, S. K. S., Pandian, S. K., and Ravi, A. V. (2012). Inhibition of quorum sensing mediated virulence factor production in urinary pathogen *Serratia marcescens* PS1 by marine sponges. *Indian J. Microbiol.* 52, 160–166. doi: 10.1007/s12088-012-0272-0

Biovia, D. S. (2015). *Discovery Studio Modeling Environment*. San Diego, CA: Dassault Systemes.

Bjarnsholt, T., and Givskov, M. (2008). Quorum sensing inhibitory drugs as next generation antimicrobials: worth the effort? *Curr. Infect. Dis. Rep.* 10, 22–28. doi: 10.1007/s11908-008-0006-y

Blosser, R. S., and Gray, K. M. (2000). Extraction of violacein from *Chromobacterium violaceum* provides a new quantitative bioassay for N-acyl homoserine lactone autoinducers. *J. Microbiol. Methods* 40, 47–55. doi: 10.1016/S0167-7012(99)00136-0

Brint, J. M., and Ohman, D. E. (1995). Synthesis of multiple exoproducts in *Pseudomonas aeruginosa* is under the control of RhlR-RhlI, another set of regulators in strain PAO1 with homology to the autoinducer-responsive LuxR-LuxI family. *J. Bacteriol.* 177, 7155–7163. doi: 10.1128/jb.177.24.7155-7163.1995

Burt, S. A., Ojo-Fakunle, V. T., Woertman, J., and Veldhuizen, E. J. (2014). The natural antimicrobial carvacrol inhibits quorum sensing in *Chromobacterium violaceum* and reduces bacterial biofilm formation at sub-lethal concentrations. *PLoS ONE* 9:e93414. doi: 10.1371/journal.pone.0093414

Choo, J. H., Rukayadi, Y., and Hwang, J. K. (2006). Inhibition of bacterial quorum sensing by vanilla extract. *Lett. Appl. Microbiol.* 42, 637–641. doi: 10.1111/j.1472-765X.2006.01928.x

Chopra, B., Dhingra, A. K., and Dhar, K. L. (2013). *Psoralea corylifolia L.* (Buguchi)-Folklore to modern evidence: review. *Fitoterapia* 90, 44–56. doi: 10.1016/j.fitote.2013.06.016

Cosconati, S., Forli, S., Perryman, A. L., Harris, R., Goodsell, D. S., and Olson, A. J. (2010). Virtual screening with autodock: theory and practice. *Expert Opin. Drug Discov.* 5, 597–607. doi: 10.1517/17460441.2010.484460

D'Almeida, R. E., Molina, R. D. I., Viola, C. M., Luciardi, M. C., Penalver, C. N., Bardon, A., et al. (2017). Comparison of seven structurally related coumarins on the inhibition of quorum sensing of *Pseudomonas aeruginosa* and *Chromobacterium violaceum*. *Bioorg. Chem.* 73, 37–42. doi: 10.1016/j.bioorg.2017.05.011

Datta, S., Jana, D., Maity, T. R., Samanta, A., and Banerjee, R. (2016). *Piper betle* leaf extracts affects the quorum sensing and hence virulence of *Pseudomonas aeruginosa* PAO1. *3 Biotech.* 6, 18. doi: 10.1007/s13205-015-0348-8

de la Fuente-Núñez, C., Reffuveille, F., Haney, E. F., Straus, S. K., and Hancock, R. E. W. (2014). Broad-spectrum anti-biofilm peptide that targets a cellular stress response. *PLoS Pathog.* 10:e1004152. doi: 10.1371/journal.ppat.1004152

Eloff, J. N. (1998). Sensitive and quick microplate method to determine the minimum inhibitory concentration of plant extracts for bacteria. *Planta Med.* 64, 711–713. doi: 10.1055/s-2006-957563

Fothergill, J. L., Panagea, S., Hart, C. A., Walshaw, M. J., Pitt, T. L., and Winstanley, C. (2007). Widespread pyocyanin overproduction among isolates of a cystic fibrosis epidemic strain. *BMC Microbiol.* 7:45. doi: 10.1186/1471-2180-7-45

Gallagher, L. A., and Manoil, C. (2001). *Pseudomonas aeruginosa* PAO1 kills *Caenorhabditis elegans* by cyanide poisoning. *J. Bacteriol.* 183, 6207–6214. doi: 10.1128/JB.183.21.6207-6214.2001

Ganesh, P. S., and Rai, R. V. (2016). Inhibition of quorum-sensing-controlled virulence factors of *Pseudomonas aeruginosa* by *Murraya koenigii* essential oil: a study in a *Caenorhabditis elegans* infectious model. *J. Med. Microbiol.* 65, 1528–1535. doi: 10.1099/jmm.0.000385

Gramany, V., Khan, F. I., Govender, A., Bisetty, K., Singh, S., and Permaul, K. (2016). Cloning, expression, and molecular dynamics simulations of a xylosidase obtained from Thermomyces lanuginosus. *J. Biomol. Struct. Dyn.* 34, 1681–1692. doi: 10.1080/07391102.2015.1089186

Hentzer, M., and Givskov, M. (2003). Pharmacological inhibition of quorum sensing for the treatment of chronic bacterial infections. *J. Clin. Invest.* 112, 1300–1307. doi: 10.1172/JCI20074

Hubbard, R. E., and Kamran Haider, M. (2001). *Hydrogen Bonds in Proteins: Role and Strength eLS*. Chichester: John Wiley & Sons, Ltd.

Huerta, V., Mihalik, K., Crixell, S. H., and Vattem, D. A. (2008). Herbs, spices and medicinal plants used in hispanic traditional medicine can decrease quorum sensing dependent virulence in *Pseudomonas aeruginosa*. *Int. J. Appl. Res. Nat. Prod.* 1, 9–15.

Humphrey, W., Dalke, A., and Schulten, K. (1996). VMD: visual molecular dynamics. *J. Mol. Graph.* 14, 33–38, 27–38.

Husain, F. M., and Ahmad, I. (2013). Quorum sensing inhibitors from natural products as potential novel anti-infective agents. *Drugs Fut.* 38, 691–705. doi: 10.1358/dof.2013.038.10.2025393

Husain, F. M., Ahmad, I., Al-thubiani, A. S., Abulreesh, H. H., AlHazza, I. M., and Aqil, F. (2017). Leaf extracts of *Mangifera indica* L. inhibit quorum sensing-regulated production of virulence factors and biofilm in test bacteria. *Front. Microbiol.* 8:727. doi: 10.3389/fmicb.2017.00727

Husain, F. M., Ahmad, I., Khan, M. S., Ahmad, E., Tahseen, Q., Khan, M. S., et al. (2015b). Sub-MICs of *Mentha piperita* essential oil and menthol inhibits

AHL mediated quorum sensing and biofilm of Gram-negative bacteria. *Front. Microbiol.* 6:420. doi: 10.3389/fmicb.2015.00420

Husain, F. M., Ahmad, I., Khan, M. S., and Al-Shabib, N. A. (2015a). *Trigonella foenum-graceum* (Seed) extract interferes with quorum sensing regulated traits and biofilm formation in the strains of *Pseudomonas aeruginosa* and *Aeromonas hydrophila*. *Evid. Based Complement. Alternat. Med.* 2015:879540. doi: 10.1155/2015/879540

Issac Abraham, S, V., Palani, A., Ramaswamy, B. R., Shunmugiah, K. P., and Arumugam, V. R. (2011). Antiquorum sensing and antibiofilm potential of *Capparis spinosa*. *Arch. Med. Res.* 42, 658–668. doi: 10.1016/j.arcmed.2011.12.002

Kalia, V. C. (2013). Quorum sensing inhibitors: an overview. *Biotechnol. Adv.* 31, 224–245. doi: 10.1016/j.biotechadv.2012.10.004

Kessler, E., Safrin, M., Olson, J. C., and Ohman, D. E. (1993). Secreted LasA of *Pseudomonas aeruginosa* is a staphylolytic protease. *J. Biol. Chem.* 268, 7503–7508.

Khan, F. I., Govender, A., Permaul, K., Singh, S., and Bisetty, K. (2015). Thermostable chitinase II from *Thermomyces lanuginosus* SSBP: cloning, structure prediction and molecular dynamics simulations. *J. Theor. Biol.* 374, 107–114. doi: 10.1016/j.jtbi.2015.03.035

Khan, F. I., Lan, D., Durrani, R., Huan, W., Zhao, Z., and Wang, Y. (2017a). The lid domain in lipases: structural and functional determinant of enzymatic properties. *Front. Bioeng. Biotechnol.* 5:16. doi: 10.3389/fbioe.2017.00016

Khan, F. I., Nizami, B., Anwer, R., Gu, K. -R., Bisetty, K., Hassan, M. I., et al. (2017b). Structure prediction and functional analyses of a thermostable lipase obtained from *Shewanella putrefaciens*. *J. Biomol. Struct. Dyn.* 35, 2123–2135. doi: 10.1080/07391102.2016.1206837

Khan, F. I., Shahbaaz, M., Bisetty, K., Waheed, A., Sly, W. S., Ahmad, F., et al. (2016a). Large scale analysis of the mutational landscape in beta-glucuronidase: a major player of mucopolysaccharidosis type VII. *Gene* 576(1 Pt 1), 36–44. doi: 10.1016/j.gene.2015.09.062

Khan, F. I., Wei, D. Q., Gu, K. R., Hassan, M. I., and Tabrez, S. (2016b). Current updates on computer aided protein modeling and designing. *Int. J. Biol. Macromol.* 85, 48–62. doi: 10.1016/j.ijbiomac.2015.12.072

Khan, S., Khan, F. I., Mohammad, T., Khan, P., Hasan, G. M., Lobb, K. A., et al. (2018). Exploring molecular insights into the interaction mechanism of cholesterol derivatives with the Mce4A: a combined spectroscopic and molecular dynamic simulation studies. *Int. J. Biol. Macromol.* 111, 548–560. doi: 10.1016/j.ijbiomac.2017.12.160

Lan, D., Xu, H., Xu, J., Dubin, G., Liu, J., Iqbal Khan, F., et al. (2017). Malassezia globosa MgMDL2 lipase: crystal structure and rational modification of substrate specificity. *Biochem. Biophys. Res. Commun.* 488, 259–265. doi: 10.1016/j.bbrc.2017.04.103

LaSarre, B., and Federle, M. J. (2013). Exploiting quorum sensing to confuse bacterial pathogens. *Microbiol. Mol. Biol. Rev.* 77, 73–111. doi: 10.1128/MMBR.00046-12

Laskowski, R. A., and Swindells, M. B. (2011). LigPlot+: multiple ligand–protein interaction diagrams for drug discovery. *J. Chem. Inf. Model.* 51, 2778–2786. doi: 10.1021/ci200227u

Lister, E., and Wilson, P. (2001). *Measurement of Total Phenolics and ABTS Assay for Antioxidant Activity*. Lincoln: Crop Research Institute.

Lowery, C. A., Salzameda, N. T., Sawada, D., Kaufmann, G. F., and Janda, K. D. (2010). Medicinal chemistry as a conduit for the modulation of quorum sensing. *J. Med. Chem.* 53, 7467–7489. doi: 10.1021/jm901742e

Masada, Y. (1976). *Analysis of Essential Oils by Gas Chromatography and Mass Spectrometry*. New York, NY: John Wiley & Sons.

Mazola, Y., Guirola, O., Palomares, S., Chinea, G., Menendez, C., Hernandez, L., et al. (2015). A comparative molecular dynamics study of thermophilic and mesophilic beta-fructosidase enzymes. *J. Mol. Model.* 21:228. doi: 10.1007/s00894-015-2772-4

McLean, R. J., Pierson, L. S. III., and Fuqua, C. (2004). A simple screening protocol or the identification of quorum sensing signal antagonists. *J. Microbiol Methods* 58, 351–360. doi: 10.1016/j.mimet.2004.04.016

Morohoshi, T., Shiono, T., Takidouchi, K., Kato, M., Kato, N., Kato, J., et al. (2007). Inhibition of quorum sensing in *Serratia marcescens* AS-1 by synthetic analogs of N-acyl homoserine lactone. *Appl. Environ. Microbiol.* 73, 6339–6344. doi: 10.1128/AEM.00593-07

Musthafa, K. S., Balamurugan, K., Pandian, S. K., and Ravi, A. V. (2012). 2, 5 Piperazinedione inhibits quorum sensing-dependent factor production in *Pseudomonas aeruginosa* PAO1. *J. Basic Microbiol.* 52, 1–8. doi: 10.1002/jobm.201100292

Musthafa, K. S., Ravi, A. V., Annapoorani, A., Packiavathy, I. S. V., and Pandian, S. K. (2010). Evaluation of anti-quorum-sensing activity of edible plants and fruits through inhibition of the N-acyl-homoserine lactone system in *Chromobacterium violaceum* and *Pseudomonas aeruginosa*. *Chemotherapy* 56, 333–339. doi: 10.1159/000320185

Musthafa, K. S., Sianglum, W., Saising, J., Lethongkam, S., and Voravuthikunchai, S. P. (2017). Evaluation of phytochemicals from medicinal plants of Myrtaceae family on virulence factor production by *Pseudomonas aeruginosa*. *APMIS* 125, 482–490 doi: 10.1111/apm.12672

Naz, F., Khan, F. I., Mohammad, T., Khan, P., Manzoor, S., Hasan, G. M., and Hassan, M. I. (2018). Investigation of molecular mechanism of recognition between citral and MARK4: a newer therapeutic approach to attenuate cancer cell progression. *Int. J. Biol. Macromol.* 107(Pt B), 2580–2589. doi: 10.1016/j.ijbiomac.2017.10.143

Norberto de Souza, O., and Ornstein, R. L. (1999). Molecular dynamics simulations of a protein-protein dimer: particle-mesh Ewald electrostatic model yields far superior results to standard cutoff model. *J. Biomol. Struct. Dyn.* 16, 1205–1218. doi: 10.1080/07391102.1999.10508328

Omwenga, E. O., Hensel, A., Pereira, S., Shitandi, A. A., and Goycoolea, F. M. (2017). Antiquorum sensing, antibiofilm formation and cytotoxicity activity of commonly used medicinal plants by inhabitants of Borabu sub-county, Nyamira County, Kenya. *PLoS ONE* 12:e0185722. doi: 10.1371/journal.pone.0185722

O'Toole, G. A., and Kolter, R. (1998). Initiation of biofilm formation in *Pseudomonas fluorescens* WCS365 proceeds via multiple, convergent signaling pathways: a genetic analysis. *Mol. Microbiol.* 28, 449–461.

Papenfort, K., and Bassler, B. L. (2016). Quorum sensing signal-response systems in Gram-negative bacteria. *Nat. Rev. Microbiol.* 14, 576–588. doi: 10.1038/nrmicro.2016.89

Pearson, J. P., Pesci, E. C., and Iglewski, B. H. (1997). Roles of *Pseudomonas aeruginosa las* and *rhl* quorum-sensing systems in control of elastase and rhamnolipid biosynthesis genes. *J. Bacteriol.* 179, 5756–5767. doi: 10.1128/jb.179.18.5756-5767.1997

Rabin, N., Zheng, Y., Opoku-Temeng, C., Du, Y., Bonsu, E., and Sintim, H. O. (2015). Biofilm formation mechanisms and targets for developing antibiofilm agents. *Future Med. Chem.* 7, 493–512. doi: 10.4155/fmc.15.6

Rasmussen, T. B., and Givskov, M. (2006). Quorum sensing inhibitors: a bargain of effects. *Microbiology* 152, 895–904. doi: 10.1099/mic.0.28601-0

Rasmussen, T. B., Manefield, M., Andersen, J. B., Eberl, L., Anthoni, U., Christophersen, C., et al. (2000). How *Delisea pulchra* furanones affect quorum sensing and swarming motility in *Serratia liquefaciens* MG1. *Microbiology* 146, 3237–3244. doi: 10.1099/00221287-146-12-3237

Reen, F. J., Gutiérrez-Barranquero, J. A., Parages, M. L., and O'Gara, F. (2018). Coumarin a novel player in microbial quorum sensing and biofilm formation inhibition. *Appl. Microbiol. Biotechnol.* 102, 2063–2073. doi: 10.1007/s00253-018-8787-x

Rigsby, R. E., and Parker, A. B. (2016). Using the PyMOL application to reinforce visual understanding of protein structure. *Biochem. Mol. Biol. Educ.* 44, 433–437. doi: 10.1002/bmb.20966

Salini, R., and Pandian, S. K. (2015). Interference of quorum sensing in urinary pathogen *Serratia marcescens* by *Anethum graveolens*. *FEMS Pathog. Dis.* 73:ftv038. doi: 10.1093/femspd/ftv038

Sarabhai, S., Sharma, P., and Capalash, N. (2013). Ellagic acid derivatives from *Terminalia chebula retz.* downregulate the expression of quorum sensing genes to attenuate *Pseudomonas aeruginosa* PAO1 virulence. *PLoS ONE* 8:53441. doi: 10.1371/journal.pone.0053441

Sarkar, R., Mondal, C., Bera, R., Chakraborty, S., Barik, R., Roy, P., et al. (2015). Antimicrobial properties of *Kalanchoe blossfeldiana*: a focus on drug resistance with particular reference to quorum sensing-mediated bacterial biofilm formation. *J. Pharm. Pharmacol.* 67, 951–962. doi: 10.1111/jphp.12397

Schüttelkopf, A. W., and van Aalten, D. M. (2004). PRODRG: a tool for high-throughput crystallography of protein-ligand complexes. *Acta Crystallogr.*

D Biol. Crystallogr. 60(Pt 8), 1355–1363. doi: 10.1107/S09074449040 11679

Singh, B. N., Singh, H. B., Singh, A., Singh, B. R., Mishra, A., and Nautiyal, C. S. (2012). *Lagerstroemia speciosa* fruit extract modulates quorum sensing-controlled virulence factor production and biofilm formation in *Pseudomonas aeruginosa*. *Microbiology* 158, 529–538. doi: 10.1099/mic.0.052985-0

Spanos, G. A., and Wrolstad, R. E. (1990). Influence of processing and storage on the phenolic composition of Thompson seedless grape juice. *J. Agri. Food Chem.* 38, 1565–1571. doi: 10.1021/jf00097a030

Stephens, D. E., Khan, F. I., Singh, P., Bisetty, K., Singh, S., and Permaul, K. (2014). Creation of thermostable and alkaline stable xylanase variants by DNA shuffling. *J. Biotechnol.* 187, 139–146. doi: 10.1016/j.jbiotec.2014.07.446

Stewart, P. S., and Costerton, J. W. (2001). Antibiotic resistance of bacteria in biofilms. *Lancet* 358, 135–138. doi: 10.1016/S0140-6736(01)05321-1

Syed, S. B., Khan, F. I., Khan, S. H., Srivastava, S., Hasan, G. M., Lobb, K. A., et al. (2018). Mechanistic insights into the urea-induced denaturation of kinase domain of human integrin linked kinase. *Int. J. Biol. Macromol.* 111, 208–218. doi: 10.1016/j.ijbiomac.2017.12.164

Trott, O., and Olson, A. J. (2010). AutoDock vina: improving the speed and accuracy of docking with a new scoring function, efficient optimization, and multithreading. *J. Comput. Chem.* 31, 455–461. doi: 10.1002/jcc.21334

Van Der Spoel, D., Lindahl, E., Hess, B., Groenhof, G., Mark, A. E., and Berendsen, H. J. (2005). GROMACS: fast, flexible, and free. *J Comput Chem,* 26, 1701–1718. doi: 10.1002/jcc.20291

Vandeputte, O. M., Kiendrebeogo, M., Rajaonson, S., Diallo, B., Mol, A., Jaziri, M. E., et al. (2010). Identification of catechin as one of the flavonoids from *Combretum albiflorum* bark extract that reduces the production of quorum-sensing-controlled virulence factors in *Pseudomonas aeruginosa PAO1*. *Appl. Environ. Microbiol.* 71, 243–253. doi: 10.1128/AEM.01059-09

Vandeputte, O. M., Kiendrebeogo, M., Rasamiravaka, T., Stévigny, C., Duez, P., Rajaonson, S., et al. (2011). The flavanone naringenin reduces the production of quorum sensing-controlled virulence factors in *Pseudomonas aeruginosa* PAO1. *Microbiology* 157, 2120–2132. doi: 10.1099/mic.0.049338-0

Vasavi, H. S., Arun, A. B., and Rekha, P. D. (2016). Anti-quorum sensing activity of flavonoid-rich fraction from *Centella asiatica* L. against *Pseudomonas aeruginosa* PAO1. *J. Microbiol. Immunol. Infect.* 49, 8–15. doi: 10.1016/j.jmii.2014.03.012

Whiteley, M., Diggle, S. P., and Greenberg, E. P. (2017). Progress in and promise of bacterial quorum sensing research. *Nature* 551, 313–320. doi: 10.1038/nature24624

WHO (2011). Regional Committee for Europe 2011. *European Strategic Action Plan on Antibiotic Resistance*. Copenhagen:WHO.

WHO (2012). *The Evolving Threat of Antimicrobial Resistance: Options for Action*. Geneva: World Health Organization.

Widmer, K. W., Soni, K. A., Hume, E. A., Beier, R. C., Jesudhasan, P., and Pillai, S. D. (2007). Identification of poultry meat-derived fatty acids functioning as quorum sensing signal inhibitors to autoinducer-2 (AI-2). *J. Food Sci.* 72, 363–368. doi: 10.1111/j.1750-3841.2007.00527.x

Williams, P. (2007). Quorum sensing, communication and cross kingdom signaling in the bacterial world. *Microbiology* 153, 3923–3928. doi: 10.1099/mic.0.2007/012856-0

Winans, S. C., and Bassler, B. L. (2002). Mob psychology. *J. Bacteriol.* 184, 873–883. doi: 10.1128/jb.184.4.873-883.2002

Wu, H., Song, Z., Hentzer, M., Andersen, J. B., Molin, S., Givskov, M., et al. (2004). Synthetic furanones inhibit quorum-sensing and enhance bacterial clearance in *Pseudomonas aeruginosa* lung infection in mice. *J. Antimicrob. Chemother.* 53, 1054–1061. doi: 10.1093/jac/dkh223

Zhang, A., and Chu, W. H. (2017). Anti-quorum sensing activity of *Forsythia suspense* on *Chromobacterium violaceum* and *Pseudomonas aeruginosa*. *Phcog. Mag.* 13, 321–325. doi: 10.4103/0973-1296.204547

Zhang, J., Rui, X., Wang, L.i., Guan, Y., Sun, X., and Dong, M. (2014). Polyphenolic extract from *Rosa rugosa* tea inhibits bacterial quorum sensing and biofilm formation. *Food Cont.* 42, 125–131. doi: 10.1016/j.foodcont.2014.02.001

Zhao, Z., Hou, S., Lan, D., Wang, X., Liu, J., Khan, F. I., et al. (2017). Crystal structure of a lipase from Streptomyces sp. strain W007-implications for thermos stability and regiospecificity. *FEBS J.* 284, 3506–3519. doi: 10.1111/febs.14211

Zhou, L., Zheng, H., Tang, Y., Yu, W., and Gong, Q. (2013). Eugenol inhibits quorum sensing at sub-inhibitory concentrations. *Biotechnol. Lett.* 35, 631–637. doi: 10.1007/s10529-012-1126-x

Conflict of Interest Statement: The authors declare that the research was conducted in the absence of any commercial or financial relationships that could be construed as a potential conflict of interest.

frontiers in Cellular and Infection Microbiology

ORIGINAL RESEARCH
published: 04 September 2018
doi: 10.3389/fcimb.2018.00292

Virtual Screening and Biomolecular Interactions of CviR-Based Quorum Sensing Inhibitors Against *Chromobacterium violaceum*

Vinothkannan Ravichandran†, Lin Zhong†, Hailong Wang, Guangle Yu, Youming Zhang and Aiying Li**

State Key Laboratory of Microbial Technology, Shandong University–Helmholtz Institute of Biotechnology (SHIB), School of Life Science, Shandong University, Qingdao, China

The rise of bacterial multi drug resistance becomes a global threat to the mankind. Therefore it is essential to find out alternate strategies to fight against these "super bugs." Quorum sensing (QS) is a cell-to-cell communication mechanism by which many bacteria regulate their biofilm and virulence factors expression to execute their pathogenesis. Hence, interfering the quorum sensing is an effective alternate strategy against various pathogens. In this study, we aimed to find out potential CviR-mediated quorum sensing inhibitors (QSIs) against *Chromobacterium violaceum*. Virtual screening from a natural products database, *in vitro* biofilm and violacein inhibition assays have been performed. Biofilm formation was investigated using confocal microscopy and gene expression studies were carried out using qRT-PCR. Further, to study the biomolecular interaction of QSIs with purified CviR Protein (a LuxR homologue), microscale thermophoresis (MST) analysis was performed. Results suggested that phytochemicals SPL, BN1, BN2, and C7X have potential GScore when compared to cognate ligand and reduced the biofilm formation and violacein production significantly. Especially, 100 μM of BN1 drastically reduced the biofilm formation about 82.61%. qRT-PCR studies revealed that *cviI, cviR, vioB, vioC, vioD* genes were significantly down regulated by QSIs. MST analysis confirmed the molecular interactions between QSIs and purified CviR protein which cohere with the docking results. Interestingly, we found that BN2 has better interaction with CviR (K_d = 45.07 ±1.90 nm). Overall results suggested that QSIs can potentially interact with CviR and inhibit the QS in a dose dependent manner. Since, LuxR homologs present in more than 100 bacterial species, these QSIs may be developed as broad spectrum anti-infective drugs in future.

Keywords: ***Chromobacterium violaceum*, quorum sensing, quorum sensing inhibition, virtual screening, biofilm inhibition and microscale thermophoresis**

OPEN ACCESS

Edited by:
Rodolfo García-Contreras, Universidad Nacional Autónoma de México, Mexico

Reviewed by:
John Pinney, Imperial College London, United Kingdom
Yael González Tinoco, Universidad Nacional Autónoma de México, Mexico

***Correspondence:**
Youming Zhang
zhangyouming@sdu.edu.cn
Aiying Li
ayli@sdu.edu.cn

†These authors have contributed equally to this work

Received: *04 May 2018*
Accepted: *30 July 2018*
Published: *04 September 2018*

Citation:
Ravichandran V, Zhong L, Wang H, Yu G, Zhang Y and Li A (2018) Virtual Screening and Biomolecular Interactions of CviR-Based Quorum Sensing Inhibitors Against Chromobacterium violaceum. Front. Cell. Infect. Microbiol. 8:292. doi: 10.3389/fcimb.2018.00292

INTRODUCTION

Antibiotic resistance has become a global health issue and considered to be a leading health challenge in recent years (Ferri et al., 2017). Hence, efforts have to be taken to identify novel strategies which could curb bacterial pathogenesis in order to tackle multi drug resistant (MDR) "super bugs" (Wagner et al., 2016). Bacteria coordinates their behavior through quorum sensing

(QS), a mechanism that helps bacterial populations to enable harmonious responses including biofilm formation and virulence factors expressions. Since, QS regulates the virulence arsenal of many pathogenic bacteria, it seems to be a captivating drug target to combat bacterial infections (Rasmussen and Givskov, 2006; Williams, 2017). Drugs targeting the virulence pathways could curb the bacterial pathogenesis and thereby prevents the disease development.

N-acylhomoserine lactones (AHLs) and peptides are the autoinducers in gram-negative bacteria and gram-positive bacteria respectively. Furthermore, autoinducer-2 (AI-2) are reported as interspecies communication signal (Miller and Bassler, 2001). AHLs contains a homoserine lactone ring with varying length of acyl chains (C4 to C18) via amide bonds (Bassler, 2002). In LuxI/LuxR- based QS systems, AHLs are synthesized by LuxI synthases and LuxR encodes the receptor proteins. Once synthesized, AHLs will be internalized, accumulated and recognized by LuxR-type receptor and this will modulate the regulation of target genes (Paul et al., 2017).

Chromobacterium violaceum, a gram-negative, facultative anaerobic, non-sporing coccobacillus has a quorum-sensing system consists of CviI/CviR, a LuxI/LuxR homolog (McClean et al., 1997; Stauff and Bassler, 2011). It is demonstrated that inhibitors able to interact with CviR could prevent the nematode from *C. violaceum*-mediated killing. Hence, it is apparent that the quorum sensing plays a vital role in *C. violaceum* pathogenesis and it is established that QSIs could be potent drug candidates in the battle against MDR pathogens including *C. violaceum* (Swem et al., 2009; Chen et al., 2011).

The advantages of QSIs over conventional antibiotics are as follows. Firstly, it is believed that the pathogens would not develop resistance to QSIs as this strategy may create only no or little selective pressure to the bacteria (Defoirdt et al., 2010). Secondly, QS seems to be essential for spreading bacterial resistance as it is directly or indirectly influencing the horizontal gene transfer. Thirdly, the LuxI/LuxR homologs have been reported in more than 100 Gram-negative bacterial species and over 200 different Gram-negative bacteria have been described to use AHLs as QS signals. Thereby QSIs may have the competence to be a broad range anti-virulent drugs (Adonizio et al., 2006). Taken together, interfering this mechanism would have an astounding impact over the bacterial resistance and its control (Uroz et al., 2009; Kalia, 2015). Numerous studies have been published related to quorum sensing inhibitors (QSIs) which rationalize the capability of this strategy (Ren et al., 2005; Rasmussen and Givskov, 2006; Ni et al., 2008; Kalia, 2013; Brackman and Coenye, 2015; Coughlan et al., 2016; Delago et al., 2016).

Natural products have always been fascinating source for the drug discovery. It is reported that more than 80% of drugs were natural products or inspired by a natural compound (Harvey, 2008). It is evident that almost half of the drugs approved in last two decades are based on natural products (Butler, 2008). Hence, it is crucial to screen natural products to discover potential QSIs against MDR pathogens. Despite the fact, several studies revealed that numerous plant extracts and natural products inhibit the quorum sensing of various pathogens (Adonizio et al., 2006; Vattem et al., 2007; Bouyahya et al., 2017; Paul et al., 2017), in-depth investigations are much essential to take-up these QSIs to the next level of drug discovery.

Here, we report high-throughput virtual screening of QSIs against CviR, the quorum regulator of *C. violaceum* and their biological evaluation through *in vitro* assays including qRT-PCR. To the best of our knowledge, this is the first study to discuss the molecular interactions of QSIs with purified quorum sensing target protein, CviR using microscale thermophoresis (MST) analysis.

MATERIALS AND METHODS

Bacterial Strains and Growth Conditions

C. violaceum 31532, *E.coli* BL21 (DE3) were used in this study. All the bacterial strains were grown in Luria-Bertani (LB) medium, and *C. violaceum* 31532 and *E.coli* BL21 (DE3) were grown at 30° and 37°C respectively, for 24 h. Quorum sensing inhibitors (QSIs) Sappanol (SPL), Butein (BN1), Bavachin (BN2), and Catechin 7-xyloside (C7X) were purchased from Chemfaces, China.

High Throughput Virtual Screening (HTVS)

The virtual screening was performed against CviR using Schrodinger software (Maestro v10.6, Glide module) to screen the natural product database containing 4687 compounds. The energy minimized 3D ligand file was prepared using LigPrep module (Friesner et al., 2006). The three-dimensional structure of CviR protein was retrieved from Protein Data Bank (PDB: 3QP1 and 3QP5). Coordinates of CviR structure was prepared by using protein preparation wizard. Docking was performed using GLIDE (Grid Based Ligand Docking with Energetics) module in Schrodinger suite. Grid files were generated using the C_6HSL, the native ligand (C_6HSL) to the center of both the grid boxes. Tyr 80, Trp 84, Asp 97, and Ser 155 were found to be the active site residues. The compounds were subjected to HTVS ligand docking using the pre-computed grid files and then XP docking was also performed for top ranking compounds. The XP docking helps to remove the false positives with much stricter scoring function than the HTVS. Hits having least GScore (Glide score) and more number of H-bonds were analyzed further. To investigate the binding pocket of LuxR homologs, CviR from *C. violaceum* and LasR from *Pseudomonas aeruginosa* were compared using RCSB PDB Protein Comparison Tool.

Biofilm Inhibition Assay

The effect of QSIs on biofilm formation was measured by microtitre plate assay (O'toole and Kolter, 1998). Briefly, overnight cultures (0.4 OD at 600 nm) of *C.violaceum* were added into 1 mL of fresh LB medium and grown with or without QSIs with varying concentrations (1, 10 and 100 μM) for 24 h at 30°C. After incubation, microtitre plates were washed with PBS ($_p$H 7.4) to remove the free-floating planktonic cells. The biofilm was stained using 200 μL of 0.1% crystal violet (CV) solution. After 15 min, CV

solution was removed and 200 μL of 95% ethanol was added. The biofilm was then quantified by measuring the absorbance at OD 470 nm using microplate reader (Infinite M200, Tecan).

Violacein Quantification Assay

Production of violacein pigment by *C. violaceum* in the presence and absence of QSIs was analyzed by violacein extraction and quantification (Blosser and Gray, 2000). Briefly, overnight culture (OD_{600} nm = 0.1) was incubated in conical flask containing LB broth with or without QSIs (1, 10, and 100 μM) and incubated at 30°C for 24 h. Bacterial cells were then collected and the pellet was dissolved in 1 mL DMSO. Cell debris was removed by centrifugation at 13,000 g for 10 min and the absorbance of soluble violacein was read at 585 nm using microplate reader (Infinite M200, Tecan).

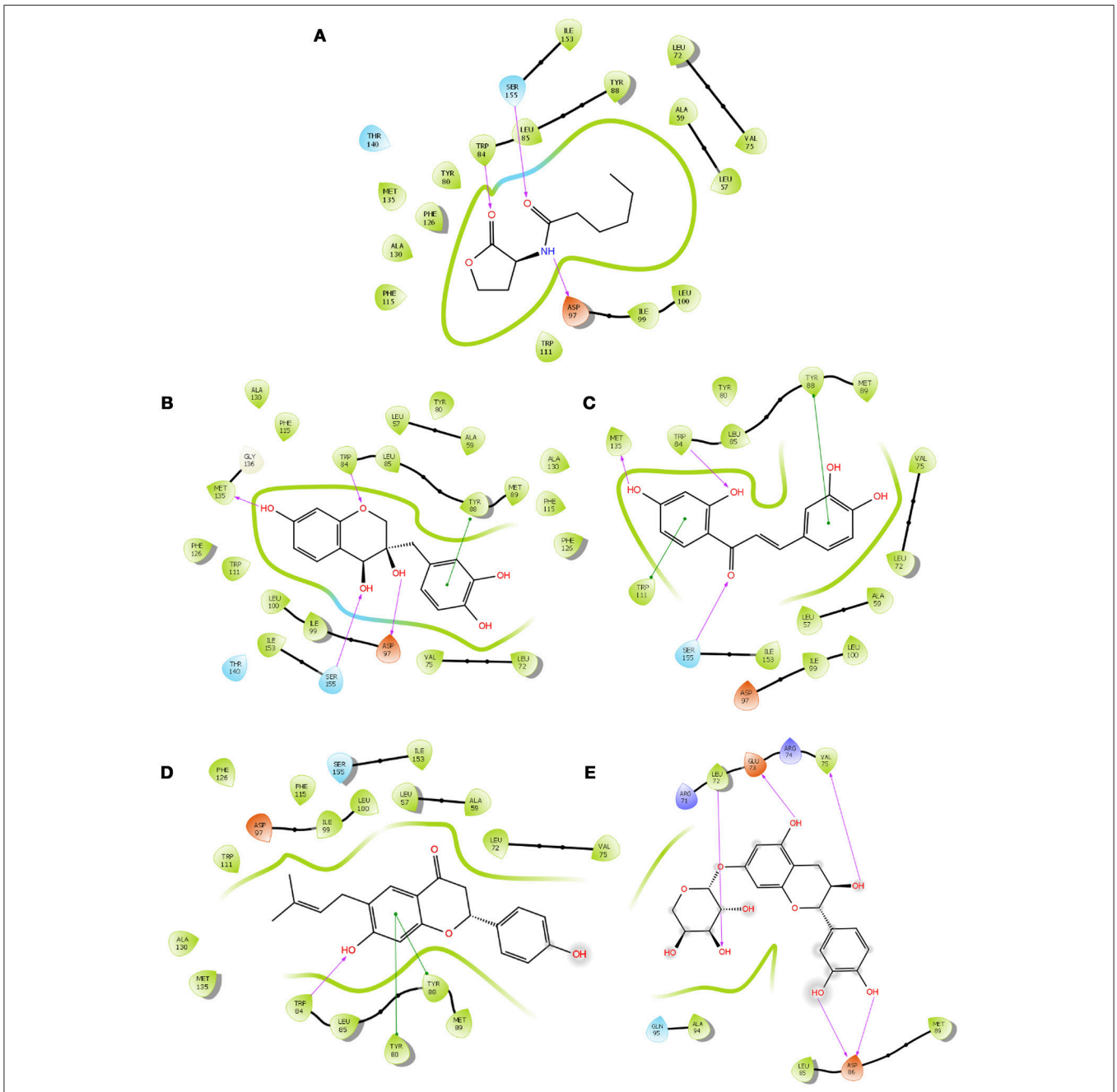

FIGURE 1 | The 2D interaction diagrams of QSIs against CviR. The purple arrows shows the H-bonds whereas the green lines shows the π-π stacking. **(A)** is for interaction map of C_6HSL, **(B)** for interaction map of SPL, **(C)** for interaction map of BN1, **(D)** for interaction map of BN2 and **(E)** for interaction map of C7X against CviR. Most of the QSIs have at least one common bond forming aminoacid with C_6HSL (Trp 84, Asp 97, Ser 155) and all of them have least GScore than C_6HSL.

Confocal Laser Scanning Microscopy (CLSM) Studies

Confocal Laser Scanning Microscopy (CLSM) analysis of the *C.violaceum* biofilms was performed as described by (Zhao and Liu, 2010). Static biofilms were grown on a glass cover slips (1: 100 diluted culture of *C.violaceum* inoculated in LB broth and incubated overnight at 30°C in stationary condition) in 6-well cell culture plates either with or without QSIs (100 μM). The developed biofilms were washed twice to remove loosely bound cells and stained with FITC-ConA for 15 min. Cells were rinsed twice in PBS to remove the excess stains and the adhered cells were analyzed using CLSM (Zeiss L800, Japan) with the excitation and emission wavelength set at 488 and 520 nm respectively.

qRT-PCR Studies

Total RNA was extracted from *C. violaceum* biofilm cells using the RNAprep Pure Kit (Tiangen, China) as per manufacturer's instructions. Biofilm cells were grown in 1 mL LB medium with or without QSIs (100 μM) at 30°C for 24 h. Total RNA was extracted with the RNA isolation kit (TIANGEN Biotech Co., Ltd., Beijing, China). Primers for *cviI, cviR,vioB, vioC, vioD,* and *rpoD* (**Table S1**) were synthesized by Sangon Biotech (Shanghai, China). Total RNA was used as a template for the reverse transcription reaction using a Prime Script RT Reagent Kit (TaKaRa, Japan) at 37°C for 15 min, three times (reverse transcription), and at 85°C for 5 min (reverse transcriptase inactivation) as per the manufacturer's protocol, with a total volume of 20 μL.

The qRT-PCR was performed according to the manufacturer's protocol for the SYBR® Premix Ex TaqTM II Kit (TaKaRa, Japan). Reverse transcriptase was used as a template for RT-qPCR, and the total reaction system (20 μL) was made up as the following: 10 μL SYBR® Premix Ex TaqTM II (2×), 0.8 μL forward primer, 0.8 μL reverse primer, 0.4 μL ROX Reference Dye (50×), 2 μL DNA template, and 6 μL double-distilled H_2O (ddH_2O). Afterwards, qRT-PCR was performed using Applied Biosystems Quant Studio™ 3 Real-Time PCR System (Applied Biosystems Inc., CA, USA). The reaction conditions are as follows: pre-denaturation at 95°C for 30 s, followed by 40 cycles of denaturation at 95°C for 5 s and annealing and extension at 60°C for 30 s. *rpoD* was used as an internal reference. The relative mRNA expression of all the genes were calculated using the $2^{-\Delta Ct}$ method. The experiment was independently conducted 3 times.

Expression and Purification of CviR

The DNA fragment encoding CviR (GQ398094) was amplified using the primers 5′-CGATATTATTGAGGCTCACAGAG AACAGATTGGTGGATCCATGGTGATCTCGAAACCCA

TABLE 1 | Docking analysis of Quorum sensing inhibitors against CivR, the quorum regulator of *Chromobacterium violaceum*.

S.No	Name	Structure	GScore	Number of H-bonds	Bond forming amino acids
1	C_6HSL	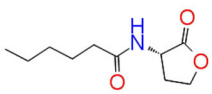	−7.052	3	Trp 84 Asp97 Ser 155
2	Sappanol	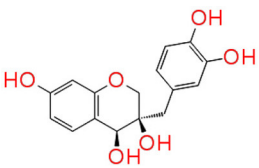	−12.140	4	Trp 84 Asp 97 Met 135 Ser 155
3	Butein	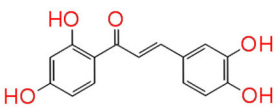	−11.246	3	Trp 84 Met 135 Ser 155
4	Bavachin	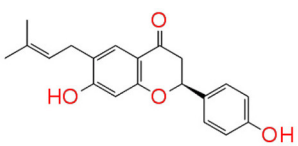	−8.056	1	Trp 84
5	Catechin 7-xyloside	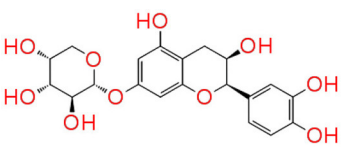	−7.414	4	Glu73 Val 75 Asn 77 Asp 86

TCAACG-3′ and 5′-TAGCAGCCGGATCTCAGTGGTGGT GGTGGTGGTGCTCGAGTTATTCGTTCGCTACGGTCGA G-3′. Primers having homology arm were used for the Red/ET recombination (Wang et al., 2016). PCR products were cloned into the expression plasmid pET28a (Novagen) linearized with BamHI and XhoI restriction enzymes by LLHR method (linear plus linear homologs recombination) of Red/ET in GBdir as per our previous reports (Wang et al., 2016). The resulting plasmid was termed as pET28-CviR and was verified by DNA sequencing of the insert and flanking regions. Produced protein corresponds to a fusion of CviR with the SUMO tag and His-tag as well. *E. coli* BL21 (DE3) was transformed with pET28-CviR. 5L Erlenmeyer flasks containing 2L LB medium supplemented with 5 μg/ml of kanamycin were inoculated with an overnight culture of *E. coli* BL21 (DE3) pET28-CviR to an initial OD_{660} of 0.05. Growth was carried out at 37°C until the OD_{660} of 0.4. The temperature was then lowered to 18°C and growth continued until an OD_{660} of 0.6 – 0.8, and then induced with 0.1 mM IPTG and growth was continued overnight at 18°C. All subsequent manipulations were conducted at 4°C. The cells were harvested by centrifugation at 4,200 rpm and ultrasonicated for 14 min in 80 mL of washing buffer with 14% of machine power (250 mM Tris-HCl, 150 mM NaCl, 20 mM imidazole, 5% glycerol, $_{p}$H 7.8) to break the cell wall for purification. Further, samples were centrifuged at 11,000 rpm for 1 h and washed twice with washing buffer after flow-through the supernatant through Ni-sepharose 6 Fast flow (GE Healthcare, USA. 20 mL wash buffer was used to elute the CviR protein once digested with ULP proteinase. The protein was stored at −80°C for further use.

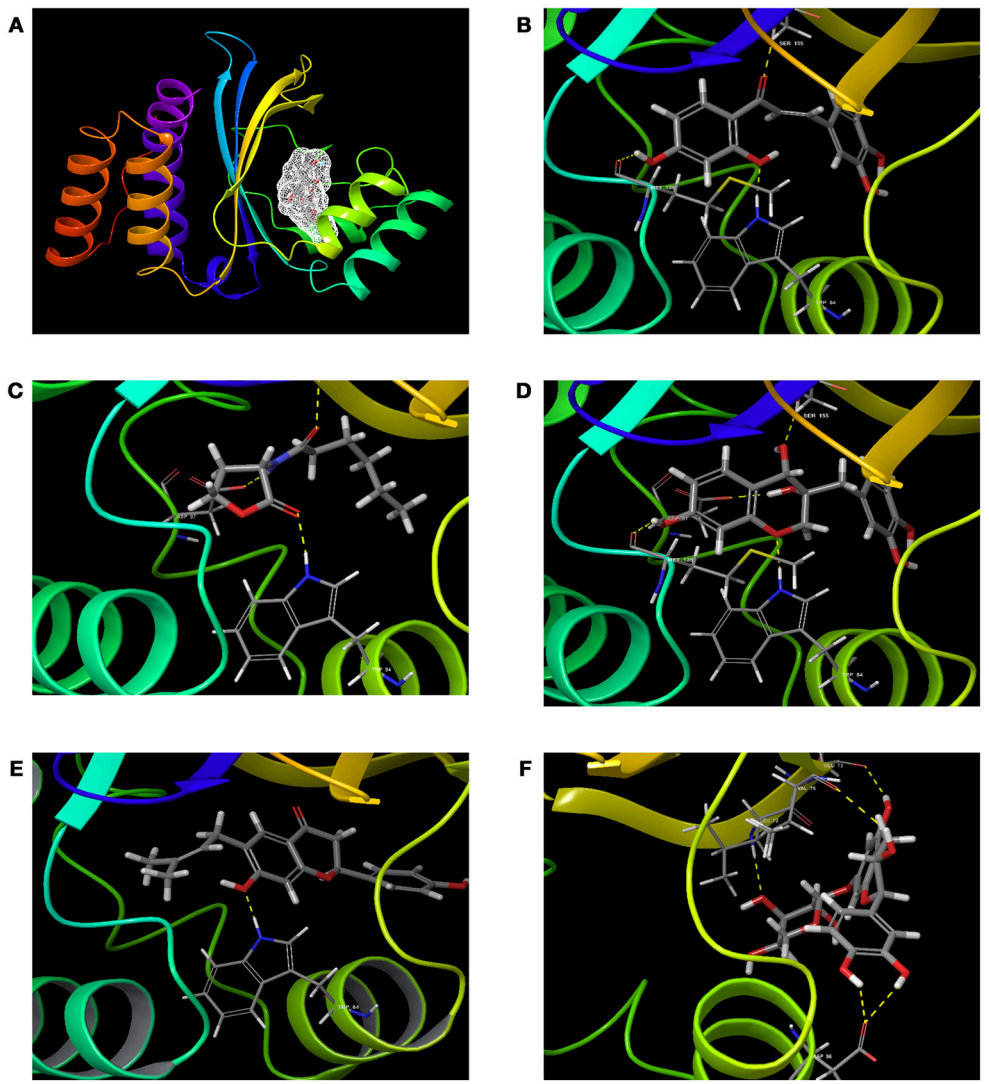

FIGURE 2 | The 3D molecular interactions of QSIs against CviR **(A)** is for CviR, the LuxR homolog of *C. violaceum* where the ligand binding pocket is depicted in light gray **(B)** is for molecular interaction of C_6HSL with CviR (3 H bonds) **(C)** for molecular interaction of SPL (4 H bonds) **(D)** for molecular interaction of BN1 (3 H bonds) **(E)** for molecular interaction of BN2 (1 H bond) and **(F)** for molecular interaction of C7X against CviR (4 H Bonds). H-bonds represented in yellow dotted line.

MST Analysis

All the compounds were analyzed with the concentration gradient of 50 μM with 20 μM of CviR which was labeled Monolith NT™ Protein Labeling Kit RED–NHS (Cat Nr: L001) before instrumental analysis. LED power was 20% and MST optimized buffer was used for the analysis (50 mM Tris-HCl, 150 mM NaCl, 10 mM MgCl2, 0,05% Tween-20).

Analysis was performed on Monolith NanoTemper (NT) 115 and its accessory, i.e., standard-treated 4 μL volume glass capillaries were employed to measure the molecular interaction (NanoTemper Technologies GmbH, Munich, Germany). Means of fluorescence intensity obtained by the MST measurements were fitted and the resultant K_d values were given together with an error estimation from the fit by the built-in formula of NT 1.5.41 analysis software (Cai et al., 2017).

Statistical Analysis

Graph pad prism software (version 6.01) was used for statistical analysis. One way ANOVA and multiple comparisons were carried out wherever required. *P*-values (<0.05 and <0.01) were considered as statistically significant. All the assays were conducted in triplicates and the results were expressed as mean ± SD.

RESULTS

Computational Studies

Molecular Interaction of QSIs Against CviR

To screen quorum sensing inhibitors against CviR, QS regulator of *C. violaceum*, virtual screening was performed using a natural product database. GScore for the native ligand (C_6HSL) was −7.052 and C_6HSL was able to form three H-bonds with Trp 84, Asp 97, Ser 155 (**Figures 1A–E**) which was used as reference value and pattern of interaction for the pose analysis. SPL, BN1, BN2, C7X were having the GScore −12.140, −11.246, −8.056, −7.414 (**Table 1**) respectively. SPL was able to form 4 H-bonds with amino acids Trp 84, Asp 97, Met 135 and Ser 155 along with a pi-pi stacking with Tyr 88. BN1 was able to form 3 H-bonds

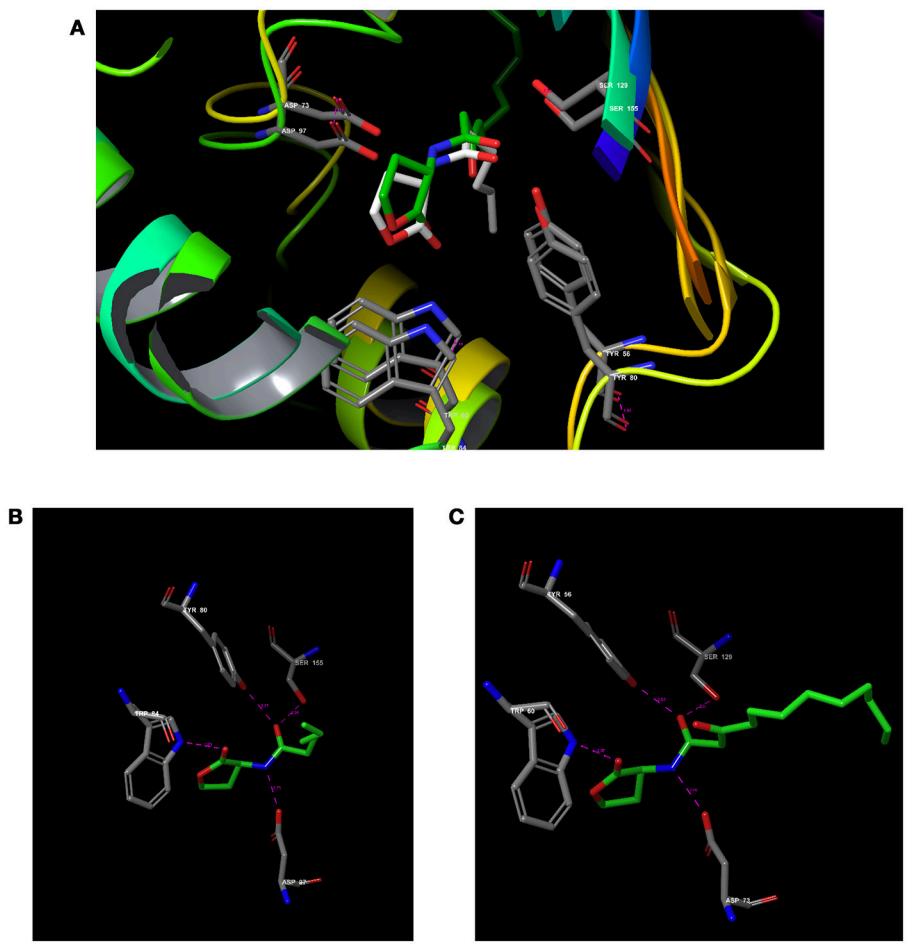

FIGURE 3 | Comparative analysis of CviR with LasR using RCSB PDB Protein Comparison Tool. **(A)** Molecular comparison of CviR vs LasR. **(A)** The alignment of the active site residues (Tyr, Trp, Asp, Ser) which are crucial for the interactions. **(B)** The molecular interaction of (N-hexanoyl-L-Homoserine lactone (C_6HSL) against CviR **(C)** The molecular interaction of N-(3-Oxododecanoyl)-L-homoserine lactone (3-Oxo-C_{12}-HSL) with LasR.

with Trp 84, Met 135 and Ser 155 along with 2 pi-pi stacking with Trp 84 and Tyr 88. Whereas, BN2 was able to form only one H-bond with two pi-pi interaction with Tyr80 and Tyr 88 (**Figures 2A–F**). In contrast, C7X has a very unusual pattern of interaction and it was able to form 4 H-bonds with Glu73, Val 75, Asn 77, and Asp 86. After pose analysis, based on GScore and H-bond forming ability, the ligands were chosen for further studies.

Comparative Analysis of CviR vs. LasR

To verify how close the binding pocket LuxR homologs are, the PDB structure of CviR and LasR were analyzed. As expected, both cognate ligands were interacting with the very similar amino acids in both receptors. C_6HSL was interacting with Tyr 80, Trp 84, Asp 97, and Ser 155 in CviR and 3-oxo-C_{12}HSL was interacting with Tyr 56, Trp 60, Asp 73 and Ser 129 (**Figure 3A**). Further, positional changes of these residues were calculated and found to have very minute change. The distance between Tyr 80-56 was 1.43 Å and the distance between Trp84-60 was 1.14 Å (**Figures 3B,C**). Asp 97-73 were in a distance of 1.00 Å. Surprisingly, Ser155-129 were in a distance less than 1 Å (0.75 Å). Further, we found that SPL and BN1 were able to interact with Ser 155, which is crucial for CviR and LasR as well.

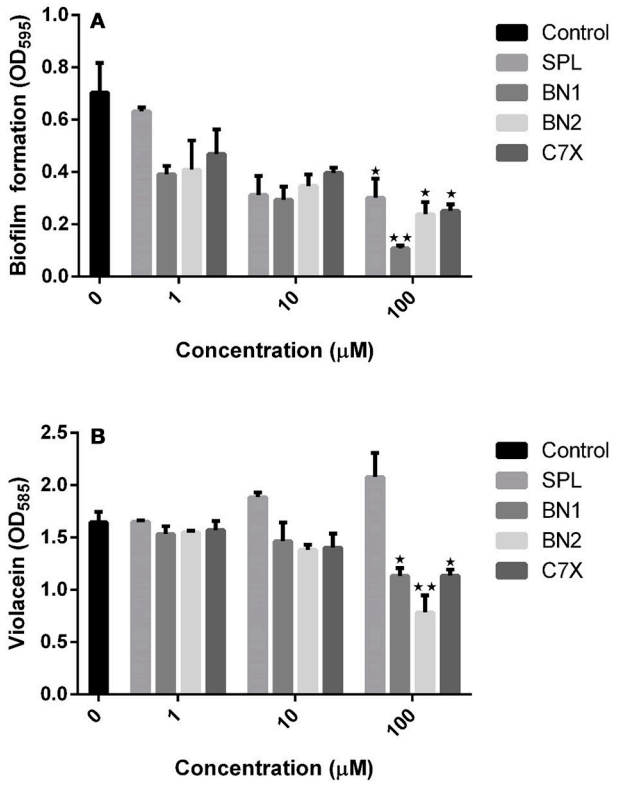

FIGURE 4 | The effect of QSI on biofilm formation and violacein. **(A)** The biofilm formation was inhibited by QSIs. Especially, BN2 and C7X have reduced the biofilm formation significantly whereas BN1 decreased the biofilm formation drastically (~50%). **(B)** The similar trend was followed in violacein production also. Though all the three QSIs reduce the violacein production, the SPL found be increased. $^*P < 0.05$ and $^{**}P < 0.01$.

Influence of QSIs on Biofilm, Growth, and Violacein

It is essential to verify the efficacy of QSIs against quorum sending regulated phenotypes in *C.violaceum*. Biofilm is one of the major factor that is under the control of quorum sensing and plays a crucial role in pathogenesis and drug resistance. All the tested QSIs reduced the biofilm formation significantly at varying concentrations (1, 10 and 100 μM). Except C7X, all the QSIs reduced more than 50% of biofilm at 10 μM concentrations (**Figure 4A**). Especially, BN1 significantly reduced the biofilm formation about 82.61% when supplied with 100 μM. Whereas, BN2 and C7X reduced the biofilm by about 66 and 64.26% respectively with the similar treatment. To differentiate the quorum sensing inhibition activity of these QSIs from antibiotic activity, the growth was analyzed. Except SPL, none of the QSIs found to have influence on the growth of *C. violaceum* (**Figure S1**). Violacein, a purple pigment produced by the *C. violaceum* which is reported to be under the control of QS mechanism via *vioABCDE* operon. Violacein quantification analysis revealed that all the tested QSIs have potentially suppressed the violacein production. BN2 reduced the violacein drastically by 52.50% when treated with 100 μM (**Figure 4B**). A concentration-dependent reduction in the violacein production was observed. Unfortunately, SPL was found to increase the production of violacein by 14.51 and 26.26% when treated with 10 and 100 μM respectively.

Confocal Studies

The efficacy of the QSIs on biofilm development was examined using the confocal laser scanning microscopy (CLSM). It was found that all the QSIs except SPL were negatively regulating the biofilm formation when treated with 100 μM concentrations (**Figures 5A–E**). To be specific, BN2 and BN2 have significantly reduced the biofilm formation when administered with 100 μM.

Gene Expression Studies

To investigate the impact of QSIs (100 μM) on the genes expression related to *C.violaceum* quorum sensing, qRT-PCR studies have been performed. First of all, the effect of QSIs on *cviI* and *cviR* was evaluated. Data suggest that the BN1 and C7X were able to significantly suppress the expression of *cviI* (**Figure 6A**). Whereas in case of cviR, the similar pattern of decrement was observed which is comparable to that of *cviI*. It is noteworthy, that SPL increased the expression of *cviI* but comparatively less in *cviR*.

To study further the effect of QSIs on *vioABCD* operon, genes including *vioB, vioC, vioD* were analyzed. All the QSIs were significantly reduced the expression of *vioB, vioC, vioD* genes (**Figure 6B**). Especially, BN2 decreased the expression of these genes very significantly. Surprisingly, SPL also decreased the expressions.

Expression and Purification of CviR

RecET based direct cloning and Redαβ based recombineering were used for heterologous expression of CviR Protein. The *cviR* gene was cloned into the expression vector pET28a and the protein was expressed in *E. coli* (**Figure 7**). The purification were

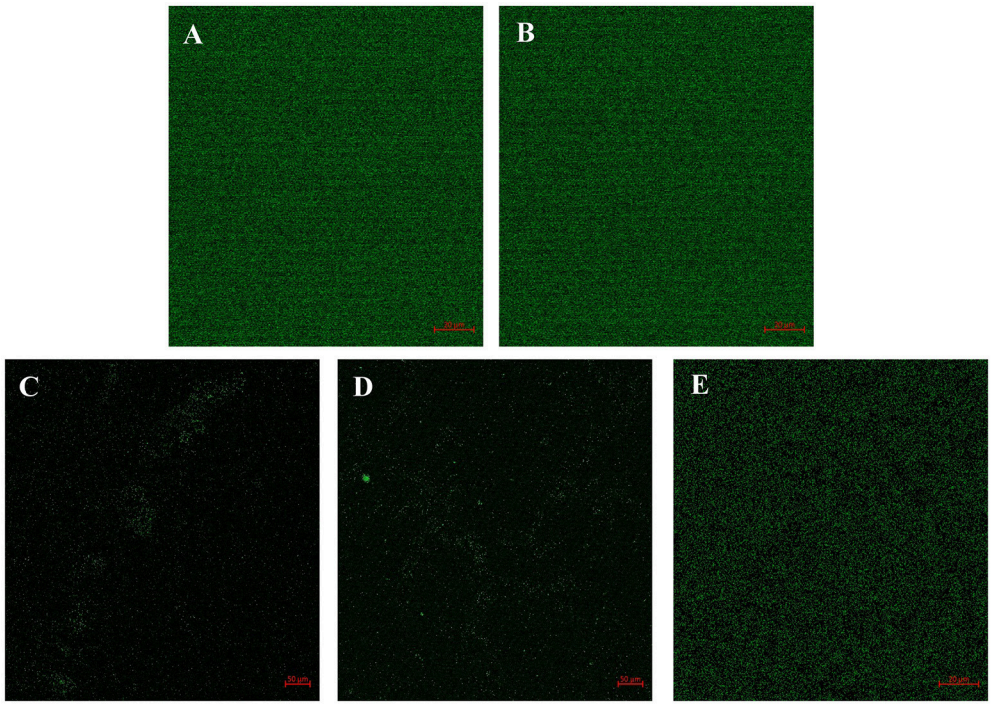

FIGURE 5 | Confocal image shows the efficacy of QSIs to curb the biofilm formation. **(A)** Control **(B)** SPL **(C)** BN1 **(D)** BN2 and **(E)** C7X.

carried out under different conditions of cell growth and buffers. The purified protein was further investigated by polyacrylamide gel electrophoresis (PAGE) (**Figure S2**).

Microscale Thermophoresis

MST experiment was carried out to detect the molecular interaction between QSIs and CviR. Differences in normalized fluorescence of the bound and unbound state will allow determination of the fraction bound and thus the dissociation constant is calculated. All values are multiplied by a factor of 1,000 which yields the relative fluorescence change in per thousand. MST results suggested that all the QSIs except C7X have significant binding ability. It is noteworthy to mention that the dissociation constant (K_d) of BN2 is 45.07 $\pm$1.90 nm (**Figure 8C**). Surprisingly, the F_{norm} value of BN1 is increased when the concentration increased and having a sigmoidal curve suggests a competitive interaction pattern (**Figure 8B**).

DISCUSSION

Due to misuse and overuse of antibiotics along with complex bacterial drug resistance mechanisms, antimicrobial resistance has emerged as a global threat (Soukarieh et al., 2018). According to WHO's Global Antimicrobial Surveillance System (GLASS), occurrence of MDR infections was found among half a million people all around the world. Resistance to penicillin has raised up to 51% whereas ciprofloxacin resistance raised from 8 to 65%. The recent report from GLASS confirms that there is a serious situation of antibiotic resistance worldwide (Tornimbene et al., 2018). Many case reports on *C.violaceum* infections were published with variety of health complications and it is resistant to a broad range of antibiotics including rifampin, vancomycin, ampicilin and cephalosporins (Fantinatti-Garboggini et al., 2004; Justo and Durán, 2017). Hence, alternatives to antibiotics is the "need of the hour" which will ultimately reduce morbidity, mortality and economic burden (Laxminarayan et al., 2016). Recently, disarming the bacterial virulence seems to be a potential alternate strategy to combat MDR (Rangel-Vega et al., 2015; Mookherjee et al., 2018). AHL mediated quorum sensing inhibition was reported to be effective in many pathogens including *C.violaceum*, *Pseudomonas aeruginosa* (Kim et al., 2015; Deryabin and Inchagova, 2018; Pérez-López et al., 2018; Soukarieh et al., 2018; Zhou et al., 2018). Since, natural products are the alluring sources of drug discovery, we intended to screen the CviR inhibitors from phytochemicals.

Virtual screening results suggested that numerous chemical moieties were able to interact with the CviR. Based on the GScore and the ability to form H-Bonds, four natural products have been chosen for further studies. Our *in silico* data revealed that molecular docking is in consistent with Crystallographic structures and in coherence with previous report (Kimyon et al., 2016). Generally, LuxR-type proteins are homodimers and each monomer consists of two domains, a ligand-binding domain (LBD) and a DNA-binding domain (DBD). Upon reception of cognate signal via LBD, they will undergo certain conformational changes, thereby allowing gene expression (Chen et al., 2011). All the QSIs SPL, BN1, BN2, C7X have better GScore than that of C_6HSL (−7.052). SPL and BN1 have a very similar pattern of

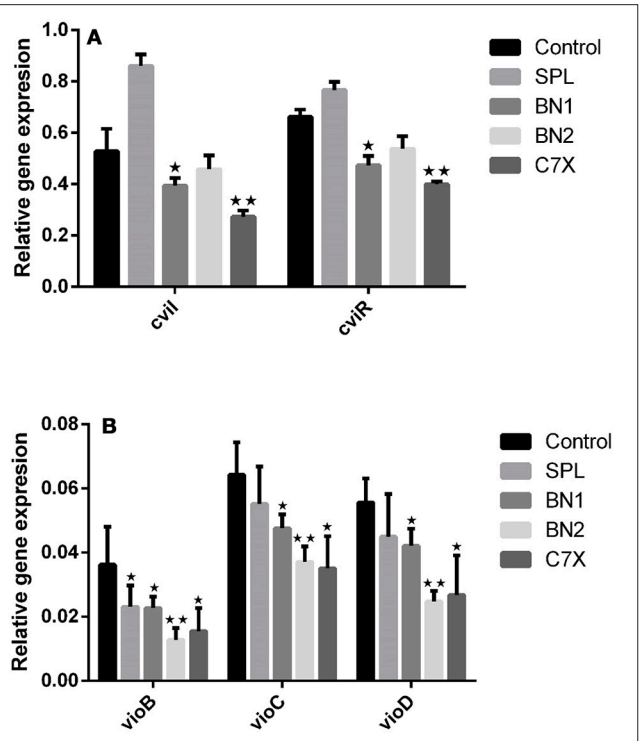

FIGURE 6 | The influence of QSIs on the genes which are under the control of CviI/CviR mediated quorum sensing. **(A)** The *cvil* and *cviR* genes were significantly suppressed by BN1 and C7X. **(B)** The genes involved in violacein biosynthesis were significantly suppressed by BN2. $^{*}P < 0.05$ and $^{**}P < 0.01$.

interaction alike C_6HSL along with H-bond Met 135. BN2 has a single H-bond with Trp 84, one of the key residue in the binding pocket of C_6HSL and it is observed to have two pi-pi interactions as well (**Figures 1D**, **2E**). It is speculated that, BN1 and BN2 may induce a closed conformation of CviR, hence it cannot interact with the DNA and thus inhibiting the QS as similar as chlorolactone (CL). It is demonstrated that CL potentially inhibits the *C.violaceum* QS by interacting with Trp 84 and Asp 97 along with a pi-pi stacking with Tyr 88 which is very similar to the pattern of interaction of BN1 (Swem et al., 2009). Whereas C7X has entirely different pattern of interaction with 4H bonds and surprisingly, C7X has interaction with Arg 74, which was reported to be present in DBT. Hence, it is hypothesized C7X could inhibit the QS by occupying the DBD and inducing a closed conformation.

Our findings showed that the AHLs (C_6 HSL and 3-oxo-C_{12}HSL) have four crucial point of interactions such as lactone carbonyl group which forms an H-bond with Trp84 residue, the acyl group amine forms a H-bond with Asp 97 and the carbonyl oxygen which forms H-bonds with Tyr80 and Ser155 which coheres with the results of Ahmed et al. (2013) (**Figures 3A–C**). Further, it is found that $Ser155_{CviR}$ and $Ser129_{LasR}$ were in a distance less than 1 Å (0.75 Å) and this suggested that Ser in the LBD must be a very essential point of interaction. Even though docking relies on many approximations, lead optimization was often in concert with evaluations and moreover this virtual screening approach saves time, manpower and cost when compared to the traditional approaches.

In AHL mediated QSIs identification process via virtual screening, biofilm formation and violacein quantification assays are the basic and crucial steps. Since violacein pigment is under the control of QS mechanism, *C.violacum* is considered to be one of the best and easily accessible biomonitor strains to screen QSIs of any origin. Our *in vitro* studies demonstrated that the QSIs have a potential influence on QS regulated phenotypes at the tested concentrations (1, 10, 100 μM) without affecting the growth (**Figures 4A,B** and **Figure S1**). Numerous studies have been reported that the plant-based natural products, such as Vanillin, Naringin, Naringenin, Quercetin, Ellagic acid and Curcumin, reduced the biofilm formation without affecting the growth (Bouyahya et al., 2017). Curcumin was reported to reduce the biofilm and virulence related traits in various uropathogens in a concentration dependent manner (Packiavathy et al., 2014). Carvacrol significantly reduced the biofilm formation (0.1–0.3 mM) of *C.violaceum* and other pathogens (Burt et al., 2014). Quercetin and quercetin-3-O-arabinoside inhibited violacein production in *C. violaceum*, at 50 and 100 μg/mL, respectively (Vasavi et al., 2014). Isoprenyl caffeate, from *manuka propolis* found to reduce violacein in agar diffusion assays (Gemiarto et al., 2015). Studies revealed that tannin rich fractions of *Terminalia catappa* inhibited violacein production (50%) at 62.5 μg per mL without significantly affecting growth (Taganna et al., 2011). It is observed that our QSIs, have suppressed the QS at minimal concentrations when compared to most of the earlier reports. To demonstrate the effect of QSIs on biofilm, CLSM studies have been performed. Results revealed that the QSIs, BN1 and BN2 have drastically reduced the biofilm (**Figures 5D,E**), which is in consistent with *in vitro* biofilm assay. Unfortunately, SPL increased the biofilm formation which is comparable to the control. Though many reports available on biofilm and violacein inhibition of various plant extracts in search of QSIs, the active principle responsible for such effects have not been investigated further in most of the cases. Many synthetic chemicals have also been explored for QSI activity but still they are not taken for further studies.

To investigate the efficacy of QSIs on the genes which are under the control of QS mechanism, qRT-PCR experiment was conducted. The *cviI* gene which produces the C_6HSL and the gene *cviR* which produces CviR protein were taken into consideration. Data suggest that significant suppression by BN1 and C7X is in consistent with the *in vitro* study results. Our results are in agreement with (Burt et al., 2014) which was observed that 0.3 mM of carvacrol inhibited the *cviI* gene expression. Hence, these results indicated that QSIs inhibited the production of AHL at gene expression level.

In violacein biosynthetic pathway, the *vioB* produces a polyketide synthase, which is very essential for biosynthesis of violacein, as it catalyzes the condensation of two tryptophan derivatives. Whereas *vioD, vioC* are nucleotide-dependent monooxygenases. *vioD* seems to catalyze the hydroxylation of one tryptophan moiety, whereas *VioA* seems to catalyze an oxidative deamination in the second tryptophan moiety, and *vioC* catalyzes intermediate violacein oxidation (August

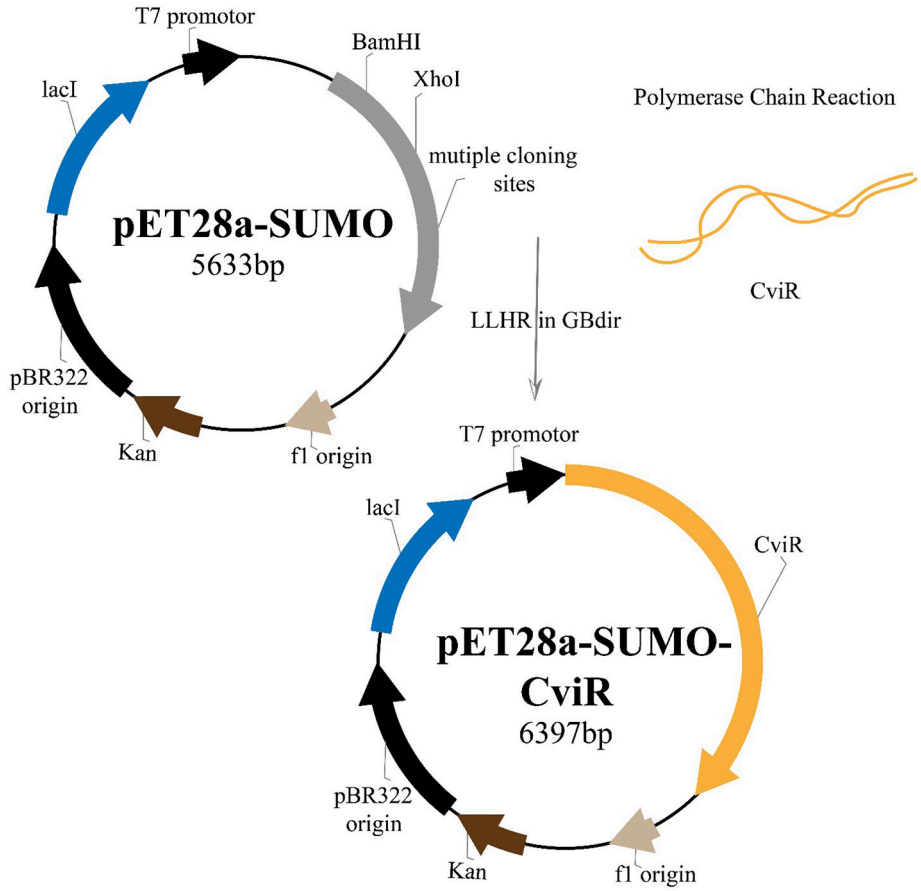

FIGURE 7 | Plasmid construction and the recombineering strategy followed for the heterologous expression of CviR protein.

et al., 2000). To study the effect of these QSIs on genes involved in violacein biosynthetic pathway, we have tested the gene expression of *vioB*, *vioC*, and *vioD*. All the QSIs have significantly suppressed the genes tested. BN1 significantly reduced the expression of *vioB*, *vioC*, and *vioD* (**Figures 6A,B**). It is documented that *Manuka propolis* PF5 treatment (300 μg/ml) down-regulated *vioD*, and the key residue was found to be isoprenyl caffeate (Gemiarto et al., 2015). Gene expression study showed the efficacy of QSIs in down regulating the QS related genes which play roles in biofilm formation and virulence directly or indirectly.

Further, to study the molecular interactions between these QSIs and CviR, CviR protein was expressed, isolated and purified for microscale thermophoresis (MST) analysis. For the CviR protein expression, RecET from Rac prophage mediated linear–linear homologous recombination (LLHR) method was followed as per our previous report, which can be used to clone large DNA regions directly from genomic DNA into expression vectors (Wang et al., 2016). MST is a powerful technique to measure biomolecular interactions which based on thermophoresis, the movement of molecules in a temperature gradient. This technique was reported to be highly sensitive that allows precise quantification of molecular interactions (Jerabek-Willemsen et al., 2014). MST results suggest that all the QSIs have potential molecular interaction with purified CviR (**Figures 8A–C**). The dissociation constant (K_d) of the BN2 is 45.07 ±1.90 nm (**Figure 8C**). These data suggest that BNI having a very similar interaction pattern to that of C_6HSL along with 2 pi-pi interactions, shows very significant interaction with CviR. According to Seidel et al. (2013), the fitting curve may be either S-shaper or mirror S-shaped. The reversal sign of MST amplitude (change in normalized fluorescence) depends on the chemistry of the compound that is titrated (e.g., Charge), its binding site and the conformational change induced upon binding. SPL and BN2 have negative slope suggesting interaction that don't alter the conformation significantly. Whereas the BN1 shows a positive slope suggesting a strong conformational change induced upon complex formation. Probably two pi-pi interactions play a major role in conformational change. Though C7X was not able to fit into the CviR binding pocket, we speculate that it might interfere the QS mechanism by negatively influencing the conformational changes required for the QS activation by interacting with the region near DNA binding domain (DBD) of CviR.

Overall results suggest that except SPL, BN1, BN2, and C7X significantly suppressed the QS of *C. violaceum*. Sappanol (SPL) is a 3, 4-dihydroxyhomoisoflavan, can be found in *Caesalpinia sappan*. Butein (BN1) is a chalcone, can be found in *Toxicodendron vernicifluum*. Bavachin (BN2) is a flavonoid,

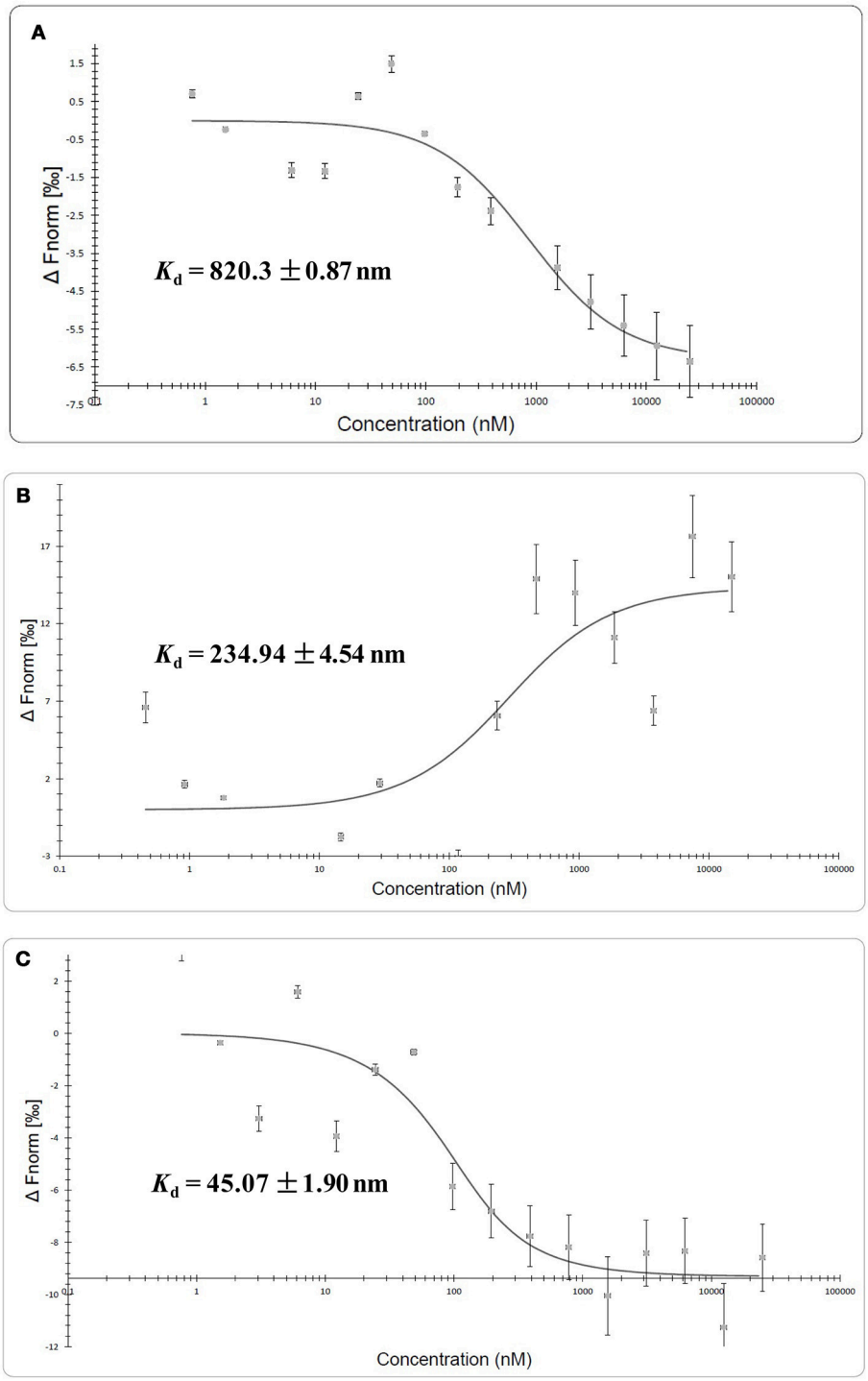

FIGURE 8 | Molecular interaction of QSIs using microscale thermophoresis analysis. **(A)** Molecular interaction of SPL **(B)** molecular interaction BN1 **(C)** molecular interaction BN2. Unfortunately we could not find any such interaction with C7X.

can be found in *Psoralea corylifolia*. Catechin-7-Xyloside (C7X) is flavan-3-ols, can be found in *Spiraea hypericifolia L.* All the natural products have their own biological activity profile. Virtual screening, *in vitro* studies, CLSM analysis of biofilm, qRT-PCR studies and molecular interaction studies using MST, suggest that BN1, BN2 significantly inhibited the CviR-mediated QS, whereas C7X might have a different mode of action and has to be explored further. Though QSIs are potential alternative to antibiotics in

the battle against MDR pathogens, it is essential to have an eye on the chances for QSIs getting resistance (Kalia et al., 2014; García-Contreras, 2016).

CONCLUSION

To summarize, our present data from virtual screening, docking analysis, qRT-PCR and MST measurement proved that the phytochemicals BN1, BN2, C7X inhibit CviR-mediated quorum against *C.violaceum* and represent potential CviR-mediated quorum sensing inhibitors against *C.violaceum*. Since LuxR homologs are present in more than 100 gram negative pathogens, these QSIs may be developed as a broad spectrum anti-infective drug candidates. Considering the emergence of multi drug resistant pathogens, it is very essential to develop novel drug discovery strategies to find potent drugs against these deadly pathogens. Since natural products always play a major role in medicine and human health, virtual screening of natural products against the molecular drug targets will be a productive approach. It is evident that starting with biological evaluation, gene expression studies and molecular interactions using MST, will help us to get an in-depth understanding of the mode of action of these moieties. It is concluded that BN1 and BN2 inhibiting the *C.violaceum* by interacting with LBD of CviR. In contrast, C7X interacting with DBD of CviR and show comparatively less inhibition than BN1 and BN2. Finally thus, this approach will help us to find out effective QSI against various pathogens.

AUTHOR CONTRIBUTIONS

YZ and VR conceived the idea and planned the experiments. VR, LZ and GY performed the experiment. YZ, VR, HW and AL contributed in data interpretation, AL, YZ and VR wrote the manuscript.

FUNDING

VR received China post-doctoral grant (2015M582103) from China Postdoctoral Science Foundation.

ACKNOWLEDGMENTS

VR was supported by China post-doctoral grant (2015M582103). We would like to thank Prof. Wei Qian, State Key Laboratory of Plant Genomics, Institute of Microbiology, Chinese Academy of Sciences, Beijing, China for providing the MST facility. We also thank the support from National Natural Science Foundation of China (31670097) and Key Research and Development Program of Shandong Province (2015 GSF12101).

SUPPLEMENTARY MATERIAL

The Supplementary Material for this article can be found online at: https://www.frontiersin.org/articles/10.3389/fcimb.2018.00292/full#supplementary-material

REFERENCES

Adonizio, A. L., Downum, K., Bennett, B. C., and Mathee, K. (2006). Anti-quorum sensing activity of medicinal plants in southern Florida. *J. Ethnopharmacol.* 105, 427–435. doi: 10.1016/j.jep.2005.11.025

Ahmed, M., Bird, S., Wang, F., and Palombo, E. A. (2013). *In silico* investigation of lactone and thiolactone inhibitors in bacterial quorum sensing using molecular modeling. *Int. J. Chem.* 5, 9–26. doi: 10.5539/ijc.v5n4p9

August, P. R., Grossman, T. H., Minor, C., Draper, M. P., MacNeil, I. A., Pemberton, J. M., et.al. (2000). Sequence analysis and functional characterization of the violacein biosynthetic pathway from *Chromobacterium violaceum*. *J. Mol. Microbiol. Biotechnol.* 2, 513–519.

Bassler, B. L. (2002). Small talk: cell-to-cell communication in bacteria. *Cell.* 109, 421–424. doi: 10.1016/S0092-8674(02)00749-3

Blosser, R. S., and Gray, K. M. (2000). Extraction of violacein from *Chromobacterium violaceum* provides a new quantitative bioassay for N-acyl homoserine lactone autoinducers. *J. Microbiol. Method.* 40, 47–55. doi: 10.1016/S0167-7012(99)00136-0

Bouyahya, A., Dakka, N., Et-Touys, A., Abrini, J., and Bakri, Y. (2017). Medicinal plant products targeting quorum sensing for combating bacterial infections. *Asian Pac. J. Trop. Med.* 10, 729–743. doi: 10.1016/j.apjtm.2017.07.021

Brackman, G., and Coenye, T. (2015). Quorum sensing inhibitors as anti-biofilm agents. *Curr. Pharm. Design.* 21, 5–11. doi: 10.2174/1381612820666140905114627

Burt, S. A., Ojo-Fakunle, V. T., Woertman, J., and Veldhuizen, E. J. (2014). The natural antimicrobial carvacrol inhibits quorum sensing in *Chromobacterium violaceum* and reduces bacterial biofilm formation at sub-lethal concentrations. *PLoS ONE* 9:e93414. doi: 10.1371/journal.pone.0093414

Butler, M. S. (2008). Natural products to drugs: natural product-derived compounds in clinical trials. *Nat. Prod. Rep.* 25, 475–516. doi: 10.1039/b514294f

Cai, Z., Yuan, Z. H., Zhang, H., Pan, Y., Wu, Y., Tian, X. Q., et.al. (2017). Fatty acid DSF binds and allosterically activates histidine kinase RpfC of phytopathogenic bacterium *Xanthomonas campestris pv. campestris* to regulate quorum-sensing and virulence. *PLoS. Pathog.* 13:e1006304. doi: 10.1371/journal.ppat.1006304

Chen, G., Swem, L. R., Swem, D. L., Stauff, D. L., O'Loughlin, C. T.,Jeffrey, P. D., et.al. (2011). A strategy for antagonizing quorum sensing. *Mol. Cell.* 42, 199–209. doi: 10.1016/j.molcel.2011.04.003

Coughlan, L. M., Cotter, P. D., Hill, C., and Alvarez-Ordóñez, A. (2016). New weapons to fight old enemies: novel strategies for the (bio) control of bacterial biofilms in the food industry. *Front. Microbiol.* 7:1641. doi: 10.3389/fmicb.2016.01641

Defoirdt, T., Boon, N., and Bossier, P. (2010). Can bacteria evolve resistance to quorum sensing disruption?. *PLoS Pathog.* 6:e1000989. doi: 10.1371/journal.ppat.1000989

Delago, A., Mandabi, A., and Meijler, M. M. (2016). Natural quorum sensing inhibitors–small molecules, big messages. *Isr. J. Chem.* 56, 310–320. doi: 10.1002/ijch.201500052

Deryabin, D. G., and Inchagova, K. S. (2018). Inhibitory effect of aminoglycosides and tetracyclines on quorum sensing in *Chromobacterium violaceum*. *Microbiology* 87, 1–8. doi: 10.1134/S002626171801006X

Fantinatti-Garboggini, F., Almeida, R. D., Portillo Vdo, A., Barbosa, T. A., Trevilato, P. B., Neto, C. E. R., et.al. (2004). Drug resistance in *Chromobacterium violaceum*. *Genet. Mol. Res.* 3, 134–147.

Ferri, M., Ranucci, E., Romagnoli, P., and Giaccone, V. (2017). Antimicrobial resistance: a global emerging threat to public health systems. *Crit. Rev. Food. Sci.* 57, 2857–2876. doi: 10.1080/10408398.2015.1077192

Friesner, R. A., Murphy, R. B., Repasky, M. P., Frye, L. L., Greenwood, J. R., Halgren, T. A., et.al. (2006). Extra precision glide: docking and scoring incorporating a model of hydrophobic enclosure for protein–ligand complexes. *J. Med. Chem.* 49, 6177–6196. doi: 10.1021/jm051256o

García-Contreras, R. (2016). Is quorum sensing interference a viable alternative to treat *Pseudomonas aeruginosa* infections? *Front. Microbiol.* 7:1454. doi: 10.3389/fmicb.2016.01454

Gemiarto, A. T., Ninyio, N. N., Lee, S. W., Logis, J., Fatima, A., Chan, E. W., et.al. (2015). Isoprenyl caffeate, a major compound in manuka propolis, is a quorum-sensing inhibitor in *Chromobacterium violaceum*. *A. Van. Leeuw. J. Microb*. 108, 491–504. doi: 10.1007/s10482-015-0503-6

Harvey, A. L. (2008). Natural products in drug discovery. *Drug Discov. Today* 13, 894–901. doi: 10.1016/j.drudis.2008.07.004

Jerabek-Willemsen, M., André, T., Wanner, R., Roth, H. M., Duhr, S., Baaske, P., et.al. (2014). MicroScale thermophoresis: interaction analysis and beyond. *J. Mol. Struct.* 1077, 101–113. doi: 10.1016/j.molstruc.2014.03.009

Justo, G. Z., and Durán, N. (2017). Action and function of *Chromobacterium violaceum* in health and disease. *Best. Pract. Res. Cl. Ga.* 31, 649–656. doi: 10.1016/j.bpg.2017.10.002

Kalia, V. C. (2013). Quorum sensing inhibitors: an overview. *Biotechnol. Adv.* 31, 224–245. doi: 10.1016/j.biotechadv.2012.10.004

Kalia, V. C. (2015). *Quorum sensing vs quorum quenching: a battle with no end in sight.* New Delhi: Springer.

Kalia, V. C., Wood, T. K., and Kumar, P. (2014). Evolution of resistance to quorum-sensing inhibitors. *Microb. Ecol.* 68, 13–23. doi: 10.1007/s00248-013-0316-y

Kim, H. S., Lee, S. H., Byun, Y., and Park, H. D. (2015). 6-Gingerol reduces *Pseudomonas aeruginosa* biofilm formation and virulence via quorum sensing inhibition. *Sci. Rep*. 5:8656. doi: 10.1038/srep08656

Kimyon, Ö., Ulutürk, Z. I., Nizalapur, S., Lee, M., Kutty, S. K., Beckmann, S., et.al. (2016). N-Acetylglucosamine inhibits LuxR, LasR and CviR based quorum sensing regulated gene expression levels. *Front. Microbiol.* 7:1313. doi: 10.3389/fmicb.2016.01313

Laxminarayan, R., Matsoso, P., Pant, S., Brower, C., Røttingen, J. A., Klugman, K., et.al. (2016). Access to effective antimicrobials: a worldwide challenge. *Lancet*. 387, 168–175. doi: 10.1016/S0140-6736(15)00474-2

McClean, K. H., Winson, M. K., Fish, L., Taylor, A., Chhabra, S. R., Camara, M., et.al. (1997). Quorum sensing and *Chromobacterium violaceum*: exploitation of violacein production and inhibition for the detection of N-acylhomoserine lactones. *Microbiology*. 143, 3703–3711. doi: 10.1099/00221287-143-12-3703

Miller, M. B., and Bassler, B. L. (2001). Quorum sensing in bacteria. *Annu. Rev. Microbiol.* 55, 165–199. doi: 10.1146/annurev.micro.55.1.165

Mookherjee, A., Singh, S., and Maiti, M. K. (2018). Quorum sensing inhibitors: can endophytes be prospective sources? *Arch. Microbiol.* 200, 355–369. doi: 10.1007/s00203-017-1437-3

Ni, N., Choudhary, G., Li, M., and Wang, B. (2008). Pyrogallol and its analogs can antagonize bacterial quorum sensing in *Vibrio harveyi*. *Bioorg. Med. Chem. Lett*. 18, 1567–1572. doi: 10.1016/j.bmcl.2008.01.081

O'toole, G. A., and Kolter, R. (1998). Flagellar and twitching motility are necessary for *Pseudomonas aeruginosa* biofilm development. *Mol. Microbiol.* 30, 295–304. doi: 10.1046/j.1365-2958.1998.01062.x

Packiavathy, I. A., Priya, S., Pandian, S. K., and Ravi, A. V. (2014). Inhibition of biofilm development of uropathogens by curcumin–an anti-quorum sensing agent from *Curcuma longa*. *Food Chem.* 148, 453–460. doi: 10.1016/j.foodchem.2012.08.002

Paul, D., Gopal, J., Kumar, M., and Manikandan, M. (2017). Nature to the natural rescue: silencing microbial chats. *Chem-Biol. Interact*. 280, 86–98. doi: 10.1016/j.cbi.2017.12.018

Pérez-López, M., García-Contreras, R., Soto-Hernández, M., Rodríguez-Zavala, J. S., Martínez-Vázquez, M., Prado-Galbarro, F. J., et.al. (2018). Antiquorum sensing activity of seed oils from oleaginous plants and protective effect during challenge with *Chromobacterium violaceum*. *J. Med. Food*. 21, 356–363. doi: 10.1089/jmf.2017.0080

Rangel-Vega, A., Bernstein, L. R., Mandujano Tinoco, E. A., García-Contreras, S. J., and García-Contreras, R. (2015). Drug repurposing as an alternative for the treatment of recalcitrant bacterial infections. *Front. Microbiol.* 6:282. doi: 10.3389/fmicb.2015.00282

Rasmussen, T. B., and Givskov, M. (2006). Quorum sensing inhibitors: a bargain of effects. *Microbiology*. 152, 895–904. doi: 10.1099/mic.0.28601-0

Ren, D., Zuo, R., González Barrios, A. F., Bedzyk, L. A., Eldridge, G. R., Pasmore, M. E., et al. (2005). Differential gene expression for investigation of *Escherichia coli biofilm* inhibition by plant extract ursolic acid. *Appl. Environ. Microbiol.* 71, 4022–4034. doi: 10.1128/AEM.71.7.4022-4034.2005

Seidel, S. A., Dijkman, P. M., Lea, W. A., van den Bogaart, G., Jerabek-Willemsen, M., Lazic, A., et al. (2013). Microscale thermophoresis quantifies biomolecular interactions under previously challenging conditions. *Methods* 59, 301–315. doi: 10.1016/j.ymeth.2012.12.005

Soukarieh, F., Vico Oton, E., Dubern, J. F., Gomes, J., Halliday, N., de Pilar Crespo, M., et.al. (2018). *In silico* and *in vitro*-guided identification of inhibitors of alkylquinolone-dependent quorum sensing in *Pseudomonas aeruginosa*. *Molecules*. 23:257. doi: 10.3390/molecules23020257

Stauff, D. L., and Bassler, B. L. (2011). Quorum sensing in *Chromobacterium violaceum*: DNA recognition and gene regulation by the CviR receptor. *J. Bacteriol.* 193, 3871–3878. doi: 10.1128/JB.05125-11

Swem, L. R., Swem, D. L., O'Loughlin, C. T., Gatmaitan, R., Zhao, B., Ulrich, S. M., et.al. (2009). A quorum-sensing antagonist targets both membrane-bound and cytoplasmic receptors and controls bacterial pathogenicity. *Mol. Cell*. 35, 143–153. doi: 10.1016/j.molcel.2009.05.029

Taganna, J. C., Quanico, J. P., Perono, R. M. G., Amor, E. C., and Rivera, W. L. (2011). Tannin-rich fraction from Terminalia catappa inhibits quorum sensing (QS) in *Chromobacterium violaceum* and the QS-controlled biofilm maturation and LasA staphylolytic activity in *Pseudomonas aeruginosa*. *J. Ethnopharmacol.* 134, 865–871. doi: 10.1016/j.jep.2011.01.028

Tornimbene, B., Eremin, S., Escher, M., Griskeviciene, J., Manglani, S., and Pessoa-Silva, C. L. (2018). WHO global antimicrobial resistance surveillance system early implementation 2016–17. *Lancet Infect. Dis.* 18, 241–242. doi: 10.1016/S1473-3099(18)30060-4

Uroz, S., Dessaux, Y., and Oger, P. (2009). Quorum sensing and quorum quenching: the yin and yang of bacterial communication. *Chem. Bio. Chem*. 10, 205–216. doi: 10.1002/cbic.200800521

Vasavi, H. S., Arun, A. B., and Rekha, P. D. (2014). Anti-quorum sensing activity of Psidium guajava L. flavonoids against *Chromobacterium violaceum* and *Pseudomonas aeruginosa* PAO1. *Microbiol. Immunol.* 58, 286–293. doi: 10.1111/1348-0421.12150

Vattem, D. A., Mihalik, K., Crixell, S. H., and McLean, R. J. C. (2007). Dietary phytochemicals as quorum sensing inhibitors. *Fitoterapia*. 78, 302–310. doi: 10.1016/j.fitote.2007.03.009

Wagner, S., Sommer, R., Hinsberger, S., Lu, C., Hartmann, R. W., Empting, M., et.al. (2016). Novel strategies for the treatment of *Pseudomonas aeruginosa* infections. *J. Med. Chem.* 59, 5929–5969. doi: 10.1021/acs.jmedchem.5b01698

Wang, H., Li, Z., Jia, R., Hou, Y., Yin, J., Bian, X., et al. (2016). RecET direct cloning and Redαβ recombineering of biosynthetic gene clusters, large operons or single genes for heterologous expression. *Nat. Protoc.* 11, 1175–1190. doi: 10.1038/nprot.2016.054

Williams, P. (2017). Strategies for inhibiting quorum sensing. *Emerg. Top. Life Sci.* 1, 23–30. doi: 10.1042/ETLS20160021

Zhao, T., and Liu, Y. (2010). N-acetylcysteine inhibit biofilms produced *by Pseudomonas aeruginosa*. *BMC Microbiol.* 10:140. doi: 10.1186/1471-2180-10-140

Zhou, J. W., Luo, H. Z., Jiang, H., Jian, T. K., Chen, Z. Q., and Jia, A. Q. (2018). Hordenine, a novel quorum sensing inhibitor and anti-biofilm agent against *Pseudomonas aeruginosa*. *J. Agr. Food. Chem*. 66, 1620–1628. doi: 10.1021/acs.jafc.7b05035

Conflict of Interest Statement: The authors declare that the research was conducted in the absence of any commercial or financial relationships that could be construed as a potential conflict of interest.

The reviewer YGT and handling Editor declared their shared affiliation.

frontiers in Cellular and Infection Microbiology

ORIGINAL RESEARCH
published: 05 December 2017
doi: 10.3389/fcimb.2017.00498

Exploring the Anti-quorum Sensing and Antibiofilm Efficacy of Phytol against *Serratia marcescens* Associated Acute Pyelonephritis Infection in Wistar Rats

Ramanathan Srinivasan[1], *Ramar Mohankumar*[2], *Arunachalam Kannappan*[1], *Veeramani Karthick Raja*[1], *Govindaraju Archunan*[3], *Shunmugiah Karutha Pandian*[1], *Kandasamy Ruckmani*[2]* *and Arumugam Veera Ravi*[1]*

[1] *Department of Biotechnology, Alagappa University, Karaikudi, India,* [2] *Department of Pharmaceutical Technology, National Facility for Drug Development for Academia, Pharmaceutical and Allied Industries, Bharathidasan Institute of Technology, Anna University, Tiruchirappalli, India,* [3] *Department of Animal Science, Centre for Pheromone Technology, Bharathidasan University, Tiruchirappalli, India*

OPEN ACCESS

Edited by:
Rodolfo García—Contreras, Universidad Nacional Autónoma de México, Mexico

Reviewed by:
Rafael Coria Jimenez, Instituto Nacional de Pediatria, Mexico
Kenneth Warwick Nickerson, University of Nebraska Lincoln, United States

***Correspondence:**
Kandasamy Ruckmani
hodpharma@gmail.com
Arumugam Veera Ravi
aveeraravi@rediffmail.com

Received: *12 September 2017*
Accepted: *20 November 2017*
Published: *05 December 2017*

Citation:
Srinivasan R, Mohankumar R, Kannappan A, Karthick Raja V, Archunan G, Karutha Pandian S, Ruckmani K and Veera Ravi A (2017) Exploring the Anti-quorum Sensing and Antibiofilm Efficacy of Phytol against Serratia marcescens Associated Acute Pyelonephritis Infection in Wistar Rats. Front. Cell. Infect. Microbiol. 7:498. doi: 10.3389/fcimb.2017.00498

Quorum Sensing (QS) mechanism, a bacterial density-dependent gene expression system, governs the *Serratia marcescens* pathogenesis through the production of virulence factors and biofilm formation. The present study demonstrates the anti-quorum sensing (anti-QS), antibiofilm potential and *in vivo* protective effect of phytol, a diterpene alcohol broadly utilized as food additive and in therapeutics fields. *In vitro* treatment of phytol (5 and 10 μg/ml) showed decreasing level of biofilm formation, lipase and hemolysin production in *S. marcescens* compared to their respective controls. More, microscopic analyses confirmed the antibiofilm potential of phytol. The biofilm related phenomenons such as swarming motility and exopolysccharide productions were also inhibited by phytol. Furthermore, the real-time analysis elucidated the molecular mechanism of phytol which showed downregulation of *fimA*, *fimC*, *flhC*, *flhD*, *bsmB*, *pigP,* and *shlA* gene expressions. On the other hand, the *in vivo* rescue effect of phytol was assessed against *S. marcescens* associated acute pyelonephritis in Wistar rat. Compared to the infected and vehicle controls, the phytol treated groups (100 and 200 mg/kg) showed decreased level of bacterial counts in kidney, bladder tissues and urine samples on the 5th post infection day. As well, the phytol treatment showed reduced level of virulence enzymes such as lipase and protease productions compared to the infected and vehicle controls. Further, the infected and vehicle controls showed increasing level of inflammatory markers such as malondialdehyde (MDA), nitric oxide (NO) and myeloperoxidase (MPO) productions. In contrast, the phytol treatment showed decreasing level of inflammatory markers. In histopathology, the uninfected animal showed normal kidney and bladder structure, wherein, the infected animals showed extensive infiltration of neutrophils in kidney and bladder tissues. In contrast, the phytol treatment showed normal kidney and bladder tissues. Additionally, the toxic effect of phytol (200 mg/kg) was assessed by single dose toxicity analysis. No changes were

observed in hematological, biochemical profiles and histopathological analysis of vital organs in phytol treated animals compared to the untreated controls. Hence, this study suggested the potential use of phytol for its anti-QS, antibiofilm and anti-inflammatory properties against *S. marcescens* infections and their associated inflammation reactions.

Keywords: acute pyelonephritis, antibiofilm, anti-inflammatory agents, anti-quorum sensing, phytol, *Serratia marcescens*, Wistar rat

INTRODUCTION

Urinary tract infection (UTI) is one among the utmost commonly detected infections in clinical settings (Hvidberg et al., 2000). In divergence to men, women are more vulnerable to UTI (Derbie et al., 2017). Almost 1 in 3 women will have had UTI by the age of 24 years. Nearly half of all female population will experience with UTI throughout their lifetime. The expenses have extended for the treatment of UTI infection is $2.4 billion a year by means of 4.5–6.8 million cases in worldwide (Foxman and Brown, 2003). The way of UTI is well-known, which starts from urethral to bladder and then moving up the ureters into the kidneys. Cystitis, a predominant UTI, takes place in the bladder of the lower urinary tract whereas the pyelonephritis, a severe kidney infection, that targets the upper urinary tract. Pyelonephritis is a potentially life threatening infection that often leads to renal damaging (Katsiari et al., 2012). Pyelonephritis occurs subsequently a sequence of events carrying the bacteria from outside of the human body, up to the bladder and finally settles down into the kidneys. If the pyelonephritis is not treated, this can lead to severe renal abscesses and sepsis along with renal failure (Ramakrishnan and Scheid, 2005). Most pyelonephritis infections are occurred by bacterial pathogens ascent through the urethra and urinary bladder. The etiologic agents of pyelonephritis are *Escherichia coli*, *Proteus mirabilis*, *Pseudomonas aeruginosa,* and *Serratia marcescens* (Ohno et al., 2003; Mittal et al., 2009; Chen et al., 2012; Kufel et al., 2016).

Serratia marcescens, a Gram-negative bacterium, belongs to the family Enterobacteriaceae, frequently isolated from urinary and respiratory tracts and it can function as an opportunistic pathogen in immunocompromised patients (Kida et al., 2007). The infections caused by *S. marcescens* are hard to treat since it possesses inherent resistance to an extensive variety of antibiotics (Lee et al., 2005; Kim et al., 2013; Leclercq et al., 2013; Liou et al., 2014; González-Juarbe et al., 2015). Development of antibiotic resistance in *S. marcescens* demands the urgent need for the alternative treatment approaches. Host-pathogen interaction and the ability of pathogens to modify the host response is a crucial factor for establishing successful infections (Youn et al., 1992). This capability of a pathogen is typically attributed to their ability to secrete several of virulence factors and to alter host immune response (McMillen et al., 1996). The prominence of these responses has been exposed in several biological processes through an assortment of inflammatory mediators and cytokines, which include tissue inflammation, wound healing and immune defense (McMillen et al., 1996; Rumbaugh et al., 2004). Recently, several reports specified that the quorum sensing (QS) mediated virulence factors are important for successful establishment of bacterial infection in animal models (Kumar et al., 2009; Gupta et al., 2013b). QS is a vital global gene regulatory machinery in bacteria that allows discrete bacteria to coordinate their virulence behavior in a cell density depended manner, which depends on self-produced signaling molecules called autoinducers (Rumbaugh et al., 1999). *Serratia marcescens* has a well described QS system (SmaI/SmaR) which utilizes different homoserine lactones (HSLs) such as C4-HSL, C6-HSL, and C8-HSL as signal molecules and governs the secretion of extensive range of virulence factors such as prodigiosin, lipase, protease, chitinase, nuclease, siderophore production, hemolysin production and most importantly biofilm formation (Hines et al., 1988; Eberl et al., 1996; Horng et al., 2002; Rice et al., 2005).

Research targeting the bacterial QS system has paid a great deal of attention for the identification of effective anti-quorum sensing (anti-QS) and antibiofilm agents. These anti-QS agents aim the virulence factors production rather the growth of the bacterial pathogen, hence the emergence of selective pressure for the development of antibiotic resistance strain is nullified. Thus, it is foreseen that the inhibition of such QS mechanism would warrant as an effective approach to reduce the *S. marcescens* pathogenicity and infection (Labbate et al., 2007). Recently, numerous studies have been continuously reported the anti-QS and antibiofilm potential of several natural compounds from plant origin. Plant sources play a vital role in delivering the novel drugs candidates in medicinal field. Phytol, a diterpene alcohol compound majorly found in essential oils, extensively used as fragrant ingredient in shampoos, cosmetics, fragrances and other toiletries (Islam et al., 2015). As well, it is also used in the production of Vitamin K and E. In therapeutic field, phytol has shown antioxidant and antinociceptive activities as well as antiallergic, antimicrobial, antiradical, anti-cholinesterase, antiamyloidogenic, and anti-inflammatory properties along with adequate safety (Inoue et al., 2005; Lim et al., 2006; Ryu et al., 2011; Santos et al., 2013; Pejin et al., 2014; Lee et al., 2016; Sathya et al., 2017). Also, the phytol is a tremendous immuno stimulant, in respect of long term memory stimulation of both acquired and innate immunity. However, the report on anti-QS potential of phytol against bacterial pathogens is very much scarce (Pejin et al., 2015) and the protective effect of phytol on bacterial pathogens in animal model is nil. Based on these facts, this pioneering study primarily focused on assessing the *in vitro* anti-QS and antibiofilm potential of phytol against *S. marcescens* and the *in vivo* protective effect of phytol against *S. marcescens* associated acute pyelonephritis infection in rat model.

MATERIALS AND METHODS

Uropathogenic *Serratia marcescens* and Its Growth Conditions

Serratia marcescens strain PS1, a clinical strain isolated from urine sample collected from a clinical diagnosis laboratory in Meenakshi General Hospital, Chennai by Nithya et al. (2010) and identified through 16S rRNA gene sequencing with the GenBank accession number of FJ584421. *Serratia marcescens* was cultured in Luria- Bertani (LB) medium (pH 7.0) for overnight at 28°C. For the experimental purposes, the *S. marcescens* strain was sub cultured in LB medium until it reached 0.4 OD at 600 nm (1×10^8 CFU/ml).

Compound Preparation

For *in vitro* study, one milligram of phytol (97%, mixture of isomers, catalog no. 139912, Sigma-Aldrich, St. Louis, MO, USA) was dissolved in 1 ml of methanol as stock solution and stored at 4°C till further use. For *in vivo* study, 200 mg of phytol was dissolved in 5 ml of corn oil as stock solution and stored at room temperature till further use. The maximum amount of methanol (10 µl, 1%) and corn oil (750 µl) was used as the vehicle controls (negative controls) for *in vitro* and *in vivo* assays, respectively.

Biofilm Cells Quantification by XTT Reduction Assay

The effect of phytol on the metabolically active cells involved in biofilm formation of *S. marcescens* was evaluated by modified XTT reduction assay (Sivaranjani et al., 2016). The XTT sodium salt was prepared in phosphate buffer saline (PBS) at a concentration of 0.2 mg/ml and menadione in acetone at 0.172 mg/ml concentration. For each experiment, the XTT/menadione reagent was freshly prepared in the ratio of 12.5:1. *Serratia marcescens* culture was inoculated in 24-well microtitre plate (MTP) containing 1 ml of respective growth medium in the absence and presence of phytol (5&10 µg/ml) and incubated at 28°C for 24 h. Following incubation, the planktonic cells were discarded from 24-well MTP. Then, the biofilm cells on MTP wells were washed and resuspended in 200 µl of 0.9% NaCl. 25 µl of XTT-menadione solution was added in 96-well MTP containing biofilm cell suspensions and incubated at 37°C for 3 h in dark. Finally, the absorbance of biofilm cell suspensions together with XTT-menadione solution was measured at 490 nm by Multilabel Reader (Molecular devices, SpectraMax M3, USA).

Growth Curve Analysis

The effect of phytol on *S. marcescens* growth was assessed by growth curve analysis. One percent of *S. marcescens* culture was added in to 100 ml of LB broth supplemented with (5 and 10 µg/ml) and without of phytol and the flasks were incubated in constant shaking at 120 rpm for 18 h in 28°C. The cell density was read at 600 nm for every 1 upto 18 h using Multilabel Reader (Packiavathy et al., 2013).

Microscopic Investigation of *S. marcescens* Biofilm Formation

To evaluate the antibiofilm potential of phytol, the light and confocal laser scanning microscopic (CLSM) analyses were done by following the method of Srinivasan et al. (2017a). After the growth of *S. marcescens* biofilm with and without of phytol on 1 × 1 cm glass slides, the planktonic cells were removed by washing with distilled water. Then the glass slides were stained with 0.4% crystal violet and 0.2% acridine orange for light and confocal microscopes, respectively. After 2 min of incubation, the excess stain was removed by distilled water wash and biofilms on glass slides were imaged under light (Nikon Eclipse Ti 100, Tokyo, Japan) and CLSM (Model LSM 710, Carl Zeiss, Oberkochen, Germany) at a magnification of 400× and 200×, respectively. The Z-Stack CLSM images were analyzed using COMSTAT software to obtain the average thickness, biofilm biomass and surface to volume ratio of the phytol treated and untreated *S. marcescens* biofilm (Heydorn et al., 2000).

Effect of Phytol on *S. marcescens* Swarming Motility

The inhibitory effect of phytol on *S. marcescens* swarming motility was assessed by the method of Packiavathy et al. (2013). Briefly, the 5 µl of *S. marcescens* culture was inoculated in the center of swarming agar plate (1% peptone, 0.5% NaCl, and 0.5% agar) with the absence and presence of phytol (5 and 10 µg/ml). Then, the swarming plates were incubated for 16 h at 28°C and observed for inhibition in swarming motility.

EPS Quantification

Extraction of EPS from phytol treated and untreated *S. marcescens* culture was carried out by phenol-sulfuric acid method as described by Hirs (1967) with slight modification. Briefly, the *S. marcescens* culture was grown with the absence and presence of phytol (5 and 10 µg/ml) for 18 h at 28°C in 24 well MTP. After incubation, the planktonic cells were washed-out by sterile distilled water. Then the biofilm cells were dissolved by 0.9% NaCl (1 ml) and equilibrated phenol (1 ml). Afterward, 5 volume of H_2SO_4 was added to mix and incubated in dark at room temperature for 1 h. Then the absorbance was taken at 490 nm. The percentage of EPS inhibition was calculated by using the following formula.

$$((\text{ControlOD} - \text{TreatedOD})/\text{ControlOD}) \times 100.$$

Lipase Quantification Assay

The phytol treated (5 and 10 µg/ml) and untreated *S. marcescens* culture was centrifuged at 10,000 rpm for 10 min. Then 100 µl of phytol treated and untreated CFCS was added to 900 µl of buffered substrate mixture having 9 volumes of 0.1% gummi arabicum and 0.2% sodium deoxycholate in 50 mM Na_2PO_4 buffer (pH 8.0) and 1 volume of 0.3% *p*-nitrophenyl palmitate in isopropanol and incubated at room temperature for 1 h. After incubation, the reaction was dismissed by adding 1 ml of 1 M Na_2CO_3 following which the mixture was centrifuged at 10,000 rpm for 10 min. Then, the absorbance of the supernatant was measured by Multilabel Reader at 410 nm (Srinivasan et al.,

2017b). The percentage of lipase inhibition was calculated by using the formula as mentioned above.

Haemolysin Quantification Assay

Fresh sheep blood was washed twice with PBS (pH 7.4) and resuspended in the same to a final concentration of 2% (v/v). To the 500 µl of 2% washed sheep erythrocytes, an equal volume of bacterial CFCS (treated with and without phytol) were added together and incubated at 37°C for 2 h. Then, the tubes were centrifuged and the hemolytic activity was determined by measuring the total amount of hemoglobin released in the supernatant at OD 405 nm in Multilabel Reader. The percent lysis was achieved by incubating the erythrocytes with distilled water (positive control) and background lysis was determined by incubating the erythrocytes with PBS (negative control). The percentage of lysis was determined by using the following formula (Kannappan et al., 2017).

$$[(A_{405}\text{ of sample} - A_{405}\text{ of background})/(A_{405}\text{ of total} - A_{405}\text{ of background})]\times 100.$$

Quantitative Real-Time PCR (qPCR) Analysis

Total RNA was extracted from phytol treated (10 µg/ml) and untreated *S. marcescens* by TRIzol method and isolated RNA was converted into cDNA using Invitrogen — superscript III kit. qPCR was done on an Applied Biosystems thermal cycler by Power SYBR Green PCR master mix in 7500 Sequence Detection System (Applied Biosystems Inc. Foster, CA, USA). PCR cycles comprised an initial denaturation at 95°C for 10 min followed by 40 cycles of denaturation at 95°C for 45 s; annealing at 57°C for 45 s; extension at 72°C for 50 s. The expression patterns of candidate virulence genes were normalized against *rplU* gene (housekeeping gene) expression and quantified by calculating 2-ΔCt. Details of the primer sequences of the candidate and housekeeping genes (*fimA*, *fimC*, *flhC*, *flhD*, *bsmB*, *rssB*, *rsmA*, *pigP*, *shlA,* and *rplU*) used in this study are given in **Table 1** and their efficiency was confirmed through 1.5% agarose gel electrophoresis (**Supplementary Figure 1**) (Salini and Pandian, 2015).

TABLE 1 | Nucleotide sequences of *S. marcescens* primers used in this study.

Gene	Primer sequence (5′-3′)	
	Forward	**Reverse**
rplU	GCTTGGAAAAGCTGGACATC	TACGGTGGTGTTTACGACGA
fimA	ACTACACCCTGCGTTTCGAC	GCGTTAGAGTTTGCCTGACC
fimC	AAGATCGCACCGTACAAACC	TTTGCACCGCATAGTTCAAG
flhC	AAGAAGCCAAGGACATTCAG	TTCCCAGGTCATAAACCAGT
flhD	TGTCGGGATGGGGAATATGG	CGATAGCTCTTGCAGTAAATGG
bsmB	CCGCCTGCAAGAAAGAACTT	AGAGATCGACGGTCAGTTCC
rssB	TAACGAACTGCTGATGCTGT	GATCTTGCGCCGTAAATTAT
rsmA	TTGGTGAAACCCTCATGATT	GCTTCGGAATCAGTAAGTCG
pigP	GAACATGTTGGCAATGAAAA	ATGTAACCCAGGAATTGCAC
shlA	GCGGCGATAACTATCAAAAT	ATTGCCAGGAGTAGAACCAG

In Vivo therapeutic Potential of Phytol on *S. marcescens* Associated Acute Pyelonephritis

Animals

Female Wistar rat (*Rattus norvegicus*) weighing 100–150 g, 6–8 weeks old were used in this study. They were kept in Central Animal House, Bharathidasan University, Tiruchirappalli, India. Rats were housed in polypropylene cages and were fed with standard rat synthetic diet (Sai Durga feeds, Bangalore) and water *ad libitum*. Ethical clearance was approved by the Institutional Animal Ethics Committee of Bharathidasan University, Tiruchirappalli, India (Approval ID: BDU/IAEC/2016/NE/37/Dt. 17.03.2016). All the experimental protocols were followed as per the guidelines of the Committee for the purpose of Control and Supervision of Experiments on Animals (CPCSEA), Government of India.

Establishment of Experimental Acute Pyelonephritis in Rat

An experimental model of acute pyelonephritis infection was established in female Wistar rat as described by Brown (2011). Briefly, the rats were anesthetized with a ketamine-xylazine cocktail (90 mg ketamine + 9 mg xylazine) administered intraperitoneally at a dosage of 0.1 ml/100 g of body weight. Then, the rat was controlled in dorsal recumbency to facilitate way of the catheter. The rat body was hold in the nondominant hand with the tail positioned between the index and middle fingers and applies trivial pressure to the tail to spread. The exterior urethral orifice was identified. Then, the thumb has placed on the ventral stomach 1 cm forward to the urethral opening and gentle pressure was applied to pull the skin toward the head. This help to make the urethral opening further protruding as well to stretch the urethra to enable way of the catheter (**Figure 1B**). A small amount of lubricant was applied at the tip of the urethral orifice and the 20-gauge IV angiocatheter (**Figure 1A**) has inserted into the urethral opening in the direction of the tail till it reaches the vaginal opening (**Figure 1C**). After reaching the vaginal opening, the catheter was gently rotated upward to the rat (**Figure 1D**) and then 200 µl of *S. marcescens* bacterial inoculum (1×10^8 CFU/ml) was gently injected into the bladder (**Figure 1E**) to avoid leak and reflux, kept in room for 10 min and then withdrawn prudently.

For experimental purpose animals were divided into four groups consisting of 5 animals each: (i) Group I — Infection control (Infection was given with *S. marcescens* cells to bladder through urethra); (ii) Group II — Vehicle control (Infection was given with *S. marcescens* cells and corn oil was given orally to infected animals after 24 h post infection (p.i.) until the 5th post-infection day (p.i.d.) for daily); (iii) Group III — Animals treated with phytol (Infected animals were treated daily with an oral dose of phytol (100 mg/kg body weight) after 24 h p.i. until the 5th p.i.d.); (iv) Group IV — Animals treated with phytol (Infected animals were treated daily with an oral dose of phytol (200 mg/kg body weight) after 24 h p.i. until the 5th p.i.d). After 5th p.i.d, the urine from each rat was collected in microfuge tubes by mild compression of the abdomen. Then the animals were sacrificed and organs were collected for further assays.

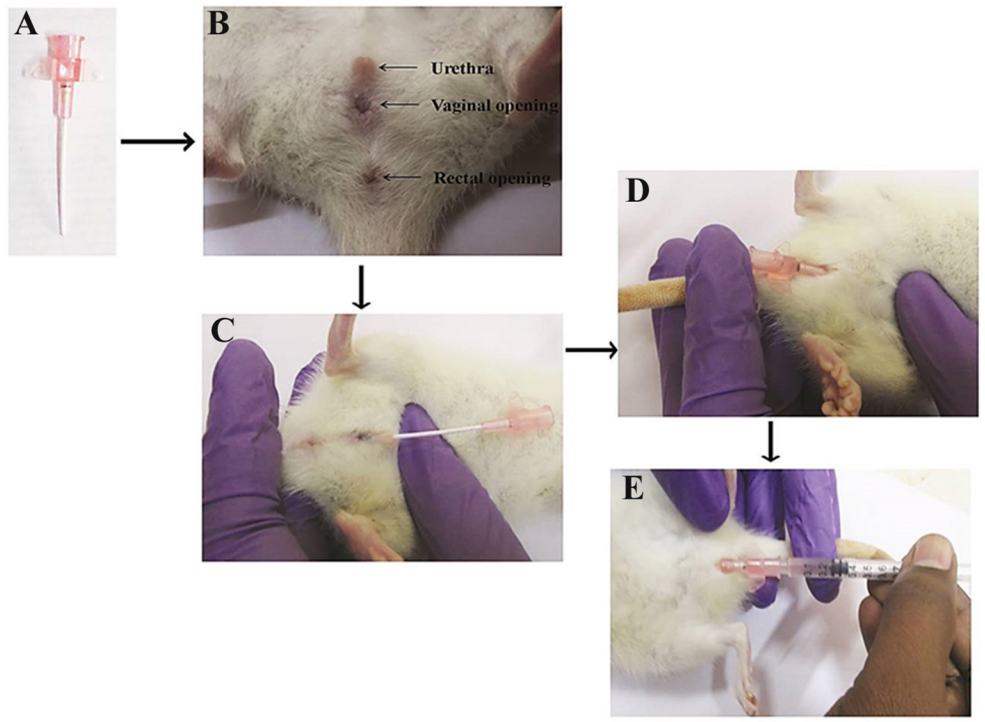

FIGURE 1 | Urinary catheterization of angiocatheter into the bladder through the urethra. Twenty-gauge IV angiocatheter **(A)**, three visible urethral, vaginal and rectal opening **(B)**, insertion of angiocatheter into the urethral opening till it reaches the vaginal opening **(C)**, rotation of angiocatheter upward to the rat **(D)**, and injection of *S. marcescens* bacterial inoculum into the bladder **(E)**.

Bacteriological Examination of Urine, Kidney, and Bladder Tissues

On the 5th p.i.d., animals from the all the groups were sacrificed. Kidney and bladder were removed aseptically, weighed and homogenized in 1 ml of phosphate buffered saline. Bacterial count was made afterward plating the appropriate dilutions of tissue homogenates and urine samples on Serratia differential agar (SD agar) plates (Himedia, India). Log bacterial counts were calculated per gram of tissue and per ml of urine as reported by Kumar et al. (2009). Further, the tissue homogenates were spun at 10,000 rpm for 10 min and filtered by 0.22 μm cellulose acetate membrane filter (Millipore, Bangalore, India). The obtained tissue homogenate filtrate was used for the estimation of protease and lipase production.

Estimation of Protease Production

Proteolytic activity was estimated by the method of Gupta et al. (2013a) with little modification. Briefly, the reaction mixture containing 200 μl of tissue homogenate diluted in 250 μl of buffered substrate [2% of azocasein (Sigma, USA) as substrate in 1 M Tris-HCl (pH-8.0)] was incubated at 37°C for 1 h. After subsequent incubation, the reaction mixture was added with 600 μl of 10% trichloro acetic acid to stop the reaction. The tubes were then spun at 10,000 rpm for 10 min and 600 μl of supernatant was added to 700 μl of 1 M NaOH. Absorbance was read at 440 nm in Multilabel reader and results were expressed in OD value.

Estimation of Lipase Production

Lipolytic activity of kidney and bladder tissue homogenized were determined using *p*-nitro phenyl palmitate (*p*-NPP) as the substrate. Two hundred microliter of tissue homogenate were added with 900 μl of reaction mix containing 1 volume of 0.3% *p*-NPP in propanol, 9 volumes of 0.1% gummi arabicum and 0.2% sodium deoxycholate in 50 mM Na_2PO_4 buffer (pH-8.0). The reaction mix was incubated for 1 h at room temperature in dark and then centrifuged at 10,000 rpm for 10 min. The reaction was dismissed by adding 1 ml of 1 M Na_2CO_3. Then, the absorbance was read at 410 nm and results were expressed in OD value (Srinivasan et al., 2017b).

Preparation of Cell Lysate

The kidney and bladder tissues from the experimental groups were homogenized using lysis buffer (10 mM Tris (pH-8.0), 20 mM EDTA and 0.25% Triton X-100). Then the supernatants were collected separately by centrifuging the tissue homogenate at 5,000 rpm for 30 min at 4°C and the protein quantification for the supernatant was done by Bradford method for all the samples. The cell lysate was kept at −80 °C until further analysis.

Malondialdehyde Estimation

Induction of pathology was assessed on the base of malondialdehyde by the method of Ohkawa et al. (1979). Briefly, an equal volume of 10% ice-cold TCA was added to the cell lysate (protein concentration−100 μg) and centrifuged at

5,000 rpm for 15 min. MDA of five different concentrations (10–50 ng) were used as standard. To the supernatant and standard solution, same volume of 0.67% thiobarbituric acid in 50% glacial acetic acid was added and samples were incubated at 100°C for 20 min. After cooling, absorbance of the supernatant and standards were measured at 532 nm. The values were expressed as μM of TBARS/mg of protein determined by calibration curve prepared using different concentrations of MDA standards.

Quantification of Myeloperoxidase (MPO) Activity

Quantification of tissue neutrophils through the myeloperoxidase assay was done by the method of Kim et al. (2012) with slight modification. Briefly, the tissue homogenate was centrifuged at 8,000 rpm for 20 min at 4°C. The supernatant was discarded and 10 ml of ice-cold 50 mM potassium phosphate buffer (pH 6.0) comprising 0.5% hexadecyltrimethylammonium bromide and 10 mM EDTA was added to the pellet. It was then subjected to sonication and the solution was centrifuged at 10,000 rpm for 20 min. Then, 50 μl of supernatant was added with 50 μl of diluted H_2O_2 (4 μl of 30% H_2O_2 diluted in 96 μl of d H_2O) and 200 μl of O-dianisidine mixture (16.7 mg of O-dianisidine, 90 ml of d H_2O and 10 ml of potassium phosphate buffer). Three subsequent readings were taken at 450 nm at 30 s intervals. One unit of MPO defined as that degrading 1 μM of H_2O_2 per min at room temperature and myeloperoxidase activity was expressed as U/mg of tissue.

Estimation of Nitrite Content

Nitrite was estimated in the kidney and bladder tissues of experimental groups by the method of Rockett et al. (1994) with slight modification. Briefly, the cell lysate (100 μg of protein) in phosphate buffer (pH-7.4) was incubated with Griess reagent (Sigma Aldrich Chemicals Ltd., St Louis, MO, USA) for 30 min in dark at room temperature. The supernatant was collected and the optical density was measured at 540 nm along with the standard (5–20 μM sodium nitrite). The nitrite content was calculated with the help of sodium nitrite standard curve and the results were showed as μM of nitrite/mg of protein.

Histopathological Analysis of Kidney and Bladder Tissues

Kidney and bladder tissues were fixed in 10% buffered normal saline and dehydrated in gradient ethanol (30–100%). Paraffin wax blocks were prepared and thin sections were stained by hematoxylin and eosin. The pathological observations of all tissues were done through microscopy analysis by a pathologist.

Pilot Single-Dose Toxicity Testing of Phytol in Wistar Rat

The rats were accommodated at a temperature of 25 ± 2°C in a 12 h light-dark cycle and acclimatized to laboratory conditions for 10 days without presenting any abnormality or pathological variations prior to experiments. Ten rats were arbitrarily divided into two groups; each containing five rats. The first group was the animal control which received the normal water, whereas the second group was orally administered with single dose of phytol (200 mg/kg body weight) for 14 days. The animals were observed for toxic signs for the first 2 h afterward dosing. Finally, the number of survivors was recorded after 24 h and animals were then maintained for additional 13 days with regular daily observations.

Hematological and Biochemical Analysis

On the day 15, all animals were anesthetized by urethane solution and blood samples were collected through retro-orbital puncture. Blood samples were collected into 2 tubes; heparinized and non-heparinized centrifuge tubes. The heparinized blood samples were used for a hematological study which includes hemoglobin concentration, white blood cell counts (WBC), red blood cell counts (RBC), and hematocrit. The serum detached from non-heparinized blood was used for a biochemical study which includes glucose, blood urea, creatinine, Alkaline phosphatase (ALP), Serum glutamic pyruvic transaminase (SGPT), Serum glutamic oxaloacetic transaminase (SGOT), triglycerides, Very low density lipoprotein (VLDL), Low density lipoprotein (LDL), High density lipoprotein (HDL), total bilirubin, direct bilirubin, indirect bilirubin, total cholesterol, total protein, albumin and globulin.

Histopathological Analysis of Vital Organs

Immediately after collecting the blood samples, the vital organs such as kidney, liver, heart, lungs, and spleen were removed for histopathological analysis. Tissues from the animal control and the group treated with the phytol (200 mg/kg) were embedded in paraffin wax for sectioning. Further, the tissue sections were subjected to hematoxylin-eosin staining. The pathological observations of all tissues were performed through microscopic analysis by a pathologist.

Statistical Analysis

All the *in vitro* experiments were conducted in triplicates and repeated thrice and the *in vivo* experiments were conducted in quintuplicates. The statistical analyses were done by SPSS statistics v17.0. Values were expressed as mean ± standard deviation. Student-*t* test was used to compare the control and treated samples.

RESULTS

Quantification of Biofilm Cells by XTT Reduction Assay

The metabolically active cells involved in *S. marcescens* biofilm formation were quantified by XTT reduction assay. Results revealed that 5 and 10 μg/ml of phytol treatment showed lower level of optical density (OD 0.45 and 0.37, respectively) when compared to the untreated and vehicle controls (OD 1.32 and 1.24, respectively) (**Figure 2A**), which clearly indicates that phytol treatment reduces the number of metabolically active cells involved in biofilm formation.

Effect of Phytol on *S. marcescens* Growth

To check the non-antibacterial activity of phytol, the bacterial growth curve assay was performed with *S. marcescens* in the

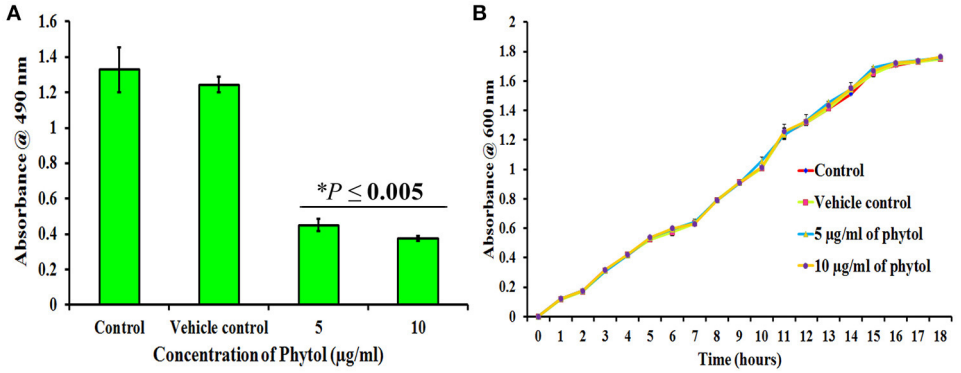

FIGURE 2 | Effect of phytol on *S. marcescens* biofilm formation and growth. Phytol treatment (5 and 10 µg/ml) significantly inhibited the biofilm formation **(A)**, without affecting the growth of *S. marcescens* **(B)**. One percent of methanol was used as vehicle control. Error bar indicates standard deviations from the mean. Student-*t* test was used to compare the control and treated samples. *Indicates significant at $p \leq 0.005$.

absence and presence of phytol (5 and 10 µg/ml). Even after 18 h of incubation, no substantial differences were observed in the cell densities between untreated, vehicle controls and phytol treated samples (**Figure 2B**), which confirms that phytol did not have any antibacterial activity against *S. marcescens* at tested concentration.

Light Microscopic and CLSM Analysis of *S. marcescens* Biofilm Formation

Light microscopic observation of biofilm formation after treatment with phytol revealed their antibiofilm potential against *S. marcescens*. A thick coating of biofilm formation was observed in untreated and vehicle control samples, whereas a noticeable reduction of biofilm was observed in phytol treated samples (**Figure 3A**). In addition to this, the 2, 2.5, and 3 D CLSM images indicated the reduced in thickness and architecture of biofilms upon phytol treatment (**Figure 3B**). COMSTAT analysis was done to determine the 3D features like average thickness, biomass and surface volume ratio of *S. marcescens* biofilms with the absence and presence of phytol. The average thickness of the biofilm was reduced from 19.3 ± 0.29 to 12.1 ± 0.51 µm after treatment with phytol (10 µg/ml). Similarly, 5 and 10 µg/ml of phytol treatment showed reduced level of biofilm biomass (14.8 ± 0.38 and 12.0 ± 0.63 $\mu m^3/\mu m^2$, respectively) compare to the untreated and vehicle controls (20.0 ± 0.19 and 19.6 ± 0.4 $\mu m^3/\mu m^2$, respectively). Furthermore, 5 and 10 µg/ml of phytol treatment displayed increasing level of surface volume ratio (0.13 ± 0.08 and 0.20 ± 0.01, respectively) due to their biofilm disintegration property, wherein the surface volume ratio of untreated and vehicle control samples were 0.06 ± 0.01 and 0.07 ± 0, respectively (**Table 2**).

Effect of Phytol on *S. marcescens* Swarming Motility

Swarming motility is a QS mediated virulence attribute in *S. marcescens*. Obtained results clearly evident that the phytol (5 and 10 µg/ml) was able to reduce the *S. marcescens* swarming efficiency in a concentration dependent manner when compared to the untreated and vehicle controls (**Figure 3C**).

Effect of Phytol on EPS Production

Microbial cells cocooned themselves in self-secreted extra polymeric substances, which play a vital role in formation of biofilms. Phytol significantly ($P \leq 0.0005$) inhibited the EPS production to the level of 32 and 39% at 5 and 10 µg/ml concentrations, respectively. Where, the vehicle control did not show any significant level of EPS inhibition (**Figure 4A**).

Effect of Phytol on Lipase and Hemolysin Productions

S. marcescens is known to harbor important virulence factors including hemolysin production, which helps the bacteria in lysing human red blood cells and production of QS controlled extracellular virulence enzyme lipase. Therefore, the efficacy of phytol to inhibit the lipase and hemolytic virulence property of *S. marcescens* was assessed by lipolytic and hemolytic activities. The obtained results showed that phytol significantly ($P \leq 0.0005$) inhibited the lipase and hemolysin productions to the level of 42 and 31% respectively, at 10 µg/ml concentration (**Figures 4A,B**).

Expression of QS Regulated Genes in *S. marcescens* upon Treatment with Phytol

The expression level of QS-regulated genes was assessed in the *S. marcescens* in the presence of phytol (10 µg/ml) using real-time quantitative PCR. Phytol at tested concentration, downregulated the expression of *fimA, fimC, flhC, flhD, bsmB, pigP,* and *shlA* genes by 0.42, 0.32, 0.25, 0.46, 0.36, 0.48, and 0.15 fold, respectively in *S. marcescens* relative to the untreated controls. In divergence, phytol upregulated the *rssB* and *rsmA* gene expressions to the level of 0.96 and 0.84 fold respectively compared to the controls (**Figure 5**).

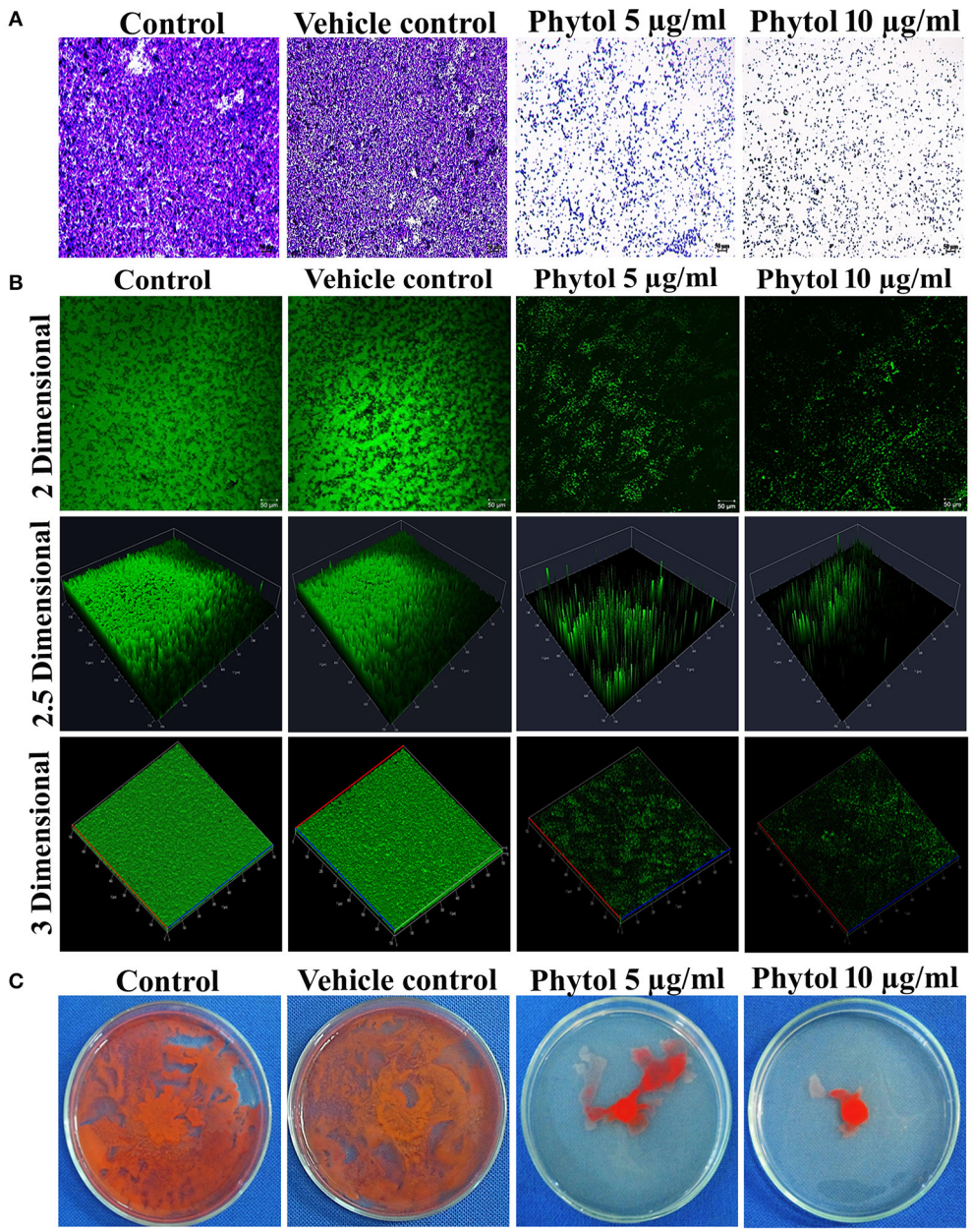

FIGURE 3 | Microscopic analyses of *S. marcescens* biofilm formation. Light microscopic **(A)** and CLSM **(B)** images of phytol treatment slides (5 and 10 µg/ml) showed disintegration of *S. marcescens* biofilm formation compared to their untreated controls. Effect of phytol on *S. marcescens* swarming motility: The control plate exhibited extensive swarming motility on soft agar. In contrast, the phytol treatment (5 and 10 µg/ml) considerably inhibited the *S. marcescens* swarming motility **(C)**. One percent of methanol was used as a vehicle control.

In Vivo Protective Effect of Phytol on *S. marcescens* Associated Acute Pyelonephritis

Morphological Changes in Kidney and Bladder of Infected and Phytol Treated Animals

Healthy kidney with smooth and normal bean shaped contours were observed in the normal uninfected rat, whereas, rat infected with *S. marcescens* by transurethral inoculation showed damaged kidney with severe abscess and pus formation. In contrast, the infected rat treated with phytol showed undamaged kidney which is similar like uninfected rat kidney (**Figure 6A**).

Assesment of Bacterial Burden in Urine, Kidney, and Bladder Tissues

The tissue homogenates of kidney, bladder and the urine samples were plated on SD agar plates for estimation of bacterial load.

TABLE 2 | COMSTAT analysis of phytol treated and untreated *S. marcescens* biofilm.

Parameter	Control	Vehicle control	Phytol 5 μg/ml	Phytol 10 μg/ml
Biomass ($\mu m^3/\mu m^2$)	20.08641 ± 0.19	19.68098 ± 0.4	14.85047 ± 0.38*	12.06844 ± 0.63*
Average thickness (μm)	19.3204 ± 0.29	19.12131 ± 0.59	14.78937 ± 0.14*	12.1517 ± 0.51***
Surface volume ratio ($\mu m^2/\mu m^3$)	0.06664 ± 0.01	0.07418 ± 0.00	0.131617 ± 0.08	0.203123 ± 0.01

*Phytol treatment (5 and 10 μg/ml) decreased the biofilm biomass, average thickness and increased the surface volume ratio of S. marcescens biofilm, compared to their untreated control. Data are expressed as mean ± SD. Student-t test was used to compare the control and treated samples. *Indicates significant at $p \leq 0.005$. ***Indicates significant at $p \leq 0.0005$.*

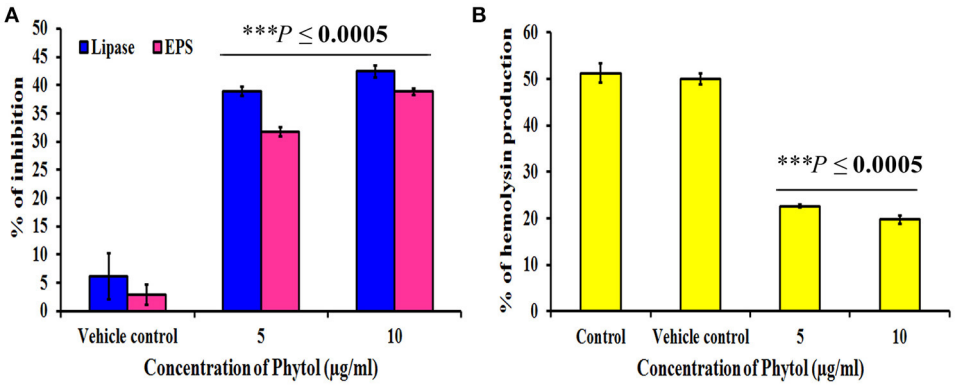

FIGURE 4 | Effect of phytol on QS mediated virulence factors production in *S. marcescens*. Phytol treatment (5 and 10 μg/ml) significantly inhibited the lipase, EPS **(A)** and hemolysin **(B)** productions in *S. marcescens*. One percent of methanol was used as a vehicle control. Error bar indicates standard deviations from the mean. Student-*t* test was used to compare the control and treated samples. ***Indicates significant at $p \leq 0.0005$.

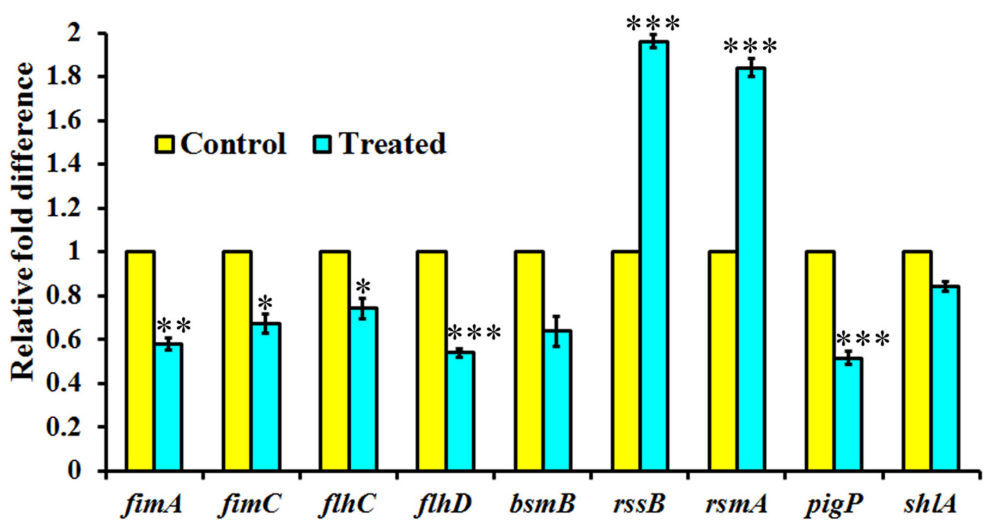

FIGURE 5 | Effect of phytol treatment on the virulence gene expression of *S. marcescens*. Phytol treatment (10 μg/ml) modulated the expression of QS controlled genes involved in virulence factors production and biofilm formation in *S. marcescens*. Error bar indicates standard deviations from the mean. Student-*t* test was used to compare the control and treated samples. *Indicates significant at $p \leq 0.005$, **indicates significant at $p \leq 0.001$, and ***indicates significant at $p \leq 0.0005$.

The 100 and 200 mg/kg body weight of phytol treatment showed a significant ($P \leq 0.0005$) decline in kidney bacterial load by log 6 and 6.5, respectively on the 5th p.i.d compared to infected control group. On the other hand, a same level of bacterial load was observed in vehicle control group compared to the infected control (**Figure 6B**). A similar decreasing drift was observed with bladder and urine bacterial counts in phytol treated groups on the 5th p.i.d. The 100 and 200 mg/kg body weight of phytol treatment decreased the bladder bacterial count by log 5.3 and 6.2, respectively compared with the infected control group (**Figure 6C**). In urine sample, the 100 and 200 mg/kg body weight of phytol treatment decreased the bacterial count by log 2.7

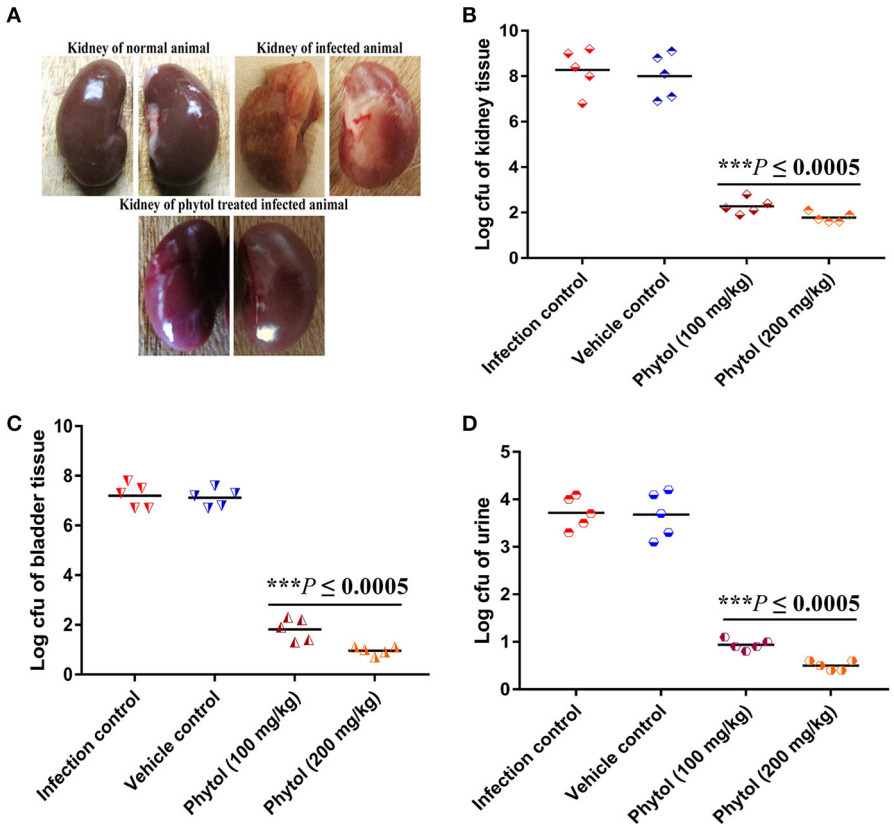

FIGURE 6 | Morphological changes in rat kidney upon treatment with and without of phytol against *S. marcescens* associated acute pyelonephritis infection. The image of untreated infected animal showed damaged kidney along with pus formation and severe abscess. In contrast, the image of phytol treated infected animal showed healthy kidney like normal animal **(A)**. Quantitative bacterial load in kidney, bladder tissues, and urine samples: Compare to the infection controls, 100 and 200 mg/kg body weight of phytol treatment showed decreased level of bacterial load in kidney **(B)**, bladder **(C)** tissues, and urine **(D)** samples. Corn oil was used as the vehicle control. Data are expressed as mean ± SD. Student-*t* test was used to compare the control and treated samples. ***Indicates significant at $p \leq 0.0005$.

and 3.2, respectively compared with the infected control group (**Figure 6D**).

Level of Protease Production in Kidney and Bladder Tissues of Phytol Treated and Untreated Infected Animals

The protease is an extracellular virulence enzyme and its production is regulated by QS mechanism in *S. marcescens*. Therefore, the level of protease production in phytol treated and untreated kidney and bladder tissues were assessed. The results showed a decreased level of protease production in phytol treatment groups than the infected and vehicle controls (**Figures 7A,B**).

Level of Lipase Production in Kidney and Bladder Tissues of Phytol Treated and Untreated Infected Animals

Alike to protease, the production of an extracellular virulence lipase enzyme is controlled by QS mechanism. Therefore, the effect of phytol in lipase production of *S. marcescens* was assessed by lipolytic assay. The results revealed a decreased level of lipase production in phytol treatment groups compared to the infected and vehicle controls (**Figures 7C,D**).

Effect of Phytol on MDA Production

Free radicals mediated lipid peroxidation produces a large number of reactive aldehydes. MDA is one among the reactive aldehydes involved in pathophysiological modifications occurred during oxidative stress in tissues. Hence, the level of MDA production was estimated to assess the level of cellular injury in kidney and bladder tissues. Kidney and bladder tissues of rat infected with *S. marcescens* showed increasing level of MDA production. In contrast, phytol treatment significantly ($P \leq 0.0005$) decreased the MDA production and protected the tissues from lipid peroxidation mediated damages (**Figure 8A**).

Effect of Phytol on MPO Level

Infiltration of neutrophils in the kidney and bladder tissues of infected rat treated with and without phytol was assessed by estimating the MPO production. MPO is an enzyme produced by neutrophils, which involves in neutralizing the deleterious effect of H_2O_2 that cause tissue injury. Assessment levels of MPO in kidney and bladder tissues of infected rats displayed augmented

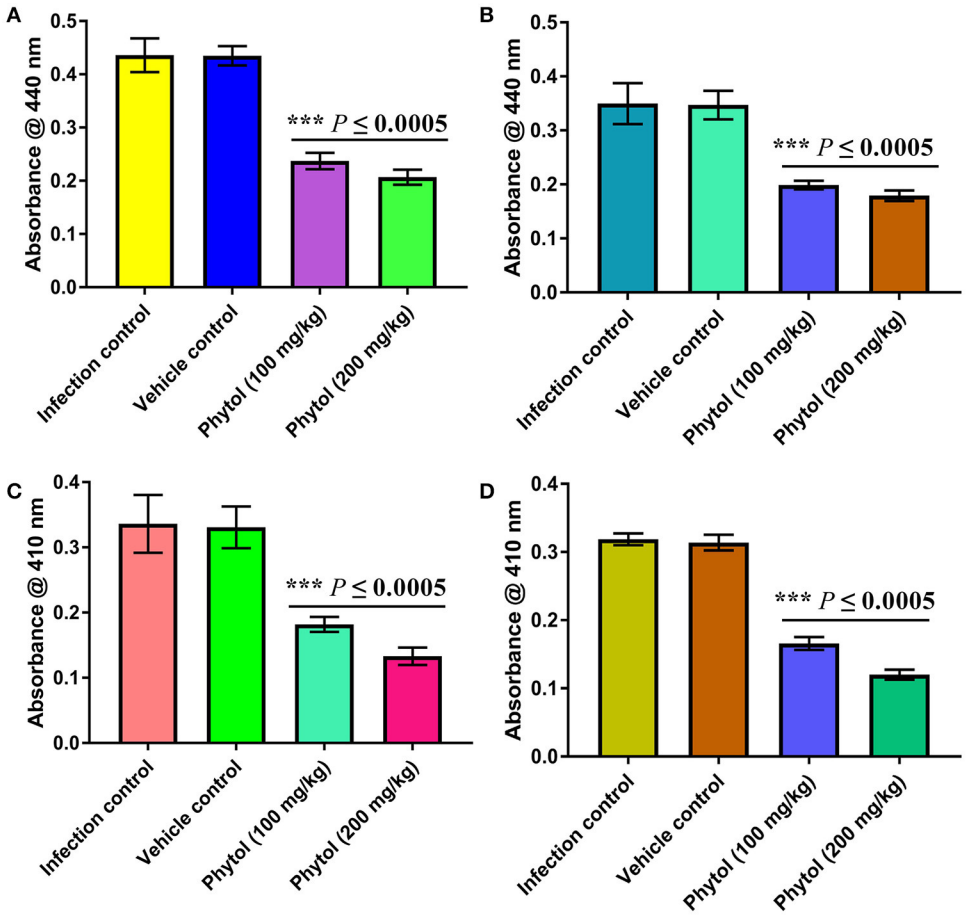

FIGURE 7 | Inhibitory effect of phytol on protease and lipase productions in kidney and bladder tissues. Phytol treatment (100 and 200 mg/kg) significantly decreased the protease **(A,B)** and lipase **(C,D)** productions in kidney **(A,C)** and bladder **(B,D)** tissues of pyelonephritis induced rats, compared to their infection controls. Corn oil was used as the vehicle control. Error bar indicates standard deviations from the mean. Student-*t* test was used to compare the control and treated samples. ***Indicates significant at $p \leq 0.0005$.

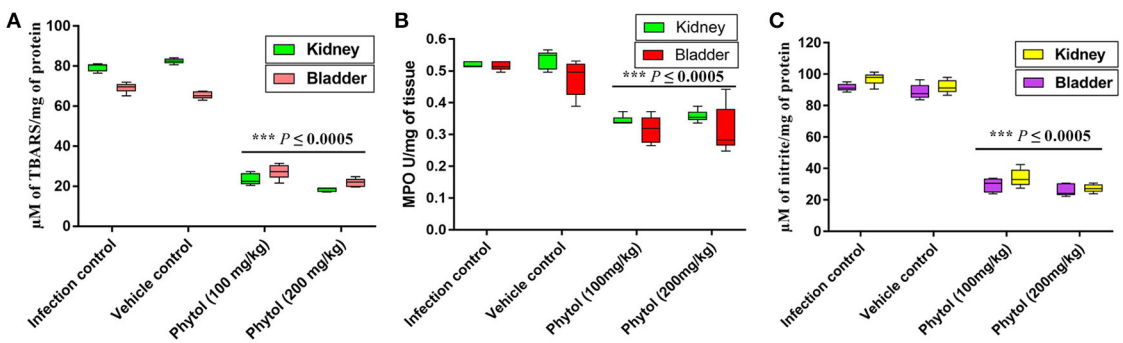

FIGURE 8 | Levels of MDA, MPO, and NO productions in kidney and bladder tissues. Phytol treatment (100 and 200 mg/kg) significantly decreased the MDA **(A)**, MPO **(B)**, and NO **(C)** levels in kidney and bladder tissues of pyelonephritis induced rats, compared to their infection controls. Corn oil was used as the vehicle control. Error bar indicates standard deviations from the mean. Student-*t* test was used to compare the control and treated samples. ***Indicates significant at $p \leq 0.0005$.

level of MPO production, while, the phytol treatment exhibited a diminution level of MPO production in both kidney and bladder tissues (**Figure 8B**).

Effect of Phytol on Nitrite Content

Reactive nitrogen intermediates are an index of nitrite produced by macrophages and neutrophils with the help of nitric oxide

(NO) synthase. Increased level of nitrite production was observed in the *S. marcescens* infected kidney and bladder tissues, whereas, the phytol treatment showed a decreased level of nitrite production in kidney and bladder tissues (**Figure 8C**).

Kidney Tissue Histology

Normal uninfected rat showed normal glomeruli (**Figure 9Aa**), whereas the rat infected with *S. marcescens* showed severe inflammation and dilation of Bowman's capsule, obliteration of renal tubules and widespread infiltration of neutrophils in the kidney tissue (**Figure 9Ab**). In vehicle control, infiltration of lymphocytes were observed near glomeruli and is representing an extensive inflammation. Destruction of renal tubules, dilatation of Bowman's capsule and glomeruli shrinkage were also observed (**Figure 9Ac**). In contrast, the infected rat treated with 100 mg/kg body weight of phytol showed mild infiltration of neutrophils. While, dilated Bowman's space and shrinkage of glomeruli were not observed (**Figure 9Ad**). Similarly, infected rat treated with 200 mg/kg body weight of phytol showed reduced level of infiltration of neutrophil and is similar to the normal animal control (**Figure 9Ae**).

Bladder Tissue Histology

Histological section of normal animal bladder showed normal structure of urinary bladder. The three layers of TEp, mucosa and muscularis appear to be normal (**Figure 9Ba**). In infection control, the increased infiltration of neutrophils was observed in the bladder wall. Also, severe mucosal abrasion was observed due to infiltration of neutrophils (**Figure 9Bb**). Similarly in vehicle control, marked inflammation and infiltration of neutrophil was observed in the transitional epithelium layer and larger areolar connective tissue was observed (**Figure 9Bc**). In contrast, the 100 mg/kg body weight of phytol treatment group showed no remarkable inflammation in the transitional epithelium layer, while, slight abrasion was observed in the urothelium (**Figure 9Bd**). Histological section of urinary bladder in 200 mg/kg body weight of phytol treatment showed clear pathological changes (**Figure 9Be**).

Single Dose Toxicity Study

Hematological and Biochemical Parameters

The haematopoietic system is one of the utmost sensitive targets for toxic compounds and considered as a vital index of pathological and physiological status in living systems. Similarly, assessment of biochemical profile acts as valuable indicator to assess the toxic nature of drugs in man and animals. In the pilot single dose toxicity study, no noteworthy difference was observed in the hematological and biochemical profile between the animal control and the phytol treated group (200 mg/kg) (**Table 3**). Compared to animal control, a slight increament was observed in ALP and SGPT levels in the phytol treated group (200 mg/kg). There was a significant decrease in triglycerides and total cholesterol level in the group treated with 200 mg/kg of phytol, when compared to the animal control.

Histological Evaluation of Vital Organs of Normal and Phytol Treated Animals

Histological micrographs of kidney from untreated animal showed normal glomeruli size and the proximal and distal convoluted tubules exhibit a normal fine structures (**Figure 10Aa**), while 200 mg/kg phytol treatment showed intact glomeruli with normal structure (**Figure 10Ba**). The liver sectioning of control animals portrayed normal architecture and hepatic cells with granulated cytoplasm. The hepatocytes were polygonal shape with a rounded nucleus, arranged in cords with the portal tract exhibiting a normal structure (**Figure 10Ab**). The rats administered with 200 mg/kg body weight of phytol showed only a moderate degeneration of hepatocytes (**Figure 10Bb**). Similarly, sections of heart from control and phytol treated animals showed normal muscle fibers with acidophilic cytoplasm

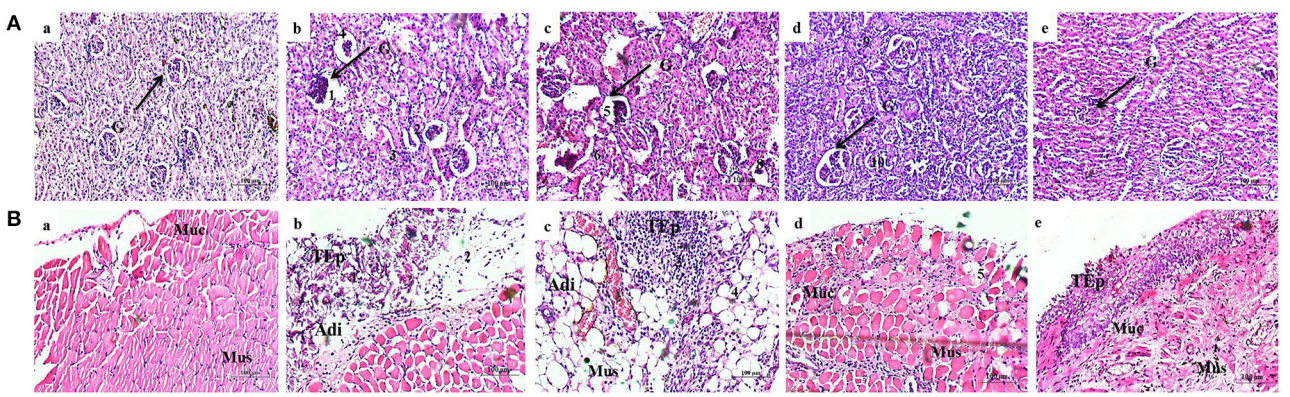

FIGURE 9 | Histopathology analysis of kidney tissue **(A)**. Normal uninfected rat **(a)**, infection control **(b)**, vehicle control **(c)**, phytol treatment (100 mg/kg) **(d)**, phytol treatment (200 mg/kg) **(e)**. 1 and 5, Dilation of Bowman's capsule; 2 and 6, Destruction of renal tubules; 3 and 7, Extensive infiltration of neutrophils; 4 and 8, Shrinkage of glomeruli; 9, Mild infiltration of neutrophils; 10, Well rejuvenated renal tubules; G, Glomeruli. Histopathology analysis of bladder tissue **(B)**. Normal uninfected rat **(a)**, Infection control **(b)**, Vehicle control **(c)**, Phytol treatment (100 mg/kg) **(d)**, Phytol treatment (200 mg/kg) **(e)**. 1 and 3, Extensive infiltration of neutrophils in the bladder wall; 2, Severe abrasion due to infiltration of neutrophils; 4, Larger areolar connective tissue interlaced with the muscular coat; 5, Slight abrasion; Muc, mucosa; Mus, muscularis; TEp, transitional epithelium; Adi, Adipose tissue. Corn oil was used as the vehicle control.

and centrally located nuclei (**Figures 10A,Bc**). The lung sections appears to be normal in phytol treated and control animals with typical alveoli (**Figures 10A,Bd**). The spleen from control and phytol treated animals showed normal granular hemosiderin pigment predominantly within macrophages in the red pulp. The white pulp containing lymphocytes surrounded by a red pulp (**Figures 10A,Be**).

TABLE 3 | Hematological and biochemical profiles of animal control and animal treated with phytol.

Hematological and biochemical parameters	Control	Phytol 200 mg/kg
Hemoglobin (gm/dL)	12.16 ± 1.8	11.84 ± 3.4
WBC ($\times 10^3$) (μL^{-1})	7.52 ± 0.6	7.18 ± 1.5
RBC ($\times 10^6$) (μL^{-1})	3.94 ± 0.6	3.92 ± 1.1
Hematocrit (%)	35.48 ± 7.03	35.58 ± 10.2
Glucose (mg/dL)	80.6 ± 16.1	76.8 ± 15.1
Blood urea (mg/dL)	48.24 ± 4.6	53.2 ± 4.6
Creatinine (mg/dL)	0.542 ± 0.3	0.48 ± 0.07
ALP (IU/L)	107.8 ± 9.8	127.6 ± 23.9
SGOT (U/L)	39.4 ± 7.2	44.4 ± 10.5
SGPT (U/L)	20.2 ± 5.1	27 ± 10.4
Triglycerides (mg/dL)	96.4 ± 6.4	91 ± 17.4
HDL (mg/dL)	16.8 ± 4.1	16.6 ± 1.4
LDL (mg/dL)	113.84 ± 20.3	105.2 ± 10.6
VLDL (mg/dL)	18.96 ± 1.6	18.2 ± 3.4
Total bilirubin (mg/dL)	0.384 ± 0.1	0.48 ± 0.1
Direct bilirubin (mg/dL)	0.246 ± 0.08	0.3 ± 0.06
Indirect bilirubin (mg/dL)	0.124 ± 0.04	0.18 ± 0.07
Total cholesterol (mg/dL)	152.4 ± 21.0	140 ± 8.9
Total Protein (gm/dL)	5.22 ± 0.4	5.14 ± 0.9
Albumin (gm/dL)	3.58 ± 0.4	3.56 ± 0.3
Globulin (gm/dL)	1.64 ± 0.3	1.58 ± 0.5

Phytol treatment (200 mg/kg) did not show any significance variations in hematological and biochemical profiles, compared to the animal control. Data are expressed as mean ± SD.

DISCUSSION

UTI is an infection occurred wherever in the urinary system typically exposed to bacterial pathogens. Once bacterial pathogens reach the kidney through ascending infection, they are capable to adhere to the urothelium before raiding the renal tissue with subsequent pyelonephritis (Nickel et al. (1987). Such sort of infections are reported to be caused by Gram-negative bacteria like *P. mirabilis, E. coli*, *Klebsiella pneumoniae*, *P. aeruginosa*, *S. marcescens,* and Gram-positive bacteria such as *Staphylococcus aureus* and *Enterococcus faecalis* (Su et al., 2003; Behzadi et al., 2010; Kaur et al., 2014).

Among which, *S. marcescens* is an important human opportunistic bacterial pathogen, causing numerous nosocomial infections such as respiratory tract infections, blood stream infections, ocular infections and most importantly urinary tract infections (Hejazi and Falkiner, 1997). It secretes array of virulence factors and forms biofilm via signal mediated QS mechanism. In our previous study, we assessed the anti-QS potential of phytol through primary assays such as prodigiosin production, protease inhibition assays and biofilm cells quantification by crystal violet assay (Srinivasan et al., 2016). Nevertheless, the present study further evaluated the potentials of phytol against *S. marcescens* by assessing various virulence assays such as biofilm cells quantification by XTT reduction assay, microscopic analyses of biofilm formation, swarming motility analysis, lipase, hemolysin and EPS quantification assays. In addition, the current study elucidated the molecular mechanism of phytol on QS system in *S. marcescens* through real-time expression analysis and confirmed its *in vivo* protective effect on acute pyelonephritis infection in rat model with satisfactory safety evaluated by single dose toxicity studies.

Biofilms are the aggregation of microorganism, wherein the microbial cells stick to each other on biotic and abiotic surfaces and composed of extracellular DNA, polysaccharides and proteins (Abdel-Aziz and Aeron, 2014). Therefore, we tested the effect of phytol on biofilm formation and EPS production in *S. marcescens* by XTT reduction and EPS quantification assays. The

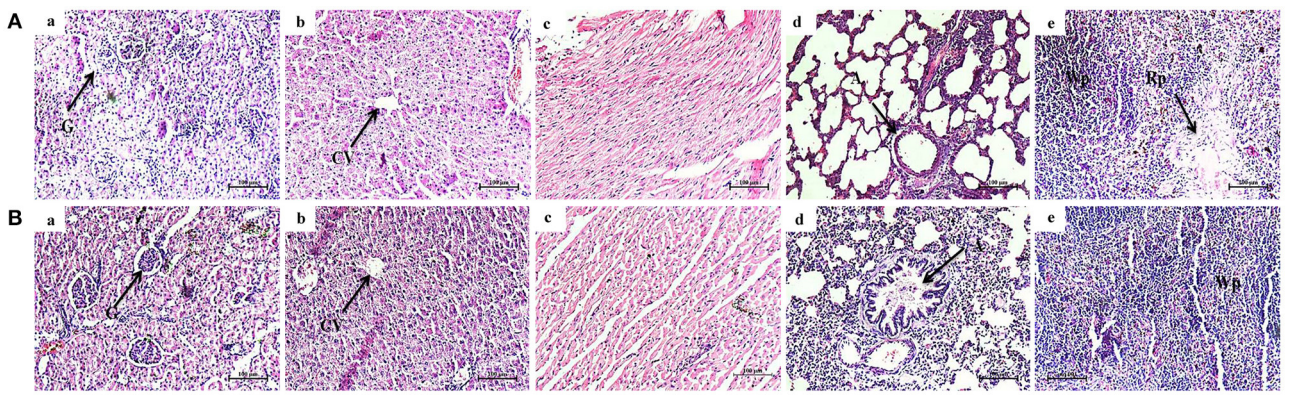

FIGURE 10 | Histopathology analysis of vital organs. Phytol treatment (200 mg/kg) **(B)** did not show any considerable histology varitions in vital organs such as kidney **(a)**, liver **(b)**, heart **(c)**, lungs **(d)**, and spleen **(e)**, compared to the vital organs of animal control **(A)**. G, Glomeruli; CV, Central Vein; A, Alveolar; Wp, White pulp; Rp, Red pulp.

obtained results showed decreasing level of metabolically active cells involved in biofilm formation and EPS production in phytol treatment compared to their respective controls (**Figures 2A**, **4A**). Further, the light and CLSM (2, 2.5, and 3 D) images confirmed the antibiofilm potential of phytol, in which, the 5 and 10 μg/ml of phytol treatment showed disintegration of biofilm formation. Divergently, the control slides showed thick coating of biofilm formation (**Figures 3A,B**). Our results are going well with the findings of the previous researches, who have reported that the morin reduced the metabolically active cells involved in *Listeria monocytogenes* biofilm formation (Sivaranjani et al., 2016) and marine bacterial extract G-16 effectively inhibited the *S. marcescens* EPS production (Padmavathi et al., 2014).

Several bacterial pathogens simultaneously grow and spread rapidly over a surface through the pattern of movement called swarming motility. This diminishes competition between bacterial cells for nutrients and speeding their growth (Kaiser, 2007). This typical virulent phenomenon in *S. marcescens* plays a vital role in catheter associated urinary tract infections. In this bacterial species the phenomenon of swimming and swarming motility is associated with QS. Hence, an attempt was made to examine the QSI potential of phytol in inhibiting the swarming movement. Results of the current study showed vigorous swarming motility in the untreated *S. marcescens* control plate, wherein the 5 and 10 μg/ml of phytol treatment showed concentration dependent swarming motility inhibition (**Figure 3C**). Consistent with this result, Srinivasan et al. (2016) have reported that *Piper betle* extract effectively inhibited the *S. marcescens* swarming motility in a concentration dependent manner.

Lipase is the secreted extracellular virulence enzyme in *S. marcescens* and their production is regulated by QS. Hemolysin production is accountable for the pathogenesis of various bacterial pathogens. Hemolysin produced by *S. marcescens* (ShlA), is a group of pore forming toxins, targets the cell membrane permeability (Shimuta et al., 2009). The result of lipase and hemolysin inhibition assays indicated a significant ($P \leq 0.0005$) decline in lipase and hemolysin production in *S. marcescens* upon treatment with 5 and 10 μg/ml of phytol (**Figures 4A,B**). Previously, *Anethum graveolens* extract and farnesol were tested for their effects on lipase and hemolysin production in *S. marcescens* and *P. aeruginosa* respectively, and which showed promising lipase and hemolysin inhibitory properties (Hassan Abdel-Rhman et al., 2015; Salini and Pandian, 2015).

Further to understand the anti-QS and antibiofilm potential of phytol at molecular level and to support the outcome of *in vitro* results, the real-time PCR analysis was performed. It is known that *fimA* and *fimC* are the major fimbrial subunits in *S. marcescens*. In 2007, a study done by Labbate et al. disclosed that the *fimA* disruption mutant unable to produce fimbriae and likewise they confirmed the absence of fimbrial structure in *S. marcescens* by electron microscopy. The products of the *flhDC* master operon, FlhD and FlhC are global gene regulators in *S. marcescens*, which expressed several inherent determinants such as cell differentiation, cell division, swimming and swarming motilities (Liu et al., 2000). Therefore, the impact of phytol on the *fimA*, *fimC*, *flhC,* and *flhD* gene expression levels were tested and the obtained real-time data showed a substantial downregulation of these fimbrial and motility genes expression in *S. marcescens*. The *bsmB* is a QS controlled virulence gene in *S. marcescens*. Labbate et al. (2007) reported that the *bsmB* mutant lacked biofilm formation, lipase, protease and S-layer protein productions. Phytol treatment decreases the expression level of *bsmB* gene up to 0.36-fold compare to the control. The RssA-RssB (RssA-sensor kinase and RssB -response regulator) is a two component system and it negatively regulates the *S. marcescens* swarming motility. RssB binds directly to the *flhDC* promoter and suppresses the *flhDC* transcription, leading to reduced production of hemolysin and flagellar mediated motilities (Lin et al., 2010). In Ang et al. (2001) stated that the overexpression of *rsmA* gene in *S. marcescens* inhibits the swarming motility and prodigiosin production. The *pigP* is the master transcriptional regulator and which controls the regulation of prodigiosin pigment production in *S. marcescens* under the QS mechanism (Gristwood et al., 2011). RssB binds directly to the promoter region of the pig operon, leading to negative regulation of prodigiosin production (Soo et al., 2014). The outcome of real-time data showed upregulation of *rssB* and *rsmA* genes expression and support the *in vitro* data of hemolysin, swarming motility and prodigiosin inhibition due to their binding on *flhDC* and *pigP* promoter regions. Likewise, phytol decreases the expression level of *pigP* gene upto 0.48 fold compare to the control. ShlA is a key virulence factor of *S. marcescens*, which has shown to wield cytotoxic effects on fibroblasts and epithelial cells (Di Venanzio et al., 2014) and *shlBA* mutant strains were extremely reduced in virulence in mice, *Drosophila melanogaster* and *Caenorhabditis elegans* models (Kurz et al., 2003). In *S. marcescens*, hemolysis and swarming motility are co-regulated (Shanks et al., 2013). In the current study the phytol inhibited the hemolysin production along with swarming motility inhibition. Similarly, the real-time data showed downregulation of *shlA* gene upon treatment with phytol (**Figure 5**).

The recent reports stated that the QS mediated virulence factors are very important for establishment of successful UTI infection in animal models (Kumar et al., 2009; Gupta et al., 2013b, 2016; Saini et al., 2015). Only limited studies specified the pathogenesis of *S. marcescens* in animal models and also no reports are available on the protective effect of plant extracts or pure compounds against *S. marcescens* associated infection in animal models. To the best of our knowledge, the present study is the first of its kind has been made with a prime objective to establish the *S. marcescens* associated acute pyelonephritis in rat and assessing the protective effect of phytol against acute pyelonephritis induced rat.

After successful establishment of acute pyelonephritis in rat model, the bacterial count in phytol treated and untreated rats were quantified by bacteriological assay. The infected control had 8.28×10^4, 7.2×10^4, and 3.72×10^4 CFU in kidney, bladder and urine samples, respectively compare to the 200 mg/kg body weight of phytol treated group in which 1.78×10^4, 0.96×10^4, and 0.5×10^4 CFU were observed in kidney, bladder and urine samples, respectively (**Figures 6B–D**). This corresponds to nearly 4.6, 7.5 and 7.4 fold decrease in bacterial count in

phytol (200 mg/kg body weight) treated kidney, bladder and urine samples respectively, compared to the infected control. These results correlate with the findings of Hvidberg et al. (2000), who have reported that the antibiotic gentamicin treatment significantly decreased the bacterial count in kidney, bladder and urine samples in UTI induced mice compare to the infection control.

Colonization of bacterial pathogens on host tissue during the early stage of infection is an essential factor for the establishment of very infection. Virulence factors produced by the bacterial pathogens help in the host colonization and subsequent infection progress. The extracellular virulence enzyme protease plays a pivotal role in the pathogenesis of *S. marcescens* during infection and induces interleukin-6 and interleukin-8 mRNA expression through protease-activated receptor 2 (PAR-2) (Kida et al., 2007). A study made by Lyerly and Kreger (1983) state that the highly purified protease enzyme obtained from *S. marcescens* induced the acute pneumonia in mice and guinea pigs. A finding made by Ishii et al. (2014) revealed that the protease intricate in the pathogenesis of *S. marcescens* and leads to a huge loss of hemolymph in silkworm larvae. Like protease, the extracellular lipase enzyme also an extensive virulence factor and which involved in the pathogenesis of *S. marcescens* (Hejazi and Falkiner, 1997). Both of these virulence enzyme productions are controlled by the QS mechanism (Labbate et al., 2007). In support, the result stated by Elsheikh et al. (1987) indicated that the virulence enzyme protease enhances the pathogenesis of *P. aeruginosa* in experimental mouse burn infection. In Gupta et al. (2013a) suggested that the QS mediated virulence enzymes such as protease and elastase are involved in the establishment and colonization of *P. aeruginosa* in mice during experimental UTI. Therefore, the inhibitory effect of phytol on virulence enzyme production in rat acute pyelonephritis model was evaluated. As expected the phytol treatment showed decreased level of protease and lipase enzymes production in both kidney and bladder tissues compared to the infected and vehicle controls (**Figure 7**). The extreme reduction in virulence enzyme productions of kidney and bladder tissues in phytol treated groups is go well with bacteriological assay. Hence, it is envisaged that the decreasing level of virulence enzymes in phytol treated groups might be due to the decreasing level of invading *S. marcescens* cells.

MDA is an indicator of lipid peroxidation and which is a steady product of oxidative stress of reactive oxygen species on unsaturated fatty acid, a vital constituent of cell membrane. In the current study, the kidney and bladder tissues from infected and vehicle control groups showed a substantial increase in MDA level on 5th p.i.d, whereas the phytol treated groups showed decreasing level of MDA production in kidney and bladder tissues (**Figure 8A**). Consistent with our results, synergistic combination of azithromycin and ciprofloxacin has been shown to decrease the MDA level in kidney tissue homogenates of *P. aeruginosa* infected mice on the 3rd and 5th p.i.d (Saini et al., 2015).

MPO is an enzyme deposited in azurophilic granules of polymorphonuclear neutrophils and macrophages, which released during inflammatory process and oxidative stress into extracellular fluid. The MPO is a possible pathological marker for the confirmation of inflammation (Loria et al., 2008). In the present study, the MPO level was considerably low in case of infected rats treated with phytol compare to the infected and vehicle controls in both kidney and bladder tissues (**Figure 8B**). The results of MPO assay go well with the findings of Vadekeetil et al. (2016), who have reported that the ajoene-ciprofloxacin combination effectively decreasing the MPO production in the mice infected from *P. aeruginosa* biofilm associated murine acute pyelonephritis.

NO is produced by a different cell types by NO synthases, which are involved in the inflammatory processes. Stimulation of NO production during inflammatory progression signifies a protection mechanism against invading bacterial pathogens, however extreme formation of NO has also been involved in host tissue injury (Van Der Vliet et al., 1997). A significant ($P \leq 0.0005$) decline of nitrite in the levels of protein was observed in kidney and bladder tissues of phytol treatment groups compare to the infection and vehicle controls. Similar to the observed results, recently the combination therapy with ajoene and ciprofloxacin has been found to show decreasing level of NO production in mice infected with *P. aeruginosa* (Vadekeetil et al., 2016).

To support the decreasing level of virulence enzymes and inflammatory markers in phytol treated groups, the histopathology analysis was done. Kidney sections of the normal uninfected rats looked histologically normal with no substantial pathological variations (**Figure 9Aa**). The kidney sections of infection and vehicle control rats had extensive infiltration of neutrophils with destruction of renal tubules and shrinkage of glomeruli (**Figures 9Ab,c**). In case of 100 mg/kg body weight of phytol treated group, a mild infiltration of neutrophils was noted and 200 mg/kg body weight of phytol treatment showed no considerable pathological changes (**Figures 9Ad,e**). Recently, Balamurugan et al. (2015) found that the treatment of UTI^{QQ} with gentamicin against rats infected with *S. aureus* showed minimal dilatation of renal tubules with no considerable pathological changes in kidney section. The bladder histology section of infection and vehicle controls showed extensive infiltration of neutrophils with severe abrasion in transitional epithelium (**Figures 9Bb,c**). In contrast, the uninfected rat and infected rat treated with phytol showed no considerable pathological changes (**Figures 9Ba,d,e**). Outcome of this bladder histology supports the results of Sabharwal et al. (2016), who have not observed any adverse pathological changes in divalent flagellin treated mice bladder tissue.

The toxicological property of phytol has been tested in different animal models for different clinical applications (Hidiroglou and Jenkins, 1972; McGinty et al., 2010). The acute oral LD_{50} of phytol in rats was described to be more than 5.0 g/kg body weight (McGinty et al., 2010). However, the rats were dosed for 28-day in sub chronic toxicity study showed the no-observed-adverse-effect-level (NOAEL) of phytol to be 500 mg/kg/day, based on organ weight changes. In contrast, the rats were dosed for a longer period of time (52–108 days) in a one-generation reproductive toxicity study, the lowest-observed-adverse-effect level (LOAEL) of phytol was to be 250 mg/kg/day, based on renal changes in male and female rats (Api et al., 2016). The overall mammalian toxicity of phytol is considered to be low only in least

concentration. Hence, the protective effect of phytol was tested against *S. marcescens* associated acute pyelonephritis infection at the concentration of 100 and 200 mg/kg. On the other hand, we assessed the toxic effect of phytol (200 mg/kg) by single dose acute toxicity study. No significant differences were observed in the hematological profile of phytol treated group compared to the animal control (**Table 3**). The oral administration of phytol in rats did not show any significant changes in biochemical profile when compared to the animal control group (**Table 3**). However, an increase in ALP and SGPT serum blood levels were observed in the phytol treatment. ALP and SGPT are generally used as markers for liver function and indicators of liver toxicity. ALP and SGPT levels elevate in the blood when the hepatic cellular permeability is changed or cellular injury occurs in liver. The histopathological analysis of vital organs (Kidney, Liver, Heart, Lungs, and Spleen) in phytol treated group did not show any adverse pathological effects compared to the animal control, except liver section (**Figure 10**). The liver section of phytol treatment showed moderate degeneration of hepatocytes (**Figure 10Bb**) and it was due to the increasing level of ALP and SGPT. The degeneration of hepatocytes and increasing level of liver enzymes support the outcome of Mackie et al. (2009), who have reported that the phytol induced the hepatotoxicity in mice.

To the best of our knowledge, this is the pioneering study annex the anti-QS and antibiofilm capability of phytol in the counteractive action on *S. marcescens* infection through the serious of virulence inhibition assays. The real-time analysis disclosed the molecular mechanism of phytol on QS intervened virulence factors productions in *S. marcescens*. Further, the *S. marcescens* associated acute pyelonephritis infection in rat model unveiled the protective effect of phytol by reducing the bacterial counts, virulence enzymes and inflammatory markers productions with adequate safety. Therefore, the utilization of phytol is promising in the advancement of novel antipathogenic medications to control acute pyelonephritis infection caused by *S. marcescens*. However, further studies will be needed to reveal the mode of action of phytol against *S. marcescens* associated acute pyelonephritis infection.

AUTHOR CONTRIBUTIONS

AV and RS conceived and designed the research; RS, AK, and VK performed the experiments; RM, KR, and GA offered advice and technical assistance for carrying out the studies on experimental animals; AV and RS analyzed the data; AV, SK, and KR contributed reagents/materials/analysis tools; RS wrote the paper and AV approved the manuscript after careful analysis.

ACKNOWLEDGMENTS

The authors RS, AK, SK, and AV thankfully acknowledge the Bioinformatics Infrastructure Facility provided by the Alagappa University [Funded by Department of Biotechnology, Government of India; Grant No. BT/BI/25/015/2012(BIF)]. The author RS sincerely thanks the University Grants Commission, New Delhi, India, for the financial support in the form of UGC-BSR fellowship [F.4-1/2006(BSR)/7-326/2011(BSR)]. The author GA thankfully acknowledges UGC for the award UGC-BSR faculty fellow. The author KR thank the DST supported "National Facility on Drug development for Academia, Pharmaceutical and Allied Industries" established at BIT Campus, Anna University, Tiruchirappalli. The authors thankfully acknowledge Dr. Claus Sternberg, DTU Systems Biology, Technical University of Denmark for providing the COMSTAT software.

SUPPLEMENTARY MATERIAL

The Supplementary Material for this article can be found online at: https://www.frontiersin.org/articles/10.3389/fcimb.2017.00498/full#supplementary-material

Supplementary Figure 1 | PCR amplification for the checking the primer efficiencies of QS controlled virulence genes in *S. marcescens*.

REFERENCES

Abdel-Aziz, S. M., and Aeron, A. (2014). Bacterial biofilm: dispersal and inhibition strategies. *SaJ Biotechnol*. 1:105. doi: 10.18875/2375-6713.1.105

Ang, S., Horng, Y. T., Shu, J. C., Soo, P. C., Liu, J. H., Yi, W. C., et al. (2001). The role of RsmA in the regulation of swarming motility in *Serratia marcescens*. *J. Biomed. Sci.* 8, 160–169. doi: 10.1159/000054028

Api, A. M., Belsito, D., Bhatia, S., Bruze, M., Calow, P., Dagli, M. L., et al. (2016). RIFM fragrance ingredient safety assessment, α-Ionone, CAS Registry Number 127-41-3. *Food Chem. Toxicol.* 97, S1–S10. doi: 10.1016/j.fct.2015.12.010

Balamurugan, P., Hema, M., Kaur, G., Sridharan, V., Prabu, P. C., Sumana, M. N., et al. (2015). Development of a biofilm inhibitor molecule against multidrug resistant *Staphylococcus aureus* associated with gestational urinary tract infections. *Front Microbiol.* 6:832. doi: 10.3389/fmicb.2015.00832

Behzadi, P., Behzadi, E., Yazdanbod, H., Aghapour, R., Cheshmeh, M. A., and Omran, D. S. (2010). A survey on urinary tract infections associated with the three most common uropathogenic bacteria. *Maedica* 5:111.

Brown, C. (2011). Urethral catheterization of the female rat. *Lab. Anim.* 40:111. doi: 10.1038/laban0411-111

Chen, C. Y., Chen, Y. H., Lu, P. L., Lin, W. R., Chen, T. C., and Lin, C. Y. (2012). *Proteus mirabilis* urinary tract infection and bacteremia: risk factors, clinical presentation, and outcomes. *J. Microbiol. Immunol. Infect.* 45, 228–236. doi: 10.1016/j.jmii.2011.11.007

Derbie, A., Hailu, D., Mekonnen, D., Abera, B., and Yitayew, G. (2017). Antibiogram profile of uropathogens isolated at Bahir Dar Regional Health Research Laboratory Centre, Northwest Ethiopia. *Pan. Afr. Med. J.* 26:134. doi: 10.11604/pamj.2017.26.134.7827

Di Venanzio, G., Stepanenko, T. M., and Véscovi, E. G. (2014). *Serratia marcescens* ShlA pore-forming toxin is responsible for early induction of autophagy in host cells and is transcriptionally regulated by RcsB. *Infect. Immun.* 82, 3542–3554. doi: 10.1128/IAI.01682-14

Eberl, L., Winson, M. K., Sternberg, C., Stewart, G. S., Christiansen, G., Chhabra, S. R., et al. (1996). Involvement of N-acyl-l-homoserine lactone autoinducers in controlling the multicellular behaviour of *Serratia liquefaciens*. *Mol. Microbiol.* 20, 127–136. doi: 10.1111/j.1365-2958.1996.tb02495.x

Elsheikh, L. E., Kronevi, T., Wretlind, B., Abaas, S., and Iglewski, B. H. (1987). Assessment of elastase as a *Pseudomonas aeruginosa* virulence factor in experimental lung infection in mink. *Vet Microbiol.* 13, 281–289. doi: 10.1016/0378-1135(87)90090-3

Foxman, B., and Brown, P. (2003). Epidemiology of urinary tract infections: transmission and risk factors, incidence, and costs. *Infect. Dis. Clin. North Am.* 17, 227–241. doi: 10.1016/S0891-5520(03)00005-9

González-Juarbe, N., Mares, C. A., Hinojosa, C. A., Medina, J. L., Cantwell, A., Dube, P. H., et al. (2015). Requirement for *Serratia marcescens* cytolysin in a murine model of hemorrhagic pneumonia. *Infect. Immun.* 83, 614–624. doi: 10.1128/IAI.01822-14

Gristwood, T., McNeil, M. B., Clulow, J. S., Salmond, G. P., and Fineran, P. C. (2011). PigS and PigP regulate prodigiosin biosynthesis in *Serratia* via differential control of divergent operons, which include predicted transporters of sulfur-containing molecules. *J. Bacteriol.* 193, 1076–1085. doi: 10.1128/JB.00352-10

Gupta, P., Gupta, R. K., and Harjai, K. (2013a). Multiple virulence factors regulated by quorum sensing may help in establishment and colonisation of urinary tract by *Pseudomonas aeruginosa* during experimental urinary tract infection. *Ind. J. Med. Microbiol.* 31:29. doi: 10.4103/0255-0857.108715

Gupta, P., Gupta, R. K., and Harjai, K. (2013b). Quorum sensing signal molecules produced by *Pseudomonas aeruginosa* cause inflammation and escape host factors in murine model of urinary tract infection. *Inflammation* 36, 1153–1159. doi: 10.1007/s10753-013-9650-y

Gupta, R. K., Harjai, K., and Chhibber, S. (2016). Rhl quorum sensing affects the virulence potential of *Pseudomonas aeruginosa* in an experimental urinary tract infection. *Antonie Leeuwenhoek* 109, 1535–1544. doi: 10.1007/s10482-016-0755-9

Hassan Abdel-Rhman, S., Mostafa El-Mahdy, A., and El-Mowafy, M. (2015). Effect of tyrosol and farnesol on virulence and antibiotic resistance of clinical isolates of *Pseudomonas aeruginosa*. *BioMed. Res. Int*. 2015:456463. doi: 10.1155/2015/456463

Hejazi, A., and Falkiner, F. R. (1997). *Serratia marcescens*. *J. Med. Microbiol.* 46, 903–912. doi: 10.1099/00222615-46-11-903

Heydorn, A., Nielsen, A. T., Hentzer, M., Sternberg, C., Givskov, M., Ersbøll, B. K., et al. (2000). Quantification of biofilm structures by the novel computer program COMSTAT. *Microbiology* 146, 2395–2407. doi: 10.1099/00221287-146-10-2395

Hidiroglou, M., and Jenkins, K. J. (1972). Fate of 14 C-phytoI Administered Orally to Sheep. *Can. J. Physiol. Pharmacol.* 50, 458–462. doi: 10.1139/y72-069

Hines, D. A., Saurugger, P. N., Ihler, G. M., and Benedik, M. J. (1988). Genetic analysis of extracellular proteins of *Serratia marcescens*. *J. Bacteriol.* 170, 4141–4146. doi: 10.1128/jb.170.9.4141-4146.1988

Hirs, C. H. W. (1967). [45] Glycopeptides. *Methods Enzymol.* 11, 411–413. doi: 10.1016/S0076-6879(67)11047-1

Horng, Y. T., Deng, S. C., Daykin, M., Soo, P. C., Wei, J. R., Luh, K. T., et al. (2002). The LuxR family protein SpnR functions as a negative regulator of N-acylhomoserine lactone-dependent quorum sensing in *Serratia marcescens*. *Mol. Microbiol.* 45, 1655–1671. doi: 10.1046/j.1365-2958.2002.03117.x

Hvidberg, H., Struve, C., Krogfelt, K. A., Christensen, N., Rasmussen, S. N., and Frimodt-Møller, N. (2000). Development of a long-term ascending urinary tract infection mouse model for antibiotic treatment studies. *Antimicrob. Agents Chemother.* 44, 156–163. doi: 10.1128/AAC.44.1.156-163.2000

Inoue, Y., Hada, T., Shiraishi, A., Hirose, K., Hamashima, H., and Kobayashi, S. (2005). Biphasic effects of geranylgeraniol, teprenone, and phytol on the growth of *Staphylococcus aureus*. *Antimicrob. Agents Chemother*. 49, 1770–1774. doi: 10.1128/AAC.49.5.1770-1774.2005

Ishii, K., Adachi, T., Hara, T., Hamamoto, H., and Sekimizu, K. (2014). Identification of a *Serratia marcescens* virulence factor that promotes hemolymph bleeding in the silkworm, *Bombyx mori*. *J Invertebr Pathol.* 117, 61–67. doi: 10.1016/j.jip.2014.02.001

Islam, M. T., de Alencar, M. V. O. B., da Conceição Machado, K., da Conceição Machado, K., de Carvalho Melo-Cavalcante, A. A., de Sousa, D. P., et al. (2015). Phytol in a pharma-medico-stance. *Chem. Biol. Interact*. 240, 60–73. doi: 10.1016/j.cbi.2015.07.010

Kaiser, D. (2007). Bacterial swarming: a re-examination of cell-movement patterns. *Curr. Biol.* 17, R561–R570. doi: 10.1016/j.cub.2007.04.050

Kannappan, A., Gowrishankar, S., Srinivasan, R., Pandian, S. K., and Ravi, A. V. (2017). Antibiofilm activity of *Vetiveria zizanioides* root extract against methicillin-resistant *Staphylococcus aureus*. *Microb. Pathog*. 110, 313–324. doi: 10.1016/j.micpath.2017.07.016

Katsiari, M., Nikolaou, C., Roussou, Z., Triantopoulou, C., Apessou, D., Platsouka, E. D., et al. (2012). Community acquired quinolone-resistant *Escherichia coli* pyelonephritis complicated with multiple renal abscesses: a case report. *Hippokratia.* 16:381.

Kaur, N., Sharma, S., Malhotra, S., Madan, P., and Hans, C. (2014). Urinary tract infection: aetiology and antimicrobial resistance pattern in infants from A Tertiary Care Hospital in North India. *J. Clin. Diagn. Res*. 8, DC01–DC03. doi: 10.7860/JCDR/2014/8772.4919

Kida, Y., Inoue, H., Shimizu, T., and Kuwano, K. (2007). *Serratia marcescens* serralysin induces inflammatory responses through protease-activated receptor 2. *Infect. Immun.* 75, 164–174. doi: 10.1128/IAI.01239-06

Kim, J. J., Shajib, M. S., Manocha, M. M., and Khan, W. I. (2012). Investigating intestinal inflammation in DSS-induced model of IBD. *J. Vis. Exp.* e3678. doi: 10.3791/3678

Kim, S. Y., Shin, J., Shin, S. Y., and Ko, K. S. (2013). Characteristics of carbapenem-resistant Enterobacteriaceae isolates from Korea. *Diagn. Microbiol. Infect. Dis.* 76, 486–490. doi: 10.1016/j.diagmicrobio.2013.04.006

Kufel, W. D., Scrimenti, A., and Steele, J. M. (2016). A case of septic shock due to *Serratia marcescens* pyelonephritis and bacteremia in a patient receiving empagliflozin. *J. Pharm. Pract.* 30, 672–675. doi: 10.1177/0897190016679760

Kumar, R., Chhibber, S., and Harjai, K. (2009). Quorum sensing is necessary for the virulence of *Pseudomonas aeruginosa* during urinary tract infection. *Kidney Int.* 76, 286–292. doi: 10.1038/ki.2009.183

Kurz, C. L., Chauvet, S., Andrès, E., Aurouze, M., Vallet, I., Michel, G. P. F., et al. (2003). Virulence factors of the human opportunistic pathogen *Serratia marcescens* identified by *in vivo* screening. *EMBO J.* 22, 1451–1460. doi: 10.1093/emboj/cdg159

Labbate, M., Zhu, H., Thung, L., Bandara, R., Larsen, M. R., Willcox, M. D., et al. (2007). Quorum-sensing regulation of adhesion in *Serratia marcescens* MG1 is surface dependent. *J. Bacteriol.* 189, 2702–2711. doi: 10.1128/JB.01582-06

Leclercq, R., Cantón, R., Brown, D. F., Giske, C. G., Heisig, P., MacGowan, A. P., et al. (2013). EUCAST expert rules in antimicrobial susceptibility testing. *Clin. Microbiol. Infect.* 19, 141–160. doi: 10.1111/j.1469-0691.2011.03703.x

Lee, H. K., Park, Y. J., Kim, J. Y., Chang, E., Cho, S. G., Chae, H. S., et al. (2005). Prevalence of decreased susceptibility to carbapenems among *Serratia marcescens*, *Enterobacter cloacae*, and *Citrobacter freundii* and investigation of carbapenemases. *Diagn. Microbiol. Infect. Dis.* 52, 331–336. doi: 10.1016/j.diagmicrobio.2005.04.012

Lee, W., Woo, E. R., and Lee, D. G. (2016). Phytol has antibacterial property by inducing oxidative stress response in *Pseudomonas aeruginosa*. *Free Radic Res.* 50, 1309–1318. doi: 10.1080/10715762.2016.1241395

Lim, S. Y., Meyer, M., Kjonaas, R. A., and Ghosh, S. K. (2006). Phytol-based novel adjuvants in vaccine formulation: 1. assessment of safety and efficacy during stimulation of humoral and cell-mediated immune responses. *J. Immune Based Ther. Vaccines* 4:6. doi: 10.1186/1476-8518-4-6

Lin, C. S., Horng, J. T., Yang, C. H., Tsai, Y. H., Su, L. H., Wei, C. F., et al. (2010). RssAB-FlhDC-ShlBA as a major pathogenesis pathway in *Serratia marcescens*. *Infect Immun.* 78, 4870–4881. doi: 10.1128/IAI.00661-10

Liou, B. H., Duh, R. W., Lin, Y. T., Lauderdale, T. L. Y., and Fung, C. P. (2014). A multicenter surveillance of antimicrobial resistance in *Serratia marcescens* in Taiwan. *J. Microbiol. Immunol. Infect.* 47, 387–393. doi: 10.1016/j.jmii.2013.04.003

Liu, J. H., Lai, M. J., Ang, S., Shu, J. C., Soo, P. C., Horng, Y. T., et al. (2000). Role of flhDC in the expression of the nuclease gene nucA, cell division and flagellar synthesis in *Serratia marcescens*. *J. Biomed. Sci*. 7, 475–483. doi: 10.1159/000025483

Loria, V., Dato, I., Graziani, F., and Biasucci, L. M. (2008). Myeloperoxidase: a new biomarker of inflammation in ischemic heart disease and acute coronary syndromes. *Mediat. Inflamm.* 2008:135625. doi: 10.1155/2008/135625

Lyerly, D. M., and Kreger, A. S. (1983). Importance of serratia protease in the pathogenesis of experimental *Serratia marcescens* pneumonia. *Infect Immun.* 40, 113–119.

Mackie, J. T., Atshaves, B. P., Payne, H. R., McIntosh, A. L., Schroeder, F., and Kier, A. B. (2009). Phytol-induced hepatotoxicity in mice. *Toxicol. Pathol.* 37, 201–208. doi: 10.1177/0192623308330789

McGinty, D., Letizia, C. S., and Api, A. M. (2010). Fragrance material review on phytol. *Food Chem. Toxicol.* 48, S59–S63. doi: 10.1016/j.fct.2009.11.012

McMillen, M. A., Huribal, M., Cunningham, M. E., Bala, R. J., Pleban, W. E., and D'aiuto, M. L. (1996). Endothelin-1, interleukin-6, and interleukin-8 levels increase in patients with burns. *J. Burn. Care Res.* 17, 384–389. doi: 10.1097/00004630-199609000-00003

Mittal, R., Aggarwal, S., Sharma, S., Chhibber, S., and Harjai, K. (2009). Urinary tract infections caused by *Pseudomonas aeruginosa*: a minireview. *J. Infect. Public Health.* 2, 101–111. doi: 10.1016/j.jiph.2009.08.003

Nickel, J. C., Olson, M., McLean, R. J. C., Grant, S. K., and Costerton, J. W. (1987). An ecological study of infected urinary stone genesis in an animal model. *BJU Int.* 59, 21–30. doi: 10.1111/j.1464-410X.1987.tb04573.x

Nithya, C., Aravindraja, C., and Pandian, S. K. (2010). *Bacillus pumilus* of Palk Bay origin inhibits quorum-sensing-mediated virulence factors in Gram-negative bacteria. *Res. Microbiol.* 161, 293–304. doi: 10.1016/j.resmic.2010.03.002

Ohkawa, H., Ohishi, N., and Yagi, K. (1979). Assay for lipid peroxides in animal tissues by thiobarbituric acid reaction. *Anal. Biochem.* 95, 351–358. doi: 10.1016/0003-2697(79)90738-3

Ohno, N., Ota, Y., Hatakeyama, S., Yanagimoto, S., Morisawa, Y., Tsukada, K., et al. (2003). A patient with *E. coli*-induced pyelonephritis and sepsis who transiently exhibited symptoms associated with primary biliary cirrhosis. *Intern. Med.* 42, 1144–1148. doi: 10.2169/internalmedicine.42.1144

Packiavathy, I. A. S. V., Sasikumar, P., Pandian, S. K., and Ravi, A. V. (2013). Prevention of quorum-sensing-mediated biofilm development and virulence factors production in *Vibrio* spp. by *curcumin*. *Appl. Microbiol. Biotechnol.* 97, 10177–10187. doi: 10.1007/s00253-013-4704-5

Padmavathi, A. R., Abinaya, B., and Pandian, S. K. (2014). Phenol, 2, 4-bis (1, 1-dimethylethyl) of marine bacterial origin inhibits quorum sensing mediated biofilm formation in the uropathogen *Serratia marcescens*. *Biofouling* 30, 1111–1122. doi: 10.1080/08927014.2014.972386

Pejin, B., Ciric, A., Glamoclija, J., Nikolic, M., and Sokovic, M. (2015). *In vitro* anti-quorum sensing activity of phytol. *Nat. Prod. Res.* 29, 374–377. doi: 10.1080/14786419.2014.945088

Pejin, B., Savic, A., Sokovic, M., Glamoclija, J., Ciric, A., Nikolic, M., et al. (2014). Further *in vitro* evaluation of antiradical and antimicrobial activities of phytol. *Nat. Prod. Res.* 28, 372–376. doi: 10.1080/14786419.2013.869692

Ramakrishnan, K., and Scheid, D. C. (2005). Diagnosis and management of acute pyelonephritis in adults. *Am. Fam. Physician* 71, 933–942.

Rice, S. A., Koh, K. S., Queck, S. Y., Labbate, M., Lam, K. W., and Kjelleberg, S. (2005). Biofilm formation and sloughing in *Serratia marcescens* are controlled by quorum sensing and nutrient cues. *J. Bacteriol.* 187, 3477–3485. doi: 10.1128/JB.187.10.3477-3485.2005

Rockett, K. A., Awburn, M. M., Rockett, E. J., Cowden, W. B., and Clark, I. A. (1994). Possible role of nitric oxide in malarial immunosuppression. *Parasite Immunol.* 16, 243–249. doi: 10.1111/j.1365-3024.1994.tb00346.x

Rumbaugh, K. P., Griswold, J. A., Iglewski, B. H., and Hamood, A. N. (1999). Contribution of quorum sensing to the virulence of *pseudomonas aeruginosa* in burn wound infections. *Infect. Immun.* 67, 5854–5862.

Rumbaugh, K. P., Hamood, A. N., and Griswold, J. A. (2004). Cytokine induction by the *P. aeruginosa* quorum sensing system during thermal injury. *J. Surg. Res.* 116, 137–144. doi: 10.1016/j.jss.2003.08.009

Ryu, K. R., Choi, J. Y., Chung, S., and Kim, D. H. (2011). Anti-scratching behavioral effect of the essential oil and phytol isolated from *Artemisia princeps* Pamp in mice. *Planta Med.* 77, 22–26. doi: 10.1055/s-0030-1250119

Sabharwal, N., Chhibber, S., and Harjai, K. (2016). Divalent flagellin immunotherapy provides homologous and heterologous protection in experimental urinary tract infections in mice. *Int. J. Med. Microbiol.* 306, 29–37. doi: 10.1016/j.ijmm.2015.11.002

Saini, H., Chhibber, S., and Harjai, K. (2015). Azithromycin and ciprofloxacin: a possible synergistic combination against *Pseudomonas aeruginosa* biofilm-associated urinary tract infections. *Int. J. Antimicrob. Agents* 45, 359–367. doi: 10.1016/j.ijantimicag.2014.11.008

Salini, R., and Pandian, S. K. (2015). Interference of quorum sensing in urinary pathogen *Serratia marcescens* by *Anethum graveolens*. *Pathog. Dis.* 73:ftv038. doi: 10.1093/femspd/ftv038

Santos, C. C., Salvadori, M. S., Mota, V. G., Costa, L. M., de Almeida, A. A., de Oliveira, G. A., et al. (2013). Antinociceptive and antioxidant activities of phytol *in vivo* and *in vitro* models. *Neurosci. J.* 2013:949452. doi: 10.1155/2013/949452

Sathya, S., Shanmuganathan, B., Saranya, S., Vaidevi, S., Ruckmani, K., and Pandima Devi, K. (2017). Phytol-loaded PLGA nanoparticle as a modulator of Alzheimer's toxic Aβ peptide aggregation and fibrillation associated with impaired neuronal cell function. *Artif. Cells Nanomed. Biotechnol.* 1–12. doi: 10.1080/21691401.2017.1391822

Shanks, R. M., Lahr, R. M., Stella, N. A., Arena, K. E., Brothers, K. M., Kwak, D. H., et al. (2013). A *Serratia marcescens* PigP homolog controls prodigiosin biosynthesis, swarming motility and hemolysis and is regulated by cAMP-CRP and HexS. *PLoS ONE* 8:e57634. doi: 10.1371/journal.pone.0057634

Shimuta, K., Ohnishi, M., Iyoda, S., Gotoh, N., Koizumi, N., and Watanabe, H. (2009). The hemolytic and cytolytic activities of *Serratia marcescens* phospholipase A (PhlA) depend on lysophospholipid production by PhlA. *BMC Microbiol.* 9:261. doi: 10.1186/1471-2180-9-261

Sivaranjani, M., Gowrishankar, S., Kamaladevi, A., Pandian, S. K., Balamurugan, K., and Ravi, A. V. (2016). Morin inhibits biofilm production and reduces the virulence of *Listeria monocytogenes*-An *in vitro* and *in vivo* approach. *Int. J. Food Microbiol.* 237, 73–82. doi: 10.1016/j.ijfoodmicro.2016.08.021

Soo, P. C., Horng, Y. T., Chang, Y. L., Tsai, W. W., Jeng, W. Y., Lu, C. C., et al. (2014). ManA is regulated by RssAB signaling and promotes motility in *Serratia marcescens*. *Res. Microbiol.* 165, 21–29. doi: 10.1016/j.resmic.2013.10.005

Srinivasan, R., Devi, K. R., Kannappan, A., Pandian, S. K., and Ravi, A. V. (2016). *Piper betle* and its bioactive metabolite phytol mitigates quorum sensing mediated virulence factors and biofilm of nosocomial pathogen *Serratia marcescens in vitro*. *J. Ethnopharmacol.* 193, 592–603. doi: 10.1016/j.jep.2016.10.017

Srinivasan, R., Durgadevi, R., Kannappan, A., and Ravi, A. V. (2017b). Inhibition of quorum sensing-dependent biofilm and virulence genes expression in environmental pathogen *Serratia marcescens* by petroselinic acid. *Antonie van Leeuwenhoek.* doi: 10.1007/s10482-017-0971-y. [Epub ahead of print].

Srinivasan, R., Santhakumari, S., and Ravi, A. V. (2017a). *In vitro* antibiofilm efficacy of *Piper betle* against quorum sensing mediated biofilm formation of luminescent *Vibrio harveyi*. *Microb. Pathog.* 110, 232–239. doi: 10.1016/j.micpath.2017.07.001

Su, L. H., Ou, J. T., Leu, H. S., Chiang, P. C., Chiu, Y. P., Chia, J. H., et al. (2003). Extended epidemic of nosocomial urinary tract infections caused by *Serratia marcescens*. *J. Clin. Microbiol.* 41, 4726–4732. doi: 10.1128/JCM.41.10.4726-4732.2003

Vadekeetil, A., Saini, H., Chhibber, S., and Harjai, K. (2016). Exploiting the antivirulence efficacy of an ajoene-ciprofloxacin combination against Pseudomonas *aeruginosa* biofilm associated murine acute pyelonephritis. *Biofouling* 32, 371–382. doi: 10.1080/08927014.2015.1137289

Van Der Vliet, A., Eiserich, J. P., Halliwell, B., and Cross, C. E. (1997). Formation of reactive nitrogen species during peroxidase-catalyzed oxidation of nitrite a potential additional mechanism of nitric oxide-dependent toxicity. *J. Biol. Chem.* 272, 7617–7625. doi: 10.1074/jbc.272.12.7617

Youn, Y. K., LaLonde, C., and Demling, R. (1992). The role of mediators in the response to thermal injury. *World J. Surg.* 16, 30–36. doi: 10.1007/BF02067111

Conflict of Interest Statement: The authors declare that the research was conducted in the absence of any commercial or financial relationships that could be construed as a potential conflict of interest.

frontiers in Cellular and Infection Microbiology

ORIGINAL RESEARCH
published: 20 March 2018
doi: 10.3389/fcimb.2018.00088

Regulation of Nicotine Tolerance by Quorum Sensing and High Efficiency of Quorum Quenching Under Nicotine Stress in *Pseudomonas aeruginosa* PAO1

Huiming Tang[1], *Yunyun Zhang*[1,2], *Yifan Ma*[1], *Mengmeng Tang*[1], *Dongsheng Shen*[1,2] *and Meizhen Wang*[1,2]*

[1] School of Environmental Science and Engineering, Zhejiang Gongshang University, Hangzhou, China, [2] Zhejiang Provincial Key Laboratory of Solid Waste Treatment and Recycling, Hangzhou, China

Quorum sensing (QS) regulates the behavior of bacterial populations and promotes their adaptation and survival under stress. As QS is responsible for the virulence of vast majority of bacteria, quorum quenching (QQ), the interruption of QS, has become an attractive therapeutic strategy. However, the role of QS in stress tolerance and the efficiency of QQ under stress in bacteria are seldom explored. In this study, we demonstrated that QS-regulated catalase (CAT) expression and biofilm formation help *Pseudomonas aeruginosa* PAO1 resist nicotine stress. CAT activity and biofilm formation in wild type (WT) and Δ*rhlR* strains are significantly higher than those in the Δ*lasR* strain. Supplementation of Δ*lasI* strain with 3OC12-HSL showed similar CAT activity and biofilm formation as those of the WT strain. LasIR circuit rather than RhlIR circuit is vital to nicotine tolerance. Acylase I significantly decreased the production of virulence factors, namely elastase, pyocyanin, and pyoverdine under nicotine stress compared to the levels observed in the absence of nicotine stress. Thus, QQ is more efficient under stress. To our knowledge, this is the first study to report that QS contributes to nicotine tolerance in *P. aeruginosa*. This work facilitates a better application of QQ for the treatment of bacterial infections, especially under stress.

Keywords: nicotine tolerance, quorum sensing, antioxidant-producing ability, biofilm formation, quorum quenching, virulence

OPEN ACCESS

Edited by:
Rodolfo García-Contreras, Universidad Nacional Autónoma de México, Mexico

Reviewed by:
Fohad Mabood Husain, King Saud University, Saudi Arabia
Miguel Cocotl-Yañez, Universidad Nacional Autónoma de México, Mexico

***Correspondence:**
Meizhen Wang
wmz@zjgsu.edu.cn

Received: *07 January 2018*
Accepted: *06 March 2018*
Published: *20 March 2018*

Citation:
Tang H, Zhang Y, Ma Y, Tang M, Shen D and Wang M (2018) Regulation of Nicotine Tolerance by Quorum Sensing and High Efficiency of Quorum Quenching Under Nicotine Stress in Pseudomonas aeruginosa PAO1. Front. Cell. Infect. Microbiol. 8:88. doi: 10.3389/fcimb.2018.00088

INTRODUCTION

Cell density-dependent cell-to-cell communication, termed as quorum sensing (QS), regulates the behavior of bacterial populations (Waters and Bassler, 2005). Bacteria secrete and share QS signaling molecules that bind to cognate receptors, and upon reaching critical concentration induce cell density-dependent adaptive responses within the population (Albuquerque et al., 2014). QS is responsible for a number of collective behavioral properties, including virulence factor secretion, biofilm formation, and horizontal gene transfer (Antonova and Hammer, 2011; Joo and Otto, 2012; Yang et al., 2017). Compared to individuality, sociality, regulated by QS, significantly increases the bacterial fitness in various environment (Darch et al., 2012). Despite increasing recognition on

bacterial QS, the roles that they play in the response of environmental stress are far from fully understood (García-contreras et al., 2015).

Quorum sensing (QS) regulates the secretion of virulence factors from a broad spectrum of bacterial pathogens, including *Pseudomonas aeruginosa* (De Kievit and Iglewski, 2000). QS also participates in the development of biofilms, which are responsible for resistance to antibiotics, in many infections (Hazan et al., 2016). Due to the role of QS in pathogenicity and antibiotic resistance, the different factors involved in these pathways are considered to be attractive targets for novel antimicrobial agents (Starkey et al., 2014; Wang et al., 2016; Whiteley et al., 2017). Interruption of QS, which is known as quorum quenching (QQ), has been explored to control bacterial pathogenicity (Chan et al., 2015). As QS is an active process in response to environmental changes, QQ will have to be applicable under various conditions. Therefore, analysis of the QS response under different environmental conditions is vital for developing an efficient strategy involving QQ to control pathogenicity of bacteria.

Pseudomonas aeruginosa, one of the most common pathogenic bacteria in the world, not only infects humans, but also plants (Valentini et al., 2017). Its pathogenicity is mainly regulated by QS (Girard and Bloemberg, 2008; Whiteley et al., 2017). *P. aeruginosa* has two acyl-homoserine lactones (AHLs) QS circuits, LasIR and RhlIR (Stover et al., 2000). In LasIR circuit, LasI catalyzes the synthesis of *N*-3-oxo-dodecanoyl homoserine lactone (3OC12-HSL), which binds to its cognate receptor LasR and subsequently induces the expression of elastase-encoding genes involved in the development of pathogenicity of the bacteria (Pearson et al., 1994). For RhlIR circuit, RhlI catalyzes the synthesis of butyryl-HSL (C4-HSL), which binds to RhlR and subsequently activates a series of virulence factors including pyocyanin (Mukherjee et al., 2017). The well-elucidated mechanism of QS in *P. aeruginosa* allows us to study the feasibility of applying QQ to reduce the pathogenicity of the bacteria.

Though *P. aeruginosa* causes infection in both, humans and plants, they are exposed to various conditions. *P. aeruginosa* is known to inhabit hypoxic mucus plugs in the lungs of cystic fibrosis (CF) patient. Nearly 30% of smokers were involved in the population of CF patient (Ortega-García et al., 2012). In addition, the growth of *P. aeruginosa* in stems and rots leads to systemic infection and ultimately to the development of severe soft-rot symptoms in tobacco (Pfeilmeier et al., 2016). Nicotine is one of the main alkaloid in tobacco. Recent evidence has demonstrated that *P. aeruginosa* could grow under nicotine stress in tobacco plants or human being, but few studies regarding the role of QS in nicotine tolerance in *P. aeruginosa* have been performed (Hutcherson et al., 2015), limiting the development and application of strategies involving QQ to control its pathogenicity under nicotine-stress conditions.

Thus, we employed *P. aeruginosa* PAO1 as the model bacteria and nicotine as the typical stress. First, the growth and antioxidant-producing and biofilm-formation ability of wild-type (WT) strains and their signal-blind mutants were compared to investigate the role of QS in nicotine tolerance. Second, competition assay under nicotine stress and complementation experiment using a signal-deficient mutant were performed to analyze the possible mechanism. Finally, the efficiency of a QS inhibitor was analyzed under the presence and absence of nicotine stress to evaluate the application of QQ under these conditions. To our knowledge, this is the first study to report that QS plays an important role in nicotine tolerance, and demonstrates that LasIR circuit, rather than the RhlIR circuit, is responsible for nicotine tolerance in *P. aeruginosa* PAO1. This information will help to improve our understanding of the role of bacterial QS under stress, and to develop and apply QQ-based strategies for combating bacterial infection in the future.

Abbreviations: CAT, Catalase; CV, Crystal violet; EPS, Extracellular polymeric substances; LB, Luria-Bertani; 3OC12-HSL, *N*-3-oxo-dodecanoyl homoserine lactone; OD, Optical density; QQ, Quorum quenching; QS, Quorum sensing; ROS, Reactive oxygen species; SOD, Superoxide dismutase; TNBSA, Trinitrobenzene sulfonic acid; WT, Wildtype.

MATERIALS AND METHODS

Bacterial Strains, Media, and Culture

The bacterial strains used in this study were *P. aeruginosa* PAO1 WT strain and its QS mutants Δ*lasR*, Δ*rhlR*, and Δ*lasI* (Wang et al., 2015).

Luria-Bertani (LB) medium with or without nicotine was used in this study. LB medium was composed of tryptone (10 g), yeast extract (5 g), NaCl (5 g) in 1 L distilled water. Filtered-sterile nicotine (0–2.0 g/L) was replenished according to requirement.

Inocula were obtained from overnight LB cultures. The initial optical density (OD) was 0.001 (600 nm), except where noted. The culture was incubated in a shaker, at 37°C with 250 rpm.

The Detection of Reactive Oxygen Species (ROS)

Wildtype strain, PAO1, was inoculated into LB with initial OD_{600} of 0.01. After the growth of the cells entered the logarithmic phase ($OD_{600} = 1$), 0, 1.6, and 2.0 g/L nicotine was added into the culture. To measure ROS, 2′,7′-dichlorofluorescin diacetate (DCFH-DA) was added at a final concentration of 10 mM. Within 1 h of incubation, DCFH-DA was hydrolyzed into dichlorofluorescin (DCFH) in the cells. Then DCFH was oxidized by ROS into dichlorofluorescein (DCF). DCF was measured using SpectraMax® i3 plate reader at 488 nm of excitation and 525 nm of emission (Molecular Devices, Sunnyvale, CA, USA) (Yu et al., 2014). H_2O_2 treatment was used as a positive control. We calculated the relative ROS level by dividing the value of the DCF level obtained for experimental samples by that for LB medium.

The Measurement of the Activity of Catalase (CAT) and Superoxide Dismutase (SOD)

After exposure to 0, 1.6, and 2.0 g/L of nicotine, cells in logarithmic phase were harvested to detect the activity of CAT

and SOD, respectively. Cells were washed thrice with 0.9% NaCl and ultrasonically lysed. Subsequently, crude enzymes were obtained by centrifugation at 4°C and 12,000 rpm for 10 min. The activity of CAT and SOD was detected using the ammonium molybdate method (A007) and hydroxylamine method (A001-1-1), respectively. The total protein content was determined using a modified Bradford assay (Kit A045). All assays were performed according to manufacturer's instructions. These kits were purchased from the Nanjing Jiancheng Bioengineering Institute (Jiangsu, China).

One unit of CAT activity was defined as the amount of lysate that catalyzes the decomposition of 1 μM of H_2O_2 per minute at 37°C. One unit of SOD activity was defined as the amount of lysate that inhibits the rate of xanthine/xanthine oxidase-dependent cytochrome-c reduction at 25°C by 50%. The activities of both enzymes were expressed as units per mg of cellular protein.

Biofilm Formation Analysis

After exposure to 0, 1.6, and 2.0 g/L of nicotine, the biofilm formation in 10-mL tubes was evaluated. Biofilm biomass was analyzed by crystal violet (CV) staining method described by Wang et al. (2012). After 24 h of incubation, the tubes were carefully washed twice with phosphate-buffered saline (PBS) to remove planktonic cells. After air drying for 5 min, biofilms were stained with 1 mL of 0.1% CV for 10 min, then the tubes were rinsed thoroughly thrice with distilled water to remove the unabsorbed CV. Finally, adhered CV was solubilized with 3 mL of alcohol acetone (4:1, v/v) and measured at 570 nm using a SpectraMax® i3 plate reader (Molecular Devices, Sunnyvale, CA, USA).

The polysaccharides, protein and DNA component of biofilm was analyzed according to Wang et al. (2012). In brief, the biofilm was washed thrice and resuspended in PBS. Subsequently, the suspension was heated to 80°C for 45 min, and the mixture was centrifuged at 13,000 rpm for 20 min to remove solid residues. The extracellular polysaccharides (EPS) and extracellular protein as the two main components of biofilm were determined using the phenol/sulfuric acid method (Dubois et al., 1956) and Coomassie brilliant blue assay (Bradford, 1976), respectively. The content of extracellular DNA as the other component of biofilm was quantified using a Nano-drop 2000 spectrophotometer after purification with a phenol/chloroform/isoamyl reagent.

The morphology of biofilm was observed by confocal laser scanning microscopy (CLSM, Leica, Germany). For ease of observation, crude glass slides were placed in flasks containing 0, 1.6, and 2.0 g/L of nicotine, and biofilms formed on these slides. The cell viability in biofilm was determined using a double live/dead staining kit containing nucleic acid stains SYTO 9 and propidium iodide (PI). After biofilm formation, the glass slides were gently rinsed by immersing them in PBS, removing all unadhered cells, and subsequently, stained for 15 min. Viable bacteria with intact cell membrane were stained with green, whereas dead bacteria with damaged membrane were stained with red. Stained samples were visualized with the following excitation/emission detectors and filter sets: for SYTO 9, 480/500 and for PI, 490/635 (Shi et al., 2016).

Coculture Assay

WT, Δ*lasR,* and Δ*rhlR* strains were grown to mid-logarithmic phase, respectively. WT *vs.* Δ*lasR*, and Δ*rhlR vs.* Δ*lasR* with the ratio of 1:1 (cell number) were separately cocultured in LB media with 0, 0.4, 0.8, 1.2, 1.6, and 2.0 g/L nicotine under 37°C for 24 h. The initial OD_{600} was 0.05. Then, skim milk agars were used to differentiate the Δ*lasR* strains from WT or Δ*rhlR* strains, where a clear zone appeared around WT and Δ*rhlR* colonies but not around Δ*lasR* colonies (Wang et al., 2015). Skim milk agar was prepared as follows (/L): 1.25 g NaCl, 1.25 g yeast extract, 2.5 g tryptone, 80 g skim milk powder, and 15 g agar. For each value reported, at least 300 colonies were screened.

QQ Assay

Acylase I (Kit A8376-1G, Sigma, Germany) was used for QQ (Yeon et al., 2008) Overnight culture of the WT strain was inoculated into LB with 0, 1.6, and 2.0 g/L of nicotine. After 12 h of incubation, 0.25 mg/L acylase I was replenished to interrupt both, 3OC12-HSL and C4-HSL-mediated QS circuits. After another 12 h of incubation, the production of QS-regulated products including elastase, pyocyanin, and pyoverdine was compared among different culture conditions.

Elastase was detected by Pierce Fluorescent Protease Assay kit (Thermo). In brief, the culture was centrifuged at 12,000 rpm for 15 min. Subsequently, 100 μL of the supernatant was mixed with 100 μL of succinylated-casein solution (1:500 mixture of 2 g/L lyophilized succinylated casein and trinitrobenzene sulfonic acid, pH = 8.5) and incubated for 45 min in the dark at room temperature. The fluorescence was detected at 450 nm using a plate reader (SpectraMax® i3, Molecular Devices, Sunnyvale, CA, USA).

Pyocyanin was measured by chloroform and hydrochloric acid extraction (Pearson et al., 1994). A total of 1.5 mL of chloroform was used to extract 2.5 mL of the supernatant. The pyocyanin was re-extracted from the chloroform using 1 mL of 0.2 M hydrochloric acid. Finally, the absorbance of the supernatant was measured at 520 nm. The concentration of pyocyanin was equal to the absorbance multiplied by 12.8 mg/L.

Pyoverdine was detected using the method described by Wurst et al. (2014). In brief, the cultures were centrifuged at 12,000 rpm for 15 min. The absorbance of the supernatant was measured at 405 nm.

The level of elastase, pyocyanin, and pyoverdine were expressed as units per OD_{600} unit in order to avoid the interference of cell density. All experiments were in triplicate.

Statistical Analysis

GraphPad Prism 6.0 software was used for statistical analyses. Two-way ANOVA and *t*-test were performed. Differences with a value of $p < 0.05$ were considered to be statistically significant.

RESULTS

QS Plays an Important Role in Nicotine Tolerance

QS is involved in the regulation of the behavior of a bacterial population, whereby the cells secrete diffusible substances that

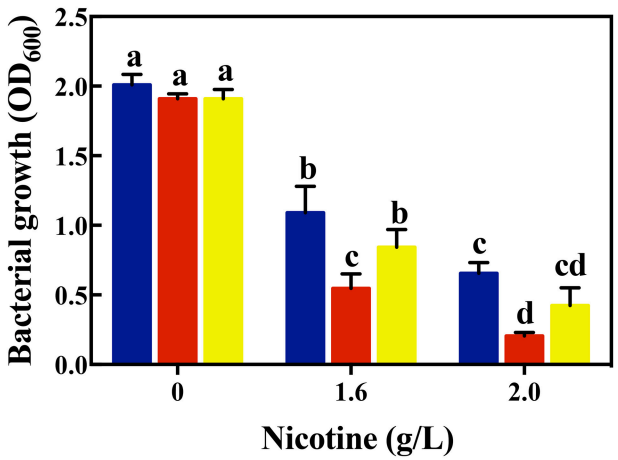

FIGURE 1 | Comparison of bacterial growth among different strains (WT, blue bars; Δ*lasR*, red bars; Δ*rhlR*, yellows bars) under exposure to different concentrations of nicotine. Different letters indicate significant difference at $p < 0.05$ and the same letter indicates no significant difference.

generate phenotypic responses in the living group. Compared to individuality, sociality confers a 100–1,000-fold increase in resistance to stress (Hazan et al., 2016). Thus, our hypothesis is that QS possibly plays an important role in nicotine tolerance. To confirm this hypothesis, a simple experiment comparing the growth of the WT strain with complete QS circuits and the signal-blind mutants under nicotine stress, was performed. Signal-blind mutants cannot respond to their cognate signals, and therefore, the expression of their corresponding regulons is inhibited.

As shown in **Figure 1**, there was no difference of bacterial growth between the WT and signal-blind mutant Δ*lasR and* Δ*rhlR* strains in the absence of nicotine. Under a 1.6 g/L-nicotine treatment, the growth of the WT, Δ*lasR, and* Δ*rhlR* strains was inhibited. However, the growth of the Δ*lasR* strain was significantly lower than that of the WT and Δ*rhlR* strains. Similar to the result of the 1.6 g/L-nicotine treatment, the growth of all three strains was inhibited under a 2.0 g/L-nicotine treatment. The lowest growth was observed in Δ*lasR* culture. Though other mechanisms possibly exist, the results indicated that QS played an important role in nicotine tolerance by *P. aeruginosa* PAO1.

Antioxidant Ability Regulated by QS Benefit for Nicotine Tolerance

Nicotine is a carcinogenic, teratogenic, and mutagenic substance, which can induce the production of a large number of free radicals, resulting in oxidative damage to cells (Haussmann and Fariss, 2016). The comparison of bacterial growth indicated that QS played an important role in nicotine tolerance. According to García-contreras et al. (2015), QS is able to exert a robust anti-oxidative response. Thus, one possibility could be that the role of QS in anti-oxidative response was beneficial for nicotine tolerance.

In order to validate this assumption, we first evaluated the ROS generation under nicotine exposure. As shown in

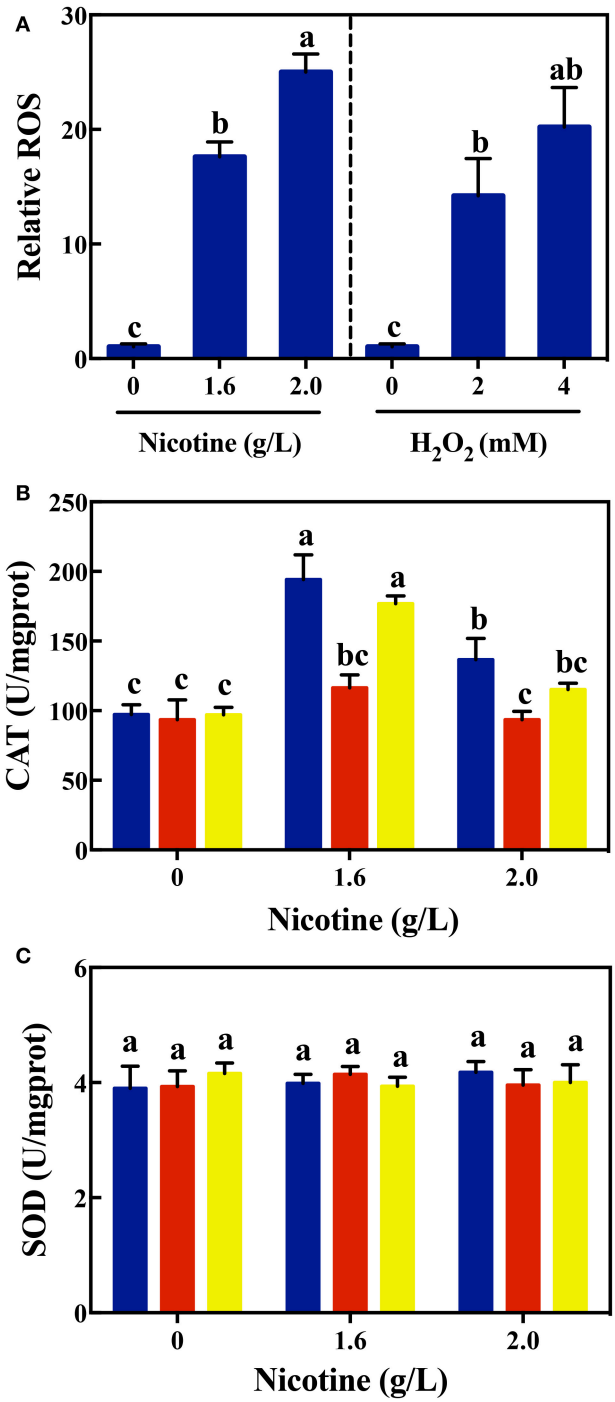

FIGURE 2 | Relative ROS levels **(A)** in WT on exposure to different concentrations of nicotine (left) and H_2O_2 (right); CAT activity **(B)** and SOD activity **(C)** among different strains (WT, blue bars; Δ*lasR*, red bars; Δ*rhlR*, yellows bars) under exposure to different concentrations of nicotine. Different letters indicate significant difference at $p < 0.05$ and the same letter indicates no significant difference.

Figure 2A, the level of intracellular ROS in WT cells increased significantly with the increase in nicotine. Nicotine-treated WT cells exhibited a higher level of ROS compared to the untreated

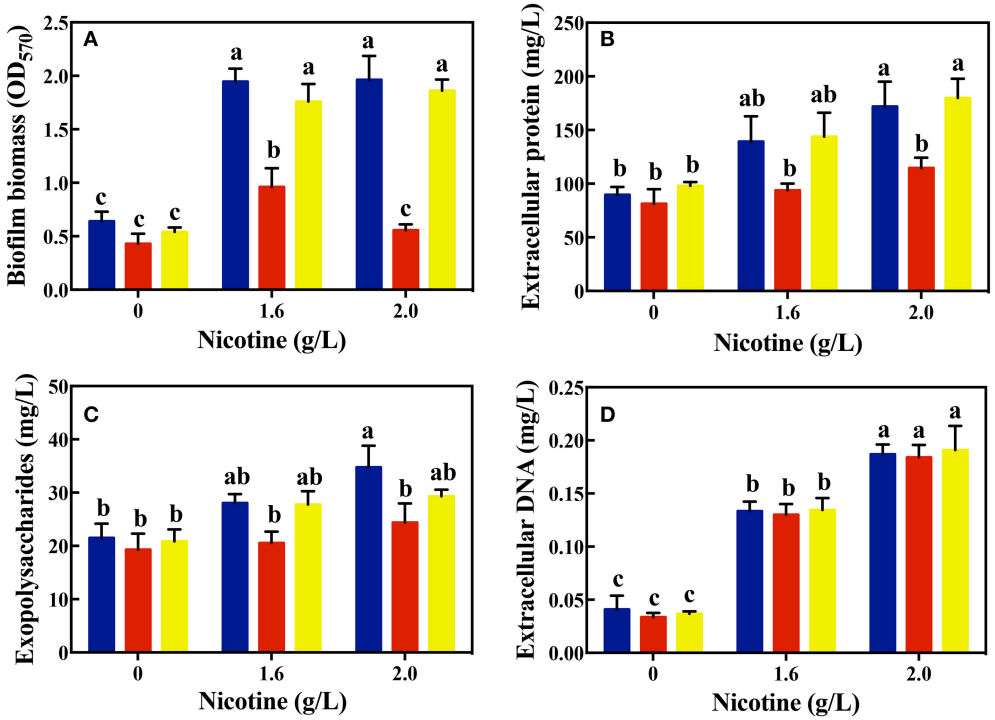

FIGURE 3 | Comparison of biofilm biomass **(A)** and its components: extracellular protein **(B)**, polysaccharides **(C)**, and extracellular DNA **(D)** among different strains (WT, blue bars; Δ*lasR*, red bars; Δ*rhlR*, yellows bars) on exposure to different concentrations of nicotine. Different letters indicate significant difference at $p < 0.05$ and the same letter indicates no significant difference.

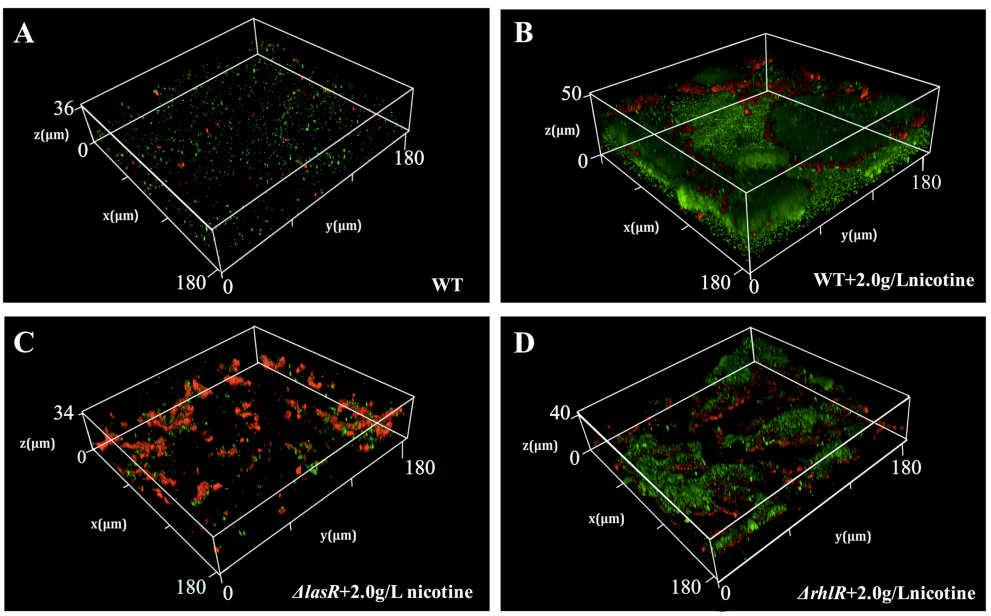

FIGURE 4 | Comparison of biofilm structure and proportion of live/dead cells (green, live cells; red, dead cells) in biofilm among WT **(A)**, WT + 2.0 g/L nicotine **(B)**, Δ*lasR* + 2.0 g/L nicotine **(C)**, and Δ*rhlR* + 2.0 g/L nicotine **(D)**.

WT cells. Especially a 2.0 g/L-nicotine treatment led to the increase in the level of ROS in nicotine-treated cells, and this level was 24.4 times higher than that in untreated cells. Using H_2O_2 as positive control, it was observed that the level of ROS produced by 2.0 g/L-nicotine treatment, is higher than that produced by 2 mM-H_2O_2 treatment. Therefore, it can be inferred that the

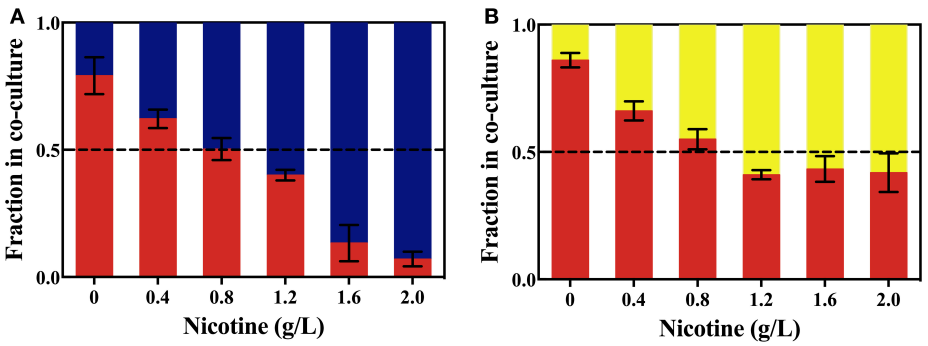

FIGURE 5 | The competition between the WT (blue bars) and Δ*lasR* (red bars) strains **(A)**, or between the Δ*rhlR* (yellows bars) and Δ*lasR* strains **(B)** on exposure to different concentrations of nicotine.

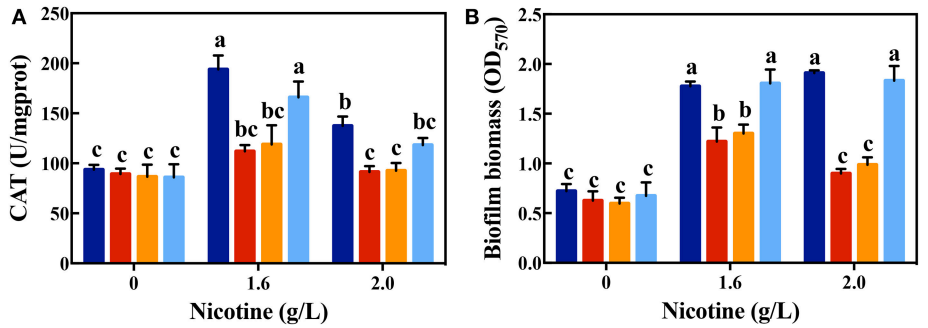

FIGURE 6 | CAT activity **(A)** and biofilm formation **(B)** after complementing Δ*lasI* strain with 3OC12-HSL on exposure to different concentrations of nicotine (WT: dark blue bars; Δ*lasR*: red bars; Δ*lasI*: orange bars; Δ*lasI* + 3OC12-HSL: light blue bars). Different letters indicate significant difference at $p < 0.05$ and the same letter indicates no significant difference.

higher the concentration of nicotine, the stronger the oxidative stress induced.

To confirm that QS could contribute to nicotine tolerance by activating antioxidant defense system, the activity of antioxidant enzymes were measured among WT, Δ*lasR,* and Δ*rhlR* strains. As shown in **Figure 2B**, there was no difference in the activity of CAT among the WT and mutant strains without nicotine stress. The activity of CAT significantly increased on exposure to 1.6 g/L of nicotine in the WT and Δ*rhlR* strains compared to that in the Δ*lasR* strain. Though the CAT activity decreased under a 2.0 g/L-nicotine treatment due to toxicity, the WT strain showed a significantly higher activity of CAT than that observed in Δ*lasR,* and this activity had no significant difference with that observed in Δ*rhlR* strain.

Additionally, we measured the SOD activity among these three strains. However, no significant increase was observed for this parameter (**Figure 2C**). Taking the above-mentioned data into account, bacterial QS involving the LasIR and RhlIR circuits, regulate the anti-oxidative response to nicotine stress in WT strain. Further studies are required to explain why QS promotes CAT activity, and not SOD activity.

QS-Regulated Biofilm Formation Favored of Nicotine Tolerance

Biofilm formation, mainly regulated by QS, could be another reason for stress tolerance (Hammer and Bassler, 2003; Daniels et al., 2004; Shrout and Nerenberg, 2012). Compared to planktonic cells, biofilm formation increases stress tolerance up by 10–1,000 folds (Hazan et al., 2016). Another parallel assumption is that QS-regulated biofilm formation is beneficial for nicotine tolerance. Therefore, to clearly understand the effect from QS-regulated biofilm formation on nicotine tolerance, we compared the biofilm formation of WT and Δ*lasR* and Δ*rhlR* strains on exposure to nicotine.

As shown in **Figure 3A**, there was no significant difference in the biofilm formation of WT and Δ*lasR* and Δ*rhlR* strains in absence of nicotine. On treating with 1.6 and 2.0 g/L of nicotine, the biofilm biomass of WT and Δ*rhlR* increased significantly. There was no difference of biofilm biomass between WT and Δ*rhlR*. However, the biofilm biomass of Δ*lasR* was significantly lower than that of the other two strains.

In addition, the amount of certain biofilm components was analyzed. As shown in **Figures 3B–D**, the level of EPS and extracellular proteins in the biofilms of the WT and Δ*rhlR* strains was significantly higher than that of the Δ*lasR* strains

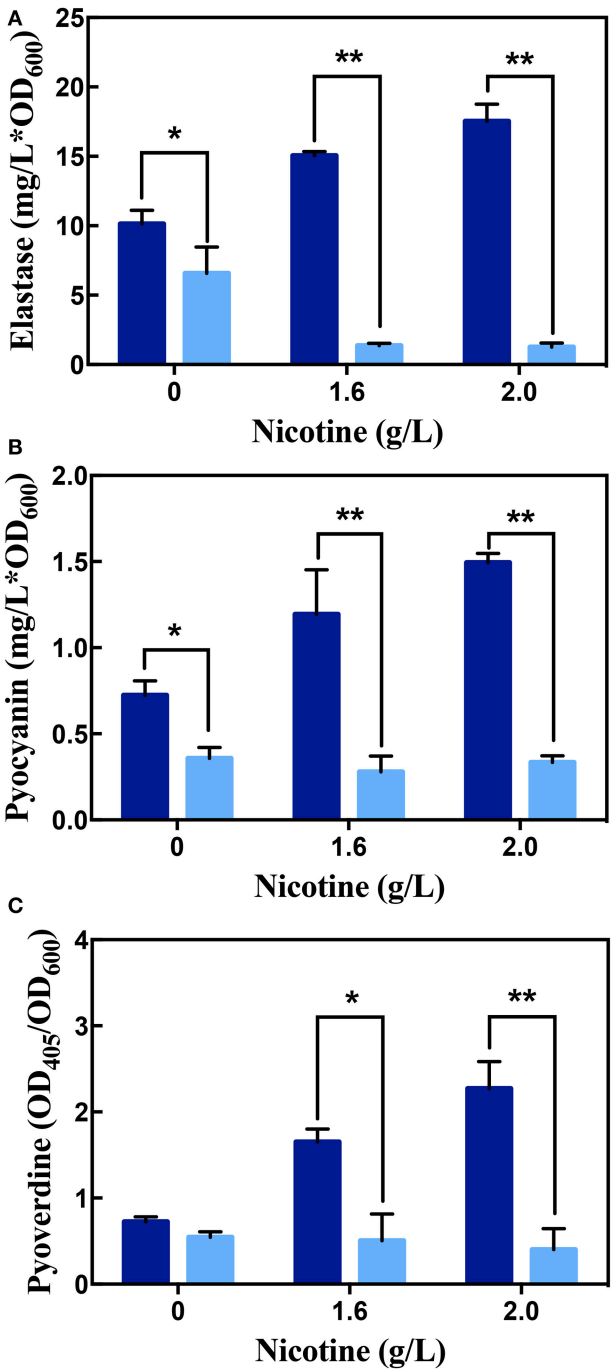

FIGURE 7 | The production of elastase **(A)**, pyocyanin **(B)**, and pyoverdine **(C)** in WT on exposure to different concentrations of nicotine, with (light blue bars) or without (dark blue bars) acylase I. ** and * indicate significant difference at $p < 0.01$ and $p < 0.05$, respectively.

under a 1.6 g/L-nicotine treatment. After exposure to 2.0 g/L of nicotine, no significant difference in the level of EPS between the biofilms of Δ*lasR* and Δ*rhlR* was observed. The level of EPS and extracellular protein in the biofilm of the WT strain was significantly higher than that in the biofilm of Δ*lasR* under a 2.0 g/L-nicotine treatment. The extracellular DNA content was almost equivalent among three strains, indicated by an extremely small amount of extracellular DNA in the biofilm.

Moreover, we used the CLSM to observe the structure of biofilm and employed a double live/dead staining to determine cell viability in biofilm. As shown in **Figure 4**, the biofilm thickness of WT and Δ*rhlR* strains increased under nicotine stress. However, the biofilm formation of Δ*lasR* was significantly inhibited under nicotine stress. Compared to WT and Δ*rhlR* biofilm, the number of dead cells dramatically increased in the Δ*lasR* biofilm. All above data demonstrated that QS-regulated biofilm formation was also involved in enhancement of nicotine tolerance.

LasIR Being Responsible for Nicotine Tolerance

As seen in **Figures 2B**, **3A**, the CAT activity and biofilm biomass in the Δ*lasR* strain was significant lower than the WT and Δ*rhlR* strain. Meanwhile there were no significant differences for the same parameters between the WT and Δ*rhlR* strains. It suggested that the LasIR circuit played more important role in nicotine tolerance than the RhlIR circuit. Bacteria lacking a functional LasIR circuit, are sensitive to nicotine. To confirm these, competition experiments between the WT and Δ*lasR* strains or between the Δ*rhlR* and Δ*lasR* strains were conducted.

As shown in **Figure 5**, without nicotine stress, Δ*lasR* growth was higher than that of the WT or Δ*rhlR* strains. After 24 h, 79.1 and 86.1% of the total population in the WT competition system and the Δ*rhlR* competition system, respectively, were Δ*lasR* cells. With the increase in nicotine concentration, the proportion of Δ*lasR* population significantly decreased. It was reduced to 16.7% in WT competition system under 2.0 g/L-nicotine stress. The decrease of Δ*lasR* fitness advantage with the increase of nicotine is consistent with the above hypothesis.

For the competition experiment, other factors except the nicotine tolerance could affect the advantageous fitness. Thus, Δ*lasI* supplementation with 3OC12-HSL was implemented in further experiments. Δ*lasI* is a signal-deficient mutant, without the ability to synthesize 3OC12-HSL, but with the functional signal receptors, LasR. According to the mechanism of QS, exogenous additional of 3OC12-HSL also could bind to LasR and trigger the expression of the corresponding regulon (Wang et al., 2015). As shown in **Figure 6**, the CAT activity and biofilm formation in the Δ*lasI* strain was similar to those in the Δ*lasR* strain. However, addition of 3OC12-HSL significantly increased the CAT activity and biofilm formation in the Δ*lasI* strain, and they were nearly identical with those in the WT strain. Both competition systems in coculture and signal complementary assays for Δ*lasI* confirm that LasIR circuit is important for nicotine tolerance in *P. aeruginosa*.

QQ Acting Even Better Under Nicotine Stress

Quorum quenching (QQ) was widely used for controlling pathogenicity in *P. aeruginosa*, and reducing the level of virulence factors such as elastase, pyocyanin, and pyoverdine (Lee and

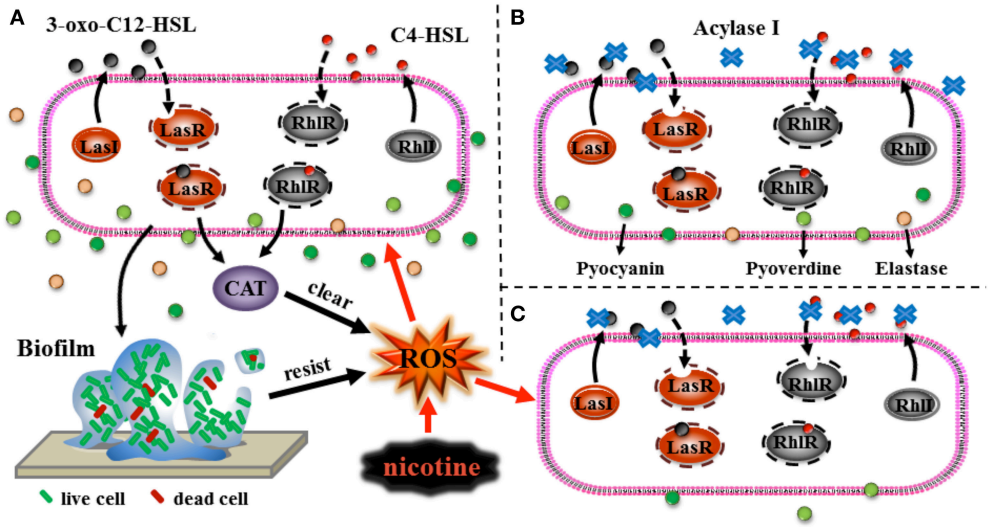

FIGURE 8 | Schematic representations of the role of QS in nicotine tolerance **(A)**, QQ leading to reduction of virulence **(B)**, and the high efficiency of QQ under nicotine exposure leading to reduction of virulence **(C)**. Black arrows represent the direction of signals transduction or direction of transport of the virulence factors, black dotted arrows represent the process of the binding of ligands to the respective receptors, black thick arrows represent clearing of ROS or resistance to stress, and red arrows represent induction of ROS production or induction of stress to cells.

Zhang, 2015). As the above-mentioned results indicate, QS played important role in nicotine tolerance. A rational deduction was that QQ could act efficiently under nicotine stress. To prove it, the production of elastase, pyocyanin, and pyoverdine was compared with or without QQ treatments.

As seen in **Figure 7**, along with the increasing of nicotine, the content of elastase, pyocyanin, and pyoverdine enhanced. It suggested that nicotine induces the QS pathway in *P. aeruginosa*. Addition of the acylase I, interrupted these pathways and decreased the production of elastase and pyocyanin. Without nicotine treatments, there was a 35.14 and 43.13% reduction in the level of elastase and pyocyanin after acylase I treatment, respectively, compared to non-addition of the acylase I. There were no significant differences between the level of pyoverdine before and after acylase I treatments.

Under nicotine stress, acylase I significantly decreased the secretion of all virulence factors. After acylase I treatment, the proportion of elastase, pyocyanin, and pyoverdine reduced to 18.23, 23.31, and 30.53% under 1.6 g/L of nicotine, respectively, compared to the levels before the acylase I treatment. After exposure to 2.0 g/L nicotine, the proportion of elastase, pyocyanin, and pyoverdine reduced to 7.13, 22.39, and 17.69%, respectively, compared to the levels before the acylase I treatment. Among all virulence factors, the production of elastase was inhibited the most. Compared to untreated cells, there was a greater decrease for all tested virulence factors under nicotine-treated cells.

DISCUSSION

The toxicity of nicotine on bacteria, through high permeability in cell membrane, oxidative stress, and macromolecular (protein and DNA) damage, has been well-studied (Huang et al., 2014). In this study, we compared the nicotine tolerance between WT and QS mutant strains, and found that the bacterial growth was significantly inhibited by nicotine if the QS pathway was nonfunctional. In addition, significantly higher CAT activity, biofilm biomass, and number of live cells in biofilm were found for the WT strain than for Δ*lasR*. These results confirmed that QS played an important role in nicotine tolerance. Besides nicotine stress, Walawalkar et al. (2016) showed that QS of *Salmonella typhi* aided in oxidative stress management. According to Lin et al. (2016), DqsIR QS mediated gene regulation of the extremophilic bacterium *Deinococcus radiodurans* in response to oxidative stress. This indicates that QS could protect bacteria from a wide range of stress.

Under nicotine stress, different strains had variant CAT activity. Highest CAT activity was observed in the WT strain, while the lowest in the Δ*lasR* strain. QS controls expression of CAT genes and mediates susceptibility to H_2O_2 (Hassett et al., 1999). Compared to individuality, cells in biofilm could help each other to protect themselves from different kinds of stress (Oliveira et al., 2015). Several studies have shown that biofilm development was regulated by QS (Tseng et al., 2016). Moreover, weakening of biofilm structure in *P. aeruginosa* has been linked to the disruption of LasIR circuit (Sunder et al., 2017). From **Figure 3A**, it can be observed that biofilm biomass increased in nicotine stress when LasIR circuit is functional. Both, antioxidant-production ability and biofilm formation, which are regulated by QS, enhance the nicotine tolerance.

Taking the CAT activity and biofilm biomass into account, LasIR circuit promotes nicotine tolerance rather than the RhlIR circuit. We also conducted competition experiments between

the Δ*rhlR* and Δ*lasR* strains. In LB media without nicotine, the Δ*lasR* strain had a significant fitness than the Δ*rhlR* strain. However, with the increase in nicotine concentration in LB media, the growth of the Δ*rhlR* strain increased significantly compared to that of the Δ*lasR* strain (**Figure 5**). From **Figure 6**, supplementation of the Δ*lasI* strain with 3OC12-HSL led to the culture showing similar CAT activity and biofilm formation to those of the WT strain, under nicotine stress. Both competition in coculture and signal complementary assays for Δ*lasI* confirmed that LasIR circuit was more important than the RhlIR circuit in the response to nicotine stress.

The members of the QS pathway are promising targets for treatment of pathogenic infection (Köhler et al., 2010). Several QQ reagents have been developed (O'Loughlin et al., 2013). As shown in **Figure 7**, the inhibition efficiencies of acylase I are different for various of virulence factors. According to the genetic network of the PAO1 strain, *lasR*, *rhlR,* and *pqsE* have been reported to be involved in the production of pyocyanin (O'Loughlin et al., 2013; Rampioni et al., 2016), while *ampR*, *ppyR, mexT,* and *lasR* are involved in the production of elastase (Van Delden et al., 1998; Maseda et al., 2004; Kong et al., 2005; Attila et al., 2008). There are much more genes contributing to elastase production than those contributing to pyocyanin production. Thus, the inhibition efficiency for pyocyanin was higher, while less elastase production was inhibited. The production of pyoverdine was regulated by PQS, a type of a QS pathway that is not mediated by AHLs, in *P. aeruginosa* (Lee and Zhang, 2015). Acylase I can only interrupt AHLs-mediated QS (Zhang et al., 2015). Thus, acylase I did not inhibit the production of pyoverdine under no nicotine treatment conditions. Different QS circuits regulate the secretion of different virulence factors (Chugani et al., 2001). One virulence factor is regulated by completely or partially regulated by QS (O'Loughlin et al., 2013; Husain et al., 2017). QQ was successful in reducing the production of certain, but not all, kinds of tested virulence factors in *P. aeruginosa*.

Various conditions, such as pH and temperature, possibly affect the application of QQ in pathogenicity control. pH and temperature could affect the existence of QS signal in the environment (Yates et al., 2002). Few studies have focused on the efficiency of QQ under stress. In this study, the QQ showed a higher efficiency in decreasing the production of virulence factors, including elastase, pyocyanin, and pyoverdine under nicotine stress compared to no stress. Nicotine is toxic to most kinds of bacteria. QS contributes to nicotine tolerance (**Figure 8A**). Interruption of QS led to the decrease in both, nicotine tolerance and virulence (**Figures 8B,C**). After loss of nicotine tolerance, the bacterial population possibly reduces their virulence in order to survive as a trade-off. Though we can not apply of QQ under nicotine stress due to its addiction, it gives us an explanation that the combination of QQ with antibiotics is higher efficient than only one treatment (Wang et al., 2018). Therefore, this study not only improves our understanding regarding the role of QS in environmental stress tolerance, but also provides a foundation for the development of QQ-based strategies to control or reduce the pathogenicity of bacteria (**Figure 8**).

AUTHOR CONTRIBUTIONS

MW, HT, and DS conceived and designed the experiments. HT, YZ, YM, and MT performed the experiments. HT and MW analyzed the data. MW and DS contributed reagents, materials, and analysis tools. MW and HT wrote the paper.

ACKNOWLEDGMENTS

This study was supported by the National Science Foundation of China (Grant no. 31570490, 51478432, 41403080) and National Undergraduate Training Program for Innovation and Entrepreneurship (Grant no. LY201710353032). We also thank Professor E. Peter Greenberg and Professor Ajai A. Dandekar for providing us with the strains and for their helpful assistance.

REFERENCES

Albuquerque, P., Nicola, A. M., Nieves, E., Paes, H. C., Williamson, P. R., Silva-Pereira, I., et al. (2014). Quorum sensing-mediated, cell density-dependent regulation of growth and virulence in *Cryptococcus neoformans*. *MBio.* 5, e00986–e00913. doi: 10.1128/mBio.00986-13

Antonova, E. S., and Hammer, B. K. (2011). Quorum-sensing autoinducer molecules produced by members of a multispecies biofilm promote horizontal gene transfer to *Vibrio cholerae*. *FEMS Microbiol. Lett.* 322, 68–76. doi: 10.1111/j.1574-6968.2011.02328.x

Attila, C., Ueda, A., and Wood, T. K. (2008). PA2663 (PpyR) increases biofilm formation in *Pseudomonas aeruginosa* PAO1 through the *psl* operon and stimulates virulence and quorum-sensing phenotypes. *Appl. Microbiol. Biotechnol.* 78, 293–307. doi: 10.1007/s00253-007-1308-y

Bradford, M. M. (1976). A rapid and sensitive method for the quantitation of microgram quantities of protein utilizing the principle of protein-dye binding. *Anal. Biochem.* 72, 248–254. doi: 10.1016/0003-2697(76)90527-3

Chan, K. G., Liu, Y. C., and Chang, C. Y. (2015). Inhibiting *N*-acyl-homoserine lactone synthesis and quenching *Pseudomonas quinolone* quorum sensing to attenuate virulence. *Front. Microbiol.* 6:1173. doi: 10.3389/fmicb.2015.01173

Chugani, S. A., Whiteley, M., Lee, K. M., D'Argenio, D., Manoil, C., and Greenberg, E. P. (2001). QscR, a modulator of quorum-sensing signal synthesis and virulence in *Pseudomonas aeruginosa*. *Proc. Natl. Acad. Sci. U.S.A.* 98, 2752–2757. doi: 10.1073/pnas.051624298

Daniels, R., Vanderleyden, J., and Michiels, J. (2004). Quorum sensing and swarming migration in bacteria. *FEMS Microbiol. Rev.* 28, 261–289. doi: 10.1016/j.femsre.2003.09.004

Darch, S. E., West, S. A., Winzer, K., and Diggle, S. P. (2012). Density-dependent fitness benefits in quorum-sensing bacterial populations. *Proc. Natl. Acad. Sci. U.S.A.* 109, 8259–8263. doi: 10.1073/pnas.1118131109

De Kievit, T. R., and Iglewski, B. H. (2000). Bacterial quorum sensing in pathogenic relationships. *Infect. Immun.* 68, 4839–4849. doi: 10.1128/IAI.68.9.4839-4849.2000

Dubois, A. B., Brody, A. W., Lewis, D. H., and Burgess, J. B. F. (1956). Oscillation mechanics of lung and chest in man. *J. Appl. Physiol.* 8, 587–594. doi: 10.1152/jappl.1956.8.6.587

García-contreras, R., Nuñezlópez, L., Jassochávez, R., Kwan, B. W., Belmont, J. A., Rangelvega, A., et al. (2015). Quorum sensing enhancement of the stress response promotes resistance to quorum quenching and prevents social cheating. *ISME J.* 9, 115–125. doi: 10.1038/ismej.2014.98

Girard, G., and Bloemberg, G. V. (2008). Central role of quorum sensing in regulating the production of pathogenicity factors in *Pseudomonas aeruginosa*. *Future Microbiol.* 3, 97–106. doi: 10.2217/17460913.3.1.97

Hammer, B. K., and Bassler, B. L. (2003). Quorum sensing controls biofilm formation in *Vibrio cholerae*. *Mol. Microbiol.* 50, 101–104. doi: 10.1046/j.1365-2958.2003.03688.x

Hassett, D. J., Ma, J. F., Elkins, J. G., McDermott, T. R., Ochsner, U. A., West, S. E., et al. (1999). Quorum sensing in *Pseudomonas aeruginosa* controls expression of catalase and superoxide dismutase genes and mediates biofilm susceptibility to hydrogen peroxide. *Mol. Microbiol.* 34, 1082–1093. doi: 10.1046/j.1365-2958.1999.01672.x

Haussmann, H. J., and Fariss, M. W. (2016). Comprehensive review of epidemiological and animal studies on the potential carcinogenic effects of nicotine perse. *Crit. Rev. Toxicol.* 46, 701–734. doi: 10.1080/10408444.2016.1182116

Hazan, R., Que, Y. A., Maura, D., Strobel, B., Majcherczyk, P. A., Hopper, L. R., et al. (2016). Auto poisoning of the respiratory chain by a quorum-sensing-regulated molecule favors biofilm formation and antibiotic tolerance. *Curr. Biol.* 26, 195–206. doi: 10.1016/j.cub.2015.11.056

Huang, R., Li, M., Ye, M., Yang, K., Xu, X., and Gregory, R. L. (2014). Effects of nicotine on *Streptococcus gordonii* growth, biofilm formation, and cell aggregation. *Appl. Environ. Microbiol.* 80, 7212–7218. doi: 10.1128/AEM.02395-14

Husain, F. M., Ahmad, I., Al-Thubiani, A. S., Abulreesh, H. H., Alhazza, I. M., and Aqil, F. (2017). Leaf extracts of mangiferaindica l. inhibit quorum sensing-regulated production of virulence factors and biofilm in test bacteria. *Front. Microbiol.* 8:727. doi: 10.3389/fmicb.2017.00727

Hutcherson, J. A., Scott, D. A., and Bagaitkar, J. (2015). Scratching the surface – tobacco-induced bacterial biofilms. *Tob. Induc. Dis.* 13:1. doi: 10.1186/s12971-014-0026-3

Joo, H. S., and Otto, M. (2012). Molecular basis of *in vivo* biofilm formation by bacterial pathogens. *Chem. Biol.* 19, 1503–1513. doi: 10.1016/j.chembiol.2012.10.022

Köhler, T., Perron, G. G., Buckling, A., and Van Delden, C. (2010). Quorum sensing inhibition selects for virulence and cooperation in *Pseudomonas aeruginosa*. *PLoS Pathog.* 6:e1000883. doi: 10.1371/journal.ppat.1000883

Kong, K. F., Jayawardena, S. R., Indulkar, S. D., Del, P. A., Koh, C. L., and Høiby, N. (2005). *Pseudomonas aeruginosa ampr* is a global transcriptional factor that regulates expression of *ampC* and *poxB* beta-lactamases, proteases, quorum sensing, and other virulence factors. *Antimicrob. Agents Chemother.* 49:4567. doi: 10.1128/AAC.49.11.4567-4575.2005

Lee, J., and Zhang, L. (2015). The hierarchy quorum sensing network in *Pseudomonas aeruginosa*. *Protein Cel* 6, 26–41. doi: 10.1007/s13238-014-0100-x

Lin, L., Dai, S., Tian, B., Li, T., Yu, J., Liu, C., et al. (2016). DqsIR quorum sensing-mediated gene regulation of the extremophilic bacterium *Deinococcus radiodurans*in response to oxidative stress. *Mol. Microbiol.* 100, 527–541. doi: 10.1111/mmi.13331

Maseda, H., Sawada, I., Saito, K., Uchiyama, H., Nakae, T., and Nomura, N. (2004). Enhancement of the mexab-oprm efflux pump expression by a quorum-sensing autoinducer and its cancellation by a regulator, mext, of the mexef-oprn efflux pump operon in *Pseudomonas aeruginosa*. *Antimicrob. Agents Chemother.* 48, 1320–1328. doi: 10.1128/AAC.48.4.1320-1328.2004

Mukherjee, S., Moustafa, D., Smith, C. D., Goldberg, J. B., and Bassler, B. L. (2017). The RhlR quorum-sensing receptor controls *Pseudomonas aeruginosa* pathogenesis and biofilm development independently of its canonical homoserine lactone autoinducer. *PLoS Pathog.* 13:e1006504. doi: 10.1371/journal.ppat.1006504

O'Loughlin, C. T., Miller, L. C., Siryaporn, A., Drescher, K., Semmelhack, M. F., and Bassler, B. L. (2013). A quorum-sensing inhibitor blocks *Pseudomonas aeruginosa* virulence and biofilm formation. *Proc. Natl. Acad. Sci. U.S.A.* 110, 17981–17986. doi: 10.1073/pnas.1316981110

Oliveira, N. M., Martinez-Garcia, E., Xavier, J., Durham, W. M., Kolter, R., Kim, W., et al. (2015). Biofilm formation as a response to ecological competition. *PLoS Biol.* 13:e1002191. doi: 10.1371/journal.pbio.1002191

Ortega-García, J. A., López-Fernández, M. T., Llano, R., Pastor-Vivero, M. D., Mondéjar-López, P., and Sánchez-Sauco, M. F. (2012). Smoking prevention and cessation programme in cystic fibrosis: integrating an environmental health approach. *J. Cyst. Fibros.* 11, 34–39. doi: 10.1016/j.jcf.2011.09.005

Pearson, J. P., Gray, K. M., Passador, L., Tucker, K. D., Eberhard, A., Iglewski, B. H., et al. (1994). Structure of the autoinducer required for expression of *Pseudomonas aeruginosa* virulence genes. *Proc. Natl. Acad. Sci. U.S.A.* 91, 197–201.

Pfeilmeier, S., Saur, I. M., Rathjen, J. P., Zipfel, C., Malone, J. G. (2016). High levels of cyclic-di-GMP in plant-associated *Pseudomonas* correlate with evasion of plant immunity. *Mol. Plant Pathol.* 17, 521–531. doi: 10.1111/mpp.12297

Rampioni, G., Falcone, M., Heeb, S., Frangipani, E., Fletcher, M. P., Dubern, J. F., et al. (2016). Unravelling the genome-wide contributions of specific 2-alkyl-4-quinolones and PqsE to quorum sensing in *Pseudomonas aeruginosa*. *PLoS Pathog.* 12:e1006029. doi: 10.1371/journal.ppat.1006029

Shi, S. F., Jia, J. F., Guo, X. K., Zhao, Y. P., Chen, D. S., Guo, Y. Y., et al. (2016). Reduced *Staphylococcus aureus* biofilm formation in the presence of chitosan-coated iron oxide nanoparticles. *Int. J. Nanomed.* 11, 6499–6506. doi: 10.2147/IJN.S41371

Shrout, J. D., and Nerenberg, R. (2012). Monitoring bacterial twitter: does quorum sensing determine the behavior of water and wastewater treatment biofilms? *Environ. Sci. Technol.* 46, 1995–2005. doi: 10.1021/es203933h

Starkey, M., Lepine, F., Maura, D., Bandyopadhaya, A., Lesic, B., He, J., et al. (2014). Identification of anti-virulence compounds that disrupt quorum-sensing regulated acute and persistent pathogenicity. *PLoS Pathog.* 10:e1004321. doi: 10.1371/journal.ppat.1004321

Stover, C. K., Pham, X. Q., Erwin, A. L., Mizoguchi, S. D., Warrener, P., Hickey, M. J., et al. (2000). Complete genome sequence of *Pseudomonas aeruginosa* PAO1, an opportunistic pathogen. *Nature* 406, 959–964. doi: 10.1038/35023079

Sunder, A. V., Utari, P. D., Ramasamy, S., van Merkerk, R., Quax, W., and Pundle, A. (2017). Penicillin V acylases from gram-negative bacteria degrade N-acylhomoserine lactones and attenuate virulence in *Pseudomonas aeruginosa*. *Appl. Microbiol. Biotechnol.* 101, 2383–2395. doi: 10.1007/s00253-016-8031-5

Tseng, B. S., Majerczyk, C. D., da Silva, D. P., Chandler, J. R., Greenberg, E. P., and Parsek, M. R. (2016). Quorum sensing influences *Burkholderia thailandensis* biofilm development and matrix production. *J. Bacteriol.* 198, 2643–2650. doi: 10.1128/JB.00047-16

Van Delden, C., Pesci, E. C., Pearson, J. P. and Iglewski, B. H. (1998). Starvation selection restores elastase and rhamnolipid production in a *Pseudomonas aeruginosa* quorum-sensing mutant. *Infect. Immun.* 66, 4499–4502.

Valentini, M., Gonzalez, D., Mavridou, D. A., and Filloux, A. (2017). Lifestyle transitions and adaptive pathogenesis of *Pseudomonas aeruginosa*. *Curr. Opin. Microbiol.* 41, 15–20. doi: 10.1016/j.mib.2017.11.006

Walawalkar, Y. D., Vaidya, Y., and Nayak, V. (2016). Response of *salmonella typhi* to bile generated oxidative stress: implication of quorum sensing and persister cell populations. *Pathog. Dis.* 74:ftw090. doi: 10.1093/femspd/ftw090

Wang, D., Shi, J., Xiong, Y., Hu, J., Lin, Z., Qiu, Y., et al. (2018). A QSAR-based mechanistic study on the combined toxicity of antibiotics and quorum sensing inhibitors against *Escherichia coli*. *J. Hazard. Mater.* 341, 438–447. doi: 10.1016/j.jhazmat.2017.07.059

Wang, M. Z., Schaefer, A. L., Dandekar, A. A., and Greenberg, E. P. (2015). Quorum sensing and policing of *Pseudomonas aeruginosa* social cheaters. *Proc. Natl. Acad. Sci. U.S.A.* 112, 2187–2191. doi: 10.1073/pnas.1500704112

Wang, M. Z., Zheng, X., He, H. Z., Shen, D. S., and Feng, H. J. (2012). Ecological roles and release patterns of acylatedhomoserine lactones in *Pseudomonas* sp. HF-1 and their implications in bacterial bioaugmentation. *Bioresource Technol.* 125, 119–126. doi: 10.1016/j.biortech.2012.08.116

Wang, T., Liu, Y., Wang, D., Lin, Z., An, Q., Yin, C., et al. (2016). The joint effects of sulfonamides and quorum sensing inhibitors on *Vibrio fischeri*: differences between the acute and chronic mixed toxicity mechanisms. *J. Hazard. Mater.* 310, 56–67. doi: 10.1016/j.jhazmat.2016.01.061

Waters, C. M., and Bassler, B. L. (2005). Quorum sensing: cell-to-cell communication in bacteria. *Annu. Rev. Cell Dev. Biol.* 21, 319–346. doi: 10.1146/annurev.cellbio.21.012704.131001

Whiteley, M., Diggle, S. P., and Greenberg, E. P. (2017). Progress in and promise of bacterial quorum sensing research. *Nature* 551, 313–320. doi: 10.1038/nature24624

Wurst, J. M., Drake, E. J., Theriault, J. R., Jewett, I. T., Verplank, L., Perez, J. R., et al. (2014). Identification of inhibitors of pvdq, an enzyme involved in

the synthesis of the siderophore pyoverdine. *ACS Chem. Biol.* 9, 1536–1544. doi: 10.1021/cb5001586

Yang, C. X., Cui, C. Y., Ye, Q. M., Kan, J. H., Fu, S. N., Song, S. H., et al. (2017). *Burkholderia cenocepacia* integrates *cis*-2-dodecenoic acid and cyclic dimericguanosine monophosphate signals to control virulence. *Proc. Natl. Acad. Sci. U.S.A.* 114, 13006–13011. doi: 10.1073/pnas.1709048114

Yates, E. A., Philipp, B., Buckley, C., Atkinson, S., Chhabra, S. R., Sockett, R. E., et al. (2002). *N*-acylhomoserine lactones undergo lactonolysis in a pH-, temperature-, and acyl chain length-dependent manner during growth of *Yersinia pseudotuberculosis* and *Pseudomonas aeruginosa*. *Infect. Immun.* 70, 5635–5646. doi: 10.1128/IAI.70.10.5635-5646.2002

Yeon, K. M., Cheong, W. S., Oh, H. S., Lee, W. N., Hwang, B. K., Lee, C. H., et al. (2008). Quorum sensing: a new biofouling control paradigm in a membrane bioreactor for advanced wastewater treatment. *Environ. Sci. Technol.* 43, 380–385. doi: 10.1021/es8019275

Yu, Y., Duan, J., Yu, Y., Li, Y., Liu, X., Zhou, X., et al. (2014). Silica nanoparticles induce autophagy and autophagic cell death in HepG2 cells triggered by reactive oxygen species. *J. Hazard. Mater.* 270, 176–186. doi: 10.1016/j.jhazmat.2014.01.028

Zhang, K., Zheng, X., Shen, D. S., Wang, M. Z., Feng, H. J., He, H. Z., et al. (2015). Evidence for existence of quorum sensing in a bioaugmented system by acylatedhomoserine lactone-dependent quorum quenching. *Environ. Sci. Pollut. Res. Int.* 22, 6050–6056. doi: 10.1007/s11356-014-3795-6

Conflict of Interest Statement: The authors declare that the research was conducted in the absence of any commercial or financial relationships that could be construed as a potential conflict of interest.

The reviewer MC-Y and handling Editor declared their shared affiliation.

frontiers in Cellular and Infection Microbiology

ORIGINAL RESEARCH
published: 26 April 2018
doi: 10.3389/fcimb.2018.00119

PvdQ Quorum Quenching Acylase Attenuates *Pseudomonas aeruginosa* Virulence in a Mouse Model of Pulmonary Infection

Putri D. Utari[1], *Rita Setroikromo*[1], *Barbro N. Melgert*[2] *and Wim J. Quax*[1]*

[1] Department of Chemical and Pharmaceutical Biology, University of Groningen, Groningen, Netherlands, [2] Department of Pharmacokinetics, Toxicology and Targeting, University of Groningen, Groningen, Netherlands

Pseudomonas aeruginosa is the predominant pathogen in pulmonary infections associated with cystic fibrosis. Quorum sensing (QS) systems regulate the production of virulence factors and play an important role in the establishment of successful *P. aeruginosa* infections. Inhibition of the QS system (termed quorum quenching) renders the bacteria avirulent thus serving as an alternative approach in the development of novel antibiotics. Quorum quenching in Gram negative bacteria can be achieved by preventing the accumulation of *N*-acyl homoserine lactone (AHL) signaling molecule via enzymatic degradation. Previous work by us has shown that PvdQ acylase hydrolyzes AHL signaling molecules irreversibly, thereby inhibiting QS in *P. aeruginosa in vitro* and in a *Caenorhabditis elegans* model of *P. aeruginosa* infection. The aim of the present study is to assess the therapeutic efficacy of intranasally instilled PvdQ acylase in a mouse model of pulmonary *P. aeruginosa* infection. First, we evaluated the deposition pattern of intranasally administered fluorochrome-tagged PvdQ (PvdQ-VT) in mice at different stages of pulmonary infection by *in vivo* imaging studies. Following intranasal instillation, PvdQ-VT could be traced in all lung lobes with 42 ± 7.5% of the delivered dose being deposited at 0 h post-bacterial-infection, and 34 ± 5.2% at 72 h post bacterial-infection. We then treated mice with PvdQ during lethal *P. aeruginosa* pulmonary infection and that resulted in a 5-fold reduction of lung bacterial load and a prolonged survival of the infected animals with the median survival time of 57 hin comparison to 42 h for the PBS-treated group. In a sublethal *P. aeruginosa* pulmonary infection, PvdQ treatment resulted in less lung inflammation as well as decrease of CXCL2 and TNF-α levels at 24 h post-bacterial-infection by 15 and 20%, respectively. In conclusion, our study has shown therapeutic efficacy of PvdQ acylase as a quorum quenching agent during *P. aeruginosa* infection.

Keywords: *Pseudomonas aeruginosa*, PvdQ acylase, quorum sensing, quorum quenching, mouse model, pulmonary infection

OPEN ACCESS

Edited by:
Rodolfo García-Contreras, Universidad Nacional Autónoma de México, Mexico

Reviewed by:
Israel Castillo Juárez, Colegio de Postgraduados (COLPOS), Mexico
Younes Smani, Instituto de Biomedicina de Sevilla (IBiS), Spain

***Correspondence:**
Wim J. Quax
w.j.quax@rug.nl

Received: *13 February 2018*
Accepted: *03 April 2018*
Published: *26 April 2018*

Citation:
Utari PD, Setroikromo R, Melgert BN and Quax WJ (2018) PvdQ Quorum Quenching Acylase Attenuates Pseudomonas aeruginosa Virulence in a Mouse Model of Pulmonary Infection. Front. Cell. Infect. Microbiol. 8:119. doi: 10.3389/fcimb.2018.00119

INTRODUCTION

Pseudomonas aeruginosa is an opportunistic Gram negative bacterium that is mainly associated with hospital-acquired infections and known as the major pathogen in cystic fibrosis (CF) patients (Driscoll et al., 2007). Nearly all pulmonary *P. aeruginosa* infections in CF patients will develop into chronic, persistent infections that require aggressive antibiotic treatments (Van Delden and Iglewski, 1998). The intrinsic traits of this bacterium coupled with complex adaptive behaviors such as biofilm formation make it resilient to many antibiotic treatments (Breidenstein et al., 2011). All of these elements propelled *P. aeruginosa* into a significant multidrug-resistant pathogen worldwide.

In numerous pathogens, production of bacterial virulence determinants is tightly regulated in a cell density-dependent manner, aided by a quorum sensing (QS) signaling system (Fuqua and Greenberg, 2002). By detecting the accumulation of signal molecules, each individual cell is capable of sensing the population density and subsequently responds by producing an arsenal of virulence factors when a critical population mass is reached (Cámara et al., 2002). The most studied signaling molecules in Gram-negative bacteria are *N*-acyl homoserine lactones (AHLs) (Papenfort and Bassler, 2016). The AHLs are produced by AHL-synthases (e.g., LuxI-type family) and sensed by transcriptional regulators (LuxR-type family) (Fuqua and Greenberg, 2002). The core of QS in *P. aeruginosa* consists of two LuxRI-based signaling systems that work in a hierarchal fashion, namely LasRI and RhlRI with 3-oxo-C12-HSL and C4-HSL as their respective cognate AHL (Jimenez et al., 2012). Deletion of either the AHL synthases or AHL receptors resulted in a downregulation of QS-regulated virulence factors, such as rhamnolipids, elastase protease, pyocyanin siderophore, and biofilm formation (Passador et al., 1993; Whiteley et al., 1999). These QS mutants are less pathogenic in animal models in comparison to the wild-type (Wu et al., 2001; Imamura et al., 2005), revealing the importance of this system for establishing successful infections. These findings opened up a possibility of attacking QS system as a new antivirulence drug therapy.

Quorum sensing (QS) inhibition (termed quorum quenching, QQ) can be performed by employing small molecule inhibitors to block the AHL productions or to avoid the interaction between AHLs and the response regulators. Bioactive compounds isolated from natural sources, or ones that are synthetized chemically, have shown therapeutic efficacy as QS inhibitors (QSIs) both *in vitro* and *in vivo* (Hentzer et al., 2002; Bjarnsholt et al., 2005; Rasmussen et al., 2005; Jakobsen et al., 2012a,b). However, some well-known small molecules inhibitors (QSIs), such as patulin and furanones, are toxic for mammals (Hentzer and Givskov, 2003; Puel et al., 2010) diminishing their potential for use humans. Another obvious approach for QS inhibition is by preventing accumulation of signal molecules by means of enzymatic degradation (Kalia, 2013). So far, three classes of enzymes have been identified that are known to inactivate AHLs, namely (i) AHL-lactonases [that cleave the ester bond in the homoserine lactone (HSL) ring moiety; Dong et al., 2000; Wang et al., 2010], (ii) AHL-acylases (that irreversibly hydrolyze the amide bond between the acyl chain and HSL; LaSarre and Federle, 2013), and the least studied (iii) AHL-oxidoreductases (that modify the 3-oxo-substituents of the AHLs; Uroz et al., 2005).

Numerous AHL-inactivating enzymes (QQ enzymes) were characterized, but only lactonase has been tested for its efficacy in mammalian models of pulmonary infection (Migiyama et al., 2013; Hraiech et al., 2014). Due to the large size of the enzyme molecules, the only possible route of administration is via the upper respiratory tract. Combining the procedures of establishing the infection and delivering the drug via the upper respiratory tract is challenging to be performed in small animals. Therefore, the recent study on the administration of an AHL-lactonase was done in rats using intubation of trachea. It successfully reduced mortality in the rat model of pneumonia (Hraiech et al., 2014). However, there is yet no study that employs a non-invasive drug administration method that closely mimics the actual procedure in human.

The purpose of our study was to determine the efficacy of one of the other AHL-inactivating enzymes, an AHL-acylase that was instilled intranasally in a mouse model of pulmonary *P. aeruginosa* infection. Our enzyme of interest is PvdQ acylase, a periplasmic enzyme from *P. aeruginosa* that is suggested to be involved in the maturation of pyoverdine siderophore (Drake and Gulick, 2011). Beside this function, PvdQ is a well-studied AHL-hydrolyzing enzyme, with specificity to long chain AHLs (Sio et al., 2006; Bokhove et al., 2010). PvdQ, either overexpressed in, or exogenously supplemented to *P. aeruginosa*, could significantly attenuate the virulence production, both *in vitro* (Sio et al., 2006), and *in vivo* in a *Caenorhabditis elegans* model (Papaioannou et al., 2009). In this report, we show results of PvdQ acylase deposition in the respiratory tract after intranasal administration and its efficacy in lethal and sublethal models of pulmonary *P. aeruginosa* infection.

MATERIALS AND METHODS

Bacterial Strains and Growing Condition

Enzymatic hydrolysis of long chain AHL was monitored by employing a reporter strain *E. coli* pSB1075 (Amp^R) (Winson et al., 1998). Determination of PvdQ inhibition strength was performed by reporter strains *P. aeruginosa PlasB::lux* (Koch et al., 2014) and *PrhlA::lux* (Tet^R) (this study). *P. aeruginosa* PAO1 was obtained from Barbara Iglewski (University of Rochester Medical Center, Rochester, NY) (Sio et al., 2006). The overnight cultures of the biosensors were prepared by inoculating a loop of frozen glycerol stock in Luria Bertani (LB) medium, followed by incubation at 37°C, 200 rpm. For the animal experiments, *P. aeruginosa* PAO1 from a frozen glycerol stock was grown in *Pseudomonas* isolation agar (PIA) selection medium (BD Difco™) overnight at 37°C. A single colony was used to inoculate a 100 mL LB medium in a 250 mL erlenmeyer flask, at 37°C, 200 rpm for 18 h. When necessary, 100 μL/mL tetracycline or 50 μL/mL ampicillin was added to the media.

Preparation of PvdQ

Production and Purification of PvdQ

PvdQ was produced and purified as reported previously (Bokhove et al., 2010), with modifications. *E. coli* DH10B

harboring pMCT_*pvdQ* was grown in 2xTY medium with chloramphenicol supplementation (50 μg/mL) for 30 h at 30°C, 200 rpm. The harvested cells were sonicated in a three times volume of lysis buffer (50 mM Tris Cl pH 8.8; 2 mM EDTA), followed by centrifugation at 17.000 rpm for 1 h. The clear lysate was applied to an anion exchange HiTrap Q-sepharose column and the flowthrough containing PvdQ was collected. After adjusting the ammonium sulfate concentration to 750 mM, the solution containing PvdQ was applied to a phenyl sepharose column. PvdQ eluted at the end of the 1,000–0 mM ammonium sulfate gradient. The buffer was exchanged into 50 mM sodium phosphate pH 6.5 and the sample was applied to a HiTrap Q-sepharose column. The collected flowthrough was subsequently concentrated and applied to a gel filtration superdex 16/60 75. A major peak containing PvdQ was collected, snap frozen and stored at −80°C until further use. All protein chromatography columns were obtained from GE Healthcare Life Sciences.

Endotoxin Removal From the Purified PvdQ

For animal experiments, endotoxin contamination in purified PvdQ was eliminated using a Pierce™ High Capacity Endotoxin Removal Resin (Thermo Scientific) following the manufacturer's manual. To adjust the PvdQ concentration, an endotoxin-free PBS buffer (Millipore, Merck) was used. The endotoxin content of purified PvdQ was analyzed with the LAL test at the University Medical Center Groningen, the Netherlands.

Fluorochrome Labeling of PvdQ

For the purpose of the PvdQ deposition study in mice, PvdQ was labeled with VivoTag 680 XL Fluorochrome (Perkin Elmers). 0.5 mg PvdQ (1 mg/mL) was labeled according to the manufacturer's manual. The calculated degree of labeling was 2, indicating that in average 2 dye molecules were coupled to one molecule of PvdQ.

In Vitro Quorum Quenching Activity of PvdQ

Enzymatic Activity of PvdQ in Hydrolyzing 3-oxo-C12-HSL

The enzymatic activity of PvdQ in deacylating 3-oxo-C12-HSL (Cayman Chemical) was validated using a bioassay procedure as previously described (Wahjudi et al., 2011). *E. coli* JM109 (pSB1075) biosensor that emits luminescence in the presence of long-chain AHLs was employed to detect the remaining 3-oxo-C12-HSL. Briefly, 2 μL of 0.5 mg/mL 3-oxo-C12-HSL in acetonitrile was spotted onto a flat-bottom μClear white microplate (Greiner Bio-One) and incubated at the room temperature until the acetonitrile evaporated. The remaining AHL was solubilized in 100 μL PBS buffer pH 7.4 containing 5 μg of PvdQ. A control reaction was prepared in identical conditions using heat-inactivated PvdQ. After 4 h at 30°C with slow agitation, 100 μL of the 100 times diluted overnight biosensor was added to each well. The emitted luminescence and the bacterial growth (OD_{600}) were monitored in a FLUOstar Omega platereader (BMG Labtech).

Quorum Quenching Activity of PvdQ in *P. aeruginosa* Reporter Strains

The following assays were performed to determine the quorum sensing inhibition activity of PvdQ by employing *P. aeruginosa* biosensors. *P. aeruginosa* P*rhlA::lux* and P*lasB::lux* each containing a chromosomal insertion of a luciferase gene under the control of a *rhlA* rhamnolipid promoter or a *lasB* elastase promoter, respectively (Koch et al., 2014). Two-fold serial dilutions of PvdQ in PBS (100 μL) were made in a flat-bottom μClear white microplate (Greiner Bio-One), covering PvdQ concentration of 0–16 μM. Overnight cultures of the biosensors were diluted 100 times in LB, and 100 μL was added to the wells containing PvdQ. The emitted luminescence and the bacterial growth (OD_{600}) were monitored in a FLUOstar Omega platereader (BMG Labtech).

Epithelial Cell Viability Assay

The effect of PvdQ on the cell viability was assessed in the lung epithelial cell lines A549 and H460. Serial 2-fold dilutions of PvdQ with a maximum concentration of 10 μM were added to 10^5 cells, followed by incubation at 37°C for 48 h. The level of cell proliferation was determined by a 3-(4,5-dimethylthiazol-2-yl)-5-(3-carboxymethoxyphenyl)-2-(4-sulfophenyl)-2H-tetrazolium (MTS salt, Promega) proliferation assay according to the manufacturer's manual.

Preparation of the Agarose-Embedded Bacteria

One day prior to infection of animals, *P. aeruginosa* PAO1 was embedded in agarose as explained elsewhere (van Heeckeren and Schluchter, 2002; Kukavica-Ibrulj et al., 2014), with modifications. Cell pellets from 100 mL overnight culture of *P. aeruginosa* PAO1 were washed twice with a sterile PBS, and were resuspended in 5 mL LB. A volume of 1 mL bacterial suspension was added to 10 mL 1.5% sterilized, pre-warmed (48–50°C) agarose (Type I Low EEO, Sigma-Aldrich) and mixed thoroughly. To prepare sterile agarose beads, a sterile LB medium was added to the agarose solution. The mixture was pipetted dropwise into the center of stirred vegetable oil (200 mL) that was equilibrated at ∼50°C. The stirring was kept at 1500 rpm for 6 min at ∼50°C. Afterwards, the emulsion was stirred slowly at 4°C for 20 min, followed by incubation on ice for 20 min. 100 mL oil in the top layer was discarded, and the remaining agarose beads were washed with PBS, followed by centrifugation in a swinging bucket rotor at 2,700 × *g*, 4°C for 15 min. The beads were subsequently washed one time with 0.5% sodium deoxycholic acid (SDC, Sigma-Aldrich) in PBS, one time with 0.25% SDC, and 4 times with PBS. After the last wash, PBS was added to the agar beads in a ratio of 2:1. The agarose beads slurry was stored at 4°C prior to use the following day. A homogenized aliquot of the agarose beads was serially diluted and plated onto PIA medium, followed by incubation at 37°C for 24 h. Based on the counted colony forming unit (CFU) on PIA plates, the original agarose beads slurry was adjusted with PBS to 1.25×10^7 CFU/mL (lethal dose) or 6.25×10^6 CFU/mL (sublethal dose) and 40 μL of the bacterial preparation was administered per animal.

Animal Experiments

Animal experiments were conducted in accordance with the Dutch Animal Protection Act and were approved by the Netherlands National Committee for the protection of animals used for scientific purposes (DEC6692, AVD105002017854). The experiments were performed in a BSL-2 area in the Central Animal Facility (CDP) of the University Medical Center Groningen (UMCG). Female BALB/c mice aged 11–12 weeks old with a minimum weight of 20 grams (at the start of experiment) were purchased from Charles River, France. Groups of 4–6 mice were housed in individual ventilator cages with unrestricted access to food and water. Infected animals were placed in cages with warming pads at the bottom of the cage.

Infection Procedure and Intranasal PvdQ Administration

The procedure for developing pulmonary infection in our study was a combination between intratracheal instillation of bacteria at the start of the experiment, and a daily intranasal delivery of the drug.

Intratracheal Instillation of Bacteria

Sterile agarose beads or agarose beads laden with *P. aeruginosa* PAO1 were instilled into the lungs via nonsurgical intratracheal administration (Bivas-Benita et al., 2005; Munder and Tümmler, 2014). Mice were anesthetized by isoflurane inhalation and the depth of anesthesia was checked by the foot reflex toward pinching. Mice were then placed vertically by the upper teeth on an intubation stand, with continuous anesthesia through a nose cone. Cold light was placed in front of the throat and the tongue was retracted to the side using forceps. When the trachea was visualized, a disposable sterile intravenous G20 catheter (BD Insyte-W) with an adjusted length was inserted into the trachea. To confirm that the catheter was indeed inside the trachea, a ventilator (Harvard Minivent) was connected. Correct catheter placement will show the chest, but not the abdomen, moving in synch with the ventilator's programmed rate. Afterwards, 40 μL of agarose beads were carefully administered into the catheter, followed by blowing 200–400 μL of air into the catheter to ensure that all beads were delivered into the lungs. While the animal was still under anesthesia, a transponder microchip (IPTT-300, BMDS) for temperature measurement was implanted subcutaneously. This transponder allows body temperature measurement with a portable reader device (DAS-7006s, BMDS) by scanning the mice without direct contact. The mice were weighed daily and their general appearance (body temperature, coat condition, behavior and locomotion) was monitored 2–3 times a day. At designated time points, the mice were anesthetized with isoflurane and euthanized by cardiac exsanguination. Blood, bronchoalveolar lavage fluid, kidney, spleen, and lungs were collected aseptically from the animals.

Intranasal PvdQ Administration

Mice were lightly anesthetized with isoflurane and held in a ∼60° inclined supine position. Subsequently, 50 μL PvdQ was instilled dropwise onto the nose of the anesthetized animal. The control group (PBS-treated) received an intranasal administration of 50 μL PBS.

Study Design

The *in vivo* study consisted of three parts: Study 1. Mouse tolerance of PvdQ; Study 2. *In vivo* imaging to monitor deposition of intranasally administered PvdQ; Study 3. An efficacy study of PvdQ in a mouse pulmonary infection model.

Study 1. Mouse Tolerance of the Intranasally Administered PvdQ

To determine tolerance of PvdQ, groups of mice were intratracheally challenged with sterile agarose beads and received a daily intranasal administration of PvdQ (25 and 250 ng/g body weight) or PBS. Animals from each group was sacrificed at 24, 48, or 72 h after the first intranasal administration for analysis of immune responses or inflammation. Experiments were performed in duplicate, totaling to 4 animals per group.

Study 2. *In Vivo* Imaging to Monitor Deposition of Intranasally Administered PvdQ

As PvdQ is a protein, special attention was given to proper delivery to the location of infection, i.e., the lungs. Deposition of intranasally administered PvdQ in airways of mice was examined by employing a VivoTag 680XL-labeled PvdQ (PvdQ-VT). Groups of animals were infected with a sublethal dose of *P. aeruginosa* PAO1 and received 50 μL of 1 mg/mL PvdQ-VT intranasally at 0 and 72 h post-bacterial inoculation. The animals were allowed to recover for 5 min after PvdQ-VT administration, followed by *in vivo* imaging as previously described (Tonnis et al., 2014). First, the animal was placed in a Fluorescence Molecular Tomography (FMT, PerkinElmer, Waltham, USA) that permits localization of PvdQ-VT in a three-dimensional visual of the animal. The fluorescence was measured at an excitation wavelength of 660 nm and an emission wavelength of 680 nm. Next, the animal was sacrificed and the isolated lungs were placed on a petri dish, followed by visualization in the *In Vivo* Imaging System (IVIS® Spectrum, PerkinElmer, Waltham, USA). The fluorescence was measured at an excitation wavelength of 675 nm and an emission wavelength of 720 nm. The acquired data from FMT and IVIS were analyzed by TrueQuant™ v3.1 software and Living Image® Software v3.2, respectively. The relative deposition of PvdQ-VT in a certain region of interest was calculated by dividing the fluorescence intensity in the region of interest by intensity of the total area times 100%. Experiments were performed in duplicate, totaling to 6 animals per group.

Study 3. Efficacy of PvdQ in a Mouse Pulmonary Infection Model

The efficacy of PvdQ as a quorum sensing inhibitor was assessed in a lethal ($n = 6$ per group) and a sublethal pulmonary infections with *P. aeruginosa* PAO1. Groups of infected animals received a daily intranasal administration of PvdQ (25 ng/g and 250 ng/g body weight) starting immediately after bacterial inoculation. At 24 and 48 h, mice were sacrificed for quantitative analysis of bacteriology, immune responses and histopathological

analysis, unless otherwise stated. Efficacy test in the lethal infection was performed as one experiment ($n = 6$ per group), while experiments for the sublethal infection were performed in triplicate, totaling to 22–23 animals per group.

Analysis of Animal Samples

Bronchoalveolar Lavage

For bronchoalveolar lavage (BAL), the lungs were flushed three times with a total volume of 2 mL PBS supplemented with protease inhibitor (cOmplete™, EDTA-free Protease Inhibitor Cocktail, Roche). Cytospin preparations from 100 μL of unprocessed BAL fluid sample were stained with May Grünwald and Giemsa staining for differential cell counts. Levels of TNF-α and CXCL2 in the cell-free supernatant of BAL fluid (600 rpm slow acceleration, room temperature for 5 min) were measured by ELISA in accordance to the manufacturer's instructions (Duoset, R&D systems).

Quantitative Bacteriology

Isolated lungs were homogenized in 5 mL PBS using a mechanical homogenizer (IKA-RW15 potter system). Blood, BAL fluid and serial dilution of lung homogenates were plated on the selective media *Pseudomonas* Isolation Agar (PIA) for quantitative bacteriology.

Histopathology

Lungs were inflated with cryocompound (Klinipath) and fixed in 4% formaldehyde (Sigma-Aldrich) overnight. Afterwards, the lobes were separated and trimmed prior to paraffin-embedding (Ruehl-Fehlert et al., 2004). Sections of 3–4 μm were stained with haematoxylin and eosin (Sigma-Aldrich). 10–15 areas of the lung sections were scored blindly for peribronchial infiltrates and alveolar involvement at a 40x magnification using an adapted histological scoring system (**Table 1**; Bayes et al., 2016) that was originally mentioned in Dubin et al. (Dubin and Kolls, 2007).

Statistical Analysis

Comparisons between two groups were carried out using Mann Whitney U (non-parametric data). Survival graph was created using the method of Kaplan-Meier, and the comparison of survival between groups was analyzed by the χ^2-test. Statistical analysis was performed using Graphpad Prism version 5 or SPSS statistics version 25. A probability value (P) ≤ 0.05 was considered statistically significant.

TABLE 1 | Histological scoring system for lung inflammation in infected animals.

Score	Peribronchial infiltrate	Alveolar involvement
0	None	None
1	Low (infiltrate ≤ 4 cells thick)	Low (<25% examined lung with increased cellularity/thickening)
2	Medium (infiltrate 5–10 cells thick)	Medium (25–50% examined lung with increased cellularity/thickening)
3	High (25–50% visualized lumen)	High (>50% examined lung with increased cellularity/thickening)
4	Diffuse (>50% visualized lumen)	

RESULTS

In Vitro Study of PvdQ

Purified PvdQ Is Active and Quenches the Virulence of *P. aeruginosa* Biosensors in a Dose-Dependent Manner

PvdQ was purified with a yield of 30 mg L^{-1} of cell culture. The protein was >95% pure judged from SDS PAGE with a Coomassie blue staining (Supplementary Figure 1). Purified PvdQ for animal experiments underwent an endotoxin removal step, resulting in a final endotoxin level of 1.6 EU/mg PvdQ, well below the recommended limit for endotoxin in preclinical research (Maylyala and Singh, 2008). The endotoxin removal procedure did not affect the AHL-hydrolyzing activity of PvdQ (Supplementary Figure 2), as shown by the equal degradation of 3-oxo-C12-HSL substrate in both enzymatic reactions.

Effectivity of PvdQ in attenuating virulence of *P. aeruginosa* was monitored by employing biosensors with a chromosomal integration of a luciferase gene controlled by the QS-regulated *lasB* promoter or *rhlA* promoter. Emitted luminescence reflects activation of the quorum sensing system, thus the amount of produced light is inversely proportional to the inhibitory strength of PvdQ. The chosen PvdQ doses did not affect growth of the biosensors. Dose-response curves were created by plotting the response of the biosensors as a relative luminescence unit per cell density (**Figure 1**). The IC50 value could not be calculated since complete signal abolishment was not reached. We could not test a higher concentration of PvdQ to reach a greater signal reduction, because PvdQ precipitates at concentrations above 4 mg/mL.

Purified PvdQ Does Not Affect the Viability of Epithelial Cell Lines

The toxicity of PvdQ to mammalian cells was assessed *in vitro*, using A549 and H460 human epithelial cell lines. Incubation of cells with up to 10 μM PvdQ for 48 h did not affect the number of viable cells in comparison to control without PvdQ treatment (Supplementary Figure 3), suggesting that PvdQ exhibits minimal to no cytotoxicity toward epithelial cells.

Validation of the Animal Model and PvdQ Administration Procedure

The Mouse Infection Model

In principle, the severity of infection in the model depends on the bacterial inoculation dose and the stress level experienced by the animals. In our procedure, the infected animals were receiving a daily administration of PvdQ via intranasal route. Based on pilot experiments, we found that an inoculation dose lower than 10^5 CFU/lungs resulted in no development of infection, whereas an inoculation dose of 10^6 CFU/lungs resulted in a severe infection. For the present study we therefore adjusted the inoculation dose to 2.5×10^5 CFU/lungs as a sublethal dose and to twice that

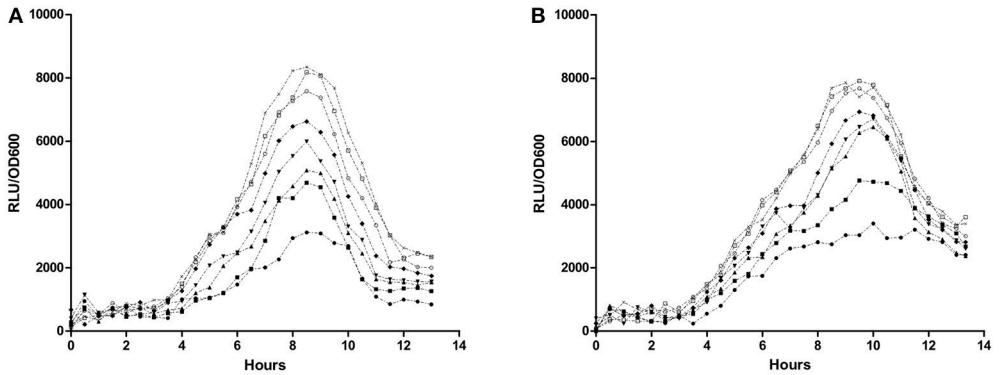

FIGURE 1 | Dose-response curve of PvdQ acylase. Biosensors **(A)** *P. aeruginosa rhlA::lux* and **(B)** *P. aeruginosa lasB::lux* were incubated with various concentration of PvdQ, as follows: 16 μM (●), 8 μM (■), 4 μM (▲), 2 μM (▼), 1 μM (♦), 0.5 μM (○), 0.25 μM (□), and 0 μM (×).

amount (5×10^5 CFU/lungs) as a lethal dose. Due to the high discomfort in the lethal infection, the PvdQ distribution study was only performed in the sublethal infection model, while the efficacy of PvdQ was investigated in both levels of infections.

Study 1. Mouse Tolerance of Intranasally Administered PvdQ

Our studies with mammalian epithelial showed that PvdQ was not toxic to these cells *in vitro*. Based on these results we performed the first part of an *in vivo* study to further ensure safety of intranasally administered PvdQ in mice. Tolerance of non-infected mice to intranasally administered PvdQ was determined with 2 doses of PvdQ (25 and 250 ng/g per animal). Both doses did not induce breathing difficulties, inactivity, poor posture or a drop of body temperature. Mild fluctuations of body weight were observed, with an average of 4% increase or decrease from the initial body weight, which was comparable to the control group receiving sterile beads and a daily intranasal PBS administration. Lungs harvested at 24, 48, and 72 h after the first PvdQ administration showed no macroscopic injury. Histological examination of lungs 72 h after PvdQ administration showed no inflammatory lesions or abnormalities (data not shown).

Study 2. *In Vivo* Imaging to Monitor the Deposition of Intranasally Administered PvdQ

A fluorochrome-tagged PvdQ (PvdQ-VT) was used to ascertain the deposition of the intranasally administered PvdQ-VT in mouse lung tissue. To determine whether infection influences enzyme deposition, PvdQ-VT was intranasally administered to infected animals at different stages of infection (0 and 72 h post-infection) followed by *in vivo* imaging analyses. The Fluorescence Molecular Tomography (FMT) allows a three-dimensional visualization of the whole animal and the typical result is shown in **Figure 2A**. PvdQ-VT could be traced along the respiratory tract of the animals and 42 ± 7.5% of the delivered dose was deposited in the lungs at 0 h post-infection. At 72 h post-infection, a slightly lower lung deposition was observed (34 ± 5.2%, n.s. compared to 0 h post-infection), and the majority of PvdQ-VT was found in the upper respiratory tract and the head. Afterwards, the lungs were isolated for a more thorough visualization in the *In Vivo* Imaging System (IVIS) and typical data are shown in **Figure 2B**. PvdQ-VT can be found in all lung lobes with a nearly equal distribution between the right lobes (combined, 47 ± 10.7%) and the left lobe (53 ± 10.7%) at 0 h post-infection. However, at 72 h post-infection, the distribution was shifted with the left lobe containing slightly more (60 ± 8.8%) than the right lobes (40 ± 8.7%).

Efficacy of PvdQ in a Mouse Model of Pulmonary Infection

Study 3. (i) Treatment With PvdQ Results in a Longer Survival Time and Higher Bacterial Clearance During Lethal Pulmonary Infection

Having established a pulmonary infection model and the safety of the PvdQ treatment, the next step was to investigate efficacy of PvdQ treatment in this infection model. Treatment of lethally infected animals with PvdQ (25 ng/g) resulted in a 5-fold lower bacterial load for the PvdQ-treated groups than for the PBS-treated group at the end of experiment ($P = 0.0465$, **Figure 3A**). Furthermore, the PvdQ treatment significantly prolonged the survival time, with a median survival time of 57 h as compared to 42 h in the PBS-treated animals ($P = 0.004$, **Figure 3B**). The same extent of efficacy was observed with the treatment of 250 ng/g PvdQ (data not shown).

Study 3. (ii) PvdQ Treatment Results in Less Lung Inflammation in a Model of Sublethal Pulmonary Infection

Inoculation with a sublethal bacterial dose resulted in a moderately severe infection, with no mortality as a consequence. Using this model, the efficacy of PvdQ treatment was assessed within 48 h post-infection by performing multiple analyses, including quantitative bacteriology, analyses of immune responses and histopathological analysis.

No significant differences were observed in bacterial load between the PvdQ-treated group and the PBS-treated group at 24 or 48 h post-bacterial-infection (Supplementary Figure 4). No

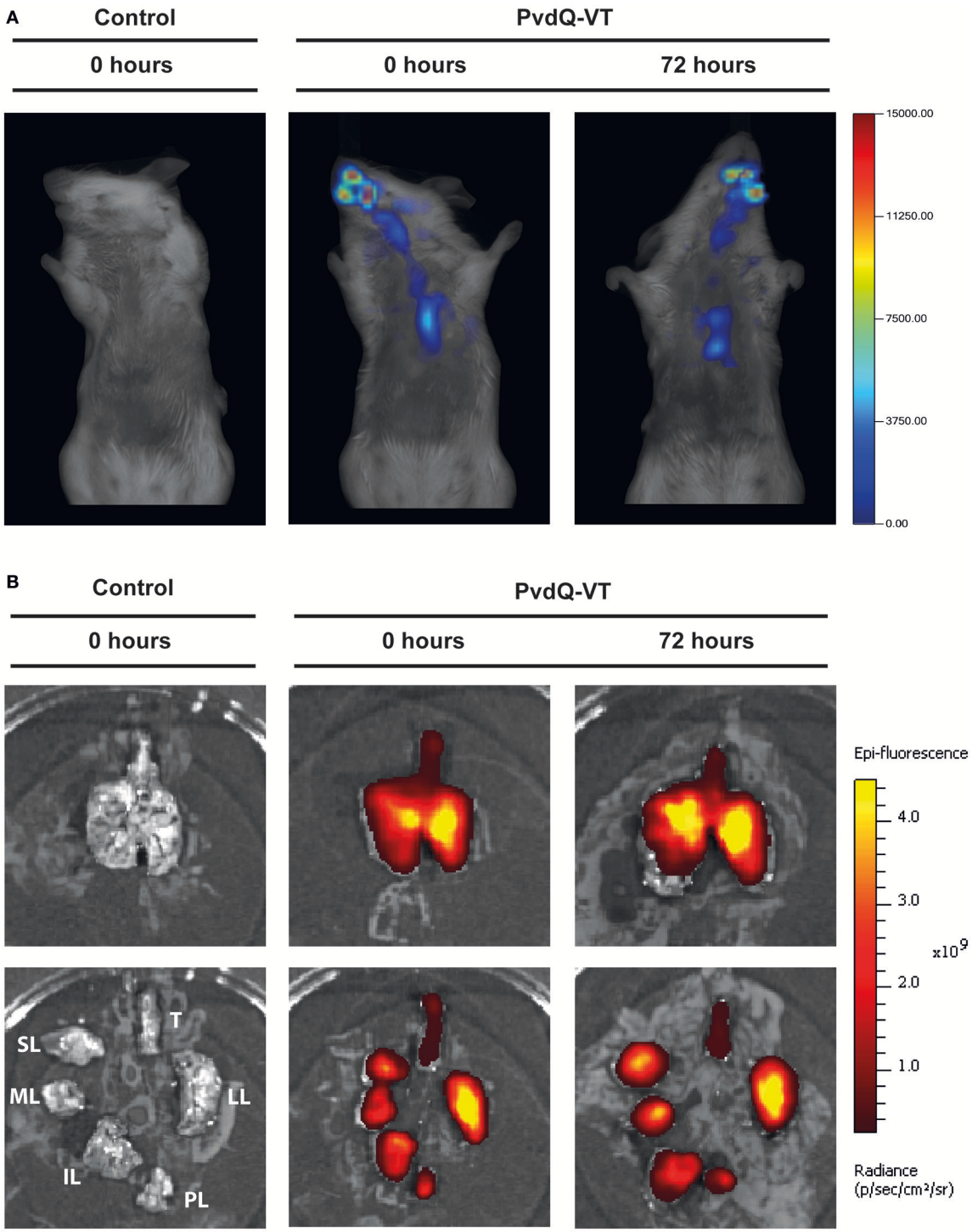

FIGURE 2 | Typical imaging results of animals after intranasal administration of PBS (control, left panel) or PvdQ-VT at different stages of infection (middle and right panels). **(A)** Results from FMT; **(B)** Results from IVIS. Upper panels show intact lungs, while lower panels show trachea and the separated lobes. Legend: Trachea (T), left lung (LL), post-caval lobe (PL), inferior lobe (IL), middle lobe (ML), and superior lobe (SL).

bacteria were found in the blood, spleen or kidney, indicating that the infection was restricted to the lungs. Histopathological analysis of lung tissue showed milder inflammation in the PvdQ-treated group than in the PBS-treated group 24 and 48 h post-infection (**Figure 4**). Lung tissue of mice treated with PBS showed a higher level of lung injury with diffuse inflammation

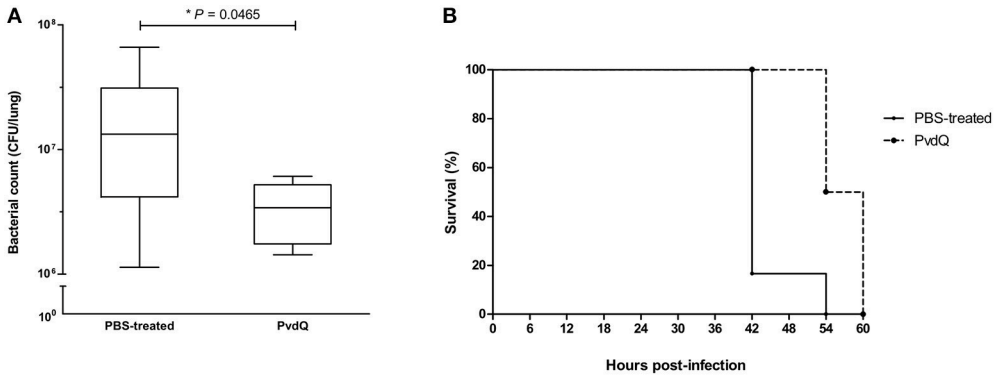

FIGURE 3 | Effects of PvdQ treatment in a lethal *P. aeruginosa* infection mouse model ($n = 6$ animals). **(A)** PvdQ treatment results in a lower load of *P. aeruginosa* in infected animals as compared to PBS-treatment. The bacterial count was obtained 42–60 h post-bacterial-infection. The box and whiskers respectively represent 25–75th percentiles, and range of the data. The horizontal lines represent the median. **(B)** PvdQ-treated animals have a significantly longer survival time than PBS-treated animals.

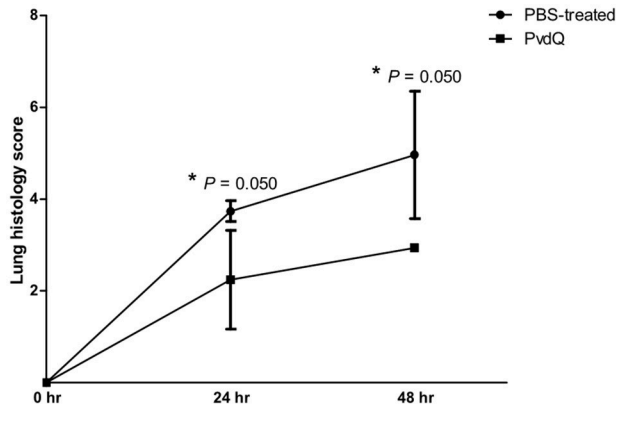

FIGURE 4 | Lung histology scores of lungs of mice treated with PBS (●) or PvdQ (■) at 24 and 48 h post bacterial-infection in a model of sublethal pulmonary infection with *P. aeruginosa*. Three animals were sacrificed from each group at each time point. The graph represents mean and standard deviation.

and swollen alveolar walls, while mice treated with PvdQ showed only small restricted lesions and hardly any alveolar involvement (**Figure 5**). In line with this finding, the levels of CXCL2 and TNF-α in BAL fluid of PvdQ-treated mice were significantly lower compared to PBS-treated mice at 24 h post-infection. At 48 h post-infection the levels of immune response indicators were similar between both groups and almost back to the levels found in non-infected animals (**Figure 6**). The total number of inflammatory cells in BAL fluid of PvdQ and PBS-treated animals was higher as compared to non-infected animals (Supplementary Figure 5A), but no differences were seen between PBS- and PvdQ-treated animals. In addition, the number of neutrophils in BAL fluid was assessed, but again no differences were seen between PBS and PvdQ treatment (Supplementary Figure 5B). The same extent of efficacy was observed with the treatment of 250 ng/g PvdQ (data not shown).

DISCUSSION

Pseudomonas aeruginosa infection is a growing problem in the healthcare, as well as being the predominant pathogen in pulmonary infections of cystic fibrosis patients. Multiple factors are contributing to the tenacity of *P. aeruginosa* as a human pathogen, including its remarkable adaptability that allows this bacterium to establish a successful infection and to escape antibiotic treatments. In the wake of the antibiotic resistance problem, relatively much attention has been given to the study of quorum sensing inhibitors (QSIs) as novel antibacterial candidates (Kalia, 2013; LaSarre and Federle, 2013; Fetzner, 2014). They fall into the category of antivirulence drugs that generate less selective pressure for evoking resistance in comparison to conventional antibiotics. AHL-hydrolyzing enzymes prevent accumulation of AHLs and the QQ effects by some of these enzymes are evident in infection models. Nevertheless, the number of the documented studies in mammals is relatively small, given the abundance of the characterized QQ enzymes. The first study in a pulmonary infection model was conducted by Migiyama and colleagues, showing that a *P. aeruginosa* strain overexpressing AiiM lactonase is less virulent than the wild-type (Migiyama et al., 2013). This finding was followed by a report from Hraiech and colleagues who employed a purified *Sso*Pox-I lactonase as a therapeutic agent in a lethal *P. aeruginosa* pulmonary infection model in rats (Hraiech et al., 2014). The purified *Sso*Pox-I lactonase was administered through the intubation of the exposed trachea and could reduce the mortality of the infected animals. Although these studies excellently demonstrated the therapeutic value of AHL-hydrolyzing enzymes, there is yet no study using a non-invasive administration route of the enzymes that closely mimics the possible drug administration route in human. In the present study, we have shown that PvdQ is well-tolerated by human lung epithelial cell lines, indicating that PvdQ has minimal or no cytotoxic effects on human cells. Furthermore, intranasally administered PvdQ acylase is well-tolerated and distributes well in lung tissue of mice, even during infection. Most importantly,

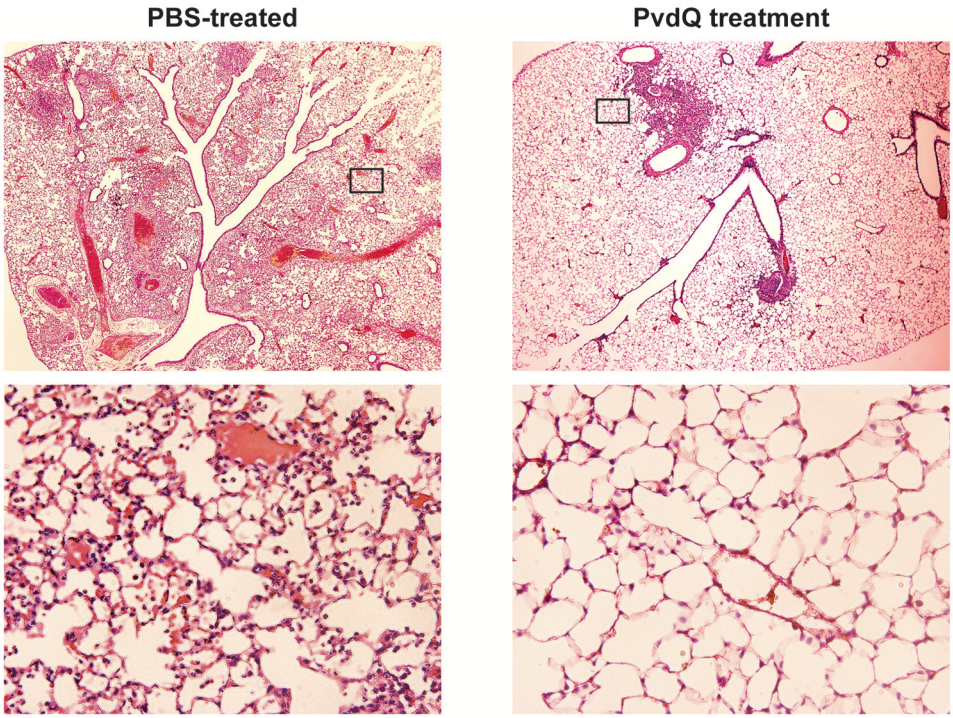

FIGURE 5 | Histological examination of lung tissue of animals infected by sublethal *P. aeruginosa* dose and treated with either PBS or PvdQ at 48 h post-bacterial-infection. Upper panels represent images of H&E stainings at 20x magnification, and the areas marked with rectangular are shown in 200x magnification in the lower panels.

intranasally administered PvdQ acylase alleviates *P. aeruginosa* pulmonary infection in mice, which may lead to faster resolution of the infection.

Prior studies have confirmed that supplementation of PvdQ to cultures of *P. aeruginosa* inhibits accumulation of 3-oxo-C12-HSL and in turn blocks production of elastase and pyocyanin (Sio et al., 2006). Furthermore, PvdQ showed a therapeutic effect in a *C. elegans* model of *P. aeruginosa* infection (Papaioannou et al., 2009). In order to test the preclinical efficacy of PvdQ in a more relevant animal model, we developed a mouse model combining the *P. aeruginosa* pulmonary infection with an administration procedure that can be translated to the human situation. A pulmonary infection model is very challenging to be developed in mouse (van Heeckeren and Schluchter, 2002), even more so when the infection is combined with a topical drug administration method. Lung-targeted delivery systems of large molecules in animal can be performed via pulmonary inhalation by different procedures, such as passive inhalation of aerosolized drugs (whole body, head-only, or nose-only exposure system), direct intratracheal administration or intranasal administration (Fernandes and Vanbever, 2009). Arguably, among these methods, a nose-only aerosol system would be of highest resemblance to that of in human, such as the inhalation of aerosolized DNAse Pulmozyme® for cystic fibrosis patients. However, the major drawback of this method is the requirement of highly accurate instruments, an ample amount of drugs, and a long exposure time (30–45 min) that could subject the infected animals to high level of stress. Intranasal delivery is one of the most common, and the least intrusive method for this purpose (Southam et al., 2002; Fernandes and Vanbever, 2009), hence it was chosen as the drug administration procedure in our experiment. Despite its simplicity, the downside of this intranasal delivery is the difficulty in controlling the dose deposition efficiency, because the drugs have to travel all the way through the upper respiratory tract before finally reaching the lungs.

Lung deposition efficiency from intranasal administration of fluorochrome-tagged PvdQ (PvdQ-VT) at 0 h post-bacterial-inoculation is in concordance to the study of Eyles and colleagues. They observed 48 ± 12.1% of radiolabeled 7-μm-diameter polymer microspheres in the healthy mouse lungs after an intranasal challenge (Eyles et al., 1999). In our study, the reduced lung deposition efficiency at the later stage of infection might be a repercussion of lung function deterioration caused by bacterial infection, such as a decrease of the inspired air volume as seen in other studies (Wölbeling et al., 2010, 2011). At 72 h post-bacterial infection, a shift of deposition toward the left lobe was observed. This finding is presumably related to the structural changes experienced by each lobe. However, to explain specific regional functions of the lungs, further research with a more elaborate function-related physiology study (e.g., determination of airspace diameters) is required.

The efficacy of PvdQ was assessed in mouse models with different levels of infection lethality. PvdQ administered via

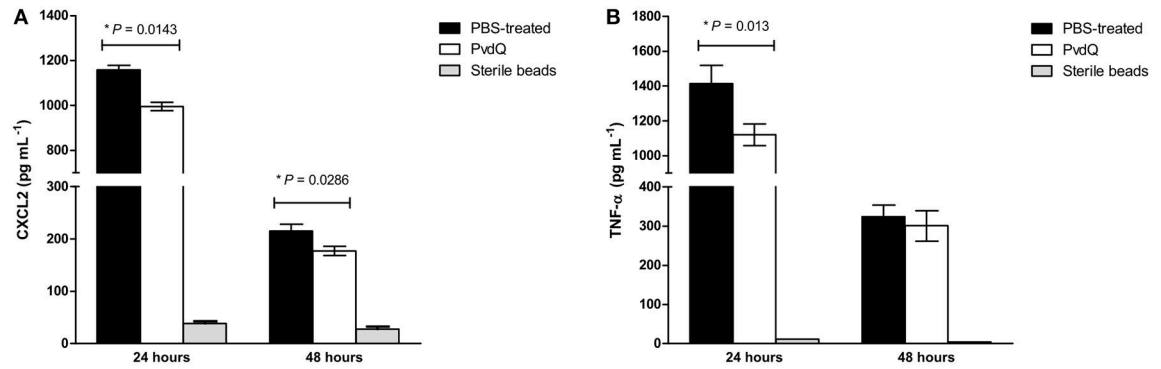

FIGURE 6 | Amounts of **(A)** CXCL2 and **(B)** TNF-α in cell-free BAL fluid from the infected animals treated with PBS (black bars) or PvdQ (white bars). The level of both CXCL2 and TNF-α of PvdQ treatment group was lower in comparison to the PBS-treated group at 24 h post-infection. Three animals were sacrificed from each group at every time point. The bars represent mean and standard deviation.

an intranasal route during lethal infection resulted in a lower bacterial load in the lungs, demonstrating a role of PvdQ in promoting bacterial clearance (**Figure 3**). Since the delivered PvdQ is a sub-MIC dose that did not affect bacterial growth *in vitro* and in a *C. elegans* infection model, we strongly believe that PvdQ does not clear the infection itself but is helping the immune system by disarming the bacteria in the mouse infection model. As a result of the lowered bacterial load, survival time of PvdQ treatment group was increased, in agreement with other murine studies of AHL-lactonases AiiM (Migiyama et al., 2013) and *Sso*Pox-I (Hraiech et al., 2014). In addition, our results also corroborate with the findings from animal studies of small molecule QSIs, such as furanone, patulin and garlic extracts (Wu et al., 2004; Bjarnsholt et al., 2005; Rasmussen et al., 2005). However, some of these QSIs such as patulin and furanone are known to be toxic for mammals (Hentzer and Givskov, 2003; Puel et al., 2010). In addition, the small molecule QSIs having intracellular targets are prone to development of resistance via upregulated efflux pumps (García-Contreras et al., 2013). The median survival after PvdQ treatment is longer than shown for the group of animals receiving a deferred *Sso*Pox-I lactonase treatment (45 h) in the study of Hraiech and colleagues (Hraiech et al., 2014). Direct comparisons with the group receiving an immediate treatment is not possible because the median survival cannot be calculated from their data as they stopped their observation after 50 h post-bacterial infection. The fact that our mice eventually were still dying even though the bacterial load is lower, may be related to an overwhelming inflammatory response. The high bacterial load may induce an excess of inflammatory responses that cannot be counteracted by PvdQ disarming virulence factors anymore.

In order to perform an extensive analysis of immune responses, we extended our study with a more thorough examination during a sublethal infection. The experimental setup was similar to that of the lethal infection, but with a smaller bacterial inoculum. Consequently, the sublethal infection was milder and the defense mechanisms themselves could clear the infection, resulting in a 1,000-fold lower bacterial CFU in comparison to the lethal infection. The treatment with PvdQ in the sublethal *P. aeruginosa* infection did not lead to a lower bacterial count in comparison to the PBS-treated group (Supplementary Figure 4), but resulted in less lung inflammation (**Figures 4**, **5**) as well as lower levels of CXCL2 and TNF-α (**Figure 6**) suggesting that virulence has been suppressed. High levels of proinflammatory cytokines are observed during bacterial infection in CF patients, including IL-8 (a human analog of CXCL2 in mouse) and TNF-α (Richman-Eisenstat, 1996). The high levels of IL-8 and TNF-α in the sputum positively correlate with clinical symptoms of deterioration in CF patients and antibiotic treatment resulted in lower levels of both cytokines (Karpati et al., 2000; Colombo et al., 2005). Numerous bacterial virulence factors are known to activate innate immune responses, while others are responsible for tissue damage during infection. This includes 3-oxo-C12-HSL that is not only a potent chemoattractant of neutrophils (Karlsson et al., 2012) but also can induce an inflammatory response by macrophages (Telford et al., 1998; Thomas et al., 2006). Many QS-regulated virulence determinants are known for their tissue destructive properties, among them is elastase that hydrolyses protein elastin of lung tissue (Van Delden and Iglewski, 1998). Our observations in the sublethal infection model indicate that PvdQ treatment may reduce lung inflammation by preventing the accumulation of 3-oxo-C12-HSL and thereby diminishing the production of virulence factors that contribute to lung injury. We observed no difference in the number of inflammatory cells in BAL fluid from the PBS treatment group, even though a considerably higher amount of cells was found at the epithelial tissue of the PBS-treated group (**Figure 5**). Extracellular factors of *P. aeruginosa* such as 3-oxo-C12-HSL (Tateda et al., 2003), rhamnolipid (Jensen et al., 2007), and pyocyanin (Allen et al., 2005) potentially induced apoptosis of the neutrophils that migrated to the alveolar space, reducing the number of cells in BAL fluid. The dose of 25 ng/g is presumably sufficient to fully hydrolyze extracellular AHLs in the lungs. Hence, increasing the PvdQ dose further did not improve the therapeutic efficacy in both lethal and sublethal infections.

Taken together, our study shows that the intranasally administered PvdQ acylase can act as a therapeutic QQ enzyme to attenuate *P. aeruginosa* in a mouse pulmonary infection model. The inhibition of *P. aeruginosa* virulence clearly contributed to bacterial clearance and an improved condition of the lungs. Hence, PvdQ by itself can be a potential candidate as a part of the treatment of pulmonary infection. Increasing the shelf-life of PvdQ is achievable by formulating it into a dry powder that is suitable for inhalation (Wahjudi et al., 2012). Another interesting approach is to employ PvdQ in the combination therapy to increase the efficacy of conventional antibiotics. Therefore, in the future studies, expanding the therapeutic application of PvdQ would be of high interest.

AUTHOR CONTRIBUTIONS

WQ is the principal investigator who initiated the project of quorum quenching. All authors contributed in designing the experiments. PU and RS performed the experiments and analyzed the data. The manuscript was written by PU and was carefully revised by BM and WQ.

ACKNOWLEDGMENTS

This study is supported by Beasiswa Unggulan Luar Negeri DIKTI Indonesia (PU) and the European Union's Horizon 2020 research and innovation programme under the Marie Sklodowska Curie grant agreement No. 713482 (ALERT). The authors thank Carian Boorsma, Michel Weij and Annemieke van Oosten for their technical help during animal experiments. We also thank Miriam van der Meulen-Frank, Wouter Hinrichs, and Jasmine Tomar for discussions during the experimental design.

SUPPLEMENTARY MATERIAL

The Supplementary Material for this article can be found online at: https://www.frontiersin.org/articles/10.3389/fcimb.2018.00119/full#supplementary-material

REFERENCES

Allen, L., Dockrell, D. H., Pattery, T., Lee, D. G., Cornelis, P., Hellewell, P. G., et al. (2005). Pyocyanin production by *Pseudomonas aeruginosa* induces neutrophil apoptosis and impairs neutrophil-mediated host defenses *in vivo*. *J. Immunol.* 174, 3643–3649. doi: 10.4049/jimmunol.174.6.3643

Bayes, H. K., Ritchie, N., Irvine, S., and Evans, T. J. (2016). A murine model of early *Pseudomonas aeruginosa* lung disease with transition to chronic infection. *Sci. Rep.* 6:35838. doi: 10.1038/srep35838

Bivas-Benita, M., Zwier, R., Junginger, H. E., and Borchard, G. (2005). Non-invasive pulmonary aerosol delivery in mice by the endotracheal route. *Eur. J. Pharm. Biopharm.* 61, 214–218. doi: 10.1016/j.ejpb.2005.04.009

Bjarnsholt, T., Jensen, P. Ø., Rasmussen, T. B., Christophersen, L., Calum, H., Hentzer, M., et al. (2005). Garlic blocks quorum sensing and promotes rapid clearing of pulmonary *Pseudomonas aeruginosa* infections. *Microbiology* 151, 3873–3880. doi: 10.1099/mic.0.27955-0

Bokhove, M., Nadal Jimenez, P., Quax, W. J., and Dijkstra, B. W. (2010). The quorum-quenching *N*-acyl homoserine lactone acylase PvdQ is an Ntn-hydrolase with an unusual substrate-binding pocket. *Proc. Natl. Acad. Sci. U.S.A.* 107, 686–691. doi: 10.1073/pnas.0911839107

Breidenstein, E. B., de la Fuente-Núñez, C., and Hancock, R. E. (2011). *Pseudomonas aeruginosa*: all roads lead to resistance. *Trends Microbiol.* 19, 419–426. doi: 10.1016/j.tim.2011.04.005

Cámara, M., Williams, P., and Hardman, A. (2002). Controlling infection by tuning in and turning down the volume of bacterial small-talk. *Lancet Infect. Dis.* 2, 667–676. doi: 10.1016/S1473-3099(02)00447-4

Colombo, C., Costantini, D., Rocchi, A., Cariani, L., Garlaschi, M. L., Tirelli, S., et al. (2005). Cytokine levels in sputum of cystic fibrosis patients before and after antibiotic therapy. *Pediatr. Pulmonol.* 40, 15–21. doi: 10.1002/ppul.20237

Dong, Y. H., Xu, J. L., Li, X. Z., and Zhang, L. H. (2000). AiiA, an enzyme that inactivates the acylhomoserine lactone quorum-sensing signal and attenuates the virulence of *Erwinia carotovora*. *Proc. Natl. Acad. Sci. U.S.A.* 97, 3526–3531. doi: 10.1073/pnas.97.7.3526

Drake, E. J., and Gulick, A. M. (2011). Structural characterization and high-throughput screening of inhibitors of PvdQ, an Ntn hydrolase involved in pyoverdine synthesis. *ACS Chem. Biol.* 6, 1277–1286. doi: 10.1021/cb2002973

Driscoll, J. A., Brody, S. L., and Kollef, M. H. (2007). The epidemiology, pathogenesis and treatment of *Pseudomonas aeruginosa* infections. *Drugs* 67, 351–368. doi: 10.2165/00003495-200767030-00003

Dubin, P. J., and Kolls, J. K. (2007). IL-23 mediates inflammatory responses to mucoid *Pseudomonas aeruginosa* lung infection in mice. *Am. J. Physiol. Lung Cell. Mol. Physiol.* 292, L519–L528. doi: 10.1152/ajplung.00312.2006

Eyles, J. E., Williamson, E. D., and Alpar, H. O. (1999). Immunological responses to nasal delivery of free and encapsulated tetanus toxoid: studies on the effect of vehicle volume. *Int. J. Pharm.* 189, 75–79. doi: 10.1016/S0378-5173(99)00239-2

Fernandes, C. A., and Vanbever, R. (2009). Preclinical models for pulmonary drug delivery. *Expert Opin. Drug Deliv.* 6, 1231–1245. doi: 10.1517/17425240903241788

Fetzner, S. (2014). Quorum quenching enzymes. *J. Biotechnol.* 201, 2–14. doi: 10.1016/j.jbiotec.2014.09.001

Fuqua, C., and Greenberg, E. P. (2002). Listening in on bacteria: acyl-homoserine lactone signalling. *Nat. Rev. Mol. Cell Biol.* 3, 685–695. doi: 10.1038/nrm907

García-Contreras, R., Maeda, T., and Wood, T. K. (2013). Resistance to quorum-quenching compounds. *Appl. Environ. Microbiol.* 79, 6840–6846. doi: 10.1128/AEM.02378-13

Hentzer, M., and Givskov, M. (2003). Pharmacological inhibition of quorum sensing for the treatment of chronic bacterial infections. *J. Clin. Invest.* 112, 1300–1307. doi: 10.1172/JCI20074

Hentzer, M., Riedel, K., Rasmussen, T. B., Heydorn, A., Andersen, J. B., Parsek, M. R., et al. (2002). Inhibition of quorum sensing in *Pseudomonas aeruginosa* biofilm bacteria by a halogenated furanone compound. *Microbiology* 148, 87–102. doi: 10.1099/00221287-148-1-87

Hraiech, S., Hiblot, J., Lafleur, J., Lepidi, H., Papazian, L., Rolain, J.-M., et al. (2014). Inhaled lactonase reduces *Pseudomonas aeruginosa* quorum sensing and mortality in rat pneumonia. *PLoS ONE* 9:e107125. doi: 10.1371/journal.pone.0107125

Imamura, Y., Yanagihara, K., Tomono, K., Ohno, H., Higashiyama, Y., Miyazaki, Y., et al. (2005). Role of *Pseudomonas aeruginosa* quorum-sensing systems in a mouse model of chronic respiratory infection. *J. Med. Microbiol.* 54, 515–518. doi: 10.1099/jmm.0.46004-0

Jakobsen, T. H., Bragason, S. K., Phipps, R. K., Christensen, L. D., van Gennip, M., Alhede, M., et al. (2012a). Food as a source for quorum sensing inhibitors: iberin from horseradish revealed as a quorum sensing inhibitor of *Pseudomonas aeruginosa*. *Appl. Environ. Microbiol.* 78, 2410–2421. doi: 10.1128/AEM.05992-11

Jakobsen, T. H., van Gennip, M., Phipps, R. K., Shanmugham, M. S., Christensen, L. D., Alhede, M., et al. (2012b). Ajoene, a sulfur-rich molecule from garlic, inhibits genes controlled by quorum sensing. *Antimicrob. Agents Chemother.* 56, 2314–2325. doi: 10.1128/AAC.05919-11

Jensen, P. Ø., Bjarnsholt, T., Phipps, R., Rasmussen, T. B., Calum, H., Christoffersen, L., et al. (2007). Rapid necrotic killing of polymorphonuclear leukocytes is caused by quorum-sensing-controlled production of rhamnolipid by *Pseudomonas aeruginosa*. *Microbiology* 153, 1329–1338. doi: 10.1099/mic.0.2006/003863-0

Jimenez, P. N., Koch, G., Thompson, J. A., Xavier, K. B., Cool, R. H., and Quax, W. J. (2012). The multiple signaling systems regulating virulence in *Pseudomonas aeruginosa*. *Microbiol. Mol. Biol. Rev.* 76, 46–65. doi: 10.1128/MMBR.05007-11

Kalia, V. C. (2013). Quorum sensing inhibitors: an overview. *Biotechnol. Adv.* 31, 224–245. doi: 10.1016/j.biotechadv.2012.10.004

Karlsson, T., Musse, F., Magnusson, K.-E., and Vikström, E. (2012). *N*-Acylhomoserine lactones are potent neutrophil chemoattractants that act via calcium mobilization and actin remodeling. *J. Leukoc. Biol.* 91, 15–26. doi: 10.1189/jlb.0111034

Karpati, F., Hjelte, L., and Wretlind, B. (2000). TNF-α and IL-8 in consecutive sputum samples from cystic fibrosis patients during antibiotic treatment. *Scand. J. Infect. Dis.* 32, 75–79. doi: 10.1080/00365540050164263

Koch, G., Nadal-Jimenez, P., Cool, R. H., and Quax, W. J. (2014). *Deinococcus radiodurans* can interfere with quorum sensing by producing an AHL-acylase and an AHL-lactonase. *FEMS Microbiol. Lett.* 356, 62–70. doi: 10.1111/1574-6968.12479

Kukavica-Ibrulj, I., Facchini, M., Cigana, C., Levesque, R. C., and Bragonzi, A. (2014). Assessing *Pseudomonas aeruginosa* virulence and the host response using murine models of acute and chronic lung infection. *Methods Mol. Biol.* 1149, 757–771. doi: 10.1007/978-1-4939-0473-0_58

LaSarre, B., and Federle, M. J. (2013). Exploiting quorum sensing to confuse bacterial pathogens. *Microbiol. Mol. Biol. Rev.* 77, 73–111. doi: 10.1128/MMBR.00046-12

Maylyala, P., and Singh, M. (2008). Endotoxin limits in formulations for preclinical research. *J. Pharm. Sci.* 97, 2041–2044. doi: 10.1002/jps.21152

Migiyama, Y., Kaneko, Y., Yanagihara, K., Morohoshi, T., Morinaga, Y., Nakamura, S., et al. (2013). Efficacy of AiiM, an N-acylhomoserine lactonase, against *Pseudomonas aeruginosa* in a mouse model of acute pneumonia. *Antimicrob. Agents Chemother.* 57, 3653–3658. doi: 10.1128/AAC.00456-13

Munder, A., and Tümmler, B. (2014). Assessing *Pseudomonas* virulence using mammalian models: acute infection model. *Methods Mol. Biol.* 1149, 773–791. doi: 10.1007/978-1-4939-0473-0_59

Papaioannou, E., Wahjudi, M., Nadal-Jimenez, P., Koch, G., Setroikromo, R., and Quax, W. J. (2009). Quorum-quenching acylase reduces the virulence of *Pseudomonas aeruginosa* in a *Caenorhabditis elegans* infection model. *Antimicrob. Agents Chemother.* 53, 4891–4897. doi: 10.1128/AAC.00380-09

Papenfort, K., and Bassler, B. L. (2016). Quorum sensing signal-response systems in Gram-negative bacteria. *Nat. Rev. Microbiol.* 14, 576–588. doi: 10.1038/nrmicro.2016.89

Passador, L., Cook, J. M., Gambello, M. J., Rust, L., and Iglewski, B. H. (1993). Expression of *Pseudomonas aeruginosa* virulence genes requires cell-to-cell communication. *Science* 260, 1127–1130. doi: 10.1126/science.8493556

Puel, O., Galtier, P., and Oswald, I. P. (2010). Biosynthesis and toxicological effects of patulin. *Toxins* 2, 613–631. doi: 10.3390/toxins2040613

Rasmussen, T. B., Skindersoe, M. E., Bjarnsholt, T., Phipps, R. K., Christensen, K. B., Jensen, P. O., et al. (2005). Identity and effects of quorum-sensing inhibitors produced by *Penicillium* species. *Microbiology* 151, 1325–1340. doi: 10.1099/mic.0.27715-0

Richman-Eisenstat, J. (1996). Cytokine soup: making sense of inflammation in cystic fibrosis. *Pediatr. Pulmonol.* 21, 3–5. doi: 10.1002/1099-0496(199601)21:1<3::AID-PPUL1950210103>3.0.CO;2-B

Ruehl-Fehlert, C., Kittel, B., Morawietz, G., Deslex, P., Keenan, C., Mahrt, C. R., et al. (2004). Revised guides for organ sampling and trimming in rats and mice–Part 2. A joint publication of the RITA* and NACAD** groups. *Exp. Toxic Pathol.* 55, 91–106. doi: 10.1078/0940-2993-00311

Sio, C. F., Otten, L. G., Cool, R. H., Diggle, S. P., Braun, P. G., Bos, R., et al. (2006). Quorum quenching by an *N*-acyl-homoserine lactone acylase from *Pseudomonas aeruginosa* PAO1. *Infect. Immun.* 74, 1673–1682. doi: 10.1128/IAI.74.3.1673-1682.2006

Southam, D. S., Dolovich, M., O'Byrne, P. M., and Inman, M. D. (2002). Distribution of intranasal instillations in mice: effects of volume, time, body position, and anesthesia. *Am. J. Physiol. Lung Cell. Mol. Physiol.* 282, L833–L839. doi: 10.1152/ajplung.00173.2001

Tateda, K., Ishii, Y., Horikawa, M., Matsumoto, T., Miyairi, S., Pechere, J. C., et al. (2003). The *Pseudomonas aeruginosa* autoinducer *N*-3-oxododecanoyl homoserine lactone accelerates apoptosis in macrophages and neutrophils. *Infect. Immun.* 71, 5785–5793. doi: 10.1128/IAI.71.10.5785-5793.2003

Telford, G., Wheeler, D., Williams, P., Tomkins, P. T., Appleby, P., Sewell, H., et al. (1998). The *Pseudomonas aeruginosa* quorum-sensing signal molecule *N*-(3-oxododecanoyl)-L-homoserine lactone has immunodulatory activity. *Inf. Immun.* 66, 36–42.

Thomas, G. L., Böhner, C. M., Williams, H. E., Walsh, C. M., Ladlow, M., Welch, M., et al. (2006). Immunomodulatory effects of *Pseudomonas aeruginosa* quorum sensing small molecule probes on mammalian macrophages. *Mol. Biosyst.* 2, 132–137. doi: 10.1039/B517248A

Tonnis, W. F., Bagerman, M., Weij, M., Sjollema, J., Frijlink, H. W., Hinrichs, W. L. J., et al. (2014). A novel aerosol generator for homogenous distribution of powder over the lungs after pulmonary administration to small laboratory animals. *Eur. J. Pharm. Biopharm.* 88, 1056–1063. doi: 10.1016/j.ejpb.2014.10.011

Uroz, S., Chhabra, S. R., Cámara, M., Williams, P., Oger, P., and Dessaux, Y. (2005). *N*-acylhomoserine lactone quorum-sensing molecules are modified and degraded by *Rhodococcus erythropolis* W2 by both amidolytic and novel oxidoreductase activities. *Microbiology* 151, 3313–3322. doi: 10.1099/mic.0.27961-0

Van Delden, C., and Iglewski, B. H. (1998). Cell-to-cell signaling and *Pseudomonas aeruginosa* infections. *Emerging Infect. Dis.* 4, 551–560. doi: 10.3201/eid0404.980405

van Heeckeren, A. M., and Schluchter, M. D. (2002). Murine models of chronic *Pseudomonas aeruginosa* lung infection. *Lab. Anim.* 36, 291–312. doi: 10.1258/002367702320162405

Wahjudi, M., Murugappan, S., van Merkerk, R., Eissens, A. C., Visser, M. R., Hinrichs, W. L. J., et al. (2012). Development of a dry, stable and inhalable acyl-homoserine-lactone-acylase powder formulation for the treatment of pulmonary *Pseudomonas aeruginosa* infections. *Eur. J. Pharm. Sci.* 48, 637–643. doi: 10.1016/j.ejps.2012.12.015

Wahjudi, M., Papaioannou, E., Hendrawati, O., van Assen, A. H. G., van Merkerk, R., Cool, R. H., et al. (2011). PA0305 of *Pseudomonas aeruginosa* is a quorum quenching acylhomoserine lactone acylase belonging to the Ntn hydrolase superfamily. *Microbiology* 157, 2042–2055. doi: 10.1099/mic.0.043935-0

Wang, W. Z., Morohoshi, T., Ikenoya, M., Someya, N., and Ikeda, T. (2010). AiiM, a novel class ot *N*-acylhomosenne lactonase from the leaf-associated bacterium *Microbacterium testaceum*. *Appl. Environ. Microbiol.* 76, 2524–2530. doi: 10.1128/AEM.02738-09

Whiteley, M., Lee, K. M., and Greenberg, E. P. (1999). Identification of genes controlled by quorum sensing in *Pseudomonas aeruginosa*. *Proc. Natl. Acad. Sci. U.S.A.* 96, 13904–13909. doi: 10.1073/pnas.96.24.13904

Winson, M. K., Swift, S., Fish, L., Throup, J. P., Jørgensen, F., Chhabra, S. R., et al. (1998). Construction and analysis of *lux*CDABE-based plasmid sensors for investigating N-acyl homoserine lactone-mediated quorum sensing. *FEMS Microbiol. Lett.* 163, 185–192. doi: 10.1111/j.1574-6968.1998.tb13044.x

Wölbeling, F., Munder, A., Kerber-Momot, T., Neumann, D., Hennig, C., Hansen, G., et al. (2011). Lung function and inflammation during murine *Pseudomonas aeruginosa* airway infection. *Immunobiology* 216, 901–908. doi: 10.1016/j.imbio.2011.02.003

Wölbeling, F., Munder, A., Stanke, F., Tümmler, B., and Baumann, U. (2010). Head-out spirometry accurately monitors the course of *Pseudomonas aeruginosa* lung infection in mice. *Respiration* 80, 340–346. doi: 10.1159/000319442

Wu, H., Song, Z., Givskov, M., Doring, G., Worlitzsch, D., Mathee, K., et al. (2001). *Pseudomonas aeruginosa* mutations in lasI and rhlI quorum sensing systems result in milder chronic lung infection. *Microbiology* 147, 1105–1113. doi: 10.1099/00221287-147-5-1105

Wu, H., Song, Z., Hentzer, M., Andersen, J. B., Molin, S., Givskov, M., et al. (2004). Synthetic furanones inhibit quorum-sensing and enhance bacterial clearance in *Pseudomonas aeruginosa* lung infection in mice. *J. Antimicrob. Chemother.* 53, 1054–1061. doi: 10.1093/jac/dkh223

Conflict of Interest Statement: The authors declare that the research was conducted in the absence of any commercial or financial relationships that could be construed as a potential conflict of interest.

frontiers in Cellular and Infection Microbiology

ORIGINAL RESEARCH
published: 13 September 2018
doi: 10.3389/fcimb.2018.00310

Multiple Quorum Quenching Enzymes Are Active in the Nosocomial Pathogen *Acinetobacter baumannii* ATCC17978

Celia Mayer[1], *Andrea Muras*[1], *Manuel Romero*[1†], *María López*[2], *María Tomás*[2] *and Ana Otero*[1*]

[1] Department of Microbiology and Parasitology, Faculty of Biology-CIBUS, Universidade de Santiago de Compostela, Santiago de Compostela, Spain, [2] Department of Microbiology, Complejo Hospitalario Universitario A Coruña-INIBIC, A Coruña, Spain

Acinetobacter baumannii presents a typical *lux*I/*lux*R quorum sensing (QS) system (*abaI*/*abaR*) but the acyl-homoserine lactone (AHL) signal profile and factors controlling the production of QS signals in this species have not been determined yet. A very complex AHL profile was identified for *A. baumannii* ATCC17978 as well as for *A. nosocomialis* M2, but only when cultivated under static conditions, suggesting that surface or cell-to-cell contact is involved in the activation of the QS genes. The analysis of *A. baumanni* clinical isolates revealed a strain-specific AHL profile that was also affected by nutrient availability. The concentration of OHC12-HSL, the major AHL found in *A. baumannii* ATCC17978, peaked upon stationary-phase establishment and decreases steeply afterwards. Quorum quenching (QQ) activity was found in the cell extracts of *A. baumannii* ATCC17978, correlating with the disappearance of the AHLs from the culture media, indicating that AHL concentration may be self-regulated in this pathogen. Since QQ activity was observed in strains in which AidA, a novel α/β-hydrolase recently identified in *A. baumannii*, is not present, we have searched for additional QQ enzymes in *A. baumannii* ATCC17978. Seven putative AHL-lactonase sequences could be identified in the genome and the QQ activity of 3 of them could be confirmed. At least six of these lactonase sequences are also present in all clinical isolates as well as in *A. nosocomialis* M2. Surface-associated motility and biofilm formation could be blocked by the exogenous addition of the wide spectrum QQ enzyme Aii20J. The differential regulation of the QQ enzymes in *A. baumannii* ATCC17978 and the full dependence of important virulence factors on the QS system provides a strong evidence of the importance of the AHL-mediated QS/QQ network in this species.

Keywords: ***Acinetobacter baumannii*, quorum sensing, AHL, quorum quenching, lactonase**

OPEN ACCESS

Edited by:
Margaret E. Bauer, Indiana University Bloomington, United States

Reviewed by:
Sunil D. Saroj, Symbiosis International University, India
Amit Kumar Mandal, Raiganj University, India

***Correspondence:**
Ana Otero
anamaria.otero@usc.es

***Present Address:**
Manuel Romero, Centre for Biomolecular Sciences, School of Life Sciences, University of Nottingham, Nottingham, United Kingdom

Specialty section:
This article was submitted to Molecular Bacterial Pathogenesis, a section of the journal Frontiers in Cellular and Infection Microbiology

Received: *04 May 2018*
Accepted: *14 August 2018*
Published: *13 September 2018*

Citation:
Mayer C, Muras A, Romero M, López M, Tomás M and Otero A (2018) Multiple Quorum Quenching Enzymes Are Active in the Nosocomial Pathogen Acinetobacter baumannii ATCC17978. Front. Cell. Infect. Microbiol. 8:310. doi: 10.3389/fcimb.2018.00310

INTRODUCTION

Acinetobacter spp. are Gram-negative, strictly aerobic coccobacilli belonging to the Gammaproteobacteria class and *Pseudomonales* order, broadly distributed in the natural environment, including soil, water and vegetation (Bergogne-Bérézin and Towner, 1996). Although the genus *Acinetobacter* includes non-pathogenic species that are present in the human skin, several *Acinetobacter* species cause a variety of opportunistic nosocomial infections including septicemia, pneumonia, endocarditis, meningitis, skin, wound, and urinary tract infections (Bergogne-Bérézin and Towner, 1996; Towner, 2009). *Acinetobacter baumannii*, the most relevant pathogenic species in the genus, has emerged as one of the most troublesome hospital-acquired pathogens (Peleg et al., 2008). Since the increase in the prevalence of multidrug resistant strains has reduced the treatment options for this pathogen (Rice, 2006; Peleg et al., 2008), *A. baumannii* is considered as an ESKAPE pathogen (Rice, 2008). Therefore, a better understanding of the mechanisms controlling the expression of virulence traits and propagation in *Acinetobacter* spp. has become critical for the discovery and development of new therapeutic strategies for these bacteria.

Important virulence traits such as motility and biofilm formation have been proposed to be under control of an *N*-acyl-homoserine lactone (AHL)-mediated quorum sensing (QS) system in different species of the *A. calcoaceticus-A. baumannii* complex (Niu et al., 2008; Kang and Park, 2010; Clemmer et al., 2011; Anbazhagan et al., 2012; Bhargava et al., 2012; Chow et al., 2014; Oh and Choi, 2015). *A. nosocomialis* M2, formerly identified as *A. baumannii* (Carruthers et al., 2013), presents a typical LuxI/LuxR-type QS network, constituted by the AHL-synthase AbaI and the AHL-receptor and transcriptional activator AbaR (Niu et al., 2008; Bhargava et al., 2010). Genes homologous to *abaI* and *abaR* of *A. nosocomialis* M2 can be found in *A. baumannii* (Smith et al., 2007; Niu et al., 2008) and in the genomes of other *Acinetobacter* species (Kang and Park, 2010; Bitrian et al., 2012; How et al., 2015; Oh and Choi, 2015). Moreover, a number of studies have described the generation of AHL signals in members of the genus (Niu et al., 2008; Chan et al., 2011, 2014; How et al., 2015). In *A. nosocomialis* M2, the signal *N*-hydroxydodecanoyl-L-homoserine lactone (OHC12-HSL) has been identified as the major AHL together with minor amounts of five additional signals (Niu et al., 2008). OHC10-HSL was identified as the major AHL produced when the synthase of a clinical isolate of *A. baumannii* was over-expressed in *Escherichia coli* (Chow et al., 2014), but the profile and factors affecting AHL production in cultures of *A. baumannii* has not been reported yet.

The capacity to degrade AHL-type QS signals, an activity known as Quorum Quenching (QQ) has been described in several environmental *Acinetobacter* isolates: the acylase AmiE, identified in *Acinetobacter* sp. Ooi24, isolated from activated sludge in a wastewater treatment plant (Ochiai et al., 2014) and the lactonase AidE, identified in *Acinetobacter* sp. 77 (Liu et al., 2017). Several other environmental strains with QQ activity have been described, but the enzymes responsible for the activity were not identified (Kang et al., 2004; Chan et al., 2011; Ochiai et al., 2013; Kim et al., 2014; Arivett et al., 2015). Putative lactonases have been identified in *A. baumannii* genomes of environmental and clinical origin (Vallenet et al., 2008; Kang and Park, 2010; Arivett et al., 2015), but the QQ activity of the strains or the catalytic activity of the enzyme has not been demonstrated. Recently, a novel enzyme capable of degrading AHLs has been identified in *A. baumannii* (López et al., 2017). The enzyme, named AidA, is a novel α/β hydrolase and is present in several clinical isolates of *A. baumannii*, but could not be identified in isolate Ab7, the only motile strain under permissive conditions. The role of AHL-mediated QS in motility has been previously described in *A. nosocomialis* M2 (Clemmer et al., 2011) and therefore, the absence of AidA could have explained the increase in motility capacity in this strain (López et al., 2017). This hypothesis was further supported by the fact that the addition of the wide spectrum AHL-degrading enzyme Aii20J (Mayer et al., 2015) completely blocked motility in Ab7 (López et al., 2017). Nevertheless, an analysis of the genomes of the well-studied strain *A. baumannii* ATCC17978, that is motile under permissive conditions (unpublished results), revealed that AidA is present, opening a question on the role of AidA in the control of QS-related phenotypes.

Therefore, in this work we have analyzed the production of QS signals and QQ capacity in *A. baumannii* ATCC17978 and compare it with the well-studied species *A. nosocomialis* M2 (formerly classified as *A. baumannii*). AHL production and QQ activity was also studied in 7 clinical isolates of *A. baumannii* (López et al., 2017). Since the analysis revealed the presence of QQ activity in *A. nosocomialis* M2, but the QQ enzyme AidA is not present in the genome of this strain, we also carried out a search in order to identify possible additional QQ enzymes in *A. baumannii* ATCC17978. We provide evidence that growth under static conditions is critical for AHL production in these pathogens and that QQ activity could be responsible for the decrease of AHL concentration observed in the onset of stationary phase. Three AHL-lactonases could be cloned and over-expressed in *E. coli*, confirming its QQ activity. The exogenous addition of the wide-spectrum QQ enzyme Aii20J (Mayer et al., 2015) completely blocked surface-associated motility and biofilm formation in *A. baumannii* ATCC17978, confirming the relevance of the QS system for key virulence traits in this species.

MATERIALS AND METHODS

Bacterial Strains, Culture Conditions, and Genetic Methods

Bacterial strains, plasmids, and primers used in this study are listed in **Table 1**. LB broth and agar were used to routinely grow and maintain *Acinetobacter* spp. at 37°C. *Chromobacterium violaceum* biosensor strains were routinely cultured on LB medium at 30°C. Antibiotics were added at final concentrations of 25–50 μg/mL kanamycin or 25 μg/mL tetracycline as required.

TABLE 1 | Bacterial strains, plasmids, and primers used in this study.

Strain or plasmid	Description	Source or references
STRAINS		
Acinetobacter baumannii		
ATCC17978		ATCC[a]
Ab1 (ROC013)	*A. baumannii* clinical isolate (respiratory). TM: ST2	INIBIC[b]
Ab2 (COR005)	*A. baumannii* clinical isolate (ulcer). TM: ST186	INIBIC[b]
Ab3 (PON002)	*A. baumannii* clinical isolate (respiratory). TM: ST52	INIBIC[b]
Ab4 (VAL001)	*A. baumannii* clinical isolate (respiratory). TM: ST169	INIBIC[b]
Ab5 (DOM009)	*A. baumannii* clinical isolate (respiratory). TM: ST80	INIBIC[b]
Ab6 (HMV001)	*A. baumannii* clinical isolate (exudate). TM: ST181	INIBIC[b]
Ab7 (HUI001)	*A. baumannii* clinical isolate (blood). TM: ST79	INIBIC[b]
Acinetobacter nosocomialis		
M2		Niu et al., 2008
Chromobacterium violaceum		
CV026	AHL biosensor, Km^r	McClean et al., 1997
VIR07	AHL biosensor, Km^r	Morohoshi et al., 2008
Escherichia coli		
BL21(DE3)plysS	F– *ompT hsdS*$_B$ (r_B-, m_B-) *dcm gal* λ(DE3) pLysS Cm^r	Promega
XL1blue	*recA1 endA1 gyrA96 thi-1 hsdR17 supE44 relA1 lac* [*F′ proAB lacIq ZΔM15* Tn10 (Tet^r)]	Agilent
PLASMIDS		
pET28c(+)	Cloning vector, Km^r	Novagen
pET28c(+)-*aidA*	pET28c(+) containing *aidA* gene from *A. baumannii* ATCC17978	This study
pET28c(+)-*aii20J*	pET28c(+) containing *aii20J* gene from *Tenacibaculum* sp. 20J	Mayer et al., 2015
pET28c(+)-A1S_0383	pET28c(+) containing *a1s_0383* gene from *A. baumannii* ATCC17978	This study
pET28c(+)-A1S_1876	pET28c(+) containing *a1s_1876* gene from *A. baumannii* ATCC17978	This study
pET28c(+)-A1S_2662	pET28c(+) containing *a1s_2662* gene from *A. baumannii* ATCC17978	This study
Primers	**Sequence (5′-3′)**	**Use in this work**
*abaI*_Fwd	TGTGCCAGACTACTACCCAC	qRT-PCR
*abaI*_Rev	TGCTAGAGGAAGGCGGATTT	qRT-PCR
*abaR*_Fwd	TTGGTCGAGTCAATCTGCAA	qRT-PCR (Eijkelkamp et al., 2013)
*abaR*_Rev	CTCGGGTCCCAATAAAATCA	qRT-PCR (Eijkelkamp et al., 2013)
*csuD*_Fwd	AGTCACAACATCGGTCCCAT	qRT-PCR
*csuD*_Rev	AAGTTCGGTGCGTCCTTCTA	qRT-PCR
*rpoB*_Fwd	GTGCTGACTTGACGCGTGAT	qRT-PCR (Park and Ko, 2015)
*rpoB*_Rev	AGCGTTCAGAAGAGAAGAACAAGTT	qRT-PCR (Park and Ko, 2015)
A1S_0383_Fwd	ACCAGGTCACGTCATGTTCT	qRT-PCR
A1S_0383_Rev	TGGTACTCATTGGCCCATGT	qRT-PCR
A1S_1708_Fwd	ATTGAAGCGCGTTACACACC	qRT-PCR
A1S_1708_Rev	ATAGTGTTGTCAGGCAGGCT	qRT-PCR
A1S_1876_Fwd	GCAGTCATATGGTCCGCATG	qRT-PCR
A1S_1876_Rev	TTAGCAACCCGTCAATGTGC	qRT-PCR
A1S_2194_Fwd	TCCCTGGCATTACTCATCCC	qRT-PCR
A1S_2194_Rev	TTCAAATAGTCGCCCGCATC	qRT-PCR
A1S_2662_Fwd	TCTGCTTCACGTTCATGAGC	qRT-PCR
A1S_2662_Rev	CTGCGAGTTGTTTTGGTCCA	qRT-PCR
A1S_2864_Fwd	GCCACTGAATACAATGCTGC	qRT-PCR
A1S_2864_Rev	TCGCAATACCACAATGTCCG	qRT-PCR
*aidA*_Fwd	TCGCTGCACGTTTTGTACTC	qRT-PCR
*aidA*_Rev	CCATCGGCGTAGTGCTTAAT	qRT-PCR
0383Fwd	GATTAACCATGGTACTGCAAGTCAAAATTGTTCCAG (NcoI)[c]	Cloning
0383Rev	GCTATGAATTCAAACCCGCTTTACCTGCGACAAACG (EcoRI)[c]	Cloning

(Continued)

TABLE 1 | Continued

Primers	Sequence (5′-3′)	Use in this work
1876Fwd	GATTAACCATGGTACAACAACCTCTAGTAAAAGA(NcoI)[c]	Cloning
1876Rev	GCTATGAATTCAAAAAGTAATTAAATGGGATT (EcoRI)[c]	Cloning
2662Fwd	GATTAACCATGGTAAAAAAACTATTTGTAGCCTTAGG (NcoI)[c]	Cloning
2662Rev	GCTATGAATTCAATTTATCAAGACTGTTATTA (EcoRI)[c]	Cloning
*aidA*Fwd	GATTAACCATGGTA.GGTAAAAGTCTAAATAATGT	Cloning
*aidA*Rev	GCTATGAATTCAACTTGACTGGAACGATGCGTTTA	Cloning
T7Fwd	TAATACGACTCACTATAGGGGAA	Universal primer
T7Rev	GCTAGTTATTGCTCAGCGG	Universal primer
luxI PF	GGTTGGGAGTTGAACTGTCC	*abaI* amplification (Bitrian et al., 2012)
luxI PR	GGTTGGGAGTTGAACTGTCC	*abaI* amplification (Bitrian et al., 2012)
luxR PF	TCGGATTTGATTATTGCGCTTATG	*abaI* amplification (Bitrian et al., 2012)
luxR PR	ACAGCTCGAATAGCTGCTG	*abaI* amplification (Bitrian et al., 2012)

[a] *American Type Culture Collection.*
[b] *Instituto de Investigación Biomédica (A Coruña).*
[c] *Restriction sites for indicated enzymes are underlined.*

AHL Profile Identification

The AHL profiles of *A. baumannii* ATCC17978 and *A. nosocomialis* M2 were obtained from 100 mL static and shaken liquid cultures grown for 0, 6, 12, 17, 24, 36, and 48 h at 37°C in LB. To compare the effect of culture media static and shaken cultures of *A. baumannii* ATCC17978 were also grown in LB (1% NaCl, 1% tryptone, and 0.5% yeast extract), low-nutrient low-salt LB (0.5% NaCl, 0.2% tryptone, and 0.1% yeast extract; LNLS-LB), low-salt LB (0.5% NaCl, 1% tryptone, and 0.5% yeast extract; LS-LB), or buffered LB (PIPES buffer, 200 mM, pH 6.7) for 17 h at 37°C. Cells were removed by centrifugation and supernatants were extracted twice with an equal volume of dichloromethane. Solvent was evaporated to dryness in a rotary evaporator at 40°C. Extracts were then dissolved in 1 mL of acetonitrile and signals were identified and quantified by HPLC-MS methodology using AHL synthetic standards as reference (Romero et al., 2014). Extracts from non-inoculated culture media incubated the same way were used as controls.

Detection of Quorum Quenching Activity

C. violaceum-based solid plate assays were carried out to detect AHL degradation activity in *A. baumannii* ATCC17978 and *A. nosocomialis* M2 as described before (Romero et al., 2010). In brief, *Acinetobacter* spp. pellets were collected from LB cultures at different times of the same growth curve of the previous section (6, 12, 17, 24, 36, and 48 h), washed in phosphate buffer saline (PBS) pH 6.7, disrupted by sonication on ice, centrifuged and filtered (0.20 μm) to obtain the cell extracts. Five hundred microliters of aliquots from each cell extract were exposed to 10 μM C6 or C12-HSL and incubated for 24 h at 22°C with shaking. In order to detect AHL inactivation activity, 100 μL of the reaction mixtures were spotted in wells made in LB plates overlaid with 5 mL of a 1/100 dilution of an overnight culture of *C. violaceum* CV026 for C6-HSL or VIR07 for C12-HSL in soft agar (0.8%). Plates were incubated for 24 h at 30°C, and the production of violacein was examined. PBS buffer plus AHLs incubated the same way were used as controls in all plates.

Confirmation of the QQ activity of *A. baumannii* ATCC17978 was performed by HPLC-MS analysis. The cell extract from a 50 mL culture in LB of ATCC17978 grown for 24 h was obtained. Then, C12 and OHC12-HSL signals (10 μM) were incubated with the cell extract at 22°C with shaking. After 24 h exposure, 200 μL of the reaction mixtures were extracted three times with the same volume of ethyl acetate with or without previous acidification to pH 2.0 for 24 h. Solvent was evaporated under nitrogen flux and suspended in acetonitrile for AHL quantification as previously described (Romero et al., 2014). PBS plus the same amount of C12 or OHC12-HSL were used as controls.

Identification and Cloning of QQ Sequences

The genomic DNA from different clinical isolates and *A. baumannii* ATCC17978 was used as template for PCR detection of *abaI*/*abaR* homologous. Genomic DNA was extracted with Wizard® Genomic DNA Purification Kit (Promega). Primers *luxI* PF, *luxI* PR, *luxR* PF, and *luxR* PR were used for *abaI*/*abaR* homologous amplification with the PCR conditions used by Bitrian et al. (2012). PCR products of the synthase and receptor (about 370 and 600 bp, respectively) were then sequenced, and analyzed using the MEGA 6 phylogenetic tool software package (Tamura et al., 2013) using the default parameters.

Bioinformatic tools such as blast (https://blast.ncbi.nlm.nih.gov/Blast.cgi) and cd-search (https://www.ncbi.nlm.nih.gov/Structure/cdd/wrpsb.cgi) from NCBI were used for identification of new QQ sequences in the *A. baumannii* ATCC17978 genome. Sequences were aligned with Clustal Omega (https://www.ebi.ac.uk/Tools/msa/clustalo/) or MUSCLE programs from EMBL-EMI (https://www.ebi.ac.uk/Tools/msa/muscle/) and shaded using the GeneDoc 2.7 program.

QQ sequences were amplified by PCR using genomic DNA and primers listed in **Table 1**. PCR conditions included denaturation at 94°C, 5min; 30 cycles of 95°C, 45 s; 55°C, 45 s; and 72°C, 1 min, with a final extension for 10 min. The PCR products from QQ enzymes were purified, digested with EcoRI and NcoI (Thermo Scientific), and cloned into the EcoRI and NcoI sites of vector pET28c(+) using T4DNA ligase (Thermo Scientific), to introduce six histidine residues in the C terminus of the protein, and transformed by electroporation into *E. coli* XL1blue and then in *E. coli* BL21(DE3) plysS. The *E. coli* BL21(DE3)plysS strains expressing recombinant proteins were inoculated into fresh LB medium with kanamycin (25 μg/mL) at 37°C with shaking. After the OD600 of the culture reached 0.6, the protein expression was induced by the addition of isopropyl-D-thiogalatopyranoside (IPTG) to a final concentration of 1 mM followed by further incubation for 5 h. After incubation, cells were harvested by centrifugation, resuspended with 20 mL of PBS buffer, lysed by sonication on ice, and centrifuged at 4°C (2,000×g for 5 min). QQ enzymes were purified using the His GraviTrap™ affinity column (GE Healthcare) protein purification kit. Purified proteins were measured by a UV-Vis Spectrophotometer Q5000 (Quawell) and analyzed with 12% SDS-PAGE.

Characterization of QQ Enzymes

QQ activity of QQ purified enzymes was confirmed with *C. violaceum* based assays. Purified proteins concentration was measured and the minimum active concentration (MAC) of each enzyme was stablished as the protein concentration in the highest decimal dilution being able to completely remove the activity of a 10 μM solution of C12-HSL in 24 hours, as detected by the *C. violaceum* VIR07 biosensor assay.

In order to determinate the specificity of purified QQ proteins a 10xMAC concentration of each enzyme was mixed with several AHLs at 10 μM in PBS pH 6.7, for 24 h, and incubated at 22°C, with shaking. The remaining signal was detected in solid plate assay with *C. violaceum* CV026 or VIR07 as explained before. Controls of PBS with the same amount of AHL were processed in the same way. AHL degradation specificity of purified enzymes was evaluated with synthetic signals: *N*-hexanoyl-L-homoserine lactone (C6-HSL), *N*-octanoyl-L-homoserine lactone (C8-HSL), *N*-decanoyl-L-homoserine lactone (C10-HSL), *N*-3-oxodecanoyl-homoserine lactone (OC10-HSL), *N*-hydroxydecanoyl-L- homoserine lactone (OHC10-HSL), *N*-dodecanoyl-L- homoserine lactone (C12-HSL), *N*-3-oxododecanoyl-L- homoserine lactone (OC12-HSL), *N*-hydroxydodecanoyl-L- homoserine lactone (OHC12-HSL), *N*-3-oxotridecanoyl-L- homoserine lactone (OC13-HSL), *N*-tetradecanoyl-L-homoserine lactone (C14-HSL), and *N*-3-oxotetradecanoyl-L-homoserine lactone (OC14-HSL).

Bacterial RNA Isolation and Quantitative Real Time PCR (qPCR)

For relative transcript levels quantification of selected genes, quantitative PCR (qPCR) was performed using cDNA from cultures of *A. baumannii* ATCC17978 grown at 37°C in LB or LS-LB with or without agitation. *Acinetobacter baumannii* cells were grown up to an optical density (600 nm) of 0.6 and total RNA was isolated using the RNase Mini Kit (Qiagen) and then treated with the Turbo DNA-free DNase kit (Ambion) following manufacture's instructions. DNA contamination was evaluated by PCR with 1 μL of purified RNA as template. RevertAid Reverse Transcriptase and random hexamers (Thermo Fisher Scientific) were used to synthesize complementary deoxyribonucleic acid (cDNA) according to the manufacturer's protocol.

qPCR was performed by using FastStart SYBR Green Master (Roche). Each 20 μL reaction mixture contained 1X FastStart SYBR Green Master, 300 nM primers, and 2 ng cDNA template. The oligonucleotides used in this study for qPCR were designed using the software Primer3 (http://bioinfo.ut.ee/primer3/) and are listed in **Table 1**. The efficiency of each primer pair was determined by carrying out RT-PCR on serial dilutions of cDNA, and the specificity was verified by melting-curve analyses (1 cycle of 95°C for 1 min and another cycle of 60°C for 1 min followed by melting at 0.5°C increments for 10 s to 95°C). Following the verification of primer efficiency and specificity, qPCR analyses were routinely carried out with an iCycler iQ5 real-time PCR detection system (Bio-Rad) according to the following amplification protocol: 95°C for 10 min followed by 40 cycles of 95°C for 20 s, 56°C for 30 s, and 72°C or 40 s. qPCRs were performed in duplicate and samples containing no reverse transcriptase or template RNA were included as negative controls. Data were analyzed by using iQ5 Optical System software (Bio-Rad), and the relative quantification was determined by the $\Delta\Delta C_T$ method normalizing to the transcription levels of the housekeeping *rpoB* gene (Livak and Schmittgen, 2001).

Motility and Biofilm Assays

Surface-associated motility assays were performed on Petri dishes with LB or LNLS-LB in 0.25% Eiken Agar (Eiken Chemical Co. Ltd. Japan). One microliter of 17-h cultures at an OD600 of 0.3 was inoculated in the center of the plates. The QQ enzyme Aii20J was mixed with the inoculum at a concentration of 20 μg/mL (López et al., 2017). Plates were incubated at 37°C for 14 h. Three plates were inoculated for each condition and experiments were repeated at least twice.

Biofilm was formed on the surface of suspended 18x18 mm coverslips using a modification of the Amsterdam active attachment model (Exterkate et al., 2010). Coverslips were submerged vertically in 3 mL of low-salt (0.5%) LB medium in 12-well cell culture plates inoculated with 17 h cultures at an OD600 of 0.05. Cultures were maintained for 4 days at 37°C and culture medium was exchanged daily. The QQ enzyme Aii20J (Mayer et al., 2015) was added with every medium exchange at a concentration of 20 μg/mL. For each condition two coverslips were stained with crystal-violet (Muras et al., 2018b) and another two were stained with LIVE/DEAD® BacLight™ Bacterial Viability Kit (Invitrogen) and observed with a Leica TCS SP5 X confocal laser scanning microscope (Leica Microsystem Heidelberg GmbH, Mannheim, Germany) with an HC PL APO 10×/0.4 CS objective.

Statistical Methods

Student's *t*-test for independent samples ($P < 0.05$) were applied for all statistical analyses.

RESULTS

Identification of AHL Profile in *A. baumannii* ATCC17978

We first analyzed the AHL profile and production kinetics in *A. baumannii* ATCC17978 by sampling at different time points during the growth curve. The cultures were done in LB and LB buffered with PIPES (pH 6.5) in order to avoid the spontaneous hydrolysis of the AHLs as basic pH (Yates et al., 2002). The same experiment was carried out with the well-studied species *A. nosocomialis* M2 in order to compare the production kinetics between both strains. Surprisingly, no AHL signal could be detected in 100-fold-concentrated extracts of culture media supernatants in shaken cultures for both, *A. baumannii* ATCC17978 and *A. nosocomialis* M2, as well as in the other *A. baumannii* clinical isolates analyzed (data not shown). On the contrary, a complex AHL profile was detected when the strains were grown under static conditions (**Tables S1**, **S2**). The differences in growth under static and shaken conditions were small after the first 10 h of culture, and therefore oxygen limitation can be disregarded as the main factor affecting AHL production under static conditions (**Figure S1**).

OHC12-HSL was identified as the major AHL signal found in the culture medium of *A. baumannii* ATCC17978 static cultures (**Figure S2**, **Table S1**). This AHL was also the main signal detected in *A. nosocomialis* M2, as reported previously (**Table S1;** Niu et al., 2008). Several additional signals were identified in both species, including OHC10-HSL, OC12-HSL and OHC14-HSL, although at much lower concentrations (**Table S1**). Minor amounts (0.2–1.5 nM) of C6, OC6, and C8, were also present in *A. baumannii* ATCC17978 only in LB medium in the 17 h sample (data not shown). Besides these 3 short-chain AHLs, OC8, and OHC8 were also found at concentrations lower than 1 nM in *A. nosocomialis* M2 in the same conditions. The concentration of AHLs peaked around 17–24 h of culture, coinciding with late logarithmic phase/early stationary phase, and suffered a steep decrease thereafter, being almost undetectable in supernatant samples after 36 h in unbuffered cultures (**Figure 1A**). Buffering of the culture media produced a higher maximal concentration of OHC12-HSL that reached 64.56 ng mL^{-1} while only 30.74 ng mL^{-1} were achieved in the unbuffered medium (**Figure 1A**). In any case, buffering the culture medium did not prevent the decrease in the signal concentration, suggesting an active AHL degradation. Furthermore, as for OHC12-HSL, the concentration of the other AHLs peaked around 17–24 h and decreased thereafter (**Table S1**). The production kinetics of OHC12-HSL was very similar in *A. nosocomialis* M2 in LB medium, but a lower maximal concentration was achieved: 17.23 ng mL^{-1}. Surprisingly, buffering the culture medium almost completely abolished the production of AHLs in this species (**Figure S3**).

To assess the possible effect of culture media on AHL production, AHL concentration was quantified after 17 h in liquid cultures of ATCC17978 grown in LB, nutrient-depleted, low-salt LB (LNLS-LB), and low-salt LB (LS-LB) with or without shaking (**Figure 2**). Previous results indicated that the expression of QS-related phenotypes, such as motility or biofilm formation, was enhanced with low-salt media (Pour et al., 2011; McQueary et al., 2012) and therefore we intended to see if these phenotypic changes were accompanied by an increase in AHL concentration. Supporting the importance of the static conditions for AHL production, no signal could be detected in supernatants of shaken cultures in any of the culture media tested (data not shown). In contrast, the major signal OHC12-HSL was produced in static cultures with a remarkable increase of concentration in LS-LB medium (**Figure 2**), a condition that enhances QS-related traits such as motility and biofilm formation (Pour et al., 2011; McQueary et al., 2012). The reduction of NaCl concentration did not affect growth in ATCC17978 (**Figure S1**).

As for ATCC17978 and *A. nosocomialis* M2, no AHL could be detected in the supernatants of shaken cultures of different *A. baumannii* clinical isolates. In static cultures the AHL profile changed among the clinical isolates analyzed. OHC12-HSL could be detected in only 3 of the 7 strains analyzed after 24 h in LB. This signal could be detected in all strains in LNLS-LB, although at much lower concentration. OHC10-HSL, OC12-HSL, OC14-HSL, and OHC14-HSL were also present in the clinical strains, but with a variable pattern (**Table S2**). The gene *abaI* could be amplified by PCR in all strains, sharing more than 98% of identity with the *abaI* gene of *A. baumannii* ATCC17978 (**Figure S4**). *abaR* genes could also be amplified by PCR in all clinical strains, sharing a 99% of identity with the *abaR* gene of ATCC17978 (data not shown).

Expression of *abaI*/*abaR* Under Different Conditions

To assess whether the presence of AHLs only under static conditions was derived from differences in the expression of QS genes, a qPCR was performed with RNA extracted after 6 h from static and shaken cultures of *A. baumannii* ATCC17978 in LB or LS-LB media. Results showed that static cultures and especially static cultures in LS-LB induced the expression of the AHL synthase gene *abaI* (A1S_0109) (**Figure 3A**), correlating with the presence of AHLs in the culture media. On the contrary, the expression of the synthase in shaken cultures was very low, independently of the culture media used. These results support a correlation between AHL production in ATCC17978 and growth in static conditions, excluding that the absence of AHL production observed in shaken cultures is derived from a fast turn-over of the signals. In contrast, the expression of the AHL receptor *abaR* did not show significant changes except for a slight increase in static cultures with LS-LB medium (**Figure 3A**). The *csuD* gene, an outer membrane protein required for type I pili biogenesis that is under the control of QS in *Acinetobacter* spp. (Tomaras et al., 2003, 2008; Clemmer et al., 2011; Luo et al., 2015; Chen et al., 2017), showed an expression pattern similar to the QS synthase (**Figure 3B**), which confirms that static conditions result in the overexpression of the QS operon and their related genes.

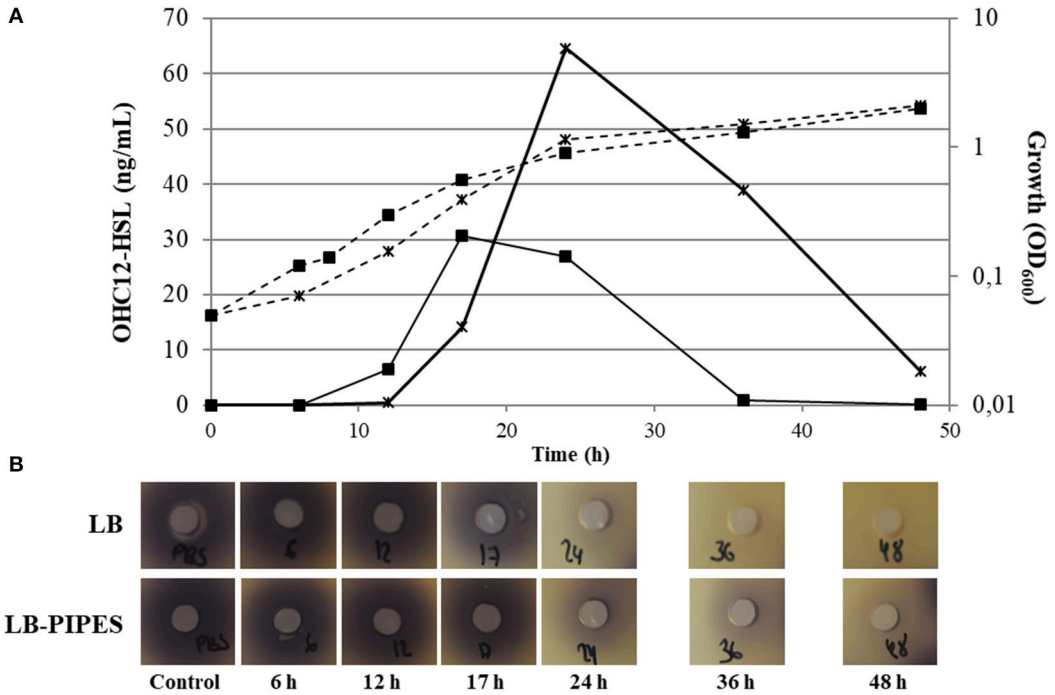

FIGURE 1 | (A) OHC12-HSL production kinetics (continuous lines) and growth curves (discontinuous lines) in static cultures of *A. baumannii* ATCC17978 grown in LB (filled squares) or buffered LB (black cross) (200 mM PIPES buffer, pH 6.7) at 37°C for 48h. **(B)** Bioassay with *C. violaceum* VIR07 to detect QQ activity in cell extracts of *A. baumannii* ATCC17978. The degradation activity against exogenous C12-HSL (10 μM) was assayed in cell extracts obtained at different time points of the growth curve (6, 12, 17, 24, 36, and 48 h) under static conditions. The presence of QQ activity is revealed by the absence of violacein around the wells. PBS plus AHL samples were treated in the same way and were used as negative controls (Control).

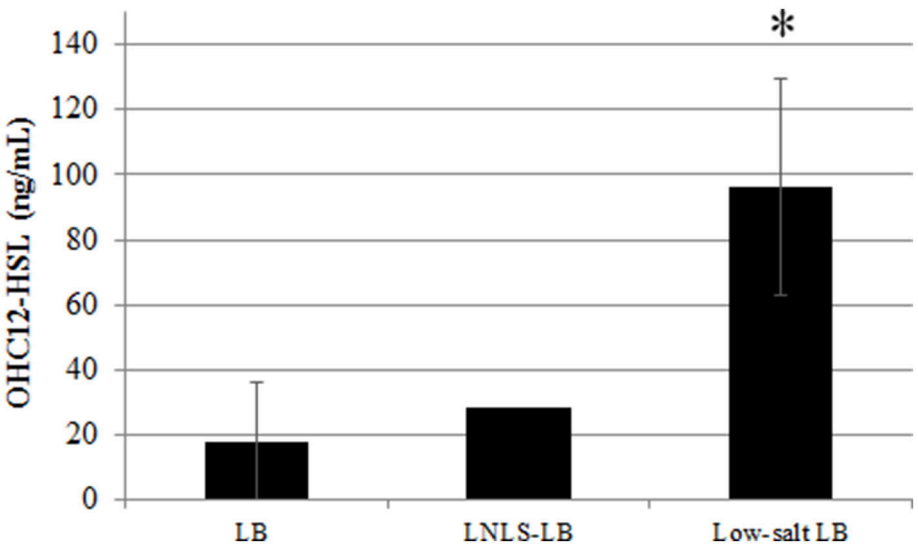

FIGURE 2 | OHC12-HSL concentration of *A. baumannii* ATCC17978 grown in LB, low-nutrient low-salt LB (LNLS-LB), and low-salt LB in static cultures maintained at 37°C during 17 h. Data are means ± SD of three independent experiments. Asterisk indicate statistically significant changes (Student's *t*-test, $p < 0.05$) with respect to the LB control.

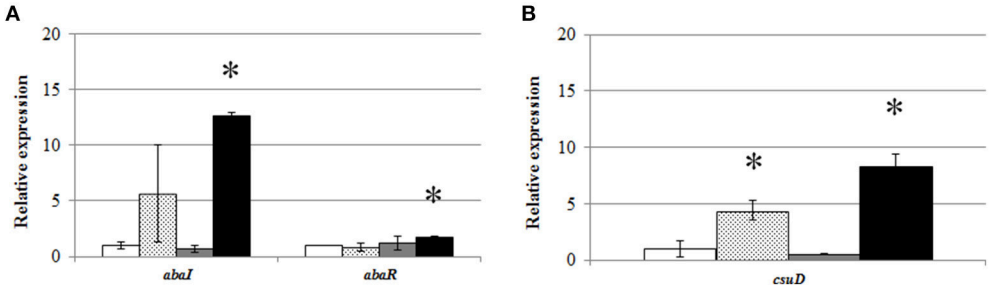

FIGURE 3 | Relative expression of **(A)** *abaI* and *abaR,* and **(B)** *csuD,* genes from *A. baumannii* ATCC17978 in shaken LB (white bars), static LB (dotted bars), shaken low-salt LB (gray bars), or static low-salt LB (black bars) cultures. Gene expression was normalized in relation to the *rpoB* gene and gene expression values in static LB were adjusted to 1.0. Error bars represent the standard deviations. Asterisk indicate statistically significant changes (Student's *t*-test, $p < 0.05$) with respect to the static LB condition.

Quorum Quenching Activity in *A. baumannii* ATCC17978 and *A. nosocomialis* M2

On the basis of the recent identification of the novel α/β hydrolase AidA in several clinical isolates of *A. baumanni* (López et al., 2017), that is also present in the genome of *A. baumannii* ATCC17978, we hypothesized that an enzymatic degradation of AHLs could cause the steep drop of OHC12-HSL concentration observed in static cultures (**Figure 1A**). To test this, QQ assays against the signals *N*-hexanoyl-L-homoserine lactone (C6-HSL) and *N*-dodecanoyl-L-homoserine lactone (C12-HSL) were performed using cell extracts obtained at different points of the growth curve under static conditions. QQ activity against C12-HSL was detected in cell extracts of *A. baumannii* ATCC17978 in 24-h cultures in both LB and buffered LB, showing a clear correlation with the disappearance of the AHLs (**Figure 1B**). In ATCC17978 no QQ activity could be found in earlier samples even in 50-fold concentrated cell extracts (data not shown). Interestingly, none of the cell extracts was able to degrade C6-HSL, suggesting that the QQ present is specific for long-chain AHLs and could be responsible for the steep drop in OHC12-HSL concentration observed in supernatants of ATCC17978 cultures. The activity was also present in cell extracts obtained from shaken cultures, indicating that high AHL concentration is not required for the expression of QQ genes. The analysis of QQ activity in the supernatants of ATCC17978 cultures revealed QQ activity against long-chain AHL with a time-dependent pattern similar to the one observed in cell extracts. QQ activity against C6-HSL was also observed in the supernatants starting at the 24-h samples (data not shown). Since the pH of supernatants reached pH values of 7.8, the experiment was repeated buffering the media at pH 6.7 to avoid the spontaneous lactonolysis of the QS signals. The QQ against C6-HSL was maintained in these buffered supernatants, demonstrating the presence of enzymatic activity (data not shown). QQ activity against long-chain AHLs was also found in the cell extracts of *A. nosocomialis* M2, correlating with the concentration of the major AHL (**Figure S3**). QQ activity against long-chain AHLs was also found in all the *A. baumannii* clinical isolates studied (**Figure S5**), despite one of them (Ab7) does not possess an AidA sequence (López et al., 2017). As observed for ATCC17978, none of the clinical isolates could eliminate C6-HSL activity (**Figure S5**).

In order to further confirm that the QQ activity detected in *A. baumannii* ATCC17978 is enzymatic and preferentially degrades long-chain AHLs, the signals C6, C12, and OHC12-HSL were exposed to a cell extract from a 24 h culture of ATCC17978 for 3 h and the remaining AHL concentration was quantified using HPLC-MS. ATCC17978 extracts completely degraded C12-HSL and around 75% of OHC12-HSL in 3 h, confirming the QQ enzymatic activity in *A. baumannii* ATCC17978 (**Figure 4**). On the contrary, the activity against C6-HSL in the extracts was very low. Additionally, aliquots of the reaction mixtures were acidified to pH 2 to facilitate the recircularization of the lactonized homoserine ring in degraded AHLs (Yates et al., 2002). If a lactonase is responsible for the QQ enzymatic activity against AHLs, an increase in the concentration of AHL after acidification would be expected, as shown for the purified lactonase Aii20J (**Figure 4**). In *A. baumannii* ATCC17978, the recovery after the acidification of the reaction mixtures could only be obtained for OHC12-HSL (**Figure 4**), confirming the presence of an AHL-lactonase in the extracts. On the contrary, the acidification did not allow the recovery of C12-HSL, indicating the possible existence of several QQ enzymes with distinct AHL-degrading activity in ATCC17978, which could explain the differences in recovery between both signals.

Identification and Cloning of Putative QQ Sequences in *A. baumannii* ATCC17978

The results obtained from the acidification assays, together with the fact that QQ activity was found in the clinical isolate *A. baumannii* Ab7 that does not possess an AidA sequence in its genome, prompted us to search the genome of *A. baumannii* ATCC17978 for additional QQ sequences. The genome was searched using a collection of QQ sequences including both, acylases and lactonases, with demonstrated or putative activity (Romero et al., 2015; Muras et al., 2018a). The search specifically included the acylase AmiE described in *Acinetobacter* sp. Ooi24 (Ochiai et al., 2014), the lactonase AidE from *Acinetobacter* sp. 77 and the putative lactonases YtnP from *A. baumannii* A155,

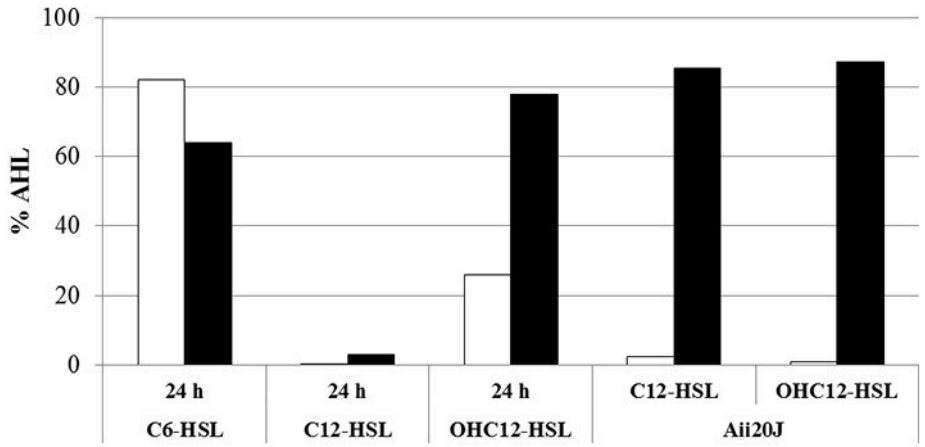

FIGURE 4 | QQ activity against C6-HSL, C12, and OHC12-HSL (10 μM) in cell extracts of *A. baumannii* ATCC17978 obtained from 24 h cultures in LB. The purified Aii20J lactonase (20 μg/mL) was used as positive control. The remaining AHL concentration after 3 h of exposure to cell extracts was quantified by HPLC-MS from reaction mixtures aliquots with (black bars) or without (white bars) acidification to reverse the lactonolysis. PBS was used as negative control. Values reported are normalized to the percentage of AHL retrieved from PBS reaction mixtures incubated the same way.

belonging to the metallo-β-lactamases family and containing the conserved domain HXHXDH (Arivett et al., 2015; Liu et al., 2017) and Y2-AiiA, that presents an aspartate instead of the second histidine in the conserved domain (HXDXDH) (Arivett et al., 2015). No putative acylase sequence was found in the genome of ATCC17978. On the contrary, besides de α/β hydrolase AidA (A1S_1757), seven sequences of putative lactonases were found, sharing ID percentages between 23 and 30% at aminoacidic level with the sequence of the AiiA lactonase of *Bacillus* sp. 240B1 (Dong et al., 2000; **Table S3**). The sequence A1S_2662 corresponds to the putative lactonase YtnP from *A. baumannii* strain A155 deposited in NCBI database (ID 99%, cover 100%), while the sequence A1S_2864 corresponds to the putative lactonase Y2-AiiA from the same strain (Arivett et al., 2015; **Table S3**). These two sequences are present in several *Acinetobacter* strains (Vallenet et al., 2008; Kang and Park, 2010; **Figure S6**) although the QQ activity has not been proved in any of them. The remaining 5 sequences presented the zinc-binding domain characteristic of the superfamily of metallo-β-lactamases (Bebrone, 2007). *A. nosocomialis* M2 does not possess a gene identical to AidA, but an α/β-hydrolase sharing a 35% of identity with AidA was found (Access number WP_022575648.1). The 7 lactonase sequences found in ATCC17978 could be also found in the genome of *A. nosocomialis* M2, sharing % ID higher than 95% in five cases: A1S_2270, A1S_1708, A1S_2194, A1S_2864, and A1S_2662. Lower ID percentages were found in M2 sequences for two of the enzymes with demonstrated activity: A1S_1876 (ID 29%, cover 31%) and A1S_0383 (ID 34%, cover 85%). All lactonase sequences could be amplified in the *A. baumannii* clinical isolates except for A1S_2194, probably due to the PCR conditions. The conservation of these sequences within and between species of *Acinetobacter* indicates a relevant physiological role of these enzymes.

Cloning and Over-Expression of the Putative QQ Enzymes in *E. coli*

In order to certify the QQ activity of the putative lactonases found in the genome of ATCC17978, we attempted to amplify and subclone in *E. coli* the 6 sequences presenting the highest identity to the *Bacillus* enzyme AiiA, A1S_2270 was dismissed due to the low cover percentage of identity of the sequence, although presenting the typical conserved domain (**Table S3**). AidA was also subcloned in *E. coli* in order to compare the specificity of the different QQ enzymes. Only 5 of the 6 selected genes could be amplified by PCR using specific primers. Sequence A1S_2194 could not be amplified even when the annealing temperature was lowered. The amplified sequences were subcloned in pET28c(+) in order to add a poly-Histidine tag to the sequence to facilitate the purification of the transgenic enzyme. Finally, recombinant *E. coli* colonies could be obtained for 3 lactonase sequences: A1S_2662 (YtnP), A1S_0383, and A1S_1876 as well as for the already described α/β hydrolase AidA. After checking the correct size and sequence of the inserts, the 4 enzymes were over-expressed and purified. The 4 enzymes were produced as soluble protein in *E. coli* BL21(DE3)plysS with the expected molecular weight taking into account the addition of the poly-His tag: ∼25.88 kDa for A1S_0383, ∼35.17 KDa for A1S_1876, ∼37.60 kDa for A1S_2662 (YtnP) and ∼33.3 kDa for AidA (**Figure S7**).

The 4 purified enzymes showed quorum quenching activity *in vitro*, although important differences were found regarding substrate specificity. Two of the enzymes, A1S_0383 and A1S_2662 were able to degrade all the AHLs tested, while A1S_1876 and AidA were not able to degrade the short-chain AHL C6-HSL (**Figure 5**). The minimum active concentration, defined as the amount of enzyme required to fully eliminate the activity of a 10 μM solution of C12-HSL in 24 h, as detected by the *C. violaceum* plate assay, was also very different among the different enzymes: 15 μg/mL for A1S_0383, 0.3 μg/mL for

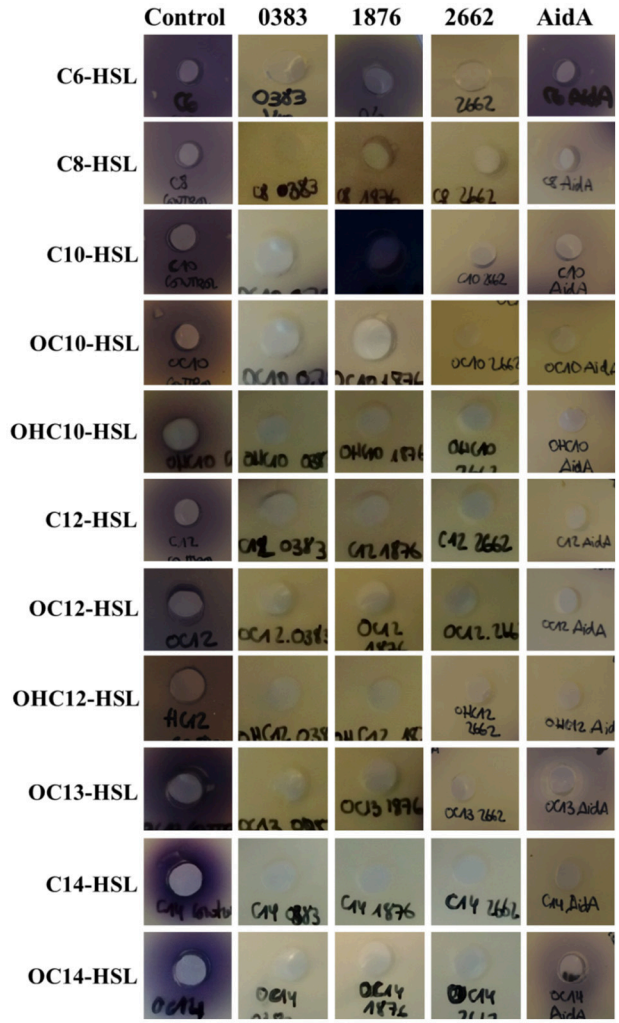

FIGURE 5 | Substrate specificity of the purified lactonases A1S_0383, A1S_1876, A1S_2662, and AidA from *A. baumannii* ATCC17978. Purified lactonases were mixed at 10xMAC concentration with AHLs (10 μM) for 24 h and the remaining AHL was evaluated in bioassays with *C. violaceum* CV026 or VIR07 biosensors. Each signal in PBS pH 6.7 was used as negative control.

A1S_1876, 1.7 μg/mL for A1S_2662, and 0.8 μg/mL for AidA (data not shown).

Expression of QQ Sequences in *A. baumannii* ATCC17978

In order to evaluate if the expression of the identified lactonases was actively regulated in *A. baumannii,* a qPCR analysis was carried out under different culture conditions. The RNA was extracted after 6 h from shaken and static cultures in LB and LS-LB (**Figure 6**) and the expression of AidA and the additional 6 lactonase sequences found in the genome was analyzed. No significant change in expression of the 6 new lactonases was observed between static and shaken conditions, but AidA was significantly over-expressed in static conditions in LB medium (**Figure 6**) suggesting an activation of this enzyme as a consequence of the activation of the QS system. The wide-spectrum lactonase A1S_2662 was expressed at high levels in all conditions, but as for A1S_1876 and the putative lactonases A1S_0383, A1S_2194, the expression only increased in LS-LB under shaken conditions, indicating that the expression of these two genes is not under the control of the QS system.

In order to further evaluate if the expression of the identified lactonases was activated by the presence of AHLs, we added OHC12-HSL, the major AHL found in *A. baumannii* ATCC17978, either from the beginning of the cultures or after 6 h (**Figure 7**). When the AHL was added at the beginning of the cultures no significant change in the expression of the lactonases was found, except for AidA that suffered a slight but significant decrease in its expression. On the contrary, the addition of the AHL to 6-h cultures caused a rapid decrease in the expression of all lactonases, except for A1S_1876, a lactonase with a low basal level of expression, that suffered a three-fold increase after the addition of OHC12-HSL (**Figure 7**).

Effect of Exogenous Quorum Quenching on Motility and Biofilm Formation

As a first approach to assess the importance of the QS system in the control of the expression of virulence factors in *A. baumannii* ATCC17978, the wide spectrum QQ enzyme Aii20J (Mayer et al., 2015) was used to try to block surface-associated motility and biofilm formation, two phenotypes previously described as being QS-controlled in different *Acinetobacter* spp. Previously, the capacity of Aii20J to effectively eliminate OHC12-HSL, the major AHL present in ATCC17978, was confirmed (**Figure 4**).

Surface-associated motility in *A. baumannii* ATCC17978 could only be observed in LNLS-LB medium in Eiken agar (**Figure 8**), presenting a characteristic tentacle-like pattern. The addition of the QQ enzyme Aii20J to the inoculum of the plates was enough to completely block the motility in these conditions. On the contrary, *A. nosocomialis* M2 presented a hyper-motile phenotype in LB medium at 37°C, being able to cover the whole plate in 14 h. This phenotype changed to a tentacle-like phenotype in the LNLS-LB medium (**Figure S8**). In the case of *A. nosocomialis* M2, the QQ enzyme Aii20J was not able to counteract the motility phenotype in any of the culture media tested, indicating important differences in the role of the QS system in the motility among *Acinetobacter* spp.

Despite differences in the structure of the biofilm formed in the presence of the QQ enzyme could be observed macroscopically (**Figure 9A**), the quantification of crystal violet staining could not detect significant differences in biofilm formation in *A. baumannii* ATCC17978 between the control and the Aii20J-treated cultures (data not shown). On the contrary, confocal microscopy observations revealed important differences: while a continuous biofilm of live bacteria could be observed in the control cultures, mainly close to the interface liquid-air, the coverslips incubated in the presence of Aii20J showed almost no presence of attached live cells (**Figure 9B**). The OD of the culture

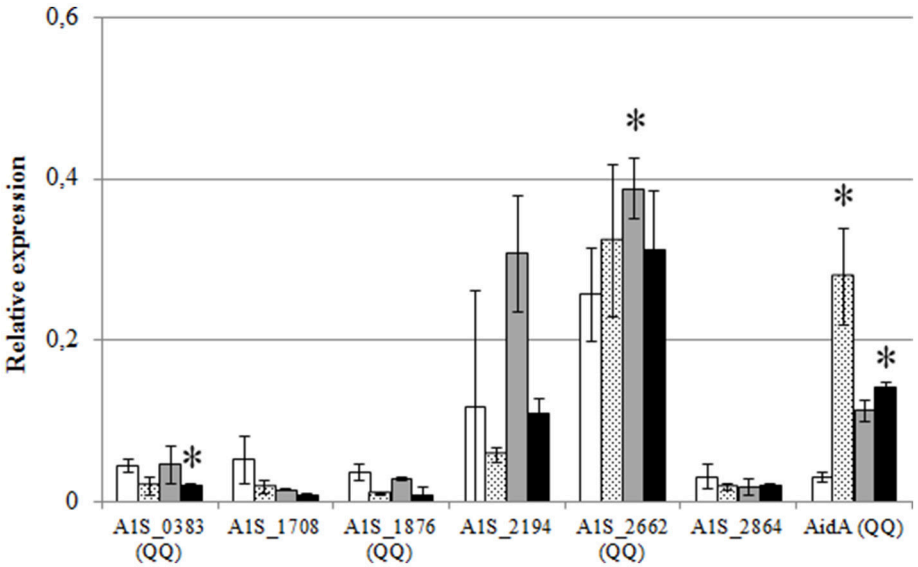

FIGURE 6 | Relative expression of the QQ lactonase genes and the α/β hydrolase AidA gene from *A. baumannii* ATCC17978, in shaken LB (white bars), static LB (dotted bars), shaken low-salt LB (gray bars), or static low-salt LB (black bars). Gene expression was normalized related to the *rpoB* gene. Error bars represent the standard deviations. Asterisks indicate statistically significant changes (Student's *t*-test, $p < 0.05$) with respect to the static LB condition.

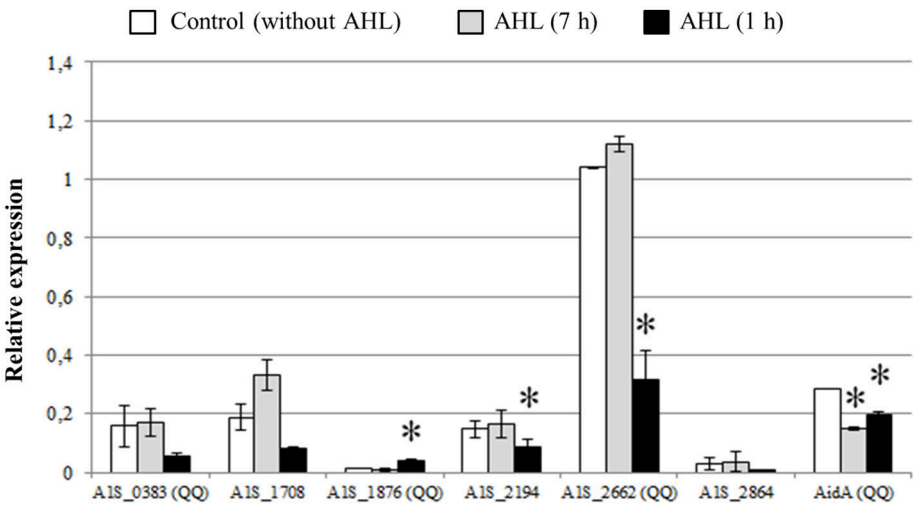

FIGURE 7 | Relative expression of QQ lactonase genes and α/β hydrolase AidA gene from *A. baumannii* ATCC17978 in response to OHC12-HSL. The AHL was added at 0 h (for 7 h) or 6 h (for 1 h) of culture growth. Gene expression was normalized related to the *rpoB* gene. Error bars represent the standard deviations. Asterisks indicate statistically significant changes (Student's *t*-test, $p < 0.05$) with respect to the static LB condition.

media was equal between control and QQ-treated cultures during the 4 days of incubation, and therefore the observed differences are not derived from growth inhibition (data not shown).

DISCUSSION

Our results strongly indicate that AHL production in *A. baumannii* ATCC17978 and *A. nosocomialis* M2 is up-regulated only when grown in static culture conditions, since no AHLs could be detected in the supernatants from shaken cultures even in 100-fold-concentrated extracts. The small differences in growth obtained between shaken and static cultures do not justify this dramatic change in AHL production (**Figure S1**). Moreover, none of 7 clinical *A. baumannii* isolates produced AHLs in shaken cultures, while significant amounts of AHLs could be found in the culture media of all of them in static conditions. In many cases, the identification of the AHLs produced by different *Acinetobacter* spp. was only possible after the over-expression of the AbaI synthase in *E. coli* (Niu et al., 2008; Chan et al.,

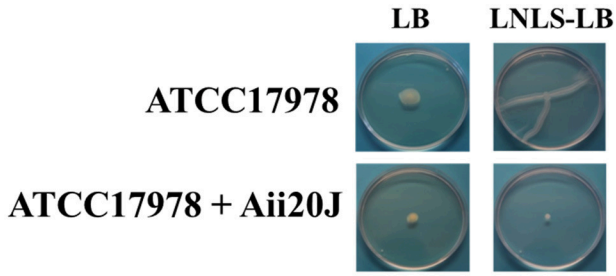

FIGURE 8 | Surface-motility assay of *A. baumannii* ATCC17978, with or without the addition of the QQ enzyme Aii20J (20 μg/mL). Cells were inoculated on LB or LNLS-LB 0.25% Eiken agar plates. Surface-associated motility was inspected after 14 h of incubation at 37°C. Images are representative results of 3 independent experiments.

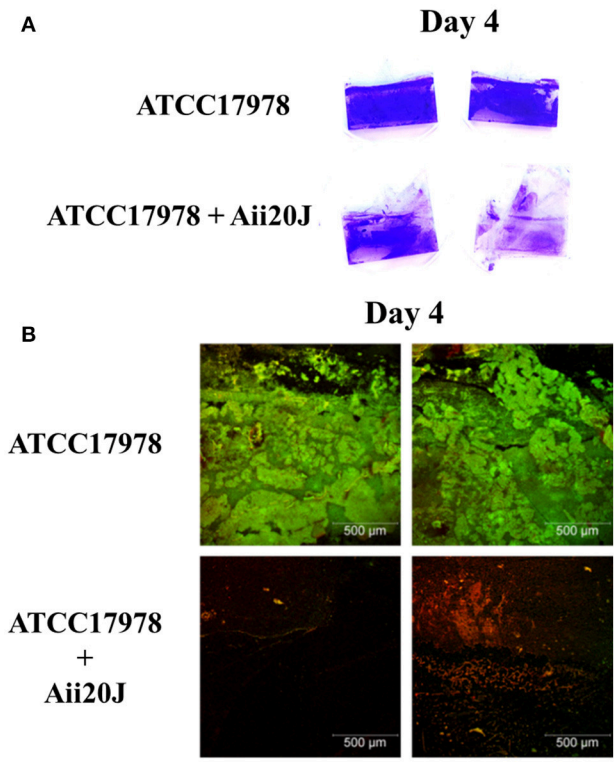

FIGURE 9 | Biofilm formation of *A. baumannii* ATCC17978 in the Amsterdam active attachment model. After 4 days of growth in low-salt LB medium, with or without QQ enzyme Aii20J (20 μg/mL), biofilm was stained with **(A)** crystal violet or **(B)** SYTO9^{TM} and propidium iodide to distinguish live cells from dead cells. Images corresponding with the biofilm formed close to the interface liquid-air are representative of several replicates.

2014). Niu et al. (2008) could obtain a dim response of the *A. tumefaciens* biosensor in 8,000- to 10,000-fold concentrated extracts of the culture medium in *A. nosocomialis* M2, although the culture conditions (shaken/not shaken) were not specified. Since AbaI is still expressed at low level in shaken cultures (**Figure 3**), we cannot completely disregard that a very small amount of AHLs is still produced in shaken cultures, although the biological significance of such low concentration of QS signals could be considered neglectable in comparison with the concentrations achieved in static cultures. The need of static culture conditions for AHL production could also explain the low percentages of AHL-producing strains found among 55 *Acinetobacter* clinical isolates (Anbazhagan et al., 2012). The absence of AHL signals in shaken cultures seems to be the result of the low expression of the AHL synthase AbaI, that is clearly up-regulated in static conditions, and not derived from a fast turn-over of the signals. These results indicate that the activation of the AHL-mediated QS system could be dependent on surface or cell-to-cell attachment in *Acinetobacter* spp. The inactivation of the QS system in shaken cultures is coherent with a previous observation reporting that pellicle formation or motility, two traits that are QS-dependent in *Acinetobacter* spp., were impaired when *A. baumannii* ATCC17978 was pre-incubated under shaking conditions. On the contrary, un-shaken cultures produced both QS dependent phenotypes (Chen et al., 2017).

To our knowledge, this is the first time that the requirement of static conditions for the activation of QS system is described. The need of mechanical cues for the detection of host cell surfaces and the expression of virulence factors has been already described in *E. coli* O157:H7 (Alsharif et al., 2015). A similar requirement was also observed in *Pseudomonas aeruginosa* that needs both, surface attachment and an active QS system for the expression of virulence genes (Siryaporn et al., 2014). In *P. aeruginosa* the chemotaxis-like chemosensor system Chp regulates the Type IV pili, that act as surface mechanosensors, and also regulates cAMP, that acts as a messenger through the virulence factor regulator (Vfr) to activate the QS circuits (Persat et al., 2015). In *A. baumannii* cAMP has been suggested to act as a regulator of the QS operon (Giles et al., 2015), and recently the two-component system CheA/Y (A1S_2811), homologous to Chp system in *P. aeruginosa* (Whitchurch et al., 2004) has been described (Chen et al., 2017). Indeed, the mutation of CheA in ATCC17978 results in a lower transcription of *abaI* and the *csu* operon and in the inhibition of motility and pellicle formation. The addition of C10-HSL restores these activities in the mutant, indicating that CheA may be controlling the expression of the motility-related *csu* operon through the expression of the QS operon (Chen et al., 2017). The *csu* operon is necessary for type I pili formation, cell attachment to plastic surfaces and latter formation of biofilms by *A. baumannii* and is thought to be under the control of the QS system (Tomaras et al., 2003; Clemmer et al., 2011; Eijkelkamp et al., 2011; Luo et al., 2015). It has been previously described that QS and *csu* operons are over-expressed in biofilms in comparison with planktonic cultures of *A. baumannii* ATCC17978 (Rumbo-Feal et al., 2013). These observations together with the fact that both, *abaI* and *csuD* are up-regulated under the static conditions required to trigger the presence of AHLs in the culture media (**Figure 3**), strongly support the possibility that CheA constitutes the attachment-dependent master regulator of the QS operon in *A. baumannii* ATCC17978, an hypothesis that should be further explored.

HPLC-MS analysis of the QS signals produced by *A. baumannii* ATCC17978 and *A. nosocomialis* M2 in static conditions revealed a similar complex AHL profile in both species, with OHC12-HSL as the major AHL, reaching a concentration around 1–2 orders of magnitude higher than the secondary AHLs. Only small differences in AHL profile are found between the two species that presented a more complex AHL profile in the rich LB medium than in the low-nutrient-low salt medium. Several studies have reported variations in the QS signals produced by *Acinetobacter* spp. using different species and media, however in most cases more than one AHL was reported (González et al., 2001, 2009; Sarkar and Chakraborty, 2007; Kang and Park, 2010; Chan et al., 2011, 2014; Bitrian et al., 2012; Kim and Park, 2013; How et al., 2015). A wide range of intraspecific variability was also found in the AHL profile within *A. baumannii* clinical isolates, since OHC12-HSL was present in only 4 of 7 strains when cultured in the rich LB medium. Intraspecific variation in AHL profile has been also reported in other important pathogens, such as *Serratia liquefaciens* (Remuzgo-Martínez et al., 2015). In the case of *A. baumannii*, these differences could be derived from differences in the control of the expression of the *abaI* synthase that is present in all isolates, or in the QQ activity, that was also present in all of them. Decreasing the salinity of the culture medium produced a five-fold increase in the concentration of the major AHL in *A. baumannii* ATCC17978, although no changes in growth rate were observed. This increase in signal concentration also seems to be derived from an increase in the expression of *abaI* (**Figure 3A**). Low salinity also activates the expression of *csuD*, which is related to surface-associated motility, a trait that has been reported to be negatively affected by high salinity values in *A. baumannii* ATCC17978 (Pour et al., 2011; McQueary et al., 2012). It is therefore plausible that additional regulators are interacting downstream the hypothetical surface-attachment sensor in order to fine-tune signal production. The complexity of this signal network that changes depending on culture conditions indicates the existence of an intricate net of signals that integrate information from several physicochemical and nutritional factors. A single channel which specifically discriminates between the presence of single and multiple autoinducers, leading to synergistic responses has been described before in *Vibrio harveyi* (Mok et al., 2003). In *P. aeruginosa*, nutritional and environmental signals selectively affect the different QS systems (Welsh and Blackwell, 2016). Therefore, it appears likely that a similar mechanism could be present in other bacteria producing different signals under different environmental stimuli.

The sharp decrease in AHL concentration upon stationary-phase achievement that correlates with the appearance of QQ activity in the cell extracts strongly indicates an active endogenous regulation of the AHL signals through enzymatic degradation. A rapid turnover of OC12-HSL was also observed in the QQ-active *Acinetobacter* sp. isolate GG2 (Chan et al., 2011). The self-regulation of AHL concentration has been already reported in *Agrobacterium tumefaciens* that activates the lactonase AttM to degrade its own signal as a response to starvation signals (Zhang et al., 2002; Uroz et al., 2009). A marine strain of *Shewanella* also degrades its own AHLs during stationary phase through a lactonase and acylase/amidase activities (Tait et al., 2009). Recently, a novel QQ enzyme, the α/β hydrolase AidA that is over-expressed in response to the non-cognate OC12-HSL has been identified in several clinical isolates of *A. baumannii* (López et al., 2017). AidA is also present in *A. baumannii* ATCC17978 and our results confirm that it is up-regulated in early-stages of the AHL-producing static cultures (**Figure 6**). It should be noted that AidA expression is lower under low-salt conditions that results in a higher OHC12-HSL concentration, which may indicate a direct involvement of AidA in signal degradation. Nevertheless, since AidA is not present in *A. noscomialis* M2 that presents the same pattern of AHL self-degradation, it is possible that several enzymes are active in the self-degradation process. Importantly, the addition of the cognate OHC12-HSL did not cause any significant change in AidA expression (**Figure 7**). It is therefore plausible that AidA is not under the direct control of the QS operon, but its expression may be controlled by additional environmental cues.

A surprisingly high number of lactonase sequences was found in the genome of *A. baumannii* ATCC17978, all of them belonging to the metallo-β-lactamase family, although only 3 of them could be subcloned in *E. coli* to confirm its AHL-lactonase activity. The presence of lactonase-like activity has been reported in other members of the genus *Acinetobacter* isolated from plant rhizosphere (Kang et al., 2004; Chan et al., 2011) that degrade both, long and short chain AHLs, and can be recovered after acidification (Chan et al., 2011). Multiple QQ enzymes have been found in *P. aeruginosa* (Huang et al., 2006) as well as in *Deinococcus radiodurans*, *Hyphomonas neptunium, Photorhabdus luminescens,* and *Rhizobium* sp. (Kalia et al., 2011; Krysciak et al., 2011). In *Rhizobium* sp. up to 5 QQ enzymes, including the two lactonases DhlR and QsdR1 have been described, although the involvement on the self-control of the AHL signals could not be demonstrated (Krysciak et al., 2011). The presence of 5 of the 6 lactonase sequences could be confirmed in all the clinical isolates as well as in *A. nosocomialis* M2. Among the 3 lactonases that could be subcloned and purified to prove its QQ activity, the lactonase A1S_2662, that corresponds to the putative lactonase YtnP found in the genome of *A. baumannii* strain A155 (Arivett et al., 2015) and is also highly conserved in *A. nosocomialis* M2, is expressed at high levels in all culture conditions (**Figure 6**). The only lactonase that is clearly activated by the addition of the cognate OHC12-HSL is A1S_1876, while all the others are down-regulated or unaffected (**Figure 7**), being therefore a good candidate to be under the control of the QS system. A1S_1876 is transcribed at low levels in early log-phase static cultures (**Figure 6**), but it should be noted that the transgenic enzyme presents the highest specific activity among the 4 enzymes that have been subcloned and purified.

Due to lack of recovery observed after acidification of C12-HSL treated with *A. baumannii* cell extracts (**Figure 4**), we cannot completely exclude the presence of additional acylase-type QQ enzymes in this species. Enzymatic activity against long chain AHLs had been identified previously in the wastewater

isolate *Acinetobacter* sp. Ooi24 and the QQ enzyme responsible was identified as an AHL-acylase (Ochiai et al., 2014). The lack of conserved domains in AHL-acylases difficult the identification of the sequences in the bacterial genomes, and therefore, the number of QQ enzymes present in *A. baumannii* could be even greater than described here. Despite substrate promiscuity has been already described in members of the metallo-β-lactamase family with AHL degradation capacity (Miraula et al., 2016), and therefore additional metabolic activities of the lactonases identified in *A. baumannii* cannot be completely disregarded, the redundancy and differential regulation of the QQ enzymes found in ATCC17978 provide a strong evidence of the importance of the AHL-mediated QS/QQ network in this species. Since some differences in the substrate specificity have been found among the 4 QQ enzymes that could be cloned, it is possible that *A. baumannii* uses this battery of QQ enzymes to differentially regulate the relative concentration of exogenous, short-chain AHLs and the endogenous principal long-chain AHL. Further studies are required to assess the role of the QQ activity present in *A. baumannii* strains in controlling the QS regulation cascade.

The exogenous addition of the wide-spectrum lactonase Aii20J completely blocked motility and biofilm formation in *A. baumannii* ATCC17978, confirming a key role of AHL-mediated QS in the expression of these two important virulence factors in this strain. Important intra-species variability in surface-associated motility and its response to QQ has been recently reported in clinical isolates of *A. baumannii* (López et al., 2017). *A. baumannii* ATCC17978 behaves in the same way as the clinical isolate Ab7, that does not possess an AidA sequence in its genome, and therefore the intrinsic QQ system does not seem to be involved in *in vitro* motility pattern and response to extrinsic QQ. Results indicate that the endogenous QQ activity present in this strain serves only to fine-tune the AHL production and that QQ strategies can be suitable as anti-pathogenic strategy in this species. In the case of *A. nosocomialis* M2, the mutation of the *abaI* gene resulted in a decrease in motility at 30°C, indicating that this trait is also under the control of the QS system in this strain (Clemmer et al., 2011). Although this effect was also observed in our experiments at 30°C (data not shown), the sensitivity of the strain to QQ was lost at 37°C, indicating important differences in the control of surface-associated motility between these two species. Regarding the effect of QQ on biofilm formation, the transgenic expression of the *Geobacillus kaustophilus* lactonase GKL in a clinical isolate of *A. baumannii* disrupted biofilm formation (Chow et al., 2014) and the addition of the QQ lactonase MomL also diminished, but not abolished biofilm formation in *A. baumannii* LMG 10531 as measured with the crystal violet staining method (Zhang et al., 2017). In the case of *A. baumannii* ATCC17978 the number of attached live cells decreases dramatically in the presence of the exogenous added QQ enzyme Aii20J (**Figure 9**). These differences were not so obvious at macroscopic level with the crystal violet staining method. A more detailed study on the effect of inactivating the QS system through both, external QQ and the generation of isogenic mutants is necessary in order to ascertain the role of the QS system in biofilm formation in this important nosocomial pathogen and to further explore the potential antipathogenic capacity of QQ strategies.

AUTHOR CONTRIBUTIONS

CM and AM carried out the experimental work. CM, MR, and AO contributed to the design, and interpretation of data. CM and AO wrote the manuscript while MR revised the manuscript. ML and MT contributed to the interpretation of the data related to QS and provided the clinical strains of *Acinetobacter*.

FUNDING

This study was financially supported by Consellería de Cultura, Educación e Ordenación Universitaria, Xunta de Galicia GPC2014/019 and co-financed by ISCIII European Regional Development Fund and Instituto de Salud Carlos III. MT was financially supported by the Miguel Servet Research Programme (CHU A Coruña and ISCIII). AM was supported by a predoctoral fellowship from Xunta de Galicia (Plan I2C). MR was supported by a Postodoctoral fellowship from Xunta de Galicia (Plan I2C).

ACKNOWLEDGMENTS

We would like to thank Prof. Paul Williams from the University of Nottingham and Prof. Tomohiro Morohoshi from the Utsunomiya University for kindly providing us with *Chromobacterium violaceum*-CV026 and VIR07 biosensor strains, respectively.

SUPPLEMENTARY MATERIAL

The Supplementary Material for this article can be found online at: https://www.frontiersin.org/articles/10.3389/fcimb.2018.00310/full#supplementary-material

REFERENCES

Alsharif, G., Ahmad, S., Islam, M. S., Shah, R., Busby, S. J., and Krachler, A. M. (2015). Host attachment and fluid shear are integrated into a mechanical signal regulating virulence in *Escherichia coli* O157:H7. *Proc. Natl. Acad. Sci. U.S.A.* 112, 5503–5508. doi: 10.1073/pnas.1422986112

Anbazhagan, D., Mansor, M., Yan, G. O., Md Yusof, M. Y., Hassan, H., and Sekaran, S. D. (2012). Detection of quorum sensing signal molecules and identification of an autoinducer synthase gene among biofilm forming clinical isolates of *Acinetobacter* spp. *PLoS ONE* 7:e36696. doi: 10.1371/journal.pone.0036696

Arivett, B. A., Fiester, S. E., Ream, D. C., Centrón, D., Ramírez, M. S., Tolmasky, M. E., et al. (2015). Draft genome of the multidrug-resistant *Acinetobacter baumannii* strain A155 clinical isolate. *Genome Announc.* 3:e00212–15. doi: 10.1128/genomeA.00212-15

Bebrone, C. (2007). Metallo-β-lactamases (classification, activity, genetic organization, structure, zinc coordination) and their superfamily. *Biochem. Pharmacol.* 74, 1686–1701. doi: 10.1016/j.bcp.2007.05.021

Bergogne-Bérézin, E., and Towner, K. J. (1996). *Acinetobacter* spp. as nosocomial pathogens: microbiological, clinical, and epidemiological features. *Clin. Microbiol. Rev.* 9, 148–165.

Bhargava, N., Sharma, P., and Capalash, N. (2010). Quorum sensing in *Acinetobacter*: an emerging pathogen. *Crit. Rev. Microbiol.* 36, 349–360. doi: 10.3109/1040841XX.2010.512269

Bhargava, N., Sharma, P., and Capalash, N. (2012). *N*-acyl homoserine lactone mediated interspecies interactions between *A. baumannii* and *P. aeruginosa*. *Biofouling* 28, 813–822. doi: 10.1080/08927014.2012.714372

Bitrian, M., Solari, C. M., González, R. H., and Nudel, C. B. (2012). Identification of virulence markers in clinically relevant strains of *Acinetobacter* genospecies. *Int. Microbiol.* 15, 79–88. doi: 10.2436/20.1501.01.161

Carruthers, M. D., Harding, C. M., Baker, B. D., Bonomo, R. A., Hujer, K. M., Rather, P. N., et al. (2013). Draft genome sequence of the clinical isolate *Acinetobacter nosocomialis* strain M2. *Genome Announc.* 1:e00906-13. doi: 10.1128/genomeA.00906-13

Chan, K. G., Atkinson, S., Mathee, K., Sam, C. K., Chhabra, S. R., Cámara, M., et al. (2011). Characterization of *N*-acylhomoserine lactone-degrading bacteria associated with the *Zingiber officinale* (ginger) rhizosphere: co-existence of quorum quenching and quorum sensing in *Acinetobacter* and *Burkholderia*. *BMC Microbiol.* 11:51. doi: 10.1186/1471-2180-11-51

Chan, K. G., Cheng, H. J., Chen, J. W., Yin, W. F., and Ngeow, Y. F. (2014). Tandem mass spectrometry detection of quorum sensing activity in multidrug resistant clinical isolate *Acinetobacter baumannii*. *Sci. World J.* 2014:891041. doi: 10.1155/2014/891041

Chen, R., L. V. R., Xiao, L., Wang, M., Du, Z., Tan, Y., et al. (2017). A1S_2811, a CheA/Y-like hybrid two-component regulator from *Acinetobacter baumannii* ATCC17978, is involved in surface motility and biofilm formation in this bacterium. *Microbiologyopen* 6:e510. doi: 10.1002/mbo3.510

Chow, J. Y., Yang, Y., Tay, S. B., Chua, K. L., and Yew, W. S. (2014). Disruption of biofilm formation by the human pathogen *Acinetobacter baumannii* using engineered quorum-quenching lactonase. *Antimicrob. Agent Chemother.* 58, 1802–1805. doi: 10.1128/AAC.02410-13

Clemmer, K. M., Bonomo, R. A., and Rather, P. N. (2011). Genetic analysis of surface motility in *Acinetobacter baumannii*. *Microbiology* 157, 2534–2544. doi: 10.1099/mic.0.049791-0

Dong, Y. H., Xu, J. L., Li, X. Z., and Zhang, L. H. (2000). AiiA, an enzyme that inactivates the acylhomoserine lactone quorum-sensing signal and attenuates the virulence of *Erwinia carotovora*. *Proc. Natl. Acad. Sci. U.S.A* 97, 3526–3531. doi: 10.1073/pnas.97.7.3526

Eijkelkamp, B. A., Hassan, K. A., Paulsen, I. T., and Brown, M. H. (2011). Investigation of the human pathogen *Acinetobacter baumannii* under iron limiting conditions. *BMC Genomics* 12:126. doi: 10.1186/1471-2164-12-126

Eijkelkamp, B. A., Stroeher, U. H., Hassan, K. A., Elbourne, L. D., Paulsen, I. T., and Brown, M. H. (2013). H-NS plays a role in expression of *Acinetobacter baumannii* virulence features. *Infect. Immun.* 81, 2574–2783. doi: 10.1128/IAI.00065-13

Exterkate, R. A., Crielaard, W., and Ten Cate, J. M. (2010). Different response to amine fluoride by *Streptococcus mutans* and polymicrobial biofilms in a novel high-throughput active attachment model. *Caries Res.* 44, 372–379. doi: 10.1159/000316541

Giles, S. K., Stroeher, U. H., Eijkelkamp, B. A., and Brown, M. H. (2015). Identification of genes essential for pellicle formation in *Acinetobacter baumannii*. *BMC Microbiol.* 15:116. doi: 10.1186/s12866-015-0440-6

González, R. H., Dijkshoorn, L., Van den Barselaar, M., and Nudel, C. (2009). Quorum sensing profile of *Acinetobacter* strains from nosocomial and environmental sources. *Rev. Argent Microbiol.* 41, 73–78.

González, R. H., Nusblat, A., and Nudel, B. C. (2001). Detection and characterization of quorum sensing signal molecules in *Acinetobacter* strains. *Microbiol. Res.* 155, 271–277. doi: 10.1016/S0944-5013(01)80004-5

How, K. Y., Hong, K. W., Sam, C. K., Koh, C. L., Yin, W. F., and Chan, K. G. (2015). Unravelling the genome of long chain *N*-acylhomoserine lactone-producing *Acinetobacter* sp. strain GG2 and identification of its quorum sensing synthase gene. *Front. Microbiol.* 6:240. doi: 10.3389/fmicb.2015.00240

Huang, J. J., Petersen, A., Whiteley. M., and Leadbetter, J.R. (2006). Identification of QuiP, the product of gene PA1032, as the second acyl-homoserine lactone acylase of Pseudomonas aeruginosa PAO1. *Appl. Environ. Microbiol.* 72, 1190–1197. doi: 10.1128/AEM.72.2.1190-1197.2006

Kalia, V. C., Rahu, S. C., and Purohit, H. J. (2011). Genomic analysis reveals versatile organisms for quorum quenching enzymes: acyl-homoserine lactone-acylase and –lactonase. *Open Microbiol. J.* 5, 1–13. doi: 10.2174/1874285801105010001

Kang, B. R., Lee, J. H., Ko, S. J., Lee, Y. H., Cha, J. S., Cho, B. H., et al. (2004). Degradation of acyl-homoserine lactone molecules by *Acinetobacter* sp. strain C1010. *Can. J. Microbiol.* 50, 935–941. doi: 10.1139/w04-083

Kang, Y. S., and Park, W. (2010). Contribution of quorum-sensing system to hexadecane degradation and biofilm formation in *Acinetobacter* sp. strain DR1. *J. Appl. Microbiol.* 109, 1650–1659. doi: 10.1111/j.1365-2672.2010.04793.x

Kim, A. L., Park, S. Y., Lee, C. H., Lee, C. H., and Lee, J. K. (2014). Quorum quenching bacteria isolated from sludge of a wastewater treatment plant and their application for controlling biofilm formation. *J. Microbiol. Biotechnol.* 24, 1574–1582. doi: 10.4014/jmb.1407.07009

Kim, J., and Park, W. (2013). Identification and characterization of genes regulated by AqsR, a LuxR-type regulator in *Acinetobacter oleivorans* DR1. *Appl. Microbiol. Biotechnol.* 97, 6967–6978. doi: 10.1007/s00253-013-5006-7

Krysciak, D., Schmeisser, C., Preuss, S., Riethausen, J., Quitschau, M., Grond, S., et al. (2011). Involvement of multiple loci in quorum quenching of autoinducer I molecules in the nitrogen-fixing symbiont *Rhizobium (Sinorhizobium)* sp. strain NGR234. *Appl. Environ. Microbiol.* 77, 5089–5099. doi: 10.1128/AEM.00112-11

Liu, C., Guo, S., Turak, A., Zhang, J., and Zhang, L. (2017). AidE encodes an *N*-acyl homoserine lactonase in *Acinetobacter*. *Sheng Wu Gong Cheng Xue Bao* 33, 1625–1639. doi: 10.13345/j.cjb.170156

Livak, K. J., and Schmittgen, T. D. (2001). Analysis of relative gene expression data using real-time quantitative PCR and the 2(-Delta Delta C(T)) method. *Methods* 25, 402–408. doi: 10.1006/meth.2001.1262

López, M., Mayer, C., Fernández-García, L., Blasco, L., Muras, A., Ruiz, F. M., et al. (2017). Quorum sensing network in clinical strains of *A. baumannii*: AidA is a new quorum quenching enzyme. *PLoS ONE* 12:e0174454. doi: 10.1371/journal.pone.0174454

Luo, L. M., Wu, L. J., Xiao, Y. L., Zhao, D., Chen, Z. X., Kang, M., et al. (2015). Enhancing pili assembly and biofilm formation in *Acinetobacter baumannii* ATCC19606 using non-native acyl-homoserine lactones. *BMC Microbiol.* 15:62. doi: 10.1186/s12866-015-0397-5

Mayer, C., Romero, M., Muras, A., and Otero, A. (2015). Aii20J, a wide-spectrum termostable *N*-acylhomoserine lactonase from the marine bacterium *Tenacibaculum* sp. 20J, can quench AHL-mediated acid resistance in *Escherichia coli*. *Appl. Microbiol. Biotechnol.* 99, 9523–9539. doi: 10.1007/s00253-015-6741-8

McClean, K. H., Winson, M. K., Fish, L., Taylor, A., Chhabra, S. R., Cámara, M., et al. (1997). Quorum sensing and *Chromobacterium violaceum*: exploitation of violacein production and inhibition for the detection of *N*-acylhomoserine lactones. *Microbiology* 143, 3703–3711. doi: 10.1099/00221287-143-12-3703

McQueary, C. N., Kirkup, B. C., Si, Y., Barlow, M., Actis, L. A., Craft, D. W., et al. (2012). Extracellular stress and lipopolysaccharide modulate *Acinetobacter* surface-associated motility. *J. Microbiol.* 50, 434–443. doi: 10.1007/s12275-012-1555-1

Miraula, M., Schenk, G., and Mitić N. (2016). Promiscuous metallo-β-lactamases: MIM-1 and MIM-2 may play an essential role in quorum sensing networks. *J. Inorg. Biochem.* 162, 366–375. doi: 10.1016/j.jinorgbio.2015.12.014

Mok, K. C., Wingreen, N. S., and Bassler, B. L. (2003). *Vibrio harveyi* quorum sensing: a coincidence detector for a two autoinducers controls gene expression. *EMBO J.* 22, 870–881. doi: 10.1093/emboj/cdg085

Morohoshi, T., Kato, M., Fukamachi, K., Kato, N., and Ikeda, T. (2008). *N*-acylhomoserine lactone regulates violacein production in *Chromobacterium violaceum* type strain ATCC12472. *FEMS Microbiol. Lett.* 279, 124–130. doi: 10.1111/j.1574-6968.2007.01016.x

Muras, A., López-Pérez, M., Mayer, C., Parga, A., Amaro-Blanco, J., and Otero, A. (2018a). High prevalence of quorum-sensing and quorum-quenching activity among cultivable bacteria and metagenomic sequences in the Mediterranean Sea. *Genes* 9:E100. doi: 10.3390/genes9020100

Muras, A., Mayer, C., Romero, M., Camino, T., Ferrer, M. D., Mira, A., et al. (2018b). Inhibition of *Streptococcus mutans* biofilm formation by extracts of *Tenacibaculum* sp. 20J, a bacterium with wide-spectrum quorum quenching activity. *J. Oral Microbiol.* 10:1429788. doi: 10.1080/20002297.2018.1429788

Niu, C., Clemmer, K. M., Bonomo, R. A., and Rather, P. N. (2008). Isolation and characterization of an autoinducer synthase from *Acinetobacter baumannii*. *J. Bacteriol.* 190, 3386–3392. doi: 10.1128/JB.01929-07.

Ochiai, S., Morohoshi, T., Kurabeishi, A., Shinozaki, M., Fujita, H., Sawada, I., et al. (2013). Production and degradation of *N*-acylhomoserine lactone quorum sensing signal molecules in bacteria isolated from activated sludge. *Biosci. Biotechnol. Biochem.* 77, 2436–2340. doi: 10.1271/bbb.130553

Ochiai, S., Yasumoto, S., Morohoshi, T., and Ikeda, T. (2014). AmiE, a novel *N*-acylhomoserine lactone acylase belonging to the amidase family, from the activated-sludge isolate *Acinetobacter* sp. strain Ooi24. *Appl. Environ. Microbiol.* 80, 6919–6925. doi: 10.1128/AEM.02190-14

Oh, M. H., and Choi, C. H. (2015). Role of LuxIR homologue AnoIR in *Acinetobacter nosocomialis* and the effect of virstatin on the expression of *anoR* gene. *J. Microbiol. Biotechnol.* 25, 1390–1400. doi: 10.4014/jmb.1504.04069

Park, Y. K., and Ko, K. S. (2015). Effect of carbonyl cyanide 3-chlorophenylhydrazone (CCCP) on killing *Acinetobacter baumannii* by colistin. *J. Microbiol.* 53, 53–59. doi: 10.1007/s12275-015-4498-5

Peleg, A. Y., Seifert, H., and Paterson, D. L. (2008). *Acinetobacter baumannii*: emergence of a successful pathogen. *Clin. Microbiol. Rev.* 21, 538–582. doi: 10.1128/CMR.00058-07

Persat, A., Inclan, Y. F., Engel, J. N., Stone, H. A., and Gitai, Z. (2015). Type IV pili mechanochemically regulate virulence factors in *Pseudomonas aeruginosa*. *Proc. Natl. Acad. Sci. U.S.A.* 112, 7563–7568. doi: 10.1073/pnas.1502025112

Pour, N. K., Dusane, D. H., Dhakephalkar, P. K., Zamin, F. R., Zinjarde, S. S., and Chopade, B. A. (2011). Biofilm formation by *Acinetobacter baumannii* strains isolated from urinary tract infection and urinary catheters. *FEMS Immunol. Med. Microbiol.* 62, 328–338. doi: 10.1111/j.1574-695XX.2011.00818.x

Remuzgo-Martínez, S., Lázaro-Díez, M., Mayer, C., Aranzamendi-Zaldumbide, M., Padilla, D., Calvo, J., et al. (2015). Biofilm formation and quorum-sensing-molecule production by clinical isolates of *Serratia liquefaciens*. *Appl. Environ. Microbiol.* 81, 3306–3315. doi: 10.1128/AEM.00088-15

Rice, L. B. (2006). Challenges in identifying new antimicrobial agents effective for treating infections with *Acinetobacter baumannii* and *Pseudomonas aeruginosa*. *Clin. Infect. Dis.* 43, S100–S105. doi: 10.1086/504487

Rice, L. B. (2008). Federal funding for the study of antimicrobial resistance in nosocomial pathogens: no ESKAPE. *J. Infect. Dis.* 197, 1079–1081. doi: 10.1086/533452

Romero, M., Avendaño-Herrera, R., Magariños, B., Cámara, M., and Otero, A. (2010). Acyl homoserine lactone production and degradation by the fish pathogen *Tenacibaculum maritimum*, a member of the *Cytophaga-Flavobacterium-Bacteroides* (CFB) group. *FEMS Microbiol. Lett.* 304, 131–139. doi: 10.1111/j.1574-6968.2009.01889.x

Romero, M., Mayer, C., Muras, A., and Otero, A. (2015). "Silencing bacterial communication through enzymatic quorum sensing inhibition," in *Quorum Sensing vs Quorum Quenching: A Battle With No End In Sight,* ed V. Kalia (New Delhi: Springer), 219–236.

Romero, M., Muras, A., Mayer, C., Buján, N., Magariños, B., and Otero, A. (2014). *In vitro* quenching of fish pathogen *Edwarsiella tarda* AHL production using marine bacterium *Tenacibaculum* sp. strain 20J cell extracts. *Dis. Aquat. Org.* 108, 217–225. doi: 10.3354/dao02697

Rumbo-Feal, S., Gómez, M. J., Gayoso, C., Álvarez-Fraga, L., Cabral, M. P., Aransay, A. M., et al. (2013). Whole transcriptome analysis of *Acinetobacter baumannii* assessed by RNA-sequencing reveals different mRNA expression profiles in biofilm compared to planktonic cells. *PLoS ONE* 8:e72968. doi: 10.1371/journal.pone.0072968

Sarkar, S., and Chakraborty, R. (2007). Quorum sensing in metal tolerance of *Acinetobacter junii* BB1A is associated with biofilm production. *FEMS Microbiol. Lett.* 282, 160–165. doi: 10.1111/j.1574-6968.2008.01080.x

Siryaporn, A., Kuchma, S. L., O'Toole, G. A., and Gitai, Z. (2014). Surface attachment induces *Pseudomonas aeruginosa* virulence. *Proc. Natl. Acad. Sci. U.S.A.* 111, 16860–16865. doi: 10.1073/pnas.1415712111

Smith, M. G., Gianoulis, T. A., Pukatzki, S., Mekalanos, J. J., Ornston, L. N., Gerstein, M., et al. (2007). New insights into *Acinetobacter baumannii* pathogenesis revealed by high-density pyrosequencing and transposon mutagenesis. *Genes Dev.* 21, 601–614. doi: 10.1101/gad.1510307

Tait, K., Williamson, H., Atkinson, S., Williams, P., Cámara, M., and Joint, I. (2009). Turnover of quorum sensing signal molecules modulates cross-kingdom signalling. *Environ. Microbiol.* 11, 1792–1802. doi: 10.1111/j.1462-2920.2009.01904.x.

Tamura, K., Stecher, G., Peterson, D., Filipski, A., and Kumar, S. (2013). MEGA6: molecular evolutionary genetics analysis version 6.0. *Mol. Biol. Evol.* 30, 2725–2729 doi: 10.1093/molbev/mst197

Tomaras, A. P., Dorsey, C. W., Edelmann, R. E., and Actis, L. A. (2003). Attachment to and biofilm formation on abiotic surfaces by *Acinetobacter baumannii*: involvement of a novel chaperone-usher pili assembly system. *Microbiology* 149, 3473–3484. doi: 10.1099/mic.0.26541-0

Tomaras, A. P., Flagler, M. J., Dorsey, C. W., Gaddy, J. A., and Actis, L. A. (2008). Characterization of a two-component regulatory system from *Acinetobacter baumannii* that controls biofilm formation and cellular morphology. *Microbiology* 154, 3398–3409. doi: 10.1099/mic.0.2008/019471-0

Towner, K. J. (2009). *Acinetobacter*: an old friend, but a new enemy. *J. Hosp. Infect.* 73, 355–363. doi: 10.1016/j.jhin.2009.03.032

Uroz, S., Dessaux, Y., and Oger, P. (2009). Quorum sensing and quorum quenching: the yin and yang of bacterial communication. *Chembiochem* 10, 205–216. doi: 10.1002/cbic.200800521

Vallenet, D., Nordmann, P., Barbe, V., Poirel, L., Mangenot, S., Bataille, E., et al. (2008). Comparative analysis of *Acinetobacters*: three genomes for three lifestyles. *PLoS ONE* 3:e1805. doi: 10.1371/journal.pone.0001805

Welsh, M. A., and Blackwell, H. E. (2016). Chemical genetics reveals environment-specific roles for quorum sensing circuits in *Pseudomonas aeruginosa*. *Cell Chem. Biol.* 23, 361–369. doi: 10.1016/j.chembiol.2016.01.006

Whitchurch, C. B., Leech, A. J., Young, M. D., Kennedy, D., Sargent, J. L., Bertrand, J. J., et al. (2004). Characterization of a complex chemosensory signal transduction system which controls twitching motility in *Pseudomonas aeruginosa*. *Mol. Microbiol.* 52, 873–893. doi: 10.1111/j.1365-2958.2004.04026.x

Yates, E. A., Philipp, B., Buckley, C., Atkinson, S., Chhabra, S. R., Sockett, R. E., et al. (2002). *N*-acylhomoserine lactones undergo lactonolysis in a pH-, temperature-, and acyl chain length-dependent manner during growth of *Yersinia pseudotuberculosis* and *Pseudomonas aeruginosa*. *Infect. Immun.* 70, 5635–5646. doi: 10.1128/IAI.70.10.5635-5646.2002

Zhang, H. B., Wang, L. H., and Zhang, L. H. (2002). Genetic control of quorum-sensing signal turnover in *Agrobacterium tumefaciens*. *Proc. Natl. Acad. Sci. U.S.A.* 99, 4638–4643. doi: 10.1073/pnas.022056699

Zhang, Y., Brackman, G., and Coenye, T. (2017). Pitfalls associated with evaluating enzymatic quorum quenching activity: the case of MomL and its effect on *Pseudomonas aeruginosa* and *Acinetobacter baumannii* biofilms. *PeerJ* 5:e3251. doi: 10.7717/pperj.3251

Conflict of Interest Statement: The authors declare that the research was conducted in the absence of any commercial or financial relationships that could be construed as a potential conflict of interest.

frontiers in Cellular and Infection Microbiology

REVIEW
published: 07 May 2018
doi: 10.3389/fcimb.2018.00139

"In-Group" Communication in Marine *Vibrio*: A Review of N-Acyl Homoserine Lactones-Driven Quorum Sensing

Jianfei Liu[†], *Kaifei Fu*[†], *Chenglin Wu, Kewei Qin, Fei Li and Lijun Zhou*[*]

Central Laboratory, Navy General Hospital of Chinese People's Liberation Army, Beijing, China

N-Acyl Homoserine Lactones (N-AHLs) are an important group of small quorum-sensing molecules generated and released into the surroundings by Gram-negative bacteria. N-AHLs play a crucial role in various infection-related biological processes of marine *Vibrio* species, including survival, colonization, invasion, and pathogenesis. With the increasing problem of antibiotic abuse and subsequently the emergence of drug-resistant bacteria, studies on AHLs are therefore expected to bring potential new breakthroughs for the prevention and treatment of *Vibrio* infections. This article starts from AHLs generation in marine *Vibrio*, and then discusses the advantages, disadvantages, and trends in the future development of various detection methods for AHLs characterization. In addition to a detailed classification of the various marine *Vibrio*-derived AHL types that have been reported over the years, the regulatory mechanisms of AHLs and their roles in marine *Vibrio* biofilms, pathogenicity and interaction with host cells are also highlighted. Intervention measures for AHLs in different stages are systematically reviewed, and the prospects of their future development and application are examined.

Keywords: N-acyl homoserine lactone, quorum sensing (QS), *Vibrio*, pathogenicity, intervention

OPEN ACCESS

Edited by:
Rodolfo García-Contreras, Universidad Nacional Autónoma de México, Mexico

Reviewed by:
Efstathios D. Giaouris, University of the Aegean, Greece
Yael González Tinoco, Universidad Nacional Autónoma de México, Mexico

***Correspondence:**
Lijun Zhou
hzzhoulj@126.com

[†]*These authors have contributed equally to this work.*

Received: *17 January 2018*
Accepted: *18 April 2018*
Published: *07 May 2018*

Citation:
Liu J, Fu K, Wu C, Qin K, Li F and Zhou L (2018) "In-Group" Communication in Marine Vibrio: A Review of N-Acyl Homoserine Lactones-Driven Quorum Sensing. Front. Cell. Infect. Microbiol. 8:139. doi: 10.3389/fcimb.2018.00139

Quorum Sensing (QS) is a phenomenon that allows bacterial communities to sense small auto-secreting molecules in the environment, allowing monitoring of population density and then regulating expressions of related genes (Bassler, 1999). These small molecules involved in bacterial QS, also known as AutoInducers (AIs) (Nealson, 1977), are classified into three types based on their synthesis pathways, namely AutoInducer-1 (AI-1), AutoInducer-2 (AI-2), and AutoInducing Peptides (AIPs) (Williams, 2007). Different bacterial species generate different AIs to carry out their QS-dependent regulatory functions.

Abbreviations: N-AHL, N-Acyl Homoserine Lactone; QS, Quorum Sensing; AI, AutoInducer; AI-1, AutoInducer-1; AI-2, AutoInducer-2; AIP, AutoInducing Peptide; MS, Mass Spectrometry; X-Gal, 5-bromo-4-chloro-3-indole-β-D-galactopyranoside; LOD, Limits of Detection; TLC, Thin Layer Chromatography; LSAC, Liquid-Solid Absorption Chromatography; HPLC, High-Performance Liquid Chromatography; UHPLC, Ultra-High-Performance Liquid Chromatography; DAD, Diode Array Detector; QTOFMS, Quadrupole Time-Off-Flight Mass Specrometer; GC, Gas Chromatography; ESI, Electrospray Ionization; NMR, Nuclear Magnetic Resonance; IS, Infrared Spectroscopy; FRET, Fluorescence Resonance Energy Transfer; mAb, monoclonal Antibody; SAM, S-Adenosyl-Methionine; ACP, Acyl Carrier Protein; Qrr sRNA, Quorum regulatory small RNA; EPS, Extracellular Polysaccharides; T3SS1 system, Type III Secretion System 1; BEMPs, Bacterial Extracellular Metalloproteases; VvhA, *Vibrio vulnificus* Hemolysin A; VCC, *Vibrio Cholerae* Cytolysin; AJ, Adherens Junction; TJ, Tight Junction; SSTIs, Skin and Soft Tissue Infections; MDR, Multi-Drug Resistance.

Gram-negative bacteria can mainly produce AI-1 and AI-2 signaling molecules that mediate QS signal transduction via different pathways (Mok et al., 2003; Liaqat et al., 2014). For example, they produce N-Acyl Homoserine Lactones (N-AHLs, AI-1) to mediate QS, to regulate various functions such as biofilm formation, toxin expression, and to escape from host immune response. Increasing studies on the role and underlying mechanism of AHLs in recent years revealed that AHLs are closely associated with the survival and the pathogenicity of most bacteria (Horng et al., 2002; Lumjiaktase et al., 2006; García-Aljaro et al., 2012a).

Vibrio are Gram-negative bacteria commonly found in the marine environment, and 12 of them have been reported as marine pathogen (Balows et al., 1991). They are not only pathogenic to many animal species used in the aquaculture industry, but also are responsible for a number of human gastrointestinal, wound, and even severe acute infections (Tarr et al., 2015). Since QS is common among marine *Vibrio*, understanding the generation, characteristics, functional regulation, and intervention means of AHLs will help increase knowledge not only on the species but also on the prevention and treatment of infections caused by *Vibrio*. This article provides an overview of the current progress and knowledge gaps on the generation characteristics, detection, regulatory functions of AHLs in marine *Vibrio*, and several different AHL-related intervention measures as well.

CHARACTERISTICS AND DETECTION OF MARINE *VIBRIO* AHLs

AHLs are a group of amphipathic small molecules (**Figure 1**), and their common structure is comprised of a hydrophilic homoserine lactone ring and a hydrophobic acyl side chain (O'Connor et al., 2015). Differences in molecular structures depend on the number of carbon (4–18), the substituent group on the third carbon (-H, -OH or -oxo), and the presence or absence of unsaturated double bonds in the acyl side chains (Kumari et al., 2006). These differences cause the diversity in the molecular structures of AHLs and in their secretion pathways. While short side-chain AHLs (<8 carbon atoms on acyl side chain, C_{4-8}-HSL) can directly penetrate cell membrane and be released into the surrounding environment upon synthesis, long side-chain AHLs (>8 carbons on acyl side chain, C_{10-18}-HSL) on the contrary can only be released through active efflux pathways, such as 3-oxo-C_{12}-HSL being exported from membranes via an active *mexAB-oprM*-encoded MexAB-OprM pump (Pearson et al., 1999). Therefore, diversity of AHLs not only indicates differences in the application of detection methods, but also serves as the basis for various functional regulation.

AHLs being generated by *Vibrio* species and AHL types being accurately detected are two important questions in QS-related studies in marine *Vibrio*. Common detection methods for AHLs include microbiosensor-based biological detection and chromatography/Mass Spectrometry (MS)-based physicochemical detection. Based on current literatures, a total of 32 AHLs-producing marine *Vibrio* species have already been identified using different detection methods. Out of the 32, 23 AHLs were definitely classified, including 10 short side-chain and 13 long side-chain AHLs (**Figure 2**;**Tables 1**,**2**).

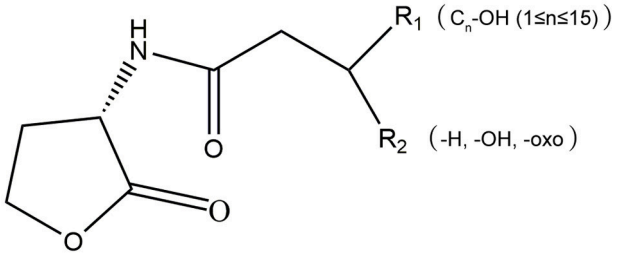

FIGURE 1 | The molecular structure of AHLs. **R1**: one at least and 15 at most are included from the 4th carbon atom on the acyl side chain of AHL molecule; **R2**: the unsubstituted (-H) or substituent groups (-OH, -oxo) on the 3rd carbon of the acyl side chain.

Characteristics of AHLs Generation in Marine *Vibrio*

AHLs generation differs among different marine *Vibrio* species (Eberhard, 1972; Nealson, 1977). For example, *V. anguillarum* produces more than 12 types of AHLs (Milton et al., 1997, 2001; Buch et al., 2003; Buchholtz et al., 2006; Purohit et al., 2013; Rasmussen et al., 2014), whereas *V. scophthalmi* and *V. harveyi* only produce one type of detectable AHL (Tait et al., 2010; Garcia-Aljaro et al., 2012b), indicating that the number of AHLs generated largely varies among marine *Vibrio*. Furthermore, only long side-chain AHLs have so far been detected in *V. scophthalmi* (García-Aljaro et al., 2008). In contrast, only short side-chain AHLs are produced in 12 *Vibrio* spp., such as *V. tubiashii* and *V. fischeri* (Eberhard et al., 1981; Kuo et al., 1994; Shaw et al., 1997; Rasmussen et al., 2014), further indicating that the AHL types and proportions also largely differ among marine *Vibrio*.

AHLs generation is also significantly different between various strains of the same species (Greenberg et al., 1979). Tait et al. (2010) isolated several strains of *V. campbelii* from coral-associated *Vibrio* (Tait et al., 2010), and found out that the AHLs detected and identified in the different strains of *V. campbelii* varied significantly, indicating that AHL generation is diverse and complex even within the same environment. This pattern of AHL generation may be associated with the rapid adaptation of *Vibrio* to environmental changes (Persat et al., 2014).

The composition of AHLs generated by marine *Vibrio* is significantly different from those found in terrestrial bacteria. Apart from the AHLs that are commonly generated in terrestrial bacteria, marine *Vibrio* generate many types of ultra-long side-chain AHLs, such as C_{14}-HSL (Girard et al., 2017), 3-OH-C_{14}-HSL (Rasmussen et al., 2014), and 3-oxo-C_{14}-HSL (Morin et al., 2003). On the other hand, AHLs such as C_7-HSL, 3-OH-C_9-HSL, 3-oxo-C_9-HSL, 3-OH-C_{11}-HSL, and 3-oxo-C_{11}-HSL are rarely identified or reported in terrestrial bacteria, but are also detected in marine *Vibrio* (Rasmussen et al., 2014).

The environmental conditions that induce generation of AHLs in marine *Vibrio* are also different from those required

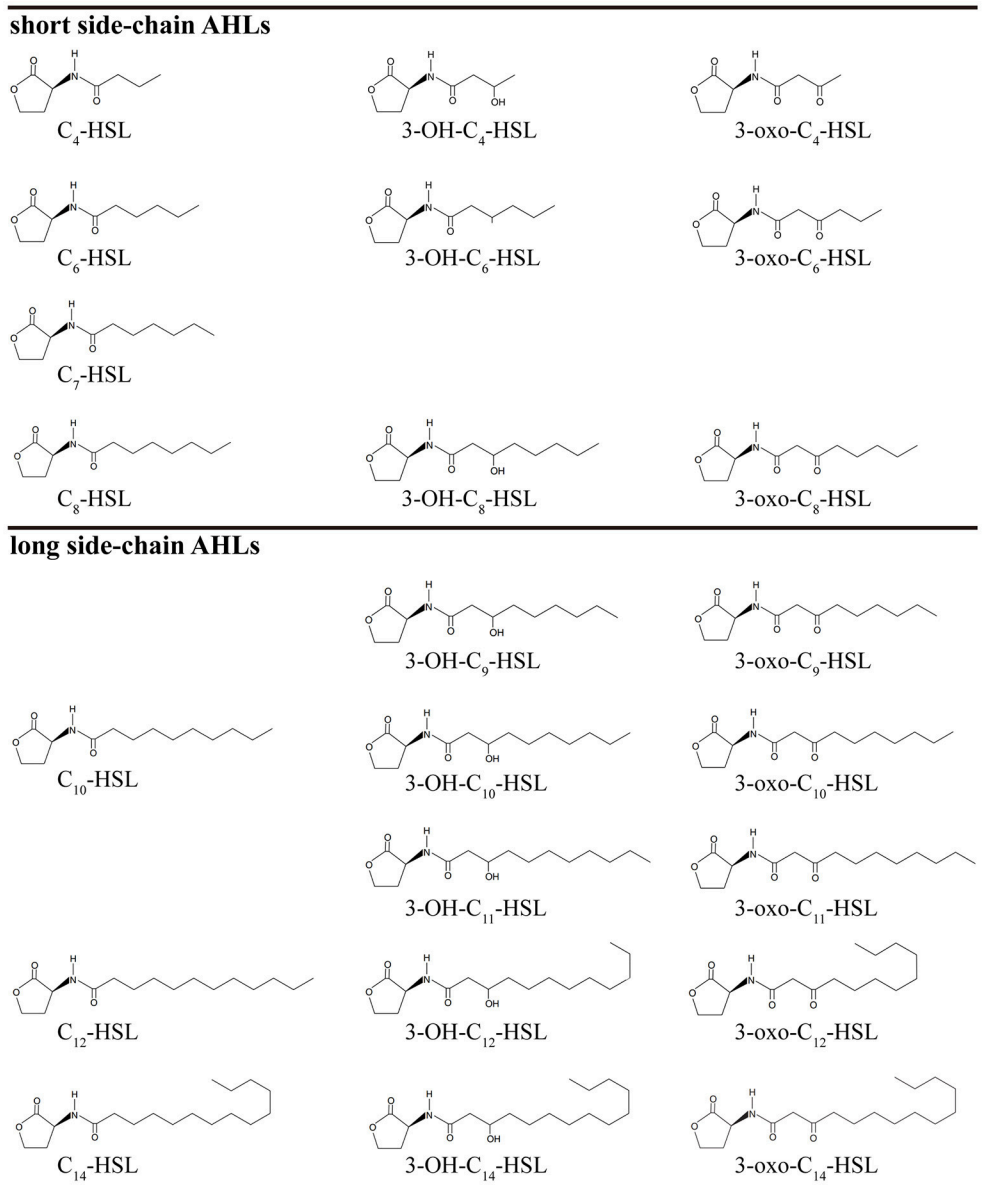

FIGURE 2 | Chemical structure of 23 AHLs produced by marine *Vibrio*.

by terrestrial bacteria. Firstly, the optimum temperature needed in marine *Vibrio* is lower than that of common terrestrial bacteria to produce AHLs. In fact, marine *Vibrio* produce more types and higher concentrations of AHLs at lower temperatures (<16°C). Thus, the AHLs diversity and concentration decrease with increasing temperature (Tait et al., 2010). Secondly, marine *Vibrio*-derived AHL types are affected more by changes in ion levels than those generated by common terrestrial bacteria (Buchholtz et al., 2006), which may be associated with greater seasonal variation in temperature and ion levels in marine environment because of complex ocean hydrography. In addition, the dominant AHL alters as the colonization state of marine *Vibrio* changes, and no report has been described by evidence on this alteration in dominant AHL in terrestrial bacteria to this day. For example, when free *V. anguillarum* infects the host, its dominant AHL changes from 3-oxo-C_{10}-HSL to 3-OH-C_6-HSL (Buchholtz et al., 2006). This change in dominant AHL types could be associated with the various regulatory mechanisms in which AHLs are involved.

Biological Detection of AHLs

Previously, AHLs generation was measured indirectly by real-time monitoring of bacterial growth rate and AHL-related gene expression, which are time and energy consuming, and has low efficiency and poor accuracy (Bainton et al., 1992; Pearson et al., 1994). With the increasing understanding of the

TABLE 1 | Statistics of the AHL types and detection methods produced by marine *Vibrio*.

Vibrio spp.	C_n-HSL							3-OH-C_n-HSL							3-oxo-C_n-HSL								References
	4	6	7	8	10	12	14	4	6	8	9	10	11	12	14	4	6	8	9	10	11	12	14	
V. aestuarianus				+[a]														+[a]						Yang et al., 2011; Garcia-Aljaro et al., 2012b
V. anguilarum	+[b]	+[ba]		+[da]				+[a]	+[dba]	+[ba]		+[db]				+[da]	+[a]	+[da]		+[dba]		+[dba]		Milton et al., 1997, 2001; Buch et al., 2003; Buchholtz et al., 2006; Garcia-Aljaro et al., 2012b; Purohit et al., 2013; Rasmussen et al., 2014
V. brasiliensis	+[d]	+[db]						+[d]												+[b]				Rasmussen et al., 2014; Tan W. S. et al., 2014
V. campbellii	+[a]	+[ae]				+[d]		+[d]	+[d]					+[d]			+[ae]							Taylor et al., 2004; Tait et al., 2010; Rasmussen et al., 2014
V. coralliilyticus	+[a]																							Tait et al., 2010
V. fischeri		+[b]		+[f]													+[afhi]	+[a]						Eberhard et al., 1981; Kuo et al., 1994; Shaw et al., 1997
V. fluvialis		+[a]		+[da]	+[g]							+[d]	+[d]			+[d]		+[d]	+[d]	+[dg]	+[d]	+[dg]		Yang et al., 2011; Wang et al., 2013; Rasmussen et al., 2014
V. furnissii				+[a]								+[a]		+[a]				+[a]						Yang et al., 2011; Viswanath et al., 2015
V. gaogenes		+[a]																						Yang et al., 2011
V. harveyi	+[a]																							Tait et al., 2010; Garcia-Aljaro et al., 2012b
V. mediterranei				+[a]													+[a]					+[a]		Taylor et al., 2004; Yang et al., 2011; Garcia-Aljaro et al., 2012b
V. metschnikovii				+[a]																		+[a]		Garcia-Aljaro et al., 2012b
V. pacinii	+[d]							+[d]																Rasmussen et al., 2014
V. proteolyticus				+[a]												+[a]								Yang et al., 2011; Garcia-Aljaro et al., 2012b; Viswanath et al., 2015
V. rotiferianus	+[da]	+[d]	+[d]	+[da]																				Tait et al., 2010; Garcia-Aljaro et al., 2012b; Rasmussen et al., 2014
V. salmonicida		+[ab]															+[ab]							Bruhn et al., 2005
V. scophthalmi														+[b]										García-Aljaro et al., 2008
V. shiloi	+[a]																							Tait et al., 2010
V. sinaloensis	+[b]																							Tan P. W. et al., 2014
V. splendidus	+[b]	+[db]	+[d]	+[a]				+[db]	+[db]	+[b]	+[d]	+[d]		+[d]	+[d]									Garcia-Aljaro et al., 2012b; Purohit et al., 2013; Rasmussen et al., 2014
V. tasmaniensis	+[a]				+[c]		+[c]							+[c]								+[c]		Tait et al., 2010; Girard et al., 2017
V. tubiashii		+[d]	+[d]					+[d]	+[d]							+[d]								Rasmussen et al., 2014
V. vulnificus	+[b]	+[b]																+[b]		+[b]		+[b]	+[b]	Morin et al., 2003; Valiente et al., 2009; Garcia-Aljaro et al., 2012b
V. xiamenensis		+[a]		+[a]								+[a]		+[a]										Viswanath et al., 2015

+, detectable; a, TLC-biosensor; b, HPLC-MS; c, UHPLC-MS; d, UHPLC-DAD-QTOFMS; e, GC-MS; f, NMR; g, ESI-MS; h, IS; i, FRET.

AHL-QS regulatory mechanisms, microbial-derived biosensors gradually replaced the above detection methods and became the conventional and standard technique for AHLs identification (O'Connor et al., 2015). Microbiosensors lack AHLs synthesis proteins but still contain the related AHL receptor proteins and functional genes. Under exogeneous AHLs stimulation, the expression of reporter genes can be initiated, which are then reflected by the changes in colony color, luminescence or enzyme activities. Microbiosensors are mainly obtained in two ways: (1) natural environmental mutation, and (2) genome editing.

For the mutation, although bacterial strains can no longer synthesize AHLs and have lost the characteristic functional expression due to gene mutation, they are still able to initiate QS regulation via exogenous AHLs recognition, leading to characteristic changes in pigments, bioluminescence and protease activities. An example of this type of biosensor is *Chromobacterium violaceum* CV026, which is a mini-Tn5 mutant of *C. violaceum* ATCC31532. *C. violaceum* CV026 has lost the ability to synthesize purple pigments itself but can proliferate purple colonies under exogenous AHLs stimulation. It is highly sensitive to short side-chain AHLs without substituents on the 3rd carbon of the acyl side chain, and with C_6-HSL as the AHL having the strongest activating capability. Furthermore, its sensitivity to short side-chain AHLs is decreased

TABLE 2 | Chemical structure information of AHLs produced by marine *Vibrio*.

AHL name	Abbreviation	Molecular formula	Molecular weight
N-Butyryl-DL-homoserine lactone	C_4-HSL	$C_8H_{13}NO_3$	171.2
N-Hexanoyl-L-homoserine lactone	C_6-HSL	$C_{10}H_{17}NO_3$	199.2
N-heptanoyl-L-homoserine lactone	C_7-HSL	$C_{11}H_{19}NO_3$	213.3
N-Octanoyl-L-homoserine lactone	C_8-HSL	$C_{12}H_{21}NO_3$	227.3
N-Decanoyl-DL-homoserine lactone	C_{10}-HSL	$C_{14}H_{25}NO_3$	255.4
N-Dodecanoyl-DL-homoserine lactone	C_{12}-HSL	$C_{16}H_{29}NO_3$	283.4
N-Tetradecanoyl-DL-homoserine lactone	C_{14}-HSL	$C_{18}H_{33}NO_3$	311.5
N-(3-Hydroxybutyryl)-L-homoserine lactone	3-OH-C_4-HSL	$C_8H_{13}NO_4$	187.2
N-(3-Hydroxyhexanoyl)-L-homoserine lactone	3-OH-C_6-HSL	$C_{10}H_{17}NO_4$	215.2
N-(3-Hydroxyoctanoyl)-DL-homoserine lactone	3-OH-C_8-HSL	$C_{12}H_{21}NO_4$	243.3
N-(3-Hydroxynonanoyl)-L-Homoserine lactone	3-OH-C_9-HSL	$C_{13}H_{23}NO_4$	257.3
N-(3-Hydroxydecanoyl)-L-Homoserine lactone	3-OH-C_{10}-HSL	$C_{14}H_{25}NO_4$	271.4
N-(3-Hydroxyundecanoyl)-L-Homoserine lactone	3-OH-C_{11}-HSL	$C_{15}H_{27}NO_4$	269.4
N-(3-Hydroxydodecanoyl)-DL-homoserine lactone	3-OH-C_{12}-HSL	$C_{16}H_{29}NO_4$	299.4
N-(3-Hydroxytetradecanoyl)-DL-homoserine lactone	3-OH-C_{14}-HSL	$C_{18}H_{33}NO_4$	327.4
N-(3-Oxoburtyryl)-L-homoserine lactone	3-oxo-C_4-HSL	$C_8H_{11}NO_4$	185.2
N-(β-Ketocaproyl)-DL-homoserine lactone	3-oxo-C_6-HSL	$C_{10}H_{15}NO_4$	213.2
N-(3-Oxooctanoyl)-L-homoserine lactone	3-oxo-C_8-HSL	$C_{12}H_{19}NO_4$	241.3
N-(3-Oxononanoyl)-L-homoserine lactone	3-oxo-C_9-HSL	$C_{13}H_{21}NO_4$	255.3
N-(3-Oxodecanoyl)-L-homoserine lactone	3-oxo-C_{10}-HSL	$C_{14}H_{23}NO_4$	269.3
N-(3-Oxoundecanoyl)-L-homoserine lactone	3-oxo-C_{11}-HSL	$C_{15}H_{25}NO_4$	283.3
N-(3-Oxododecanoyl)-L-homoserine lactone	3-oxo-C_{12}-HSL	$C_{16}H_{27}NO_4$	297.4
N-(3-Oxotetradecanoyl)-L-homoserine lactone	3-oxo-C_{14}-HSL	$C_{18}H_{31}NO_4$	325.4

by approximately 10-fold when carbonyl substituent is present on the 3rd carbon of the acyl side chains. In contrast, short side-chain AHLs with hydroxyl substituents on the 3rd carbon of the acyl side chain are not recognized by *C. violaceum* CV026 (McClean et al., 1997).

In the second type of microbiosensors construction, artificial plasmid insertion based on direct genome editing is carried out in bacterial cells to sense exogenous AHLs that induce reporter gene expression via the recombinant plasmid, leading to changes in biological characteristics of microbiosensors of this type. *Agrobacterium tumefaciens* KYC55 is a biosensor with broad-spectrum AHLs detection capacity acquired artificially, and is highly sensitive to long side-chain AHLs. *A. tumefaciens* KYC55 contains the p*T7-traR* plasmid, which has a p*tral-lacZ* promotor triggered by broad-spectrum AHLs to initiate the expression of the *lacZ* gene. The *lacZ* gene encodes β-galactosidase, which then hydrolyzes 5-bromo-4-chloro-3-indole-β-D-galactopyranoside (X-Gal) to produce a blue color in the bacterial colony (Zhu et al., 2003).

Given the diversity in microbiosensors, the types of detectable AHLs and their Limits of Detection (LOD) would also vary. Therefore, the detection of different AHLs generated by marine *Vibrio* would then be performed one by one across multiple microbiosensors for several times, with the concentrations of the generated AHLs being indirectly calculated. Although this method is not precise, its low cost and ease of use make it a popular technique for the crude screening of AHLs in marine *Vibrio*. Previously reported microbiosensors used for detecting AHLs generated by marine *Vibrio* are listed in **Table 3**.

Physicochemical Detection of AHLs

Thin Layer Chromatography (TLC) is a type of Liquid-Solid Absorption Chromatography (LSAC) commonly used in combination with microbiosensors. Generally, AHL standards and test samples are loaded onto the TLC plate and immersed in the developing solution, causing samples to migrate with different speed. After the plate is dried, the culture media containing microbiosensor is then added onto the plate for culture. Color changes or luminescence in the colonization sites of the microbiosensor are used as the reporter signals for determining the types of AHL via comparison with the AHL standards (Huang et al., 2012). The TLC-biosensor combination is a cheap, rapid and highly efficient detection method that qualitatively and semi-quantitatively identifies the types and concentrations of AHLs in mixtures (Sun et al., 2010). This makes it a favored common preliminary screening technique for AHLs detection in marine *Vibrio*. Shaw et al. (1997) was the first to utilize the TLC-biosensor method to show the generation of 3-oxo-C_6-HSL and 3-oxo-C_8-HSL from *V. fischeri* (Shaw et al., 1997). In 2015, Viswanath et al. (2015) also used the same method to identify two other AHLs (3-OH-C_{10}-HSL, 3-OH-C_{12}-HSL) synthesized by *V. fischeri*, and accurately classified the AHLs generated by *V. xiamenensis* and *V. proteolyticus* (Viswanath et al., 2015). To date, 18 marine *Vibrio* species were shown to generate AHLs using the TLC-biosensor method (**Table 1**).

TABLE 3 | The biosensors and specific traits for the detection of AHLs produced by marine *Vibrio*.

Microbiosensors	Plasmid	Sensing system	AHL types	Report system	Functional expression	References
						author, year
C. violaceum CV026	—	CviI/RC	C_6-HSL*; C_4-HSL; C_8-HSL; 3-oxo-C_{4-8}-HSL	endogenous pigment	purple colony	McClean et al., 1997
E. coli	pSB 536	AhyI/R	C_4-HSL*	LuxCDABE	bioluminescence	Tait et al., 2010
E. coli	pSB 401	LuxI/R	3-oxo-C_6-HSL*; C_6-HSL; C_8-HSL	LuxCDABE	bioluminescence	Tait et al., 2010
E. coli MT102	pSB403	LuxI/R	3-oxo-C_6-HSL*; C_6-HSL; C_8-HSL; 3-oxo-C_8-HSL	LuxCDABE	bioluminescence	Charlesworth et al., 2015
E. coli	pSB 1075	LasI/R	3-oxo-C_{12}-HSL*; C_{12}-HSL; 3-oxo-C_{10}-HSL	LuxCDABE	bioluminescence	Tait et al., 2010
A. tumefaciens NTL1	pDCI41E33	TraI/R	3-oxo-C_4-HSL - 3-oxo-C_{12}-HSL*; C_6-HSL – C_{12}-HSL	*lacZ*	β-galactosidase expression	O'Connor et al., 2015
A. tumefaciens NTL4	pZLR4	TraI/R	3-oxo-C_8-HSL*; C_{6-14}-HSL; 3-OH-C_{6-10}-HSL; 3-oxo-C_{4-14}-HSL	*lacZ*	β-galactosidase expression	Kumar et al., 2016
A. tumefaciens KYC55	pJZ372 pJZ384 pJZ410	TraI/R T7 T7	3-oxo-C_8-HSL*; C_{6-10}-HSL; 3-OH-C_{6-10}-HSL; 3-oxo-C_6-HSL; 3-oxo-C_{12}-HSL	*lacZ*	β-galactosidase expression	Joelsson and Zhu, 2006
P. putida F117	pAS-C8	CepI/R	C_8-HSL*; C_{10}-HSL	*gfp*	green fluorescence	Steidle et al., 2001
P. putida F117	pKR-C12	LasI/R	3-oxo-C_{12}-HSL*; 3-oxo-C_{10}-HSL	*gfp*	green fluorescence	Krick et al., 2007

**most sensitive AHLs.*

Despite the approval of many researchers on its qualitative detection capacity, some drawbacks remain. For example, due to the poor specificity of microbiosensor strains, migrations without matching any of colored or luminous colonization sites of the microbiosensors can easily occur when used in combination with TLC, leading to the inaccurate identification of AHL types (Buch et al., 2003).

Lately, High-Performance Liquid Chromatography tandem Mass Spectrometry (HPLC-MS) with higher sensitivity and specificity was introduced and widely applied for AHLs detection in marine *Vibrio*. HPLC-MS is a physicochemical detection method based on the different retention times of AHLs due to their molecular weights. The AHLs successively enter the mass spectrometer, and their molecular structures are determined based on ion charge-to-mass ratio. HPLC-MS has the LOD in pg level and can provide abundant information on the structures of AHLs. In 1981, Eberhard et al. used HPLC-MS to confirm that 3-oxo-C_6-HSL was the dominant AHL type produced by *V. fischeri* regulating the bioluminescence of the bacterial community (Eberhard et al., 1981). Kuo et al. (1994) subsequently demonstrated that 3-oxo-C_6-HSL was superior to C_6-HSL and C_8-HSL in inducing the bioluminescence in *V. fischeri* (Kuo et al., 1994). Since the 1990s, the TLC-biosensor method combined with HPLC-MS was commonly used across numerous AHL detection-related studies of marine *Vibrio* for the preliminary screening of AHLs generation and the accurate determination of AHLs types and concentrations (**Table 1**).

In recent years, Ultra-High-Performance Liquid Chromatography (UHPLC) has been used increasingly as the faster and more sensitive chromatography in detecting AHLs for its great application potentials. UHPLC-MS or UHPLC-Diode Array Detector-Quadrupole Time-Off-Flight Mass Spectrometer (DAD-QTOFMS) even provides accurate identification and quantification of the tested AHLs. Its ultra-high precision, stability and scan quality do not only detect common AHL types but also AHLs with ultra-long acyl side chains ($>C_{14}$) or covalent double bonds (Rasmussen et al., 2014; **Table 1**). In 2017, Girard et al. first reported the generation of C_{14}-HSL in *V. tasmaniensis*, and used UHPLC-MS/MS to confirm the presence of an unsaturated double bond in its acyl side chain (Girard et al., 2017). UHPLC not only overcomes the time-consuming disadvantage of HPLC, but it also greatly increases the types of detectable AHLs, and is therefore a milestone in the study of marine *Vibrio* AHLs.

Moreover, other physicochemical and photochemical methods, such as Gas Chromatograph tandem MS (GC-MS) and Electrospray Ionization tandem MS (ESI-MS), are also widely applied in the detection of marine *Vibrio* AHLs

(Taylor et al., 2004; Wang et al., 2013; **Table 1**). GC-MS analyzes the molecular structures of AHLs based on the differences in adsorption intensity to inert gas and thereby their sequential entrance into the mass spectrometer. However, certain AHL types in the mixture sample may be lost during this process since they are sensitive to temperature change and may degrade during gasification. On the other hand, ESI-MS accurately determines the structure of AHLs via AHL gasification and analysis of the resulting ion fragments. Since AHLs are often a mixture of various types, it is difficult to accurately isolate each of them during gasification and could be missed. Furthermore, other physicochemical methods such as Nuclear Magnetic Resonance (NMR) (Kuo et al., 1994), Infrared Spectroscopy (IS), and Fluorescence Resonance Energy Transfer (FRET)were also used in some studies (Zhang and Ye, 2014). However, these methods are unable to meet the demands of rapid AHLs detection owing to their complicated operation procedures and high requirements on sample preparation. As a result, only few laboratories were able to use these methods for AHLs detection and analysis in marine *Vibrio*, making them unpopular in the research field.

Immunological Approaches

Apart from the aforementioned methods, some studies also attempted detection using immunological approaches. Although several antibodies against AHLs are now available, many limitations still exist. The RS2-IG9 antibody for example, developed against 3-oxo-C_{12}-HSL (antigen) from *Pseudomonas aeruginosa* by Kaufmann et al. (2008), has a limited AHL detection range due to its inability to bind other AHLs (Kaufmann et al., 2008). Despite the subsequent emergence of several patented monoclonal Antibodies (mAbs) targeting the homoserine lactone ring or carboxylic acid derivatives on the acyl side chain of AHLs (Janda et al., 2010; Charlton and Porter, 2012; Bhardwaj et al., 2013), many of these mAbs are still under experimental investigation and are therefore not yet applicable for conventional detection.

SYNTHESIS AND REGULATORY MECHANISMS OF MARINE *VIBRIO* AHLs

Synthesis of AHLs

AHLs can be catalytically synthesized by LuxI homologous proteins (Gilson et al., 1995; Henke and Bassler, 2004; Bruhn et al., 2005; Rasmussen et al., 2014; O'Connor et al., 2015). While some synthtic proteins of AHLs were found in terrestrial bacterial species, such as TraI in *A. tumefaciens* (White and Winans, 2007), RhlI and LasI in *P. aeruginosa* (Brint and Ohman, 1995; Seed et al., 1995), other synthtic proteins of AHLs were present in *Vibrio* species, such as VanI in *V. anguilarum* (Milton et al., 1997), LuxI and AinS in *V. fischeri* (Schaefer et al., 1996; Hanzelka et al., 1999). As **Figure 3** shows, LuxI-type proteins first synthesize AHL precursors via the acylation of S-Adenosyl-Methionine (SAM), which removes methylthioadenosine through internal nucleophilic substitution to form the homoserine lactone ring of AHL. Then, Acyl Carrier Protein (ACP)-fatty acyl group derivatives are transferred onto the amino groups of SAM to form

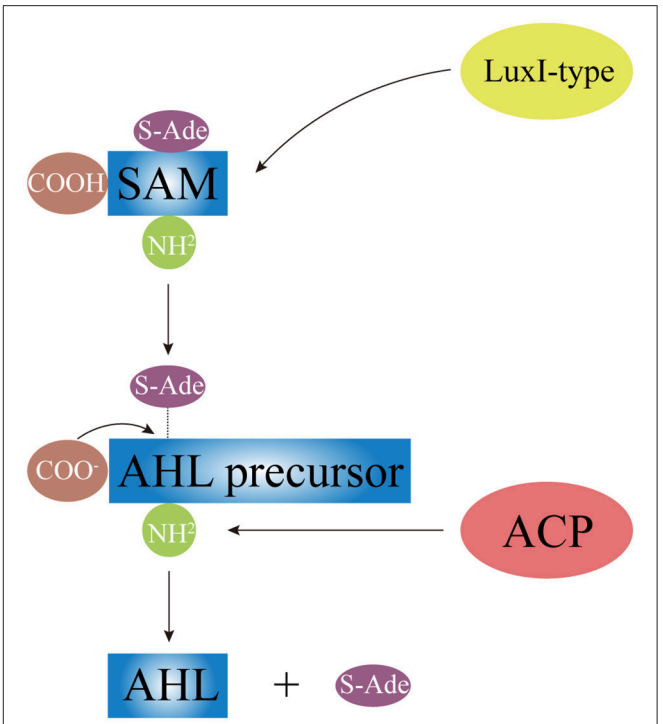

FIGURE 3 | The schematic diagram of AHL synthesis. Under the catalysis of LuxI-type protein, AHL precursor (the HSL ring) is formed via acylating of SAM and removing the S-Ade; the acyl side chain is formed by the transferring of ACP-fatty acyl group derivative onto SAM. SAM, S-Adenosyl-Methionine; S-Ade, methylthioadenosine; ACP, Acyl Carrier Protein.

acyl side chains with various carbon numbers and chain lengths, which ultimately forms the entire AHL molecule. Difference in the geometric location of the binding site among different LuxI-type proteins determines the status of the third carbon on the acyl side chain, such as saturation (C_3-H) or oxidation (C_3-OH, C_3-oxo), as well as the degree of methylation.

Regulatory Mechanisms of AHLs

As Chapter 1 has mentioned, AHLs are secreted to environment immediately via different secretion pathways after being produced. Short side-chain AHLs are directly released out of the cell upon synthesis while long side-chain AHLs are actively secreted to the environment. Both AHL types are involved in QS signal transduction. There are more than three QS transduction systems existed in *Vibrio*, which present the complexity of diversification and precise regulatory mechanisms in *Vibrio* species (see a review by Milton, 2006). Among all the QS systems, there are two AHL-mediated QS transduction systems in *Vibrio* including the direct "LuxI/R" system and the cascade regulatory system. Of the two the direct "LuxI/R" system first explored in *V. fischeri* is the most known one (Engebrecht and Silverman, 1984). The bioluminescence of *V. fischeri* as an example is the result of LuxR-mediated activation of the LuxCDABE protein, which was also the first QS regulation identified in bacteria. In the LuxI/R QS system, LuxI protein acted as the AHL synthase,

and LuxR protein acted as the direct ligand protein of AHLs. The "LuxI/R" system allows bacterial cells to form AHL-receptor complex, which could then bind the functional DNA domain to the subsequent QS related genes (Choi and Greenberg, 1992).

Studies on *V. fluvialis*, *V. harveyi,* and *V. cholerae* showed that marine *Vibrio* species share similar AHLs regulatory cascades. In an intact AHLs regulatory cascade, the concentration of AHLs increasing to a sensing threshold level of LuxN protein is the key to form AHL-receptor complex in subsequently and to lead a successful QS signal transduction. There are three key molecule types involved in the regulatory cascade of AHLs. The first one is the "two-component" phosphorelay system (Ronson et al., 1987; Parkinson and Kofoid, 1992), where AHLs-sensing LuxN (a cytoplasmic membrane-bound protein) presents as the "input" element and its response regulator LuxO protein as the "output" element (Freeman et al., 2000). LuxN is responsible for sensing AHLs using its "input" domain and for modulating the transmitter activity by changing phosphorylation status of the histidine residue using its transmitter domain (Freeman and Bassler, 1999). LuxO is in response to receive and pass the transmitter signals to the "output" domain by changing phosphorylation status of the aspartate residue. The second one is the Quorum regulatory small RNAs (Qrr sRNAs), and they are in response to degrade the LuxR-type receptor proteins of AHLs via interacting with the chaperone molecule Hfq. The last one is the LuxR-type proteins, which are in charge of activate downstream signaling cascade.

As shown in **Figure 4**, when the concentration of AHLs is too low to be detected, LuxN presents as kinase, and the autophosphorylation of it occurs normally, activating its downstream transcription factor LuxO via the prior phosphorylation of histidine phosphotransfer protein LuxU (Freeman and Bassler, 1999). This then leads to the expression of Qrr sRNAs (Lilley and Bassler, 2000; Lenz et al., 2004), which sustains the degradation of LuxR-type AHL receptor proteins via interaction with Hfq (Tu and Bassler, 2007). In addition, under the role of two-component phosphorelay system, the phosphorylation of LuxO protein directly promotes the competitive binding of the downstream transcriptional regulators AphA (against OpaR) to the membrane fusion operon *mfpABC* via the activation of Qrr sRNAs expression, which finally inhibits bacterial biofilm formation (Zhou et al., 2013). There are also several feedback mechanisms on Qrr sRNA-related QS cascade (**Figure 4**; Ball et al., 2017). The increased expression of Qrr sRNAs could directly suppress the expression of LuxO and LuxN protein to maintain the whole dynamic accommodation system (Feng et al., 2015). Coincidentally, the feedback regulation between transcriptional regulator AphA and Qrr sRNAs is almost the same (Rutherford et al., 2011).

On the other hand, when the concentration of environmental AHLs gradually increases to the sensing threshold of LuxN protein, its spontaneous autophosphorylation is inhibited. That in turn inhibits the phosphorylation of downstream proteins (Timmen et al., 2006) such as LuxU protein, which further interferes the phosphorylation of LuxO, leading to the inhibition of Qrr sRNAs expression. As a result, LuxR-type receptor protein is continuously synthesized, and it binds to the acyl side chain of free AHLs to form AHL-receptor transcription complex. The complex regulates the expression of multiple downstream target genes, such as the master regulating gene *luxR* of *V. harveyi* (Van Kessel et al., 2013), the elastase coding gene *lasR* of *P. aeruginosa* (Gambello and Iglewski, 1991), the curvature coding gene *crvA* of *V. cholerae* (Bartlett et al., 2017), and the QS regulon coding gene *esaR* of *Pantoea stewartii* (Ramachandran et al., 2014). Thus, those aforementioned regulations ultimately initiate or silence RNA transcription and protein translation to express related functions (Bassler et al., 1994; Anetzberger et al., 2009; **Figure 5**).

REGULATORY FUNCTIONS OF MARINE *VIBRIO* AHLs

AHL and Biofilm Formation

When the environmental surface is suitable for bacterial survival, biofilm formation starts from the adhesion of bacterial cells. Along with the enhanced secretion of extracellular enzymes, biofilm matrix builds and biofilm reaches to its mature stage eventually. At the end stage of biofilm formation circle, biofilm starts to collapse, leading to the increased motility of the bacterial cells within the matrix. The collapsing allows bacteria to attach to suitable environmental surfaces, followed by a new period of biofilm formation, including enhanced secretion of extracellular enzymes and formation of biofilm matrix (**Figure 6**). Biofilm formation is also connected to changes in colony morphology, proliferative metabolism, and drug resistance. Bacteria within the biofilm have significantly slower metabolism and present antibiotic resistance properties. The structure of the biofilm matrix protects bacteria from host cell-mediated or drug-induced phagocytic clearance, allowing the bacteria to evade the host's immune system (Bhardwaj et al., 2013).

Indeed, previous studies have shown that AHLs increases the survival of marine *Vibrio* by regulating key processes of biofilm formation in many ways (McDougald et al., 2006). First, AHLs regulate the excretion of Extracellular Polymeric Substances (EPS) to constitute the cage construction of biofilm matrix. The matrix provides a suitable space for bacterial colonization and stable metabolism. Its porous nature and complex structure allow bacteria cells to hide deeply within the matrix, allowing avoidance of host immune cell-mediated cytotoxicity or phagocytosis and to effectively block the permeation of antibiotics. AHLs such as C_4-HSL and C_6-HSL also upregulate the expression of ESP-related genes via binding to AHL receptor proteins, which in turn increase EPS production by forming denser biofilm matrix and reinforced defense barrier (Jamuna and Ravishankar, 2016). Second, AHLs regulate the ability of adhesion or detachment of marine *Vibrio*, allowing the colonization changes for a better adaption to the environment, thus EPS excretion changes in order to quicken or reduce a new period of biofilm formation (Phippen and Oliver, 2015). When the bacteria are in a harsh environment, AHLs enhance bacterial adhesion to adjacent solid surfaces so as to promote clonal proliferation and to speed up the EPS excretion. Once the environmental condition is improved, Qrr sRNAs degrade LuxR-type AHL receptor proteins to reduce *Vibrio* adhesion and enhance their mobility (Phippen and

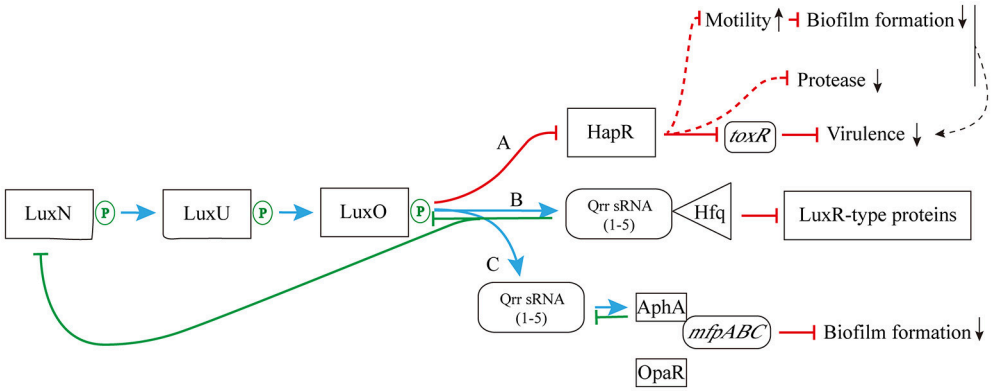

FIGURE 4 | The pathway of phosphorylation for LuxN protein**. (A)** The LuxN phosphorylation inhibits the expression of HapR, and further influences the expression of virulence factor ToxR; **(B)** The LuxN phosphorylation promotes the combination of Qrr sRNA and Hfq, and it constantly degrades LuxR-type proteins; **(C)** The LuxN phosphorylation activates the expression of Qrr sRNAs, allowing competitive combination of transcriptional regulator AphA and membrane fusion operon *mfpABC*, and inhibiting biofilm formation. Blue arrow: positive regulation; red solid T-connector: direct negative regulation; red dashed T-connector: indirect negative regulation; green solid T-connector: direct negative regulation in the feedback pathway; black dashed arrow: indirect positive regulation; green P-circle: phosphorylation; down arrow: weakened expression.

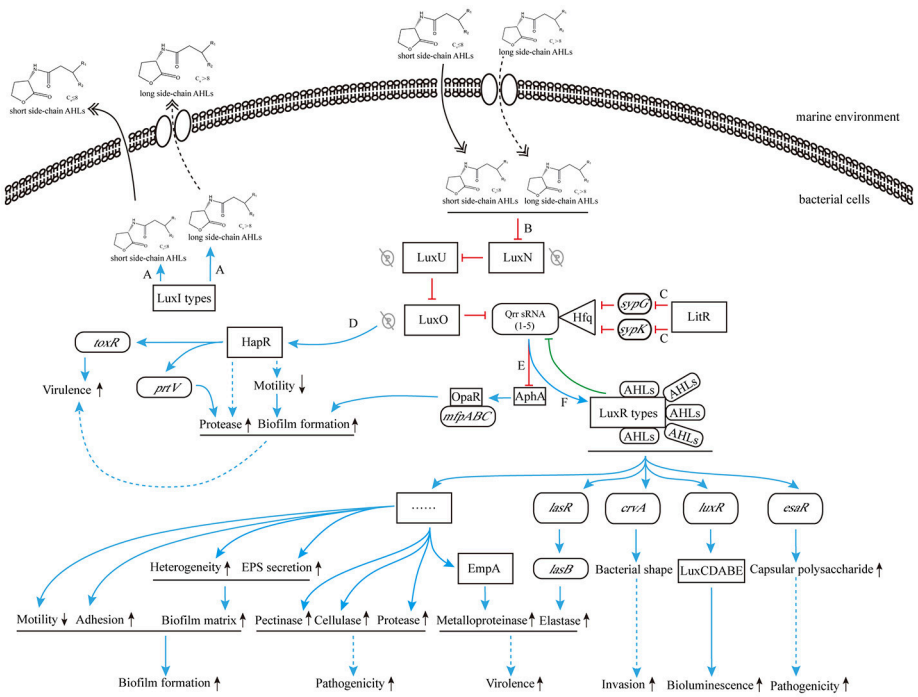

FIGURE 5 | The cascade control mechanism of AHLs produced by marine *Vibrio*. **(A)** LuxI-type proteins synthesize and release AHLs to the environment; **(B)** high concentration of AHLs inhibit the phosphorylation for LuxN protein; **(C)** the transcription inhibition of *sypG* and *sypK* by LitR inhibit the combination of Qrr sRNAs and Hfq, and promote the production of LuxR-type protein; **(D)** the inhibition of phosphorylation for LuxN protein removes the surpression of HapR, resulting to direct increased ToxR expression and indirect down regulation of bacterial motility and subsequent increased regulation of biofilm formation and protease production, and promotes bacterial virulence; **(E)** the inhibition of Qrr sRNAs expression is in favor of combining OpaR to *mfpABC*, further increases biofilm formation; **(F)** the AHL-LuxR protein complex activates downstream functional pathways. Blue solid arrow: positive regulation; blue dashed arrow: indirect positive regulation; red T-connector: negative regulation; green T-connector: negative regulation in the feedback pathway; double-headed solid arrow: direct release; double-headed dashed arrow: active transmembrane transport; gray P-circle with a strikethrough: unhappened phosphorylation; up arrow: enhanced expression; down arrow: weakened expression.

Oliver, 2015), resulting to migration and proliferation of colony to compatible environments. Third, AHLs alter *Vibrio* colony morphology to facilitate biofilm formation. Changes in the colony morphology dynamically regulate the surface area of the biofilm. Compared with a smooth colony, a wrinkled one can effectively increase its surface area to enhance bacterial adhesion

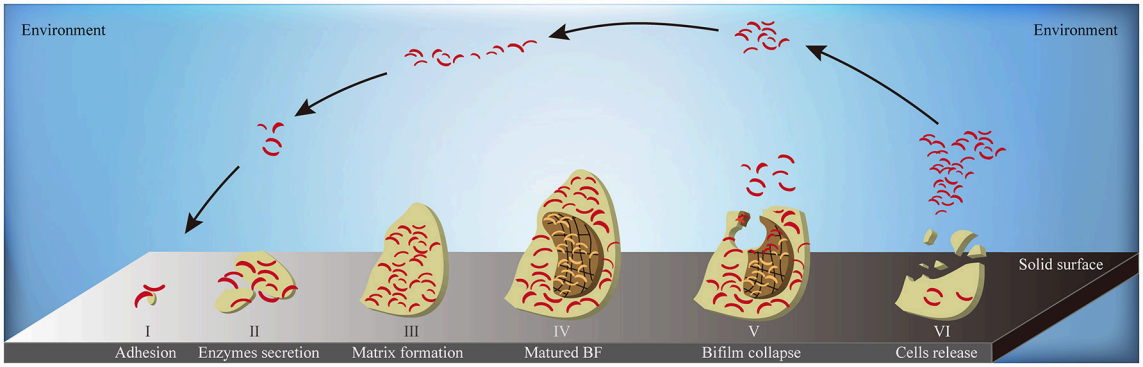

FIGURE 6 | The schematic diagram of biofilm formation. A complete circle of biofilm formation contains: (I) the adhesion of bacterial cells to suitable solid surface; (II) the enhanced secretion of extracellular enzymes; (III) the formation of biofilm matrix; (IV) the formation of matured biofilms; (V) the collapse of biofilm in the middle-end stage; (VI) the release of bacterial cells inside the biofilm to environment in the end stage. BF, biofilm; yellow flat, the entire biofilm; borrow flat, the biofilm matrix; red bend pole, bacterial cells.

to the biofilm. Furthermore, active proliferation of the surface bacteria increases the heterogeneity of the biofilm, which in turns positively regulates its associated functions (Anetzberger et al., 2009). LitR, a transcription inhibitor of the *syp* gene family, inhibits *syp*-mediated transcription of Qrr sRNAs to promote the formation of the AHL-LuxR receptor transcription complex (Miyashiro et al., 2014), which regulates the transformation of smooth to wrinkled *V. salmonicida* colonies, and thus, enhancing biofilm formation (Hansen et al., 2014).

AHL and Bacterial Pathogenicity

Bacterial virulence is associated with the strength of bacterial pathogenicity in the host. The invasiveness level and the expression of virulence genes are two critical factors on bacterial virulence, which could exercise either combined effects or solo effects. In most *Vibrio* species, the above-mentioned factors often coordinate with each other. Taken wound infection by *V. vulnificus* as an example, the strong invasive capacity of *V. vulnificus* determines the accurate path and rapid efficiency when entering host bloodstream, and along with *V. vulnificus* proliferation, the subsequent accumulation and regulation of toxin expression via various virulence genes would lead to a high risk of *V. vulnificus*-related death (Lubin et al., 2015). However, as a non-bacteremia *Vibrio* species, *V. cholerae* doesn't cause septicemia but severe diarrhea, acute acidosis and vomiting, which is resulted in the solo-effects of its toxins (Rai and Chattopadhyay, 2014), such as the canonical *Vibrio cholerae* Cytolysin (VCC; He and Olson, 2010).

Substances related to bacterial invasiveness include extracellular enzymes, capsular polysaccharides and other proteins, which play crucial roles in breaking the defense barrier of the host. Bacterial virulence-related proteins encoded by virulence genes could induce the apoptosis of host cells during pathogen infection and lead to the development of various symptoms such as systemic infection and multiple-organ failure. For example, the transcriptional activator ExsA activates the expression of Type III Secretion System 1 (T3SS1 system) and causes disease progression of *V. parahaemolyticus* (Zhou et al., 2008); the pore forming toxin *Vibrio vulnificus* Hemolysin A (VvhA) is an important exotoxin of *V. vulnificus* and causes apoptosis in epithelial cells (Lohith et al., 2015); VCC of *V. cholerae* has potent cell-killing activity and is listed as its prominent membrane-damaging cytolysin (Khilwani and Chattopadhyay, 2015). Early in 1993, the study of Jones et al. (1993) had already revealed the virulence regulation of QS system, and in recent years, more studies have further shown that the expression of virulence-related pathogenic factors of *Vibrio* is strictly regulated by QS system and the environment (Bhardwaj et al., 2013; Lee et al., 2014; Hema et al., 2015; Jung et al., 2015).

Bacterial Extracellular Metalloproteases (BEMPs) are an important type of invasive exocytotic enzymes, and the dependence on the iron acquisition is a key factor for the expression and regulation of BEMPs (Nguyen and Jacq, 2014). BEMPs can be divided into 63 families based on differences in the homologous sequence (Zhang Y. Y. et al., 2017). Elastase is currently the most widely studied enzyme despite no studies or reports of it being produced by *Vibrio*, the production of which is closely related to QS system. As one of the important pathogenic determinants in *P. aeruginosa*, the elastase production is regulated by *lasB* gene, which is activated by the AHL-LasR receptor complex mediated through the binding of the QS signaling molecule 3-oxo-C_{12}-HSL to its receptor LasR (Gambello and Iglewski, 1991). During this process, 3-oxo-C_{12}-HSL reaching threshold concentration and activating relevant regulatory cascade provide an important intercellular transport pathway for the expression of elastase (Passador et al., 1993).

As reported in the newly published MEROPS database (January 2017)[1], *Vibrio* species can produce multiple families of BEMPs including M4, M48 and S1. Taken EmpA—a metalloprotease in the BEMP family—as an example, it is a AHL-regulated virulence factor of *Vibrio* (Denkin and Nelson, 2004). Croxatto et al. (2002) have demonstrated that LuxR-type QS

[1]https://www.ebi.ac.uk/merops/index.shtml

transcriptional regulator VanT is required for EmpA expression in *V. anguillarum*. The positive regulation of VanT could enhance EmpA expression, and thereby increase the total secretion of BEMPs from *Vibrio* (Croxatto et al., 2002). QS-mediated regulation of BEMPs has been well exploited in some terrestrial bacteria, such as *lasB*-mediated regulation of elastase via AHL-LasR receptor complex in *P. aeruginosa* (Gambello and Iglewski, 1991; Wei et al., 2015); *Clostridium perfringens* hemolysins CPA and PFO are regulated by the CpAL QS system (Vidal et al., 2015). In *Vibrio* species, HapR protein, a master regulator in *V. cholerae*, has been found to positively regulate *V. cholerae* protease production via upgrading the coding activity of a downstream BEMP related gene *prtV* under the high cell density condition (**Figure 5**; Nguyen and Jacq, 2014). However, since there are fewer studies on the AHLs-mediated regulation of *Vibrio* BEMPs than there are on common terrestrial bacteria, further supplementary data and investigation are required to elucidate the relevant phenotypes and mechanisms.

Besides the regulation of AHLs on BEMPs, many studies have shown that AHLs participate in the regulation of marine *Vibrio* pathogenicity via regulating other virulence-related proteins. For example, ToxR, a classic *Vibrio* virulence factor encoded by the virulence-related gene *toxR*, is directly regulated by AHLs. ToxR was first discovered in *V. cholerae*, and subsequent studies showed that homologous genes of *toxR* also exist in many pathogenic *Vibrio* species such as *V. parahaemolyticus*, *V. vulnificus,* and *V. alginolyticus*. When AHLs concentration is below threshold, the regulator LuxO affects the expression of *toxR* gene through inhibition of the production of its upstream protein—HapR, thereby keeping *Vibrio* virulence at a relatively attenuated level (**Figure 4**). In contrast, when AHLs concentration is higher than the threshold, LuxO is no longer capable of inhibiting the generation of HapR protein, leading to increased toxin synthesis by the *toxR* gene. Meanwhile, bacterial pathogenicity is also synergistically enhanced by the combined regulation of various biological activities, including the down regulation of bacterial motility and subsequent increased regulation of biofilm formation and protease production (**Figure 5**; Ball et al., 2017).

The curvature determinant protein CrvA, which is another virulence factor, is also regulated by QS signaling molecules. CrvA could alter the vibrioid shape of *V. cholerae* based on the changes occurring in the environment. *V. cholerae* invasiveness increases when CrvA changing the cell from a rod to a bent shape, allowing effective entrance into the host's gut for colonization and proliferation (Bartlett et al., 2017).

Apart from virulence factors ToxR and CrvA, the expressions of various *Vibrio* toxins, such as *Vibrio vulnificus* Hemolysin (VVH) and toxin A (Elgaml et al., 2014), are also directly regulated by AHLs. The synergistic expression of *Vibrio* toxins and virulence factors could enhance bacterial pathogenicity. However, relevant reports on this field remain scarce compared to those done on terrestrial bacteria, which merits further investigation and research.

Interaction Between AHL and Host

With an interaction called inter-kingdom signaling (Hughes and Sperandio, 2008), AHLs could modify various types of eukaryotic host cells and modulate host's defense system so as to exert multiple regulatory functions to higher organisms (Hartmann and Schikora, 2012). AHL-mediated regulation of the immune system is a common topic among many current studies.

AHLs directly regulate immune cell proliferation. Taken the signaling molecule 3-oxo-C_{12}-HSL as an example, it could inhibit the proliferation of T lymphocytes and human dendritic cells in a dose-dependent manner (10–100 μm; Boontham et al., 2008). Besides, different AHLs have significantly different regulatory efficiency on host cells. AHLs-related comparative study by Gupta et al. (2011) showed that C_4-HSL and 3-oxo-C_{12}-HSL within a certain dose range (1–30 μm) could both inhibit splenic T cell proliferation in mice, while this inhibitory effect could only be detected at high concentration of C_4-HSL addition alone. In contrast, low concentration of 3-oxo-C_{12}-HSL alone was sufficient to inhibit T cell proliferation (Gupta et al., 2011). The study of Gupta et al. (2011) indicates that long side-chain AHLs have better regulatory efficiency than short side-chain AHLs, and the combination of both types has greater inhibitory effect than either AHLs alone.

As well as the regulation of cell proliferation, 3-oxo-C_{12}-HSL also affects immune cell survival by inducing apoptosis of neutrophils (Tateda et al., 2003; Li et al., 2010), mast cells and phagocytes in a dose-dependent manner (10–100 μm). 3-oxo-C_{12}-HSL could as well activate phagocytosis in human phagocytes via activation of the p38-MAPK pathway, leading to inflammation (Vikström et al., 2005). In the meantime, 3-oxo-C_{12}-HSL acts as a chemokine to promote neutrophil migration to the inflammation site and induces host inflammatory response (Zimmermann et al., 2006).

AHLs could alter the host immune response pattern (Rumbaugh et al., 2004). Specifically, high concentration of synthesized AHLs could modulate the immune response of host cells by switching from the Th_1 immune response, which protects host cells, to the Th_2 immune response, which is more suitable for bacteria survival (Moser et al., 2002; Hooi et al., 2004). At the same time, these signaling molecules inhibit the activation of Th_1-type immune response to enhance the AHLs-QS phenomenon (Gupta et al., 2011). During host immune response, other than inducing changes in immune cells, 3-oxo-C_{12}-HSL also acts on several cells such as epithelial cells, fibroblasts and lung fibroblasts to synergistically mediate transformation to Th_2 immune response (Smith et al., 2001, 2002).

In addition to the immune system, AHLs also regulate other cell types such as epithelial cells. 3-oxo-C_{12}-HSL is the most commonly studied AHL molecule as it could (1) directly damage the barrier function of intestinal epithelial cells Caco-2 (Vikström et al., 2006), and (2) modify the integrity of epithelial cells via altering tyrosine, serine and threonine phosphorylation in Adherens Junction (AJ) transmembrane protein E-cadherin, cytoplasmic protein β-catenin, Tight Junction (TJ) transmembrane protein occluding,

and TJ cytoplasmic protein Zonula Occludens-1 (ZO-1) in a time-dependent manner (Vikström et al., 2009).

AHLs-RELATED INTERVENTION MEASURES

Vibrio genus included pathogenic species that are widely found in the marine environment (see a review by Milton, 2006), and their infections cause a series of diseases such as acute gastroenteritis (Shimohata and Takahashi, 2010), septicemia (Horseman and Surani, 2011), and Skin and Soft Tissue Infections (SSTIs; Diaz, 2014). These diseases have acute onset, rapid progression, and may lead to multiple organ failure or even death in severe cases (Janda et al., 2015). As a consequence of increased antibiotic abuse worldwide, the gradual development of Multi-Drug Resistance (MDR) in marine *Vibrio* renders the current measures for *Vibrio* infection less effective, making the search for new anti-*Vibrio* infection measures an urgent focus of research (Elmahdi et al., 2016). As previously discussed in this article, AHLs not only regulate many physiological functions in marine *Vibrio*, but also cause damages to the host cells and immune system, thereby playing a key role in the infection process. With the increased understanding of the regulatory mechanisms of AHLs, blocking key factors in their regulatory pathways and hence inhibiting the downstream effects of AHLs may serve as potential prevention measures and treatments for *Vibrio* infections.

Intervention measures for AHLs-mediated regulation reported in the current literature could be divided into three strategies. The first involves the inhibition of AHLs generation via blocking the synthesis pathway (including the synthesis proteins and the two-component phosphorelay system; Kalia and Purohit, 2011). Specifically, triclosan could inhibit the production of ACP protein by disrupting the chromosomal *fabI* gene, which in turn hinders the function of AHL synthase RhlI and blocks C_4-HSL synthesis (Hoang and Schweizer, 1999); closantel inhibits the two-component phosphorelay system by altering the structure of histidine kinase sensor "in-put" element (Stephenson et al., 2000), leading to a suppression of AHL synthesis genes (Zhang, 2003). Furthermore, *V. harveyi* R-21446 and *V. harveyi* Fav 2-50-7 isolated from coral-associated microbial colonies could either interfere with the color change of bacterial colony or inhibit biofilm formation of other bacterial groups by blocking AHLs synthesis of the tested bacteria, while the AHL production of themselves was not influenced (Tait et al., 2010; Golberg et al., 2013), and are then considered natural anti-AHL *Vibrio*.

The second intervention type involves the degradation of synthesized AHLs. For example, the AHL-degrading enzyme AiiA produced by *Bacillus* spp. is a lactonase presenting broad spectrum anti-AHL characteristics and displays natural tolerance to acidic environments (Augustine et al., 2010). AiiA inhibits biofilm formation by degrading AHL and blocking its signaling pathway, and significantly reducing the pathogenicity of *Vibrio* in the host, making it a potential AHL inhibitor (Augustine et al., 2010). Further, some higher organisms, such as brine shrimp, have the ability to inactivate AHLs by at least two methods: (1) by providing a highly alkaline intestinal environment, the synthesized AHLs could be hydrolyzed immediately; (2) by producing AHL-inactivating enzymes to reduce the formation of AHL-receptor complex (Defoirdt et al., 2008).

The third-class functions by interfering with AHL-receptor complex formation. Based on the mechanistic pattern of AHL inhibitors, AHL-receptor complex formation could be intervened via four main approaches. (A) Via reducing the binding efficiency of AHL-receptor to its promoter sequence. For example, cinnamylaldehyde and its derivatives block the binding efficiency of transcriptional regulator LuxR-type protein to its promoter sequence, which then affects the expression of the latter, leading to the forming inhibition of AHL-receptor complex, and eventually hinder the downstream regulatory functions of AHLs (Brackman et al., 2008). (B) Via performing the competitive binding to AHL receptor between AHL inhibitor and AHL, and the downstream pathway of gene expression could be eventually blocked. For example, thiazolidinedione analog competitively binds to the binding sites on the amino group or carboxyl group of LuxR protein to block the formation of AHL-LuxR receptor complex (Rajamanikandan et al., 2017), ultimately decreasing the expression of downstream genes. (C). Via changing the structure of AHL receptors. QS inhibitors such as Furanone C-30, which reduces the stability of LuxR receptor and facilitate the structural change of the latter prevent the formation of the AHL-receptor complex (Ren et al., 2001; Lowery et al., 2008). (D) Via modulating AHL receptor-mediated regulation of downstream genes. For example, coumarin significantly reduces LuxR-mediated regulation of downstream genes, and alters the protease activity and hemolytic capacity of *V. splendidus*, resulting in reduced virulence expression (Zhang et al., 2017).

The three major intervention measures target different parts of the AHLs regulatory cascade to inhibit regulation of downstream functions, leading to interference of the infection process and reduced pathogenicity of marine *Vibrio* (Bhardwaj et al., 2013; Chu and McLean, 2016).

CONCLUSION AND PROSPECTS

AHLs are important QS signaling molecules produced by many bacteria genera, especially as the foremost type of QS molecules in a variety of Gram negative bacteria, such as *P. aeruginosa* and *Acinetobacter baumannii* (Smith et al., 2002; Chan et al., 2014). AHLs are not solely restricted to terrestrial bacteria, but are commonly found among marine *Vibrio*. They are involved in many key regulations and play crucial roles in the progress of *Vibrio* infections. With the increased emergence of antibiotic-resistant *Vibrio* species in recent years, studies on QS system have become the new breakthrough for the prevention and treatment of marine *Vibrio* infections.

From the detection methods of AHLs to their production diversity, there are several features about AHLs characterization in *Vibrio* summarized in this article, including types, concentrations, and dominance alteration. Among these features

of *Vibrio*, an article by Buchholtz et al. (2006) discussed about the dominant AHL change in *V. anguillarum* along with differing environments, which so far has only been reported once. Yet, is this dominance changing of AHLs only happening in *Vibrio*? Or, is there any close relationship between this phenomenon and *Vibrio* adaption to different environments? There is still no further research continuing with these hypotheses. Currently, from AHLs regulating functions to AHL-related QS prevention strategies, most studies focus on common terrestrial pathogens such as *P. aeruginosa* and other bacteria especially on the interaction between AHLs and host cells, while the fewer studies in *Vibrio* are still on their exploration stage based on the similar researches in terrestrial bacteria. This means either a stagnate or a slow-moving forward in this field, which is expected to be seen for a breakthrough in the future.

Since the research direction is somewhat limited as above-mentioned, further studies will be required to determine other specific AHLs-related functions and regulatory mechanisms that may be present in *Vibrio* species. Therefore, expansion of research on the generation, regulation and relevant functions of AHLs in marine *Vibrio* has great application potentials and deserve further in-depth investigations.

AUTHOR CONTRIBUTIONS

JL and LZ conceptualized this review. KF and LZ designed the frame structure of this review based on the idea. JL and KF organized the original writing of this review. CW and KQ confirmed the logic validity of this review. FL and LZ proofread the paper. JL and KF contributed equally to this work. All authors discussed the conclusion and commented on the manuscript.

FUNDING

This work is supported by the Key Foundation of Navy General Hospital (Grant No.: 14J004) and National Natural Science Foundation of China (Grant No.: 81273311 and 31400107).

ACKNOWLEDGMENTS

We thank our colleagues, MS. Yuxiao Wang, Dr. Xiaojie Yu, Dr. Weizheng Shuai, MS. Yan Liu, MS. Qian Pu, for their generous suggestions to this paper and the great help in the preparation of this review.

REFERENCES

Anetzberger, C., Pirch, T., and Jung, K. (2009). Heterogeneity in quorum sensing-regulated bioluminescence of *Vibrio harveyi*. *Mol. Microbiol.* 73, 267–277. doi: 10.1111/j.1365-2958.2009.06768.x

Augustine, N., Kumar, P., and Thomas, S. (2010). Inhibition of *Vibrio cholerae* biofilm by AiiA enzyme produced from *Bacillus* spp. *Arch. Microbiol.* 192, 1019–1022. doi: 10.1007/s00203-010-0633-1

Bainton, N. J., Bycroft, B. W., Chhabra, S. R., Stead, P., Gledhill, L., Hill, P. J., et al. (1992). A general role for the lux autoinducer in bacterial cell signaling: control of antibiotic biosynthesis in *Erwinia*. *Gene* 116, 87–91. doi: 10.1016/0378-1119(92)90633-Z

Ball, A. S., Chaparian, R. R., and van Kessel, J. C. (2017). Quorum sensing gene regulation by LuxR/HapR master regulators in vibrios. *J. Bacteriol.* 199, e00105–e00117. doi: 10.1128/JB.00105-17

Balows, A., Hausler, W. J. Jr., Herrmann, K. L., and Isenberg, H. D. (1991). *Manual of Clinical Microbiology*. Washington, DC: American Society for Microbiology.

Bartlett, T. M., Bratton, B. P., Duvshani, A., Miguel, A., Sheng, Y., Martin, N. R., et al. (2017). A periplasmic polymer curves *Vibrio cholerae* and promotes pathogenesis. *Cell* 168, 172.e115–185.e115. doi: 10.1016/j.cell.2016.12.019

Bassler, B. L. (1999). How bacteria talk to each other: regulation of gene expression by quorum sensing. *Curr. Opin. Microbiol.* 2, 582–587. doi: 10.1016/S1369-5274(99)00025-9

Bassler, B. L., Wright, M., and Silverman, M. R. (1994). Multiple signalling systems controlling expression of luminescence in *Vibrio harveyi*: sequence and function of genes encoding a second sensory pathway. *Mol. Microbiol.* 13, 273–286. doi: 10.1111/j.1365-2958.1994.tb00422.x

Bhardwaj, A. K., Vinothkumar, K., and Rajpara, N. (2013). Bacterial quorum sensing inhibitors: attractive alternatives for control of infectious pathogens showing multiple drug resistance. *Recent Pat. Antiinfect. Drug Discov.* 8, 68–83. doi: 10.2174/1574891X11308010012

Boontham, P., Robins, A., Chandran, P., Pritchard, D., Cámara, M., Williams, P., et al. (2008). Significant immunomodulatory effects of *Pseudomonas aeruginosa* quorum-sensing signal molecules: possible link in human sepsis. *Clin. Sci.* 115, 343–351. doi: 10.1042/CS20080018

Brackman, G., Defoirdt, T., Miyamoto, C., Bossier, P., Van Calenbergh, S., Nelis, H., et al. (2008). Cinnamaldehyde and cinnamaldehyde derivatives reduce virulence in *Vibrio* spp. by decreasing the DNA-binding activity of the quorum sensing response regulator LuxR. *BMC Microbiol.* 8:149. doi: 10.1186/1471-2180-8-149

Brint, J. M., and Ohman, D. E. (1995). Synthesis of multiple exoproducts in *Pseudomonas aeruginosa* is under the control of RhlR-RhlI, another set of regulators in strain PAO1 with homology to the autoinducer-responsive LuxR-LuxI family. *J. Bacteriol.* 177, 7155–7163.

Bruhn, J. B., Dalsgaard, I., Nielsen, K. F., Buchholtz, C., Larsen, J. L., and Gram, L. (2005). Quorum sensing signal molecules (acylated homoserine lactones) in Gram-negative fish pathogenic bacteria. *Dis. Aquat. Org.* 65, 43–52. doi: 10.3354/dao065043

Buch, C., Sigh, J., Nielsen, J., Larsen, J. L., and Gram, L. (2003). Production of acylated homoserine lactones by different serotypes of *Vibrio anguillarum* both in culture and during infection of rainbow trout. *Syst. Appl. Microbiol.* 26, 338–349. doi: 10.1078/072320203322497365

Buchholtz, C., Nielsen, K. F., Milton, D. L., Larsen, J. L., and Gram, L. (2006). Profiling of acylated homoserine lactones of *Vibrio anguillarum in vitro* and *in vivo*: influence of growth conditions and serotype. *Syst. Appl. Microbiol.* 29, 433–445. doi: 10.1016/j.syapm.2005.12.007

Chan, K. G., Cheng, H. J., Chen, J. W., Yin, W. F., and Ngeow, Y. F. (2014). Tandem mass spectrometry detection of quorum sensing activity in multidrug resistant clinical isolate *Acinetobacter baumannii*. *Sci. World J.* 2014:891041. doi: 10.1155/2014/891041

Charlesworth, J., Kimyon, O., Manefield, M., and Burns, B. P. (2015). Detection and characterization of N-acyl-l-homoserine lactones using GFP-based biosensors in conjunction with thin-layer chromatography. *J. Microbiol. Methods* 118, 164–167. doi: 10.1016/j.mimet.2015.09.012

Charlton, K. A., and Porter, A. J. R. (2012). *Methods for the Treatment of an Infectious Bacterial Disease With an Anti-lactone or Lactone Derived Signal Molecules Antibody. U.S. Patent No 8,168,397*. Washington, DC: U.S. Patent and Trademark Office.

Choi, S. H., and Greenberg, E. P. (1992). Genetic dissection of DNA binding and luminescence gene activation by the *Vibrio fischeri* LuxR protein. *J. Bacteriol.* 174, 4064–4069. doi: 10.1128/jb.174.12.4064-4069.1992

Chu, W., and McLean, R. J. (2016). Quorum signal inhibitors and their potential use against fish diseases. *J. Aquat. Anim. Health* 28, 91–96. doi: 10.1080/08997659.2016.1150907

Croxatto, A., Chalker, V. J., Lauritz, J., Jass, J., Hardman, A., Williams, P., et al. (2002). VanT, a homologue of *Vibrio harveyi* LuxR, regulates serine,

metalloprotease, pigment, and biofilm production in *Vibrio anguillarum*. *J. Bacteriol.* 184, 1617–1629. doi: 10.1128/JB.184.6.1617-1629.2002

Defoirdt, T., Boon, N., Sorgeloos, P., Verstraete, W., and Bossier, P. (2008). Quorum sensing and quorum quenching in *Vibrio harveyi*: lessons learned from *in vivo* work. *ISME J.* 2, 19–26. doi: 10.1038/ismej.2007.92

Denkin, S. M., and Nelson, D. R. (2004). Regulation of *Vibrio anguillarum* empA metalloprotease expression and its role in virulence. *Appl. Environ. Microbiol.* 70, 4193–4204. doi: 10.1128/aem.70.7.4193-4204.2004

Diaz, J. H. (2014). Skin and soft tissue infections following marine injuries and exposures in travelers. *J. Travel Med.* 21, 207–213. doi: 10.1111/jtm.12115

Eberhard, A. (1972). Inhibition and activation of bacterial luciferase synthesis. *J. Bacteriol.* 109, 1101–1105.

Eberhard, A., Burlingame, A. L., Eberhard, C., Kenyon, G. L., Nealson, K. H., and Oppenheimer, N. J. (1981). Structural identification of autoinducer of *Photobacterium fischeri* luciferase. *Biochemistry* 20, 2444–2449. doi: 10.1021/bi00512a013

Elgaml, A., Higaki, K., and Miyoshi, S. (2014). Effects of temperature, growth phase and luxO-disruption on regulation systems of toxin production in *Vibrio vulnificus* strain L-180, a human clinical isolate. *World J. Microbiol. Biotechnol.* 30, 681–691. doi: 10.1007/s11274-013-1501-3

Elmahdi, S., DaSilva, L. V., and Parveen, S. (2016). Antibiotic resistance of *Vibrio parahaemolyticus* and *Vibrio vulnificus* in various countries: a review. *Food Microbiol.* 57, 128–134. doi: 10.1016/j.fm.2016.02.008

Engebrecht, J., and Silverman, M. (1984). Identification of genes and gene products necessary for bacterial bioluminescence. *Proc. Natl. Acad. Sci. U.S.A.* 81, 4154–4158. doi: 10.1073/pnas.81.13.4154

Feng, L., Rutherford, S. T., Papenfort, K., Bagert, J. D., van Kessel, J. C., Tirrell, D. A., et al. (2015). A qrr noncoding RNA deploys four different regulatory mechanisms to optimize quorum-sensing dynamics. *Cell* 160, 228–240. doi: 10.1016/j.cell.2014.11.051

Freeman, J. A., and Bassler, B. L. (1999). A genetic analysis of the function of LuxO, a two-component response regulator involved in quorum sensing in *Vibrio harveyi*. *Mol. Microbiol.* 31, 665–677. doi: 10.1046/j.1365-2958.1999.01208.x

Freeman, J. A., Lilley, B. N., and Bassler, B. L. (2000). A genetic analysis of the functions of LuxN: a two-component hybrid sensor kinase that regulates quorum sensing in *Vibrio harveyi*. *Mol. Microbiol.* 35, 139–149. doi: 10.1046/j.1365-2958.2000.01684.x

Gambello, M. J., and Iglewski, B. H. (1991). Cloning and characterization of the *Pseudomonas aeruginosa* lasR gene, a transcriptional activator of elastase expression. *J. Bacteriol.* 173, 3000–3009. doi: 10.1128/jb.173.9.3000-3009.1991

García-Aljaro, C., Eberl, L., Riedel, K., and Blanch, A. R. (2008). Detection of quorum-sensing-related molecules in *Vibrio scophthalmi*. *BMC Microbiol.* 8:138. doi: 10.1186/1471-2180-8-138

García-Aljaro, C., Melado-Rovira, S., Milton, D. L., and Blanch, A. R. (2012a). Quorum-sensing regulates biofilm formation in *Vibrio scophthalmi*. *BMC Microbiol.* 12:287. doi: 10.1186/1471-2180-12-287

Garcia-Aljaro, C., Vargas-Cespedes, G. J., and Blanch, A. R. (2012b). Detection of acylated homoserine lactones produced by *Vibrio* spp. and related species isolated from water and aquatic organisms. *J. Appl. Microbiol.* 112, 383–389. doi: 10.1111/j.1365-2672.2011.05199.x

Gilson, L., Kuo, A., and Dunlap, P. V. (1995). AinS and a new family of autoinducer synthesis proteins. *J. Bacteriol.* 177, 6946–6951. doi: 10.1128/jb.177.23.6946-6951.1995

Girard, L., Blanchet, É., Intertaglia, L., Baudart, J., Stien, D., Suzuki, M., et al. (2017). Characterization of N-Acyl homoserine lactones in *Vibrio tasmaniensis* LGP32 by a biosensor-based UHPLC-HRMS/MS Method. *Sensors* 17:906. doi: 10.3390/s17040906

Golberg, K., Pavlov, V., Marks, R. S., and Kushmaro, A. (2013). Coral-associated bacteria, quorum sensing disrupters, and the regulation of biofouling. *Biofouling* 29, 669–682. doi: 10.1080/08927014.2013.796939

Greenberg, E. P., Hastings, J. W., and Ulitzur, S. (1979). Induction of luciferase synthesis in *Beneckea harveyi* by other marine bacteria. *Arch. Microbiol.* 120, 87–91. doi: 10.1007/BF00409093

Gupta, R. K., Chhibber, S., and Harjai, K. (2011). Acyl homoserine lactones from culture supernatants of *Pseudomonas aeruginosa* accelerate host immunomodulation. *PLoS ONE* 6:e20860. doi: 10.1371/journal.pone.0020860

Hansen, H., Bjelland, A. M., Ronessen, M., Robertsen, E., and Willassen, N. P. (2014). LitR is a repressor of syp genes and has a temperature-sensitive regulatory effect on biofilm formation and colony morphology in *Vibrio* (*Aliivibrio*) *salmonicida*. *Appl. Environ. Microbiol.* 80, 5530–5541. doi: 10.1128/AEM.01239-14

Hanzelka, B. L., Parsek, M. R., Val, D. L., Dunlap, P. V., Cronan, J. E. Jr., and Greenberg, E. P. (1999). Acylhomoserine lactone synthase activity of the *Vibrio fischeri* AinS protein. *J. Bacteriol.* 181, 5766–5770.

Hartmann, A., and Schikora, A. (2012). Quorum sensing of bacteria and trans-kingdom interactions of N-acyl homoserine lactones with eukaryotes. *J. Chem. Ecol.* 38, 704–713. doi: 10.1007/s10886-012-0141-7

He, Y., and Olson, R. (2010). Three-dimensional structure of the detergent-solubilized *Vibrio cholerae* cytolysin (VCC) heptamer by electron cryomicroscopy. *J. Struct. Biol.* 169, 6–13. doi: 10.1016/j.jsb.2009.07.015

Hema, M., Balasubramanian, S., and Princy, S. A. (2015). Meddling *Vibrio cholerae* murmurs: a neoteric advancement in cholera research. *Indian J. Microbiol.* 55, 121–130. doi: 10.1007/s12088-015-0520-1

Henke, J. M., and Bassler, B. L. (2004). Three parallel quorum-sensing systems regulate gene expression in *Vibrio harveyi*. *J. Bacteriol.* 186, 6902–6914. doi: 10.1128/JB.186.20.6902-6914.2004

Hoang, T. T., and Schweizer, H. P. (1999). Characterization of *Pseudomonas aeruginosa* enoyl-acyl carrier protein reductase (FabI): a target for the antimicrobial triclosan and its role in acylated homoserine lactone synthesis. *J. Bacteriol.* 181, 5489–5497.

Hooi, D. S., Bycroft, B. W., Chhabra, S. R., Williams, P., and Pritchard, D. I. (2004). Differential immune modulatory activity of *Pseudomonas aeruginosa* quorum-sensing signal molecules. *Infect. Immun.* 72, 6463–6470. doi: 10.1128/IAI.72.11.6463-6470.2004

Horng, Y. T., Deng, S. C., Daykin, M., Soo, P. C., Wei, J. R., Luh, K. T., et al. (2002). The LuxR family protein SpnR functions as a negative regulator of N-acylhomoserine lactone-dependent quorum sensing in *Serratia marcescens*. *Mol. Microbiol.* 45, 1655–1671. doi: 10.1046/j.1365-2958.2002.03117.x

Horseman, M. A., and Surani, S. (2011). A comprehensive review of *Vibrio vulnificus*: an important cause of severe sepsis and skin and soft-tissue infection. *Int. J. Infect. Dis.* 15, e157–e166. doi: 10.1016/j.ijid.2010.11.003

Huang, Y., Zhang, J., Yu, Z., Zeng, Y., and Chen, Y. (2012). Isolation and characterization of acyl homoserine lactone-producing bacteria during an urban river biofilm formation. *Arch. Microbiol.* 194, 1043–1048. doi: 10.1007/s00203-012-0849-3

Hughes, D. T., and Sperandio, V. (2008). Inter-kingdom signalling: communication between bacteria and their hosts. *Nat. Rev. Microbiol.* 6, 111–120. doi: 10.1038/nrmicro1836

Jamuna, B. A., and Ravishankar, R. V. (2016). Effect of small chain N acyl homoserine lactone quorum sensing signals on biofilms of food-borne pathogens. *J. Food Sci. Technol.* 53, 3609–3614. doi: 10.1007/s13197-016-2346-1

Janda, J. M., Newton, A. E., and Bopp, C. A. (2015). Vibriosis. *Clin. Lab. Med.* 35, 273–288. doi: 10.1016/j.cll.2015.02.007

Janda, K. D., Kaufmann, G. F., and Park, J. (2010). *Antibody-Mediated Disruption of Quorum Sensing in Bacteria. U.S. Patent No 9,394,371*. Washington, DC: U.S. Patent and Trademark Office.

Joelsson, A. C., and Zhu, J. (2006). LacZ-based detection of acyl-homoserine lactone quorum-sensing signals. *Curr. Protoc. Microbiol.* Chapter 1:Unit 1C.2. doi: 10.1002/9780471729259.mc01c02s3

Jones, S., Yu, B., Bainton, N. J., Birdsall, M., Bycroft, B. W., Chhabra, S. R., et al. (1993). The lux autoinducer regulates the production of exoenzyme virulence determinants in *Erwinia carotovora* and *Pseudomonas aeruginosa*. *EMBO J.* 12, 2477–2482.

Jung, S. A., Chapman, C. A., and Ng, W. L. (2015). Quadruple quorum-sensing inputs control *Vibrio cholerae* virulence and maintain system robustness. *PLoS Pathog.* 11:e1004837. doi: 10.1371/journal.ppat.1004837

Kalia, V. C., and Purohit, H. J. (2011). Quenching the quorum sensing system: potential antibacterial drug targets. *Crit. Rev. Microbiol.* 37, 121–140. doi: 10.3109/1040841X.2010.532479

Kaufmann, G. F., Park, J., Mee, J. M., Ulevitch, R. J., and Janda, K. D. (2008). The quorum quenching antibody RS2-1G9 protects macrophages from the cytotoxic effects of the *Pseudomonas aeruginosa* quorum sensing signalling molecule N-3-oxo-dodecanoyl-homoserine

lactone. *Mol. Immunol.* 45, 2710–2714. doi: 10.1016/j.molimm.2008.01.010

Khilwani, B., and Chattopadhyay, K. (2015). Signaling beyond punching holes: modulation of cellular responses by *Vibrio cholerae* cytolysin. *Toxins* 7, 3344–3358. doi: 10.3390/toxins7083344

Krick, A., Kehraus, S., Eberl, L., Riedel, K., Anke, H., Kaesler, I., et al. (2007). A marine *Mesorhizobium* sp. produces structurally novel long-chain N-acyl-L-homoserine lactones. *Appl. Environ. Microbiol.* 73, 3587–3594. doi: 10.1128/AEM.02344-06

Kumar, J. S., Umesha, S., Prasad, K. S., and Niranjana, P. (2016). Detection of quorum sensing molecules and biofilm formation in *Ralstonia solanacearum*. *Curr. Microbiol.* 72, 297–305. doi: 10.1007/s00284-015-0953-0

Kumari, A., Pasini, P., Deo, S. K., Flomenhoft, D., Shashidhar, H., and Daunert, S. (2006). Biosensing systems for the detection of bacterial quorum signaling molecules. *Anal. Chem.* 78, 7603–7609. doi: 10.1021/ac061421n

Kuo, A., Blough, N. V., and Dunlap, P. V. (1994). Multiple N-acyl-L-homoserine lactone autoinducers of luminescence in the marine symbiotic bacterium *Vibrio fischeri*. *J. Bacteriol.* 176, 7558–7565. doi: 10.1128/jb.176.24.7558-7565.1994

Lee, M. N., Kim, S. K., Li, X. H., and Lee, J. H. (2014). Bacterial virulence analysis using brine shrimp as an infection model in relation to the importance of quorum sensing and proteases. *J. Gen. Appl. Microbiol.* 60, 169–174. doi: 10.2323/jgam.60.169

Lenz, D. H., Mok, K. C., Lilley, B. N., Kulkarni, R. V., Wingreen, N. S., and Bassler, B. L. (2004). The small RNA chaperone Hfq and multiple small RNAs control quorum sensing in *Vibrio harveyi* and *Vibrio cholerae*. *Cell* 118, 69–82. doi: 10.1016/j.cell.2004.06.009

Li, G., Dong, S., Qu, J., Sun, Z., Huang, Z., Ye, L., et al. (2010). Synergism of hydroxyapatite nanoparticles and recombinant mutant human tumour necrosis factor-α in chemotherapy of multidrug-resistant hepatocellular carcinoma. *Liver Int.* 30, 585–592. doi: 10.1111/j.1478-3231.2009.02113.x

Liaqat, I., Bachmann, R. T., and Edyvean, R. G. (2014). Type 2 quorum sensing monitoring, inhibition and biofilm formation in marine microrganisms. *Curr. Microbiol.* 68, 342–351. doi: 10.1007/s00284-013-0484-5

Lilley, B. N., and Bassler, B. L. (2000). Regulation of quorum sensing in *Vibrio harveyi* by LuxO and sigma-54. *Mol. Microbiol.* 36, 940–954. doi: 10.1046/j.1365-2958.2000.01913.x

Lohith, G. K., Kingston, J. J., Singh, A. K., Murali, H. S., and Batra, H. V. (2015). Evaluation of recombinant leukocidin domain of VvhA exotoxin of *Vibrio vulnificus* as an effective toxoid in mouse model. *Immunol. Lett.* 167, 47–53. doi: 10.1016/j.imlet.2015.06.015

Lowery, C. A., Dickerson, T. J., and Janda, K. D. (2008). Interspecies and interkingdom communication mediated by bacterial quorum sensing. *Chem. Soc. Rev.* 37, 1337–1346. doi: 10.1039/b702781h

Lubin, J. B., Lewis, W. G., Gilbert, N. M., Weimer, C. M., Almagro-Moreno, S., Boyd, E. F., et al. (2015). Host-like carbohydrates promote bloodstream survival of *Vibrio vulnificus in vivo*. *Infect. Immun.* 83, 3126–3136. doi: 10.1128/IAI.00345-15

Lumjiaktase, P., Diggle, S. P., Loprasert, S., Tungpradabkul, S., Daykin, M., Cámara, M., et al. (2006). Quorum sensing regulates dpsA and the oxidative stress response in *Burkholderia pseudomallei*. *Microbiology* 152(Pt 12), 3651–3659. doi: 10.1099/mic.0.29226-0

McClean, K. H., Winson, M. K., Fish, L., Taylor, A., Chhabra, S. R., Camara, M., et al. (1997). Quorum sensing and *Chromobacterium violaceum*: exploitation of violacein production and inhibition for the detection of N-acylhomoserine lactones. *Microbiology* 143 (Pt 12), 3703–3711. doi: 10.1099/00221287-143-12-3703

McDougald, D., Lin, W. H., Rice, S. A., and Kjelleberg, S. (2006). The role of quorum sensing and the effect of environmental conditions on biofilm formation by strains of *Vibrio vulnificus*. *Biofouling* 22, 161–172. doi: 10.1080/08927010600743431

Milton, D. L. (2006). Quorum sensing in vibrios: complexity for diversification. *Int. J. Med. Microbiol.* 296, 61–71. doi: 10.1016/j.ijmm.2006.01.044

Milton, D. L., Chalker, V. J., Kirke, D., Hardman, A., Cámara, M., and Williams, P. (2001). The LuxM homologue VanM from *Vibrio anguillarum* directs the synthesis of N-(3-hydroxyhexanoyl)homoserine lactone and N-hexanoylhomoserine lactone. *J. Bacteriol.* 183, 3537–3547. doi: 10.1128/JB.183.12.3537-3547.2001

Milton, D. L., Hardman, A., Camara, M., Chhabra, S. R., Bycroft, B. W., Stewart, G. S., et al. (1997). Quorum sensing in *Vibrio anguillarum*: characterization of the vanI/vanR locus and identification of the autoinducer N-(3-oxodecanoyl)-L-homoserine lactone. *J. Bacteriol.* 179, 3004–3012. doi: 10.1128/jb.179.9.3004-3012.1997

Miyashiro, T., Oehlert, D., Ray, V. A., Visick, K. L., and Ruby, E. G. (2014). The putative oligosaccharide translocase SypK connects biofilm formation with quorum signaling in *Vibrio fischeri*. *Microbiologyopen* 3, 836–848. doi: 10.1002/mbo3.199

Mok, K. C., Wingreen, N. S., and Bassler, B. L. (2003). *Vibrio harveyi* quorum sensing: a coincidence detector for two autoinducers controls gene expression. *EMBO J.* 22, 870–881. doi: 10.1093/emboj/cdg085

Morin, D., Grasland, B., Vallée-Réhel, K., Dufau, C., and Haras, D. (2003). On-line high-performance liquid chromatography-mass spectrometric detection and quantification of N-acylhomoserine lactones, quorum sensing signal molecules, in the presence of biological matrices. *J. Chromatogr. A* 1002, 79–92. doi: 10.1016/S0021-9673(03)00730-1

Moser, C., Jensen, P. O., Kobayashi, O., Hougen, H. P., Song, Z., Rygaard, J., et al. (2002). Improved outcome of chronic *Pseudomonas aeruginosa* lung infection is associated with induction of a Th1-dominated cytokine response. *Clin. Exp. Immunol.* 127, 206–213. doi: 10.1046/j.1365-2249.2002.01731.x

Nealson, K. H. (1977). Autoinduction of bacterial luciferase. Occurrence, mechanism and significance. *Arch. Microbiol.* 112, 73–79. doi: 10.1007/BF00446657

Nguyen, A. N., and Jacq, A. (2014). Small RNAs in the Vibrionaceae: an ocean still to be explored. *Wiley Interdiscip. Rev. RNA* 5, 381–392. doi: 10.1002/wrna.1218

O'Connor, G., Knecht, L. D., Salgado, N., Strobel, S., Pasini, P., and Daunert, S. (2015). Whole-cell biosensors as tools for the detection of quorum-sensing molecules: uses in diagnostics and the investigation of the quorum-sensing mechanism. *Adv. Biochem. Eng. Biotechnol.* 3, 181–200. doi: 10.1007/10_2015_337

Parkinson, J. S., and Kofoid, E. C. (1992). Communication modules in bacterial signaling proteins. *Annu. Rev. Genet.* 26, 71–112. doi: 10.1146/annurev.ge.26.120192.000443

Passador, L., Cook, J. M., Gambello, M. J., Rust, L., and Iglewski, B. H. (1993). Expression of *Pseudomonas aeruginosa* virulence genes requires cell-to-cell communication. *Science* 260, 1127–1130.

Pearson, J. P., Gray, K. M., Passador, L., Tucker, K. D., Eberhard, A., Iglewski, B. H., et al. (1994). Structure of the autoinducer required for expression of *Pseudomonas aeruginosa* virulence genes. *Proc. Natl. Acad. Sci. U.S.A.* 91, 197–201. doi: 10.1073/pnas.91.1.197

Pearson, J. P., Van Delden, C., and Iglewski, B. H. (1999). Active efflux and diffusion are involved in transport of *Pseudomonas aeruginosa* cell-to-cell signals. *J. Bacteriol.* 181, 1203–1210.

Persat, A., Stone, H. A., and Gitai, Z. (2014). The curved shape of *Caulobacter crescentus* enhances surface colonization in flow. *Nat. Commun.* 5:3824. doi: 10.1038/ncomms4824

Phippen, B. L., and Oliver, J. D. (2015). Clinical and environmental genotypes of *Vibrio vulnificus* display distinct, quorum-sensing-mediated, chitin detachment dynamics. *Pathog. Dis.* 73:ftv072. doi: 10.1093/femspd/ftv072

Purohit, A. A., Johansen, J. A., Hansen, H., Leiros, H. K., Kashulin, A., Karlsen, C., et al. (2013). Presence of acyl-homoserine lactones in 57 members of the Vibrionaceae family. *J. Appl. Microbiol.* 115, 835–847. doi: 10.1111/jam.12264

Rai, A. K., and Chattopadhyay, K. (2014). Trapping of *Vibrio cholerae* cytolysin in the membrane-bound monomeric state blocks membrane insertion and functional pore formation by the toxin. *J. Biol. Chem.* 289, 16978–16987. doi: 10.1074/jbc.M114.567099

Rajamanikandan, S., Jeyakanthan, J., and Srinivasan, P. (2017). Binding mode exploration of LuxR-thiazolidinedione analogues, e-pharmacophore-based virtual screening in the designing of LuxR inhibitors and its biological evaluation. *J. Biomol. Struct. Dyn.* 35, 897–916. doi: 10.1080/07391102.2016.1166455

Ramachandran, R., Burke, A. K., Cormier, G., Jensen, R. V., and Stevens, A. M. (2014). Transcriptome-based analysis of the *Pantoea stewartii* quorum-sensing regulon and identification of EsaR direct targets. *Appl. Environ. Microbiol.* 80, 5790–5800. doi: 10.1128/AEM.01489-14

Rasmussen, B. B., Nielsen, K. F., Machado, H., Melchiorsen, J., Gram, L., and Sonnenschein, E. C. (2014). Global and phylogenetic distribution of quorum sensing signals, acyl homoserine lactones, in the family of Vibrionaceae. *Mar. Drugs* 12, 5527–5546. doi: 10.3390/md12115527

Ren, D., Sims, J. J., and Wood, T. K. (2001). Inhibition of biofilm formation and swarming of *Escherichia coli* by (5Z)-4-bromo-5-(bromomethylene)-3-butyl-2(5H)-furanone. *Environ. Microbiol.* 3, 731–736. doi: 10.1046/j.1462-2920.2001.00249.x

Ronson, C. W., Nixon, B. T., and Ausubel, F. M. (1987). Conserved domains in bacterial regulatory proteins that respond to environmental stimuli. *Cell* 49, 579–581.

Rumbaugh, K. P., Hamood, A. N., and Griswold, J. A. (2004). Cytokine induction by the *P. aeruginosa* quorum sensing system during thermal injury. *J. Surg. Res.* 116, 137–144. doi: 10.1016/j.jss.2003.08.009

Rutherford, S. T., van Kessel, J. C., Shao, Y., and Bassler, B. L. (2011). AphA and LuxR/HapR reciprocally control quorum sensing in vibrios. *Genes Dev.* 25, 397–408. doi: 10.1101/gad.2015011

Schaefer, A. L., Val, D. L., Hanzelka, B. L., Cronan, J. E. Jr., and Greenberg, E. P. (1996). Generation of cell-to-cell signals in quorum sensing: acyl homoserine lactone synthase activity of a purified *Vibrio fischeri* LuxI protein. *Proc. Natl. Acad. Sci. U.S.A.* 93, 9505–9509. doi: 10.1073/pnas.93.18.9505

Seed, P. C., Passador, J., and Iglewski, B. H. (1995). Activation of the *Pseudomonas aeruginosa* lasI gene by LasR and the *Pseudomonas* autoinducer PAI: an autoinduction regulatory hierarchy. *J. Bacteriol.* 177, 654–659. doi: 10.1128/jb.177.3.654-659.1995

Shaw, P. D., Ping, G., Daly, S. L., Cha, C., Cronan, J. E. Jr., Rinehart, K. L., et al. (1997). Detecting and characterizing N-acyl-homoserine lactone signal molecules by thin-layer chromatography. *Proc. Natl. Acad. Sci. U.S.A.* 94, 6036–6041. doi: 10.1073/pnas.94.12.6036

Shimohata, T., and Takahashi, A. (2010). Diarrhea induced by infection of *Vibrio parahaemolyticus*. *J. Med. Invest.* 57, 179–182. doi: 10.2152/jmi.57.179

Smith, R. S., Fedyk, E. R., Springer, T. A., Mukaida, N., Iglewski, B. H., and Phipps, R. P. (2001). IL-8 production in human lung fibroblasts and epithelial cells activated by the *Pseudomonas* autoinducer N-3-oxododecanoyl homoserine lactone is transcriptionally regulated by NF-kappa B and activator protein-2. *J. Immunol.* 167, 366–374. doi: 10.4049/jimmunol.167.1.366

Smith, R. S., Harris, S. G., Phipps, R., and Iglewski, B. (2002). The *Pseudomonas aeruginosa* quorum-sensing molecule N-(3-oxododecanoyl)homoserine lactone contributes to virulence and induces inflammation *in vivo*. *J. Bacteriol.* 184, 1132–1139. doi: 10.1128/jb.184.4.1132-1139.2002

Steidle, A., Sigl, K., Schuhegger, R., Ihring, A., Schmid, M., Gantner, S., et al. (2001). Visualization of N-acylhomoserine lactone-mediated cell-cell communication between bacteria colonizing the tomato rhizosphere. *Appl. Environ. Microbiol.* 67, 5761–5770. doi: 10.1128/AEM.67.12.5761-5770.2001

Stephenson, K., Yamaguchi, Y., and Hoch, J. A. (2000). The mechanism of action of inhibitors of bacterial two–component signal transduction systems. *J. Biol. Chem.* 275, 38900–38904. doi: 10.1074/jbc.M006633200

Sun, L., Tang, C., and Leng, Y. P. (2010). The research progress of the novel thin layer chromatography expansion agent. *Sci. Technol. West China* 9, 47–48. doi: 10.3969/j.issn.1671-6396.2010.36.025

Tait, K., Hutchison, Z., Thompson, F. L., and Munn, C. B. (2010). Quorum sensing signal production and inhibition by coral-associated vibrios. *Environ. Microbiol. Rep.* 2, 145–150. doi: 10.1111/j.1758-2229.2009.00122.x

Tan, P. W., Tan, W. S., Yunos, N. Y., Mohamad, N. I., Adrian, T. G., Yin, W. F., et al. (2014). Short chain N-acyl homoserine lactone production in tropical marine *Vibrio sinaloensis* strain T47. *Sensors* 14, 12958–12967. doi: 10.3390/s140712958

Tan, W. S., Yunos, N. Y., Tan, P. W., Mohamad, N. I., Adrian, T. G., Yin, W. F., et al. (2014). Characterisation of a marine bacterium *Vibrio brasiliensis* T33 producing N-acyl homoserine lactone quorum sensing molecules. *Sensors* 14, 12104–12113. doi: 10.3390/s140712104

Tarr, C. L., Bopp, C. A., and Farmer, J. J. (2015). "Vibrio and related organisms," in *Manual of Clinical Microbiology, 11th Edn*, eds J. H. Jorgensen, M. A. Pfaller, K. C. Carroll, G. Funke, M. L. Landry, S. S. Richter, and D. W. Warnock (Washington, DC: American Society of Microbiology), 762–772.

Tateda, K., Ishii, Y., Horikawa, M., Matsumoto, T., Miyairi, S., Pechere, J. C., et al. (2003). The *Pseudomonas aeruginosa* autoinducer N-3-oxododecanoyl homoserine lactone accelerates apoptosis in macrophages and neutrophils. *Infect. Immun.* 71, 5785–5793. doi: 10.1128/IAI.71.10.5785-5793.2003

Taylor, M. W., Schupp, P. J., Baillie, H. J., Charlton, T. S., de Nys, R., Kjelleberg, S., et al. (2004). Evidence for acyl homoserine lactone signal production in bacteria associated with marine sponges. *Appl. Environ. Microbiol.* 70, 4387–4389. doi: 10.1128/AEM.70.7.4387-4389.2004

Timmen, M., Bassler, B. L., and Jung, K. (2006). AI-1 influences the kinase activity but not the phosphatase activity of LuxN of *Vibrio harveyi*. *J. Biol. Chem.* 281, 24398–24404. doi: 10.1074/jbc.M604108200

Tu, K. C., and Bassler, B. L. (2007). Multiple small RNAs act additively to integrate sensory information and control quorum sensing in *Vibrio harveyi*. *Genes Dev.* 21, 221–233. doi: 10.1101/gad.1502407

Valiente, E., Bruhn, J. B., Nielsen, K. F., Larsen, J. L., Roig, F. J., Gram, L., et al. (2009). *Vibrio vulnificus* produces quorum sensing signals of the AHL-class. *FEMS Microbiol. Ecol.* 69, 16–26. doi: 10.1111/j.1574-6941.2009.00691.x

Van Kessel, J. C., Ulrich, L. E., Zhulin, I. B., and Bassler, B. L. (2013). Analysis of activator and repressor functions reveals the requirements for transcriptional control by LuxR, the master regulator of quorum sensing in *Vibrio harveyi*. *mBio* 4, e00378-13. doi: 10.1128/mBio.00378-13

Vidal, J. E., Shak, J. R., and Canizalez-Roman, A. (2015). The CpAL quorum sensing system regulates production of hemolysins CPA and PFO to build *Clostridium perfringens* biofilms. *Infect. Immun.* 83, 2430–2442. doi: 10.1128/IAI.00240-15

Vikström, E., Bui, L., Konradsson, P., and Magnusson, K. E. (2009). The junctional integrity of epithelial cells is modulated by *Pseudomonas aeruginosa* quorum sensing molecule through phosphorylation-dependent mechanisms. *Exp. Cell Res.* 315, 313–326. doi: 10.1016/j.yexcr.2008.10.044

Vikström, E., Magnusson, K. E., and Pivoriunas, A. (2005). The *Pseudomonas aeruginosa* quorum-sensing molecule N-(3-oxododecanoyl)-L-homoserine lactone stimulates phagocytic activity in human macrophages through the p38 MAPK pathway. *Microbes Infect.* 7, 1512–1518. doi: 10.1016/j.micinf.2005.05.012

Vikström, E., Tafazoli, F., and Magnusson, K. E. (2006). *Pseudomonas aeruginosa* quorum sensing molecule N-(3 oxododecanoyl)-l-homoserine lactone disrupts epithelial barrier integrity of Caco-2 cells. *FEBS Lett.* 580, 6921–6928. doi: 10.1016/j.febslet.2006.11.057

Viswanath, G., Jegan, S., Baskaran, V., Kathiravan, R., and Prabavathy, V. R. (2015). Diversity and N-acyl-homoserine lactone production by Gammaproteobacteria associated with Avicennia marina rhizosphere of South Indian mangroves. *Syst. Appl. Microbiol.* 38, 340–345. doi: 10.1016/j.syapm.2015.03.008

Wang, Y., Wang, H., Liang, W., Hay, A. J., Zhong, Z., Kan, B., et al. (2013). Quorum sensing regulatory cascades control *Vibrio fluvialis* pathogenesis. *J. Bacteriol.* 195, 3583–3589. doi: 10.1128/JB.00508-13

Wei, G., Tian, N., Valery, A. C., Zhong, Y., Schuppan, D., and Helmerhorst, E. J. (2015). Identification of pseudolysin (*lasB*) as an aciduric gluten-degrading enzyme with high therapeutic potential for celiac disease. *Am. J. Gastroenterol.* 110, 899–908. doi: 10.1038/ajg.2015.97

White, C. E., and Winans, S. C. (2007). Cell-cell communication in the plant pathogen *Agrobacterium tumefaciens*. *Philos. Trans. R. Soc. Lond. B Biol. Sci.* 362, 1135–1148. doi: 10.1098/rstb.2007.2040

Williams, P. (2007). Quorum sensing, communication and cross-kingdom signalling in the bacterial world. *Microbiology* 153(Pt 12), 3923–3938. doi: 10.1099/mic.0.2007/012856-0

Yang, Q., Han, Y., and Zhang, X. H. (2011). Detection of quorum sensing signal molecules in the family Vibrionaceae. *J. Appl. Microbiol.* 110, 1438–1448. doi: 10.1111/j.1365-2672.2011.04998.x

Zhang, C., and Ye, B. C. (2014). Real-time measurement of quorum-sensing signal autoinducer 3OC6HSL by a FRET-based nanosensor. *Bioprocess Biosyst. Eng.* 37, 849–855. doi: 10.1007/s00449-013-1055-7

Zhang, L. H. (2003). Quorum quenching and proactive host defense. *Trends Plant Sci.* 8, 238–244. doi: 10.1016/S1360-1385(03)00063-3

Zhang, S., Liu, N., Liang, W., Han, Q., Zhang, W., and Li, C. (2017). Quorum sensing-disrupting coumarin suppressing virulence phenotypes in *Vibrio splendidus*. *Appl. Microbiol. Biotechnol.* 101, 3371–3378. doi: 10.1007/s00253-016-8009-3

Zhang, Y. Y., Yan, J., and Ge, Y. M. (2017). Advances in bacterial extracellular metalloproteases and their pathogenic roles. *Chin. J. Microbiol. Immunol.* 37, 161–164. doi: 10.3760/cma.j.issn.0254-5101.2017.02.013

Zhou, D., Yan, X., Qu, F., Wang, L., Zhang, Y., Hou, J., et al. (2013). Quorum sensing modulates transcription of cpsQ-mfpABC and mfpABC in *Vibrio parahaemolyticus*. *Int. J. Food Microbiol.* 166, 458–463. doi: 10.1016/j.ijfoodmicro.2013.07.008

Zhou, X., Shah, D. H., Konkel, M. E., and Call, D. R. (2008). Type III secretion system 1 genes in *Vibrio parahaemolyticus* are positively regulated by ExsA and negatively regulated by ExsD. *Mol. Microbiol.* 69, 747–764. doi: 10.1111/j.1365-2958.2008.06326.x

Zhu, J., Chai, Y., Zhong, Z., Li, S., and Winans, S. C. (2003). *Agrobacterium* bioassay strain for ultrasensitive detection of N-acylhomoserine lactone-type quorum-sensing molecules: detection of autoinducers in *Mesorhizobium huakuii*. *Appl. Environ. Microbiol.* 69, 6949–6953. doi: 10.1128/AEM.69.11.6949-6953.2003

Zimmermann, S., Wagner, C., Müller, W., Brenner-Weiss, G., Hug, F., Prior, B., et al. (2006). Induction of neutrophil chemotaxis by the quorum-sensing molecule N-(3-oxododecanoyl)-L-homoserine lactone. *Infect. Immun.* 74, 5687–5692. doi: 10.1128/IAI.01940-05

Conflict of Interest Statement: The authors declare that the research was conducted in the absence of any commercial or financial relationships that could be construed as a potential conflict of interest.

The reviewer YT and handling Editor declared their shared affiliation.

frontiers in Cellular and Infection Microbiology

ORIGINAL RESEARCH
published: 12 October 2017
doi: 10.3389/fcimb.2017.00441

Modulating the Global Response Regulator, LuxO of *V. cholerae* Quorum Sensing System Using a Pyrazine Dicarboxylic Acid Derivative ($PDCA^{py}$): An Antivirulence Approach

*M. Hema, Sahana Vasudevan, P. Balamurugan and S. Adline Princy**

Quorum Sensing Laboratory, Centre for Research in Infectious Diseases, School of Chemical and Biotechnology, SASTRA University, Thanjavur, India

Vibrio cholerae is a Gram-negative pathogen which causes acute diarrhoeal disease, cholera by the expression of virulence genes through quorum sensing (QS) mechanism. The QS circuit of *V. cholerae* is controlled by the global quorum regulator, LuxO, which at low cell density (LCD) state produces major virulence factors such as, toxin co-regulated pilus (TCP) and cholera toxin (CT) to mediate infection. On the contrary, at the high cell density (HCD) state the virulent genes are downregulated and the vibrios are detached from the host intestinal epithelial cells, promoted by HapA protease. Hence, targeting the global regulator LuxO would be a promising approach to modulate the QS to curtail *V. cholerae* pathogenesis. In our earlier studies, LuxO targeted ligand, 2,3 pyrazine dicarboxylic acid (PDCA) and its derivatives having desired pharmacophore properties were chemically synthesized and were shown to have biofilm inhibition as well as synergistic activity with the conventionally used antibiotics. In the present study, the QS modulatory effect of the PDCA derivative with pyrrolidine moiety designated as $PDCA^{py}$ against the *V. cholerae* virulence gene expression was analyzed at various growth phases. The data significantly showed a several fold reduction in the expression of the genes, *tcp* and *ct* whereas the expression of *hapR* was upregulated at the LCD state. In addition, $PDCA^{py}$ reduced the adhesion and invasion of the vibrios onto the INT407 intestinal cell lines. Collectively, our data suggest that $PDCA^{py}$ could be a potential QS modulator (QSM) for the antivirulence therapeutic approach.

Keywords: cholera toxin, LCD, HCD, qRT-PCR, adhesion, invasion

OPEN ACCESS

Edited by:
Rodolfo García-Contreras, National Autonomous University of Mexico, Mexico

Reviewed by:
Yael González Tinoco, National Autonomous University of Mexico, Mexico
Bernardo Franco, Universidad de Guanajuato, Mexico

****Correspondence:***
S. Adline Princy
adlineprinzy@biotech.sastra.edu

Received: *04 July 2017*
Accepted: *26 September 2017*
Published: *12 October 2017*

Citation:
Hema M, Vasudevan S, Balamurugan P and Adline Princy S (2017) Modulating the Global Response Regulator, LuxO of V. cholerae Quorum Sensing System Using a Pyrazine Dicarboxylic Acid Derivative ($PDCA^{py}$): An Antivirulence Approach. Front. Cell. Infect. Microbiol. 7:441. doi: 10.3389/fcimb.2017.00441

INTRODUCTION

Quorum Sensing (QS) in bacteria is a system of response and stimuli that depend on the cell density and concentration of autoinducer molecules to co-regulate the biological processes like expression of virulence factors, biofilm, motility, sporulation, bioluminescence etc. (Papenfort and Bassler, 2016; Zhang et al., 2016). Like most of the clinical pathogens, *Vibrio cholerae* which causes severe diarrheal disease, cholera, also uses QS for its virulence mechanism. Hence, manipulating the QS system of *V. cholerae* using target-specific inhibitors/modulators would be a promising anti virulence therapeutic approach, especially in the case of antimicrobial resistance (AMR) strains (Gorski et al., 2016).

In *V. cholera,* the cholera toxin (CT) and toxin-coregulated pilus (TCP) are the major virulence factors which are the under control of QS regulator, LuxO (Zhu et al., 2002). The virulence factor, CT, is encoded by the genes *ctxA* and *ctxB* located in CTXΦ prophage (Maiti et al., 2006). CT is a heterodimeric protein which belongs to an AB_5 toxin family. It has an enzymatically active single subunit that covalently binds with pentamer B subunit and interacts with GM_1, a ganglioside receptor. The interaction would translocate the A subunit in an intracellular manner to activate adenylyl cyclase (Polizzotti and Kiick, 2006). The adenylyl cyclase elevates the level of cAMP and alters the ion channels thus effluxing the ions and water (Popoff, 2011).

Colonization of bacteria on the host intestinal epithelial cells is an essential step to establish pathogenesis (Lu and Walker, 2001). The gene, *tcp* in the Vibrio pathogenicity island (VPI) encodes the type IV pilus (TCP). This is co-regulated by CT to mediate the *V. cholerae* intestinal colonization (adhesion) and microcolony formation on the surface of the host cells to promote invasion.

Unlike other pathogenic bacteria, *V. cholerae* expresses its virulence factors at its low cell density (LCD) state. At high cell density (HCD) state, the virulence factors expression is downregulated to enhance the production of the enzyme, protease that detaches the vibrios from the human intestine (Jung et al., 2016). This is facilitated by the transcriptional regulator, LuxO, which acts as a genetic switch between the two distinct modes. The quorum regulator, LuxO, is a member of NtrC type response regulatory protein that purely depends upon ATP hydrolysis as an energy source for its function (Stabb and Visick, 2013). At LCD condition, in the presence of low levels of autoinducers (AIs), the AI receptors act as kinases and transfer a phosphate group to activate the response regulator LuxO. Activated LuxO (LuxO∼P) regulates the gene encoding the small regulatory RNAs (sRNAs) Qrr1-4 along with RNA chaperone Hfq binds to the mRNA transcript of HapR (virulence repressor protein in *V. cholerae*) and represses its expression. This further up regulates the gene expression of biofilm and virulence factors including TCP and CT. At HCD state, accumulation of AI leads to the removal of phosphate from LuxO by the phosphatase activity of the AI receptors. The inactive LuxO repress the sRNAs(Qrr1-4) and activates the expression of HapR which further down-regulates the virulence genes expression (Waters et al., 2008; Hema et al., 2015a).

Hence, we propose that targeting LuxO will lead to the premature activation of HCD condition at the LCD state to reduce the level of infection at an early stage (Hema et al., 2015b). Besides, LuxO belongs to NtrC type response regulatory protein and is highly conserved across all *Vibrio* sps., the LuxO selective inhibitors would act as broad spectrum quorum quencher to fight against vibrio infections (Ng et al., 2012). In this context, through our earlier studies, we have shown that 2,3 pyrazine dicarboxylic acid (PDCA) derivatives with pyrrolidine moiety: 3-(4-(Pyrrolidin-1-yl) phenyl carbamoyl) pyrazine-2-carboxylic acid and 3-(3-Fluoro-4-(pyrrolidin-1-yl) phenyl carbamoyl) pyrazine-2- carboxylic acid exhibited anti-biofilm property. In addition, we have also shown that the presence of fluorine group in the latter derivative did not alter the activity of the compound (Hema et al., 2016). Previously, pyrazinamide (a derivative of pyrazine) was shown to have antimycobacterial activity (Mitchison, 1996). It is interesting to note that PDCA was proven to have antibacterial and antifungal properties (Beaula et al., 2015). This suggests that substituted pyrazines might possess antiinfective properties in addition to other biological important activities. Hence, in the present study, the QS modulatory effect of 3-(4-(Pyrrolidin-1-yl) phenyl carbamoyl) pyrazine-2-carboxylic acid termed as $PDCA^{py}$ (**Figure S1**) was confirmed through gene expression analysis. Further, the host-pathogen relationship was understood through adhesion and invasion studies.

MATERIALS AND METHODS

Bacterial Strains and Culture Conditions

V. cholerae AMR strain, Vc4, obtained from JSS Medical College, Mysore and reference strain, MTCC 3905, was used for this study. Received strains were cultured in TCBS agar to ascertain cell viability. Pure colonies obtained are preserved in glycerol at −80°C. Strains were grown under standard growth conditions (LB broth, 37°C, aeration) as recommended by the NCCL standard. A LCD of $OD_{600nm} = 0.2$ was used for further assays (Tyor and Kumari, 2016). For all the assays, $PDCA^{py}$ treatment was carried out at its IC_{50} concentration, 25 μM (Hema et al., 2016).

RNA Extraction and qRT-PCR Profiling of Gene Expression

Total RNA was isolated from *V. cholerae* strains at early-log phase (2 h) and late-log phase (8 h) using RNeasy® Protect Bacteria Mini Kit (Qiagen), according to the manufacturer's guidelines. Integrity and purity of the isolated RNA were checked using standard agarose gel electrophoresis and NanoDrop (Thermo Scientific, USA), respectively. The cDNA was prepared in accordance with manufacturer's instructions of iScript™ cDNA Synthesis Kit. The reaction conditions include annealing at 24°C for 5 min, extension at 42°C for 30 min and the samples were inactivated at 85°C for 5 min.

The expression level of genes under regulation of LuxO was analyzed using qRT- PCR and the primers used for the study were listed in **Table 1**. The reaction mixture of volume 20 μL contains 1 μL each of forward and reverse primers, 4 μL of diluted cDNA, and 10 μL of the sybr green master mix. The above mixture was made up to 20 μL with RNAse free water. qRT-PCR was performed for 40 cycles as follows: the initial denaturation at 95°C (2 min), denaturation at 95°C (15 s), annealing at 57.7°C (20 s), final extension at 72°C (20 s). Negative control (without cDNA) was maintained in parallel to ensure the samples were free of contamination. The 16 s rRNA was used as reference genes. Relative gene expression was calculated using the $2^{-\Delta\Delta CT}$ method (Vezzulli et al., 2015).

cAMP-Assay

Intestinal cell line INT 407 (obtained from NCCS, Pune) was grown in Minimum essential medium (MEM) supplemented

TABLE 1 | Primers used in this study.

S. no.	*Gene*	Primer code	Primer sequence (5′-3′)	References
1	*CT*	ct_F	TATGCCAAGAGGACAGAGTGAG	Sarkar et al., 2002
		ct_R	AACATATCCATCATCGTGCCTAAC	
2	*tcp*	tcp_F	CGTTGGCGGTCAGTCTTG	Sarkar et al., 2002
		tcp_R	CGGGCTTTCTTCTTGTTCG	
3	*hapA*	hapA_F	ACGGTACAGTTGCCGAATGG	Silva et al., 2006
		hapA_R	GCTGGCTTTCAATGTCAGGG	
4	*hapR*	hapR_F	CCAACTTCTTGACCGATCAC	Silva and Benitez, 2004
		hapR_R	GGTGGAAACAAACAGTGGCC	
5	*qrr-2*	qrr2_F	GGTGACCCTTGTTAAGCCGA	This study
		qrr2_R	CTATTCACTAACAACGTCAGTTGGC	
6	*qrr-4*	qrr4_F	TGACCCTTCTAAGCCGAGGG	This study
		qrr4_R	GAACAATGGTGTTCACTAACAACG	
7	*16S rRNA*	16sVC_F	ACCTTACCTACTCTTGACATCCA	Lipp et al., 2003
		16sVC_R	CCCAACATTTCACAACACGAG	

with 10% FBS and 1% (v/v) penicillin- streptomycin at 37°C in a 5% CO_2 atmosphere in T-25 cm^2 flask. All tissues reagents were purchased from the Himedia Laboratories (Sousa et al., 2001). The cAMP level was quantified using cAMP-Glo™ Promega kit. The assay was performed as per the manufacturer's instructions. In brief, INT 407 cell lines were incubated with CT extracted from the pretreated and control strains. After incubating INT 407 cells for 8 h, the cells were treated with cAMP-Glo™ lysis buffer and incubated for 15 min. Then, 40 μl of cAMP-Glo™ detection solution (2.5 μL Protein Kinase A per 1 mL of cAMP-Glo™ reaction buffer) was added to each well and incubated for 10 min. Following the incubation period, 80 μL of the Kinase-Glo® reagent was added to terminate Protein kinase A (PKA) in all reactions and detect the remaining ATP through luciferase reaction. Further, the plates were shaken for 30 s and incubated for 10 min and a blank was maintained. The luminescence was read with Synergy H1 microplate reader and expressed as RLU which is inversely proportional to cAMP level (Bratz et al., 2013).

Adhesion and Invasion Assay

INT 407 cell lines were grown to confluence in MEM medium containing 10% FBS and 1% antibiotics. Cells were grown in 24 well plate and washed three times with sterile cell culture grade PBS and MEM medium (without FBS and antibiotics). In parallel, *V. cholerae* was grown to mid-exponential phase in the presence and absence of the test compound $PDCA^{py}$. The cells were pelleted and resuspended in MEM medium containing 10% FBS without antibiotics. The culture was then added to INT 407 monolayer at a multiplicity of infection (MOI) 50 and incubated for 90 min at 37°C in a 5% CO_2 atmosphere, for the specific bacterial adherence to the cell monolayer. The non-adherent bacteria were removed by washing the cell lines repeatedly with PBS and MEM containing 10% FBS. After repeated washings, the adherent cells were then detached using 0.1% Triton X-100 in PBS followed by vigorous pipetting. The bacterial CFU was determined by serial plating the diluted suspension. All experiments were performed in triplicates (Chourashi et al., 2016).

The anti-adhesion property of $PDCA^{py}$ further could affect the bacterial invasion to the host cells (Pizarro-Cerda and Cossart, 2006). Hence for invasion assay, in an independent experiment, after infecting the monolayer cell lines with the bacterial culture, the supernatant in each well was replaced with MEM medium containing 10% FBS supplemented with 200 μg/mL gentamycin (to kill adhered extracellular bacteria) and incubated for 60 min at 37°C in a 5% CO_2 atmosphere. Subsequently, the cell lines were washed three times with PBS and MEM medium. The cell lines were lysed with Triton X-100 and the invaded bacterial cells were counted by plating on LB agar plates (Marini et al., 2015; Peng et al., 2016).

Microscopic Imaging of Adherent Bacteria Using Giemsa Stain

Sterile coverslips were placed into each well of 24 well tissue culture plates before seeding the cells. After adding the cell suspension over the coverslips, the cells were grown in MEM medium containing 10% FBS and 1% antibiotics for 60 min incubation at 37°C in a 5% CO_2 atmosphere. After infection, the monolayer was washed with PBS and fixed with methanol for 30 min. Further, the cells were washed with PBS for 3 times and stained for 30 min with Giemsa stain to examine under a microscope (Marini et al., 2015).

MTT Cell Viability Assay

The cytotoxicity effect of $PDCA^{py}$ was tested on HepG2 cell lines and the cell viability was measured using MTT assay. Hep G2 cells were maintained in Eagle's MEM supplemented with non-essential amino acids, 10% FBS and 1% Pen Strep. Briefly, the cells were resuspended to a density of 1×10^6 CFU/mL and 100 μL were seeded into 96 well plates including a positive control (media and cells without the $PDCA^{py}$) and a blank (media alone). Plates were incubated at 37°C in 5% CO_2 until the cells reached confluence. Further, the medium was replaced with varying concentration of test compound suspended in MEM medium and incubated for 24 h at 37°C in 5% CO_2. After the incubation period, 20 μL of MTT solution (5 mg/mL) was added and incubated for 4 h. To this, 100% of DMSO was added to each well, gently swirled for 10 min and the absorbance was read at 570 nm (Kim et al., 2006). The percentage cell viability of $PDCA^{py}$ treated HepG2 cells were calculated comparing with the untreated cells.

Statistical Analysis

GraphPad prism software version 6.05 (GraphPad Software Inc., SanDiego, CA) was used for all statistical analysis. Unpaired *t*-test was used to test the significance. All the assays were conducted in triplicates and the values were expressed as mean ± SD. The value of $P < 0.05$ was used to indicate the significant difference.

RESULTS

qRT-PCR Profiling of Gene Expression

The qRT-PCR studies were performed to understand the effect of PDCA^{py} over the expression level of LuxO regulated genes, in clinical isolate (Vc4) as well as in reference strain. The strains without the treatment of PDCA^{py} were taken as control. At LCD state, the LuxO regulated virulence genes *ct*, *tcp* which encodes for CT and Type-IV regulated co-pilus, respectively, along with small regulatory RNAs (*qrr1-4*) are expressed, repressing the

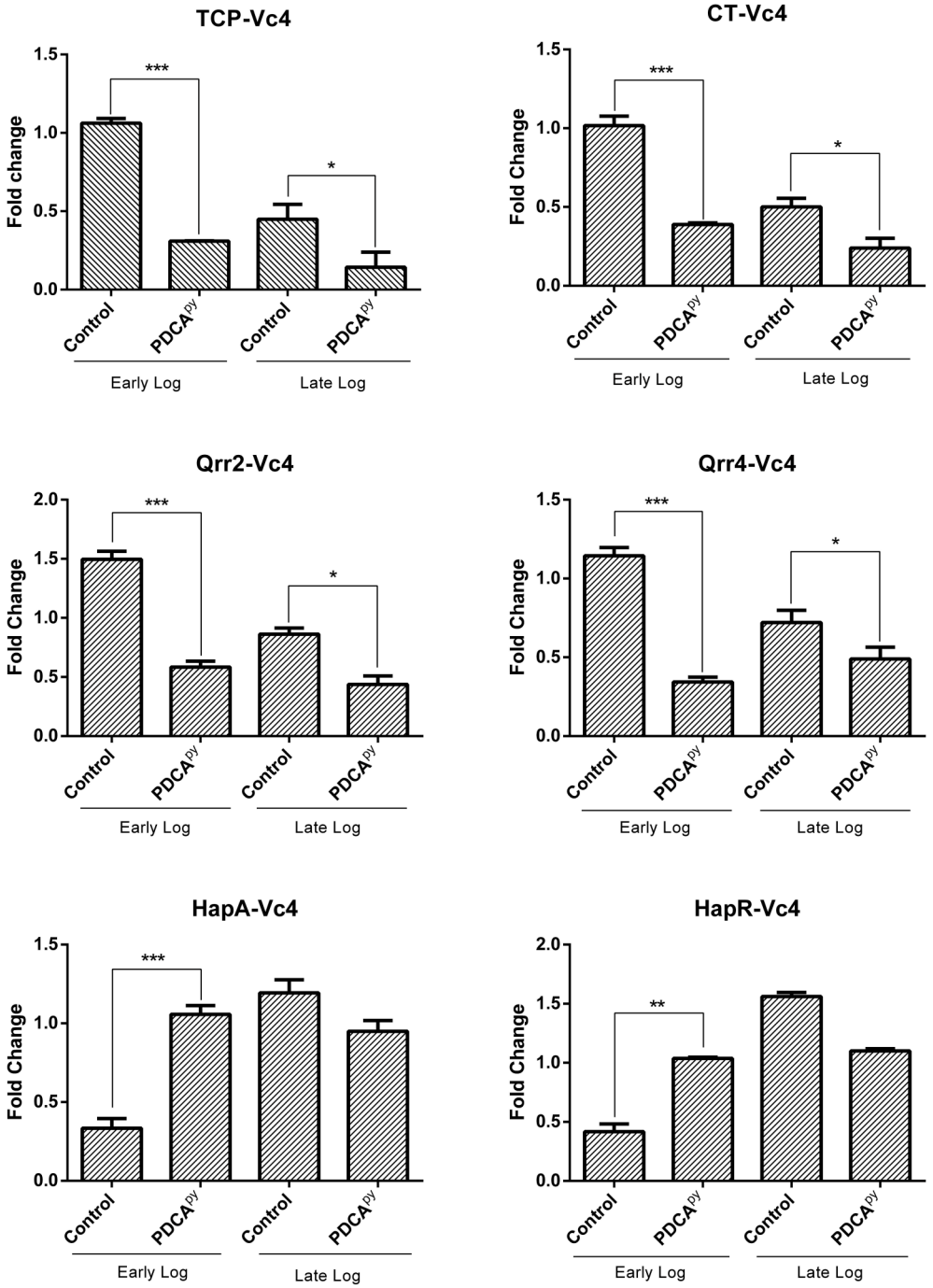

FIGURE 1 | LuxO regulated gene expression analysis by qRT- PCR. The genes *tcp, ct, qrr2,* and *qrr4* showed down-regulation and the up-regulation of *hapR* and *hapA* in the early log phase when treated with PDCA^{py} suggesting premature activation of HCD condition at LCD state. At the late log phase (HCD state), LCD condition is retained in the case of PDCA^{py} treated. 16srRNA was used as reference gene for normalization. Statistical significance denotes, $^{***}p \leq 0.001$; $^{**}p \leq 0.01$; $^{*}p \leq 0.05$.

hapR and *hapA* which encodes for protease and vice versa in the case of HCD state.

In our study, PDCA^{py} showed a LuxO selective modulation by significantly down-regulating the expression level of *ct*, *tcp*, *qrr-4*, and *qrr-2* at the early log phase. It can be also observed that the *hapR* and *hapA* genes are upregulated at LCD state. A similar trend is sustained at the late log phase (**Figure 1**). The gene expression of PDCA^{py} treated at the early log phase (LCD state) was comparable to the expression of the control seen at the late-log phase (HCD). This shows the premature activation of HCD condition at LCD state at the genetic level.

cAMP-Assay

The cellular cascade is an ATP-dependent process and the level of ATP and cAMP would directly relate the production of CT as detailed in the introduction (Polizzotti and Kiick, 2006; Popoff, 2011). **Figure 2** shows the significant increase in the relative luminescence in the treated (PDCA^{py}) cells in comparison with the control. The cell lines infected with either MTCC 3905 or Vc4 on prior treatment with PDCA^{py} showed a relative luminescence expressed as RLU to be 443 and 663, respectively. Also, in the untreated cells, the RLU of MTCC 3905 (control) and Vc4 (control) was found to be 208 and 323, respectively. This implies that the cAMP levels are reduced in the case of treated cells as cAMP levels and RLU are inversely proportional. Thus, the data shows a greater coherence with the gene expression analysis of the LuxO regulated genes by qRT-PCR.

Adhesion and Invasion Assay

From qPCR expression profiling, it was elucidated that the gene *tcp* (encoding Toxin Co-regulated Pilus; TCP) expression was down-regulated in the presence of PDCA^{py} and so we intended to examine its effect on the adhesion of *V. cholerae* to INT 407 cell monolayers. In the case of Vc4, the anti-adhesion effect of PDCA^{py} showed a significant reduction of 1.53×10^5 CFU/mL when compared to the untreated cells (3.23×10^6 CFU/mL). Similar results were observed for MTCC 3905 (**Figure 3A).** In invasion assay (**Figure 3B**), the treated cells with PDCA^{py} showed a greater reduction in the invaded cells (Vc4) of about 2.2×10^4 CFU/mL when compared to the untreated control (2.2×10^5 CFU/mL). Similar observations were made for MTCC 3905 (treated: 1.4×10^4CFU/mL, untreated: 4.1×10^5 CFU/mL). The data were in concordance with the qRT-PCR expression profile of LuxO regulated genes, where the TCP expression level was down-regulated by the quorum modulators, PDCA^{py} that invariably showed its effect in the bacterial adherence to the INT 407 cell lines.

Further, TCP-mediated cell adherence of *V. cholerae* onto the INT 407 cell lines in the presence and absence of PDCA^{py} was visualized by light microscope. The light micrographs of adhesion assay (**Figure 4**) shows that the untreated bacterial cells (comma shaped *V. cholerae* cells) are adhered onto the INT 407 cell lines. On the contrary the PDCA^{py} treated cells showed significantly reduced adherence substantiating the CFU reduction (**Figure 3A**) in the PDCA^{py} treated bacterial cells. Similarly, the invasion assay showed detachment of INT 407 cells which illustrates the invasion of the PDCA^{py} untreated bacterial cells. In the case of treated bacterial cells, invasion is reduced thereby maintaining the intact monolayer of INT 407 cell lines (**Figure 5**).

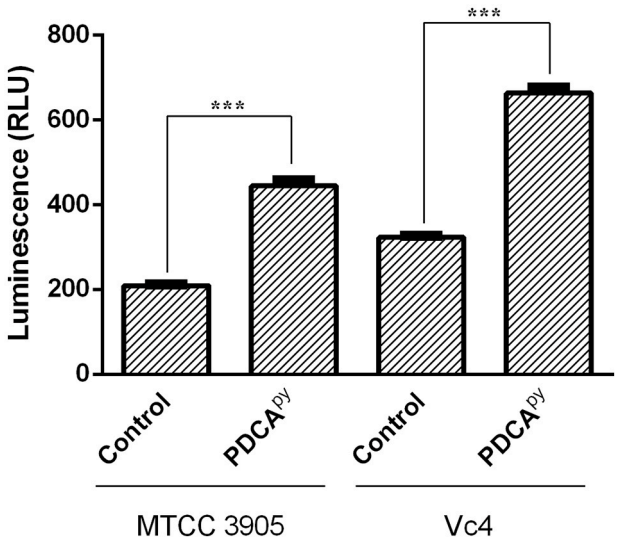

FIGURE 2 | Quorum sensing modulatory effect of PDCA^{py} using cAMP-Glo assay. PDCA^{py} treated samples showed relatively increased luminescence when compared to the untreated samples (control) in both the *V. cholerae* strains, MTCC3905 (reference strain), and Vc4 (clinical isolate).This implies low cAMP levels as it is inversely proportional to luminescence. ***Indicates significantly different ($p \leq 0.001$) compared to untreated control.

MTT Cell Viability Assay

Cell-based MTT assay was used to investigate the toxic effect of a synthesized compound, PDCA^{py} on HepG2 cell line (Soldatow et al., 2013). The reduction of yellow tetrazolium MTT (3-(4,5-dimethylthiazolyl-2)-2,5-diphenyltetrazolium bromide) is reduced in metabolically active cells as a part of an action of dehydrogenase enzymes, to generate reducing equivalents (NADH, NADPH). The results (**Figure 6**) showed that the percentage viability of the HepG2 cell line was unaffected in the presence of the test compound at its 2-fold and 4-fold IC_{50} concentrations compared to the untreated control cells.

DISCUSSION

The intestinal pathogen *V. cholerae,* encodes virulence factors like TCP, CT, and biofilm for their persistence in the host cells leading to acute diarrhoeal disease, cholera (Reidl and Klose, 2002). As QS plays a crucial role in pathogenic vibrio to regulate biofilm formation and virulence factors, chemical or natural molecules that could modulate the QS system could be a rational alternative therapy (Ng et al., 2012; Faloon et al., 2014). LuxO is the global response regulator for the known QS signaling pathways in *V. cholerae* (Cheng et al., 2015). Previous reports also state that LuxO targeted pro-quorum sensing molecules which lock the pathogenic vibrios into the HCD QS mode at the LCD state could be exploited as the aforementioned therapeutic approach (Ng et al., 2012). The premature activation of HCD condition at LCD state will prevent the biofilm formation and the expression of virulence factors promoting detachment of vibrios

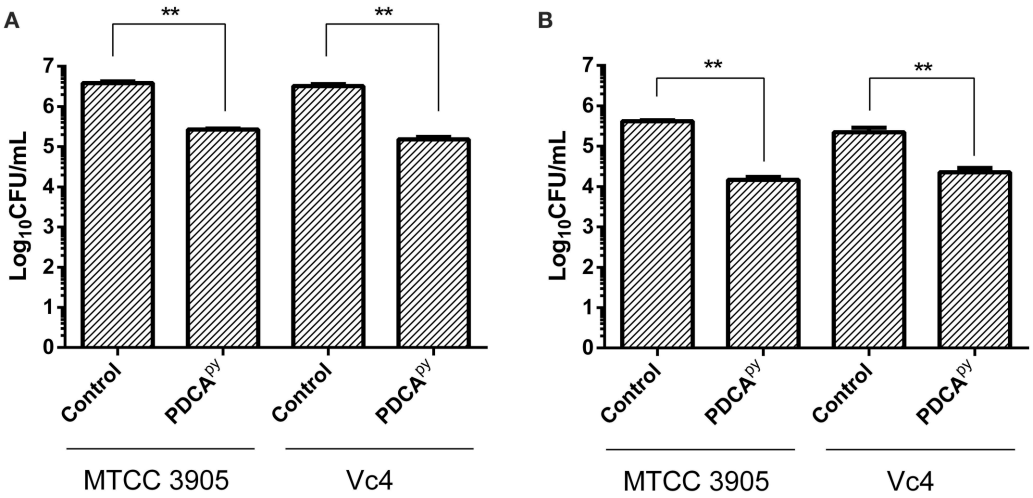

FIGURE 3 | Anti- adhesion and anti- invasion effect of PDCA^{py} treated *V. cholerae* onto INT-407 monolayer cells**. (A)** Adhesion data showing significant reduction in the number of adhered *V. cholerae* onto the intestinal epithelial cells when treated with PDCA^{py}. **(B)** Invasion results where the number of invaded cells enumerated was significantly reduced in the case of PDCA^{py} treated bacterial cells. **Indicates significantly different ($p \leq 0.01$) compared to untreated control.

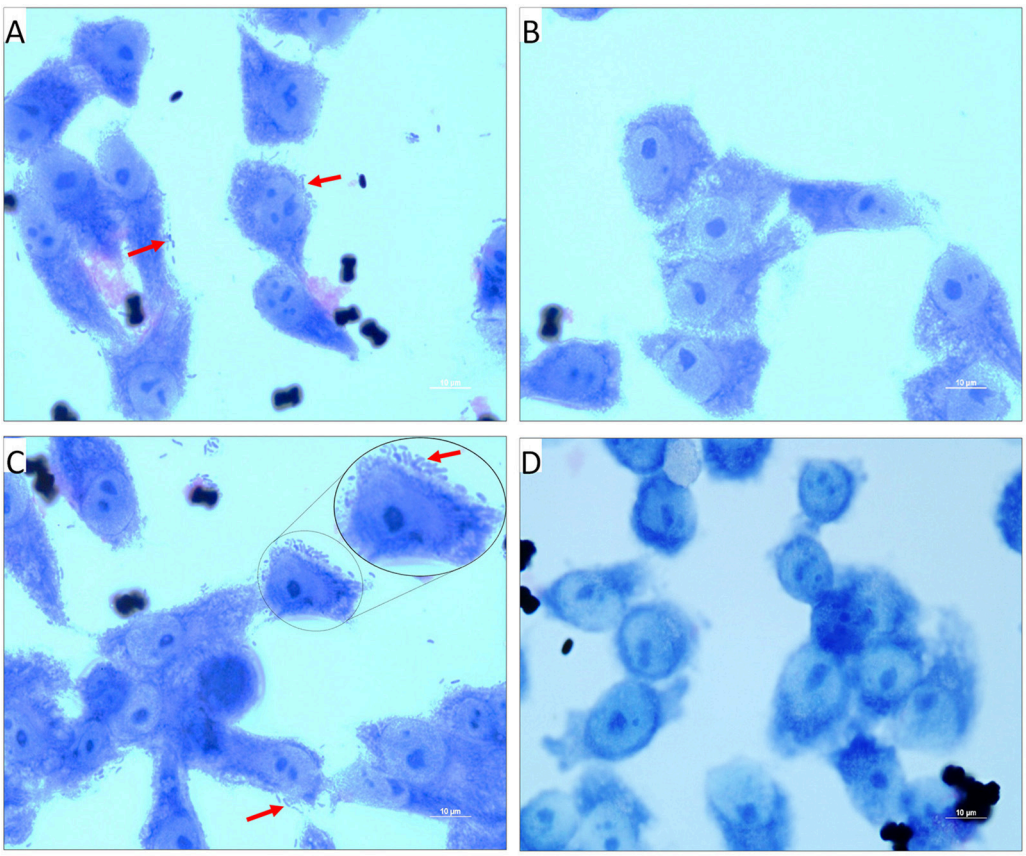

FIGURE 4 | Light micrographs showing the adhered *V. cholerae* onto INT 407 monolayer cells. **(A,C)** Control panels of INT 407 cell lines infected with MTCC3905 reference strain and clinical isolate, Vc4, respectively. The red arrow mark represents the adhered bacterial cells onto the intestinal cell lines producing a carpet like aggregate pattern. **(B,D)** PDCA^{py} treated MTCC3905 reference strain and clinical isolate, Vc4 bacterial cells adhered to INT 407 cells, respectively. PDCA^{py} treated cells, showed a significant reduction in adherence to the cell lines as compared to the control. Scale bar in micrographs represents 10 μm.

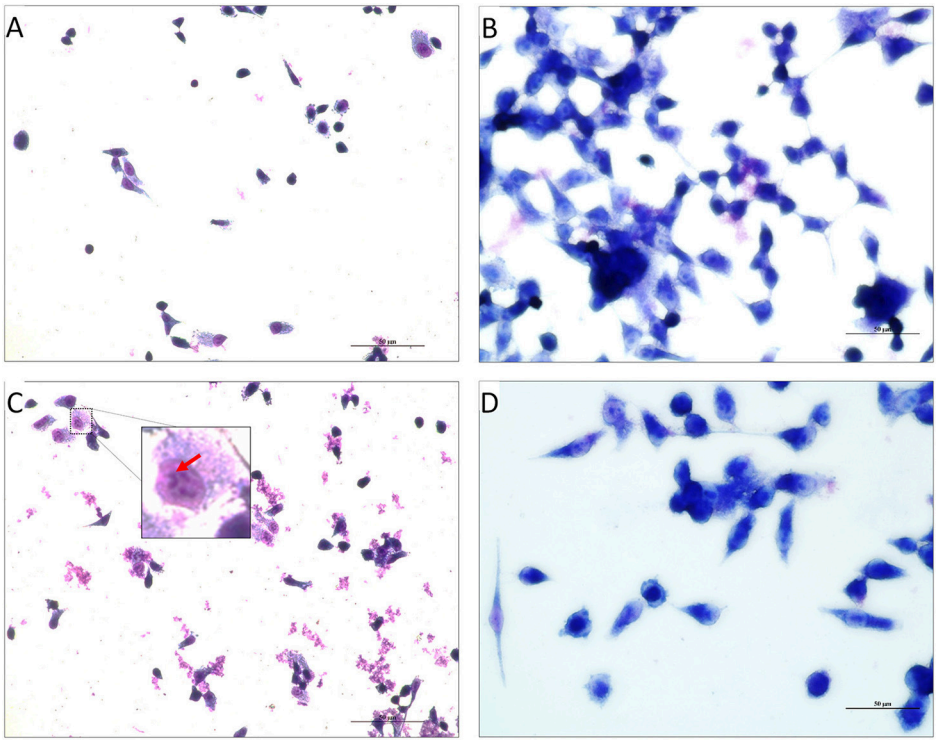

FIGURE 5 | Light Micrographs showing the invaded *V. cholerae* onto INT 407 monolayer cells. **(A,C)** INT 407 cell lines invaded by the PDCA^{py} untreated MTCC3905 and Vc4, respectively. The coma shaped *V. cholerae* cells that are invaded in the INT 407 cell lines can be distinctly seen in the untreated control (inset, enlarged image).The invasion of the *V. cholerae* cells into intestinal epithelial cells were unhealthy (rounded and detached). **(B,D)** PDCA^{py} treated *V. cholerae* showed reduced invasive property, leading to healthy intestinal cells. Scale bar in micrographs represents 50 μm.

from the intestine. Such modulators will facilitate the clearance of detached vibrios by the host immune response and prevent the overuse of antibiotics by their synergistic action with the conventional antibiotics (Hema et al., 2016). In addition, these modulators do not pose a survival stress to the bacteria, thus minimizing the resistance development. Hence, targeting LuxO would be a promising anti-virulence therapeutic strategy.

In the light of our previous *in silico* studies, we had shown that target specific modulators, PDCA and its derivatives, could impede the activity of LuxO as they interact with three key amino acids (G170, G172, and I140) present in the ATPase domain which hydrolyzes ATP molecules (Hema et al., 2015b). Further, the synthesized pyrrolidine derivative of PDCA was proven to possess anti-biofilm activity without affecting the growth of *V. cholerae* (**Figure S2**) speculating to the LuxO targeted QS modulatory effect (Hema et al., 2016). Hence, the present work is to explore the mechanism underpinning the LuxO modulatory activity by 3-(4-(Pyrrolidin-1-yl) phenyl carbamoyl) pyrazine-2-carboxylic acid (PDCA^{py}) thus providing the prelude for probing PDCA-based novel quorum-sensing modulators.

Gene expression profiling provides an insight to elucidate the pathway that could be altered by the QS modulators (QSMs). In *V. cholerae*, the infection cycle initiates at LCD state with the up-regulated virulence gene expressions like *ct*, *tcp*, regulatory RNAs *qrr1-4* and down-regulated *hapR* gene expression, thus, promoting intestinal colonization. Subsequently at HCD state, the dissemination of colonized vibrios from the human intestinal cells is facilitated with the upregulation of *hapR* and down-regulation of the other virulence genes (Ng et al., 2012).

In the present study, down-regulated gene expression of *ct*, *tcp, qrr,* and up-regulated gene expression of *hapA, hapR* is reported at the early-log phase for the PDCA^{py} treated cells (**Figure 1**). The data showed that PDCA^{py} modulates the QS genetic circuit to mimic the gene expressions of HCD condition to prevail at the LCD state. This further inhibits the phenotypic expression of CT and TCP virulence factors. In a similar study the effect of thio-azauracil based broad spectrum pro-quorum sensing molecules on down-regulation of virulence gene expression in *V. cholerae* was investigated (Ng et al., 2012).

The release of CT initiates the synthesis of cAMP by activating the adenylyl cyclase to regulate the cystic fibrosis transmembrane conductance regulator (CFTR). This leads to an instant efflux of ions and water from the infected intestinal cells to cause diarrhea (Gurney et al., 2017). Literature reports suggest that cAMP is an indirect measure to relate the expression of CT (Hyun and Kimmich, 1982; Bratz et al., 2013). Hence, here we have used cAMP-Glo assay to determine the cAMP levels in PDCA^{py} treated and untreated conditions. According to this assay, cAMP binds to protein kinase A to release the active catalytic subunits. This further catalyzes the transfer of the terminal phosphate of ATP to a protein kinase A substrate, consuming ATP in the process. Thus, the level of remaining ATP is measured in

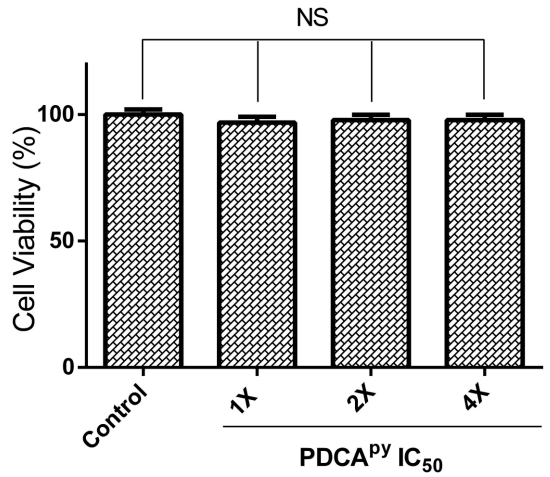

FIGURE 6 | Cell viability of HepG2 cells treated with PDCA^{py}. Cell viability of HepG2 cells was not affected as indicated by the insignificant difference between control and treated at its IC_{50} concentration, 1X = 25 μM, 2X = 50 μM, 4X = 100 μM. NS denotes no significant differences ($p > 0.05$).

terms of luminescence which is inversely proportional to cAMP levels (Bratz et al., 2013). Here we have observed increased luminescence in the PDCA^{py} treated cells as compared to the control, indicating the decreased levels of CT. This is reinforced by the evidence from gene expression studies with significant down-regulation of *ct* (**Figure 1**).

The colonization factor, type IV TCP, enhances *V. cholerae* pathogenesis promoting the formation of micro-colonies in the intestine (Millet et al., 2014). Almagro-Moreno et al. (2015) had demonstrated that Δ*tcp* strains neither colonize the human epithelial cells nor cause the key symptoms of cholera. Hence, the anti-adhesion effect of PDCA^{py} was demonstrated in the human intestinal epithelial cell line, INT 407. The reduced CFU counts from the PDCA^{py} treated bacterial cells suggest the interference in adhesion to INT 407 cell lines. This is attributed to the fact that PDCA^{py} specifically modulated the LuxO and subsequently the expression of TCP, a major colonization factor. The property of invasion can be considered as another aspect of *V. cholerae* pathogenicity, similar to enterotoxigenic *Escherichia coli* infection (Elsinghorst and Kopecko, 1992). Similar to the adhesion assay, a significant reduction in the invasion was also observed. This is corroborated from the light microscopic images (**Figures 4**, **5**) that PDCA^{py} interferes with the colonization onto the intestinal cells. These results are in concordance with the reduced gene expression of the colonization factor, *tcp* (**Figure 1**).

For a small molecule to be scored as a drug candidate, one of the essential characteristics is non-toxicity toward the host cell. In this context, MTT-based cytotoxicity studies have shown the non-toxic nature of the QSM, PDCA^{py}. Additionally, the other drug-like properties that include water solubility, cell permeability, good absorption and no host cell cytotoxicity as reported earlier through our *in silico* studies (Hema et al., 2015b).

Targeting the ATPase domain of LuxO could potentially be developed as broad spectrum NtrC family inhibitors as it is highly conserved in all *Vibrio* sp. (Boyaci et al., 2016). Ng et al. (2012) have tested their LuxO targeted pro-quorum sensing molecules of *V. cholerae* against *V. harveyi* and *Vibrio parahaemolyticus*. They have concluded that these molecules are capable of modulating QS in other *Vibrio* sp. also where LuxO functions to be the global QS regulator (Ng et al., 2012). In this context, PDCA^{py} could serve as a potent broad spectrum lead molecule for *Vibrio* sp. infections.

CONCLUSION

QS is a well-known system that regulates biofilm and various virulence factors in pathogenic bacteria. Our studies provide an insight on the QS modulatory effect of PDCA^{py} [3-(4-(Pyrrolidin-1-yl) phenyl carbamoyl) pyrazine-2-carboxylic acid] against both clinical as well as reference strains of *V. cholerae*. Thus, PDCA^{py} could serve as a potent, target-specific and non-toxic lead for drug development against Vibrio infections.

AUTHOR CONTRIBUTIONS

All authors listed, have made a substantial, direct and intellectual contribution to the work, and approved it for publication.

ACKNOWLEDGMENTS

We sincerely thank SASTRA University and its management for providing us the infrastructure needed to carry out our research work. We also acknowledge the DST-FIST program (SR/FST/ETI-331/2013) for microscope imaging facility.

SUPPLEMENTARY MATERIAL

The Supplementary Material for this article can be found online at: https://www.frontiersin.org/articles/10.3389/fcimb.2017.00441/full#supplementary-material

Figure S1 | Chemical Structure of PDCA^{py} (3-(4-(Pyrrolidin-1-yl) phenyl carbamoyl) pyrazine-2-carboxylic acid).

Figure S2 | Growth curve of *V. cholerae* MTCC 3905 and Vc4 strains in the presence and absence of PDCA^{py} at its IC_{50} Concentration, 25 μM. The growth of the *V. cholerae* strains taken was not affected in the presence of PDCA^{py}.

REFERENCES

Almagro-Moreno, S., Pruss, K., and Taylor, R. K. (2015). Intestinal colonization dynamics of *Vibrio cholerae*. *PLoS Pathog.* 11:e1004787. doi: 10.1371/journal.ppat.1004787

Beaula, T. J., Packiavathi, A., Manimaran, D., Joe, I. H., Rastogi, V. K., and Jothy, V. B. (2015). Quantum chemical computations, vibrational spectroscopic analysis and antimicrobial studies of 2, 3-Pyrazinedicarboxylic acid. *Spectrochim. Acta Mol. Biomol. Spectrosc.* 138, 723–735. doi: 10.1016/j.saa.2014.11.034

Boyaci, H., Shah, T., Hurley, A., Kokona, B., Li, Z., Ventocilla, C., et al. (2016). Structure, regulation, and inhibition of the quorum-sensing signal integrator LuxO. *PLoS Biol.* 14:e1002464. doi: 10.1371/journal.pbio.1002464

Bratz, M., Hook, B., and Schagat, T. (2013). *Measuring cAMP Levels and Cytotoxicity in a Single Plate Well*. Article Promega Corporation. Available online at: http://www.promega.in/resources/pubhub/measuring-camp-levels-and-cytotoxicity-in-a-single-plate-well-article

Cheng, A. T., Ottemann, K. M., and Yildiz, F. H. (2015). *Vibrio cholerae* response regulator VxrB controls colonization and regulates the type VI secretion system. *PLoS Pathog.* 11:e1004933. doi: 10.1371/journal.ppat.1004933

Chourashi, R., Mondal, M., Sinha, R., Debnath, A., Das, S., Koley, H., et al. (2016). Role of a sensor histidine kinase ChiS of *Vibrio cholerae* in pathogenesis. *Int. J. Med. Microbiol.* 306, 657–665. doi: 10.1016/j.ijmm.2016.09.003

Elsinghorst, E. A., and Kopecko, D. (1992). Molecular cloning of epithelial cell invasion determinants from enterotoxigenic *Escherichia coli*. *Infect. Immun.* 60, 2409–2417.

Faloon, P., Jewett, I., Youngsaye, W., Bennion, M., Ng, W.-L., Hurley, A., et al. (2014). *Discovery of ML366, an Inhibitor of Vibrio cholerae Quorum Sensing Acting via the LuxO Response Regulator. Probe Reports from the NIH Molecular Libraries Program In: Probe Reports from the NIH Molecular Libraries Program* [Internet]. Bethesda, MD: National Center for Biotechnology Information 2010. Available online at: https://www.ncbi.nlm.nih.gov/books/NBK189922/

Gorski, A., Miedzybrodzki, R., Weber-Dabrowska, B., Fortuna, W., Letkiewicz, S., Rogóz, P., et al. (2016). Phage therapy: combating infections with potential for evolving from merely a treatment for complications to targeting diseases. *Front. Microbiol.* 7:1515. doi: 10.3389/fmicb.2016.01515

Gurney, M. A., Laubitz, D., Ghishan, F. K., and Kiela, P. R. (2017). Pathophysiology of Intestinal Na^+/H^+ Exchange. *Cell. Mol. Gastroenterol. Hepatol.* 3, 27–40. doi: 10.1016/j.jcmgh.2016.09.010

Hema, M., Balasubramanian, S., and Princy, S. A. (2015a). Meddling *Vibrio cholerae* murmurs: a neoteric advancement in cholera research. *Indian J. Microbiol.* 55, 121–130. doi: 10.1007/s12088-015-0520-1

Hema, M., Karthi, S., and AdlinePrincy, S. (2015b). Design of LuxO based inhibitors to reverse engineer the genetic circuit of *Vibrio cholerae*- an anti-virulent cholera therapy. *J. Chem. Pharm. Res.* 7, 1544–1552.

Hema, M., Princy, S. A., Sridharan, V., Vinoth, P., Balamurugan, P., and Sumana, M. (2016). Synergistic activity of quorum sensing inhibitor, pyrizine-2-carboxylic acid and antibiotics against multi-drug resistant *V. cholerae*. *RSC Advances* 6, 45938–45946. doi: 10.1039/C6RA04705J

Hyun, C. S., and Kimmich, G. A. (1982). Effect of cholera toxin on cAMP levels and Na^+ influx in isolated intestinal epithelial cells. *Am. J. Physiol.* 243, C107–C115.

Jung, S. A., Hawver, L. A., and Ng, W.-L. (2016). Parallel quorum sensing signaling pathways in *Vibrio cholerae*. *Curr. Genet.* 62, 255–260. doi: 10.1007/s00294-015-0532-8

Kim, A. L., Zhu, Y., Zhu, H., Han, L., Kopelovich, L., Bickers, D. R., et al. (2006). Resveratrol inhibits proliferation of human epidermoid carcinoma A431 cells by modulating MEK1 and AP-1 signalling pathways. *Exp. Dermatol.* 15, 538–546. doi: 10.1111/j.1600-0625.2006.00445.x

Lipp, E. K., Rivera, I. N., Gil, A. I., Espeland, E. M., Choopun, N., Louis, V. R., et al. (2003). Direct detection of *Vibrio cholerae* and ctxA in Peruvian coastal water and plankton by PCR. *Appl. Environ. Microbiol.* 69, 3676–3680. doi: 10.1128/AEM.69.6.3676-3680.2003

Lu, L., and Walker, W. A. (2001). Pathologic and physiologic interactions of bacteria with the gastrointestinal epithelium. *Am. J. Clin. Nutr.* 73, 1124S–1130S.

Maiti, D., Das, B., Saha, A., Nandy, R. K., Nair, G. B., and Bhadra, R. K. (2006). Genetic organization of pre-CTX and CTX prophages in the genome of an environmental *Vibrio cholerae* non-O1, non-O139 strain. *Microbiology* 152, 3633–3641. doi: 10.1099/mic.0.2006/000117-0

Marini, E., Magi, G., Mingoia, M., Pugnaloni, A., and Facinelli, B. (2015). Antimicrobial and anti-virulence activity of capsaicin against erythromycin-resistant, cell-invasive group a streptococci. *Front. Microbiol.* 6:1281. doi: 10.3389/fmicb.2015.01281

Millet, Y. A., Alvarez, D., Ringgaard, S, von Andrian, U. H., Davis, B. M., and Waldor, M. K. (2014). Insights into *Vibrio cholerae* intestinal colonization from monitoring fluorescently labeled bacteria. *PLoS pathog.* 10:e1004405. doi: 10.1371/journal.ppat.1004405

Mitchison, D. A. (1996). Pyrazinamide—on the antituberculosis drug frontline. *Nat. Med.* 2, 635–636. doi: 10.1038/nm0696-635

Ng, W.-L., Perez, L., Cong, J., Semmelhack, M. F., and Bassler, B. L. (2012). Broad spectrum pro-quorum-sensing molecules as inhibitors of virulence in vibrios. *PLoS Pathog.* 8:e1002767. doi: 10.1371/journal.ppat.1002767

Papenfort, K., and Bassler, B. L. (2016). Quorum sensing signal-response systems in Gram-negative bacteria. *Nat. Rev. Microbiol.* 14, 576–588. doi: 10.1038/nrmicro.2016.89

Peng, Y., Wang, X., Shou, J., Zong, B., Zhang, Y., Tan, J., et al. (2016). Roles of Hcp family proteins in the pathogenesis of the porcine extraintestinal pathogenic *Escherichia coli* type VI secretion system. *Sci. Rep.* 6:26816. doi: 10.1038/srep26816

Pizarro-Cerda, J., and Cossart, P. (2006). Bacterial Adhesion and entry into host cells. *Cell* 715–727. doi: 10.1016/j.cell.2006.02.012

Polizzotti, B. D., and Kiick, K. L. (2006). Effects of polymer structure on the inhibition of cholera toxin by linear polypeptide-based glycopolymers. *Biomacromolecules* 7, 483–490. doi: 10.1021/bm050672n

Popoff, M. (2011). Multifaceted interactions of bacterial toxins with the gastrointestinal mucosa. *Future Microbiol.* 6, 763–797. doi: 10.2217/fmb.11.58

Reidl, J., and Klose, K. E. (2002). *Vibrio cholerae* and cholera: out of the water and into the host. *FEMS Microbiol. Rev.* 26, 125–139. doi: 10.1111/j.1574-6976.2002.tb00605.x

Sarkar, A., Nandy, R. K., Nair, G. B., and Ghose, A. C. (2002). Vibrio pathogenicity island and cholera toxin genetic element-associated virulence genes and their expression in non-O1 non-O139 strains of *Vibrio cholerae*. *Infect. Immun.* 70, 4735–4742. doi: 10.1128/IAI.70.8.4735-4742.2002

Silva, A. J., and Benitez, J. A. (2004). Transcriptional regulation of *Vibrio cholerae* hemagglutinin/protease by the cyclic AMP receptor protein and RpoS. *J. Bacteriol.* 186, 6374–6382. doi: 10.1128/JB.186.19.6374-6382.2004

Silva, A. J., Leitch, G. J., Camilli, A., and Benitez, J. A. (2006). Contribution of hemagglutinin/protease and motility to the pathogenesis of El Tor biotype cholera. *Infect. Immun.* 74, 2072–2079. doi: 10.1128/IAI.74.4.2072-2079.2006

Soldatow, V. Y., LeCluyse, E. L., Griffith, L. G., and Rusyn, I. (2013). *In vitro* models for liver toxicity testing. *Toxicol. Res.* 2, 23–39. doi: 10.1039/C2TX20051A

Sousa, M. C., Goncalves, C., Bairos, V., and Poiares-Da-Silva, J. (2001). Adherence of Giardia lamblia trophozoites to int-407 human intestinal cells. *Clin. Diagn. Lab. Immunol.* 8, 258–265. doi: 10.1128/CDLI.8.2.258-265.2001

Stabb, E. V., and Visick, K. L. (2013)."*Vibrio fisheri*: squid symbiosis," in *The Prokaryotes,* eds E. Rosenberg, E. F. Delong, S. Lory, E. Stackebrandt, and F. Thompson (Berlin; Heidelberg: Springer), 497–532.

Tyor, A. K., and Kumari, S. (2016). Biochemical characterization and antibacterial properties of fish skin mucus of fresh water fish, *Hypophthalmichthysnobilis*. *Int. J. Pharm. Pharm. Sci.* 8, 132–136.

Vezzulli, L., Stauder, M., Grande, C., Pezzati, E., Verheye, H. M., Owens, N. J., et al. (2015). gbpA as a novel qPCR target for the species-specific detection of *Vibrio cholerae* O1, O139, non-O1/non-O139 in environmental, stool, and historical continuous plankton recorder samples. *PLoS ONE* 10:e0123983. doi: 10.1371/journal.pone.0123983

Waters, C. M., Lu, W., Rabinowitz, J. D., and Bassler, B. L. (2008). Quorum sensing controls biofilm formation in *Vibrio cholerae* through modulation of cyclic di-GMP levels and repression of vpsT. *J. Bacteriol.* 190, 2527–2536. doi: 10.1128/JB.01756-07

Zhang, P., Lu, H., Chen, H., Zhang, J., Liu, L., Lv, F., et al. (2016). Cationic conjugated polymers-induced quorum sensing of bacteria cells. *Anal. Chem.* 88, 2985–2988. doi: 10.1021/acs.analchem.5b03920

Zhu, J., Miller, M. B., Vance, R. E., Dziejman, M., Bassler, B. L., and Mekalanos, J. J. (2002). Quorum-sensing regulators control virulence gene expression in *Vibrio cholerae*. *Proc. Natl. Acad. Sci. U.S.A.* 99, 3129–3134. doi: 10.1073/pnas.052694299

Conflict of Interest Statement: The authors declare that the research was conducted in the absence of any commercial or financial relationships that could be construed as a potential conflict of interest.

The reviewer YGT and handling Editor declared their shared affiliation.

frontiers in Cellular and Infection Microbiology

ORIGINAL RESEARCH
published: 08 November 2018
doi: 10.3389/fcimb.2018.00368

The 9*H*-Fluoren Vinyl Ether Derivative SAM461 Inhibits Bacterial Luciferase Activity and Protects *Artemia franciscana* From Luminescent Vibriosis

Alberto J. Martín-Rodríguez[1,2], Sergio J. Álvarez-Méndez[1], Caroline Overå[3], Kartik Baruah[4,5], Tânia Margarida Lourenço[4], Parisa Norouzitallab[4,6], Peter Bossier[4], Víctor S. Martín[1] and José J. Fernández[1]*

[1] Instituto Universitario de Bio-Orgánica "Antonio González", Centro de Investigaciones Biomédicas de Canarias, Universidad de La Laguna, Tenerife, Spain, [2] Department of Microbiology, Tumor and Cell Biology, Karolinska Institutet, Stockholm, Sweden, [3] Institute of Biophysics and Biophysical Chemistry, University of Regensburg, Regensburg, Germany, [4] Laboratory of Aquaculture & Artemia Reference Center, Department of Animal Sciences and Aquatic Ecology, Faculty of Bioscience Engineering, Ghent University, Ghent, Belgium, [5] Department of Animal Nutrition and Management, Faculty of Veterinary Medicine and Animal Sciences, Swedish University of Agricultural Sciences, Uppsala, Sweden, [6] Laboratory of Immunology and Animal Biotechnology, Department of Animal Sciences and Aquatic Ecology, Ghent University, Ghent, Belgium

Vibrio campbellii is a major pathogen in aquaculture. It is a causative agent of the so-called "luminescent vibriosis," a life-threatening condition caused by bioluminescent *Vibrio* spp. that often involves mass mortality of farmed shrimps. The emergence of multidrug resistant *Vibrio* strains raises a concern and poses a challenge for the treatment of this infection in the coming years. Inhibition of bacterial cell-to-cell communication or quorum sensing (QS) has been proposed as an alternative to antibiotic therapies. Aiming to identify novel QS disruptors, the 9H-fluroen-9yl vinyl ether derivative SAM461 was found to thwart *V. campbellii* bioluminescence, a QS-regulated phenotype. Phenotypic and gene expression analyses revealed, however, that the mode of action of SAM461 was unrelated to QS inhibition. Further evaluation with purified *Vibrio fischeri* and NanoLuc luciferases revealed enzymatic inhibition at micromolar concentrations. *In silico* analysis by molecular docking suggested binding of SAM461 in the active site cavities of both luciferase enzymes. Subsequent *in vivo* testing of SAM461 with gnotobiotic *Artemia franciscana* nauplii demonstrated naupliar protection against *V. campbellii* infection at low micromolar concentrations. Taken together, these findings suggest that suppression of luciferase activity could constitute a novel paradigm in the development of alternative anti-infective chemotherapies against luminescent vibriosis, and pave the ground for the chemical synthesis and biological characterization of derivatives with promising antimicrobial prospects.

Keywords: vinyl ether, luciferase, *Artemia*, vibriosis, alternative anti-infectives

OPEN ACCESS

Edited by:
Rodolfo García-Contreras, Universidad Nacional Autónoma de México, Mexico

Reviewed by:
Dana Kathleen Shaw, Washington State University, United States
Hélène Marquis, Cornell University, United States

***Correspondence:**
Alberto J. Martín-Rodríguez
ajmartinr@ull.es;
jonatan.martin.rodriguez@ki.se

Specialty section:
This article was submitted to Molecular Bacterial Pathogenesis, a section of the journal Frontiers in Cellular and Infection Microbiology

Received: *03 August 2018*
Accepted: *03 October 2018*
Published: *08 November 2018*

Citation:
Martín-Rodríguez AJ, Álvarez-Méndez SJ, Overå C, Baruah K, Lourenço TM, Norouzitallab P, Bossier P, Martín VS and Fernández JJ (2018) The 9H-Fluoren Vinyl Ether Derivative SAM461 Inhibits Bacterial Luciferase Activity and Protects Artemia franciscana From Luminescent Vibriosis. Front. Cell. Infect. Microbiol. 8:368. doi: 10.3389/fcimb.2018.00368

INTRODUCTION

Bacterial cell-to-cell communication or quorum sensing (QS) is a population-density-dependent extracellular signaling process that enables the coordination of collective behaviors in several bacterial species. This intercellular communication system relies on the synthesis, secretion and detection of signaling molecules termed autoinducers (AIs), which enable bacteria to optimize their metabolic resources and carry out tasks that are only possible at high cellular densities. Thus, QS exerts a tight control over bacterial gene expression, often involving hundreds of genes (Wilder et al., 2011; Majerczyk et al., 2016; Ball et al., 2017). Some of the QS-regulated physiological processes in diverse bacterial models include biofilm formation, host colonization and virulence factor production (Zhu and Mekalanos, 2003; Bassler and Losick, 2006; Waters et al., 2008; Ruwandeepika et al., 2011a; Bjelland et al., 2012). For this reason and given that, in principle, signal interference would not impose a selective pressure on bacterial populations, QS disruption has been proposed as a more selective target in the development of antibacterial therapies (LaSarre and Federle, 2013).

Vibrio campbellii is a marine bacterium whose bioluminescence is controlled by a complex QS regulatory system. Three hybrid sensor kinases, LuxN, LuxPQ, and CqsS responding to three different AIs converge in a response regulator, LuxO that controls the transcription of the mRNA encoding the master regulator of the QS regulon, LuxR. Upon DNA binding, LuxR enables the expression of hundreds of genes including the luciferase structural operon *luxCDABEGH*, where *luxAB* encode the two subunits of the bacterial luciferase (Meighen, 1991; Waters and Bassler, 2006). LuxG and LuxH are not essential for light production, though, and are not present in other bacterial *lux* homologs (Waidmann et al., 2011). Because of its QS-regulated light production and its well-characterized QS system, *V. campbellii* has been widely employed as a model biosensor to screen for QS inhibitors (Martín-Rodríguez and Fernández, 2016).

V. campbellii is a pernicious pathogen in aquaculture, affecting farm stocks of fish, shrimps and mollusks worldwide (Austin and Zhang, 2006; Haldar et al., 2011; Wang et al., 2015). Diseases caused by *V. campbellii* include skin ulcers, vasculitis, gastrointestinal disorders and eye lesions in fish (Austin and Zhang, 2006; Shen et al., 2017) and the so-called "luminescent vibriosis" in crustaceans and mollusks, often involving mass mortality and extensive economic loss (Travers et al., 2009; Darshanee Ruwandeepika et al., 2012; Lio-Po, 2016). This disease owes its name to the bioluminescence displayed by its causative agents, primarily *V. campbellii* and *V. harveyi*. Mortality rates between 60 and 80% have been reported in abalone (*Haliotis tuberculata*), up to 85% in white shrimp (*Litopenaeus vannamei*) and up to 100% in salmonids (Defoirdt et al., 2007a), with global estimated costs for this disease exceeding $9 billion per year (Bondad-Reantaso et al., 2005). The indiscriminate use of antibiotics over decades has resulted in the emergence of multidrug-resistant *V. campbellii* strains (Scarano et al., 2014). The need for sustainable alternative therapies is even more urgent taking into account the tight regulations and growing public health concerns associated with the use of antibiotics in aquaculture (Defoirdt et al., 2011).

Experimental characterization of novel drug candidates for aquaculture requires representative and reliable animal models. In this context, the *Artemia franciscana* naupliar gnotobiotic model is well-established, with the nauplii being relatively easy to rear under germ-free conditions and providing the additional advantage of eliminating any indirect effects caused by host microbiota, thereby allowing a direct cause-effect association during drug candidate testing (Baruah et al., 2015). In an effort to find QS antagonists from chemical libraries, SAM461 was identified as a potent inhibitor of *V. campbellii* bioluminescence with no inhibitory effect on bacterial growth at effective doses in the low-micromolar range. Here we describe our characterization of its mode of action and *in vivo* performance using axenically-hatched *A. franciscana* nauplii.

MATERIALS AND METHODS

Strains and Growth Conditions

The *V. campbellii* strains used in this study are listed in **Table 1**. Bacteria were recovered from cryopreserved stocks on marine agar (Difco). Single colonies were used to start the experiments as described below. When necessary, ampicillin (100 $\mu g\ ml^{-1}$) and isopropyl-β-D-thiogalactoside (IPTG; 200 μM) were supplemented.

Synthesis of SAM461

(*E*)-Methyl 3-((9*H*-fluoren-9-yl)oxy)acrylate (SAM461) was synthesized using 9-hydroxyfluorene (380 mg, 2.00 mmol) as

TABLE 1 | Strains and primers used in this study.

Strains	Genotype and relevant characteristics	Source or references
Vibrio campbellii ATCC-BAA 1116 (BB120)	Wild type strain.	Bassler et al., 1994
Vibrio campbellii JAF548 pAK*lux*1	Strain JAF548 (BB120 *luxO* D47E linked to Kan^r) carrying plasmid pAK*lux*1 (Amp^r), a pBBR1MCS-4 derivative containing the *luxCDABE* operon from *Photorhabdus luminescens*. Luminescence independent of quorum sensing.	Defoirdt et al., 2012
Primers	**Sequence**	**Source or references**
qVhluxR_F	TCAATTGCAAAGAGACCTCG	Defoirdt et al., 2007b
qVhluxR_R	AGCAAACACTTCAAGAGCGA	Defoirdt et al., 2007b
qVHluxA_F	ATTTGCCGCAACTTCTTGGG	This study
qVHluxA_R	TGGTGTCTTTGTGGCCTTTC	This study
qVHluxC_F	AGATGCATTCGCCGCAAAAG	This study
qVHluxC_R	AACGTTGAAGTGGTCGCATG	This study
qVhrpoA_F	CGTAGCTGAAGGCAAAGATGA	Defoirdt et al., 2007b
qVhrpoA_R	AAGCTGGAACATAACCACGA	Defoirdt et al., 2007b

starting material. Methyl propiolate (1.3 equiv) was added portionwise under Ar atmosphere (six portions, one portion every 5 min) to a solution of the alcohol (1 equiv) and DABCO (0.1 equiv) in dry dichloromethane (0.4 M). After thin-layer chromatography (TLC) analysis revealed a complete reaction (1 h approximately), the product was concentrated and purified by flash chromatography (28 cm of height of silica gel, *n*-hexane/Et_2O 85/15) affording SAM461 (515 mg, 97%) as a yellowish solid consistent with reported data (Tejedor et al., 2014). SAM461 molecular weight (MW) and octanol:water partition coefficient (cLogP) were calculated with ChemBioDraw Ultra 13.0.0.3015 (CambridgeSoft, PerkinElmer).

Spectroscopic data of SAM461: R_F 0.38 (*n*-hexane/Et_2O 80/20 two times); ^{1}H-NMR (400 MHz, δ, $CDCl_3$) 3.64 (s, 3H), 5.47 (d, $J = 12.3$ Hz, 1H), 5.94 (s, 1H), 7.28–7.35 (m, 2H), 7.40–7.47 (m, 3H), 7.55 (d, $J = 7.5$ Hz, 2H), 7.67 (d, $J = 7.5$ Hz, 2H); ^{13}C-NMR (100 MHz, δ, $CDCl_3$) 51.1 (q), 82.7 (d), 99.4 (d), 120.3 (d, 2C), 125.5 (d, 2C), 128.1 (d, 2C), 130.0 (d, 2C), 140.9 (s, 2C), 141.1 (s, 2 C), 160.8 (s), 168.0 (s); MS (EI) m/z (relative intensity) 266 $(M)^+$ (1), 166 (30), 165 (100), 163 (11), 139 (5), 115 (3); HRMS calcd for $C_{17}H_{14}O_3$ $(M)^+$ 266.0943, found 266.0942. ^{1}H and ^{13}C-NMR spectra (**Figure S1**) were recorded on Bruker Avance instruments at room temperature, and data were processed using Topspin software (version 2.1); chemical shifts (δ) are reported in parts per million (ppm), and coupling constants (*J*) are quoted in Hertz (Hz); ^{1}H-NMR spectrum is referenced to the resonance from residual $CHCl_3$ at 7.250 ppm and multiplicity is expressed by the abbreviations m (multiplet), s (singlet) and d (doublet); ^{13}C-NMR spectrum is referenced to the central peak of the signal from $CDCl_3$ at 77.00 ppm, multiplicity was assigned from DEPT135 and DEPT90 experiments and is expressed by the abbreviations s (C), d (CH) and q (CH_3). Mass spectra were recorded with an AutoSpec Micromass spectrometer by using electronic impact (EI-TOF 70 eV).

Growth Curves And Quorum Sensing Assays With *Vibrio campbellii*

Quorum sensing inhibition assays were performed in autoinducer bioassay (AB) medium (17.5 g l^{-1} NaCl, 12.3 g l^{-1} $MgSO_4$, 2.0 g l^{-1} casamino acids, 0.01 M potassium phosphate, 0.001 M L-arginine, 1% v/v glycerol) as previously described (Martín-Rodríguez and Fernández, 2016). Briefly, diluted overnight cultures (1:100) were exposed to serial dilutions of SAM461 in sealed, white, clear bottom 96-well plates (Costar 3610). To keep solvent concentration to a minimum, a highly concentrated stock solution of SAM461 in DMSO was used (80 mM). Control experiments involved non-treated cells (untreated control) and cells supplemented with a volume of DMSO equivalent to that of the highest treatment dose (solvent control). Luminescence and optical density at 600 nm were measured every 15 min for 18 h in a multimode plate reader (PerkinElmer EnSpire). Luminescence reads of treatments were normalized with respect to that of the controls, and dose-response curves were adjusted using a four-parameter non-linear regression model as implemented in GraphPad Prism v5 (Prism Software). Experiments were run in triplicate.

RNA Extraction, cDNA Synthesis And qRT-PCR

Overnight *V. campbellii* BB120 cultures were diluted 1:100 in AB medium with (8 μM) and without SAM461. The untreated control received a proportional amount of DMSO (0.01% v/v). Three biological replicates were prepared per condition. Bacterial cultures were incubated aerobically at 30°C for 8 h before RNA was isolated with the High Pure RNA Isolation Kit (Roche) as recommended by the manufacturer. Residual genomic DNA was removed after treatment with 5U RNAse-free DNAse (Promega). Complementary DNA (cDNA) synthesis was performed with the First Transcriptor cDNA synthesis kit (Roche) according to the manufacturer's instructions using 1 μg of total RNA. Expression of *luxR*, *luxA* and *luxC* and *rpoD* was determined using the primers listed in **Table 1**. Quantitative PCR reactions were prepared with the SensiMix SYBR & Fluorescein Kit (Bioline) in sealed optical 96-well plates using a Bio-Rad MyIQ instrument. Gene expression for treated and untreated cells was calculated with the qbase+ software (Biogazelle) and the statistical significance of the differences was analyzed by a two-tailed Student's *t*-test. Significance was set at $P = 0.05$.

Enzymatic Assays With *Vibrio fischeri* And NanoLuc Luciferases

Bacterial luciferase assays were conducted with commercial *Vibrio fischeri* luciferase (V_fLuc) (Sigma-Aldrich L8507), which is a close analog of that of *V. campbellii*, as described previously (Cruz et al., 2011). Briefly, 2 μl of substrate and cofactor solution (final concentrations after addition of enzyme solution: 0.06% BSA, 0.64 mM decanal, 25 μM FMN, 0.5 mM NADH) were dispensed inside the wells of a 1,536-well white/solid bottom high base plate (Greiner 789175), to which either 25 or 50 nl of compound stock solution were added from a 384-well acoustically compatible compound plate (Greiner 788876) using an ATS-100 acoustic dispenser (EDC Biosystems; 250 μM-122 nM, 12 point-titration with duplicates, DMSO, tartrazine and pifithrin-α as controls). The mixture was incubated for 5 min and then 2 μl of enzyme solution were added to each well of the 1,536-well plate (final concentrations: 1.88 g ml^{-1} bacterial luciferase and FMN reductases, approximate protein concentration of 0.75 mg ml^{-1}); enzyme buffer (100 mM pH 7.0 sodium phosphate buffer) was used as control. After a 3-min incubation period at room temperature in the dark, luminescence was monitored for 180 s using a ViewLux system (PerkinElmer) with the following settings: gain = high (23X); speed = high (0.5 μs); binning = 6X, flatfield corrected using NanoLuc (Promega) standard.

NanoLuc (NLuc) luciferase inhibition testing was performed as described previously (Dranchak et al., 2013). Thus, 2 μl of NLuc assay substrate (Nano-Glo luminescence assay, Promega) (final concentrations: 300 mM sodium ascorbate, 5 mM sodium chloride, 0.1% triton X-100, 20 μM coelenterazine in 1X PBS, pH 7.4) were dispensed into white solid-bottom 1,536 well plates (Greiner Bio One) with a BioRAPTR FRD (Beckman Coulter). Compounds were transferred to the plates in 25–50 nl by an Echo acoustic dispenser (Labcyte) in the concentration range of

244 nM to 250 μM along with DMSO and titrations of cilnidipine positive control from top concentration of 125 μM. NLuc substrate reagent and compounds were incubated for 10 min at room temperature and one volume secreted NLuc medium was added with a BioRAPTR FRD. NLuc enzyme luminescence was measured using a ViewLux plate reader (PerkinElmer).

Docking of SAM461 to *Vibrio campbellii* Luciferase and NanoLuc

Molecular docking was used to investigate the binding sites of SAM461 to both the *V. campbellii* luciferase alpha chain (V_cLuc) and NLuc, whose crystal structures are available from the Protein Data Bank (PDB). The potential binding areas (cavities) were found using CavityPlus (Xu et al., 2018), which detects cavities in the structure and informs about potential allosteric sites based on motion correlation analyses. Structure coordinates for V_cLuc (PDB ID: 3FGC; Laskowski and Swindells, 2011) and NLuc (PDB ID: 5IBO) were used, after the heteroatoms were removed prior to docking. The 3D models of the ligands were created using ChemDraw Professional (CambridgeSoft, PerkinElmer). Docking experiments were performed using VINA (Trott and Olson, 2010) via YASARA (Krieger and Vriend, 2014), and the runs were clustered according to a root-mean-square-deviation (RMSD) cut-off of 5 Å. A grid box was placed around the residues forming the cavity of interest, localizing the docking area. Interactions between protein and ligands were initially analyzed using LigPlot$^+$ (Laskowski and Swindells, 2011), and the ligand-protein complex was further examined and imaged with UCSF Chimera (Pettersen et al., 2004).

Hatching of Axenic *Artemia franciscana* Nauplii

Approximately 60 mg of *A. franciscana* cysts originating from the Great Salt Lake, Utah, USA (EG Type, batch 21452, INVE Aquaculture) were hydrated in 9 ml of sterile artificial seawater for 1 h. Sterile seawater was prepared by adding 3.5% of Instant Ocean® synthetic sea salt (Aquarium Systems) to 1 l of distilled water and filter-sterilizing. The cysts were sterilized and decapsulated by treatment with 330 μl NaOH (32%) and 5 ml NaOCl (50%) under constant, 0.2-μm filtered aeration. The reaction was stopped after 2 min by addition of 5 ml $Na_2S_2O_3$ (1%) and aeration was discontinued. The decapsulated cysts were washed, re-suspended in sterile seawater and incubated for 28 h under constant illumination (27 μE $m^{-2}s^{-1}$). The sterility of the hatched *A. franciscana* nauplii was verified by adding hatching water (500 μl) to a tube containing marine broth (Difco) as well as spread plating (100 μl) on marine agar (Difco), followed by incubation at 28°C for 5 days (Baruah et al., 2011). Experiments started with non-sterile nauplii were discarded.

Artemia franciscana Challenge Assays And Lethality Tests

A survival dose-response relationship for SAM461 was determined as described previously (Baruah et al., 2015). Briefly, a group of 20 germ-free nauplii at developmental stage II (in which their mouth is open to ingest food particles) was transferred to sterile 40 ml glass tubes containing 10 ml of sterile artificial seawater. Working 1 mM solutions of SAM461 were prepared in sterile seawater (10 ml) from a stock solution of the compounds in DMSO. The DMSO concentration in the different experimental groups was adjusted as per the solvent concentration in the highest dose group. Treatments were supplemented with SAM461 (0.125–8 μM) and challenged with *V. campbellii* at 10^7 cells ml^{-1}. *A. franciscana* survival was scored after 2 days by counting the number of live nauplii. As controls, the following groups were maintained: untreated nauplii that were not challenged with *V. campbellii* (negative control), untreated nauplii that were challenged with *V. campbellii* (positive control), and nauplii treated with DMSO and challenged with *V. campbellii* (DMSO control). Each experiment was performed in five replicates. Prior to challenge assays, the cytotoxic effect of SAM461 (2–32 μM) was determined in germ-free *A. franciscana* nauplii in the absence of *V. campbellii*, otherwise as described above. Survival data were subjected to one-way analysis of variances (ANOVA) followed by Dunnett's *post-hoc* analysis as implemented in GraphPad Prism v5 (Prism Software, La Jolla, CA). Statistical significance was set at $P = 0.05$.

RESULTS

SAM461 Inhibits Bacterial Luminescence Independently of Quorum Sensing

During the screening of diversity-oriented chemical libraries, compound SAM461 (**Figure 1A**) was identified as a bioluminescence inhibitor using *V. campbellii* BB120 as a bioreporter. SAM461 is a drug-like molecule fulfilling Lipinski's rule of 5 (Lipinski et al., 2001), a commonly used "rule of thumb" to determine the *druglikeliness* of a molecule. Therefore, SAM461 was synthesized in larger amounts to investigate its mode of action. Hence, we analyzed its effect on *V. campbellii* BB120 growth and bioluminescence in the concentration range 0.39–200 μM. SAM461 was found to be toxic to *V. campbellii* BB120 at concentrations >100 μM (data not shown), therefore these higher concentrations were excluded from further analysis. Testing of serial 2-fold dilutions of SAM461 from 50 to 0.39 μM revealed dose-dependent luminescence quenching (**Figure 1B**). The observed luminescence inhibition was not associated to alteration of bacterial growth rates at these doses, with only a slight growth delay being observed at the highest concentration of 50 μM (**Figure 1B**). To determine the potency of SAM461, dose-response curves were prepared. The IC_{50} for luminescence inhibition in *V. campbellii* BB120 was found to be 7.8 μM (**Figure 1C**). Taken together, these results indicate that SAM461 inhibits bacterial bioluminescence at non-toxic concentrations in the low micromolar range.

We initially hypothesized that SAM461 could be a QS inhibitor. Therefore, we performed the same experiment described above in a *V. campbellii* mutant displaying bioluminescence independently of QS. Thus, *V. campbellii* JAF548 is a BB120 isogenic mutant harboring a point mutation

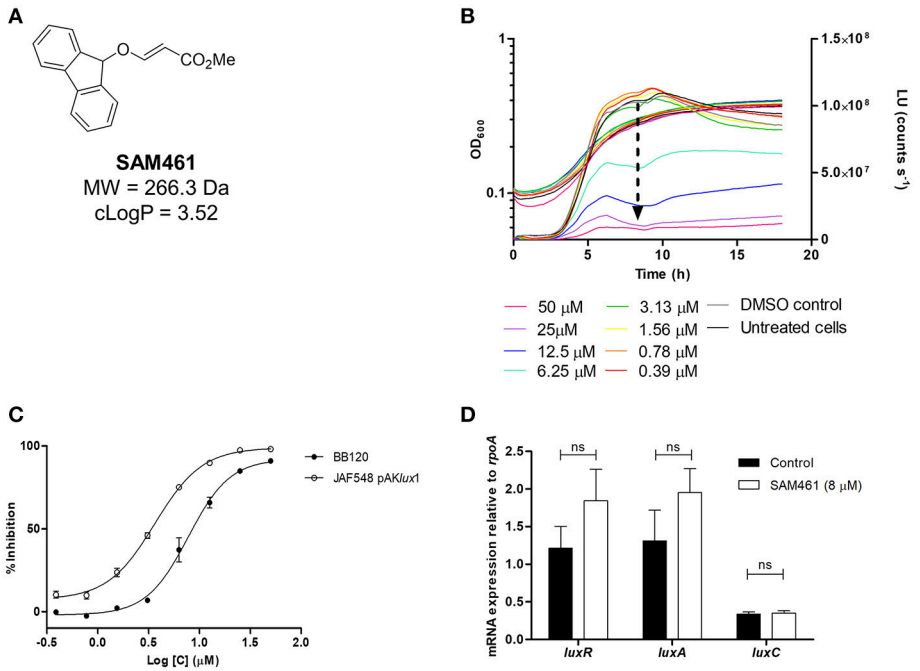

FIGURE 1 | SAM461 inhibits *Vibrio campbellii* bioluminescence independently of quorum sensing. **(A)** Chemical structure and relevant chemical properties of SAM461. **(B)** *V. campbellii* BB120 growth (left *y* axis) and luminescence curves (right *y* axis) in the presence of SAM461 (0.39–50 μM), including solvent (DMSO) and untreated controls. The arrow highlights the dose-dependent luminescence quenching induced by SAM461. **(C)** Dose-response curves for SAM461-induced luminescence inhibition in *V. campbellii* BB120 (WT strain) and JAF548 pAK*lux*1 (constitutively luminescent mutant independent of QS). **(D)** Relative expression of *luxR*, *luxA*, and *luxC* in the absence (control) and presence (8 μM) of SAM461.

in the *luxO* allele that renders the cell constitutively non-luminescent (Defoirdt et al., 2012). Bioluminescence had been restored in this strain upon introduction of plasmid pAK*lux*1 harboring the *luxCDABE* operon from *Photorhabdus luminescens* under the *lac* promoter (**Table 1**). Hence, luminescence inhibition in this strain would indicate targets outside the QS circuit. SAM461 inhibited light production in this reporter strain similarly as in *V. campbellii* BB120 (IC_{50} = 3.6 μM, **Figure 1C**), thereby indicating the existence of targets beyond cell-to-cell communication.

To confirm that QS inhibition does not contribute to SAM461-induced luminescence quenching we determined the transcript levels of *luxR*, encoding the QS master regulator, as well as *luxC* and *luxA*, two of the QS-regulated genes in the *luxCDABEGH* operon, in treated (8 μM) and untreated *V. campbellii* BB120 cultures. The expression of these three genes was found to be not significantly different in treated and untreated *V. campbellii* cells (**Figure 1D**). This confirms unambiguously that SAM461 activity is independent of QS disruption.

SAM461 Inhibits Luciferase Activity

We have shown that SAM461 displays potent bioluminescence inhibition in *V. campbellii* at low micromolar doses in a QS-independent fashion. We therefore reasoned that the potent effect observed in live bacteria (**Figure 2A**) could be due to inhibition of the bacterial luciferase enzyme. Using purified *V. fischeri* luciferase (V_fLuc), we measured enzyme activity in the presence of serial dilutions of SAM461. Indeed, SAM461 inhibited V_fLuc *in vitro* with an IC_{50} = 191.1 μM, indicating a moderately potent activity in comparison to other V_fLuc inhibitors, such as tatrazine and PFT-α used as controls (Kim and Spiegel, 2013; **Figure 2B**). To determine the specificity of SAM461, we further tested this compound against NLuc, which is structurally and biochemically different to the bacterial luciferase (**Figure 2C**). SAM461 was found to inhibit NLuc activity with an IC_{50} = 149.5 μM, a similar value to that determined for V_fLuc. Taken together, these findings suggest that SAM461 inhibits luciferase activity non-selectively.

Molecular Docking

To gain an insight on the molecular interactions of SAM461 and its luciferase protein targets, an *in silico* analysis by molecular docking was performed with the crystal structures of *V. campbellii* luciferase (V_cLuc) and NLuc.

Analysis of SAM461-V_cLuc Interactions

Putative allosteric sites in V_cLuc were detected by CavityPlus based on the cavity containing the active site. Since the X-ray structure of V_cLuc was solved in complex with the substrate $FMNH_2$, docking of $FMNH_2$ was used to test the reliability of the docking results. For both SAM461 and FMNH, 400 docking poses were generated in the putative allosteric sites and the active site. To evaluate the docking results of SAM461 and

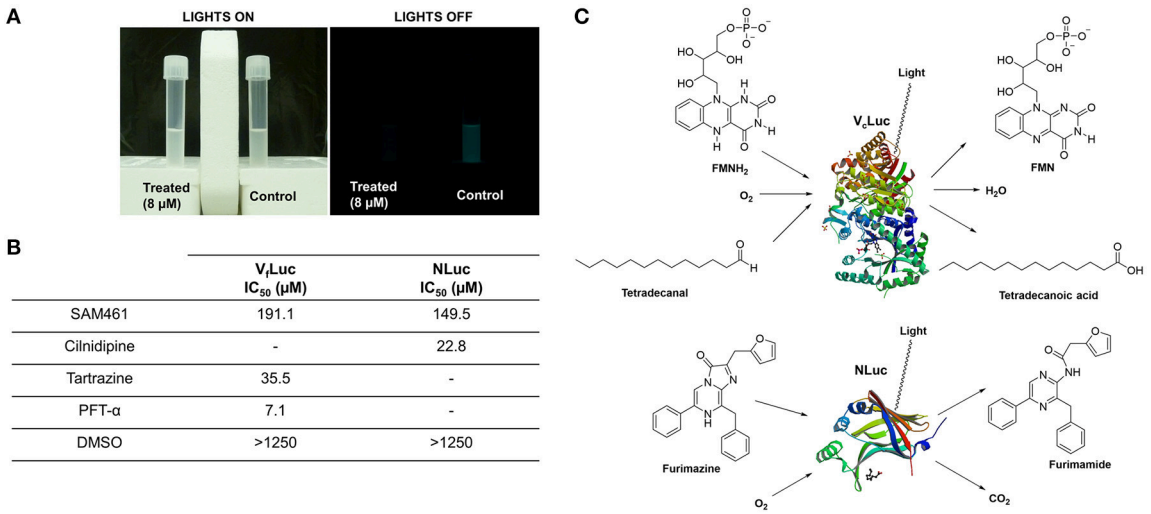

	V_fLuc IC_{50} (μM)	NLuc IC_{50} (μM)
SAM461	191.1	149.5
Cilnidipine	-	22.8
Tartrazine	35.5	-
PFT-α	7.1	-
DMSO	>1250	>1250

FIGURE 2 | SAM461 interferes with bacterial luciferase activity. **(A)** Phenotypic evidence of potent bioluminescence inhibition caused by SAM461 (8 μM) in *Vibrio campbellii* BB120. **(B)** Half-maximal inhibitory concentration of SAM461 for *Vibrio fischeri* luciferase (V_fLuc) and NanoLuc luciferase (NLuc). Tartrazine and PFT-α were used as positive controls for V_fLuc inhibition, and cilnidipine was used as positive control for NLuc inhibition. DMSO was used as solvent control. **(C)** Substrates, cofactors and products involved in the redox processes catalyzed by the bacterial luciferase (*V. campbellii*, V_CLuc) and NLuc resulting in light emission. Protein structures were retrieved from the Protein Data Bank (PDB: 3FGC–V_CLuc, and 5IBO–NLuc).

$FMNH_2$, the binding energy (kcal mol^{-1}) and calculated affinity (CA; μM) of the docked ligands were considered. Docking of SAM461 to the different cavities of V_cLuc revealed a significantly different binding energy and CA (over 15-fold) when docked in the $FMNH_2$ binding site compared to the potential allosteric cavities (**Table 2**). The highest scoring pose in the first cluster exhibited a binding energy of −8.7 kcal mol^{-1} and a CA of 0.36 μM. However, the highest scoring pose in the second cluster is hydrogen bonded, establishing an interaction of SAM461 with Arg107 and Gly108 (**Figures 3A,B**). Due to the apparent flexibility of the acrylate chain, the hydrogen bond interactions would likely stabilize this binding pose in the cavity.

Docking of $FMNH_2$ to V_cLuc yielded a similar pose as that observed in the X-ray structure (**Figure S2A**). Because the aliphatic chain in this molecule is also likely to be flexible, differences in the chain orientation were observed. Despite this apparent flexibility, both the docked and crystal resolved molecule (Laskowski and Swindells, 2011) formed very similar hydrogen bonds and residue contacts. They shared hydrogen bonds with Glu43, Ala75, Arg107, Leu109, Glu175, Ser176 and Thr179, and multiple shared hydrophobic interactions with other residues (**Figures S2B,C**). The hydrogen bond to Arg107 was also observed for SAM461. Docking of $FMNH_2$ displayed a calculated binding energy of −9.1 kcal mol^{-1} and a CA of 0.21 μM. Superposing the ligand-receptor complexes showed a similar orientation of both SAM461 and $FMNH_2$, with the rigid aromatic rings against the hydrophobic cavity, and the flexible region pointing toward the cavity opening (**Figure 3C**).

Analysis of SAM461-NLuc Interactions

NLuc does not have a confirmed substrate binding site, but it is assumed that the active site is located in the central cavity, since it should be able to accommodate the substrate coelenterazine (Laskowski and Swindells, 2011). CavityPlus detected one possible allosteric cavity based on this active site. Furimazine was docked to both the active and potential allosteric site to compare with the results of SAM461. In contrast to V_cLuc, the docked binding energy and CA for NLuc were not as different between the two cavities, but the active site provided a higher calculated affinity for both ligands (**Table 2**). The highest scoring SAM461 pose in the active site has the fluorene rings oriented toward the hydrophobic interior of the cavity, and the acrylate chain turning outwards (**Figure 3D**). This pose allows

TABLE 2 | Docking binding energy and calculated affinity of the highest scores in the different cavities of *Vibrio campbelli* luciferase (V_CLuc).

Ligand	Cavity V_CLuc	Binding energy (kcal mol^{-1})	Calculated affinity (μM)
SAM461	$FMNH_2$ binding site (hydrogen bond)	−7.6	2.3
	$FMNH_2$ binding site (highest score)	−8.7	0.36
	Potential Allosteric site 1	−6.5	14.8
	Potential Allosteric site 2	−7.0	6.6
	Potential Allosteric site 3	−7.0	6.8
$FMNH_2$	$FMNH_2$ binding site	−9.1	0.21
	Cavity NLuc		
SAM461	Potential Active Site	−6.7	11.9
	Potential Allosteric site	−5.9	41.4
Furimazine	Potential Active site	−7.4	3.8
	Potential Allosteric site	−7.0	7.1

Potential allosteric sites were detected by CavityPlus.

hydrogen bonding with Leu45 and Asp46, and hydrophobic contacts with 7 other residues (**Figure 3E**). The highest scoring pose of furimazine in the same site did not form hydrogen bonds, but 11 hydrophobic contacts, many of which are shared with the SAM461 pose (**Figure S2D**). When investigating the areas surrounding the ligand, the larger cavity housing the active site may provide better solvent protection for both furimazine and SAM461 (**Figures S2E,F**).

SAM461 Protects *Artemia franciscana* From *Vibrio Campbellii* Infection

Light production is a major metabolic endeavor, and dark mutants of pathogenic *Vibrio* are known to be less virulent than their wild-type counterparts (Phuoc et al., 2009; Ruwandeepika et al., 2011b). To determine the effect of SAM461 on *V. campbellii* infectivity we used the gnotobiotic *A. franciscana* infection model (Baruah et al., 2015). We first determined the toxicity of SAM461 toward *A. franciscana* nauplii in the range 2–32 μM. The lowest dose of the compound exerting significant toxicity was 16 μM, whereas no toxicity was detected in the range 2–8 μM (**Figure 4A**). We next challenged germ-free *A. franciscana* nauplii with *V. campbellii* in the absence and presence of SAM461 at non-toxic doses (0.125–8 μM). SAM461 fully protected *A. franciscana* from *V. campbellii* infection at concentrations as low as 2 μM ($P < 0.001$, **Figure 4B**). At this dose, *A. franciscana* survival was increased 2-fold in comparison to untreated nauplii (**Figure 4B**), thereby highlighting the therapeutic potential of this molecule.

DISCUSSION

Luminescent vibriosis caused by *V. campbellii* and close relatives is a major disease with a remarkable economic impact. Growing concerns related to the use of antibiotics in aquaculture and the emergence of multidrug resistant bacterial pathogens have motivated a global search of alternative therapeutic and prophylactic options (Defoirdt et al., 2007a, 2011). In this context, QS inhibitors have been proposed as promising candidates (Bhardwaj et al., 2013; LaSarre and Federle, 2013; Kim et al., 2018). Searching for potential QS inhibitors from in-house chemical libraries (University of La Laguna, Spain), compound SAM461 was identified as a hit during an initial screening round involving testing of the chemicals against *V. campbellii* BB120.

In this study we have delineated the mode of action of SAM461. Given the known association between light production and QS in *V. campbellii*, we initially envisioned that the activity exhibited by SAM461 could be related to QS inhibition. However, testing of SAM461 against a genetically-engineered, constitutively luminescent *V. campbellii* mutant and subsequent transcriptional analysis of *luxR* and QS-regulated genes revealed a mode of action independent of QS disruption. This was not completely surprising, though. *V. campbellii* produces three types of QS signaling molecules: AI-1, an *N*-acyl homoserine lactone; AI-2, a furanosyl borate diester; and CAI-1, a long-chain amino ketone (Anetzberger et al., 2012). Even though examples of QS inhibitors without chemical relatedness to the natural autoinducers exist, most of the known QS disruptors are chemical analogs of the native signal ligands (Galloway et al., 2011; Kalia, 2013; Martín-Rodríguez et al., 2016), which is not the case of SAM461. Nevertheless, with a half-maximal inhibition value in the single-digit μM range and no toxicity in the bacterial population as determined by growth inhibition at effective doses, the activity of this molecule deserved further characterization.

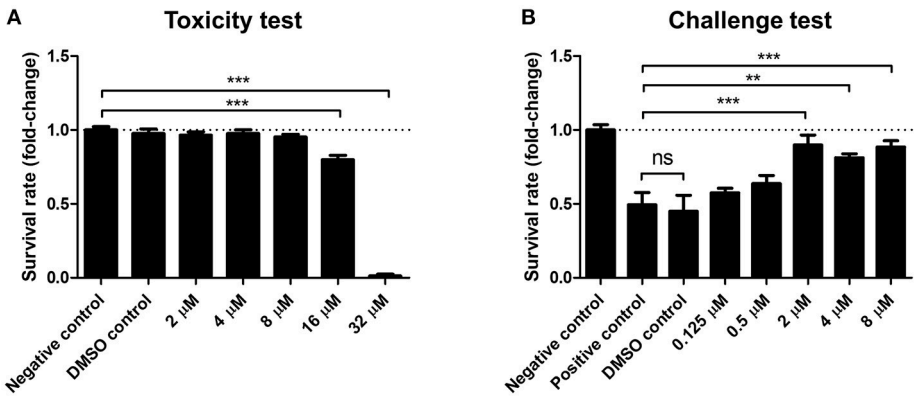

FIGURE 4 | SAM461 confers protection to *Artemia franciscana* nauplii against *Vibrio campbellii* BB120 at non-toxic concentrations. **(A)** Toxicity of SAM461 to germ-free *A. franciscana.* Nauplii were exposed to SAM461 at the indicated doses. Un-exposed nauplii served as negative control. Nauplii exposed to only DMSO served as solvent control. Survival was scored after 48 h of exposure. Data are presented as fold-change relative to the negative control, which has been normalized to 1 (dotted line). Data represent the mean ± standard error of five replicates. Asterisks indicate significant differences relative to the negative control (***$P < 0.001$). **(B)** Survival rate of *A. franciscana* nauplii during co-challenge with *V. campbellii*. SAM461 was added to the culture water at indicated concentrations. Simultaneously, the nauplii were challenged with *V. campbellii* at 10^7 cfu ml^{-1} for 48 h. Control groups included untreated nauplii challenged with *V. campbellii* (positive control), DMSO-treated nauplii challenged with *V. campbellii* (DMSO control) and non-challenged (uninfected) nauplii (negative control). Data are presented as fold-change relative to the negative control, which has been normalized to 1 (dotted line). Values represent the mean ± standard error of five replicates. Asterisks indicate significant differences with respect to the positive control (**$P < 0.01$; ***$P < 0.001$).

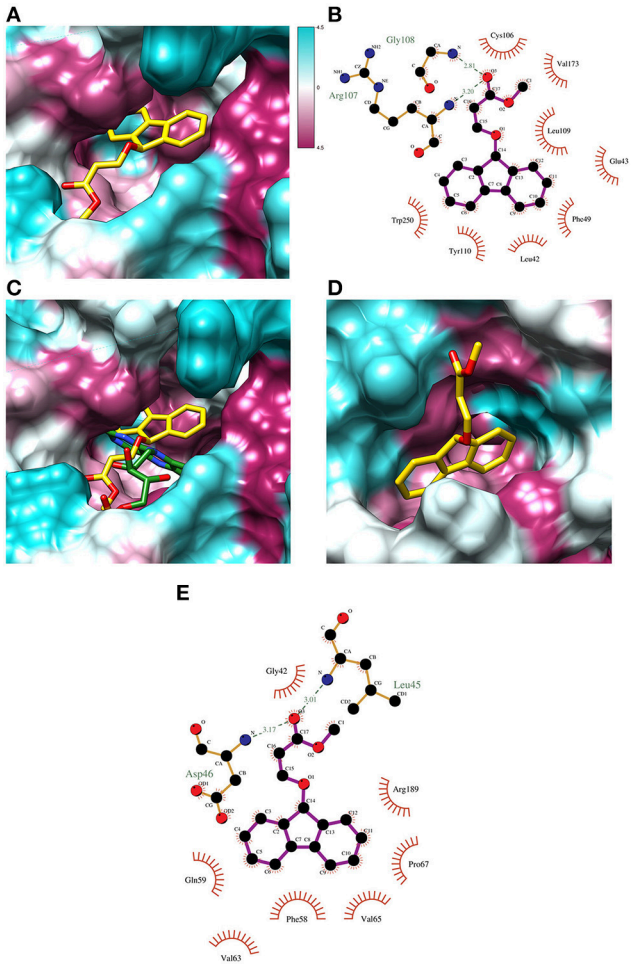

FIGURE 3 | Docking poses of ligand/substrate and their calculated interactions. **(A)** Docking pose of SAM461 (second highest scoring) in the predicted active site pocket of V_CLuc. The images show the hydrophobic surface areas marked as magenta, and hydrophilic areas in cyan based on the hydrophobicity scale of Kyte and Doolittle (57). **(B)** Interaction diagram of the docked SAM461 molecule in the V_CLuc active site. The interactions represent the second docking cluster, displaying hydrogen bonds together with hydrophobic contacts. The dotted green lines represent hydrogen bonds. Red lines indicate hydrophobic interactions between protein residues and ligand atoms. **(C)** Comparison of the X-ray structure of the FMNH-V_CLuc complex (green; PDB: 3FGC) and the docking pose of SAM461 (yellow) in the active site pocket of V_CLuc. The general poses of the molecules are similar, with the rings turned toward the cavity interior and the flexible carbon chains forming hydrogen bonds with residues closer to the cavity opening. **(D)** The docked SAM461 ligand in the active site cavity of NLuc. **(E)** Interaction diagram of the SAM461 ligand docked to the active site cavity of NLuc. The hydrogen bonds (shown as dotted green lines) likely act to stabilize the flexible region of the molecule.

We reasoned that the bioluminescence inhibition observed in *V. campbellii* JAF548 pAK*lux*1 could be due to impaired luciferase activity. Recall that in this dark mutant genetic background the *lux* operon is ectopically expressed, thus rendering the cells constitutively bright independently of the cell population density. Indeed, SAM461 inhibited bacterial luciferase activity *in vitro* with an IC_{50} of 191.1 μM. This IC_{50} was 2 orders of magnitude higher than that observed in live bacteria. These differences between *in vitro* and *in vivo* activities are not uncommon, and they have been reported for other bacterial luciferase inhibitors in *V. campbellii* as well (Kim and Spiegel, 2013).

The biochemistry behind light production in *Vibrio* spp. is complex (Kim and Spiegel, 2013). The bacterial luciferase has three substrates: reduced flavin mononucleotide ($FMNH_2$), a long-chain fatty acid aldehyde (usually tetradecanal) and molecular oxygen. $FMNH_2$ is the product of the reduction of FMN by NADPH, a reaction catalyzed by the enzyme NADPH FMN oxidoreductase. $FMNH_2$ is transferred to the bacterial luciferase, where it is oxidized by molecular oxygen. This results in the formation of hydroperoxide that reacts with a fatty acid aldehyde produced by the fatty acid reductase complex. The reaction of the aldehyde with hydroperoxide results in the generation of an excited-state intermediate that emits blue-green light and gives H_2O and FMN as products. An overview of this complex process has been presented in **Figure 2C**. Hence, interference of SAM461 with the luciferase enzyme or any of the proteins or metabolic pathways involved in substrate and cofactor biosynthesis could lead to decreased light emission. The biochemistry of the NLuc luciferase is different. This enzyme is an engineered derivative of the naturally-occurring *Oplophorus gracilirostris* luciferase and exhibits high substrate specificity. Thus, NLuc catalyzes the oxidation of furimazine to produce furimamide, carbon dioxide and an intense light output. Testing of SAM461 against NLuc revealed similar performance as against the bacterial luciferase, and therefore we deduced that SAM461 is a non-selective luciferase inhibitor.

Although the docking experiments do not aim for the validation of whether the SAM461 ligand binds in the active site of its luciferase protein targets, our *in silico* results demonstrate the chemical feasibility of such a scenario. Docking of SAM461 and $FMNH_2$ showed similar theoretical binding energies and calculated affinities when bound to the active site of V_cLuc. While these values might differ from the actual thermodynamic parameters, the 15-fold decrease of CA determined for the active site with respect to the allosteric site strongly suggest that both ligands have a preferred theoretical binding toward the former. The observation that the $FMNH_2$ substrate displays similar binding poses to the binding conformation of the flavin moiety in the X-ray protein-substrate complex, but with differences in the aliphatic chain conformation, supports the assumed flexibility. Determining the binding of NLuc was more demanding since the ligands showed similar affinity toward both the active and allosteric binding sites, with furimazine having stronger apparent affinity than SAM461 for both cavities. The larger cavity harboring the active site could provide a better binding pocket for both the native ligand furimazine and SAM461. The potential allosteric site would possibly not offer enough protection against the solvent. This together with the slightly preferred affinity toward the active site could suggest SAM461 binds to the active site of NLuc.

Luminescence has been reported to play a role in host colonization and infectivity in both commensal and pathogenic *Vibrio* spp. For example, luminescence genes have been shown

to play an important role in the symbiotic colonization of the luminescent organs of the squid host by *V. fischeri* (Visick et al., 2000; Nyholm and McFall-Ngai, 2004; Chun et al., 2008). In the fish pathogen *V. salmonicida*, *luxA* mutants showed impaired infectivity and were outcompeted by the WT strain in co-challenge tests in Atlantic salmons (Nelson et al., 2007). In *V. campbellii* BB120 specifically, non-luminescent variants have been found to be less virulent than their luminescent counterparts in *A. franciscana* (Phuoc et al., 2009; Ruwandeepika et al., 2011b). Consistent with these precedents, the luminescence inhibitor SAM461 was found to protect *A. franciscana* from *V. campbellii* infection at low micromolar doses. Previous studies have found decreased virulence factor production and increased susceptibility to host defense mechanisms in non-luminescent variants of pathogenic *Vibrio* spp. (Szpilewska et al., 2003; Katsev et al., 2004; Phuoc et al., 2009; Ruwandeepika et al., 2011b), phenomena that could contribute to the observed performance of SAM461 during *in vivo* infection experiments.

In conclusion, we have presented herein that targeting the bacterial luciferase could constitute a novel paradigm in the treatment of luminescent vibriosis. SAM461 is a small, drug-like vinyl ether that supports diverse functionalities in its skeleton (Tejedor et al., 2013; Zhu and Kirsch, 2013) thus streamlining diverse-oriented synthesis and subsequent analyses of structure-activity relationships based on this lead. The lack of chronic toxicity of SAM461 at effective doses on the bacterial pathogen as well as in the host results promising to prevent the emergence of bacterial resistance and encourages its potential use as an adjuvant chemotherapy.

ETHICS STATEMENT

This study is exempt from ethics committe approval since it only involves experimental research with invertebrate larvae, which is not subjected to animal research regulations.

AUTHOR CONTRIBUTIONS

AJM-R conceived the idea of the work. AJM-R performed the *in vitro* experiments with *V. campbellii*. SJÁ-M synthesized compound SAM461. CO conducted the molecular docking analyses. KB, TL, PN, and PB designed the *in vivo* infection studies with gnotobiotic *A. franciscana* nauplii. TL and PN performed the challenge and toxicity tests. AJM-R wrote the manuscript with the input of all co-authors. All of the authors contributed to data analysis. VSM and JJF led the projects funding the study.

FUNDING

This study was funded by the Spanish Ministry of Economy and Competitiveness, grant CTQ2014-55888-C03-01-R and CTQ2014-56362-C2-1-P.

ACKNOWLEDGMENTS

AJM-R acknowledges the Oceanic Platform of the Canary Islands (PLOCAN) for a 2 + 2 fellowship. SJÁ-M thanks the Spanish MECyD for an FPU grant. CO is grateful to Dr. M. Gregor Madej (University of Regensburg, Germany). The authors are grateful to Prof. J. Inglese, Dr. Ryan McArthur and Dr. Patricia Dranchak (National Institutes of Health, Bethesda, Maryland) for luciferase inhibition testing.

SUPPLEMENTARY MATERIAL

The Supplementary Material for this article can be found online at: https://www.frontiersin.org/articles/10.3389/fcimb.2018.00368/full#supplementary-material

REFERENCES

Anetzberger, C., Schell, U., and Jung, K. (2012). Single cell analysis of *Vibrio harveyi* uncovers functional heterogeneity in response to quorum sensing signals. *BMC Microbiol.* 12, 209. doi: 10.1186/1471-2180-12-209

Austin, B., and Zhang, X.-H. (2006). *Vibrio harveyi*: a significant pathogen of marine vertebrates and invertebrates. *Lett. Appl. Microbiol.* 43, 119–124. doi: 10.1111/j.1472-765X.2006.01989.x

Ball, A. S., Chaparian, R. R., and van Kessel, J. C. (2017). Quorum sensing gene regulation by LuxR/HapR master regulators in vibrios. *J. Bacteriol.* 199, e00105–e00117. doi: 10.1128/JB.00105-17

Baruah, K., Duy Phong, H. P. P., Norouzitallab, P., Defoirdt, T., and Bossier, P. (2015). The gnotobiotic brine shrimp (*Artemia franciscana*) model system reveals that the phenolic compound pyrogallol protects against infection through its prooxidant activity. *Free Radic. Biol. Med.* 89, 593–601. doi: 10.1016/j.freeradbiomed.2015.10.397

Baruah, K., Ranjan, J., Sorgeloos, P., MacRae, T. H., and Bossier, P. (2011). Priming the prophenoloxidase system of *Artemia franciscana* by heat shock proteins protects against *Vibrio campbellii* challenge. *Fish Shellfish Immunol.* 31, 134–141. doi: 10.1016/j.fsi.2011.04.008

Bassler, B. L., and Losick, R. (2006). Bacterially speaking. *Cell* 125, 237–246. doi: 10.1016/j.cell.2006.04.001

Bassler, B. L., Wright, M., and Silverman, M. R. (1994). Sequence and function of LuxO, a negative regulator of luminescence in *Vibrio harveyi*. *Mol. Microbiol.* 12, 403–412. doi: 10.1111/j.1365-2958.1994.tb01029.x

Bhardwaj, A. K., Vinothkumar, K., and Rajpara, N. (2013). Bacterial quorum sensing inhibitors: attractive alternatives for control of infectious pathogens showing multiple drug resistance. *Recent Pat. Antiinfect. Drug Discov.* 8, 68–83. doi: 10.2174/1574891X11308010012

Bjelland, A. M., Sørum, H., Tegegne, D. A., Winther-Larsen, H. C., Willassen, N. P., and Hansen, H. (2012). LitR of *Vibrio salmonicida* is a salinity-sensitive quorum-sensing regulator of phenotypes involved in host interactions and virulence. *Infect. Immun.* 80, 1681–1689. doi: 10.1128/IAI.06038-11

Bondad-Reantaso, M. G., Subasinghe, R. P., Arthur, J. R., Ogawa, K., Chinabut, S., Adlard, R., et al. (2005). Disease and health management in Asian aquaculture. *Vet. Parasitol.* 132, 249–272. doi: 10.1016/j.vetpar.2005.07.005

Chun, C. K., Troll, J. V., Koroleva, I., Brown, B., Manzella, L., Snir, E., et al. (2008). Effects of colonization, luminescence, and autoinducer on host transcription during development of the squid-vibrio association. *Proc. Natl. Acad. Sci. U.S.A.* 105, 11323–11328. doi: 10.1073/pnas.0802369105

Cruz, P. G., Auld, D. S., Schultz, P. J., Lovell, S., Battaile, K. P., MacArthur, R., et al. (2011). Titration-based screening for evaluation of natural product extracts:

identification of an aspulvinone family of luciferase inhibitors. *Chem. Biol.* 18, 1442–1452. doi: 10.1016/j.chembiol.2011.08.011

Darshanee Ruwandeepika, H. A., Sanjeewa Prasad Jayaweera, T., Paban Bhowmick, P., Karunasagar, I., Bossier, P., and Defoirdt, T. (2012). Pathogenesis, virulence factors and virulence regulation of vibrios belonging to the Harveyi clade. *Rev. Aquac.* 4, 59–74. doi: 10.1111/j.1753-5131.2012.01061.x

Defoirdt, T., Benneche, T., Brackman, G., Coenye, T., Sorgeloos, P., and Scheie, A. A. (2012). A quorum sensing-disrupting brominated thiophenone with a promising therapeutic potential to treat luminescent vibriosis. *PLoS ONE* 7:e41788. doi: 10.1371/journal.pone.0041788

Defoirdt, T., Boon, N., Sorgeloos, P., Verstraete, W., and Bossier, P. (2007a). Alternatives to antibiotics to control bacterial infections: luminescent vibriosis in aquaculture as an example. *Trends Biotechnol.* 25, 472–479. doi: 10.1016/j.tibtech.2007.08.001

Defoirdt, T., Miyamoto, C. M., Wood, T. K., Meighen, E., a, Sorgeloos, P., Verstraete, W., et al. (2007b). The natural furanone (5Z)-4-bromo-5-(bromomethylene)-3-butyl-2(5H)-furanone disrupts quorum sensing-regulated gene expression in *Vibrio harveyi* by decreasing the DNA-binding activity of the transcriptional regulator protein LuxR. *Environ. Microbiol.* 9, 2486–2495. doi: 10.1111/j.1462-2920.2007.01367.x

Defoirdt, T., Sorgeloos, P., and Bossier, P. (2011). Alternatives to antibiotics for the control of bacterial disease in aquaculture. *Curr. Opin. Microbiol.* 14, 251–258. doi: 10.1016/j.mib.2011.03.004

Dranchak, P., MacArthur, R., Guha, R., Zuercher, W. J., Drewry, D. H., Auld, D. S., et al. (2013). Profile of the GSK published protein kinase inhibitor set across ATP-dependent and-independent luciferases: implications for reporter-gene assays. *PLoS ONE* 8:e57888. doi: 10.1371/journal.pone.0057888

Galloway, W. R., Hodgkinson, J. T., Bowden, S. D., Welch, M., and Spring, D. R. (2011). Quorum sensing in Gram-negative bacteria: small-molecule modulation of AHL and AI-2 quorum sensing pathways. *Chem. Rev.* 111, 28–67. doi: 10.1021/cr100109t

Haldar, S., Chatterjee, S., Sugimoto, N., Das, S., Chowdhury, N., Hinenoya, A., et al. (2011). Identification of *Vibrio campbellii* isolated from diseased farm-shrimps from south India and establishment of its pathogenic potential in an *Artemia* model. *Microbiology* 157, 179–188. doi: 10.1099/mic.0.041475-0

Kalia, V. C. (2013). Quorum sensing inhibitors: an overview. *Biotechnol. Adv.* 31, 224–245. doi: 10.1016/j.biotechadv.2012.10.004

Katsev, A. M., Wegrzyn, G., and Szpilewska, H. (2004). Effects of hydrogen peroxide on light emission by various strains of marine luminescent bacteria. *J. Basic Microbiol.* 44, 178–184. doi: 10.1002/jobm.200310330

Kim, B. S., Jang, S. Y., Bang, Y.-J., Hwang, J., Koo, Y., Jang, K. K., et al. (2018). QStatin, a selective inhibitor of quorum sensing in *Vibrio* species. *MBio* 9, e02262–e02217. doi: 10.1128/mBio.02262-17

Kim, T., and Spiegel, D. A. (2013). Serendipitous discovery of two highly selective inhibitors of bacterial luciferase. *Tetrahedron* 69, 7692–7698. doi: 10.1016/j.tet.2013.05.086

Krieger, E., and Vriend, G. (2014). YASARA view–molecular graphics for all devices–from smartphones to workstations. *Bioinformatics* 30, 2981–2982. doi: 10.1093/bioinformatics/btu426

LaSarre, B., and Federle, M. J. (2013). Exploiting quorum sensing to confuse bacterial pathogens. *Microbiol. Mol. Biol. Rev.* 77, 73–111. doi: 10.1128/MMBR.00046-12

Laskowski, R. A., and Swindells, M. B. (2011). LigPlot+: multiple ligand-protein interaction diagrams for drug discovery. *J. Chem. Inf. Model.* 51, 2778–2786. doi: 10.1021/ci200227u

Lio-Po, G. D. (2016). "Luminous *Vibrio* and the greenwater culture of the tiger shrimp *Penaeus monodon* with *Tilapia*," in *Tilapia in Intensive Co-culture*, eds P. W. Perschbacher, and R. R. Stickney (Chichester: John Wiley & Sons, Ltd), 81–93.

Lipinski, C. A., Lombardo, F., Dominy, B. W., and Feeney, P. J. (2001). Experimental and computational approaches to estimate solubility and permeability in drug discovery and development settings. *Adv. Drug Deliv. Rev.* 46, 3–26. doi: 10.1016/S0169-409X(00)00129-0

Majerczyk, C., Schneider, E., and Greenberg, E. P. (2016). Quorum sensing control of type VI secretion factors restricts the proliferation of quorum-sensing mutants. *Elife* 5, e14712. doi: 10.7554/eLife.14712

Martín-Rodríguez, A., and Fernández, J. (2016). A bioassay protocol for quorum sensing studies using *Vibrio campbellii*. *Bio Protoc.* 6:e1866. doi: 10.21769/BioProtoc.1866

Martín-Rodríguez, A., Quezada, H., Aragón, G., de la Fuente-Nuñez, C., Castillo-Juarez, I., Maeda, T., et al. (2016). "Recent advances in novel antibacterial development," in *Frontiers in Clinical Drug Research: Anti-Infectives vol. 2*, ed Atta-Ur-Rahman (Sharjah: Bentham Science Publishers), 3–61.

Meighen, E. A. (1991). Molecular biology of bacterial bioluminescence. *Microbiol. Rev.* 55, 123–142.

Nelson, E. J., Tunsjø, H. S., Fidopiastis, P. M., Sørum, H., and Ruby, E. G. (2007). A novel *lux* operon in the cryptically bioluminescent fish pathogen *Vibrio salmonicida* is associated with virulence. *Appl. Environ. Microbiol.* 73, 1825–1833. doi: 10.1128/AEM.02255-06

Nyholm, S. V., and McFall-Ngai, M. J. (2004). The winnowing: establishing the squid-vibrio symbiosis. *Nat. Rev. Microbiol.* 2, 632–642. doi: 10.1038/nrmicro957

Pettersen, E. F., Goddard, T. D., Huang, C. C., Couch, G. S., Greenblatt, D. M., Meng, E. C., et al. (2004). UCSF chimera–a visualization system for exploratory research and analysis. *J. Comput. Chem.* 25, 1605–1612. doi: 10.1002/jcc.20084

Phuoc, L. H., Defoirdt, T., Sorgeloos, P., and Bossier, P. (2009). Virulence of luminescent and non-luminescent isogenic vibrios towards gnotobiotic *Artemia franciscana* larvae and specific pathogen-free *Litopenaeus vannamei* shrimp. *J. Appl. Microbiol.* 106, 1388–1396. doi: 10.1111/j.1365-2672.2008.04107.x

Ruwandeepika, H. A., Bhowmick, P. P., Karunasagar, I., Bossier, P., and Defoirdt, T. (2011a). Quorum sensing regulation of virulence gene expression in *Vibrio harveyi in vitro* and *in vivo* during infection of gnotobiotic brine shrimp larvae. *Environ. Microbiol. Rep.* 3, 597–602. doi: 10.1111/j.1758-2229.2011.00268.x

Ruwandeepika, H. A., Defoirdt, T., Bhowmick, P. P., Karunasagar, I., and Bossier, P. (2011b). Expression of virulence genes in luminescent and nonluminescent isogenic vibrios and virulence towards gnotobiotic brine shrimp (*Artemia franciscana*). *J. Appl. Microbiol.* 110, 399–406. doi: 10.1111/j.1365-2672.2010.04892.x

Scarano, C., Spanu, C., Ziino, G., Pedonese, F., Dalmasso, A., Spanu, V., et al. (2014). Antibiotic resistance of *Vibrio* species isolated from *Sparus aurata* reared in Italian mariculture. *New Microbiol.* 37, 329–337. Available online at: https://www.ncbi.nlm.nih.gov/pubmed/25180847

Shen, G. M., Shi, C. Y., Fan, C., Jia, D., Wang, S. Q., Xie, G. S., et al. (2017). Isolation, identification and pathogenicity of *Vibrio harveyi*, the causal agent of skin ulcer disease in juvenile hybrid groupers *Epinephelus fuscoguttatus* × *Epinephelus lanceolatus*. *J. Fish Dis.* 40, 1351–1362. doi: 10.1111/jfd.12609

Szpilewska, H., Czyz, A., and Wgrzyn, G. (2003). Experimental evidence for the physiological role of bacterial luciferase in the protection of cells against oxidative stress. *Curr. Microbiol.* 47, 379–382. doi: 10.1007/s00284-002-4024-y

Tejedor, D., Álvarez-Méndez, S. J., López-Soria, J. M., Martín, V. S., and García-Tellado, F. (2014). A robust and general protocol for the Lewis-base-catalysed reaction of alcohols and alkyl propiolates. *Eur. J. Org. Chem.* 2014, 198–205. doi: 10.1002/ejoc.201301303

Tejedor, D., Méndez-Abt, G., Cotos, L., and García-Tellado, F. (2013). Propargyl Claisen rearrangement: allene synthesis and beyond. *Chem. Soc. Rev.* 42, 458–471. doi: 10.1039/C2CS35311C

Travers, M.-A., Le Bouffant, R., Friedman, C. S., Buzin, F., Cougard, B., Huchette, S., et al. (2009). Pathogenic *Vibrio harveyi*, in contrast to non-pathogenic strains, intervenes with the p38 MAPK pathway to avoid an abalone haemocyte immune response. *J. Cell. Biochem.* 106, 152–160. doi: 10.1002/jcb.21990

Trott, O., and Olson, A. (2010). AutoDock VINA: improving the speed and accuracy of docking with a new scoring function, efficient optimization and multithreading. *J. Comput. Chem.* 31, 455–461. doi: 10.1002/jcc.21334

Visick, K. L., Foster, J., Doino, J., McFall-Ngai, M., and Ruby, E. G. (2000). *Vibrio fischeri lux* genes play an important role in colonization and development of the host light organ. *J. Bacteriol.* 182, 4578–4586. doi: 10.1128/JB.182.16.4578-4586.2000

Waidmann, M. S., Bleichrodt, F. S., Laslo, T., and Riedel, C. U. (2011). Bacterial luciferase reporters: the Swiss army knife of molecular biology. *Bioeng. Bugs* 2, 8–16. doi: 10.4161/bbug.2.1.13566

Wang, L., Chen, Y., Huang, H., Huang, Z., Chen, H., and Shao, Z. (2015). Isolation and identification of *Vibrio campbellii* as a bacterial pathogen for luminous vibriosis of *Litopenaeus vannamei*. *Aquac. Res.* 46, 395–404. doi: 10.1111/are.12191

Waters, C. M., and Bassler, B. L. (2006). The *Vibrio harveyi* quorum-sensing system uses shared regulatory components to discriminate between multiple autoinducers. *Genes Dev.* 20, 2754–2767. doi: 10.1101/gad.1466506

Waters, C. M., Lu, W., Rabinowitz, J. D., and Bassler, B. L. (2008). Quorum sensing controls biofilm formation in *Vibrio cholerae* through modulation of cyclic di-GMP levels and repression of *vpsT*. *J. Bacteriol.* 190, 2527–2536. doi: 10.1128/JB.01756-07

Wilder, C. N., Diggle, S. P., and Schuster, M. (2011). Cooperation and cheating in *Pseudomonas aeruginosa*: the roles of the *las*, *rhl* and *pqs* quorum-sensing systems. *ISME J.* 5, 1332–1343. doi: 10.1038/ismej.2011.13

Xu, Y., Wang, S., Hu, Q., Gao, S., Ma, X., Zhang, W., et al. (2018). CavityPlus: a web server for protein cavity detection with pharmacophore modelling, allosteric site identification and covalent ligand binding ability prediction. *Nucleic Acids Res.* 46, W374–W379. doi: 10.1093/nar/gky380

Zhu, J., and Mekalanos, J. J. (2003). Quorum sensing-dependent biofilms enhance colonization in *Vibrio cholerae*. *Dev. Cell* 5, 647–656. doi: 10.1016/S1534-5807(03)00295-8

Zhu, Z.-B., and Kirsch, S. F. (2013). Propargyl vinyl ethers as heteroatom-tethered enyne surrogates: diversity-oriented strategies for heterocycle synthesis. *Chem. Commun. (Camb).* 49, 2272–2283. doi: 10.1039/c3cc37258h

Conflict of Interest Statement: The authors declare that the research was conducted in the absence of any commercial or financial relationships that could be construed as a potential conflict of interest.

frontiers in Cellular and Infection Microbiology

REVIEW
published: 05 February 2019
doi: 10.3389/fcimb.2018.00444

Interference With Quorum-Sensing Signal Biosynthesis as a Promising Therapeutic Strategy Against Multidrug-Resistant Pathogens

Osmel Fleitas Martínez[1,2], *Pietra Orlandi Rigueiras*[2], *Állan da Silva Pires*[2], *William Farias Porto*[2,3,4], *Osmar Nascimento Silva*[3], *Cesar de la Fuente-Nunez*[5,6,7,8,9]* *and Octavio Luiz Franco*[1,2,3]*

[1] *Programa de Pós-Graduação em Patologia Molecular, Universidade de Brasília, Brasília, Brazil,* [2] *Centro de Análises Proteômicas e Bioquímicas, Universidade Católica de Brasília, Brasília, Brazil,* [3] *S-Inova Biotech, Programa de Pós-Graduação em Biotecnologia, Universidade Católica Dom Bosco, Campo Grande, Brazil,* [4] *Porto Reports, Brasília, Brazil,* [5] *Synthetic Biology Group, MIT Synthetic Biology Center, Massachusetts Institute of Technology, Cambridge, MA, United States,* [6] *Research Laboratory of Electronics, Massachusetts Institute of Technology, Cambridge, MA, United States,* [7] *Department of Biological Engineering, Department of Electrical Engineering and Computer Science, Massachusetts Institute of Technology, Cambridge, MA, United States,* [8] *Broad Institute of MIT and Harvard, Cambridge, MA, United States,* [9] *The Center for Microbiome Informatics and Therapeutics, Cambridge, MA, United States*

OPEN ACCESS

Edited by:
Rodolfo García-Contreras, National Autonomous University of Mexico, Mexico

Reviewed by:
Hanne Ingmer, University of Copenhagen, Denmark
Yael González Tinoco, Ensenada Center for Scientific Research and Higher Education (CICESE), Mexico

***Correspondence:**
Cesar de la Fuente-Nunez
cfuente@mit.edu
Octavio Luiz Franco
ocfranco@gmail.com

Specialty section:
This article was submitted to Molecular Bacterial Pathogenesis, a section of the journal Frontiers in Cellular and Infection Microbiology

Received: *21 August 2018*
Accepted: *12 December 2018*
Published: *05 February 2019*

Citation:
Fleitas Martínez O, Rigueiras PO, Pires ÁS, Porto WF, Silva ON, de la Fuente-Nunez C and Franco OL (2019) Interference With Quorum-Sensing Signal Biosynthesis as a Promising Therapeutic Strategy Against Multidrug-Resistant Pathogens. Front. Cell. Infect. Microbiol. 8:444. doi: 10.3389/fcimb.2018.00444

Faced with the global health threat of increasing resistance to antibiotics, researchers are exploring interventions that target bacterial virulence factors. Quorum sensing is a particularly attractive target because several bacterial virulence factors are controlled by this mechanism. Furthermore, attacking the quorum-sensing signaling network is less likely to select for resistant strains than using conventional antibiotics. Strategies that focus on the inhibition of quorum-sensing signal production are especially attractive because the enzymes involved are expressed in bacterial cells but are not present in their mammalian counterparts. We review here various approaches that are being taken to interfere with quorum-sensing signal production via the inhibition of autoinducer-2 synthesis, PQS synthesis, peptide autoinducer synthesis, and N-acyl-homoserine lactone synthesis. We expect these approaches will lead to the discovery of new quorum-sensing inhibitors that can help to stem the tide of antibiotic resistance.

Keywords: virulence, antibiotic resistance, quorum sensing, quorum-sensing inhibition, anti-virulence therapy

INTRODUCTION

The increase in bacterial resistance to antimicrobial compounds and the spread of drug-resistant pathogens have become serious threats to human health. Currently, most antimicrobial compounds target essential bacterial physiological processes, thereby exerting a strong selective pressure on bacteria and facilitating the emergence and dissemination of resistant strains (Munguia and Nizet, 2017). Therapeutic strategies that circumvent the emergence and spread of multidrug-resistant pathogens are, therefore, urgently needed.

New attractive approaches for generating new therapeutics have focused on interfering with bacterial virulence factors, specifically, interfering with compounds synthesized by pathogens that facilitate colonization of the host and subsequent infection (Kong et al., 2016; Vale et al., 2016; Dickey et al., 2017; Munguia and Nizet, 2017). Because interference with virulence factors does

not aim to eradicate the bacteria, it does not exert a strong selective pressure on the bacteria and probably decelerates the emergence and dissemination of resistant mutant strains (Gutierrez et al., 2009; Sully et al., 2014; Daly et al., 2015; Quave et al., 2015). However, the emergence of anti-virulence drug-resistant pathogens has been reported (Maeda et al., 2012; García-Contreras et al., 2013, 2015). Anti-virulence therapy appears all the more advantageous if we also consider that the production of virulence factors is under the control of regulatory mechanisms (e.g., quorum-sensing), and it should be possible to interfere with these mechanisms, consequently affecting the production of multiple virulence factors (Dickey et al., 2017; Defoirdt, 2018).

Quorum-sensing networks allow bacterial communication through the action of small diffusible autoinducer molecules (AI). These AI molecules comprise a diversity of molecular species such as autoinducer-2 (AI-2), acylated homoserine lactones (acyl-HSLs), oligopeptides, the *Pseudomonas* quinolone signal molecule (PQS), diffusible signal factor (DSF), γ-butyrolactone, 2-(2-hydroxyphenyl)-thiazole-4-carbaldehyde (IQS) among others (Guo et al., 2013; LaSarre and Federle, 2013; Pereira et al., 2013). Quorum-sensing systems operate in a cell density-dependent fashion, allowing the increase of AI concentration when cell density increases. After the AI concentration reaches a certain threshold, it triggers signaling events that modulate the expression of genes related to bacterial physiology, virulence, and biofilm formation (Papenfort and Bassler, 2016).

Interference with quorum-sensing systems has been envisioned as a suitable strategy to address the multi-drug resistance problem (Hirakawa and Tomita, 2013; Defoirdt, 2018). In this regard, a great diversity of compounds that interfere with quorum-sensing systems have been reported, as well as tools for their discovery (Jian and Li, 2013; Quave and Horswill, 2013; Nandi, 2016; Ali et al., 2017; Asfour, 2018). Strategies for inhibiting quorum sensing systems are designed mainly to interfere with the biosynthesis of AI, extracellular accumulation of the AI, and signal detection (LaSarre and Federle, 2013; Reuter et al., 2016; Singh et al., 2016; Haque et al., 2018). One of the most thoroughly explored strategies so far is interference with the extracellular accumulation of the signal. This interference can be achieved by using enzymes that degrade the signal or modify it, the use of antibodies that sequester the signal, as well as by synthetic polymers that sequester the signal (Fetzner, 2015; Daly et al., 2017; Ma et al., 2018). Interference in signal detection implies the use of compounds that interfere with the signal binding to the receptor (Singh et al., 2016; Wang and Muir, 2016; Kim et al., 2018). Other quorum-quenching strategies involve interfering with transcription factors binding to DNA and inhibiting the synthesis of the quorum-sensing signal (Gutierrez et al., 2009; Baldry et al., 2016; Scoffone et al., 2016; Greenberg et al., 2018).

The bacterial enzymes involved in quorum-sensing signal biosynthesis may be an attractive target for the development of anti-virulence agents because these enzymes are absent in mammals (Sun et al., 2004; Christensen et al., 2013; Pereira et al., 2013; Chan et al., 2015; Ji et al., 2016). Moreover, the inhibition of some of these enzymes could affect the production of more than one signal (Singh et al., 2006; Gutierrez et al., 2007, 2009; LaSarre and Federle, 2013). Experimental evidence suggests that dysfunctional AI-producing enzymes could turn pathogens less virulent for the host than pathogens expressing wild-type enzymes (Gallagher et al., 2002; Déziel et al., 2005; Kim et al., 2010; Komor et al., 2012). Thus, inhibiting the biosynthesis of the quorum-sensing signal could be a suitable strategy for developing anti-virulence agents. Because signal biosynthesis inhibition has emerged as an especially attractive way to perturb quorum-sensing networks, this strategy is emphasized in this review. The array of quorum-sensing signal biosynthesis inhibitors that have been developed, their main targets, the effects of these inhibitors on pathogen virulence, and new approaches for quorum-sensing signal biosynthesis inhibition will be summarized.

INHIBITION OF AUTOINDUCER-2 SYNTHESIS

AI-2 compounds have been claimed as "universal" signal molecules involved in inter- and intra-bacterial species communication. This is supported by the fact that *luxS* gene homologs are widely distributed among bacterial genomes [*luxS* encodes the S-ribosylhomocysteine lyase (LuxS) enzyme, which synthesizes AI-2] (Pereira et al., 2013; Pérez-Rodríguez et al., 2015; Kaur et al., 2018). Moreover, some bacteria that are unable to produce AI-2 (e. g., *Pseudomonas aeruginosa* and *Riemerella anatipestifer*) respond to AI-2 external supply, and AI-2 mediates the interaction between polymicrobial biofilm members (Han et al., 2015; Li et al., 2015; Laganenka and Sourjik, 2017). In addition to regulation of biofilm formation, AI-2 has been linked to the regulation of pathogen virulence factors production, colonization capacity, persistence, and adaption to host environment (Armbruster et al., 2009; Li et al., 2017; Ma Y. et al., 2017). Therefore, interference with AI-2 production could be used as a strategy to attenuate pathogen virulence. Two main enzymes participate in AI-2 biosynthesis: Methylthioadenosine/S- adenosylhomocysteine nucleosidase (MTA/SAH nucleosidase) and LuxS. Both enzymes are involved in the activated methyl cycle, and they therefore influence bacterial metabolism. Strategies focused on inhibiting AI-2 production have, therefore, targeted these enzymes (Lebeer et al., 2007; Parveen and Cornell, 2011; LaSarre and Federle, 2013; Pereira et al., 2013).

METHYLTHIOADENOSINE/ S-ADENOSYLHOMOCYSTEINE NUCLEOSIDASE INHIBITORS

MTA/SAH nucleosidase has been identified in several bacterial species but is absent from mammalian cells (Sun et al., 2004). It is also linked to the acyl-HSLs biosynthesis pathway; therefore, MTA/SAH nucleosidase inhibition could interfere with the production of these quorum-sensing signals (Singh et al., 2006; Gutierrez et al., 2007, 2009). In addition, MTA/SAH nucleosidase appears to influence pathogens' capacity to produce biofilms (Bao et al., 2015; Han et al., 2017). Therefore, MTA/SAH nucleosidase could be an excellent choice as a

target for the development of new quorum-sensing inhibitors. However, caution must be exercised, because the inhibition of MTA/SAH nucleosidase could result in the accumulation of S-adenosyl-homocysteine (SAH) and 5-methylthioadenosine (MTA) which, if present at high levels, could inhibit reactions catalyzed by polyamine synthases and S-adenosylmethionine dependent methyltransferases, interfering with bacterial growth (Heurlier et al., 2009; Parveen and Cornell, 2011). *Vibrio cholerae* MTA/SAH nucleosidase mutants with impaired growth have been reported (Silva et al., 2015). Nevertheless, experimental evidence has demonstrated that it is possible to inhibit MTA/SAH nucleosidase activity without severely affecting bacterial growth and without inducing resistance toward inhibitors (Gutierrez et al., 2009). In addition, Bourgeois et al. (2018) observed that a *Salmonella enterica* serovar Typhimurium Δ*metJ* mutant strain, which was defective in methionine metabolism, presented elevated intracellular MTA levels without affecting bacterial growth (Bourgeois et al., 2018). In a *S. aureus pfs* mutant strain (*pfs* encodes the MTA/SAH nucleosidase), growth was not impaired in nutrient-rich conditions but it was affected in zebrafish embryos (Bao et al., 2013). MTA is also a substrate of the human enzyme MTA phosphorylase, but the structural differences between the human and bacterial enzymes (in the purine, ribose and 5′-alkylthio binding sites) make it possible to develop MTA structural analogs as inhibitors that are selective for MTA/SAH nucleosidase (Lee et al., 2004; Guo et al., 2013; **Figure 1**).

The structures of MTA/SAH nucleosidase homologs in several bacterial species have been resolved; these species include *Escherichia coli*, *Helicobacter pylori*, *Streptococcus pneumoniae*, *Staphylococcus aureus*, *S. enterica*, *V. cholerae*, *Brucella melitensis*, and more recently *Aeromonas hydrophila* (Lee et al., 2003; Singh et al., 2006; Siu et al., 2008; Ronning et al., 2010; Haapalainen et al., 2013; Kang et al., 2014; Thomas et al., 2015; Xu et al., 2017). Basically, the MTA/SAH nucleosidase is a homodimer that contains two active sites in which specific sub-sites (purine, ribose and 5′-alkylthio binding sites) are involved in the interactions with the substrate (Ronning et al., 2010). MTA/SAH nucleosidase removes adenine from SAH, MTA, and 5′-deoxyadenosine yielding S-ribosyl-L-homocysteine (SRH), S-methyl-5′-thioribose, and 5′-deoxyribose, respectively. In *Neisseria meningitidis* and *H. pylori*, this reaction takes place through an early transition state while in other bacteria such as *Klebsiella pneumoniae*, *E. coli*, *S. aureus*, and *S. pneumoniae* it occurs through a late dissociative transition state (Singh et al., 2005b; Gutierrez et al., 2007). In line with this, most of the MTA/SAH nucleosidase inhibitors that have been developed are transition state analogs (Singh et al., 2005a,b, 2006; Gutierrez et al., 2007, 2009).

Several of these transition state analogs have been tested on *E. coli* and *S. pneumoniae* MTA/SAH nucleosidases (Singh et al., 2005a, 2006). The analogs were mainly based on 5′-thio-Immucillin-A and 5′-thio-DADMe-Immucillin-A derivate compounds, in which diverse chemical groups (aromatic, cycloalkyl, halogenated aliphatic and hydrophobic groups) were incorporated at the 5′-thio position. The 5′-thio-DADMe-Immucillin-A-derived analogs behaved as more potent MTA/SAH nucleosidase inhibitors than 5′-thio-Immucillin-A-derived analogs, because these analogs mimic the late dissociative transition state through which the enzymatic reaction in these bacterial species takes place (Singh et al., 2005a, 2006). Moreover, 5′-thio-DADMe-Immucillin-A-based inhibitors showed *V. cholerae* N16961 and *E. coli* O157: H7 cellular MTA/SAH nucleosidase inhibition. The inhibitors interfered with AI production without affecting bacterial growth. Although the inhibitors reach their intracellular target, a significant diffusion barrier was observed. For both *V. cholerae* and *E. coli*, the inhibition of AI-2 production by 5′-butylthio-DADMe-Immucillin-A was sustained over several bacterial generations, suggesting that bacterial resistance had not emerged toward the MTA/SAH nucleosidase inhibitor. The 5′-butylthio-DADMe-Immucillin-A inhibitor reduced biofilm production in both species of bacteria (Gutierrez et al., 2009). However, Silva et al. (2015) recently showed that *V. cholerae* N16961 was able to form biofilm when treated with 5′-methylthio-DADMe-Immucillin-A, although a high percentage of MTA/SAH nucleosidase inhibition was reached. In addition, in two MTA/SAH nucleosidase mutant strains biofilm production was similar to the wild-type strain (*V. cholerae* N16961) whereas the growth rate and swarming motility were lower than the wild-type strain (Silva et al., 2015).

In another line of research, novel inhibitors of *S. enterica* MTA/SAH nucleosidase based on transition state analogs were designed. Interestingly, *S. enterica* MTA/SAH nucleosidase presented an elongated 5′-alkylthio-binding pocket. In that case, the design of novel inhibitors involved adding elongated 5′-alkylthio groups to the DADMe-Imm-A core to fill this site. The new inhibitors were 2-hydroxyethylthio-DADMe-Imm-A, 3-hydroxypropylthio-DADMe-Imm-A, 4-hydroxybutylthio-DADMe-Imm-A and 2-(2-hydroxyethoxy)ethylthio-DADMe-Imm-A, all of which showed dissociation constants in the pM range (Haapalainen et al., 2013). Recently, the putative *Mycobacterium tuberculosis* MTA/SAH nucleosidase (Rv0091) was expressed and characterized kinetically, showing a preference for 5′-deoxyadenosine as the substrate in comparison with MTA and SAH. For Rv0091, DADMe-Imm-A inhibitors consisting of derivatized analogs with long alkyl groups at the C5′ position exerted potent inhibitory activity (Namanja-Magliano et al., 2016). Additionally, when using 5′-deoxyalkyl- and 5′-alkylthio-DADMe-Immucillin-A transition state analogs it was observed that for the 5′-deoxyalkyl-DADMe-Immucillin-A analogs, shorter 5′-alkyl-substituents led to the most potent inhibition, in contrast to 5′-alkylthio-DADMe-Immucillin-A analogs, in which longer 5′-alkyl-substituents led to the most potent inhibition. These inhibitors did not affect the growth of *M. tuberculosis* or *Mycobacterium smegmatis*; however, they showed an antimicrobial effect on *H. pylori* (due to the involvement of *H. pylori* MTA/SAH nucleosidase in the menaquinone biosynthesis pathway). The authors suggested that Rv0091 plays a role in 5′-deoxyadenosine recycling but is not essential for the growth of *M. tuberculosis* or *M. smegmatis* (Namanja-Magliano et al., 2017).

Furthermore, the MTA/SAH nucleosidase has been suggested to influence the virulence of pathogens in an AI-2-independent fashion. Based on mouse infection models and zebrafish embryo

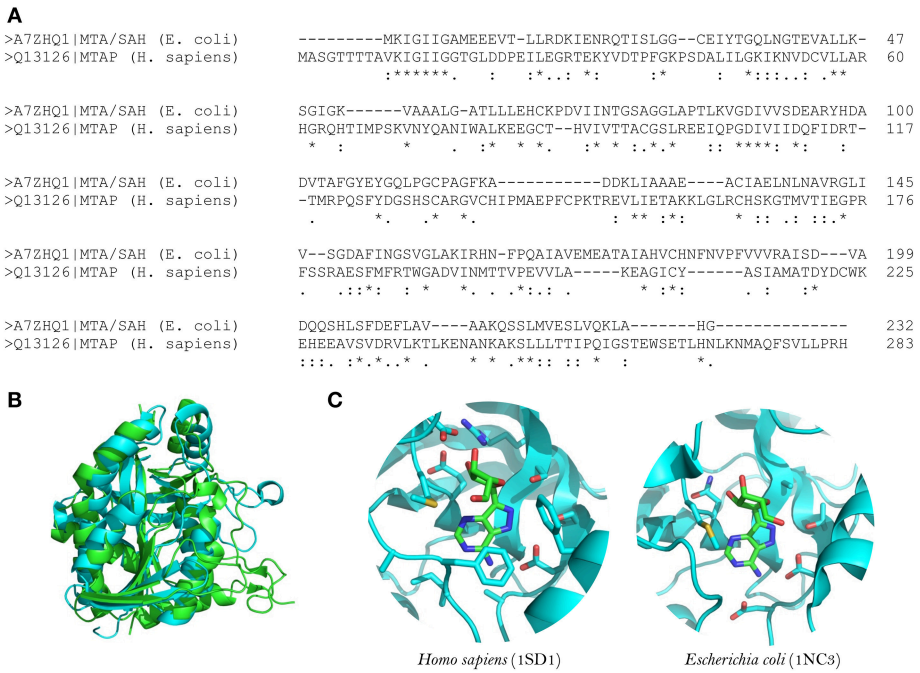

FIGURE 1 | Structural comparison between human MTA phosphorylase and *E. coli* MTA/SAH nucleosidase. **(A)** Sequence alignment between *E. coli* MTA/SAH nucleosidase (MTAN; Uniprot ID: A7ZHQ1) and human MTA phosphorylase (MTAN; Uniprot ID: Q13126). **(B)** Structural alignment between MTAN (green) and MTAP (blue). **(C)** Active site comparison between MTAN (PDB ID: 1SD1, left) and MTAP (PDB ID: 1NC3, right) with formycin. The structures were retrieved from PDB, and the visualization was done by using Pymol v.1.6.

infection models, Bao et al. (2013) demonstrated that a *S. aureus* NCTC 8325 *pfs* mutant strain displayed attenuated virulence *in vivo*. In addition, a *luxS* mutant was as virulent as the isogenic wild-type *S. aureus* NCTC8325 strain, suggesting that the effects of *pfs* deletion on *S. aureus* virulence were independent of the AI-2-based quorum sensing pathway. The attenuated virulence of the *pfs* mutant strain was associated with reduced proliferation *in vivo*. Additionally, *in vitro* analysis showed reduced extracellular protease activity in the *pfs* mutant strain linked to reduced *sspABC* operon transcription and *aur* gene transcription (Bao et al., 2013). Another study showed that *S. aureus* NCTC 8325 *pfs* mutant strain displayed reduced biofilm formation *in vitro* by AI-2-independent mechanisms. The *pfs* deletion reduced the transcription of autolysis-related genes *atlE* and *lytM* in the mutant strain; therefore, autolysis-dependent extracellular DNA release in the *pfs* mutant, and consequently biofilm formation, was affected (Bao et al., 2015).

The experimental findings reviewed above suggest that MTA/SAH nucleosidase could influence pathogen virulence via quorum-sensing-independent or –dependent mechanisms (Gutierrez et al., 2009; Bao et al., 2013, 2015; Silva et al., 2015). Therefore, for MTA/SAH nucleosidase inhibitor evaluation studies, precise experimental designs aimed at distinguishing by which mechanism (i.e., quorum sensing-independent and/or –dependent) the pathogen's virulence is affected are warranted. Moreover, most of the studies about MTA/SAH nucleosidase inhibition have been focused on designing inhibitors and evaluating their inhibitory activity via enzymatic assays using purified enzymes, but data about the real impact that such inhibitors have on pathogens virulence is scarce (Singh et al., 2005a,b, 2006; Gutierrez et al., 2007; Haapalainen et al., 2013; Namanja-Magliano et al., 2016).

Therefore, it is essential to perform studies that evaluate the effects of MTA/SAH nucleosidase inhibitors on pathogen virulence gene expression as well as testing the effectiveness of these to attenuate pathogens *in vivo*. Immucillin-based inhibitors appear to be a reasonable option as quorum quenching agents. This class of inhibitors has been used as antiviral, antibacterial (specifically in *H. pylori*), anti-malarial, and antineoplastic agents. Some of them are in clinical trials or have been approved for use in humans. Immucillin-based inhibitors are chemically stable, specific, and it is possible to chemically modify them to gain bioavailability without severely affecting their inhibitory activity (Longshaw et al., 2010; Evans et al., 2018).

S-RIBOSYLHOMOCYSTEINE LYASE INHIBITORS

The enzyme S-ribosylhomocysteine lyase (LuxS) is a potential target for the development of new therapeutic agents because it is present in numerous bacterial species but not in mammals (Pereira et al., 2013; Pérez-Rodríguez et al., 2015;

Kaur et al., 2018). In addition, LuxS also appears to modulate bacterial biofilm formation based on results obtained with *luxS* mutant bacteria (Hardie and Heurlier, 2008; Kang et al., 2017; Ma R. et al., 2017; Zuberi et al., 2017). However, through which mechanisms *luxS* influences biofilm formation is under debate. LuxS could influence biofilm formation in an AI-2-dependent fashion, in which the expression of genes associated with bacterial adherence and biofilm matrix production may be modulated through AI-2-mediated signaling (Hardie and Heurlier, 2008; Duanis-Assaf et al., 2016; Ma R. et al., 2017; Velusamy et al., 2017; Pang et al., 2018). In addition, AI-2 may promote single and mixed species biofilm formation through chemotaxis-mediated aggregation events (Laganenka et al., 2016; Laganenka and Sourjik, 2017). However, other findings suggest that *luxS* also influences biofilm formation in an AI-2 signaling-independent fashion, probably involving the activated methyl cycle, fimbriation modulation and biofilm-associated gene expression modulation (Niu et al., 2013; Hu et al., 2018; Yadav et al., 2018).

Furthermore, LuxS may influence the virulence of pathogens during the host infection process. Recently, Yadav et al. (2018) demonstrated using a rat model of otitis media that *S. pneumoniae* D39Δ*luxS* mutant strain had decreased capacity for host colonization in comparison with the wild-type strain. Similarly, in a murine model D39Δ*luxS* displayed reduced capacity of nasopharynx colonization as well as reduced dissemination toward lung and blood. Interestingly, when AI-2 was administered to the D39Δ*luxS* infected mice, the D39Δ*luxS* mutant became as virulent as the wild-type strain without AI-2 treatment, suggesting that attenuated virulence in D39Δ*luxS* was associated with impaired AI-2 production and signaling (Trappetti et al., 2017). Moreover, in mice dual-infected with wild-type *Borrelia burgdorferi* and a *luxS* mutant strain, a higher wild-type bacterial load was observed than *luxS* mutant bacterial load in distal tissues from infection site, suggesting attenuated virulence for the *luxS* mutant (Arnold et al., 2015). However, using a pneumonic plague mouse model Fitts et al. (2016) observed that a *Yersinia pestis* CO92 *ΔluxS* mutant was as virulent as the wild-type CO92 strain. In addition, deletion of l*uxS* from a *ΔrbsAΔlsrA* strain (attenuated virulence) turns it into the *ΔrbsAΔlsrAΔluxS* mutant, which was also as virulent as the wild-type strain (Fitts et al., 2016).

Taking into consideration the experimental evidence mentioned above, implementation of therapeutic strategies focused on LuxS inhibition may turn out to be complex and more difficult than initially envisioned. The effects of *luxS* on biofilm formation and virulence appear be dependent on bacterial species and genetic background (Bao et al., 2013; Fitts et al., 2016; Ma Y. et al., 2017; Trappetti et al., 2017; Velusamy et al., 2017; Hu et al., 2018). Also, LuxS could influence gene expression in an AI-2 signaling-independent fashion (Pereira et al., 2013). Moreover, LuxS inhibition could facilitate the accumulation of toxic compounds that disturb bacterial viability, and it could therefore exert selective pressure on the pathogen (Heurlier et al., 2009). In addition, the effects of *luxS* suppression on bacterial growth could be dependent on environmental stress conditions (Park et al., 2017). LuxS-independent pathways could also be involved in AI-2 formation (Tavender et al., 2008). However, *in vivo* studies have shown that it is possible to attenuate pathogen virulence via LuxS inhibition (Zhang et al., 2009; Sun and Zhang, 2016).

LuxS is a homodimer metalloenzyme that catalyzes the SRH cleavage through a proposed mechanism involving two isomerization steps (aldo-ketose and keto-ketose isomerization) followed by a β-elimination step to yielding L-homocysteine and the enol form of 4,5 dihydroxy-2,3-pentanedione (DPD) (Zhu et al., 2003, 2006; Pei and Zhu, 2004; **Figure 2**). The DPD spontaneously cyclizes and reorganizes into various furanone molecules that constitute the AI-2 (LaSarre and Federle, 2013). In this regard, most of the strategies for directly inhibiting LuxS are centered on substrate analogs that compete with the natural substrate for binding to the enzyme active site and interfere with any of the mechanistic steps that LuxS catalyzes (Alfaro et al., 2004; Wnuk et al., 2008; Malladi et al., 2011; **Figure 2**).

Some of the reported LuxS competitive inhibitors are SRH analogs that contain a modified C1 at the ribose or [4-aza]ribose, which could affect the initial ring opening and the subsequent isomerization [e.g., S-anhydroribosyl-L-homocysteine, and S-(1-Amino-1,4-anhydro-1,5-dideoxy-D-ribitol-5-yl)-L-homocysteine] (Alfaro et al., 2004; Malladi et al., 2011; **Figure 2**, compound 1). Another potential LuxS inhibitor that could affect the ring opening is the SRH analog S-(1,5-Dideoxy-4-thio-D-ribofuranos-5-yl)-L-homocysteine (Sobczak et al., 2015). Moreover, compounds that interfere with the tautomerization/isomerization steps during the catalytic cycle act as competitive inhibitors of LuxS. Some of these compounds are SRH analogs in which the hydroxyl group at ribose C3 position has been removed or modified, making it a non-enolizable hydroxyl group and therefore interfering with the formation of the 3-ketone intermediate (e.g., 3,5,6-trideoxy-6-fluoro-D-erythro-hex-5-enofuranose) (Wnuk et al., 2008; **Figure 2**, compound 2). In addition, analogs of enediolate intermediates in which the enediolate moiety was substituted by a planar hydroxamate group act as powerful reversible competitive inhibitors of LuxS (Shen et al., 2006).

Inhibitors of the LuxS catalytic β-elimination step targeted the carbon (C5)-sulfur bond or the hydrogen atom at C4 position in the SRH substrate. In the inhibitor S-homoribosyl-L-cysteine, the carbon (C5)-sulfur bond was replaced by a C5-C6 carbon-carbon bond, which interferes with the cleavage of the carbon-sulfur bond (Alfaro et al., 2004; **Figure 2**, compound 3). Recently, Chbib et al. (2016) synthesized 4-C-Alkyl/aryl-SRH analogs that potentially could inhibit LuxS at the β-elimination step. The substitution of the hydrogen atom at C4 position by alkyl/aryl groups should prevent the abstraction of the C4-proton, which is important for the β-elimination step (Chbib et al., 2016). Interestingly, these authors suggested that the 4-C-Alkyl/aryl-SRH analogs also could inhibit LuxS by interfering with the dimerization of the enzyme. Previously, SRH analogs that carried alkyl/aryl groups at the C3 position of the homocysteine moiety of SRH were suggested as LuxS dimerization inhibitors (Liu, 2012).

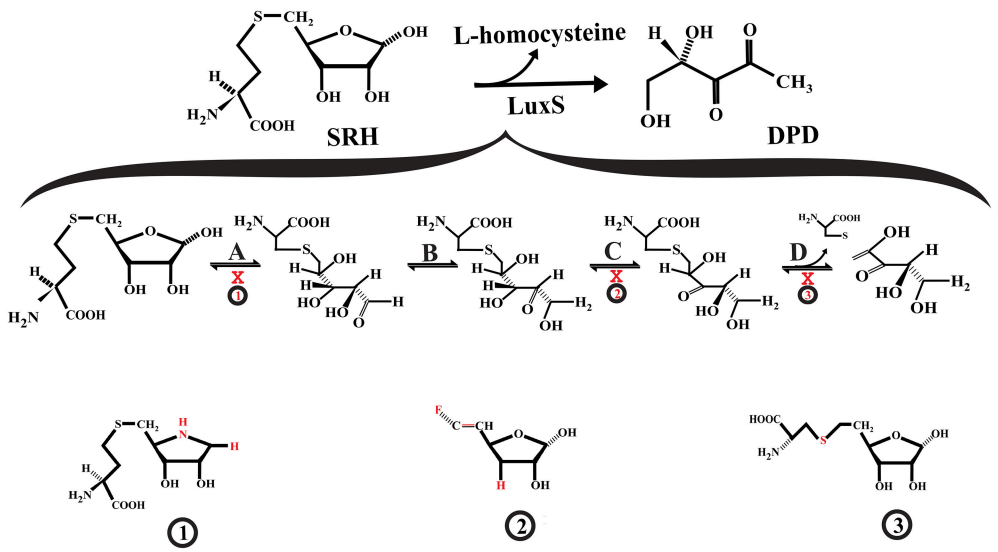

FIGURE 2 | Interference with S-ribosylhomocysteine lyase (LuxS) activity. **(A)** S-ribosyl-homocysteine (SRH) ribose ring opening. **(B)** The opened SRH molecule undergoes aldose-ketose isomerization yielding 2-keto intermediate. **(C)** The 2-keto intermediate is transformed into 3-keto intermediate via ketose-ketose isomerization. **(D)** The 3-keto intermediate suffers a β-elimination reaction releasing L-homocysteine and the enol form of DPD. The SRH analog S-(1-Amino-1,4-anhydro-1,5-dideoxy-D-ribitol-5-yl)-L-homocysteine (1) may act as a competitive inhibitor that not suffer ring opening, affecting the aldose-keto isomerization. The 3,5,6-trideoxy-6-fluoro-D-erythro-hex-5-enofuranose (2) may interfere with the formation of the 3-keto intermediate. The S-homoribosyl-L-cysteine inhibitor (3) may interfere with the β-elimination step. The red X indicates inhibition.

Indeed, LuxS inhibitors [e.g., S-xylosylhomocysteine and S-(3-deoxy-3-fluoroxylosyl) homocysteine] that exerted a time-dependent inhibition of LuxS have been identified. They act as slow-binding inhibitors of improved potency, similarly to the halogenated S-[3-Bromo-3,5-dideoxy-D-ribofuranose-5-yl]-L-homocysteine and S-[3-fluoro-3,5-dideoxy-D-ribofuranos-5-yl]-L-homocysteine analogs (Gopishetty et al., 2009; Wnuk et al., 2009). The time-dependent inhibition exerted by these halogenated analogs was produced by the enzyme-catalyzed elimination of halide ions (Gopishetty et al., 2009). Equally, time-dependent inhibition of LuxS was observed for the S-[4-Amino-4,5-dideoxy-α/β-D-ribofuranos-5-yl]-L-homocysteine hemiaminal analog. This time-dependent inhibition was suggested as a result from the formation of ketone intermediates that bind to the LuxS active site with a higher affinity than the ribose natural substrate (Malladi et al., 2011).

Molecules that covalently modify LuxS also mediate its inhibition. Along these lines, halogenated furanones have been shown to inactivate LuxS. Specifically, it was observed that furanones that contain a vinyl monobromide moiety inhibit LuxS in a concentration-dependent manner. Mechanistic studies showed that LuxS was inactivated by covalent modification (Zang et al., 2009). Recently, it was hypothesized that the 2-deoxy-2-propylthiol-S-ribosylhomocysteine potentially could inhibit LuxS via covalent modification (Chbib, 2017).

Most of these luxS inhibitors have been tested *in vitro* using enzymatic assays with the purified LuxS enzyme. However, if these inhibitors are able to inhibit luxS *in vivo* with the consequent attenuation of pathogen virulence still needs to be investigated.

In addition to the SRH substrate analogs described above, other LuxS inhibitors are substrate non-analogs. Using phage display, representative peptide sequences that bind to LuxS were found. Of these, only the peptide TNRHNPHHLHHV inhibited LuxS and, then, only weakly, showing that there is not necessarily a correlation between peptide binding to LuxS and enzyme inhibition (Han and Lu, 2009). However, two LuxS-derived peptides have been described [peptide 5411 (MHTLEHLFAGFM) and 5906 (MLFAGFM)] that acted as potential LuxS inhibitors and mediated the attenuation of *Edwardsiella tarda* TX1 virulence *in vivo* (Zhang et al., 2009). The expression of the inhibitory peptides in TX1 strain (via plasmids) affected AI-2 production, reduced biofilm formation, and reduced *esrA* and *orf26* gene expression. Additionally, the virulence of TX1 strain was attenuated in infected Japanese flounder fish. Fish infected with the TX1 strain could be attenuated either by means of a commensal *Pseudomonas* sp. strain expressing the peptide 5411 or by directly expressing such peptide in tissues of infected fish (Zhang et al., 2009). Recent findings demonstrated that peptide 5906 production by *E. coli* DH5α/p5906 or by fish tissues attenuated *E. tarda* pathogenesis in Japanese flounder. In addition, the pathogenesis of *A. hydrophila* AH1 and *V. harveyi* T4 in infected fish was attenuated by *E. coli* DH5α/p5906. However, this attenuation was moderate in comparison with the attenuation that *E. tarda* underwent. It has been suggested that differences in the LuxS sequences of these pathogens could be responsible for the observed differences in the attenuation levels (Sun and Zhang, 2016). All these findings suggest that LuxS-derived peptides have the potential to act as AI-2-based quorum sensing system inhibitors in several bacterial species and

that engineered commensal bacteria to produce LuxS-derived peptides could be a feasible strategy for quorum quenching *in vivo*.

To disturb LuxS functionality, the design of small molecule inhibitors has been the most exploited strategy. However, interference with the *luxS* gene expression represents an alternative approach to impairing LuxS function. The development of the Clustered Regularly Interspaced Short Palindromic Repeats-Cas 9 (CRISPR-Cas9) genome-editing technology now permits the expression of genes to be modulated with a high specificity and reduced off-target effect. This technology has been proposed as a promising method for fighting against antimicrobial resistance (Greene, 2018). Recently, Kang et al. (2017), using CRISPR-Cas9 genome-editing technology, obtained *E. coli* SE15Δ*luxS* mutant clones from the *E. coli* SE15 clinical strain isolated from the indwelling catheter of a patient suffering from urinary tract infections. *E. coli* SE15Δ*luxS* clones showed reduced biofilm formation in comparison to the wild-type strain. Moreover, in *E. coli* SE15Δ*luxS* mutant the expression of the genes *mqsR*, *pgaB*, *pgaC*, *csgE*, and *csgF* (involved in biofilm formation) was down-regulated (Kang et al., 2017). This work showed that by using CRISPR-Cas9 genome-editing technology it is possible to disturb the *luxS* gene expression and consequently impair one of the mechanisms of pathogenicity (biofilm formation) employed by pathogens. However, if this approach will be effective *in vivo* remains to be seen. Nevertheless, the feasibility of CRISPR-Cas9 genome-editing technology for attenuating the virulence of pathogens *in vivo* has been demonstrated. In this respect, the use of CRISPR-Cas9 phagemid vectors attenuated the virulence of enterohaemorrhagic *E. coli* in a *Galleria mellonella* infection model and *S. aureus* in a mouse skin colonization model (Bikard et al., 2014; Citorik et al., 2014).

An alternative CRISPR-Cas9-based approach, namely the CRISPR interference (CRISPRi) approach, has been applied successfully for *luxS* attenuation in clinical bacterial isolates (Zuberi et al., 2017). This system is based on the use of a Cas-9 DNA endonuclease that is not catalytically active (dCas-9) but can be directed toward the target gene by a small guide RNA and repress the expression of the target gene via interfering with the transcriptional process (Qi et al., 2013). Using a CRISPRi approach that targeted the *luxS* gene of the *E. coli* clinical strain AK-117 (isolated from urinary catheters), Zuberi et al. (2017) obtained three *luxS* knockdown strains (AK-LV1, AK-LV2, and AK-LV3) that were metabolically actives but with impaired biofilm formation capacity (Zuberi et al., 2017).

It has been described that in *E. coli* the CyaR small RNA regulated *luxS* gene expression negatively via post-transcriptional binding to the *luxS* mRNA 5′end (including the ribosome binding site), consequently, CyaR small RNA expression reduced AI-2 production (De Lay and Gottesman, 2009). Moreover, Zhang and Sun (2012) using an antisense RNA interference approach, impaired *luxS* expression in *Edwardsiella ictaluri* J901 strain, yielding the *luxS*-defective *E. ictaluri* J901Ri strain. *E. ictaluri* J901Ri showed lower AI-2 production, reduced biofilm formation, and down-regulated expression of *orf26*, *esrA*, *eseB*, *eseD, eihA,* and *wbiT* genes in comparison to *E. ictaluri* J901C control strain. Moreover, *E. ictaluri* J901Ri-infected zebrafish group showed lower accumulated mortality than *E. ictaluri* J901C- infected group, and *E. ictaluri* J901Ri infectivity on ZF4 cells was reduced in comparison to the control strain (Zhang and Sun, 2012). Therefore, it was possible that using an RNA interference approach attenuated the *E. ictaluri* J901 virulence. Based on an antisense RNA interference approach that targeted the *luxS* gene, Zhang et al. (2008), attenuated the virulence of the pathogen *E. tarda*. The *E. tarda* TX1/pJR18 strain, which contained a plasmid (pJR18) that constitutively expressed the *luxS* antisense RNA, showed lower AI-2 production, reduced biofilm formation and reduced expression of *esrA* and *orf26* genes in comparison to the control *E. tarda* TX1/pJRA strain. Furthermore, in *E. tarda* TX1/pJR18-infected Japanese flounder group the accumulated mortality, the bacteria recovered from blood and kidney, and *orf 26* and *esrA* expression were lower than the *E. tarda* TX1/pJRA-infected group (Zhang et al., 2008). Based on all these findings, it could be envisioned that antisense oligonucleotide-based inhibition could be a feasible strategy for the development of new luxS inhibitors.

INHIBITION OF PQS SYNTHESIS

Pseudomonas aeruginosa produces 2-heptyl-3-hydroxy-4(1H)-quinolone, which is commonly known as *Pseudomonas* quinolone signal (PQS) and acts as a quorum-sensing signal molecule (Déziel et al., 2004). Among the proteins involved at PQS synthesis, several of them are encoded by the *pqsABCDE* operon. The first step in the PQS biosynthesis pathway involves the formation of anthraniloyl-coenzyme A from anthranilate catalyzed by an anthranilate CoA ligase (PqsA). Subsequently, two condensation reactions take place. First, anthraniloyl-coenzyme A condenses with malonyl-CoA to form (2-aminobenzoyl) acetate with the participation of the proteins PqsD and PqsE. Second, the (2-aminobenzoyl) acetate condenses with octanoate through the PqsB and PqsC catalytic activity, producing 2-heptyl-4(1H)-quinolone (HHQ). Finally, HHQ is hydroxylated by PqsH FAD-dependent monooxygenase to form PQS (Déziel et al., 2004; Dulcey et al., 2013). Both HHQ and PQS act as signaling molecules.

Several enzyme-catalyzed reactions in the PQS biosynthesis pathway are being targeted for interference with PQS production (Sahner et al., 2013; Hinsberger et al., 2014; Ji et al., 2016; Maura et al., 2017). Anthranilate-CoA ligase (PqsA) constitutes an attractive target for developing drugs because the ortholog enzyme is absent in humans. PqsA catalyzes the conversion of anthranilate to anthraniloyl-coenzyme A in a reaction that involves an anthranilyl-AMP intermediate, which has been targeted in the design of PqsA inhibitors (Ji et al., 2016).

Recently, Ji et al. (2016) designed and evaluated the inhibitory activity of several sulfonyladenosine compounds on PqsA. These small molecules mimic the anthranilyl-AMP intermediate. The anthranilyl-AMS and anthranilyl-AMSN compounds were the most potent PqsA inhibitors that were found to reduce HHQ and PQS quinolone production by *P. aeruginosa* strain PA14; while salicyl-AMS, salicyl-AMSN, and benzoyl-AMS inhibitors

were less potent. The authors suggested that differences in cell penetration, stability, and/or target specificity could be responsible for the variations in potency observed in inhibiting HHQ and PQS quinolone production (Ji et al., 2016). Other types of PqsA inhibitors that have been studied are the substrate analogs. Challenging the *P. aeruginosa* strain PAO1 culture with the anthranilate analog methyl-anthranilate was observed to inhibit the production of PQS and to decrease activity of the virulence factor elastase in a concentration-dependent manner. Interestingly, the methyl-anthranilate treatment did not affect the growth of cultures (Calfee et al., 2001). Moreover, other anthranilic acid analogs, specifically halogenated anthranilic acid analogs, exerted inhibitory activity on the production 4-hydroxy-2-alkylquinolines (HAQs) in *P. aeruginosa* and *Burkholderia thailandensis* without significantly disturbing bacterial growth (Lesic et al., 2007). The treatment of *P. aeruginosa* with several of these halogenated analogs represses the expression of HAQ biosynthetic operons *pqsA-E* and *phnAB* as well as the virulence factors pyocyanin (*phz ABCDEFG*, *phzH*, *phzM*, and *phzS*), hydrogen cyanide (*hcnABC*), chitinase (*chiC*), lectins (*lecA and lecB*), and elastase (*lasB*). Interestingly, these compounds are also effective *in vivo*, as they limited the virulence of *P. aeruginosa* in mice, delayed mortality in the treated animals, reduced the production of HHQ, and prevented systemic dissemination of the bacteria (Lesic et al., 2007). Furthermore, Coleman et al. (2008) tested the inhibitory activity of several anthranilate analogs on PQS production in bacterial cultures as well as on PqsA activity. Most of the chloro- and fluoro-anthranilate derivatives inhibited the production of PQS in *P. aeruginosa* culture and were PqsA substrates. Additionally, the anthranilonitrile, 5-nitroanthranilonitrile, methylanthranilate, and 3-fluoro-O-anisidine analogs did not behave as PqsA substrates but inhibited the production of PQS (Coleman et al., 2008).

Another protein involved in the PQS biosynthesis pathway that has been considered for the development of anti-virulence drugs is PqsD. PqsD forms homodimers in solution and structurally is similar to *E. coli* β-ketoacyl-ACP synthase III (FabH), showing the Cys-His-Asn catalytic triad typical of FabH-like enzymes (Bera et al., 2009). PqsD catalyzes the formation of 2-aminobenzoylacetyl-CoA in the PQS biosynthesis pathway using as substrates anthraniloyl-CoA and malonyl-CoA. Initially PqsD forms an anthraniloyl-PqsD intermediate via Cys 112 in the PqsD active site; subsequently, a condensation reaction takes place with malonyl-CoA. Given the structural similarity between PqsD and FabH-like enzymes, it has been suggested that FabH inhibitors potentially could inhibit PqsD (Pistorius et al., 2011; Dulcey et al., 2013).

Along the same lines, Pistorius et al. (2011) demonstrated that the well-established FabH inhibitors, such as 2-(4-bromo-3-diethylsulfamoyl-benzoylamino)-benzoic acid and 2-[(2- phenoxybiphenyl-4-carbonyl) amino] benzoic acid, had IC_{50} in the micromolar range; therefore, they exerted a modest inhibitory activity toward PqsD (Pistorius et al., 2011). Subsequently, introducing modifications in the 2-(4-bromo-3-diethylsulfamoyl-benzoylamino)-benzoic acid inhibitor yielded a series of sulfonamide-substituted benzamidobenzoic acids that inhibited PqsD. It was suggested that the binding of these compounds within the anthraniloyl-CoA channel of PqsD (involving hydrogen bonds, π-stackings, and hydrophobic interactions) hinders the access of substrate to the catalytic site; the compounds are therefore acting as entropy-driven channel-blocker inhibitors (Weidel et al., 2013). Moreover, Hinsberger et al. (2014) identified PqsD inhibitors with preferential selectivity to PqsD over RNA polymerase. These inhibitors were derivatives of benzamidobenzoic acid. The selectivity to PqsD was favored by introducing modifications on the benzamidobenzoic acid scaffold. The development of PqsD inhibitors that minimally affect the activity of RNA polymerase is desirable, because compounds that hinder this activity could exert selective pressure on the targeted bacteria (Hinsberger et al., 2014).

Using a ligand-based approach, Storz et al. (2012), identified several PqsD inhibitors that consisted of PqsD substrates and transition state analogs. The most potent inhibitor was (2-nitrophenyl)phenyl methanol, which contained a (2-nitrophenyl)methanol core rigidified by an unsubstituted phenyl moiety. This molecule inhibited the production of HHQ and PQS by *P. aeruginosa* PA14 cultures and reduced the biovolume of biofilm formed by this bacterial strain. At a concentration of 250 μM, this molecule did not affect bacterial growth or have a toxic effect on human THP-1 macrophages (Storz et al., 2012). A subsequent study showed that the inhibition of PqsD by (2-nitrophenyl)phenyl methanol was time-dependent (Storz et al., 2013). Subsequently, Storz et al. (2014) synthesized and evaluated several (2-nitrophenyl)methanol derivatives with improved *in vitro* PqsD inhibition. However, most of these derivatives did not show similar potency in inhibiting HHQ production in a *pqsH*-deficient *P. aeruginosa* PA14 strain. The derivative that contained an ethyl group at the methanol moiety, as well as those which contained heteroaromatic pentacycles, strongly inhibited PqsD activity in cells, even though these derivatives were not among the best PqsD inhibitors *in vitro*. Therefore, for (2-nitrophenyl)methanol derivatives, improved *in vitro* PqsD inhibition does not necessarily mean improved inhibitory activity *in cellulo* (Storz et al., 2014).

Other PqsD inhibitors that have been reported are compounds of the aryl-ureidothiophene-2-carboxylic acid class. These compounds were predicted to bind to the substrate channel of PqsD via their aryloxy-moiety pointed toward the bottom of the pocket and thereby block the binding of the substrate, anthraniloyl-CoA (Sahner et al., 2013). Moreover, the chemical structure combination of ureidothiophene-2-carboxylic acids with (2-nitrophenyl)methanol inhibitors yielded some derivatives with improved PqsD inhibitory activity when activity was measured in a cell-free enzyme assay. However, these compounds were ineffective in reducing HHQ production in a whole-cell *P. aeruginosa* assay. Ureidothiophene-2-carboxylic acid-based inhibitors were suggested to be expelled by efflux pumps in *P. aeruginosa*; if this were found to be the case, they would not be suitable for development as quorum-quenching strategies (Sahner et al., 2015). Based on the similarity between PqsD and the chalcone synthase (CHS2) expressed in alfalfa (*Medicago sativa*), Allegretta et al. (2015) developed new PqsD inhibitors from substrates of CHS2. These substrate

analogs contained a catechol core that was important for inhibitory activity. Apparently, these compounds inhibited PqsD by blocking the enzyme substrate channel. Several of these inhibitors reduced the production of HHQ in bacterial cultures without affecting bacterial growth (Allegretta et al., 2015). Recently, Thomann et al. (2016) introduced an innovative and original strategy for quenching the PQS quorum-sensing system in *P. aeruginosa*. This strategy was based on the development of a dual-inhibitor compound that simultaneously inhibited both the PQS transcriptional regulator (PqsR) and PqsD. This compound acted as a dual inhibitor that affected the production of the virulence factors, pyocyanin and pyoverdine, but without affecting bacterial growth. Additionally, this compound reduced biofilm formation by *P. aeruginosa* and boosted the anti-bacterial activity of ciprofloxacin under biofilm conditions. Importantly, the dual inhibitor increased, in a dose-dependent manner and without cytotoxic effects, the survival rate of *G. mellonella* larvae challenged with lethal doses of *P. aeruginosa* (Thomann et al., 2016).

Inhibitors of the heterodimeric enzyme PqsBC have also been described. PqsBC participates in the PQS biosynthesis pathway by catalyzing the condensation of 2-aminobenzoyl acetate and octanoyl-CoA to form HHQ. Drees et al. (2016) demonstrated that 2-aminoacetophenone (secondary metabolite) acts as a competitive inhibitor of PqsBC and also inhibits HHQ production by *Pseudomonas putida* KT2440 (Drees et al., 2016). Moreover, PqsBC synthetic inhibitors more potent than 2-aminoacetophenone were recently described. This class of compounds were benzamide-benzimidazole derivatives and acted as dual inhibitors (acting simultaneously on PqsR and PqsBC). These PqsBC synthetic inhibitors attenuated *P. aeruginosa* PA14 virulence during infection of human lung epithelial cells and mouse macrophages. Some of the dual inhibitors reduced bacterial meropenem tolerance, specifically, the dual inhibitors with high anti-PqsR activity (Maura et al., 2017). Dual inhibitors with high anti-PqsR activity block 2-aminoacetophenone production more potently than dual inhibitors with low anti-PqsR activity, of particular interest because 2-aminoacetophenone has been associated with bacterial tolerance to antibiotics (Maura et al., 2017). Moreover, using two selective inhibitors to PqsBC, Allegretta et al. (2017) showed that in inhibitor-treated *P. aeruginosa* PA14 cells the 2-aminoacetophenone levels were higher than in non-treated bacteria. Consequently, the treatment with one of the PqsBC inhibitors favored *P. aeruginosa* PA14 tolerance to meropenem (Allegretta et al., 2017).

INHIBITION OF AUTOINDUCER PEPTIDE SYNTHESIS

In important Gram-positive pathogens including *S. aureus*, *Enteroccocus faecalis*, *Listeria monocytogenes*, *Clostridium difficile, Clostridium botulinum, Clostridium perfringens, Bacillus cereus, Streptococcus pyogenes* and others, the control of virulence factor expression is associated with peptide-based quorum sensing systems (Gray et al., 2013; Jimenez and Federle, 2014; Le and Otto, 2015; Singh et al., 2016; Ali et al., 2017). The *S. aureus* accessory gene regulator (*agr*) system and *E. faecalis fsr* quorum-sensing system are the most extensively characterized peptide-based quorum sensing systems (Gray et al., 2013; Ali et al., 2017; Tan et al., 2018).

The *S. aureus agr*-system controls the expression of several virulence factors, including RNAIII, δ-hemolysin, and phenol soluble modulins (PSMs). Transcription of the *agr* operon produces the RNA II and RNA III transcripts. Specifically, RNA II translation produces the proteins AgrA, AgrB, AgrC, and AgrD, which are the structural components of the *agr*-system, while RNAIII is involved in the post-transcriptional control of virulence factors expression and encodes δ-hemolysin (Tan et al., 2018). AgrD is the precursor of the autoinducer peptides (AIP) (AIP-I, AIP-II, AIP-III, and AIP-IV). AgrB is an endopeptidase involved in AIP maturation. The AgrB endopeptidase and the type I signal peptidase SpsB remove the C-terminal tail and N-terminal leader segment of AgrD, respectively, producing the thiolactone AIPs (LaSarre and Federle, 2013; Tan et al., 2018). The proteins AgrC/AgrA constitute a two-component system that is involved in AIP signaling. After AIPs are secreted, they bind to the histidine kinase AgrC receptor, which autophosphorylates with the subsequent transference of the phosphoryl group to the response regulator AgrA rendering phosphorylated AgrA. Phosphorylated AgrA forms a dimer, which at low concentration acts as a transcription factor that preferentially binds to the P2 promoter, triggering the production of RNAII transcripts. Consequently, the production of the *agr* components increases in an autocatalytic way (Wang and Muir, 2016; Tan et al., 2018). After phosphorylated AgrA accumulates to a threshold level, it binds to the P3 promoter stimulating the production of RNAIII transcripts. Additionally, phosphorylated AgrA binds to the *psmα* and *psmβ* promoters, stimulating the production of PSMs (Gray et al., 2013; Tan et al., 2018). Because the *agr* system operates as a positively regulated auto-loop system, in principle, it is possible to disturb AIP production through interfering with any step of the circuit.

In a study performed by Kavanaugh et al. (2007), which focused on the identification of peptidases involved in AIP biosynthesis in *S. aureus,* the type I signal peptidase SpsB was identified as having a role in the *S. aureus* AIP biosynthesis pathway. Specifically, two SpsB inhibitors [(P+1) and NIF] were developed that consisted of peptides that mimic the N-terminal cleavage site of AgrD. The inhibitor NIF showed improved stability and stronger inhibition of quorum sensing in comparison to inhibitor P+1 (Kavanaugh et al., 2007). On the other hand, it has been reported that ambuic acid (a secondary fungal metabolite) inhibits the production of AIP in *S. aureus* as well as the biosynthesis of GBAP in *E. faecalis* and the putative cyclic peptide pheromones LsrD698 and LsrD826 in *Listeria innocua* (Nakayama et al., 2009). Later Todd et al. (2016), using an ultraperformance liquid chromatography coupled to mass spectrometry (UPLC-MS) platform, showed that ambuic acid suppresses AIP-I production by a clinical isolate of methicillin-resistant *S. aureus* (MRSA), in a dose-dependent manner (Todd et al., 2016). More recently, an MRSA strain was genetically manipulated to constitutively

produce AIP-I without quorum-sensing control. Ambuic acid was found to effectively inhibit the biosynthesis of AIP-I by this strain. Interestingly, *in vivo* experiments in a murine model of intradermal MRSA challenge verified that ambuic acid attenuates MRSA pathogenesis and mediates quorum quenching *in vivo*. Moreover, ambuic acid proved effective in AIP biosynthesis inhibition of several pathogens besides *S. aureus*, i.e., *Staphylococcus saprophyticus*, *L. monocytogenes,* and *E. faecalis*, but did not affect commensal bacteria such as *Staphylococcus lugdunensis* and some *Staphylococcus epidermidis* strains. This selectivity is a desirable characteristic for therapeutic agents (Todd et al., 2017). In sum, all this evidence showed the potential of ambuic acid as an anti-virulence therapeutic agent.

Another target for the *agr*-system inhibition is the response regulator protein AgrA, which acts as *agr* operon transcriptional factor. The impairing of AgrA functionality might perturb the *agr* operon transcription and consequently AIP production as well as *agr*-controlled virulence factors production. Several chemical compounds including 2-(4-methylphenyl)-1,3-thiazole-4-carboxylic acid, 9H-xanthene-9-carboxylic acid, 4-phenoxyphenol, savirin, ω-hydroxyemodin, biaryl hydroxyketones, and norlichexanthone appear to act by blocking the binding of AgrA to the *agr* operon promoters via direct interaction with the AgrA C-terminal DNA binding domain (Leonard et al., 2012; Sully et al., 2014; Daly et al., 2015; Baldry et al., 2016; Greenberg et al., 2018). Moreover, other compounds like naphthalene derivatives and biaryl compounds potentially could bind to the AgrA N-terminal phosphoryl-binding pocket, interfering with ArgA phosphorylation and binding to DNA (Khodaverdian et al., 2013).

Recently, some of these AgrA inhibitors have shown be promising in attenuating bacterial virulence *in vivo*. In this regard, ω-hydroxyemodin (a polyhidroxyanthraquinone) inhibited *in vitro* all the *S. aureus* agr-system types (I–IV). Consequently, ω-hydroxyemodin treatment reduced the RNAIII, *psmα* and *hla* transcription without bactericidal and cytotoxic-associated effects. In addition, ω-hydroxyemodin inhibited the *S. epidermidis agr*-system and attenuated the virulence of *S. aureus* in a mouse skin and soft tissue infection model, apparently via disruption of the *arg*-system, facilitating the bacterial clearance by the host immune system (Daly et al., 2015). Previously, Sully et al. (2014), using an airpouch skin infection model and a dermonecrosis model, described *S. aureus*-attenuated virulence by savirin via *agr*-system disruption and improved host immune response. The treatment of *S. aureus* USA300 strain LAC with savirin down-regulated the expression of several *agr*-regulated virulence factors, including RNAIII, V8 protease, serine proteases, lipase, staphopain, PMSβ1, PMSα, PVL, and others, whereas it up-regulated the expression of Spa, SdrD and fibrinogen-binding protein. In addition, savirin treatment reduced α-hemolysin, protease and lipase activity. Clinical isolates (comprising the *agr*-systems I, II, III, and IV) treated with savirin down-regulated *psmα* transcript levels, and α-hemolysin activity was reduced in several MRSA and MSSA clinical isolates. Interestingly, resistance or tolerance to savirin were not observed, and the *S. epidermidis agr* system was not significantly disturbed (Sully et al., 2014). Moreover, two biaryl hydroxyketones (F12 and F19) have been reported that downregulated *hla*, *psmα* and RNAIII expression in the MRSA USA300 strain. The methicillin-resistant *Staphylococcus epidermidis* (MRSE) strain treated with F19 down-regulated AtlE, psmα and RNAIII transcript levels. F-19 protected monocyte and macrophage cells from the lysis caused by several Gram-positive pathogens. Importantly, in an MRSA wound infection model, compound F-19 potentiated β-lactam and fluoroquinolone antibiotic activity, whereas in an MRSA bacteremia/sepsis model, F-19 alone and in combination with cephalothin protected the animals from a lethal infection with MRSA (Greenberg et al., 2018). In a previous study, F-12 and F-19 treatment increased the survival time of MRSA-infected larvae, as well as when they were used in combination with β-lactam antibiotics. In addition, in mice, F-12 stimulated the healing of MRSA-infected wounds (Kuo et al., 2015). Antisense oligonucleotides that target the *agrA* mRNA have also been used to inhibit AgrA activity. Recently, antisense oligonucleotides against *agrA* mRNA were used as a strategy to quench the *agr*-system in a community-associated MRSA strain (CA-MRSA USA300 LAC). The antisense oligonucleotide treatment affected the *agrA* expression as well as the expression of several virulence factors, including *psmα*, *psmβ*, *hla,* and *pvl*. The CA-MRSA USA300 LAC strain virulence in a mouse subcutaneous infection model was attenuated by antisense oligonucleotide treatment (Da et al., 2017).

Disruption of the *agr*-system via interference with AgrC activity, in principle, could also influence AIP biosynthesis. The most exploited strategy to develop AgrC inhibitors is based on producing structural modifications in native AIP scaffold to yield AIP structural analogs (Singh et al., 2016; Wang and Muir, 2016). Some of the recently developed AgrC inhibitors are amide-bridged AIP-III analogs, in which the thioester bond was replaced by an amide bond conferring higher hydrolytic stability and solubility in aqueous media on them than their precursors. The introduction of the amide bridge did not severely affect the inhibitory potency of the lactam analogs toward *S. aureus* AgrC (type I-IV) (Tal-Gan et al., 2016). Simplified AIP-II peptidomimetics were developed from a truncated AIP-II by Vasquez et al. (2017). Some of these peptidomimetics were pan-group *S. aureus* AgrC inhibitors; however, the most soluble mimetic in aqueous media (a desirable characteristic for the inhibitors) did not show a potent inhibitory activity toward *S. aureus* AgrC (group III-IV) in comparison with the parental peptide (truncated AIP-II), but displayed an inhibitory activity similar to the parental peptide toward *S. aureus* group I, which is one of the main etiologic agents in human infections (Vasquez et al., 2017). Moreover, Karathanasi et al. (2018) described linear synthetic peptidomimetics that interfered with the *S. aureus agr*-system through competitive binding to the AgrC receptor (Karathanasi et al., 2018). Recently, other AgrC inhibitors described were *S. epidermidis* AIP and *S. lugdunensis* AIP analogs (Gordon et al., 2016; Yang et al., 2016). Furthermore, secondary metabolites such as WS9326A, WS9326B, and cochimicin II/III from actinomycetes, avellanin from *Hamigera ingelheimensis*, ngercheumicins and solonamides from *Photobacterium* sp. strain S2753 probably influence the AgrC activity via competitive inhibition (Mansson et al., 2011; Kjaerulff et al., 2013; Desouky

et al., 2015; Igarashi et al., 2015; Wang and Muir, 2016). Solonamide B showed to be effective in a mouse model for atopic dermatitis to attenuate *S. aureus* virulence via δ-toxin-induced immunopathologic response inhibition (Baldry et al., 2018).

INHIBITION OF N-ACYL-HOMOSERINE LACTONE SYNTHESIS

In Gram-negative bacteria, quorum-sensing systems based on acyl-HSLs as signal molecules are the most common. The category of acyl-HSLs (also known as autoinducer-1) comprises more than 30 different molecules that share a common structural scaffold, consisting of an acyl chain linked to a homoserine lactone ring. The acyl chains vary in length (4-18 carbons), oxidation state, and degree of saturation (LaSarre and Federle, 2013; Chan et al., 2015). The acyl-HSLs are biosynthesized mainly by the acyl-HSL synthases belonging to the Lux I family (Lux I-type acyl-HSL synthases). These synthases use as substrates S-adenosyl-L-methionine (SAM) and acylated acyl-carrier protein (acyl-ACP) and yield the respective acyl-HSL, the holo-ACP, and MTA, as products (Chung et al., 2011). The Lux I-type acyl-HSLs synthases are present in hundreds of bacterial species, and enzymes from different bacterial species may share conserved regions. Lux I-type acyl-HSLs synthases are not present in Eukarya, making them a potential target for the development of quorum-sensing inhibitors (Chan et al., 2015; Papenfort and Bassler, 2016).

The synthesis of butyryl-HSL is mediated by *P. aeruginosa* RhlI synthase using as substrates butyryl-ACP and SAM. An early study by Parsek et al. (1999) showed that the end products, MTA, and holo-ACP, and the SAM substrate analogs SAH, S-adenosylcysteine, and sinefungin, act as RhlI synthase inhibitors (Parsek et al., 1999). Another acyl-HSL synthase present in *P. aeruginosa* for which inhibitors have been reported is LasI. In a study by Lidor et al. (2015), the compound (z)-5-octylidenethiazolidine-2, 4-dione (TZD-C8) was found to inhibit biofilm formation by *P. aeruginosa* PAO1 in a dose-dependent manner, as well as to induce the downregulation of the expression of the *pqsABCDE* operon and the *lasI* gene. Therefore, potentially TZD-C8 could perturb both the quorum-sensing system based on PQS and that based on 3-oxo-C12-HSL. The *in vitro* swarming motility and PQS production of the bacteria were also affected. *In silico* evaluation of the interaction between TZD-C8 and LasI suggested that the inhibitory activity of TZD-C8 could result from its binding to the LasI activity pocket (Lidor et al., 2015). In the Gram-negative bacterium *Burkholderia glumae* the quorum-sensing signal octanoyl-L-HSL (C8-HSL) is synthesized by the acyl-HSL synthase TofI. Chung et al. (2011) found the TofI inhibitor J8-C8 from a library of acyl-HSL analogs. This compound reduced the production of C8-HSL by *B. glumae* BGR1 cells. In addition, J8-C8 inhibited C8-HSL synthesis in a dose-dependent manner and, together with MTA, had a synergistic inhibitory effect on TofI. X-ray crystal structure analyses showed that J8-C8 binds to the acyl-ACP binding site on TofI, specifically the binding site for the acyl chain, while MTA independently binds to the binding site for SAM (Chung et al., 2011). Moreover, Christensen et al. (2013) reported five compounds that inhibited *Burkholderia mallei* BmaI1 synthase and YspI synthase from *Y. pestis*, which is phylogenetically distant from *B. mallei* BmaI1 synthase. Additionally, two of the five compounds were found to reduce the production of octanoyl-HSL without affecting bacterial growth. The most potent compound [3-(4-methylpiperazin-1-yl)(pyridin-2-yl)methyl-2-phenyl-1H-indol-1-ol] acted as a noncompetitive inhibitor of BmaI1 synthase, and some analogs of this compound showed inhibitory activity. One interesting finding in this study was that one of the five inhibitory compounds selected was the cephalosporin antibiotic cefatrizine, suggesting that cephalosporin antibiotics may inhibit acyl-HSL synthases (Christensen et al., 2013).

It has been reported that thioether analogs of the thioester acyl-substrates of acyl-HSL synthase inhibit the enzyme. Specifically, octyl-ACP noncompetitively inhibited *B. mallei* BmaI1 synthase while the isopentyl-CoA competitively inhibited the *Bradyrhizobium japonicum* BjaI-synthase (Christensen et al., 2014). Recently, new diketopiperazine derivatives have been described that inhibit *Burkholderia cenocepacia* CepI acyl-HSL synthase. The most potent of these derivatives [(3S)-3-Benzyl-6-(3,6-dioxocyclohexa-1,4-dien-1-yl)piperazine-2,5-dione] acted as a non-competitive inhibitor toward both C8-ACP and SAM substrates. This finding was also supported by molecular docking analysis, which showed several high-affinity contact sites for the inhibitor on the CepI structure, but none of these sites was the SAM- and acyl substrate-binding site. Besides, some of these diketopiperazine derivative compounds did not exert an antimicrobial effect on *B. cenocepacia* J2315 but did interfere with the production of virulence factors such as proteases and siderophores. Furthermore, they perturbed biofilm formation, protected *Caenorhabditis elegans* nematodes against infection with *B. cenocepacia* J2315, and had low toxicity for HeLa cells (Scoffone et al., 2016). Recently, based on comparative proteomics approach, Buroni et al. (2018) demonstrated that *B. cenocepacia* J2315 treated with (3S)-3-benzyl-6-(3,6-dioxocyclohexa-1,4-dien-1-yl)piperazine-2,5-dione displayed a protein expression pattern quite similar to *B. cenocepacia* Δ*cepI* mutant (*B. cenocepacia* J2315 with deleted *cepI* gene). Interestingly, both the inhibitor-treated strain and the Δ*cepI* mutant overexpressed the giant cable pilus protein CblA, which has been associated with *B. cenocepacia* virulence *in vivo*. In addition, using site-directed mutagenesis and enzymatic activity inhibition approaches it was observed that the pocket around the Ser 41 residue on the CepI structure appears to be the inhibitor binding site (Buroni et al., 2018).

Quorum-quenching agents of plant origin have been identified as inhibitors of acyl-HSL synthases. Chang et al. (2014) identified salicylic acid, tannic acid, and trans-cinnamaldehyde as potential acyl-HSL synthase inhibitors. Subsequently, it was demonstrated that trans-cinnamaldehyde was an RhlI-specific inhibitor and did not affect the growth of *P. aeruginosa*. Molecular docking analysis of trans-cinnamaldehyde suggested that this inhibition might be mediated by the occupation of the substrate-binding pocket on the synthase (Chang et al., 2014). Recently, other plant-derived compounds have been identified as acyl-HSL synthase inhibitors. It was observed that carvacrol and eugenol reduce biofilm formation, the activity of plant cell wall

degrading enzymes, the expression of quorum-sensing-related genes, and virulence in the phytopathogens *Pectobacterium carotovorum* subsp. *brasiliense* Pcb1692 and *Pectobacterium aroidearum* PC1. Based on docking of these compounds to the computational models of ExpR (regulatory protein) and ExpI (acyl-HSL synthase), the mechanism of action of these quorum-quenching agents was suggested to involve direct interaction with ExpI/ExpR proteins and the consequent inhibition of acyl-HSL production (Joshi et al., 2016).

Even though most of the strategies for inhibiting signal production have targeted the acyl-HSL synthases, it is possible that other enzymes linked to the signal biosynthesis pathway could also be targeted. In this respect, it has been reported that triclosan inhibited the *P. aeruginosa* enoyl-acyl carrier protein reductase (FabI) *in vitro*. This inhibition reduced the production of butyryl-HSL because FabI supplies the butyryl-ACP necessary for RhlI synthase-mediated butyryl-HSL synthesis (Hoang and Schweizer, 1999). Since FabI is involved in the metabolism of the fatty acids (an essential process for the bacteria), inhibitory agents directed toward it could potentially exert selective pressure on the bacteria with the subsequent emergence of resistant mutants. In fact, resistance to triclosan by *P. aeruginosa* PAO1 has been reported; this resistance results from active efflux pumps and a triclosan-resistant enoyl-acyl carrier protein reductase (FabV) (Chuanchuen et al., 2003; Zhu et al., 2010; Huang et al., 2016).

FUTURE DIRECTIONS

The book *"Sun Tzu on The Art of War"* postulated that "*In the practical art of war, the best thing of all is to take the enemy's country whole and intact; to shatter and destroy it is not so good. So, too, it is better to recapture an army entire than to destroy it, to capture a regiment, a detachment or a company entire than to destroy them*" (Giles, 2000). In this light, the war of science against bacterial pathogens should not exclusively focus on novel bactericidal agents (which would destroy the enemy), but should also consider antivirulence factors (which would trap the enemy, leaving it without weapons and/or communication systems), allowing the human or animal host to subsequently eliminate the pathogens. Because quorum sensing is a critical process for controlling collective traits including lifestyle and biofilm formation, the synthetic modulators of quorum sensing seem to be the key to manipulating bacterial behavior on demand. This is particularly so in the case of pathogenic bacteria, whose virulence factors include quorum sensing mechanisms (Papenfort and Bassler, 2016).

In this Review, we have summarized the main targets for quorum sensing signal biosynthesis inhibition. The control of bacterial behavior by small molecules has been viewed as a promising strategy for the control of biofilms; and despite the differences among species, quorum sensing plays a crucial role in the infectious process. Although therapies that affect quorum sensing are less likely to select for resistance in comparison with traditional antibiotics, some cases reported in the literature show that bacteria can become resistant to quorum-sensing inhibitors (Defoirdt et al., 2010; Kalia et al., 2014; García-Contreras et al., 2016). Nevertheless, the selective pressure exerted by traditional antibiotics is higher than that of the quorum-sensing inhibitors; therefore, the latter may have longer functional lives and greater utility in treating bacterial infections than the former, which have been, in many cases, rendered ineffective by resistance. To date, few clinical trials of molecules that inhibit quorum sensing have been conducted (Papenfort and Bassler, 2016); therefore, it is still too early to assess the therapeutic potential of these molecules. Efforts to determine mechanisms of resistance and to screen for more effective inhibitors, as well as studies focusing on the *in vivo* application of such molecules, could lead to the next generation of antimicrobial agents.

AUTHOR CONTRIBUTIONS

OF, OS, CFN, and OLF contributed conception and design of the review. OF, PR, ÁP, WP, and OS wrote the manuscript. PR and ÁP made the figures. OLF and CFN revised the manuscript. All authors read and approved the submitted version.

FUNDING

This work was supported by CAPES, CNPq, FAPDF, FUNDECT, UCB, and UCDB. OS holds a postdoctoral scholarship from the National Council of Technological and Scientific Development (CNPq) and Fundação de Apoio ao Desenvolvimento do Ensino, Ciência e Tecnologia do Estado de Mato Grosso do Sul (FUNDECT)—Brazil [300583/2016-8]. This work was supported by the Ramon Areces Foundation (to CFN).

REFERENCES

Alfaro, J. F., Zhang, T., Wynn, D. P., Karschner, E. L., and Zhou, Z. S. (2004). Synthesis of LuxS inhibitors targeting bacterial cell– cell communication. *Org. Lett.* 6, 3043–3046. doi: 10.1021/ol049182i

Ali, L., Goraya, M. U., Arafat, Y., Ajmal, M., Chen, J. L., and Yu, D. (2017). Molecular mechanism of quorum-sensing in *Enterococcus faecalis*: its role in virulence and therapeutic approaches. *Int. J. Mol. Sci.* 18:E960. doi: 10.3390/ijms18050960

Allegretta, G., Maurer, C. K., Eberhard, J., Maura, D., Hartmann, R. W., Rahme, L., et al. (2017). In-depth profiling of MvfR-regulated small molecules in *Pseudomonas aeruginosa* after quorum sensing inhibitor treatment. *Front. Microbiol.* 8:924. doi: 10.3389/fmicb.2017.00924

Allegretta, G., Weidel, E., Empting, M., and Hartmann, R. W. (2015). Catechol-based substrates of chalcone synthase as a scaffold for novel inhibitors of PqsD. *Eur. J. Med. Chem.* 90, 351–359. doi: 10.1016/j.ejmech.2014.11.055

Armbruster, C. E., Hong, W., Pang, B., Dew, K.E., Juneau, R. A., Byrd, M. S., et al. (2009). LuxS promote biofilms maturation and persistence of nontypeable *Haemophilus influenzae in vivo* via modulation of lipooligoscharides on bacterial surface. *Infect. Immun.* 77, 4081–4019. doi: 10.1128/IAI.00320-09

Arnold, W. K., Savage, C. R., Antonicello, A. D., and Stevenson, B. (2015). Apparent role for *Borrelia burgdorferi* luxS during mammalian infection. *Infect. Immun.* 83:1347. doi: 10.1128/IAI.00032-15

Asfour, H. Z. (2018). Anti-quorum sensing natural compounds. *J. Microsc. Ultrastruct.* 6, 1–10. doi: 10.4103/JMAU.JMAU_10_18

Baldry, M., Nakamura, Y., Nakagawa, S., Frees, D., Matsue, H., Núñez, G., et al. (2018). Application of an agr-specific antivirulence compound as therapy for *Staphylococcus aureus*-induced inflammatory skin disease. *J. Infect. Dis.* 218, 1009–1013. doi: 10.1093/infdis/jiy259

Baldry, M., Nielsen, A., Bojer, M. S., Zhao, Y., Friberg, C., Ifrah, D., et al. (2016). Norlichexanthone reduces virulence gene expression and biofilm formation in *Staphylococcus aureus*. *PLoS ONE* 11:e0168305. doi: 10.1371/journal.pone.0168305

Bao, Y., Li, Y., Jiang, Q, Zhao, L., Xue, T., Hu, B., et al. (2013). Methylthioadenosine/S-adenosylhomocysteine nucleosidase (Pfs) of *Staphylococcus aureus* is essential for the virulence independent of LuxS/AI-2 system. *Int. J. Med. Microbiol.* 303, 190–200. doi: 10.1016/j.ijmm.2013.03.004

Bao, Y., Zhang, X., Jiang, Q., Xue, T., and Sun, B. (2015). Pfs promotes autolysis-dependent release of eDNA and biofilm formation in *Staphylococcus aureus*. *Med. Microbiol. Immunol.* 204, 215–226. doi: 10.1007/s00430-014-0357-y

Bera, A. K., Atanasova, V., Robinson, H., Eisenstein, E., Coleman, J. P., Pesci, E. C., et al. (2009). Structure of PqsD, a Pseudomonas quinolone signal biosynthetic enzyme, in complex with anthranilate. *Biochemistry* 48, 8644–8655. doi: 10.1021/bi9009055

Bikard, D., Euler, C. W., Jiang, W., Nussenzweig, P. M., Goldberg, G. W., Duportet, X., et al. (2014). Exploiting CRISPR-Cas nucleases to produce sequence-specific antimicrobials. *Nat Biotechnol.* 32, 1146–1150. doi: 10.1038/nbt.3043

Bourgeois, J. S., Zhou, D., Thurston, T. L. M., Gilchrist, J. J., and Ko, D. C. (2018). Methylthioadenosine suppresses Salmonella virulence. *Infect. Immun.* 86:e00429. doi: 10.1128/IAI.00429-18

Buroni, S., Scoffone, V. C., Fumagalli, M., Makarov, V., Cagnone, M., Trespidi, G., et al. (2018). Investigating the mechanism of action of diketopiperazines inhibitors of the *Burkholderia cenocepacia* quorum sensing synthase CepI: a site-directed mutagenesis study. *Front. Pharmacol.* 9:836. doi: 10.3389/fphar.2018.00836

Calfee, M. W., Coleman, J. P., and Pesci, E. C. (2001). Interference with Pseudomonas quinolone signal synthesis inhibits virulence factor expression by *Pseudomonas aeruginosa*. *Proc. Natl. Acad. Sci. U.S.A.* 98, 11633–11637. doi: 10.1073/pnas.201328498

Chan, K. G., Liu, Y.C., and Chang, C.Y. (2015). Inhibiting N-acyl-homoserine lactone synthesis and quenching Pseudomonas quinolone quorum sensing to attenuate virulence. *Front. Microbiol.* 6:1173. doi: 10.3389/fmicb.2015.01173

Chang, C. Y., Krishnan, T., Wang, H., Chen, Y., Yin, W. F., Chong, T. M., et al. (2014). Non-antibiotic quorum sensing inhibitors acting against N-acyl homoserine lactone synthase as druggable target. *Sci. Rep.* 4:7245. doi: 10.1038/srep07245

Chbib, C. (2017). Synthesis of isomeric analogues of S-ribosylhomocysteine analogues with homocysteine unit attached to C2 of ribose. *Bioorg. Med. Chem. Lett.* 27, 1681–1685. doi: 10.1016/j.bmcl.2017.03.004

Chbib, C., Sobczak, A. J., Mudgal, M., Gonzalez, C., Lumpuy, D., Nagaj, J., et al. (2016). S-Ribosylhomocysteine analogues modified at the ribosyl C-4 position. *J. Sulphur Chem.* 37, 307–327. doi: 10.1080/17415993.2015.1137921

Christensen, Q. H., Brecht, R. M., Dudekula, D., Greenberg, E. P., and Nagarajan, R. (2014). Evolution of acyl-substrate recognition by a family of acyl-homoserine lactone synthases. *PLoS ONE* 9:e112464. doi: 10.1371/journal.pone.0112464

Christensen, Q. H., Grove, T. L., Booker, S. J., and Greenberg, E. P. (2013). A high-throughput screen for quorum-sensing inhibitors that target acyl-homoserine lactone synthases. *Proc. Natl. Acad. Sci. U.S.A.* 110, 13815–13820. doi: 10.1073/pnas.1313098110

Chuanchuen, R., Karkhoff-Schweizer, R. R., and Schweizer, H. P. (2003). High-level triclosan resistance in *Pseudomonas aeruginosa* is solely a result of efflux. *Am. J. Infect. Control* 31, 124–127. doi: 10.1067/mic.2003.11

Chung, J., Goo, E., Yu, S., Choi, O., Lee, J., Kim, J., et al. (2011). Small-molecule inhibitor binding to an N-acyl-homoserine lactone synthase. *Proc. Natl. Acad. Sci. U.S.A.* 108, 12089–12094. doi: 10.1073/pnas.1103165108

Citorik, R. J., Mimee, M., and Lu, T. K. (2014). Sequence-specific antimicrobials using efficiently delivered RNA-guided nucleases. *Nat. Biotechnol.* 32, 1141–1145. doi: 10.1038/nbt.3011

Coleman, J. P., Hudson, L. L., McKnight, S. L., Farrow, J. M. III., Calfee, M. W., Lindsey, C. A., et al. (2008). *Pseudomonas aeruginosa* PqsA is an anthranilate-coenzyme A ligase. *J. Bacteriol.* 190:1247. doi: 10.1128/JB.01140-07

Da, F., Yao, L., Su, Z., Hou, Z., Li, Z., Xue, X., et al. (2017). Antisense locked nucleic acids targeting agr inhibit quorum sensing and pathogenesis of community-associated methicillin-resistant *Staphylococccus aureus*. *J. Appl. Microbiol.* 122, 257–267. doi: 10.1111/jam.13321

Daly, S. M., Elmore, B. O., Kavanaugh, J. S., Triplett, K. D., Figueroa, M., Raja, H. A., et al. (2015). ω-Hydroxyemodin limits *Staphylococcus aures* quorum sensing-mediated pathogenesis and immflamation. *Antimicrob. Agents Chemother.* 59, 2223–2235. doi: 10.1128/AAC.04564-14

Daly, S. M., Joyner, J. A., Triplett, K. D., Elmore, B. O., Pokhrel, S., Frietze, K. M., et al. (2017). VLP-based vaccine induces immune control of *Staphylococcus aureus* virulence regulation. *Sci. Rep.* 7:637. doi: 10.1038/s41598-017-00753-0

De Lay, N., and Gottesman, S. (2009). The Crp-activated small non-coding regulatory RNA CyaR (RyeE) links nutritional status to group behavior. *J. Bacteriol.* 191, 461–476. doi: 10.1128/JB.01157-08

Defoirdt, T. (2018). Quorum-sensing systems as targets for antivirulence therapy. *Trends Microbiol.* 26, 313–328. doi: 10.1016/j.tim.2017.10.005

Defoirdt, T., Boon, N., and Bossier, P. (2010). Can bacteria evolve resistance to quorum sensing disruption? *PLoS Pathog.* 6:e1000989. doi: 10.1371/journal.ppat.1000989

Desouky, S. E., Shojima, A., Singh, R. P., Matsufuji, T., Igarashi, Y., Suzuki, T., et al. (2015). Cyclodepsipeptides produced by actinomycetes inhibit cyclic-peptide-mediated quorum sensing in Gram-positive bacteria. *FEMS Microbiol. Lett.* 362:fvn109. doi: 10.1093/femsle/fnv109

Déziel, E., Gopalan, S., Tampakaki, A. P., Lépine, F., Padfield, K. E., Saucier, M., et al. (2005). The contribution of MvfR to *Pseudomonas aeruginosa* pathogenesis and quorum sensing circuitry regulation: multiple quorum sensing-regulated genes are modulated without affecting lasRI, rhlRI or the production of N-acyl-l-homoserine lactones. *Mol. Microbiol.* 55, 998–1014. doi: 10.1111/j.1365-2958.2004.04448.x

Déziel, E., Lépine, F., Milot, S., He, J., Mindrinos, M. N., Tompkins, R. G., et al. (2004). Analysis of *Pseudomonas aeruginosa* 4-hydroxy-2-alkylquinolines (HAQs) reveals a role for 4-hydroxy-2-heptylquinoline in cell-to-cell communication. *Proc. Natl. Acad. Sci. U.S.A.* 101, 1339–1344. doi: 10.1073/pnas.0307694100

Dickey, S. W., Cheung, G. Y. C., and Otto, M. (2017). Different drugs for bad bugs: antivirulence strategies in the age of antibiotic resistance. *Nat. Rev. Drug Discov.* 16, 457–471. doi: 10.1038/nrd.2017.23

Drees, S. L., Li, C., Prasetya, F., Saleem, M., Dreveny, I., Williams, P., et al. (2016). PqsBC, a condensing enzyme in the biosynthesis of the *Pseudomonas aeruginosa* quinolone signal CRYSTAL STRUCTURE, INHIBITION, AND REACTION MECHANISM. *J. Biol. Chem.* 291, 6610–6624. doi: 10.1074/jbc.M115.708453

Duanis-Assaf, D., Steinberg, D., Chai, Y., and Shemesh, M. (2016). The LuxS based quorum sensing governs lactose induced biofilm formation by *Bacillus subtilis*. *Front. Microbiol.* 6:1517. doi: 10.3389/fmicb.2015.01517

Dulcey, C. E., Dekimpe, V., Fauvelle, D. A., Milot, S., Groleau, M. C., Doucet, N., et al. (2013). The end of an old hypothesis: the Pseudomonas signaling molecules 4-hydroxy-2-alkylquinolines derive from fatty acids, not 3-ketofatty acids. *Chem. Biol.* 20, 1481–1491. doi: 10.1016/j.chembiol.2013.09.021

Evans, G. B., Tyler, P. C., and Scharmm, V. L. (2018). Immucillins in infectious diseases. *ACS Infect. Dis.* 4, 107–117. doi: 10.1021/acsinfecdis.7b00172

Fetzner, S. (2015). Quorum quenching enzymes. *J. Biotechnol.* 201, 2–14. doi: 10.1016/j.jbiotec.2014.09.001

Fitts, E. C., Andersson, J. A., Kirtley, M. L., Sha, J., Erova, T. E., Chauhan, S., et al. (2016). New insights into Autoinducer-2 signaling as a virulence regulator in a mouse model of pneumonic plague. *mSphere* 1:e00342-16. doi: 10.1128/mSphere.00342-16

Gallagher, L. A., McKnight, S. L., Kuznetsova, M. S., Pesci, E. C., and Manoil, C. (2002). Functions required for extracellular quinolone signaling by *Pseudomonas aeruginosa*. *J. Bacteriol.* 184, 6472–6480. doi: 10.1128/JB.184.23.6472-6480.2002

García-Contreras, R., Maeda, T., and Wood, T. K. (2016). Can resistance against quorum-sensing interference be selected? *ISME J.* 10, 4–10. doi: 10.1038/ismej.2015.84

García-Contreras, R., Martínez-Vázquez, M., Velázquez-Guadarrama, N., Villegas-Pañeda, A. G., Hashimoto, T., Maeda, T., et al. (2013). Resistance to the quorum-quenching compounds brominated furanone C-30 and 5-fluorouracil in *Pseudomonas aeruginosa* clinical isolates. *Pathog. Dis.* 68, 8–11. doi: 10.1111/2049-632X.12039

García-Contreras, R., Peréz-Eretza, B., Jasso-Chávez, R., Lira-Silva, E., Roldán-Sánchez, J. A., González-Valdez, A., et al. (2015). High variability in quorum quenching and growth inhibition by furanone C-30 in *Pseudomonas aeruginosa* clinical isolates from cystic fibrosis patients. *Pathog. Dis.* 73:ftv040. doi: 10.1093/femspd/ftv040

Giles, L. (2000). *Sun Tzu on The Art of War: The Oldest Military Treatise in the World*. Leicester: Allandale Online Publishing, 8. Available online at: https://sites.ualberta.ca/~enoch/Readings/The_Art_Of_War.pdf

Gopishetty, B., Zhu, J., Rajan, R., Sobczak, A. J., Wnuk, S. F., Bell, C. E., et al. (2009). Probing the catalytic mechanism of S-ribosylhomocysteinase (LuxS) with catalytic intermediates and substrate analogues. *J. Am. Chem. Soc.* 131, 1243–1250. doi: 10.1021/ja808206w

Gordon, C. P., Olson, S. D., Lister, J. L., Kavanaugh, J. S., and Horswill, A. R. (2016). Truncated autoinducing peptides as antagonists of *Staphylococcus lugdunensis* quorum sensing. *J. Med. Chem.* 59, 8879–8888. doi: 10.1021/acs.jmedchem.6b00727

Gray, B., Hall, P., and Gresham, H. (2013). Targeting agr- and agr-like quorum sensing systems for development of common therapeutics to treat multiple gram-positive bacterial infections. *Sensor* 13, 5130–5166. doi: 10.3390/s130405130

Greenberg, M., Kuo, D., Jankowsky, E., Long, L., Hager, C., Bandi, K., et al. (2018). Small molecule AgrA inhibitors F12 and F19 act as antivirulence agents against Gram-positive pathogens. *Sci. Rep.* 8:14578. doi: 10.1038/s41598-018-32829-w

Greene, A. C. (2018). CRISPR-based antibacterials: transforming bacterial defense into offense. *Trends Biotechnol.* 36, 127–130. doi: 10.1016/j.tibtech.2017.10.021

Guo, M., Gamby, S., Zheng, Y., and Sintim, H. O. (2013). Small molecule inhibitors of AI-2 signaling in bacteria: state-of-the-art and future perspectives for anti-quorum sensing agents. *Int. J. Mol. Sci.* 14, 17694–17728. doi: 10.3390/ijms140917694

Gutierrez, J. A., Crowder, T., Rinaldo-Matthis, A., Ho, M. C., Almo, S. C., and Schramm, V. L. (2009). Transition state analogs of 5′-methylthioadenosine nucleosidase disrupt quorum sensing. *Nat. Chem. Biol.* 5, 251–257. doi: 10.1038/nchembio.153

Gutierrez, J. A., Luo, M., Singh, V., Li, L., Brown, R. L., Norris, G. E., et al. (2007). Picomolar inhibitors as transition-state probes of 5′-methylthioadenosine nucleosidases. *ACS Chem. Biol.* 2, 725–734. doi: 10.1021/cb700166z

Haapalainen, A. M., Thomas, K., Tyler, P. C., Evans, G. B., Almo, S. C., and Schramm, V. L. (2013). *Salmonella enterica* MTAN at 1.36 Å resolution: a structure-based design of tailored transition state analogs. *Structure* 6, 963–974. doi: 10.1016/j.str.2013.04.009

Han, T., Li, Y., Shan, Q., Liang, W., Hao, W., Li, Y., et al. (2017). Characterization of S-adenosylhomocysteine/Methylthioadenosine nucleosidase on secretion of AI-2 and biofilm formation of *Escherichia coli*. *Microb. Pathog.* 108, 78–84. doi: 10.1016/j.micpath.2017.05.015

Han, X., Liu, L., Fan, G., Zhang, Y., Xu, D., Zuo, J., et al. (2015). *Riemerella anatipestifer* lacks luxS, but can uptake exogenous autoinducer-2 to regulate biofilm formation. *Res. Microbiol.* 166, 486–483. doi: 10.1016/j.resmic.2015.06.004

Han, X., and Lu, C. (2009). Biological activity and identification of a peptide inhibitor of LuxS from *Streptococcus suis* serotype 2. *FEMS Microbiol. Lett.* 294, 16–23. doi: 10.1111/j.1574-6968.2009.01534.x

Haque, S., Ahmad, F., Dar, S. A., Jawed, A., Mandal, R. K., Wahid, M., et al. (2018). Developments in strategies for quorum sensing virulence factor inhibition to combat bacterial drug resistance. *Microb. Pathog.* 121, 293–302. doi: 10.1016/j.micpath.2018.05.046

Hardie, K. R., and Heurlier, K. (2008). Establishing bacterial communities by 'word of mouth': LuxS and autoinducer 2 in biofilm development. *Nat. Rev. Microbiol.* 6, 635–643. doi: 10.1038/nrmicro1916

Heurlier, K., Vendeville, A., Halliday, N., Green, A, Winzer, K., Tang, C. M., et al. (2009). Growth deficiencies of *Nisseria meningitidis* pfs and luxS mutants are not due to inactivaction of quorum sensing. *J. Bacteriol.* 191:1293. doi: 10.1128/JB.01170-08

Hinsberger, S., de Jong, J. C., Groh, M., Haupenthal, J., and Hartmann, R. W. (2014). Benzamidobenzoic acids as potent PqsD inhibitors for the treatment of *Pseudomonas aeruginosa* infections. *Eur. J. Med. Chem.* 76, 343–351. doi: 10.1016/j.ejmech.2014.02.014

Hirakawa, H., and Tomita, H. (2013). Interference of bacterial cell-to-cell communication: a new concept of antimicrobial chemotherapy breaks antibiotic resistance. *Front. Microbiol.* 4:114. doi: 10.3389/fmicb.2013.00114

Hoang, T. T., and Schweizer, H. P. (1999). Characterization of *Pseudomonas aeruginosa* enoyl-acyl carrier protein reductase (FabI): a target for the antimicrobial triclosan and its role in acylated homoserine lactone synthesis. *J. Bacteriol.* 181, 5489–5497.

Hu, X., Wang, Y., Gao, L., Jiang, W., Lin, W., Niu, C., et al. (2018). The impairment of methyl metabolism from luxS mutation of *Streptococcus mutans*. *Front. Microbiol.* 9:404. doi: 10.3389/fmicb.2018.00404

Huang, Y. H., Lin, J. S., Ma, J. C., and Wang, H. H. (2016). Functional characterization of triclosan-resistant enoyl-acyl-carrier protein reductase (FabV) in *Pseudomonas aeruginosa*. *Front. Microbiol.* 7:1903. doi: 10.3389/fmicb.2016.01903

Igarashi, Y., Gohda, F., Kadoshima, T., Fukuda, T., Hanafusa, T., Shojima, A., et al. (2015). Avellanin C, an inhibitor of quorum-sensing signaling in *Staphylococcus aureus*, from *Hamigera ingelheimensis*. *J. Antibiot.* 68, 707–710. doi: 10.1038/ja.2015.50

Ji, C., Sharma, I., Pratihar, D., Hudson, L. L., Maura, D., Guney, T., et al. (2016). Designed small-molecule inhibitors of the anthranilyl-CoA synthetase PqsA block quinolone biosynthesis in *Pseudomonas aeruginosa*. *ACS Chem. Biol.* 11, 3061–3067. doi: 10.1021/acschembio.6b00575

Jian, T., and Li, M. (2013). Quorum sensing inhibitors: a patent review. *Expert Opin. Ther. Pat.* 23, 867–894. doi: 10.1517/13543776.2013.779674

Jimenez, J. C., and Federle, M. J. (2014). Quorum sensing in group A Streptococcus. *Front. Cell. Infect. Microbiol.* 4:127. doi: 10.3389/fcimb.2014.00127

Joshi, J. R., Khazanov, N., Senderowitz, H., Burdman, S., Lipsky, A., and Yedidia, I. (2016). Plant phenolic volatiles inhibit quorum sensing in pectobacteria and reduce their virulence by potential binding to ExpI and ExpR proteins. *Sci. Rep.* 6:38126. doi: 10.1038/srep38126

Kalia, V. C., Wood, T. K., and Kumar, P. (2014). Evolution of resistance to quorum-sensing inhibitors. *Microb. Ecol.* 68, 13–23. doi: 10.1007/s00248-013-0316-y

Kang, S., Kim, J., Hur, J. K., and Lee, S. S. (2017). CRISPR-based genome editing of clinically important *Escherichia coli* SE15 isolated from indwelling urinary catheters of patients. *J. Med. Microbiol.* 66, 18–25. doi: 10.1099/jmm.0.000406

Kang, X., Zhao, Y., Jiang, D., Li, X., Wang, X., Wu, Y., et al. (2014). Crystal structure and biochemical studies of *Brucella melitensis* 5′-methylthioadenosine/S-adenosylhomocysteine nucleosidase. *Biochem. Biophys. Res. Commun.* 446, 965–970. doi: 10.1016/j.bbrc.2014.03.045

Karathanasi, G., Bojer, M. S., Baldry, M., Johannessen, B. A., Wolff, S., Greco, I., et al. (2018). Linear peptidomimetics as potent antagonists of *Staphylococcus aureus* agr quorum sensing. *Sci Rep.* 8:3562. doi: 10.1038/s41598-018-21951-4

Kaur, A., Capalash, N., and Sharma, P. (2018). Quorum sensing in thermophiles: prevalence of autoinducer-2 system. *BMC Microbiol.* 18:62. doi: 10.1186/s12866-018-1204-x

Kavanaugh, J. S., Thoendel, M., and Horswill, A. R. (2007). A role for type I signal peptidase in *Staphylococcus aureus* quorum sensing. *Mol. Microbiol.* 65, 780–798. doi: 10.1111/j.1365-2958.2007.05830.x

Khodaverdian, V., Pesho, M., Truitt, B., Bollinger, L., Patel, P., Nithianantham, S., et al. (2013). Discovery of antivirulence agents against methicillin-resistant *Staphylococcus aures*. *Antimicrob. Agents Chemother.* 57, 3645–3652. doi: 10.1128/AAC.00269-13

Kim, B., Park, J. S., Choi, H. Y., Yoon, S. S., and Kim, W. G. (2018). Terrein is an inhibitor of quorum sensing and c-di-GMP in *Pseudomonas aeruginosa*: a connection between quorum sensing and c-di-GMP. *Sci. Rep.* 8:8617. doi: 10.1038/s41598-018-26974-5

Kim, K., Kim, Y. U., Koh, B. H., Hwang, S. S., Kim, S. H., Lépine, F., et al. (2010). HHQ and PQS, two *Pseudomonas aeruginosa* quorum-sensing molecules, down-regulate the innate immune responses through the nuclear factor-κB pathway. *Immunology* 129, 578–588. doi: 10.1111/j.1365-2567.2009.03160.x

Kjaerulff, L., Nielsen, A., Mansson, M., Gram, L., Larsen, T. O., Ingmer, H., et al. (2013). Identification of four new agr quorum sensing-interfering

cyclodepsipeptides from a marine Photobacterium. *Mar. Drugs*. 11, 5051–5062. doi: 10.3390/md11125051

Komor, U., Bielecki, P., Loessner, H., Rohde, M., Wolf, K., Westphal, K., et al. (2012). Biofilm formation by *Pseudomonas aeruginosa* in solid murine tumors–a novel model system. *Microbes Infect.* 14, 951–958. doi: 10.1016/j.micinf.2012.04.002

Kong, C., Neoh, H. M., and Nathan, S. (2016). Targeting *Staphylococcus aureus* toxins: a potential form of anti-virulence therapy. *Toxins* 8:E72. doi: 10.3390/toxins8030072

Kuo, D., Yu, G., Hoch, W., Gabay, D., Long, L., Ghannoum, M., et al. (2015). Novel quorum-quenching agents promote methicillin-resistant *Staphylococcus aureus* (MRSA) wound healing and sensitize MRSA to β-lactam antibiotics. *Antimicrob. Agents Chemother.* 59, 1512–1518. doi: 10.1128/AAC.04767-14

Laganenka, L., Colin, R., and Sourjik, V. (2016). Chemotaxis towards autoinducer 2 mediates autoaggregation in *Escherichia coli*. *Nat. Commun.* 7:12984. doi: 10.1038/ncomms12984

Laganenka, L., and Sourjik, V. (2017). Autoinducer 2-dependent *Escherichia coli* biofilm formation is enhanced in a dual-species co-culture. *Appl. Environ. Microbiol.* 84:AEM02638–17. doi: 10.1128/AEM.02638-17

LaSarre, B., and Federle, M. J. (2013). Exploiting quorum sensing to confuse bacterial pathogens. *Microbiol. Mol. Biol. Rev.* 77, 73–111. doi: 10.1128/MMBR.00046-12

Le, K. Y., and Otto, M. (2015). Quorum-sensing regulation in staphylococci-an overview. *Front. Microbiol.* 6:1174. doi: 10.3389/fmicb.2015.01174

Lebeer, S., De Keersmaecker, S. C., Verhoeven, T. L., Fadda, A. A., Marchal, K., and Vanderleyden, J. (2007). Functional analysis of luxS in the probiotic strain *Lactobacillus rhamnosus* GG reveals a central metabolic role important for growth and biofilm formation. *J. Bacteriol.* 189:860. doi: 10.1128/JB.01394-06

Lee, J. E., Cornell, K. A., Riscoe, M. K., and Howell, P. L. (2003). Structure of *Escherichia coli* 5′-Methylthioadenosine/S-Adenosylhomocysteine nucleosidase inhibitor complexes provide insight into the conformational changes required for substrate binding and catalysis. *J. Biol. Chem.* 278, 8761–8770. doi: 10.1074/jbc.M210836200

Lee, J. E., Settembre, E. C., Cornell, K. A., Riscoe, M. K., Sufrin, J. R., Ealick, S. E., et al. (2004). Structural comparison of MTA phosphorylase and MTA/AdoHcy nucleosidase explains substrate preferences and identifies regions exploitable for inhibitor design. *Biochemistry* 43, 5159–5169. doi: 10.1021/bi035492h

Leonard, P. G., Bezar, I. F., Sidote, D. J., and Stock, A. M. (2012). Identification of a hydrophobic cleft in the LytTR domain of AgrA as a locus for small molecule interactions that inhibit DNA binding. *Biochemestry* 51, 10035–10043. doi: 10.1021/bi3011785

Lesic, B., Lépine, F., Déziel, E., Zhang, J., Zhang, Q., Padfield, K., et al. (2007). Inhibitors of pathogen intercellular signals as selective anti-infective compounds. *PLoS Pathog.* 3:e126. doi: 10.1371/journal.ppat.0030126

Li, H., Li, X., Song, C., Zhang, Y., Wang, Z., Liu, Z., et al. (2017). Autoinducer-2 facilitates *Pseudomonas aeruginosa* PAO1 pathogenicity *in vitro* and *in vivo*. *Front. Microbiol.* 8:1944. doi: 10.3389/fmicb.2017.01944

Li, H., Li, X., Wang, Z., Fu, Y., Ai, Q., Dong, Y., et al. (2015). Autoinducer-2 regulates *Pseudomonas aeruginosa* PAO1 biofilm formation and virulence production in a dose-dependent manner. *BMC Microbiol.* 15:192. doi: 10.1186/s12866-015-0529-y

Lidor, O., Al-Quntar, A., Pesci, E. C., and Steinberg, D. (2015). Mechanistic analysis of a synthetic inhibitor of the *Pseudomonas aeruginosa* LasI quorum-sensing signal synthase. *Sci. Rep.* 5:16569. doi: 10.1038/srep16569

Liu, R. (2012). *Synthesis of S-Ribosyl-l-Homocysteine and Analogs Modified at the Homocysteine-C3 Position*. Master's thesis, San Fransisco, CA, University of San Fransisco.

Longshaw, A. I., Adanitsch, F., Gutierrez, J. A., Evans, G. B., Tyler, P. C., and Schramm, V. L. (2010). Design and synthesis of potent "sulfur-free" transition state analogue inhibitors of 5′-methylthioadenosine nucleosidase and 5′-methylthioadenosine phosphorylase. *J. Med. Chem.* 53, 6730–6746. doi: 10.1021/jm100898v

Ma, L., Feng, S., Fuente-Núñez, C., Hancock, R. E. W., and Lu, X. (2018). Development of moleculary imprinted polymers to block quorum sensing and inhibit bacterial biofilm formation. *ACS Appl. Mater. Interfaces*. 10, 18450–18457. doi: 10.1021/acsami.8b01584

Ma, R., Qiu, S., Jiang, Q., Sun, H., Xue, T., Cai, G., et al. (2017). AI-2 quorum sensing negatively regulates rbf expression and biofilm formation in *Staphylococccus aureus*. *Int. J. Med. Microbiol.* 307, 257–267. doi: 10.1016/j.ijmm.2017.03.003

Ma, Y., Hao, L., Ke, H., Liang, Z., Ma, J., Liu, Z., et al. (2017). LuxS/AI-2 in *Streptococcus agalactiae* reveals a key role in acid tolerance and virulence. *Res. Vet. Sci*. 115, 501–507. doi: 10.1016/j.rvsc.2017.07.032

Maeda, T., García-Contreras, R., Pu, M., Sheng, L., Garcia, L.R., Tomás, M., et al. (2012). Quorum quenching quandary: resistance to antivirulence compounds. *ISME J*. 6, 493–501. doi: 10.1038/ismej.2011.122

Malladi, V. L., Sobczak, A. J., Meyer, T. M., Pei, D., and Wnuk, S. F. (2011). Inhibition of LuxS by S-ribosylhomocysteine analogues containing a [4-aza] ribose ring. *Bioorg. Med. Chem.* 19, 5507–5519. doi: 10.1016/j.bmc.2011.07.043

Mansson, M., Nielsen, A., Kjaerulff, L., Gotfredsen, C. H., Wietz, M., Ingmer, H., et al. (2011). Inhibition of virulence gene expression in *Staphylococcus aureus* by novel depsipeptides from a marine photobacterium. *Mar. Drugs*. 9, 2537–2552. doi: 10.3390/md9122537

Maura, D., Drees, S. L., Bandyopadhaya, A., Kitao, T., Negri, M., Starkey, M., et al. (2017). Polypharmacology approaches against the *Pseudomonas aeruginosa* MvfR regulon and their application in blocking virulence and antibiotic tolerance. *ACS Chem. Biol.* 12, 1435–1443. doi: 10.1021/acschembio.6b01139

Munguia, J., and Nizet, V. (2017). Pharmacological targeting of the host–pathogen interaction: alternatives to classical antibiotics to combat drug-resistant superbugs. *Trends Pharmacol. Sci.* 38, 473–488. doi: 10.1016/j.tips.2017.02.003

Nakayama, J., Uemura, Y., Nishiguchi, K., Yoshimura, N., Igarashi, Y., and Sonomoto, K. (2009). Ambuic acid inhibits the biosynthesis of cyclic peptide quormones in gram-positive bacteria. *Antimicrob. Agents Chemother.* 53, 580–586. doi: 10.1128/AAC.00995-08

Namanja-Magliano, H. A., Evans, G. B., Harijan, R. K., Tyler, P. C., and Schramm, V. L. (2017). Transition state analogue inhibitors of 5′-deoxyadenosine/5′-methylthioadenosine nucleosidase from *Mycobacterium tuberculosis*. *Biochemistry* 56, 5090–5098. doi: 10.1021/acs.biochem.7b00576

Namanja-Magliano, H. A., Stratton, C. F., and Schramm, V. L. (2016). Transition state structure and inhibition of Rv0091, a 5′-Deoxyadenosine/5′-methylthioadenosine nucleosidase from *Mycobacterium tuberculosis*. *ACS Chem. Biol.* 11, 1669–1676. doi: 10.1021/acschembio.6b00144

Nandi, S. (2016). Recent advances in ligand and structure based screening of potent quorum sensing inhibitors against antibiotic resistance induced bacterial virulence. *Recent Pat. Biotechnol.* 10, 195–216. doi: 10.2174/1872208310666160728104450

Niu, C., Robbins, C. M., Pittman, K. J., Osborn, J. L., Stubblefield, B. A., Simmons, R. B., et al. (2013). LuxS influences *Escherichia coli* biofilm formation through autoinducer-2-dependent and autoinducer-2-independent modalities. *FEMS Microbiol. Ecol*. 83, 778–791. doi: 10.1111/1574-6941.12034

Pang, B., Armbruster, C. E., Foster, G., Learman, B. S., Gandhi, U., and Swords, W. E. (2018). Autoinducer 2 (AI-2) production by nontypeable *Haemophilus influenzae* 86-028NP promotes expression of a predicted glycosyltransferase that is a determinant of biofilm maturation, prevention of dispersal, and persistence *in vivo*. *Infect. Immun.* 86:e00506-18. doi: 10.1128/IAI.00506-18

Papenfort, K., and Bassler, B. L. (2016). Quorum sensing signal–response systems in Gram-negative bacteria. *Nat. Rev. Microbiol.* 14, 576–588. doi: 10.1038/nrmicro.2016.89

Park, H., Lee, K., Yeo, S., Shin, H., and Holzapfel, W. H. (2017). Autoinducer-2 quorum sensing influences viability of *Escherichia coli* O157:H7 under osmotic and *in vitro* gastrointestinal stress conditions. *Front. Microbiol.* 8:1077. doi: 10.3389/fmicb.2017.01077

Parsek, M. R., Val, D. L., Hanzelka, B. L., Cronan, J. E Jr., and Greenberg, E. P. (1999). Acyl homoserine-lactone quorum-sensing signal generation. *Proc. Natl. Acad. Sci. U.S.A.* 96, 4360–4365. doi: 10.1073/pnas.96.8.4360

Parveen, N., and Cornell, K. A. (2011). Methylthioadenosine/S-adenosylhomocysteine nucleosidase, a critical enzyme for bacterial metabolism. *Mol. Microbiol.* 79, 7–20. doi: 10.1111/j.1365-2958.2010.07455.x

Pei, D., and Zhu, J. (2004). Mechanism of action of S-ribosylhomocysteinase. *Curr. Opin. Chem. Biol.* 8, 492–497. doi: 10.1016/j.cbpa.2004.08.003

Pereira, C. S., Thompson, J. A., and Xavier, K. B. (2013). AI-2-mediated signalling in bacteria. *FEMS Microbiol. Rev.* 37, 156–181. doi: 10.1111/j.1574-6976.2012.00345.x

Pérez-Rodríguez, I., Bolognini, M., Ricci, J., Bini, E., and Vetriani, C. (2015). From deep-sea volcanoes to human pathogens: a conserved quorum-sensing signal in Epsilonproteobacteria. *ISME J.* 9, 1222–1234. doi: 10.1038/ismej.2014.214

Pistorius, D., Ullrich, A., Lucas, S., Hartmann, R. W., Kazmaier, U., and Müller, R. (2011). Biosynthesis of 2-Alkyl-4 (1H)-Quinolones in *Pseudomonas aeruginosa*: potential for therapeutic interference with pathogenicity. *Chembiochem* 12, 850–853. doi: 10.1002/cbic.201100014

Qi, L. S., Larson, M. H., Gilbert, L. A., Doudna, J. A., Weissman, J. S., Arkin, A. P., et al. (2013). Repurposing CRISPR as an RNA guide plataform for sequence-specific control of gene expression. *Cell* 152, 1173–1183. doi: 10.1016/j.cell.2013.02.022

Quave, C. L., and Horswill, A. R. (2013). Flipping the switch: tools for detecting small molecules inhibitors of staphylococcal virulence. *Front. Microbiol.* 5:706. doi: 10.3389/fmicb.2014.00706

Quave, C. L., Lyles, J. T., Kavanaugh, J. S., Nelson, K., Parlet, C. P., Crosby, H. A., et al. (2015). Castanea sativa (European Chestnut) leaf extract rich in ursene and oleanene derivatives block *Sthaphylococcus aureus* virulence and pathogenesis without detectble resistance. *PLoS ONE* 10:e0136486. doi: 10.1371/journal.pone.0136486

Reuter, K., Steinbach, A., and Helms, V. (2016). Interfering with bacterial quorum sensing. *Perspect. Med. Chem.* 8, 1–15. doi: 10.4137/PMC.S13209

Ronning, D. R., Iacopelli, N. M., and Mishra, V. (2010). Enzyme–ligand interactions that drive active site rearrangements in the *Helicobacter pylori* 5′-methylthioadenosine/S-adenosylhomocysteine nucleosidase. *Protein Sci.* 19, 2498–2510. doi: 10.1002/pro.524

Sahner, J. H., Brengel, C., Storz, M. P., Groh, M., Plaza, A., Müller, R., et al. (2013). Combining *in silico* and biophysical methods for the development of *Pseudomonas aeruginosa* quorum sensing inhibitors: an alternative approach for structure-based drug design. *J. Med. Chem.* 56, 8656–8664. doi: 10.1021/jm401102e

Sahner, J. H., Empting, M., Kamal, A., Weidel, E., Groh, M., Börger, C., et al. (2015). Exploring the chemical space of ureidothiophene-2-carboxylic acids as inhibitors of the quorum sensing enzyme PqsD from *Pseudomonas aeruginosa*. *Eur. J. Med. Chem.* 96, 14–21. doi: 10.1016/j.ejmech.2015.04.007

Scoffone, V. C., Chiarelli, L. R., Makarov, V., Brackman, G., Israyilova, A., Azzalin, A., et al. (2016). Discovery of new diketopiperazines inhibiting *Burkholderia cenocepacia* quorum sensing *in vitro* and *in vivo*. *Sci. Rep.* 6:32487. doi: 10.1038/srep32487

Shen, G., Rajan, R., Zhu, J., Bell, C. E., and Pei, D. (2006). Design and synthesis of substrate and intermediate analogue inhibitors of S-ribosylhomocysteinase. *J. Med. Chem.* 49, 3003–3011. doi: 10.1021/jm060047g

Silva, A. J., Parker, W. B., Allan, P. W., Ayala, J. C., and Benitez, J. A. (2015). Role of methylthioadenosine /S-adenosylhomocysteine nucleosidase in *Vibrio cholerae* in cellular communication and biofilm development. *Biochem. Biophys. Res. Commun.* 461, 65–69. doi: 10.1016/j.bbrc.2015.03.170

Singh, R.P., Desouky, S. E., and Nakayama, J. (2016). Quorum quenching strategy targeting Gram-positive pathogenic bacteria. *Adv. Exp. Med. Biol.* 901, 109–130. doi: 10.1007/5584_2016_1

Singh, V., Evans, G. B., Lenz, D. H., Mason, J. M., Clinch, K., Mee, S., et al. (2005a). Femtomolar transition state analogue inhibitors of 5′-methylthioadenosine/S-adenosylhomocysteine nucleosidase from *Escherichia coli*. *J. Biol. Chem.* 280, 18265–18273. doi: 10.1074/jbc.M414472200

Singh, V., Lee, J. E., Núñez, S., Howell, P. L., and Schramm, V. L. (2005b). Transition state structure of 5 ′-methylthioadenosine/S-adenosylhomocysteine nucleosidase from *Escherichia coli* and its similarity to transition state analogues. *Biochemistry* 44, 11647–11659. doi: 10.1021/bi050863a

Singh, V., Shi, W., Almo, S. C., Evans, G. B., Furneaux, R. H., Tyler, P. C., et al. (2006). Structure and inhibition of a quorum sensing target from *Streptococcus pneumoniae*. *Biochemistry* 45, 12929–12941. doi: 10.1021/bi061184i

Siu, K. K., Lee, J. E., Smith, G. D., Horvatin-Mrakovcic, C., and Howell, P. L. (2008). Structure of *Staphylococcus aureus* 5′-methylthioadenosine/S-adenosylhomocysteine nucleosidase. *Acta Crystallogr. Sect. F Struct. Biol. Cryst. Commun.* 64, 343–350. doi: 10.1107/S1744309108009275

Sobczak, A. J., Chbib, C., and Wnuk, S. F. (2015). S-ribosylhomocysteine analogs containing a [4-thio] ribose ring. *Carbohydr. Res.* 415, 39–47. doi: 10.1016/j.carres.2015.07.005

Storz, M. P., Allegretta, G., Kirsch, B., Empting, M., and Hartmann, R. W. (2014). From *in vitro* to in cellulo: structure–activity relationship of (2-nitrophenyl) methanol derivatives as inhibitors of PqsD in *Pseudomonas aeruginosa*. *Org. Biomol. Chem.* 12, 6094–6104. doi: 10.1039/C4OB00707G

Storz, M. P., Brengel, C., Weidel, E., Hoffmann, M., Hollemeyer, K., Steinbach, A., et al. (2013). Biochemical and biophysical analysis of a chiral PqsD inhibitor revealing tight-binding behavior and enantiomers with contrary thermodynamic signatures. *ACS Chem. Biol.* 8, 2794–2801. doi: 10.1021/cb400530d

Storz, M. P., Maurer, C. K., Zimmer, C., Wagner, N., Brengel, C., de Jong, J. C., et al. (2012). Validation of PqsD as an anti-biofilm target in *Pseudomonas aeruginosa* by development of small-molecule inhibitors. *J. Am. Chem. Soc.* 134, 16143–16146. doi: 10.1021/ja3072397

Sully, E. K., Malachowa, N., Elmore, B. O., Alexander, S. M., Femling, J. K., Gray, B. M., et al. (2014). Selective chemical inhibition of agr quorum sensing in *Staphylococcus aureus* promote host defense with minimal impacto on the resistance. *PLoS Pathog.* 10:e1004174. doi: 10.1371/journal.ppat.1004174

Sun, B., and Zhang, M. (2016). Analysis of the antibacterial effect of an *Edwardsiella tarda* LuxS inhibitor. *Springerplus* 5:92. doi: 10.1186/s40064-016-1733-4

Sun, J., Daniel, R., Wagner-Döbler, I., and Zeng, A. P. (2004). Is autoinducer-2 a universal signal for interspecies communication: a comparative genomic and phylogenetic analysis of the synthesis and signal transduction pathways. *BMC Evol. Biol.* 4:36. doi: 10.1186/1471-2148-4-36

Tal-Gan, Y., Ivancic, M., Cornilescu, G., Yang, T, and Blackwell, HE. (2016). Highly stable, amide bridged autoinducing peptides analogues that strongly inhibit the AgrC quorum sensing receptor in *Staphylococcus aureus*. *Angew. Chem. Int. Ed Engl.* 55, 8913–8917. doi: 10.1002/anie.201602974

Tan, L., Li, S. R., Jiang, B., Hu, X. M., and Li, S. (2018). Therapeutic targeting of the *Staphylococcus aureus* accessory gene regulator (agr) system. *Front. Microbiol.* 9:55. doi: 10.3389/fmicb.2018.00055

Tavender, T. J., Halliday, N. M., Hardie, K. R., and Winzer, K. (2008). LuxS-independent formation of AI-2 from ribulose-5-phosphate. *BMC Microbiol.* 8:98. doi: 10.1186/1471-2180-8-98

Thomann, A., de Mello Martins, A. G., Brengel, C., Empting, M., and Hartmann, R. W. (2016). Application of dual inhibition concept within looped autoregulatory systems toward antivirulence agents against *Pseudomonas aeruginosa* infections. *ACS Chem. Biol.* 11, 1279–1286. doi: 10.1021/acschembio.6b00117

Thomas, K., Cameron, S. A., Almo, S. C., Burgos, E. S., Gulab, S. A., and Schramm, V. L. (2015). Active site and remote contributions to catalysis in methylthioadenosine nucleosidases. *Biochemistry* 54, 2520–2529. doi: 10.1021/bi501487w

Todd, D. A., Parlet, C. P., Crosby, H. A., Malone, C. L., Heilmann, K. P., Horswill, A. R., et al. (2017). Signal biosynthesis inhibition with ambuic acid as a strategy to target antibiotic-resistant infections. *Antimicrob. Agents Chemother.* 61:e00263-17. doi: 10.1128/AAC.00263-17

Todd, D. A., Zich, D. B., Ettefagh, K. A., Kavanaugh, J. S., Horswill, A. R., and Cech, N. B. (2016). Hybrid Quadrupole-Orbitrap mass spectrometry for quantitative measurement of quorum sensing inhibition. *J. Microbiol. Methods* 127, 89–94. doi: 10.1016/j.mimet.2016.05.024

Trappetti, C., McAllister, J. L., Chen, A., Wang, H., Paton, W. A., Oggioni, R. M., et al. (2017). Autoinducer 2 signaling via the phosphotransferase FruA drives galactose utilization by *Streptococcus pneumoniae*, resulting in hypervirulence. *MBio* 8:e02269-16. doi: 10.1128/mBio.02269-16

Vale, P. F., McNally, L., Doeschl-Wilson, A., King, K. C., Popat, R., Domingo-Sananes, M. R., et al. (2016). Beyond killing: can we find new ways to manage infection? *Evol Med Public Health* 2016, 148–157. doi: 10.1093/emph/eow012

Vasquez, J. K., Tal-Gan, Y., Cornilescu, G., Tyler, K. A., and Blackwell, H. E. (2017). Simplified AIP-II peptidomimetics are potent inhibitors of *Staphylococcus aureus* AgrC quorum sensing receptors. *Chembiochem* 18, 413–423. doi: 10.1002/cbic.201600516

Velusamy, S. K., Sampathkumar, V., Godboley, D., and Fine, D. H. (2017). Survival of an *Aggregatibacter actinomycetemcomitans* quorum sensing luxS mutant in

the mouths of Rhesus monkeys: insights into ecological adaptation. *Mol. Oral Microbiol.* 32, 432–442. doi: 10.1111/omi.12184

Wang, B., and Muir, T. W. (2016). Regulation of virulence in *Staphylococcus aureus*: molecular mechanisms and remaining puzzles. *Cell Chem Biol.* 23, 214–224. doi: 10.1016/j.chembiol.2016.01.004

Weidel, E., de Jong, J. C., Brengel, C., Storz, M. P., Braunshausen, A., Negri, M., et al. (2013). Structure optimization of 2-benzamidobenzoic acids as PqsD inhibitors for *Pseudomonas aeruginosa* infections and elucidation of binding mode by SPR, STD NMR, and molecular docking. *J. Med. Chem.* 56, 6146–6155. doi: 10.1021/jm4006302

Wnuk, S. F., Lalama, J., Garmendia, C. A., Robert, J., Zhu, J., and Pei, D. (2008). S-Ribosylhomocysteine analogues with the carbon-5 and sulfur atoms replaced by a vinyl or (fluoro) vinyl unit. *Bioorg. Med. Chem.* 16, 5090–5102. doi: 10.1016/j.bmc.2008.03.028

Wnuk, S. F., Robert, J., Sobczak, A. J., Meyers, B. P., Malladi, V. L., Zhu, J., et al. (2009). Inhibition of S-ribosylhomocysteinase (LuxS) by substrate analogues modified at the ribosyl C-3 position. *Bioorg. Med. Chem.* 17, 6699–6706. doi: 10.1016/j.bmc.2009.07.057

Xu, Y., Wang, L., Chen, J., Zhao, J., Fan, S., Dong, Y., et al. (2017). Structural and functional analyses of Periplasmic 5′-Methylthioadenosine/S-Adenosylhomocysteine nucleosidase from *Aeromonas hydrophila*. *Biochemistry* 56, 5347–5355. doi: 10.1021/acs.biochem.7b00691

Yadav, M.K., Vidal, J. E., Go, Y. Y., Kim, S. H., Chae, S. W., and Song, J. J. (2018). The LuxS/AI-2 quorum sensing system of *Streptococcus pneumoniae* is required to cause disease, and to regulate virulence-and metabolism-related genes in a rat model of middle ear infection. *Front. Cell. Infect. Microbiol.* 8:138. doi: 10.3389/fcimb.2018.00138

Yang, T., Tal-Gan, Y., Paharik, A. E., Horswill, A. R., and Blackwell, H. E. (2016). Structure-function analyses of a *Staphylococcus epidermidis* autoinducing peptide reveals motifs critical for AgrC-type receptor modulation. *ACS Chem. Biol.* 11, 1982–1991. doi: 10.1021/acschembio.6b00120

Zang, T., Lee, B. W., Cannon, L. M., Ritter, K. A., Dai, S., Ren, D., et al. (2009). A naturally occurring brominated furanone covalently modifies and inactivates LuxS. *Bioorg. Med. Chem. Lett.* 19, 6200–6204. doi: 10.1016/j.bmcl.2009.08.095

Zhang, M., Jiao, X. D., Hu, Y. H., and Sun, L. (2009). Attenuation of *Edwardsiella tarda* virulence by small peptides that interfere with LuxS/autoinducer type 2 quorum sensing. *Appl. Environ. Microbiol.* 75:3882. doi: 10.1128/AEM.02690-08

Zhang, M., Sun, K., and Sun, L. (2008). Regulation of autoinducer 2 production and luxS expression in a pathogenic *Edwardsiella tarda* strain. *Microbiology* 154, 2060–2069. doi: 10.1099/mic.0.2008/017343-0

Zhang, M., and Sun, L. (2012). *Edwardsiella ictaluri* LuxS: activity, expression, and involvement in pathogenicity. *Pol. J. Microbiol.* 61, 263–271.

Zhu, J., Hu, X., Dizin, E., and Pei, D. (2003). Catalytic mechanism of S-ribosylhomocysteinase (LuxS): direct observation of ketones intermediates by 13C NMR spectroscopy. *J. Am Chem Soc.* 125, 13379–81. doi: 10.1021/ja0369663

Zhu, J., Knottenbelt, S., Kirk, M. L., and Pei, D. (2006). Catalytic mechanism of S-ribosylhomocysteinase: ionization state of active-site residues. *Biochemistry* 45, 12195–12203. doi: 10.1021/bi061434v

Zhu, L., Lin, J., Ma, J., Cronan, J. E., and Wang, H. (2010). Triclosan resistance of *Pseudomonas aeruginosa* PAO1 is due to FabV, a triclosan-resistant enoyl-acyl carrier protein reductase. *Antimicrob. Agents Chemother.* 54, 689–698. doi: 10.1128/AAC.01152-09

Zuberi, A., Misba, L., and Khan, A. U. (2017). CRISPR Interference (CRISPRi) inhibition of luxS gene expression in *E. coli: an approach to inhibit biofilm. Front. Cell Infect. Microbiol.* 7:214. doi: 10.3389/fcimb.2017.00214

Conflict of Interest Statement: The authors declare that the research was conducted in the absence of any commercial or financial relationships that could be construed as a potential conflict of interest.

frontiers in Cellular and Infection Microbiology

ORIGINAL RESEARCH
published: 08 May 2018
doi: 10.3389/fcimb.2018.00144

Anti-quorum Sensing Activities of Selected Coral Symbiotic Bacterial Extracts From the South China Sea

Zhi-Ping Ma[1], Yu Song[2], Zhong-Hua Cai[1], Zhi-Jun Lin[2], Guang-Hui Lin[2], Yan Wang[3] and Jin Zhou[1]**

[1] Shenzhen Public Platform for Screening and Application of Marine Microbial Resources, The Graduate School at Shenzhen, Tsinghua University, Beijing, China, [2] The Department of Earth Science, Tsinghua University, Beijing, China, [3] Biology, Shenzhen Polytechnic, Shenzhen, China

The worldwide increase in antibiotic-resistant pathogens means that identification of alternative antibacterial drug targets and the subsequent development of new treatment strategies are urgently required. One such new target is the quorum sensing (QS) system. Coral microbial consortia harbor an enormous diversity of microbes, and are thus rich sources for isolating novel bioactive and pharmacologically valuable natural products. However, to date, the versatility of their bioactive compounds has not been broadly explored. In this study, about two hundred bacterial colonies were isolated from a coral species (*Pocillopora damicornis*) and screened for their ability to inhibit QS using the bioreporter strain *Chromobacterium violaceum* ATCC 12472. Approximately 15% (30 isolates) exhibited anti-QS activity, against the indicator strain. Among them, a typical Gram-positive bacterium, D11 (*Staphylococcus hominis*) was identified and its anti-QS activity was investigated. Confocal microscopy observations showed that the bacterial extract inhibited the biofilm formation of clinical isolates of wild-type *P. aeruginosa* PAO1 in a dose-dependent pattern. Chromatographic separation led to the isolation of a potent QS inhibitor that was identified by high-performance liquid chromatography-mass spectrometry (HPLC-MS) and nuclear magnetic resonance (NMR) spectroscopy as DL-homocysteine thiolactone. Gene expression analyses using RT-PCR showed that strain D11 led to a significant down-regulation of QS regulatory genes (*lasI*, *lasR*, *rhlI,* and *rhlR*), as well as a virulence-related gene (*lasB*). From the chemical structure, the target compound (DL-homocysteine thiolactone) is an analog of the acyl-homoserine lactones (AHLs), and we presume that DL-homocysteine thiolactone outcompetes AHL in occupying the receptor and thereby inhibiting QS. Whole-genome sequence analysis of *S. hominis* D11 revealed the presence of predicted genes involved in the biosynthesis of homocysteine thiolactone. This study indicates that coral microbes are a resource bank for developing QS inhibitors and they will facilitate the discovery of new biotechnologically relevant compounds that could be used instead of traditional antibiotics.

Keywords: anti-quorum sensing, coral microbes, *S. hominis*, HPLC-MS-NMR, marine drug

OPEN ACCESS

Edited by:
Maria Tomas,
Complexo Hospitalario Universitario A Coruña, Spain

Reviewed by:
Naybi Muñoz,
Colegio de Postgraduados (COLPOS), Mexico
J. Christopher Fenno,
University of Michigan, United States

****Correspondence:***
Yan Wang
wangyanmary@szpt.edu.cn
Jin Zhou
zhou.jin@sz.tsinghua.edu.cn

Received: *29 January 2018*
Accepted: *20 April 2018*
Published: *08 May 2018*

Citation:
Ma Z-P, Song Y, Cai Z-H, Lin Z-J, Lin G-H, Wang Y and Zhou J (2018) Anti-quorum Sensing Activities of Selected Coral Symbiotic Bacterial Extracts From the South China Sea. Front. Cell. Infect. Microbiol. 8:144. doi: 10.3389/fcimb.2018.00144

INTRODUCTION

The rising problem of microbial resistance to current antibiotics and high spreading rate of resistant bacterial species has become a major public health concern. Multidrug-resistance is the biggest challenge facing the healthcare sector field (Adonizio et al., 2008). Biofilm formation is one of the mechanisms used by bacteria for developing such resistance (Vuotto et al., 2014; Arendrup and Patterson, 2017). Biofilms can act as protective membranes and are difficult to eliminate, leading to both therapy failure and disease recurrence. In recent years, it has become apparent that improved strategies and new antimicrobials are urgently needed to control infectious diseases.

Biofilm formation is controlled by cellular signals, widely known as quorum sensing (QS). Inhibition of QS is one of the many different strategies deployed to control biofilm-forming microbes without causing drug resistance (Singh et al., 2013, 2016). Some opportunistic pathogens, such as *Serratia marcescens* and *Pseudomonas aeruginosa*, control production of their virulence factors including biofilm formation by using QS systems. For example, more than 6% of the genes in the genome of *P. aeruginosa* are regulated by QS and are involved in the control of pathogenesis (Schuster et al., 2003; Wagner et al., 2003). Therefore, much work has focused on targeting microbial pathogenesis by inhibiting QS or biofilm formation. This paradigm is neither bactericidal (it does not kill bacteria) nor bacteriostatic (it does not inhibit bacterial growth). It appears to be a particularly attractive alternative to other methods because it does not impose a strong selective pressure, and thus bacterial resistance is less likely to develop (Sommer et al., 2013). For this reason, the identification of compounds that interfere with QS systems is of considerable interest in an effort to develop treatments against biofilm-associated pathogens (Christensen et al., 2007). For this reason, an approach known as QS inhibition has been developed when an efficient screening for anti-QS agents is required.

In recent years, several anti-QS compounds were reported from plants and microbes (Choo et al., 2006; Ni et al., 2009; Kalia and Purohit, 2011; Kalia, 2012). A lot of bacteria and metabolites isolated from terrestrial environments have shown anti-QS properties that can decrease the expression of virulence factors produced by some pathogens (Okuda, 2005; Adonizio et al., 2008; Tolmacheva et al., 2014). Numerous reports are emerging that provide evidence demonstrating anti-QS activity from various land sources including plants, animal extracts, fungi, and host-associated bacteria (Jiang and Li, 2013; Defoirdt, 2017; Singh et al., 2017).

Interestingly, the ocean contains a rich microbial biodiversity in which plenty of bioactive compounds are produced by various aquatic microbes, indicating that the marine environment can serve as an important resource in the search for novel anti-QS substances (Dobretsov et al., 2009; Teasdale et al., 2011; Yaniv et al., 2017). Taking coral as an example, it contains an enormous diversity of microorganisms, which render the coral microbiota ideally suited to the search for new ecological functions and bioactive metabolic compounds (Pham et al., 2016). In previous studies, the bacterial species *Oceanobacillus profundus* was isolated from the octocoral *Antillogorgia elisabethae* and was reported for its anti-QS activity by yielded compounds tyrosol and tyrosol acetate (Martínez-Matamoros et al., 2016). In addition, *Marinobacter* sp. and a Proteobacteria associated with corals have also been reported to inhibit the QS-dependent virulence factors in an environmental isolate of *S. marcescens*, which further augmented our interest in exploring coral-associated bacterial isolates (Kvennefors et al., 2012). The likelihood of finding novel bioactive compounds from coral ecosystems seems high since many such symbiotic microorganisms in this ecosystem have not been well-characterized. With this milieu, the coral ecosystem, a hitherto under-explored reserve for novel bacteria, was screened for anti-QS producers. These bacteria were then evaluated for their anti-biofilm activity, with the hope that biomolecules from such novel bacteria will be of a new and unique type.

It is worth noting that despite the abundance of active compounds from marine environments, to date the discovery and isolation of anti-QS compounds from these sources has been slow compared with the synthetic chemistry approach or terrestrial counterparts (Dobretsov et al., 2011; Yaniv et al., 2017). More importantly, a detailed identification of compounds has still not been performed (Bakkiyaraj et al., 2012, 2013). The present study stresses the importance of the coral-associated bacteria as a potential model for naturally occurring products with anti-QS properties. More specifically, given the limited knowledge available on the production of these cues by coral bacteria, the purpose of this study was to gain a clearer understanding of the ecological role of the anti-QS substances secreted by coral-symbiotic microbes.

In this study, we take the coral *Pocillopora damicornis* as the material to screen for QS-inhibiting bacteria, and one isolated bacterium was further explored for anti-QS potential. The active compounds from this bacteria were identified, expression of regulatory key genes was analyzed, and a possible mechanism of action was inferred.

MATERIALS AND METHODS

Bacterial Strains and Culture Conditions, and Coral Samples

Chromobacterium violaceum ATCC®. 12472™ and *Pseudomonas aeruginosa* PAO1 were used in this study. Both strains were cultured in lysogeny broth (LB) medium containing 1% peptone, 0.5% yeast extract, and 0.5% NaCl, either in liquid form or solidified using 1.5% agar as necessary.

Coral (*Pocillopora damicornis*) samples were collected from Xishan Islands (located at 3°57.058′E, 36°8.532′S) in the South China Sea. The samples were collected from six sites (three from Heilong Island and three from Daming Island) at a depth of 5–6 m. The salinity was around 33.1‰ (33.1 per thousand) and the seawater temperature was 29.7°C. At each site, five coral samples were collected. Samples were washed with sterile seawater, homogenized by grinding and agitation, and serially diluted in sterile seawater. Next, 50 μl of dilutions from 10^{-4} to 10^{-7} were surface-plated on marine agar 2216 (Difco, USA) and

incubated at 30°C for 3–5 days. A quantity of pre-test colonies, chosen on the basis of their different colonial morphology, were collected by sterile toothpick and incubated in the conditions described above.

Screening and Identifying Anti-QS Bacteria

A disc diffusion assay (Bauer et al., 1966) was performed with biosensor strain *C. violaceum* ATCC 12472 to detect anti-QS activity (Busetti et al., 2014). Briefly, 5 ml overnight reporter strain culture is poured into 45 ml LB media containing 0.75% agar until the temperature of the media is about 45°C. The mixture is then plated and allowed to solidify before sterile filter paper circles (5 mm diameter) are placed on the LB surface at regular intervals. The screened single colony isolates are cultured overnight in LB medium at 30°C in 1.5 ml Eppendorf tubes with constant shaking at 150 rpm. The cultured individual as the test strains (OD_{600} near 0.1) and bacterial suspension (3 μl) are pipetted onto the filter paper. 2,5-Dimethyl-4-hydroxy-3[2H]-furanone (CAS No. 3658-77-3, Sigma-Aldrich, USA) dissolved in dimethyl sulfoxide (DMSO, 1 μl), DMSO solvent, and LB broth are used as positive, negative and blank controls, respectively, in this plate-based bioassay. After incubation for 24 h at 30°C, inhibition of pigment production around the disc (a colorless ring) is checked. Positive anti-QS activity will be recorded as visible colorless haloes like furanone. The bacterial isolates showing promising positive anti-QS activities are selected for further study. To ensure reliability of the experiment, the anti-QS activities of the selected isolates are repeated three times independently.

Potential anti-QS strains were grown overnight in LB broth at 30°C, and then 200 μl from each culture was transferred into a clean 1.5 ml Eppendorf tube and centrifuged at 7,000 g for 1 min (Chang et al., 2017). The flow-through in the tube was discarded, 100 μl TE buffer was added, and the sample was mixed gently, and then boiled for 10 min. The resulting supernatant contained the crude DNA extract (OD_{260}/OD_{230} was more than 1.7, and OD_{260}/OD_{280} was between 1.8 and 2.0). The 16S rRNA gene, which is approximately 1500 bp, was amplified by PCR using the forward primer 27F (5′-AGAGTTTGATCCTGGCTCAG-3′) and the reverse primer 1492R (5′-GGTTACCTTGTTACGACTT-3′) (Lane, 1991), and sequenced at BGI-Shenzhen (BGI China, Mainland). The sequences obtained were assembled, analyzed, and manually edited using the CAP3 software package. The resulting sequences were compared against those from the NCBI database (http://www.ncbi.nlm.nih.gov) using BLAST analysis and the RDP online service (https://rdp.cme.msu.edu).

Determination of Growth and Violacein Production

The effect of the potential anti-QS bacterial extract on the growth of *C. violaceum* ATCC 12472 was determined by the colony count on plate method (Choo et al., 2006). Cultures of *C. violaceum* ATCC 12472 were serially diluted and 100 μl aliquots were spread on LB plates. The plates were incubated at 30°C for 24 h, and bacterial counts were compared with the control. For quantification of violacein production, 1 ml of culture was centrifuged at 13,000 rpm for 10 min to precipitate insoluble violacein. The culture supernatant was discarded and 1 ml DMSO was added to the pellet. The solution was vortexed vigorously for 30 s to completely solubilize violacein and was then centrifuged at 13,000 rpm for 10 min to remove cells (Choo et al., 2006). Two-hundred microliters of the violacein-containing supernatants were added to 96-well flat-bottomed microplates, three wells per sample, and the absorbance was read with a spectrophotometer (Infinite® 200 PRO, Tecan, Austria) at a wavelength of 585 nm (Blosser and Gray, 2000).

Extracting the Anti-QS Active Components

The possible anti-QS strains were incubated for 48 h in LB broth at 30°C with shaking at 200 rpm. Samples were then centrifuged at 6,000 g, 4°C for 20 min to remove bacterial cells, and the resulting supernatants were collected and extracted using an equal volume of ethyl acetate, with vigorous shaking for 15–20 min. The extraction was repeated twice and the aqueous extract fractions were discarded. The organic extract fractions (obtained by ethyl acetate extraction) were combined and evaporated in a rotary evaporator at 45°C. The organic residues were dissolved in methanol (Nithya et al., 2010c) and concentrated using nitrogen flow. All resulting extracts were sterilized using 0.22 μm filters.

A second-round of testing for anti-QS activity was carried out using the sterilized extracts and following the above-mentioned methods (see "Screening and identifying anti-QS bacteria"). The putative extracts (from the anti-QS strains identified in the preliminary screen) were pipetted onto the filter paper, and the QS inhibition activity was calculated by measuring the diameter of colorless haloes relative to equivalent furanone. Finally, the positive extracts were stored at −20°C and used for biofilm inhibition experiments at a range of concentrations.

Influence of Anti-QS Extract on *P. aeruginosa* PAO1 Biomass and Cellular Growth

The effects of the extract from the anti-QS positive strain on the biomass of biofilms produced by *P. aeruginosa* PAO1 were determined using the crystal violet (CV) method (Huber et al., 2003; Choo et al., 2006). Briefly, freshly cultured *P. aeruginosa* PAO1 was added to 96-well polystyrene plates (100 μl per well) and incubated in LB medium (Hinsa, 2006). The bacterial extracts (for example D11 strain) were added at 1, 2.5, 5, and 10 μg/ml (w/v). The mixtures were incubated at 30°C for 48 h. Planktonic cells and spent medium were removed from each culture. The remaining adherent cells were gently rinsed twice using deionized water. One-hundred microliters of 1% (w/v) CV solution was added to each well for 30 min at room temperature. The excess dye was discarded, and the plates were washed gently but thoroughly using deionized water. The CV-stained cells were solubilized in DMSO and the absorbance at 600 nm was determined using a microplate reader (Infinite® 200 PRO, Tecan). *P. aeruginosa* PAO1 cultures incubated in the absence of extract and lose QSI ability extract (ultrasonic method to destroy the chemical structure of the extract) served as negative

controls. Pure water was used as a blank control. Experiments were performed with 12 replicates (12 replicate wells in 96-well plates) for each treatment. When absorbance was determined, three readings were recorded for each well.

To determine the effects of the extract on the growth of *P. aeruginosa* PAO1, a growth curve assay was conducted. *P. aeruginosa* PAO1 was cultured in LB broth in the presence or absence of extract from strain D11 (10 μg/ml, w/v). Cultures were incubated at 30°C for 48 h. After 0, 3, 6, 9, 12, 18, 27, 36, and 48 h, the optical density at 600 nm was determined using a microplate spectrophotometer (Infinite® 200 PRO, Tecan). Bacterial abundance was measured using a flow cytometer (BD Biosciences, USA). Briefly, samples (1 ml each) were fixed with glutaraldehyde (0.5% final concentration), then stained with SYBR green I solution (Molecular Probes) (at a 1000-fold dilution of the stock solution) at room temperature in the dark for 15 min (Gasol and del Giorgio, 2000). Fluorescent 1-μm latex beads (10^5 beads per ml) were added to the samples as an internal standard. Bacterial number (cells/ml) were calculated by their signatures in a side-scatter-vs.-green-fluorescence plot, as described by Pinder et al. (1990) and Gasol and del Giorgio (2000).

Separation and Identification of Anti-QS Active Compounds

Extract compounds were separated by preparative high-performance liquid chromatography (HPLC) (Agilent 1200, USA). Samples were kept at 4°C until injection, and 100 μl extract sample was injected onto a reverse-phase C18 core-shell column (50 × 2.1 mm, Waters, CA, USA) via an auto-sampler (ThermoFisher Scientific, USA). The mobile phase was obtained using 83% methanol and 17% water at a flow rate of 0.5 ml/min at 30°C. Samples, separated every 30 s, were collected with the fraction collector. At the end of the separation process, every peak sample was taken and concentrated by nitrogen-flow method. Every purified sample was then re-tested to confirm the anti-QS activity using the procedures described above (see "Screening and identifying anti-QS bacteria").

The collected anti-QS active peaks were further purified on HPLC (Waters Delta Prep 4000, USA) using a C18 column and a linear water/acetonitrile gradient containing 0.1% trifluoroacetic acid. The residue was dissolved in 1 ml acetonitrile/water (1:1, v/v) to determine the molecular weight by mass spectrometry (MS) on a LTQ XL Orbitrap using a static nanospray (Thermo-Fisher, CA, USA) in positive-/negative-ion mode. To determine the active molecular structure, nuclear magnetic resonance spectroscopy (NMR) was performed on the purified anti-QS active sample to get a heteronuclear single quantum coherence (HSQC) and heteronuclear multiple bond coherence (HMBC) spectrogram.

Inhibition of Biofilm

Pre-sterilized glass microscope slides were used to observe biofilms by confocal laser scanning microscopy (CLSM) as described in the previous study (Ortlepp et al., 2007; Tolker-Nielsen and Sternberg, 2014). Briefly, *P. aeruginosa* PAO1 was grown in LB medium overnight and diluted with fresh medium to an OD_{600} of about 0.02. Then, 2 ml dilutions were incubated under static conditions with or without anti-QS extract (10 μg/mL, w/v) in 12-well plates with a glass microscope slide in each well. After 12 and 36 h, the glass slides were gently lifted out and rinsed with deionized water to remove loosely attached cells. The biofilms on one side were stained with 5 μM SYTO9 dye (Sigma, USA) in the dark, and those on the other side were wiped off. After 15 min, the slides were washed, and observed by CLSM (Zeiss, Germany) with a ×60 objective lens to visualize the biofilms. The 488 nm excitation and 520 nm emission filter settings were used for detection of SYTO9. Quantification of biofilm parameters was processed with the COMSTAT software using the CLSM images (Heydorn et al., 2000). Of the available parameters, we selected the three factors of total biomass, average thickness, and roughness coefficient to evaluate the biofilms (Hentzer et al., 2001). 3D transmission-fluorescence photos of the *P. aeruginosa* PAO1 biofilms were produced using FV10-ASW2.0 Viewer (Olympus, Japan). The optical sections were 5 μm apart on the Z-axis and taken at 640 × 640 pixels with a 12-bit intensity resolution (Chang et al., 2017). Digital images were processed using Leica Confocal Software Lite (Leica Microsystems, Germany).

Effect of Anti-QS Extract on the Expression of QS Genes

P. aeruginosa PAO1 was grown in 10 ml LB liquid medium to an OD_{600} of approximately 0.1. At this time point, treated groups had approximately 10 μl extract added (extract concentration was 10 μg/ml) to the *P. aeruginosa* PAO1 culture medium. The extract was dissolved in methanol and the final methanol concentration in the experimental system was 0.1% (v/v). Solvent control groups had 10 μl methanol only added. After 24–36 h, total RNA was extracted from control and treated groups using RNAiso Plus Reagent (Takara, China), and reverse-transcribed into cDNA with PrimeScript RT reagent kit (Takara) according to the manufacturer's protocol. Before performing the quantitative real-time PCR (qRT-PCR), RNA quality was determined (by measuring A_{260}/A_{280} and A_{260}/A_{230}, and by gel electrophoresis). Eight reported functional genes coding for QS regulation activity were chosen for PCR analyses. Primers were designed using Primer Express 3.0 (Applied Biosystems) and are listed in **Table 1**. Thirty-two PCR cycles were run with denaturation at 95°C for 15 s, annealing at 55°C for 30 s, and extension at 60°C for 45 s. The 16S rRNA gene was used as a control for standardization. A melt curve analysis was also done for the validation of specificity of the qRT-PCR. The relative transcription level of each gene was defined as the ratio of its transcript of biofilms grown in the indicated concentration of compounds over that in LB medium with methanol, using the $2^{-\Delta\Delta Ct}$ method (Livak and Schmittgen, 2001).

Whole-Genome Sequencing of Strain D11

Genomic DNA of strain D11 was extracted using a GenEluteTMkit (Sigma-Aldrich, USA) and converted into a next-generation sequencing library using Next-era XT (Illumina, CA, USA) according to the manufacturer's instructions. Whole-genome sequencing was performed using the MiSeq at BGI Company (Shenzhen, China). SMRT Analysis 2.3.0 was used to filter low-quality reads and the sequences were assembled using Spades v2.5 (default setting) (Bankevich et al., 2012). The

generated contigs were scaffolded and gap-closed using SSPACE and GAPFiller, respectively (Boetzer et al., 2011; Boetzer and Pirovano, 2012). Genome annotation was performed using Prokka and InterProScan5 (Jones et al., 2014; Seemann, 2014).

The software tRNAscan-SE v.1.23 and RNAmmer v.1.2 were used to identify presence of tRNA and rRNA, respectively (Lagesen et al., 2007). Gene prediction was performed by GeneMarkS with an integrated model that combined the GeneMarkS generated (native) and heuristic model parameters (Besemer et al., 2001). A whole-genome BLAST search (*E*-value less than 1×10^{-5}), minimal alignment length percentage larger than 40%, was performed against the main databases, including KEGG (Kyoto Encyclopedia of genes and genomes), COG (Clusters of Orthologous Groups), and Swiss-Prot. The annotation predictions were manually evaluated and only genes predicted with consensus from two or more annotation pipelines were trusted in order to provide gene identification with high confidence.

Statistical Analysis

Differences in various data were determined using analysis of variance (ANOVA) at the $P < 0.05$ significance level. All analyses were performed using the SPSS software package 13.0 (NY, USA).

RESULTS

Isolation and Identification of Anti-QS Coral Bacteria

The possible anti-QS bacteria were screened using *C. violaceum* ATCC 12472 as an indicator strain since it produces the purple pigment violacein unless its QS system is interrupted. Using this technique, a lack of pigmentation from the indicator organism in the vicinity of the test organism indicates a potential anti-QS result (do Valle Gomes and Nitschke, 2012). A total of 200 culturable bacteria were isolated from the *Pocillopora damicornis* symbiotic environment and screened for anti-QS ability. About 15% (30 isolates) were positive in the screen for color reduction in *C. violaceum* ATCC 12472, with representative results shown in **Figure 1**. Some isolates showed promising anti-QS activity and a distinct white opaque zone of inhibition was observed in the biosensor plate containing reference strain *C. violaceum* ATCC 12472. The activity of positive isolates was recorded as either strong, medium or weak, based on the diameter of visible colorless haloes by the biosensor (**Table 2**). The isolate D11 caused the most significant reduction (the diameter of visible colorless haloes is 18.36 mm), in which the purple pigment of *C. violaceum* ATCC 12472 was completely eliminated (**Figure 1**). In comparison, the zone of inhibition was not detected with the negative control (DMSO solvent) or blank control (LB medium only).

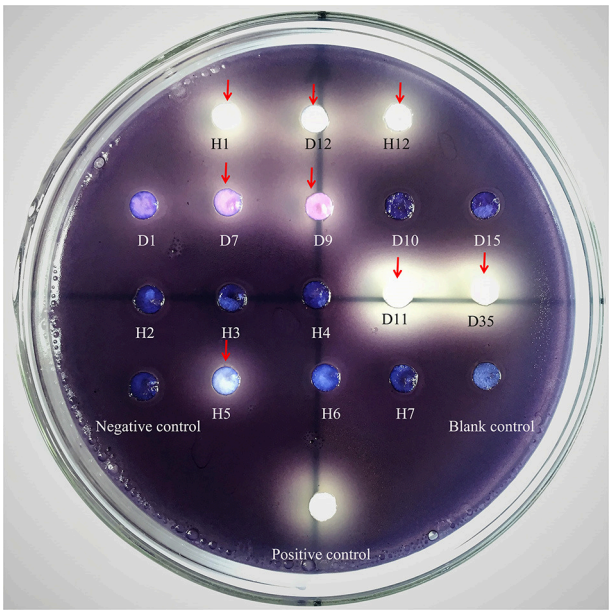

FIGURE 1 | Screening of anti-QS strains on biosensor plates containing reference strain *C. violaceum* ATCC 12472 and filter paper for sample detection. Water, LB medium and furanone (diluted 10 times with DMSO) were used as blank, negative and positive controls, respectively. The absence of purple or formation of a pigment inhibition was considered to indicate a potential QS inhibitor. The red arrows refer to the positive anti-QS strains and the pigment inhibition can be observed on a clear background on the plate. Notes: the number indicated the test isolate strains. H samples come from Heilong Island, and D samples come from Daming Island.

TABLE 1 | Primers for quantitative reverse transcriptase-PCR.

Gene	Forward primer (5′–3′)	Reverse primer (5′–3′)
rhlR	AACGCCAGATCCTGCAATG	CGGCGTCGAACTTCTTCTG
rhlI	GCAGCTGGCGATGAAGATATTC	CGAACGAAATAGCGCTCCAT
lasR	GACCAGTTGGGAGATATCGGTTA	TCCGCCGAATATTTCCCATA
lasI	GCCCCTACATGCTGAAGAACA	CGAGCAAGGCGCTTCCT
lasA	GACCAGTTGGGAGATATTAGTTA	TCCAAAGAATATTTCCCATA
lasB	CGACAACGCGTCGCAGTA	AGGTAGAACGCACGGTTGTACA
pqsA	AACGCCAGATCCTGCAATG	CGGCGTCGAACTTCTTCTG
pqsR	GCAGCTGGCGATGAAGATATTC	CGAACGAAATAGCGCTCCAT

TABLE 2 | Anti-QS activity of selected coral symbiotic bacteria and taxonomical identification.

Isolate no.	Bacterial species	% Identity	Anti-QS activity (diameter of the white opaque zone, mm)
D11	*Staphylococcus hominis*	100	18.36
D35	*Staphylococcus warneri*	99	13.08
H1	*Lysinibacillus fusiform*	99	10.39
D12	*Bacillus cereus*	99	9.84
H12	*Vibrio alginolyticus*	98	11.25

Differences in diameter of the white opaque zone indicate differences in anti-QS activity. Notes: in this study, 30 potential anti-QS strains were screened. After16S rRNA gene sequencing, five poor quality sequences were removed. The remaining25 high quality sequences were subjected to BLAST searches in the NCBI database; after dereplication, five bacteria were successful identified and are shown in this table.

The 16S rRNA gene sequences of these 30 positive isolates were aligned to the NCBI database using BLAST. Most of the representative isolates shared 99% sequence similarity with their respective reference strains. After filtering low-quality sequences and dereplication analyses, five representative strains were chosen from the candidates for anti-QS active substance studies. These five bacterial strains were *Staphylococcus hominis*, *Lysinibacillus fusiform*, *Bacillus cereus*, *Staphylococcus warneri*, and *Vibrio alginolyticus*. The 16S rRNA gene sequences for these five strains have been submitted to the GenBank database under the accession numbers MG761744–MG761748. Among the five strains, isolate D11 revealed a 100% sequence similarity to *Staphylococcus hominis* and has been tentatively named *S. hominis* D11 (GenBank accession number is MG761745). In the following experiment, we chose *S. hominis* D11, which has the most anti-QS activity, as the research object.

Effect of Anti-QS Extract on Growth and Violacein Production of *C. violaceum* ATCC 12472

The results of the colony count performed on LB plates at 24 h incubation showed no significant difference in the number of colony forming units (CFU) (**Figure 2A**). This indicates that the tested strains (D11, *S. hominis*; D35, *L. fusiform*; H1, *B. cereus;* D12, *S. warneri*; and H12, *V. alginolyticus*) have no effect on the growth of *C. violaceum* ATCC 12472. The five bacterial isolates showed a significant drop in violacein content, especially isolate D11 where violacein production was reduced by 92.3% (**Figure 2B**). Therefore, reduced production of violacein by bacterial culture was not due to the reduction of the "quorum," but due to the interruption of the "sensing."

Extract From Strain D11 Inhibits Biofilm Formation

The anti-biofilm activity of the D11 extract was tested against the widely used biofilm-forming clinical isolate *P. aeruginosa* PAO1. **Figure 3A** presents quantitative analysis of *P. aeruginosa* PAO1 biofilm inhibition. Addition of *S. hominis* D11 extract (1, 2.5, 5, and 10 μg/ml) to *P. aeruginosa* PAO1 reduced biofilm formation by 18.2, 30.3, 46.7, and 62.1%, respectively, indicating that the inhibition occurred in a dose-dependent manner. The possibility of an inhibitory effect of the D11 extract on the growth of *P. aeruginosa* PAO1 was also analyzed. However, no significant effect on growth of *P. aeruginosa* PAO1 was observed in the presence of 10 μg/ml bacterial extracts (**Figure 3B**).

Visualization of biofilms by microscopy analysis enabled precise evaluation of the biofilm 3D-structure. The topology of the biofilm developed by *P. aeruginosa* PAO1 and the effect of the D11 extract on it was analyzed by CLSM. A well-grown biofilm along with adhering bacterial cells was observed in control samples (normal biofilm developed by *P. aeruginosa* PAO1) at 12 and 36 h (**Figures 4A,C**), whereas dispersed bacterial cells were observed in treated samples (**Figures 4B,D**). Extremely thick biofilms (more cells and polysaccharides) were formed in the control relative to the experimental group. Also, the COMSTAT analysis clearly showed the disrupted surface topology and height distribution profile of the biofilm developed in the presence of the D11 extract compared to the control biofilm (taking36 h as the example) (**Figure 5**). In control groups, *P. aeruginosa* PAO1 developed a thick, dense biofilm, whereas on a surface coated with the D11 active crude extract, biofilm formation and bacterial adherence were prevented. Quantitative analysis showed that the D11 crude extract surface coating inhibited biofilm total biomass and average thickness by 43.9 and 58.7%, respectively (**Figures 5A,B**).

Identification of Anti-QS Compounds

Pre-HPLC analysis was applied to separate the crude extracts, with fractions collected every 30 s. The chromatogram from the liquid chromatography mass spectrometer (ThermoFisher Scientific™ TSQ Altis™, USA) showed that five main peaks exist (**Figure 6A**). The five fractions were collected and anti-QS activity was individually retested for each fraction using the biosensor plate containing *C. violaceum* ATCC 12472. Fraction peak 2 showed a maximum zone of QS inhibition; therefore, this fraction was selected for further characterization. Fraction peak 2 was subjected to HPLC and gas chromatography-mass spectrometry (GC-MS) analysis, and a main mass spectral peak, detected at m/z 118.03, was considered the corresponding experimental mass of the active fraction (**Figure 6B**). The detected mass spectra showed some resemblance to homocysteine thiolactone in the GC-MS library. The calculated (theoretical) or expected molecular mass of compound homocysteine thiolactone is 118. The molecular mass of the active fraction was further confirmed by NMR (C^{13} and H^{1}) (**Figures 6C,D**).

In order to confirm the QS inhibitory activity produced by strain D11 can be attributed to homocysteine thiolactone, the commercial product (DL-homocysteine thiolactone, CAS No. 6038-19-3) was purchased from the Macklin Biochemical Co., Ltd (Shanghai, China). The anti-QS activity of this commercial product was tested according to the above-mentioned methods. The inhibitory activity of DL-homocysteine thiolactone against bacterial QS was determined using violacein production by *C. violaceum* ATCC 12472. From **Figure 7A**, a concentration-dependent inhibitory activity was observed, with the tested concentrations (0.0625, 0.125, 0.25, 0.5, and 1.0 μg/ml) of DL-homocysteine thiolactone showing a significant inhibition in violacein content (ranged from 62.5 to 98.1%). A varying degree of white opaque zone of inhibition was also observed in the biosensor plate containing reference strain *C. violaceum* ATCC 12472 (**Figure 7B**).

Expression Analysis by qRT-PCR

The transcriptional level of eight specific genes (*lasI*, *lasR*, *lasA*, *lasB*, *rhlI*, *rhlR*, *pqsA*, and *pqsR*) encoding putative biofilm-forming and QS factors was determined by RT-PCR in 24 h-old *P. aeruginosa* PAO1 cultures with extract and *P. aeruginosa* PAO1 cultures with methanol only as control. Approximately 2.5- to 5.1-fold down-regulation of the genes *lasI*, *lasR*, *lasA*, and *lasB* [responsible for acyl-homoserine lactone (AHL)-based biofilm formation] were observed in *P. aeruginosa* PAO1 cultured with

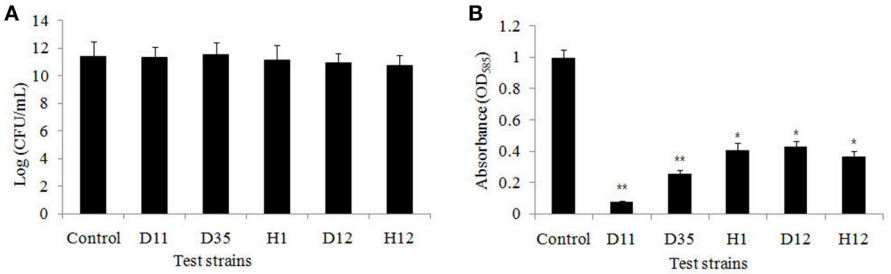

FIGURE 2 | (A) Bacterial cell count of the flask incubation assay. The five test isolates were D11 (*Staphylococcus hominis*), D35 (*Staphylococcus warneri*), H1 (*Lysinibacillus fusiform*), D12 (*Bacillus cereus*), and H12 (*Vibrio alginolyticus*). *C. violaceum* ATCC 12472 was incubated for 16 h, and 100 μl of the bacteria, adjusted to OD_{600nm} of 0.1 (approximately 1×10^8 CFU/ml), were spread on LB plates. The growth inhibition were compared with control. Data are presented as the logarithm of mean CFU ± SD. **(B)** Inhibition of violacein production by test strains. Violacein production was measured spectrophotometrically as described in the Materials and Methods. Data are presented as mean ± SD of absorbance at 585 nm. Asterisks indicate a statistically difference between experimental groups and control groups (*$P < 0.05$; **$P < 0.01$).

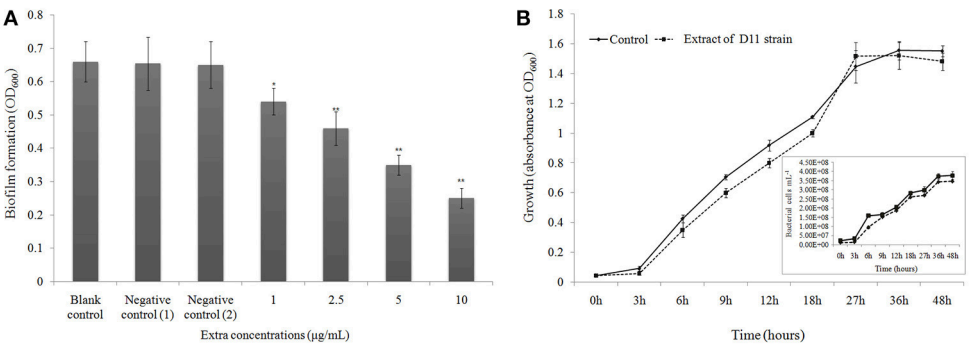

FIGURE 3 | (A) Biofilm dispersal activity (crystal violet assay) of extract from isolate *Staphylococcus hominis* D11. Different concentrations of bacterial extract (1–10 μg/ml) were tested against the widely used biofilm-forming reference strain *P. aeruginosa* PAO1. Experiments with "extract + DMSO," "lose QSI ability extract + DMSO," "DMSO only," and "no extract + no DMSO" were considered as test control, negative control (1), negative control (2), and blank control, respectively. Asterisks indicate a statistically significant difference (*$P < 0.05$; **$P < 0.01$) between experimental groups and control groups. Data are presented as mean ± SD ($n = 3$). **(B)** Effect of anti-QS compounds on growth of *P. aeruginosa* PAO1. Bacteria were grown in LB media with (dotted line) and without (solid line) D11 strain extract (10 μg/ml). The extract did not affect specific bacterial growth rate or bacterial abundance. Flow cytometry results (inset picture) show the count of bacterial cells. Data are presented as mean ± SD ($n = 3$).

the extract ($P < 0.05$ or $P < 0.01$) (**Figure 8**). Two virulence-related genes (*rhlI* and *rhlR*) also showed a significant decrease (72.3 and 88.5%, respectively) in expression level ($P < 0.01$). These results indicated that the general trend in expression for specific genes was similar between RT-PCR and biofilm state. As for the *Pseudomonas* quinolone signal (PQS) system in *P. aeruginosa* PAO1, there were no obvious differences between the experimental groups and the control groups (**Figure 8**).

Bio-Information From the Whole Genome of Strain D11

The whole genome of strain D11 comprised 5,392,014 nucleotides and the G+C content was 44.69%. It contains 71 contigs with an N50 contig length of 126,438 bp. The whole genome encodes 76 tRNA and 17 rRNA genes. The genome predicted a total of 4522 genes with 3738 protein-coding genes (Supplementary Table 1). Based on functional categories of COG (http://www.ncbi.nlm.nih.gov/COG/), a total of 593 genes were annotated to be participating in carbohydrate and amino acid metabolism, another 1018 genes were predicted to have general functions (Supplementary Figures 1, 2). In addition, 285 genes were predicted to encode signal transduction molecules.

In addition, we analyzed the candidate genes related to homocysteine thiolactone production. Homocysteine, an intermediate compound in the methionine metabolic cycle, is an amino acid that includes a thiol group. The homocysteine thiolactone forms adducts through irreversible reactions with epsilon-NH_2 groups of lysine residues. We found several methionine-related genes (*metI, metC, metF, metE*, and *mdh*) (Supplementary Figure 3) located in the upstream position (contig 1), these genes showed relatively high sequence identity to another species of the same genus, *Staphylococcus aureus* (GenBank accession numbers SACOL0431-ACOL0427) (Schoenfelder et al., 2013). Our analysis predicts the presence of these genes identified in isolate D11 might be involved in methionine (or its intermediate product homocysteine thiolactone) biosynthesis. However, the corresponding mutants need to be constructed in the future in order to confirm this assumption.

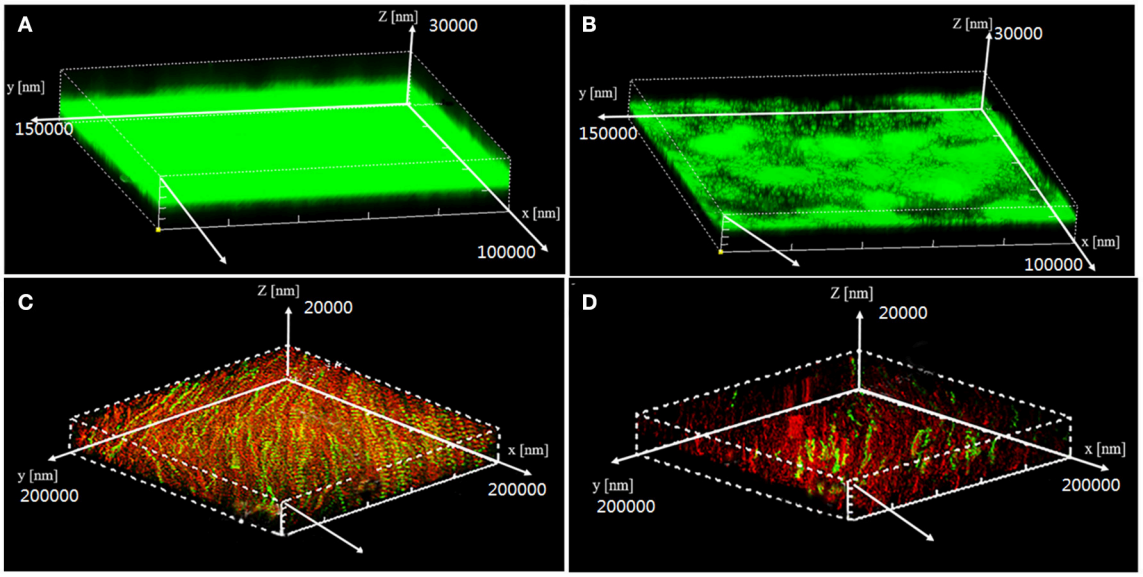

FIGURE 4 | Confocal scanning laser microscopy (CLSM) z-stack 3-D images of *P. aeruginosa* PAO1 biofilm architecture in the presence (10 μg/ml)or absence (0 μg/ml) of D11 extract in media with 2% glucose. Data shown are early stage (12 h) biofilm structure of *P. aeruginosa* PAO1 in control group **(A)** and treatment group **(B)**, and the post-stage (36 h) biofilm structure of *P. aeruginosa* PAO1 in control group **(C)** and experimental group **(D)**. In these images, live bacterial cells produced green fluorescence, whereas dead cell sproduced red fluorescence.

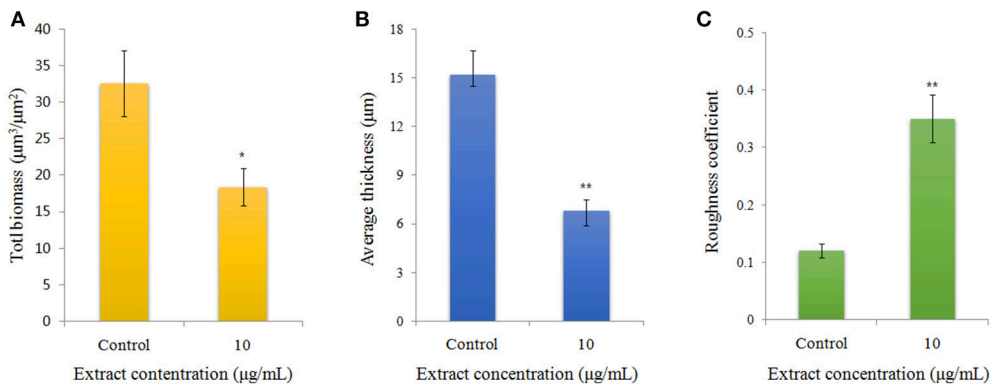

FIGURE 5 | Quantification of biofilm formation of *P. aeruginosa* PAO1 (taking 36 h as example) using COMSTAT software, including **(A)** bio-volume, **(B)** average thickness, and **(C)** roughness coefficient. Error bars indicate SD ($n = 3$). Asterisks indicate a statistically significant difference (*$P < 0.05$; **$P < 0.01$) between experimental groups and control groups.

DISCUSSION

Among the marine environment, microorganisms and their metabolic products are a crucial source for the discovery of novel anti-QS compounds (Dong and Zhang, 2005; Choo et al., 2006; Dobretsov et al., 2006). Most of studies published on the production of QS inhibitors by marine bacteria have focused on bacteria that were collected from various niches, like surfaces, biofilms, and sediments (Teasdale et al., 2009, 2011). Indeed, many of the known anti-QS compounds have been discovered in sessile marine organisms such as sponges and microalgae that interact closely with bacteria (Stowe et al., 2011; Golberg et al., 2013). In the coral surface, Skindersoe et al. (2008) demonstrated that a large number of symbiotic microbes along the Great Barrier Reef corals possess anti-QS abilities. In addition, many studies were recently published indicating that QS inhibitors may be a frequently occurring feature in coral culturable bacteria such as *Bacillus* sp. and *Vibrio* sp. (Kanagasabhapathy et al., 2009; Thenmozhi et al., 2009; Nithya and Pandian, 2010a; Romero et al., 2012). These examples indicate that coral-derived bacteria may be potential sources of anti-QS compounds. In this work, approximately 15% of isolates from the hard coral species exhibited anti-QS activity. Among them, five strains (including *S. hominis* D11) were found to have significant anti-QS activity,

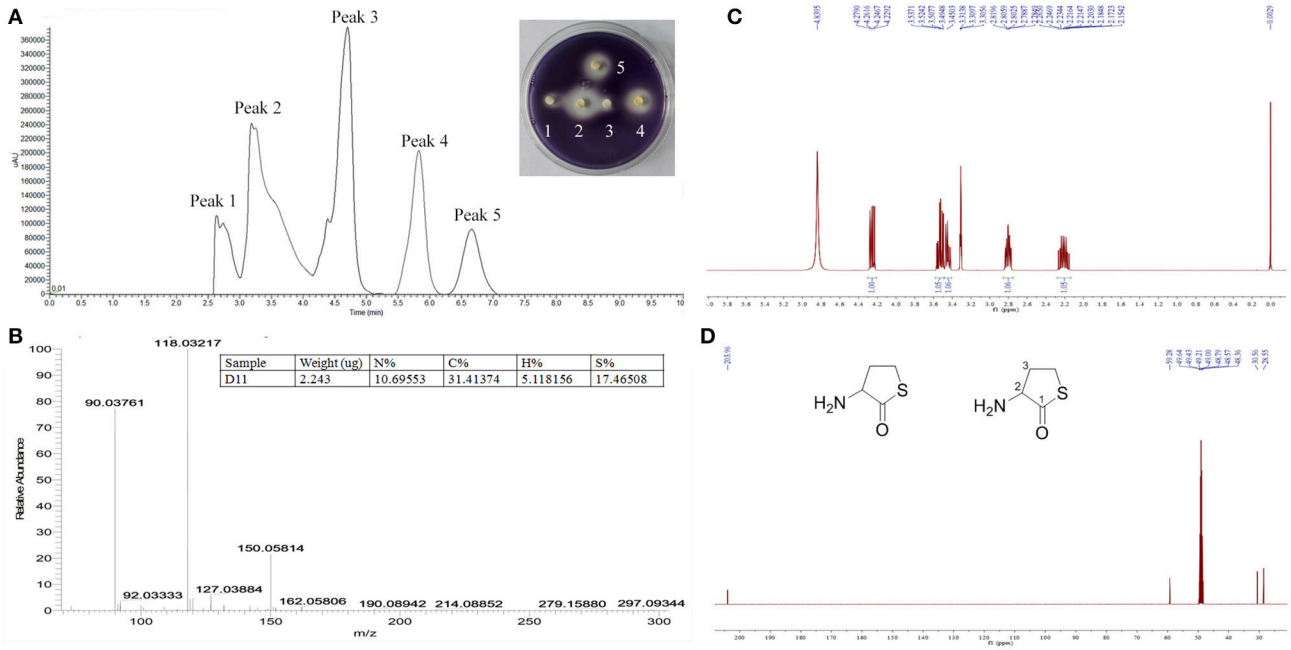

FIGURE 6 | Analysis of active fraction showing anti-QS activity. **(A)** Pre-HPLC analysis of *S. hominis* D11 extract. The chromatogram shows the five main active peaks from *S. hominis* D11. The insert picture in **(A)** is the re-test of the anti-QS activity of the five peak compounds. **(B)** GC chromatograms and ESI-MS/MS of the active fraction (peak 2) of *S. hominis* D11 extract. Peaks are a function of intensity measured in milli-absorption units over time in minutes. **(C)** ^{1}H-NMR spectrum of compound in Methanol-d_4 at 400 MHz. **(D)** ^{13}C-NMR spectrum of compound in Methanol-d_4 at 100 MHz. ^{1}H-NMR (Methanol-d_4, 400 MHz) δ:4.25 (1H, dd, J =12.9, 7.0 Hz, H-2), 3.53 (1H, td, J =11.6, 5.2 Hz, H-4), 3.45 (1H, ddd, J =11.6, 7.2, 1.1 Hz, H-4), 2.80 (1H, dddd, J = 12.2, 6.7, 5.2, 1.4 Hz, H-3), 2.21 (1H, m, H-3). ^{13}C-NMR (Methanol-d_4, 100 MHz) δ:204.0 (C-1), 59.3 (C-2), 30.6 (C-3), 28.6 (C-4). The insert picture in **(D)** is the structure of DL-homocysteine thiolactone (redrawn by ChemBioDraw Ultra 12.0).

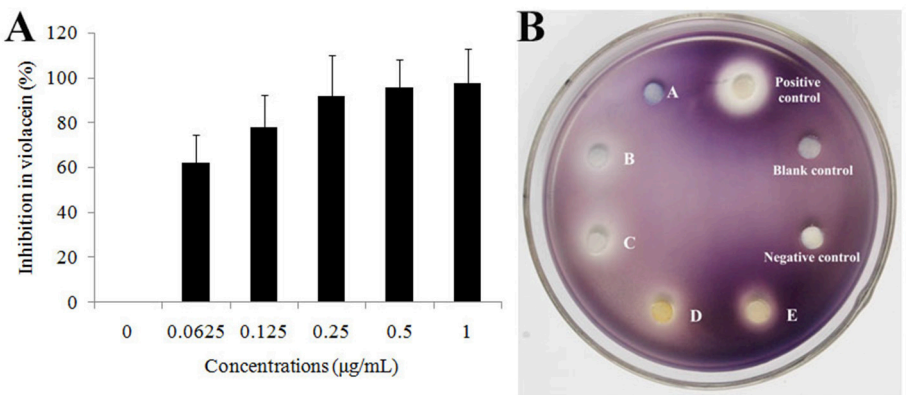

FIGURE 7 | Effect of DL-homocysteine thiolactone on violacein production by *C. violaceum* ATCC 12472. **(A)** Percentage of inhibition of the violacein pigment after incubation with different concentrations of DL-homocysteine thiolactone. A dose-response effect in the production of violacein was observed in a series of concentrations (0.0625, 0.125, 0.25, 0.5, and 1.0 μg/mL) of DL-homocysteine thiolactone. Data show the mean (±SD) of three independent experiments. **(B)** Anti-QS activity of pure DL-homocysteine thiolactone at different concentrations. A, 0.0625 μg/ml; B, 0.125 μg/ml; C, 0.25 μg/ml; D, 0.5 μg/ml; and E, 1.0 μg/ml. LB medium, DMSO only and furanone (dissolved in DMSO, 1.0 μg/ml) were used as blank, negative and positive controls, respectively.

supporting the hypothesis of Certner and Vollmer (2018), i.e., coral microbiota is a vast natural reservoir for developing new anti-QS substances.

Among the screened anti-QS bacteria, *S. hominis* D11 presented the most apparent opaque halo (growth of reporter strain with pigment inhibition) surrounding the isolate (**Figure 1**). The correlating results of violacein production (**Figure 2B**) further proved that the screened strains possess anti-QS activity against *C. violaceum* ATCC 12472. This inhibition activity seems similar to that of halogenated furanone,

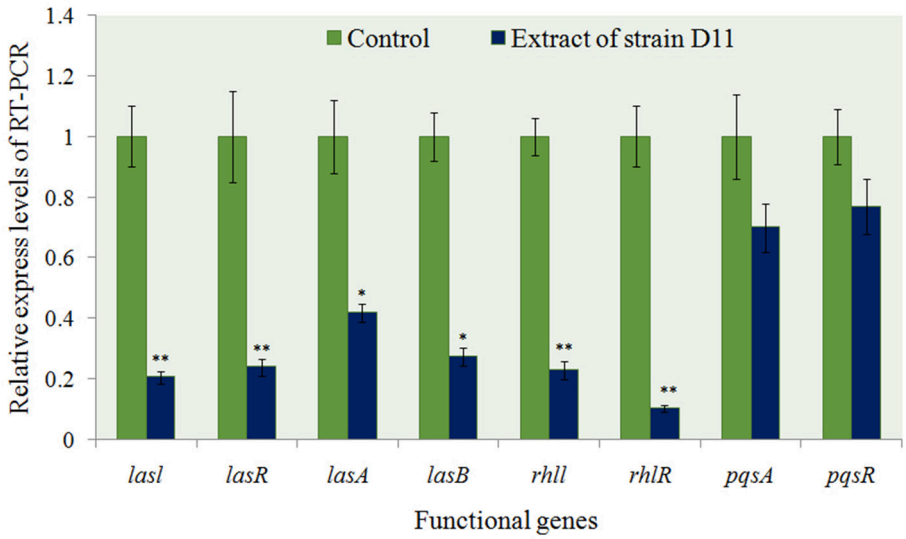

FIGURE 8 | Expression profiling of some anti-QS regulatory genes from *P. aeruginosa* PAO1 with D11 extract measured by real-time PCR. The mRNA expression of these genes in the absence of extract served as a control. Results are based on three independent experiments and error bars represent means ± SD ($n = 3$). Asterisks indicate a statistically significant difference (*$P < 0.05$; **$P < 0.01$) between experimental groups and control groups.

which inhibit QS function by interfering with *luxS*- or AI-2 system (Ren et al., 2002; Huang, 2009). Previously, some studies demonstrated that anti-QS activity and antimicrobial activity may co-occur (Busetti et al., 2014; Abudoleh and Mahasneh, 2017). In order to rule out the possibility that the inhibitory effect on the production of purple pigment was due to an antimicrobial effect, growth experiments with different test strains were performed, and no significant difference was observed among the experimental and control groups (**Figure 2A**). These results indicated that absence of violacein is mainly caused by QS disruption.

Accumulating data evidence that AHL-dependent QS is a key factor for formation of biofilms, indicating that anti-QS substances can inhibit biofilm development. Research by Adonizio et al. (2008) and Nithya et al. (2010b) suggest that *P. aeruginosa* PAO1 biofilm maturation can be inhibited by marine-derived bacterial species *Callistemon viminalis* and *Bacillus pumilus* S8-07, respectively. Teasdale et al. (2009) also found that the anti-QS properties exhibited by the marine bacterium *Halobacillus salinus* C42 were present in the solvent phase, in which the solvent was ethyl acetate. In this study, we found that addition of D11 organic extract resulted in significant reduction in the *P. aeruginosa* PAO1 biofilm (**Figure 3A**), indicating that active anti-QS extract may contain non-enzymatic compounds. In addition, inhibition of the AHL-dependent QS system by bacterial extracts was also observed. We speculated that the activity substance was associated with AHL analogs that acted as AHL-antagonists by competing with AHL for receptor binding and eventually inhibit biofilm formation of *P. aeruginosa* PAO1. In order to test the hypothesis and elucidate the possible mechanisms responsible for the inhibitory properties, related studies aimed at purifying and characterizing D11 extracts were carried out. After HPLC-MS-NMR analysis, we determined from the chemical structure that the activity substance was DL-homocysteine thiolactone (**Figure 6D**). Interestingly, this compound is very similar to homoserine lactone (HSL), produced from hydrolysis of AHLs, a common QS signal molecule (McInnis and Blackwell, 2011). This result supported our hypothesis along with further confirmation that AHL-based analogs have been extensively developed as QS modulators or anti-biofilm agents (Melvin et al., 2016). Interestingly, the violacein inhibition and anti-QS activities were confirmed by using the pure commercial DL-homocysteine thiolactone substance, which leads to the proposal that the QS inhibitory activity produced by strain D11 is homocysteine thiolactone. This is the first report of anti-biofilm activity of DL-homocysteine thiolactone on *P. aeruginosa*; further study is required to develop this substance as an anti-bacterial agent for treatment of the biofilm-forming pathogenic bacteria.

Quorum-sensing genes are key regulators of biofilm development, various extracellular virulence factors, luminescence and the antibiotic resistance of bacterial pathogens (Schuster and Greenberg, 2006; deKievit, 2009; Sharma et al., 2014). There are three well-characterized QS networks that have been identified in *P. aeruginosa*: *las*-, *rhl*-, and *pqs*-pathways. The three pathways utilize the corresponding AHLs: respectively, N-3-oxo-dodecanoyl homoserine-lactone (3OC12-HSL), N-butanoylhomoserine lactone (C4-HSL), and 2-heptyl-3-hydroxyl-4-quinolone (*Pseudomonas* quinolone signal, or PQS) (Zhang and Dong, 2004). In these systems, *lasI* and *rhlI* are involved in autoinducer synthesis, and *lasR* and *rhlR* code for transcriptional activators (Sharma et al., 2014). In our work, significantly reduced *lasI, lasR, rhlI,* and *rhlR* expression were observed (**Figure 8**), indicating that the D11

extract (DL-homocysteine thiolactone) has the ability to inhibit *lasR* and *rhlR* regulatory systems. It perhaps suggests that the mechanism for QS inhibition is via interaction with both *las* and *rhl* receptors. This result was also found by Vattem et al. (2007) who achieved the same result with extracts of *Kigelia africana*. In addition, unlike the chemically synthesized QS inhibitors, such as furanone, cyclopentanols and furanone derivatives (Givskov et al., 1996; Hentzer et al., 2002; Ishida et al., 2007; Geske et al., 2008; Kim et al., 2008), the natural compounds (for instance, DL-homocysteine thiolactone) have several advantages, including low toxicity and being environment-friendly. These features expand their potential utility in the biomedical field as natural QS inhibitors. In addition to anti-biofilm activity, strain D11 also inhibited the production of *P. aeruginosa* PAO1 virulence factors such as *las* genes (**Figure 8**). These results are similar to findings by Park et al. (2005), which showed that the *Streptomyces* strain M664 produces an AHL-degrading acylase enzyme that degrades AHL-regulated elastase and total and *lasA* proteases by 43–50%. Musthafa et al. (2011) also demonstrated that the marine-derived *Bacillus* sp. SS4 inhibited AHL-regulated production of *P. aeruginosa* virulence factors. In addition, our previous work found that the inhibition of elastase activity and siderophore production by *Rhizobium* sp. NAO1 occurs via interference with QS activity because these virulence factors are under the control of the *las*-coding gene systems (Chang et al., 2017).

For the whole-genome data of strain D11 (*S. hominis*), genome annotation on predicted genes was carried out by BLAST searches against anon-redundant protein sequence database and other databases available online, such as COG and KEGG. Based on the functional categories and gene annotation analysis (Supplementary Figure 2), 216 genes of strain D11 are involved in carbohydrate metabolism and 472 genes participate in nitrogen utilization and energy conversion, which allows this microorganism to adapt to coral-bacteria symbiosis. After gene annotation analysis, 377 genes were related to amino acids processing. Potentially, these genes are a key feature of strain D11 that enable it to biosynthesize all kinds of amino acids, including an intermediate compound (homocysteine) in methionine metabolism. For methionine or related by-products (such as homocysteine thiolactone), several *metI/E/F*-encoding genes were predicted to be located at contig1 (Supplementary Figure 3). These genes showed relatively high identity to another species of the same genus, *Staphylococcus aureus* (Grundy and Henkin, 1998). Our results further support the previous viewpoint, i.e., many microorganisms are able to synthesize methionine *de novo* and staphylococci employ the trans-sulfuration pathway to generate methionine (Rodionov et al., 2004). In this work, the whole-genome sequence of strain D11 provides deeper understanding of the molecular mechanism of the anti-QS ability of strain D11, and also may facilitate insights into the active product biosynthesis process.

CONCLUSIONS

In this work, we uncovered the anti-QS activity of a marine bacterial species isolated from the coral *Pocillopora damicornis*. The extract of strain D11 (*S. hominis*) was antagonistic to *P. aeruginosa* PAO1 QS and affected QS-regulated functional genes, including those involved in biofilm formation and virulence production. It is possible that the analog molecule DL-homocysteine thiolactone produced by strain D11 (*S. hominis*) competed with the auto-inducers produced by *P. aeruginosa* PAO1. Interestingly, DL-homocysteine thiolactone did not affect the growth of *P. aeruginosa* PAO1. These characteristics may accelerate development of QS inhibitors with broad-spectrum activity, and facilitate the discovery of novel drugs with greater efficacy to deal with bacterial infections in the current post-antibiotic era.

AUTHOR CONTRIBUTIONS

Z-PM and JZ performed the experiments and drafting of the manuscript. YS and Z-HC acquired and analyzed data. Z-JL prepared figures and tables. YW and G-HL completed critical revision.

ACKNOWLEDGMENTS

This study was supported by NSFC (41741015), as well as the S&T Projects of Shenzhen Science and Technology Innovation Committee (JCYJ20170412171959157, JCYJ20150529164918736, JCYJ20150831192329178, and JCYJ20170412171947159).

SUPPLEMENTARY MATERIAL

The Supplementary Material for this article can be found online at: https://www.frontiersin.org/articles/10.3389/fcimb.2018.00144/full#supplementary-material

REFERENCES

Abudoleh, S. M., and Mahasneh, A. M. (2017). Anti-quorum sensing activity of substances isolated from wild berry associated bacteria. *Avicenna J. Med. Biotechnol.* 9, 23–30.

Adonizio, A., Kong, K. F., and Mathee, K. (2008). Inhibition of quorum sensing controlled virulence factor production in *Pseudomonas aeruginosa* by south Florida plant extracts. *Antimicrob. Agents Chemother.* 52, 198–203. doi: 10.1128/AAC.00612-07

Arendrup, M. C., and Patterson, T. F. (2017). Multidrug-resistant candida: epidemiology, molecular mechanisms, and treatment. *J. Infect. Dis.* 216(Suppl. 3), S445–S451. doi: 10.1093/infdis/jix131

Bakkiyaraj, D., Sivasankar, C., and Pandian, S. K. (2012). Inhibition of quorum sensing regulated biofilm formation in *Serratia marcescens* causing nosocomial infections. *Bioorg. Med. Chem. Lett.* 22, 3089–3094. doi: 10.1016/j.bmcl.2012.03.063

Bakkiyaraj, D., Sivasankar, C., and Pandian, S. K. (2013). Anti-pathogenic potential of coral associated bacteria isolated from Gulf of Mannar against *Pseudomonas aeruginosa*. *Indian J. Microbiol.* 53, 111–113. doi: 10.1007/s12088-012-0342-3

Bankevich, A., Nurk, S., Antipov, D., Gurevich, A. A., Dvorkin, M., Kulikov, A. S., et al. (2012). SPAdes: a new genome assembly algorithm and its applications to single-cell sequencing. *J. Comp. Biol.* 19, 455–477. doi: 10.1089/cmb.2012.0021

Bauer, A. W., Kirby, W. M., Sherris, J. C., and Turck, M. (1966). Antibiotic susceptibility testing by a standardized single disk method. *Am. J. Clin. Pathol.* 45, 493–496. doi: 10.1093/ajcp/45.4ts.493

Besemer, J., Lomsadze, A., and Borodovsky, M. (2001). GeneMarkS: a self-training method for prediction of gene starts in microbial genomes. Implications for finding sequence motifs in regulatory regions. *Nucleic Acids Res.* 29, 2607–2618. doi: 10.1093/nar/29.12.2607

Blosser, R. S., and Gray, K. M. (2000). Extraction of violacein from *Chromobacterium violaceum* provides a new quantitative bioassay for N-acyl homoserine lactone autoinducers. *J. Microbiol. Methods* 40, 47–55. doi: 10.1016/S0167-7012(99)00136-0

Boetzer, M., Henkel, C. V., Jansen, H. J., Butler, D., and Pirovano, W. (2011). Scaffolding preassembled contigs using SSPACE. *Bioinformatics* 27, 578–579. doi: 10.1093/bioinformatics/btq683

Boetzer, M., and Pirovano, W. (2012). Toward almost closed genomes with GapFiller. *Gen. Biol.* 13:R56. doi: 10.1186/gb-2012-13-6-r56

Busetti, A., Shaw, G., Megaw, J., Gorman, S. P., Maggs, C. A., and Gilmore, B. F. (2014). Marine-derived quorum-sensing inhibitory activities enhance the antibacterial efficacy of tobramycin against *Pseudomonas aeruginosa*. *Mar. Drugs.* 13, 1–28. doi: 10.3390/md13010001

Certner, R. H., and Vollmer, S. V. (2018). Inhibiting bacterial quorum sensing arrests coral disease development and disease-associated microbes. *Environ. Microbiol.* 20, 645–657. doi: 10.1111/1462-2920.13991

Chang, H., Zhou, J., Zhu, X. S., Yu, S. C., Chen, L., Jin, H., et al. (2017). Strain identification and quorum sensing inhibition characterization of marine-derived *Rhizobium* sp. NAO1. *R. Soc. Open. Sci.* 4:170025. doi: 10.1098/rsos.170025

Choo, J. H., Rukayadi, Y., and Hwang, J. K. (2006). Inhibition of bacterial quorum sensing by vanilla extract. *Lett. Appl. Microbiol.* 42, 637–641. doi: 10.1111/j.1472-765X.2006.01928.x

Christensen, L. D., Moser, C., Jensen, P. Ø., Rasmussen, T. B., Christophersen, L., Kjelleberg, S., et al. (2007). Impact of *Pseudomonas aeruginosa* quorum sensing on biofilm persistence in an *in vivo* intraperitoneal foreign-body infection model. *Microbiology* 153, 2312–2320. doi: 10.1099/mic.0.2007/006122-0

Defoirdt, T. (2017). Quorum-sensing systems as targets for anti-virulence therapy. *Trends. Microbiol.* 26, 313–328. doi: 10.1016/j.tim.2017.10.005.

deKievit, T. R. (2009). Quorum sensing in *Pseudomonas aeruginosa* biofilms. *Environ. Microbiol.* 11, 279–288. doi: 10.1111/j.1462-2920.2008.01792.x

Dobretsov, S., Dahms, H. U., and Qian, P. Y. (2006). Inhibition of biofouling by marine microorganisms and their metabolites. *Biofouling* 22, 43–54. doi: 10.1080/08927010500504784

Dobretsov, S., Teplitski, M., Bayer, M., Gunasekera, S., Proksch, P., and Paul, V. J. (2011). Inhibition of marine biofouling by bacterial quorum sensing inhibitors. *Biofouling* 27, 893–905. doi: 10.1080/08927014.2011.609616

Dobretsov, S., Teplitski, M., and Paul, V. (2009). Mini-review: quorum sensing in the marine environment and its relationship to biofouling. *Biofouling* 25, 413–427. doi: 10.1080/08927010902853516

Dong, Y. H., and Zhang, L. H. (2005). Quorum sensing and quorum-quenching enzymes. *J. Microbiol.* 43, 101–109.

do Valle Gomes, M. Z., and Nitschke, M. (2012). Evaluation of rhamnolipid and surfactin to reduce the adhesion and remove biofilms of individual and mixed cultures of food pathogenic bacteria. *Food Control* 25, 441–447. doi: 10.1016/j.foodcont.2011.11.025

Gasol, J., del Giorgio, P. (2000). Using flow cytometry for counting natural planktonic bacteria and understanding the structure of planktonic bacterial communities. *Sci. Mar.* 64, 197–224. doi: 10.3989/scimar.2000.64n2197

Geske, G. D., O'Neill, J. C., Miller, D. M., Wezeman, R. J., Mattmann, M. E., Lin, Q., et al. (2008). Comparative analyses of N-acylated homoserine lactones reveal unique structural features that dictate their ability to activate or inhibit quorum sensing. *Chembiochem* 9, 389–400. doi: 10.1002/cbic.200700551

Givskov, M., de Nys, R., Manefield, M., Gram, L., Maximilien, R., Eberl, L., et al. (1996). Eukaryotic interference with homoserine lactone-mediated prokaryotic signaling. *J. Bacteriol.* 178, 6618–6622. doi: 10.1128/jb.178.22.6618-6622.1996

Golberg, K., Pavlov, V., Marks, R. S., and Kushmaro, A. (2013). Coral-associated bacteria, quorum sensing disrupters, and the regulation of biofouling. *Biofouling* 29, 669–682. doi: 10.1080/08927014.2013.796939

Grundy, F. J., and Henkin, T. M. (1998). The S box regulon: a new global transcription termination control system for methionine and cysteine biosynthesis genes in gram-positive bacteria. *Mol. Microbiol.* 30, 737–749. doi: 10.1046/j.1365-2958.1998.01105.x

Hentzer, M., Riedel, K., Rasmussen, T. B., Heydorn, A., Andersen, J. B., Parsek, M. R., et al. (2002). Inhibition of quorum sensing in *Pseudomonas aeruginosa* biofilm bacteria by a halogenated furanone compound. *Microbiology* 148, 87–102. doi: 10.1099/00221287-148-1-87

Hentzer, M., Teitzel, G. M., Balzer, G. J., Heydorn, A., Molin, S., Givskov, M., et al. (2001). Alginate overproduction affects *Pseudomonas aeruginosa* biofilm structure and function. *J. Bacteriol.* 183, 5395–5401. doi: 10.1128/JB.183.18.5395-5401.2001

Heydorn, A., Nielsen, A. T., Hentzer, M., Sternberg, C., Givskov, M., Ersbøll, B. K., et al. (2000). Quantification of biofilm structures by the novel computer program COMSTAT. *Microbiology* 146, 2395–2407. doi: 10.1099/00221287-146-10-2395

Hinsa, S. M. (2006). Biofilm formation by *Pseudomonas fluorescens* WCS365: a role for *LapD*. *Microbiology* 52, 1375–1383. doi: 10.1099/mic.0.28696-0

Huang, Z., Meric, G., Liu, Z., Ma, R., Tang, Z., and Lejeune, P. (2009)*luxS*-based quorum-sensing signaling affects biofilm formation in *Streptococcus mutans*. *J. Mol. Microbiol. Biotechnol.* 17, 12–19. doi: 10.1159/000159193

Huber, B., Eberl, L., Feucht, W., and Polster, J. (2003). Influence of polyphenols on bacterial biofilm formation and quorum-sensing. *Z. Naturforsch. C* 58, 879–884. doi: 10.1515/znc-2003-11-1224

Ishida, T., Ikeda, T., Takiguchi, N., Kuroda, A., Ohtake, H., and Kato, J. (2007). Inhibition of quorum sensing in *Pseudomonas aeruginosa* by N-acyl cyclopentylamides. *Appl. Environ. Microbiol.* 73, 3183–3188. doi: 10.1128/AEM.02233-06

Jiang, T., and Li, M. (2013). Quorum sensing inhibitors: a patent review. *Expert. Opin. Ther. Pat.* 23, 867–894. doi: 10.1517/13543776.2013.779674

Jones, P., Binns, D., Chang, H. Y., Fraser, M., Li, W., McAnulla, C., et al. (2014). InterProScan 5: genome-scale protein function classification. *Bioinformatics* 30, 1236–1240. doi: 10.1093/bioinformatics/btu031

Kalia, V. C. (2012). Quorum sensing inhibitors: an overview. *Biotechnol. Adv.* 31, 224–245. doi: 10.1016/j.biotechadv.2012.10.004

Kalia, V. C., and Purohit, H. J. (2011). Quenching the quorum sensing system: potential antibacterial drug targets. *Crit. Rev. Microbiol.* 37, 121–140. doi: 10.3109/1040841X.2010.532479

Kanagasabhapathy, M., Yamazaki, G., Ishida, A., Sasaki, H., and Nagata, S. (2009). Presence of quorum-sensing inhibitor-like compounds from bacteria isolated from the brown alga *Colpomenia sinuosa*. *Lett. Appl. Microbiol.* 49, 573–579. doi: 10.1111/j.1472-765X.2009.02712.x

Kim, C., Kim, J., Park, H. Y., Park, H. J., Lee, J. H., Kim, C. K., et al. (2008). Furanone derivatives as quorum-sensing antagonists of *Pseudomonas aeruginosa*. *Appl. Microbiol. Biotechnol.* 80, 37–47. doi: 10.1007/s00253-008-1474-6

Kvennefors, E. C., Sampayo, E., Kerr, C., Vieira, G., Roff, G., and Barnes, A. C. (2012). Regulation of bacterial communities through antimicrobial activity by the coral holobiont. *Microb. Ecol.* 63, 605–618. doi: 10.1007/s00248-011-9946-0

Lagesen, K., Hallin, P., Rødland, E. A., Staerfeldt, H. H., Rognes, T., and Ussery, D. W. (2007). RNAmmer: consistent and rapid annotation of ribosomal RNA genes. *Nucleic Acids Res.* 35, 3100–3108. doi: 10.1093/nar/gkm160

Lane, D. J. (1991). "16S/23S rRNA sequencing," in *Nucleic Acid Techniques in Bacterial Systematics,* eds E. Stackebrandt, W. Goodfellow (New York, NY: John Wiley & Sons, Inc.), 115–118.

Livak, K. J., and Schmittgen, T. D. (2001). Analysis of relative gene expression data using real-time quantitative PCR and the $2^{-\Delta\Delta Ct}$ method. *Methods* 25, 402–408. doi: 10.1006/meth.2001.1262

Martínez-Matamoros, D., Fonseca, M. L., Duque, C., Ramos, F. A., and Castellanos, L. (2016). Screening of marine bacterial strains as source of quorum sensing inhibitors (QSI): first chemical study of *Oceanobacillus profundus* (RKHC-62B). *Vitae* 23, 30–47. doi: 10.17533/udea.vitae.v23n1a04

McInnis, C. E., and Blackwell, H. E. (2011). Thiolactone modulators of quorum sensing revealed through library design and screening. *Bioorg. Med. Chem.* 19, 4820–4828. doi: 10.1016/j.bmc.2011.06.071

Melvin, J. A., Montelaro, R. C., and Bomberger, J. M. (2016). Clinical potential of engineered cationic antimicrobial peptides against drug resistant biofilms. *Expert. Rev. Anti. Infect. Ther.* 14, 989–991. doi: 10.1080/14787210.2016.1236687

Musthafa, K. S., Saroja, V., Pandian, S. K., and Ravi, A. V. (2011). Antipathogenic potential of marine *Bacillus* sp. SS4 on *N*-acyl-homoserine-lactone-mediated virulence factors production in *Pseudomonas aeruginosa* (PAO1). *J. Biosci.* 36, 55–67. doi: 10.1007/s12038-011-9011-7

Ni, N., Li, M., Wang, J., and Wang, B. (2009). Inhibitors and antagonists of bacterial quorum sensing. *Med. Res. Rev.* 29, 65–124. doi: 10.1002/med.20145

Nithya, C., Aravindraja, C., and Pandian, S. K. (2010b). *Bacillus pumilus* of Palk Bay origin inhibits quorum-sensing-mediated virulence factors in Gram-negative bacteria. *Res. Microbiol.* 161, 293–304. doi: 10.1016/j.resmic.2010.03.002

Nithya, C., Begum, M. F., and Pandian, S. K. (2010c). Marine bacterial isolates inhibit biofilm formation and disrupt mature biofilms of *Pseudomonas aeruginosa* PAO1. *Appl. Microbiol. Biotechnol.* 88, 341–358. doi: 10.1007/s00253-010-2777-y

Nithya, C., and Pandian, S. K. (2010a). The *in vitro* antibiofilm activity of selected marine bacterial culture supernatants against *Vibrio* spp. *Arch. Microbiol.* 192, 843–854. doi: 10.1007/s00203-010-0612-6

Okuda, T. (2005). Systematics and health effects of chemically distinct tannins in medicinal plants. *Phytochem Rev.* 66, 2012–2031. doi: 10.1016/j.phytochem.2005.04.023

Ortlepp, S., Sjögren, M., Dahlström, M., Weber, H., Ebel, R., Edrada, R., et al. (2007). Antifouling activity of bromotyrosine-derived sponge metabolites and synthetic analogues. *Mar. Biotechnol.* 9, 776–785. doi: 10.1007/s10126-007-9029-x

Park, S. Y., Kang, H. O., Jang, H. S., Lee, J. K., Koo, B. T., and Yum, D. Y. (2005). Identification of extracellular N-acylhomoserine lactone acylase from a *Streptomyces* sp. and its application to quorum quenching. *Appl. Environ. Microbiol.* 71, 2632–2641. doi: 10.1128/AEM.71.5.2632-2641.2005

Pham, T. M., Wiese, J., Wenzel-Storjohann, A., and Imhoff, J. F. (2016). Diversity and antimicrobial potential of bacterial isolates associated with the soft coral *Alcyoniumdigitatum* from the Baltic Sea. *Antonie Van Leeuwenhoek*. 109, 105–119. doi: 10.1007/s10482-015-0613-1

Pinder, A. C., Purdy, P. W., Poulter, S. A., and Clark, D. C. (1990). Validation of flow cytometry for rapid enumeration of bacterial concentrations in pure cultures. *J. Appl. Bacteriol.* 69, 92–100. doi: 10.1111/j.1365-2672.1990.tb02916.x

Ren, D., Sims, J., and Wood, T. (2002). Inhibition of biofilm formation and swarming of *Bacillus subtilis* by (5Z)-4-bromo-5-(bromomethylene)-3-butyl-2 (5H)-furanone. *Lett. Appl. Microbiol.* 34, 293–299. doi: 10.1046/j.1472-765x.2002.01087.x

Rodionov, D. A., Vitreschak, A. G., Mironov, A. A., and Gelfand, M. S. (2004). Comparative genomics of the methionine metabolism in Gram-positive bacteria: a variety of regulatory systems. *Nucleic Acids Res.* 32, 3340–3353. doi: 10.1093/nar/gkh659

Romero, M., Martin-Cuadrado, A. B., and Otero, A. (2012). Determination of whether quorum quenching is a common activity in marine bacteria by analysis of cultivable bacteria and metagenomic sequences. *Appl. Environ. Microbiol.* 78, 6345–6348. doi: 10.1128/AEM.01266-12

Schoenfelder, S. M., Marincola, G., Geiger, T., Goerke, C., Wolz, C., and Ziebuhr, W. (2013). Methionine biosynthesis in Staphylococcus aureus is tightly controlled by a hierarchical network involving an initiator tRNA-specific T-box riboswitch. *PLoS Pathog.* 9:e1003606. doi: 10.1371/journal.ppat.1003606

Schuster, M., and Greenberg, E. P. (2006). A network of networks: quorum-sensing gene regulation in *Pseudomonas aeruginosa*. *Int. J. Med. Microbiol.* 296, 73–81. doi: 10.1016/j.ijmm.2006.01.036

Schuster, M., Lohstroh, C. P., Ogi, T., and Greenberg, E. P. (2003). Identification, timing and signal specificity of *Pseudomonas aeruginosa* quorum-controlled genes: a transcriptome analysis. *J. Bacteriol.* 185, 2066–2079. doi: 10.1128/JB.185.7.2066-2079.2003

Seemann, T. (2014). Prokka: rapid prokaryotic genome annotation. *Bioinformatics* 30, 2068–2069. doi: 10.1093/bioinformatics/btu153

Sharma, I. M., Petchiappan, A., and Chatterji, D. (2014). Quorum sensing and biofilm formation in mycobacteria: role of c-di-GMP and methods to study this second messenger. *IUBMB Life* 66, 823–834. doi: 10.1002/iub.1339

Singh, V. K., Kavita, K., Prabhakaran, R., and Jha, B. (2013). Cis-9-octadecenoic acid from the rhizospheric bacterium *Stenotrophomonas maltophilia* BJ01 shows quorum quenching and anti-biofilm activities. *Biofouling* 29, 855–867. doi: 10.1080/08927014.2013.807914

Singh, V. K., Mishra, A., and Jha, B. (2016). "Marine bacterial extracellular polymeric substances: characteristics and applications," in *Marine Glycobiology: Principles and Applications*, ed S. Kim (Boca Raton, FL: Taylor and Francis Group; CRC Press), 369–377.

Singh, V. K., Mishra, A., and Jha, B. (2017). Anti-quorum sensing and anti-biofilm activity of *Delftia tsuruhatensis* extract by attenuating the quorum sensing-controlled virulence factor production in *Pseudomonas aeruginosa*. *Front. Cell. Infect. Microbiol.* 7:337. doi: 10.3389/fcimb.2017.00337

Skindersoe, M. E., Ettinger-Epstein, P., Rasmussen, T. B., Bjarnsholt, T., de Nys, R., and Givskov, M. (2008). Quorum sensing antagonism from marine organisms. *Mar. Biotechnol.* 10, 56–63. doi: 10.1007/s10126-007-9036-y

Sommer, R., Joachim, I., Wagner, S., and Titz, A. (2013). New approaches to control infections: anti-biofilm strategies against gram-negative bacteria. *Chimia* 67, 286–290. doi: 10.2533/chimia.2013.286

Stowe, S. D., Richards, J. J., Tucker, A. T., Thompson, R., Melander, C., and Cavanagh, J. (2011). Anti-biofilm compounds derived from marine sponges. *Mar. Drugs* 9, 2010–2035. doi: 10.3390/md9102010

Teasdale, M. E., Donovan, K. A., Forschner-Dancause, S. R., and Rowley, D. C. (2011). Gram-positive marine bacteria as a potential resource for the discovery of quorum sensing inhibitors. *Mar. Biotechnol.* 13, 722–732. doi: 10.1007/s10126-010-9334-7

Teasdale, M. E., Liu, J., Wallace, J., Akhlaghi, F., and Rowley, D. C. (2009). Secondary metabolites produced by the marine bacterium *Halobacillus salinus* that inhibit quorum sensing-controlled phenotypes in Gram-negative bacteria. *Appl. Environ. Microbiol.* 75, 567–572. doi: 10.1128/AEM.00632-08

Thenmozhi, R., Nithyanand, P., Rathna, J., and Karutha, P. S. (2009). Antibiofilm activity of coral-associated bacteria against different clinical M serotypes of *Streptococcus pyogenes*. *FEMS Immunol. Med. Microbiol.* 573, 284–294. doi: 10.1111/j.1574-695X.2009.00613.x

Tolker-Nielsen, T., and Sternberg, C. (2014). Methods for studying biofilm formation: flow cells and confocal laser scanning microscopy. *Methods Mol. Biol.* 1149, 615–629. doi: 10.1007/978-1-4939-0473-047

Tolmacheva, A. A., Rogozhin, E. A., and Deryabin, D. G. (2014). Antibacterial and quorum sensing regulatory activities of some traditional Eastern-European medicinal plants. *Acta Pharm.* 64, 173–186. doi: 10.2478/acph-2014-0019

Vattem, D. A., Mihalik, K., Crixell, S. H., and McLean, R. J. (2007). Dietary phytochemicals as quorum sensing inhibitors. *Fitoterapia* 78, 302–310. doi: 10.1016/j.fitote.2007.03.009

Vuotto, C., Longo, F., Balice, M. P., Donelli, G., and Varaldo, P. E. (2014). Antibiotic resistance related to biofilm formation in *Klebsiella pneumoniae*. *Pathogens* 3, 743–758. doi: 10.3390/pathogens3030743

Wagner, V. E., Bushnell, D., Passador, L., Brooks, A. I., and Iglewski, B. H. (2003). Microarray analysis of *Pseudomonas aeruginosa* quorum-sensing regulons: effects of growth phase and environment. *J. Bacteriol.* 185, 2080–2095. doi: 10.1128/JB.185.7.2080-2095.2003

Yaniv, K., Golberg, K., Kramarsky-Winter, E., Marks, R., Pushkarev, A., Béjà, O., et al. (2017). Functional marine metagenomic screening for anti-quorum sensing and anti-biofilm activity. *Biofouling* 33, 1–13. doi: 10.1080/08927014.2016.1253684

Zhang, L. H., and Dong, Y. H. (2004). Quorum sensing and signal interference: diverse implications. *Mol. Microbiol.* 53, 1563–1571. doi: 10.1111/j.1365-2958.2004.04234.x

Conflict of Interest Statement: The authors declare that the research was conducted in the absence of any commercial or financial relationships that could be construed as a potential conflict of interest.

frontiers in Cellular and Infection Microbiology

ORIGINAL RESEARCH
published: 12 July 2017
doi: 10.3389/fcimb.2017.00313

Inhibition of the Quorum Sensing System (ComDE Pathway) by Aromatic 1,3-di-m-tolylurea (DMTU): Cariostatic Effect with Fluoride in Wistar Rats

*Gurmeet Kaur, P. Balamurugan and S. Adline Princy **

Quorum Sensing Laboratory, Centre for Research in Infectious Diseases, School of Chemical and Biotechnology, SASTRA University, Thanjavur, India

Dental caries occurs as a result of dysbiosis among commensal and pathogenic bacteria leading to demineralization of enamel within a dental biofilm (plaque) as a consequence of lower pH in the oral cavity. In our previous study, we have reported 1,3-disubstituted ureas particularly, 1,3-di-m-tolylurea (DMTU) could inhibit the biofilm formation along with lower concentrations of fluoride (31.25 ppm) without affecting bacterial growth. In the present study, RT-qPCR analysis showed the target specific molecular mechanism of DMTU. *In vivo* treatment with DMTU, alone or in combination with fluoride, resulted in inhibition of caries (biofilm development of *Streptococcus mutans*) using a Wistar rat model for dental caries. The histopathological analysis reported the development of lesions on dentine in infected subjects whereas the dentines of treated rodents were found to be intact and healthy. Reduction in inflammatory markers in rodents' blood and liver samples was observed when treated with DMTU. Collectively, data speculate that DMTU is an effective anti-biofilm and anti-inflammatory agent, which may improve the cariostatic properties of fluoride.

Keywords: quorum sensing, dental caries, antibiofilm, multi-drug resistance, DMTU

OPEN ACCESS

Edited by:
Maria Tomas,
Complexo Hospitalario Universitario A Coruña, Spain

Reviewed by:
Thomas Thurnheer,
University of Zurich, Switzerland
Robson Souza Leão,
Rio de Janeiro State University, Brazil

****Correspondence:***
S. Adline Princy
adlineprinzy@biotech.sastra.edu

Received: *14 April 2017*
Accepted: *26 June 2017*
Published: *12 July 2017*

Citation:
Kaur G, Balamurugan P and Princy SA (2017) Inhibition of the Quorum Sensing System (ComDE Pathway) by Aromatic 1,3-di-m-tolylurea (DMTU): Cariostatic Effect with Fluoride in Wistar Rats. Front. Cell. Infect. Microbiol. 7:313. doi: 10.3389/fcimb.2017.00313

INTRODUCTION

Streptococcus mutans is known as one of the principal aetiological agent that plays a significant role in the transition of non-pathogenic commensal oral microbiota to highly acidic and cariogenic biofilms resulting in the development of dental caries. Worldwide, dental caries is one of the most common biofilm-dependent oral infectious diseases. The major virulence factors include acidogenicity and aciduricity along with its characteristic ability to produce dental plaque (biofilm). In *S. mutans*, biofilm formation is regulated by quorum sensing (QS) that involves ComDE two-component signal transduction system (TCSTS) which regulates the expression of virulence factors in cell density dependent manner. ComDE QS circuit in *S. mutans* specifically responds to the competence stimulating peptide (CSP; Kaur et al., 2015). The CSP is synthesized as a 21 amino acids propeptide by *comC* followed by maturation of CSP by an ABC transporter ComA along with an accessory protein ComB and finally secreted (18 amino acids long peptide signal) to the extracellular environment. Secreted peptide is detected by the histidine kinase membrane-bound protein receptor, ComD, resulting in phosphorylation of its cytoplasmic response regulator, ComE

thus, resulting in expression of various virulence genes as a response to signaling peptide (Ishii et al., 2010).

Biofilm formation protects bacteria from the host immune system and also acts a diffusion barrier providing resistance to bacteria from various antimicrobials (Senadheera and Cvitkovitch, 2008; Arya and Princy, 2013). In fact, cells existing within the biofilm community are 10–1,000 times more resistant to antimicrobials than their planktonic counterparts (Mah and O'Toole, 2001). Dental plaque (biofilm), if allowed to persist on tooth surfaces, subsequently progress to the development of periodontitis leading to the extraction of a tooth in infected individuals. *S. mutans* may enter the blood stream via injuries in oral cavity and further attach to platelet-fibrin-matrices on damaged endothelial tissue. The ability of *S. mutans* to adhere and thrive on the injured heart tissue leads to the unhindered survival and pathogenesis of chronic infective endocarditis which may cause significant morbidity and mortality (Bansal et al., 2013). Invasion by *S. mutans* in the blood stream may also result in bacteremia causing chronic inflammation and its manifestations such as rheumatoid arthritis, premature birth of babies. Targeting one of the key components involved in cell-cell signaling process can lead to inhibition of biofilm formation (Qi et al., 2005; Rasmussen and Givskov, 2006; Ravichandiran et al., 2012). Development of novel anti-biofilm drugs against biofilm forming bacteria without causing mortality of the pathogen might result in the inhibition of biofilm formation (Balamurugan et al., 2015; Chen et al., 2015). In this context, we have previously reported ComA as a potential target for drug development (Kaur et al., 2016). *In silico* findings showed 1,3-disubstituted ureas as potential ligands followed by synthesis and *in vitro* validation of parent ligand (DMTU) along with five derivative ligands revealed parent ligand i.e., 1,3-di-m-tolylurea (DMTU) as a potential inhibitor of ComA. Fluoride has been used long as an effective cariostatic agent for caries prevention in commercial formulations. However, prolonged use of high concentrations of fluoride (1,000–2,000 ppm) has led to the development of fluoride-resistant strains along with its reported side effects such as fluorosis, neurotoxicity, and weakened bones in children (Jetti et al., 2014; Spittle, 2016). Therefore, to explore the possibility of reducing the fluoride concentration, we had included fluoride in our *in vitro* assays and investigated its synergistic activity along with our synthesized compounds. Results of *in vitro* validation indicated that DMTU could act as a potent biofilm inhibitor alone as well as along with lower concentration of fluoride (31.25 ppm) among all the synthesized compounds.

Thus, to further explore the target specific activity of DMTU, the objectives of the present study were (i) to elucidate the target specific mechanism of DMTU on various quorum regulated genes and (ii) to test and validate the activity of DMTU at pre-clinical stages using Wistar rat model for dental caries.

MATERIALS AND METHODS

Cell Culture

Liver hepatocellular carcinoma (Hep G2) cells were received from National Centre for Cell Science (NCCS), Pune, India. The cells were cultured in Dulbecco's modified Eagle's medium (HiMedia) supplemented with 10% fetal bovine serum (FBS) and 1% pen/strep. The cells were incubated and maintained at 37°C in a saturated humidified incubator with 5% CO_2. MTT [3-(4,5-dimethylthiazole-2-yl)-2,5-diphenyl tetrazolium bromide] for cell proliferation assay was purchased from HiMedia, Mumbai, India.

Bacterial Strains and Growth Medium

S. mutans MTCC 497 was received from the Microbial Type Culture Collection (MTCC), Chandigarh, India and was used as a standard strain in the study. A clinical isolate of *S. mutans*, SM4 (Multidrug resistant) was received from JSS Medical College, Mysore, India. The SM4 strain was categorized to be multidrug resistant as described by Magiorakos et al. (2012). Both the strains were grown at 37°C in brain heart infusion broth/agar (HiMedia) supplemented with 2% sucrose.

Test Compounds

The synthesis of aromatic 1,3-disubstituted ureas was carried out by a simple one-pot reaction of aryl isocyanates with the selective amines has been reported previously by the authors. Further, the derivatives of the lead compound were synthesized and screened *in vitro* for their anti-biofilm activity. Amongst all the synthesized compounds, DMTU (1,3-di-m-tolylurea; **Figure 1A**) was found to be the most effective based on their biofilm inhibiting activity against *S. mutans*.

Quantification of Gene Expression Using RT-qPCR

S. mutans (MTCC 497 and SM4) were grown in BHIB in the presence and absence of DMTU (3.75 μM) and fluoride (31.35 ppm) till 24 h at 37°C. Cells were harvested by centrifugation from grown cultures (0.5 ml) at early log phase (3–5 h), mid-log phase (8–10 h) and stationary phase (24 h) and immediately stored at −80°C. RNA was isolated using a Qiagen RNeasy mini Kit in accordance with the manufacturer's instructions. RNA concentrations were determined by OD_{260} measurements in a NanoDrop (Thermo Scientific, USA). cDNA synthesis was carried out using the iScript™ cDNA Synthesis Kit according to the manufacturer's instructions. Briefly, the reaction mixture was incubated for annealing at 25°C for 5 min, extension at 42°C for 30 min and inactivation of samples at 85°C for 5 min.

RT-qPCR was used to assess the transcription levels of biofilm and virulence related genes (*comA, nlmC, immA, immB, bsmH, bsmI, comDE, comX, comB*). Sequences of the primers used in this study are furnished in **Table 1**. The reaction mixture in a total volume of 20 μl, consisted 10 μl 2X SYBR Green PCR Master Mix, forward and reverse primers (1 μl each), 4 μl of nuclease-free water and 4 μl of 20X diluted cDNA (Hasan et al., 2012). PCR conditions included an initial denaturation at 95°C for 2 min, followed by 40 cycles of denaturation (95°C for 15 s), annealing (55–57°C for 15 s), and extension (72°C for 20 s). To ensure the samples were free from contamination, negative controls containing nuclease-free water instead of cDNA were run in parallel. The relative gene expression was analyzed using the $2^{-\Delta\Delta CT}$ method with 16S r-RNA as a reference gene. RT-qPCR experiments were in compliance with the MIQE (Minimum

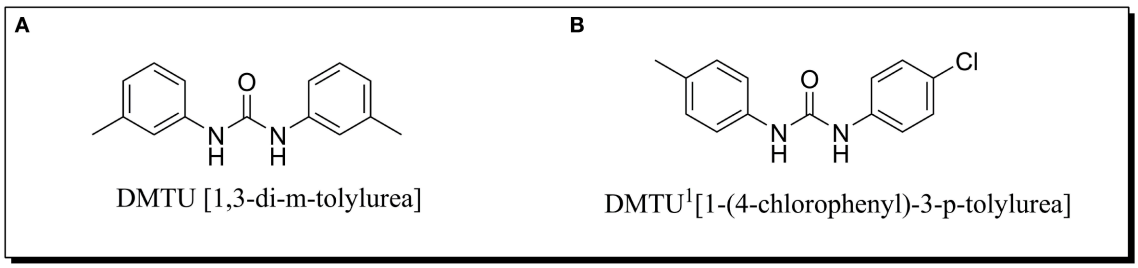

FIGURE 1 | Chemical structure of **(A)** DMTU (1,3-di-m-tolylurea) and **(B)** DMTU[1] (1-(4-chlorophenyl)-3-p-tolylurea).

TABLE 1 | Primer sequence for RT-qPCR analysis of various genes in *S. mutans*.

Gene	Forward Primer Sequence (5′–3′)	Reverse Primer Sequence (5′–3′)
comDE	ACAATTCCTTGAGTTCCATCCAAG	TGGTCTGCTGCCTGTTGC
16S rRNA	CCTACGGGAGGCAGCAGTAG	CAACAGAGCTTTACGATCCGAAA
nlmC	TTGTGCAGCAGGTATTGCTC	AAGAGCTCCTCCGATTCCTC
immA	TCTCCCCTGCTTGTTCAGAT	GCTGGCAAATTCGCTTACTT
immB	GCTAGAGAGGCAAATGCACA	CAGCAGCAGCTGAGAAGATG
bsmI	GAAACAATGGATACAGAGACG	GGAACAATAAGAGGATTTGG
bsmH	AGACATGTTAGCCGCTGTTGAAG	AAGCGCCTGTTCCAATCGTA
comX	CTGTTTGTCAAGTGGCGGTA	GCATACTTTGCCTTCCCAAA
comA	ACGAGCCTAACAAGGGGATT	CCCTGAGGCATTTGTTCAAT
comB	CCAGTCCAAACCGTCAGACT	GCTGCTTTCCTTGTCTTTCG

Information for Publication of Quantitative Real-Time PCR Experiments) guidelines as listed in the MIQE checklist (Bustin et al., 2009; Supplementary Information: Table S1).

MTT Cell Proliferation Assay

For toxicity analysis, Liver hepatocellular carcinoma (Hep G2) cells were cultured in the presence of DMTU and DMTU[1] **Figure 1B**. After trypsinization and counting the cells with a hemocytometer, 10,000 cells were seeded in 96 well plate along with 1, 3-disubstituted ureas. The cells were allowed to proliferate for 24 h at 37°C and at the endpoint, MTT reagent was added and further subjected to 4 h of incubation (Ciofani et al., 2010). The formazan crystals formed after addition of MTT were solubilized using DMSO (100 μL) and the absorbance was measured at 570 nm in a microtitre plate reader (iMark, BIORAD, Japan).

Animal Study

Acute Oral Toxicity (AOT) Analysis:

Healthy female Wistar rats aged 8 weeks used for the AOT analysis were bred and reared in the Central Animal Facility, SASTRA University, Thanjavur, Tamil Nadu, India. The animals were acclimatized to animal house conditions for 1 week prior to the treatment with DMTU. The animals were housed and maintained in polypropylene cages consisting of clean paddy husk bedding with stainless steel grill lids at a temperature of 25 ± 2°C under a 12:12 h light-dark cycle. The rats were fed with pelleted feed (M/S ATNT Laboratories, Mumbai, India) and filtered tap water *ad libitum* throughout the experiment.

The acute oral toxicity test of DMTU was evaluated in rats using the up and down procedure in accordance with OECD 425 guidelines (Maneewattanapinyo et al., 2011). Briefly, the rats were divided into five groups with the first group receiving a limited dose of 175 mg/kg orally using a suitable intubation canula. The animals were observed for toxic symptoms continuously for the first 3 h after dosing. The animals were further observed for 48 h and based on survival of the first group rats, the second group was dosed with 550 mg/kg orally. Similar observations were carried out for the second group and subsequently based on the survival of rat, the dosing was increased to 2,000 mg/kg for the next three groups. All these animals were then maintained for 14 days further with feed intake observations made on a daily basis and weight observations on a weekly basis. At the 14th day, the animal was sacrificed and vital organs were observed macroscopically by a calibrated professional histopathologist for any lesions.

Efficacy Studies

The animal experiments were reviewed and approved by Institutional Animal Ethics Committee (IAEC) with approval number 382/SASTRA/IAEC/RPP of SASTRA University, Thanjavur, Tamil Nadu, India and was performed according to the methods described previously (Murata et al., 2010). To determine the effects of DMTU on caries establishment, a total of 42 SPF female Wistar rats aged 21 days were purchased from the Central Animal Facility, SASTRA University, Thanjavur, India. After acclimatization for 5 days, the 30 animals were infected with clinical isolate of *S. mutans* SM4, using a sterile cotton swab

dipped in culture medium (10^5 CFU/mL) and randomly divided into five groups ($n = 6$ per group): a disease control, a DMTU treated group (3.75 μM), a fluoride treated group (500 ppm), a synergy group (3.75 μM DMTU and 31.25 ppm fluoride), a 10 X DMTU group (37.5 μM- to determine the long-term effects of high dose of DMTU). The swab was obtained and plated on Mitis Salivarius Agar with 0.2 U/mL bacitracin to confirm the colonization of *S. mutans* on dentine. Each group was fed with diet 2,000 (contains 56% sucrose) and 5% sucrose water *ad libitum*. In addition to these five groups, two other groups were maintained as controls ($n = 6$ per group): a control group without sucrose diet and another control group with diet 2,000 and 5% sucrose water. From this point, the molars of animals were given topical treatments with their corresponding concentrations once daily by using a camel hair brush. The animals were noted for their body weight weekly and physical appearance was noted daily. The treatment was carried out for 7 weeks, and at the end of the experimental period, animals were euthanized by CO_2 asphyxiation. The lower jawline was dissected aseptically and suspended in 10 ml of sterile phosphate buffer saline and subjected to sonication (20 s pulses at 10 s intervals for two times) to recover the maximum adhered viable counts. The solution was further serially diluted and plated on Mitis Salivarius Agar with 0.2 U/mL bacitracin to estimate the *S. mutans* population. The determination of the severity of caries developed on molars of the animals was scored according to Larson's modification of the Keyes system (Larson, 1981) and was performed by expert examiner in caries evaluation.

Histopathological Evaluation

For histopathological evaluation, the liver tissues and decalcified dentine was collected and post-fixed in 4% PFA for 24 h at 4°C, embedded in paraffin (Leica EG1150H, Leica Microsystems, Heerbrugg, Switzerland), and sectioned into ∼3 μm thick sections (Leica RM2125 RTS, Leica Microsystems, Heerbrugg, Switzerland). The sections were further stained with hematoxylin and eosin using an automated tissue processing and staining system (Leica TP 1020; Leica FG1150; Leica RM 2125 RTS and Leica ST4040) and scored blindly by a veterinary pathologist to be examined under a binocular microscope (Nikon Eclipse Ci-Ds-Fi2; Cardiff et al., 2014).

Inflammatory Parameters Evaluation

Inflammatory markers were assessed using RT-qPCR method. Blood samples (5 ml each) from all the rats were collected in EDTA-treated collection tubes, just before the necropsy was performed. The blood samples were further centrifuged at 2000 rpm for 10 min at 4°C for plasma collection (Chavali et al., 2014). The plasma samples were immediately stored at −20°C until used. RNA was isolated using a Qiagen RNeasy mini kit were assessed and cDNA synthesis was carried out using the same procedure as described in Section Quantification of Gene Expression Using RT-qPCR.

RT-qPCR analysis was carried out in 96 well plates (Thermofisher) using Realplex 2 (Eppendorf) to assess the transcription levels of genes related to inflammatory markers (IL-1, IL-6, C-Reactive Protein, TNF-α; **Table 2**). Reaction mixture in a total volume of 20 μl, consisted 10 μl 2X SYBR Green PCR Master Mix, forward and reverse primers (1 μl each), 4 μl of nuclease-free water and 4 μl of 20X diluted cDNA. PCR conditions included an initial denaturation at 95°C for 2 min, followed by 40 cycles of denaturation (95°C for 15 s), annealing (52.9°C for 15 s), extension (72°C for 20 s). To ensure the samples were free from contamination, negative controls containing nuclease-free water instead of cDNA were run in parallel. The relative gene expression was analyzed using the $2^{-\Delta\Delta CT}$ method with *Gapdh* as internal control.

TABLE 2 | Primer sequence used for RT-qPCR analysis of inflammatory markers in rat liver and blood.

Gene	Forward Primer Sequence (5′-3′)	Reverse Primer Sequence (5′-3′)
IL1	GGAAAGGGGAGAAATCCAAG	TGTTCTTTTCACCCCCTGAC
IL6	CCGGAGAGGAGACTTCACAG	ACAGTGCATCATCGCTGTTC
CRP	AACCTGGGAGAGGGTCAGAT	GACTCTGCTTCCAGGGACAC
TNF-α	AGTCCGGGCAGGTCTACTTT	GGCCACTACTTCAGCGTCTC
Gapdh	CATGGTCTACATGTTCCAGT	GGCTAAGCAGTTGGTGGTGC

Statistical Analysis

For RT-qPCR, one way ANOVA and multiple comparisons were performed. The data from *in vivo* study were analyzed by unpaired Student's *t*-test. For relative quantification of genes, the ΔΔCt mathematical model was used and normalization of RT-qPCR data was carried out using 16S-rRNA (for *S. mutans* genes) and *Gapdh* (for animal samples) as a reference gene by comparing the ratios of the gene of interest to those of a reference gene. The minimum level of significance was set at $p \leq 0.05$ (95% Confidence Interval). All the assays were carried out in triplicates and the results were expressed as mean ± SD. Graph Pad Prism software (version 6.01) was used for statistical analysis for all the experiments.

RESULTS

Gene Expression Profiling Using RT-qPCR

Gene expression study using RT-qPCR in MTCC 497 revealed that the genes which were located downstream to *comA* were down-regulated at mid-log phase and stationary phase except for *immA* and *immB* genes which were found to be up-regulated. The genes were found to have a basal level expression at the early phase (**Figure 2**). In contrast, fluoride did not show any significant effect on the expression of quorum sensing genes at mid-log phase as well as the stationary phase. Similar results were achieved in SM4 strain treated with DMTU at the tested concentration (**Figure 3**).

Cytotoxicity Analysis

In the present study, MTT assay revealed that DMTU and DMTU[1] do not have any quantitative cytotoxic effect on morphology and proliferation of Hep G2 cell lines when compared with the respective control as shown in **Figure 4**. The cells were found to have about 90 percent confluence after 24 h

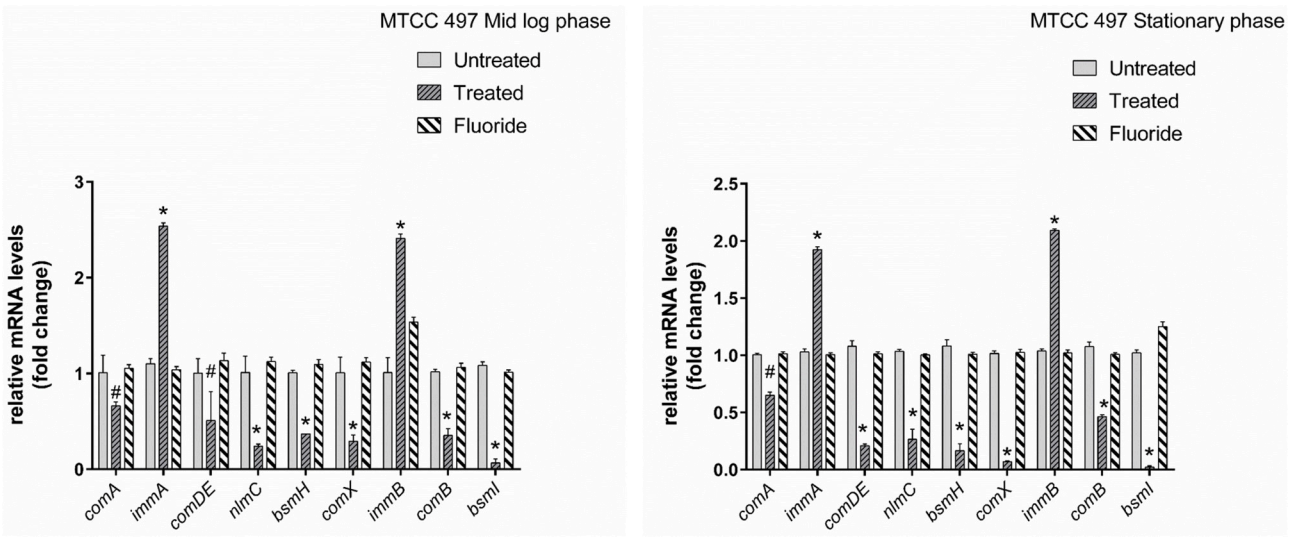

FIGURE 2 | RT-qPCR analysis of various genes involved directly and indirectly in quorum sensing circuit of MTCC 497 (*S. mutans*). The results are represented as ratios corresponding to the fold change of genes treated with DMTU (3.75 μM) and fluoride (31.25 ppm) as well as control (without treatment) at mid-log phase and stationary growth phase. 16S rRNA gene was used as an internal control for data normalization. *Indicates significantly different ($p < 0.05$) compared to untreated genes. #$p > 0.05$.

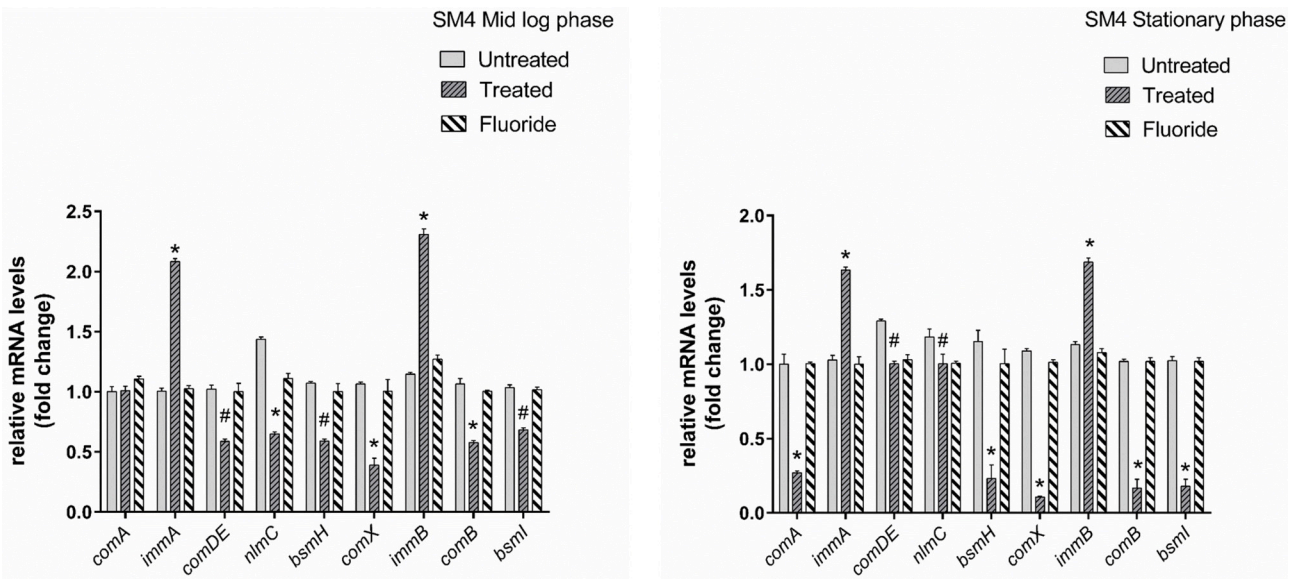

FIGURE 3 | RT-qPCR analysis of various genes involved directly and indirectly in quorum sensing circuit of clinical isolate SM4. The results are represented as ratios corresponding to the fold change of genes treated with DMTU (3.75 μM) and fluoride (31.25 ppm) as well as control (without treatment) at mid log phase and stationary growth phase. 16S rRNA gene was used as an internal control for data normalization. *Indicates significantly different ($p < 0.05$) compared to untreated genes. #$p > 0.05$.

of incubation. The results of cytotoxicity assay suggested that compounds can be further used in rodent animals for efficacy studies for validation of compounds.

Acute Oral Toxicity Studies

In acute oral toxicity study, the rats did not show toxic signs or death during the 14 day observation period. External examination of the rats did not show any signs of disease development and uptake of feed was normal without significant differences in the average weight gains among the experimental groups (data not shown). The skin and natural orifices of all experimental animals revealed no morphologic alterations. The animals did not show any variation in their general physical appearance and behavior and also,

no signs of anorexia, depression, lethargy, jaundice, dermatitis throughout the study. Macroscopic observation of organs such as heart, lung, pancreas, spleen, liver, stomach, intestine, kidney, ovary, brain, eyes, and tongue revealed indifference among all the rats without any detectable pathological symptoms.

DMTU Reduce the Incidence of Dental Caries *In vivo*

The present study has revealed that DMTU acts as a potential cariostatic agent and thus hinder the occurrence of dental caries *in vivo*. Macroscopic observations showed the development of brown and black lesions on the crown of diseased rats whereas, reduction in the development of lesions was found in DMTU treated group (**Figure 5**). Moreover, in the diseased group, the tissue around the molar root was inflamed as compared to the normal control group. The group treated with fluoride (250 ppm F, clinically proven anticaries agent) alone showed comparatively reduced lesions but not as significant as that of DMTU treated group. In this study, it is shown that DMTU (3.75 μM) in combination with lower concentrations of fluoride (31.25 ppm F) was considerably effective in reducing the occurrence of lesions and adherence of biofilm producing cells as compared to the fluoride alone. The colony count of SM4 showed significant reduction in the adherent cells in case of DMTU and combinatorial study group when compared with disease control (**Figure 6**). The total viable counts and the SM4 viable counts recovered from the rodents' plaque were not significantly affected by treatments with DMTU when compared to the normal control ($p > 0.05$).

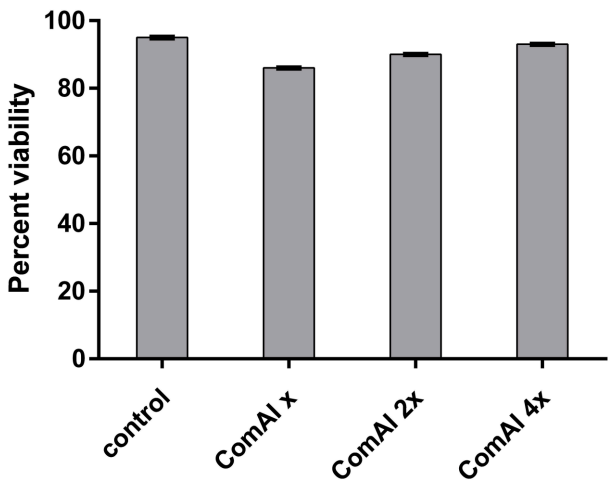

FIGURE 4 | Viability of HepG2 cells after 24 h treatment. The cells did not exhibit any significant cytotoxicity with cells treated with DMTU at two as well as four times of the effective concentration (X = 3.75 μM).

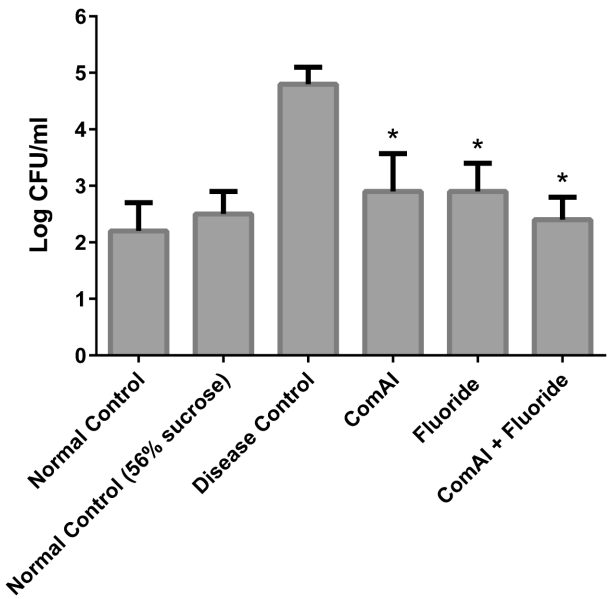

FIGURE 6 | Anti-adherent activity of DMTU in treated groups in comparison to control groups was evaluated by colony forming unit (CFU) assay and the results were plotted on a logarithmic scale. The columns in the graph represent the mean of six animals per group. Error bars represent standard deviations with $^*p < 0.05$.

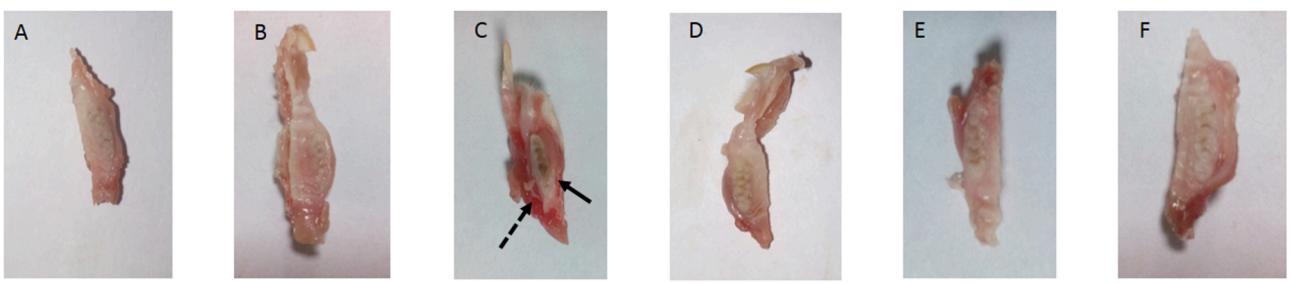

FIGURE 5 | Incidence of dental caries. The image represents the occurrence of dental caries in various groups. **(A)** Normal control group without sucrose diet; **(B)** Normal control with sucrose diet; **(C)** Disease control group, solid arrow represents the occurrence of black lesions on molar crown indicating development of caries and dotted arrow represents the inflamed gum tissue due to infection by *S. mutans*; **(D)** DMTU (3.75 μM) treated group; **(E)** Fluoride (250 ppm) treated group; **(F)** DMTU (3.75 μM) along with fluoride (31.25 ppm) treated group.

Histopathology Studies

The liver of control as well as DMTU (10 X dose; X = 3.75 μM) administered rats showed normal hepatic structure, characterized by polygonal-shape hepatocytes with well-defined boundaries, large centrally located nucleus with light stained acidophilic cytoplasm along with dispersed chromatin radially disposed in hepatic lobules (**Figure 7**). The incidence of dental lesions is summarized in **Figure 8**. Decalcified longitudinal sections of teeth of the normal group showed healthy dentine, odontoblast, and pulp, whereas in the diseased group, the carious dentine lesions were moderate to severe transcending through odontoblast into the pulp and completely decayed enamel crown.

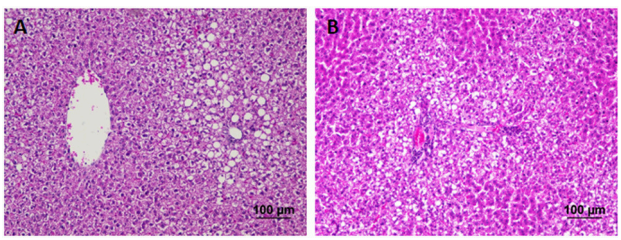

FIGURE 7 | Hematoxylin and eosin staining of liver tissue: Hematoxylin stains the nucleus blue in color and counter staining by eosin imparts pink color to the cytoplasm. **(A)** Normal control group and **(B)** the group treated with 10 X dose of DMTU (X= 3.75 μM). Normal as well as treated groups showed normal liver tissue histology without any pathological signs (Section thickness: 3 μM).

Almost no carious lesions were detected in DMTU treated as well-combinatorial treated group whereas moderate carious lesions were recorded in fluoride treated group.

Reduction in Inflammatory Markers

Inflammatory markers such as IL-1, IL-6, TNF-α, CRP showed varying expression levels in diseased as well as treated groups. In case of liver samples (**Figure 9**), levels of proinflammatory cytokines TNF-α, CRP, IL-1, and IL-6 were found significantly elevated in diseased group as compared to the control group ($p < 0.05$). Treatment with DMTU and DMTU along with fluoride significantly ($p < 0.05$) decreased the expression of TNF-α, CRP, IL-1. However, IL-6 levels were not affected by DMTU treatments but DMTU along with fluoride was able to reduce the expression significantly. Furthermore, in plasma (**Figure 10**), except IL-6, other inflammatory markers used in this study, i.e., IL-1, CRP, and TNF-α showed significant reduction in expression levels in treated groups (DMTU alone and Combinatorial group) as compared to the diseased group.

DISCUSSION

Oral cavity is one amongst the dynamic microbial community niche consisting of more than 700 species in equilibrium. Most of the species are commensal and help in maintaining the normal balance and thus avoiding pathogenic interference by opportunistic pathogens. Emergence of multidrug resistant strains has raised the concern and need for the development

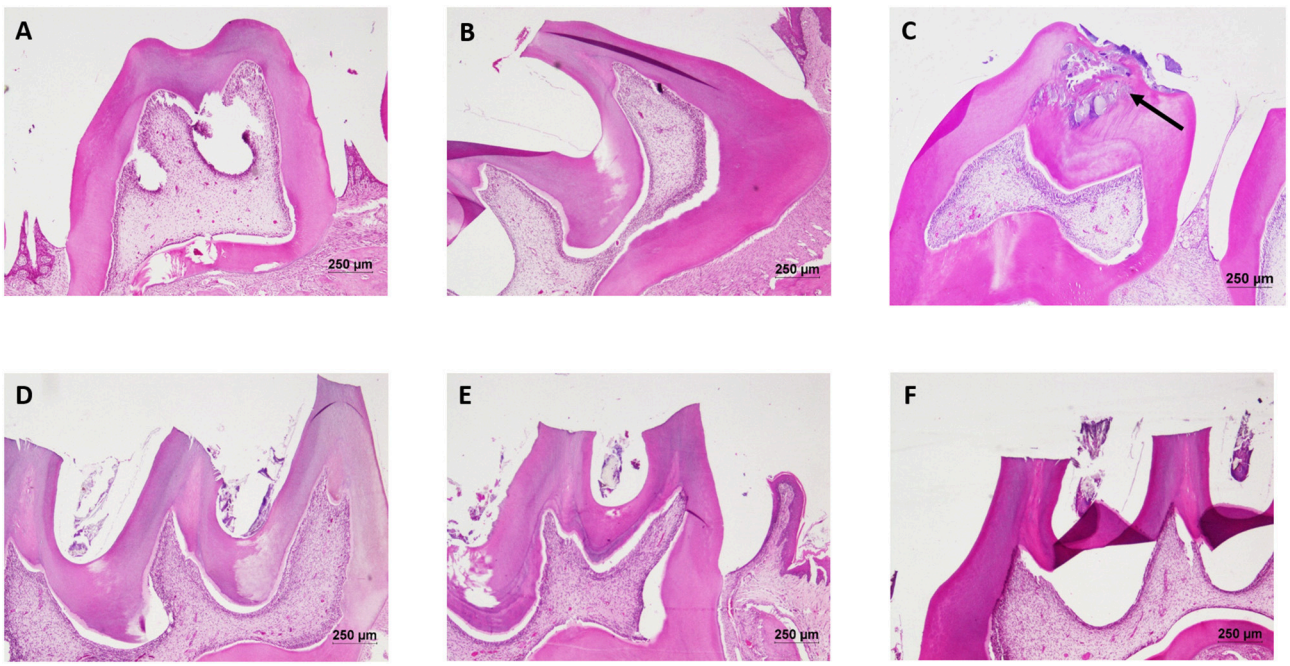

FIGURE 8 | Hematoxylin and eosin staining of dental tissue: Hematoxylin stains the nucleus blue in color and counter staining by eosin imparts pink color to the cytoplasm. **(A)** Normal control group; **(B)** Normal control with sucrose; **(C)** Diseased group, solid arrow represents the lesions developed on the dentine and penetrated up to the dental pulp tissue; **(D)** DMTU (3.75 μM) treated group; **(E)** Fluoride (250 ppm) treated group; **(F)** DMTU (3.75 μM) along with fluoride (31.25 ppm) treated group (Section thickness: 3 μM).

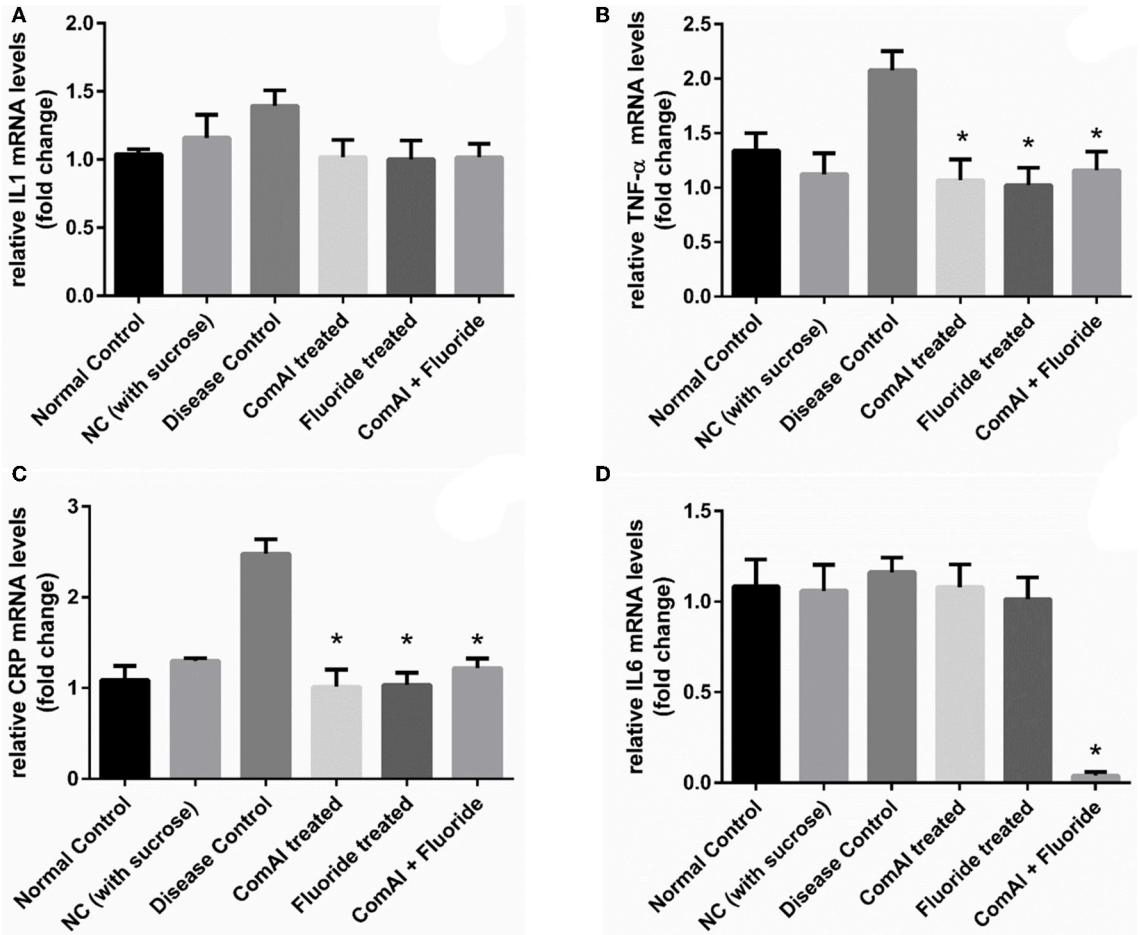

FIGURE 9 | RT-qPCR analysis of inflammatory markers in liver tissues of Wistar rats. **(A)** IL-1; **(B)** TNF-α; **(C)** C-Reactive Protein (CRP); **(D)** IL-6. The results are represented as ratios corresponding to the fold change in various treatment groups when compared with normal control group (without treatment). *Gapdh* gene was used as an internal control for data normalization. *Indicates significantly different ($p < 0.05$) compared to untreated tissues.

of better anti-virulent drugs. In this context, our present study focussed on the *in vitro* and *in vivo* validation of target specific anti-virulent drugs which were previously reported by our research group to have better binding to DMTU (Kaur et al., 2016).

Our study examined the effects of DMTU and fluoride at mid-logarithmic growth phase and stationary growth phase. The genes considered in this study are reported to be directly and indirectly involved in quorum sensing circuit of *S. mutans*. At mid-log phase, the expression of *immA* and *immB* (bacteriocin-immunity genes) were found to be up-regulated. Similar results were observed previously by Wang et al. (2013) where the group reported up-regulation of *immA* and *immB* genes upon treatment with chlorhexidine in *comC* mutant. Additionally, they also reported the enhanced sensitivity of *comC* mutant toward antimicrobials indicating the indirect involvement of quorum sensing in resistance toward various antimicrobials. In a previous study by Sztajer et al. (2008) the effect of the *luxS* mutant on the expression of bacteriocin genes was explored and was in-line context with our present data except for the *bsmH* gene which was found to be up-regulated in their study. This can be attributed to the fact *luxS* might be regulating the expression of *bsmH* in an alternative way and not through the two component ComDE TCTS system. Parallel reports by Banu et al. (2010) showed the down-regulation of *bsmH* as well as other bacteriocin related genes in *pknB* mutant strains. They have speculated that *pknB* modulates the activity of ComDE TCTS system. On the other hand, as expected, treatment of MTCC 497 and SM4 strains with DMTU, resulted in down-regulation of the genes involved in competence development and bacteriocin production through ComDE quorum sensing pathway. The effect of DMTU further transcended till stationary phase indicating that the effect is not temporary and has effect at later stages of growth in *S. mutans*. The *comA* gene was found to be down-regulated as *S. mutans* enters from early to mid and then stationary phase as a result of positive feedback loop present in ComDE QS pathway. Interestingly, on exposure to fluoride alone, the relative expression of the genes was found to be at the basal level when compared with the control samples. This signifies that fluoride does not have any effect on the ComDE pathway and it might be

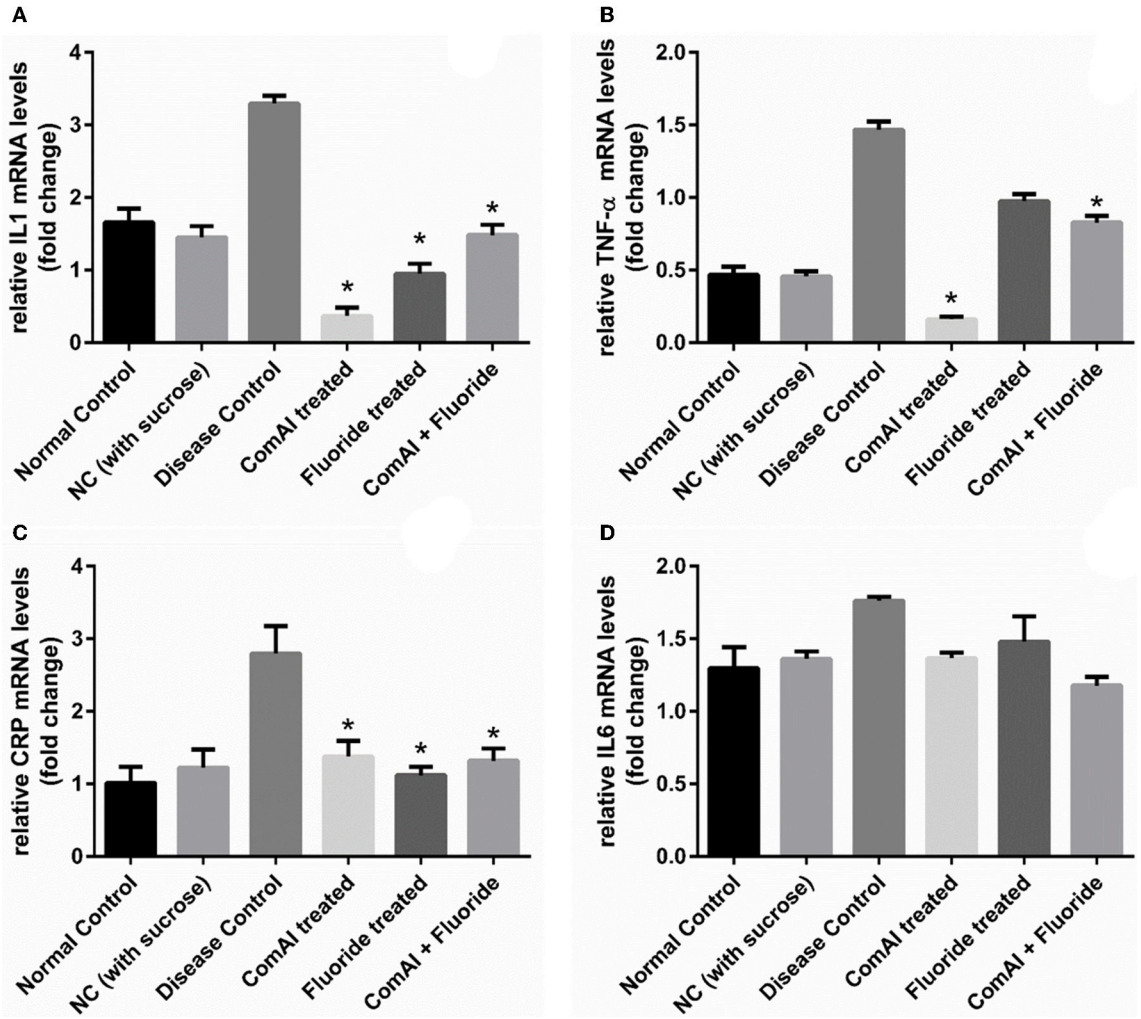

FIGURE 10 | qRT-PCR analysis of inflammatory markers in samples collected from the blood plasma of Wistar rats. **(A)** IL-1; **(B)** TNF-α; **(C)** C-Reactive Protein (CRP); **(D)** IL-6. The results are represented as ratios corresponding to the fold change in various treatment groups when compared with normal control group (without treatment). *Gapdh* gene was used as an internal control for data normalization. *Indicates significantly different ($p < 0.05$) compared to untreated tissues.

affecting alternative pathway involved in the EPS production as well as sucrose metabolism.

MTT assay was carried out to evaluate the potential toxicity of DMTU in cell lines before proceeding for *in vivo* acute oral toxicity in Wistar rats. The *in vitro* cytotoxic results revealed that DMTU was not found to have any toxic effect on mammalian cell lines making it suitable for validating the drug *in vivo*. In acute oral toxicity studies, the rats were found to be healthy till the highest dose used (2,000 mg/kg/PO) as per OECD 425 guidelines. This shows that DMTU does not have short-term as well as long-term toxic effects.

The efficacy study was carried out to evaluate whether the antibiofilm and cariostatic activity of DMTU would be similar to that of *in vitro* study, with widely used Wistar rat model for dental caries study *in vivo* (Koo et al., 2005). Topical application of DMTU significantly reduced the formation of biofilm and effectively decreased the incidence of dental caries when compared with disease control ($p < 0.05$) confirming previous *in vitro* findings (Kaur et al., 2016). The property of DMTU in reducing the development of carious lesions on the tooth surface clearly indicates anti-caries activity at the brief exposure of efficacious concentration in the presence of sucrose-rich diet when ingested by the animals when compared with disease control ($p < 0.05$). The ability of topically applied DMTU to have a persistent anti-caries effect is a desirable characteristic of a novel chemotherapeutic agent targeting biofilm oriented dental diseases such as dental caries (Bowen, 2015). It is noteworthy that colony counts of the total microflora of the oral cavity and the SM4 *S. mutans* were not affected which approves well with its lack of antibacterial activity against biofilm results of our previous findings (Kaur et al., 2016). Furthermore, these observations indicate that the caries preventive mechanisms of DMTU may be related to its effects on ComA in quorum sensing circuit resulting in down-regulation of several virulence attributes of *S.*

mutans, such as biofilm formation and bacteriocin production by this pathogen. Combinatorial study group in rodent model showed that DMTU in combination with fluoride enhances the anti-cariogenic effect of fluoride thus, clearly has potential clinical application to reduce the prevalence of dental caries at lower concentrations without increasing the concentration of fluoride exposure. As mentioned earlier, fluoride does not alter the expression of genes involved in quorum sensing of *S. mutans*. In previous reports, fluoride levels found in plaque, affect the glycolytic activity and production of Gtfs by disrupting the proton permeability of the cell membrane in *S. mutans* (Marquis et al., 2003; Koo et al., 2006). The intracellular polysaccharides (IPS) is metabolized by oral pathogens when external sources of fermentable carbon have been depleted in the oral cavity. Thus, IPS promote the occurrence of carious lesions by enhanced exposure of tooth surfaces to lower pH in the biofilm niche. IPS is synthesized as a result of ATP pools in cells of the biofilm matrix. Fluoride significantly reduces the ATP pools and results in substantial reduction in IPS synthesis and as a result reduces the incidence of lower pH in the oral cavity. In addition, fluoride also enhances the remineralization process and cause a reduction in the demineralization process at the tooth-biofilm interface. The present data not only corroborate previous *in vitro* findings but also support the hypothesis that interfering with the quorum sensing circuit possibly results in a reduction of caries by inhibition of virulence attributes and biofilm formation by *S. mutans*.

The liver is one of the major organs involved in the detoxification of the body. It was necessary to evaluate the long-term effects of higher doses of DMTU on hepatocytes to eliminate any toxicity pattern involved with the administration of DMTU. In the present study, liver sections did not show any degenerative signs thus, proving the administration of DMTU (up to 10 X doses for long term might not be toxic to the recipients at clinical stages. Histopathological examination of teeth and absence of lesions in DMTU treated group provides an evidence that topical applications of DMTU and in combination with fluoride have a cariostatic effect. In disease group, caries has penetrated enamel (decalcified), dentine and reached the depth of teeth i.e., pulp (soft connective tissue; **Figure 8**). The entrance of *S. mutans* in pulp can lead to the invasion of bacteria in the blood stream causing a systemic pro-inflammatory response in the body (Nakano et al., 2004). A review study by Esser et al. (2014), has reported the potential link between low-grade chronic inflammation and systemic diseases such as obesity and Type 2 Diabetes. High-level expression of the inflammatory response may lead to the development of systemic diseases such as cardiovascular disease, rheumatoid arthritis, type 2 Diabetes, premature birth of babies and so on (Gurenlian, 2009). To investigate this, we estimated the expression levels of inflammatory markers such as TNF-α, IL-6, IL-1, CRP in plasma as well as liver tissues. The liver has a remarkable capacity to adapt to injury stress through tissue repair when compared to any other solid organ in the body. Complex interactions of immune cell subsets regulate this repair process. Levels of pro-inflammatory cytokines TNF-α, CRP, IL-1 were significantly down-regulated in the case of plasma as compared to liver, attributing to the fact that, cytokines are more readily diffused and easily estimated by RT-qPCR analysis as compared to liver tissues. The low levels of inflammatory markers in case of treated groups can be attributed to the fact that due to inhibition of biofilm formation by DMTU alone and in combination will prevent the formation of carious lesions and further inhibit the invasion of *S. mutans* in the pulp.

Collectively, the data in our present study shows that DMTU reduces the incidence of caries development by targeting the ComA in quorum sensing pathway of *S. mutans* which further affects the major virulence factors such as biofilm formation, bacteriocin production without causing mortality of bacteria. DMTU along with lower concentrations of fluoride could be used as a potential cariostatic measure to reduce the incidence of caries without affecting the remineralization property of fluoride. The combination of DMTU with fluoride at lower concentrations may provide a potential substitute to the current chemotherapeutic approaches to prevent the incidence of dental caries. In addition, prevention of caries also results in the reduction of inflammatory markers as shown in this study at pre-clinical stages. Additional studies are warranted to link and explore pathways that link dental caries to systemic diseases and this may provide a guide to further enhance the anti-inflammatory chemotherapeutic anti-caries agents in oral formulations.

AUTHOR CONTRIBUTIONS

All authors listed have made a substantial, direct and intellectual contribution to the work, and approved it for publication.

ACKNOWLEDGMENTS

Author, GK is a recipient of the University Grants Commission Maulana Azad National Fellowship (UGC-MANF) (MANF-2014-15-SIK-PUN-31423) from the University Grants Commission, Government of India and the support is duly acknowledged. We sincerely thank Dr. DavidRaj C. and Dr. Prabhu P.C. for their support in the execution of animal studies and histopathological studies respectively. We sincerely express our gratitude toward SASTRA University and its management for providing us the infrastructure needed to carry out our research work.

SUPPLEMENTARY MATERIAL

The Supplementary Material for this article can be found online at: http://journal.frontiersin.org/article/10.3389/fcimb.2017.00313/full#supplementary-material

REFERENCES

Arya, R., and Princy, S. A. (2013). An insight into pleiotropic regulators Agr and Sar: molecular probes paving the new way for antivirulent therapy. *Future Microbiol.* 8, 1339–1353. doi: 10.2217/fmb.13.92

Balamurugan, P., Hema, M., Kaur, G., Sridharan, V., Prabu, P., Sumana, M., et al. (2015). Development of a biofilm inhibitor molecule against multidrug resistant *Staphylococcus aureus* associated with gestational urinary tract infections. *Front. Microbiol.* 6:832. doi: 10.3389/fmicb.2015.00832

Bansal, M., Rastogi, S., and Vineeth, N. S. (2013). Influence of periodontal disease on systemic disease: inversion of a paradigm: a review. *J. Med. Life* 6, 126–130.

Banu, L. D., Conrads, G., Rehrauer, H., Hussain, H., Allan, E., and van der Ploeg, J. R. (2010). The *Streptococcus mutans* serine/threonine kinase, PknB, regulates competence development, bacteriocin production, and cell wall metabolism. *Infect. Immun.* 78, 2209–2220. doi: 10.1128/IAI.01167-09

Bowen, W. (2015). Dental caries–not just holes in teeth! A perspective. *Mol. Oral. Microbiol.* 31, 228–233. doi: 10.1111/omi.12132

Bustin, S. A., Benes, V., Garson, J. A., Hellemans, J., Huggett, J., Kubista, M., et al. (2009). The MIQE guidelines:Minimum Information for publication of quantitative real-time PCR experiments. *Clin. Chem.* 55, 611–622. doi: 10.1373/clinchem.2008.112797

Cardiff, R. D., Miller, C. H., and Munn, R. J. (2014). Manual hematoxylin and eosin staining of mouse tissue sections. *Cold. Spring. Harb. Protoc.* 6, 655–658. doi: 10.1101/pdb.prot073411

Chavali, V., Tyagi, S. C., and Mishra, P. K. (2014). Differential expression of dicer, miRNAs, and inflammatory markers in diabetic Ins2+/− Akita hearts. *Cell Biochem. Biophys.* 68, 25–35. doi: 10.1007/s12013-013-9679-4

Chen, L., Ren, Z., Zhou, X., Zeng, J., Zou, J., and Li, Y. (2015). Inhibition of *Streptococcus mutans* biofilm formation, extracellular polysaccharide production, and virulence by an oxazole derivative. *Appl. Microbiol. Biotechnol.* 100, 1–11. doi: 10.1007/s00253-015-7092-1

Ciofani, G., Danti, S., D'Alessandro, D., Moscato, S., and Menciassi, A. (2010). Assessing cytotoxicity of boron nitride nanotubes: interference with the MTT assay. *Biochem. Biophys. Res. Commun.* 394, 405–411. doi: 10.1016/j.bbrc.2010.03.035.

Esser, N., Legrand-Poels, S., Piette, J., Scheen, A. J., and Paquot, N. (2014). Inflammation as a link between obesity, metabolic syndrome and type 2 diabetes. *Diabetes Res. Clin. Pract.* 105, 141–150. doi: 10.1016/j.diabres.2014.04.006

Gurenlian, J. (2009). Inflammation: the relationship between oral health and systemic disease. *Dent. Assist.* 78, 8–10.

Hasan, S., Danishuddin, M., Adil, M., Singh, K., Verma, P. K., and Khan, A. U. (2012). Efficacy of *E. officinalis* on the cariogenic properties of *Streptococcus mutans*: a novel and alternative approach to suppress quorum-sensing mechanism. *PLoS ONE* 7:e40319. doi: 10.1371/journal.pone.0040319

Ishii, S., Yano, T., Ebihara, A., Okamoto, A., Manzoku, M., and Hayashi, H. (2010). Crystal structure of the peptidase domain of Streptococcus ComA, a bifunctional ATP-binding cassette transporter involved in the quorum-sensing pathway. *J. Biol. Chem.* 285, 10777–10785. doi: 10.1074/jbc.M109.093781

Jetti, R., Raghuveer, C., Mallikarjuna Rao, C., Somayaji, S., and Prakash Babu, B. (2014). Neuroprotective effect of Ascorbic acid and Ginkgo biloba against fluoride caused neurotoxicity. *IOSR J. Environ. Sci. Toxicol. Food Technol.* 8, 30–36.

Kaur, G., Balamurugan, P., Maheswari, C. U., Anitha, A., and Princy, S. A. (2016). Combinatorial effects of aromatic 1, 3-disubstituted ureas and fluoride on *in vitro* inhibition of *Streptococcus mutans* biofilm formation. *Front. Microbiol.* 7:861. doi: 10.3389/fmicb.2016.00861

Kaur, G., Rajesh, S., and Princy, S. A. (2015). Plausible drug targets in the *Streptococcus mutans* quorum sensing pathways to combat dental biofilms and associated risks. *Indian J. Microbiol.* 55, 349–356. doi: 10.1007/s12088-015-0534-8

Koo, H., Schobel, B., Scott-Anne, K., Watson, G., Bowen, W., Cury, J., et al. (2005). Apigenin and tt-farnesol with fluoride effects on *S. mutans* biofilms and dental caries. *J. Dent. Res.* 84, 1016–1020. doi: 10.1177/154405910508401109

Koo, H., Sheng, J., Nguyen, P. T., and Marquis, R. E. (2006). Co-operative inhibition by fluoride and zinc of glucosyl transferase production and polysaccharide synthesis by mutans streptococci in suspension cultures and biofilms. *FEMS Microbiol. Lett.* 254, 134–140. doi: 10.1111/j.1574-6968.2005.00018.x

Larson, R. (1981). Merits and modifications of scoring rat dental caries by Keyes' method [Abstract]. *Anim. Models Cariol.* (special suppl.), 195–203. Abstract retrieved from Microbiology Abstracts.

Magiorakos, A., Srinivasan, A., Carey, R. B., Carmeli, Y., Falagas, M. E., Giske, C. G., et al. (2012). Multidrug-resistant, extensively drug-resistant and pandrug-resistant bacteria: an international expert proposal for interim standard definitions for acquired resistance. *Clin. Microbiol. Infect.* 18, 268–281. doi: 10.1111/j.1469-0691.2011.03570.x

Mah, T.-F. C., and O'Toole, G. A. (2001). Mechanisms of biofilm resistance to antimicrobial agents. *Trends Microbiol.* 9, 34–39. doi: 10.1016/S0966-842X(00)01913-2

Maneewattanapinyo, P., Banlunara, W., Thammacharoen, C., Ekgasit, S., and Kaewamatawong, T. (2011). An evaluation of acute toxicity of colloidal silver nanoparticles. *J. Vet. Med. Sci.* 73, 1417–1423. doi: 10.1292/jvms.11-0038

Marquis, R. E., Clock, S. A., and Mota-Meira, M. (2003). Fluoride and organic weak acids as modulators of microbial physiology. *FEMS Microbiol. Rev.* 26, 493–510. doi: 10.1111/j.1574-6976.2003.tb00627.x

Murata, R. M., Branco-de-Almeida, L. S., Franco, E. M., Yatsuda, R., dos Santos, M. H., de Alencar, S. M., et al. (2010). Inhibition of *Streptococcus mutans* biofilm accumulation and development of dental caries *in vivo* by 7-epiclusianone and fluoride. *Biofouling* 26, 865–872. doi: 10.1111/j.1574-6976.2003.tb00627.x

Nakano, K., Nomura, R., Nakagawa, I., Hamada, S., and Ooshima, T. (2004). Demonstration of *Streptococcus mutans* with a cell wall polysaccharide specific to a new serotype, k, in the human oral cavity. *J. Clin. Microbiol.* 42, 198–202. doi: 10.1128/JCM.42.1.198-202.2004

Qi, F., Kreth, J., Lévesque, C. M., Kay, O., Mair, R. W., Shi, W., et al. (2005). Peptide pheromone induced cell death of *Streptococcus mutans*. *FEMS Microbiol. Lett.* 251, 321–326. doi: 10.1016/j.femsle.2005.08.018

Rasmussen, T. B., and Givskov, M. (2006). Quorum sensing inhibitors: a bargain of effects. *Microbiology* 152, 895–904. doi: 10.1099/mic.0.28601-0

Ravichandiran, V., Shanmugam, K., Anupama, K., Thomas, S., and Princy, A. (2012). Structure-based virtual screening for plant-derived SdiA-selective ligands as potential antivirulent agents against uropathogenic *Escherichia coli*. *Eur. J. Med. Chem.* 48, 200–205. doi: 10.1016/j.ejmech.2011.12.015

Senadheera, D., and Cvitkovitch, D. G. (2008). Quorum sensing and biofilm formation by *Streptococcus mutans*. *Adv. Exp. Med. Biol.* 631, 178–188. doi: 10.1007/978-0-387-78885-2_12

Spittle, B. (2016). Dental fluorosis as a marker for fluoride-induced cognitive impairment. *Fluoride* 49, 3–4.

Sztajer, H., Lemme, A., Vilchez, R., Schulz, S., Geffers, R., Yip, C. Y. Y., et al. (2008). Autoinducer-2-regulated genes in *Streptococcus mutans* UA159 and global metabolic effect of the *luxS* mutation. *J. Bacteriol.* 190, 401–415. doi: 10.1128/JB.01086-07

Wang, W.-L., Liu, J., Huo, Y.-B., and Ling, J.-Q. (2013). Bacteriocin immunity proteins play a role in quorum-sensing system regulated antimicrobial sensitivity of *Streptococcus mutans* UA159. *Arch. Oral. Biol.* 58, 384–390. doi: 10.1016/j.archoralbio.2012.09.001

Conflict of Interest Statement: The authors declare that the research was conducted in the absence of any commercial or financial relationships that could be construed as a potential conflict of interest.

frontiers in Cellular and Infection Microbiology

MINI REVIEW
published: 24 April 2018
doi: 10.3389/fcimb.2018.00122

Quorum Sensing Signaling and Quenching in the Multidrug-Resistant Pathogen *Stenotrophomonas maltophilia*

Pol Huedo [1†], Xavier Coves [1,2†], Xavier Daura [1,3], Isidre Gibert [1,2] and Daniel Yero [1,2*]*

[1] Institut de Biotecnologia i de Biomedicina, Universitat Autònoma de Barcelona, Barcelona, Spain, [2] Departament de Genètica i de Microbiologia, Universitat Autònoma de Barcelona, Barcelona, Spain, [3] Catalan Institution for Research and Advanced Studies, Barcelona, Spain

Stenotrophomonas maltophilia is an opportunistic Gram-negative pathogen with increasing incidence in clinical settings. The most critical aspect of *S. maltophilia* is its frequent resistance to a majority of the antibiotics of clinical use. Quorum Sensing (QS) systems coordinate bacterial populations and act as major regulatory mechanisms of pathogenesis in both pure cultures and poly-microbial communities. Disruption of QS systems, a phenomenon known as Quorum Quenching (QQ), represents a new promising paradigm for the design of novel antimicrobial strategies. In this context, we review the main advances in the field of QS in *S. maltophilia* by paying special attention to Diffusible Signal Factor (DSF) signaling, Acyl Homoserine Lactone (AHL) responses and the controversial Ax21 system. Advances in the DSF system include regulatory aspects of DSF synthesis and perception by both *rpf*-1 and *rpf*-2 variant systems, as well as their reciprocal communication. Interaction via DSF of *S. maltophilia* with unrelated organisms including bacteria, yeast and plants is also considered. Finally, an overview of the different QQ mechanisms involving *S. maltophilia* as quencher and as object of quenching is presented, revealing the potential of this species for use in QQ applications. This review provides a comprehensive snapshot of the interconnected QS network that *S. maltophilia* uses to sense and respond to its surrounding biotic or abiotic environment. Understanding such cooperative and competitive communication mechanisms is essential for the design of effective anti QS strategies.

Keywords: multi-drug resistance, quorum sensing, quorum quenching, nosocomial infections, antimicrobial resistance

OPEN ACCESS

Edited by:
Maria Tomas, Complexo Hospitalario Universitario A Coruña, Spain

Reviewed by:
Beathriz Godoy Vilela Barbosa, Universidade de Pernambuco, Brazil
Jose Ramos-Vivas, Instituto de Investigación Marques de Valdecilla (IDIVAL), Spain

***Correspondence:**
Isidre Gibert
isidre.gibert@uab.cat
Daniel Yero
daniel.yero@uab.cat

[†] These authors have contributed equally to this work.

Received: *16 February 2018*
Accepted: *05 April 2018*
Published: *24 April 2018*

Citation:
Huedo P, Coves X, Daura X, Gibert I and Yero D (2018) Quorum Sensing Signaling and Quenching in the Multidrug-Resistant Pathogen Stenotrophomonas maltophilia. Front. Cell. Infect. Microbiol. 8:122. doi: 10.3389/fcimb.2018.00122

INTRODUCTION

Stenotrophomonas maltophilia is a ubiquitous multidrug resistant Gram-negative bacterium that has emerged as an important nosocomial pathogen (Brooke, 2012; Adegoke et al., 2017) and stands as one of the most common lung pathogens in cystic fibrosis patients (Amin and Waters, 2014). The most important natural reservoir of this microorganism is thought to be the rhizosphere (Berg et al., 2005; Ryan et al., 2009), a highly competitive niche that facilitates the acquisition by bacteria of antimicrobial-resistance genes (Berg et al., 2005) and favors the establishment of communication networks between neighboring organisms (Bais et al., 2006). The result of

this competitive coevolution appears to have a strong impact when translated to clinical environments.

Bacterial cells can communicate through the production and detection of signal molecules, a mechanism known as quorum sensing (QS) (Waters and Bassler, 2005; Papenfort and Bassler, 2016). Through cell-to-cell communication, bacterial populations synchronize gene expression and globally respond to changes in the environment, also during infection (Rutherford and Bassler, 2012). QS communication may also connect different bacterial species and even members of different kingdoms (Lowery et al., 2008). On the other end, the disruption of exogenous QS, a phenomenon termed Quorum Quenching (QQ), constitutes a varied and widespread protection mechanism exploited by bacterial competitors and by host defenses in case of infection (Dong et al., 2007). Indeed, interrupting bacterial QS strongly impairs bacterial pathogenic capacity (Kalia and Purohit, 2011).

Several different QS signals and QQ mechanisms have been identified in the last decades, significantly expanding our knowledge on bacterial communication (Kleerebezem et al., 1997; Dong et al., 2007; Deng et al., 2011; Kalia and Purohit, 2011; Ryan et al., 2015; Papenfort and Bassler, 2016; Zhou et al., 2017). Here, we review recent advances in the characterisation of the QS network of *S. maltophilia*, focusing on the two variants regulating the diffusible signal factor (DSF) system, as well as the QQ mechanisms in which this microorganism is involved. We also discuss the role of N-acyl homoserine lactone (AHL) signaling molecules and the controversial Ax21 system in the QS network of this species. Overall, this review provides a comprehensive picture of the signaling network that interconnects *S. maltophilia* with its surrounding environment.

DSF-QUORUM SENSING IN *S. MALTOPHILIA*

So far, the most studied QS system in *S. maltophilia* is that based on the DSF fatty acid (FA) signal *cis*-11-methyl-2-dodecenoic acid, originally described in *Xanthomonas campestris* pv. *campestris* (*Xcc*) (Barber et al., 1997). As a *Xanthomonadales* member and differently than the unrelated DSF-like-producing bacteria *Burkholderia cenocepacia and Pseudomonas aeruginosa, S. maltophilia* governs DSF communication through the genes co-localized in the *rpf* (regulation of pathogenicity factors) cluster (Huedo et al., 2015). Genes within this cluster include key enzymes of DSF synthesis, perception and signal transduction and are organized in two adjacent operons that are convergently transcribed. One operon is composed by the genes encoding for the FA ligase RpfB and the synthase RpfF, while the opposite operon encodes for a two-component system including the sensor kinase RpfC and the cytoplasmic regulator RpfG (Fouhy et al., 2007; Huedo et al., 2014b). Unlike *Xanthomonas* sp. and similar to *Xylella fastidiosa*, the *rpf* cluster in *S. maltophilia* does not encode for the transmembrane protein RpfH (Huedo et al., 2014b).

Two *rpf* Cluster Variants in *S. maltophilia*

A distinctive feature of the DSF system in *S. maltophilia* is the presence of two *rpf* cluster variants that produce and sense DSF signals distinctly and regulate important biological processes (Huedo et al., 2014b). Two initial studies investigating the relation between genotypic and phenotypic traits of *S. maltophilia* isolates suggested that a significant group of strains lacked the *rpfF* gene (Pompilio et al., 2011; Zhuo et al., 2014). Later, a population study focused on DSF-QS revealed that, unlike the other *Xanthomonadales*, *S. maltophilia* presents two *rpfF* variants (named *rpfF*-1 and *rpfF*-2) and that primers designed to PCR-amplify the *rpfF* gene didn't recognize the *rpfF*-2 variant (Huedo et al., 2014b). More recently, the existence of the two *rpfF* alleles in *S. maltophilia* clinical and environmental isolates has been further validated by a population genomic analysis (Lira et al., 2017). The two *rpfF* variants differ, in particular, in the sequence encoding for the N-terminal 108 residues (Huedo et al., 2014b). Taking all the published data together (Huedo et al., 2014b; Lira et al., 2017) and assuming that the *rpfF*$^{-}$ isolates from Pompilio et al. (2011) and Zhuo et al. (2014) belong to the *rpfF*-2 variant, the *rpfF*-1 variant has been so far identified in 98 isolates (55.5%), while *rpfF*-2 has been detected in 81 isolates (44.5%).

Investigation of the *rpf* cluster in the two *rpfF* variant strains showed that the sensor RpfC presents two variants as well, with a fixed association between the *rpfF* variant and its cognate *rpfC*, meaning that all strains harboring *rpfF*-1 necessarily carry the *rpfC*-1 variant and likewise for the *rpfFC*-2 pair (Huedo et al., 2014b). Besides differences in amino-acid sequence, the two RpfC variants vary in length and secondary structure. RpfC-1 displays 10 trans-membrane regions (TMR) in the N-terminal region that are highly related to the RpfC-RpfH complex constituting the DSF sensor domain in *Xcc* (Slater et al., 2000; Huedo et al., 2014b). On the contrary, RpfC-2 lacks 5 of these TMRs as in *Xylella fastidiosa* (*Xf*) RpfC (Chatterjee et al., 2008; Huedo et al., 2014b). Differences between the *rpf* cluster variants strongly affect DSF synthesis, perception, and regulation of biological processes in *S. maltophilia*.

rpf-1 and *rpf*-2 Strains Distinctly Synthesize and Sense DSF Signals

Remarkably, while *rpf*-1 strains display evident DSF production in standard growth conditions, *rpf*-2 isolates require extra copies of *rpfF*-2 or the absence of the sensor/repressor component RpfC-2 to achieve detectable levels of DSF (Huedo et al., 2014b). The mechanistic aspects of DSF synthesis and perception in *S. maltophilia rpf*-1 seem to be similar to those reported for the model organism *Xcc*. Both microorganisms synthesize *cis*-11-methyl-2-dodecenoic acid as the main DSF signal (He and Zhang, 2008; Huedo et al., 2014b). *Xcc* RpfF produces additional DSF signals including *cis*-2-dodecenoic acid, *cis*-11-methyldodeca-2,5-dienoic acid, and *cis*-10-methyl-2-dodecenoic acid (Deng et al., 2015, 2016; Zhou et al., 2015). The production of seven derivatives of the *cis*-11-methyl-2-dodecenoic acid by one *S. maltophilia* strain (WR-C) had been also reported (Huang and Lee Wong, 2007). More recently, however, the canonical *cis*-11-methyl-2-dodecenoic acid was the only unsaturated FA signal

identified in culture supernatants of the *S. maltophilia* strains E77 (RpfF-1) and M30 (RpfF-2) (Huedo et al., 2014a,b) (**Table 1**).

As reported for the DSF synthases of *B. cenocepacia* (Bi et al., 2012) and *Xcc* (Zhou et al., 2015), both the RpfF-1 and RpfF-2 proteins from *S. maltophilia* appear to have a double acyl-ACP dehydratase and thioesterase activity that catalyze the conversion of (*R*)-3-hydroxy-11-methyl-dodecanoyl-ACP to DSF in two steps (Huedo et al., 2015). In addition, the thioesterase activity of all RpfF proteins seems to be nonspecific, cleaving a variety of medium- and long-chain acyl-ACP substrates and thus generating free FAs that are then released to the extracellular environment (Bi et al., 2012; Huedo et al., 2015; Zhou et al., 2015). In *S. maltophilia* the major free FA released by this thioesterase activity is the 13-methyltetradecanoic acid (*iso*-15:0), which is also the most abundant FA in the phospholipids of both *Xanthomonas* sp. (Vauterin et al., 1996) and *S. maltophilia* (Kim et al., 2010). Surprisingly, *iso*-15:0 is actually considered a biomarker phospholipid FA for the Gram-positive group (Kaur et al., 2005) and seems to be present only in Gram-negative bacteria displaying DSF communication. Interestingly, DSF and *iso*-15:0 are generated through the same biosynthetic pathway (Heath and Rock, 2002), which suggests a potential connection between DSF production and membrane synthesis (Huedo et al., 2015).

In line with this observations, the presence of *iso*-15:0 in the medium appears to modulate DSF production in *rpf*-1 strains, perhaps because the intact RpfC-1 sensor (10 TMR) is able to detect this FA, thus liberating free active RpfF-1 capable of subsequent DSF synthesis (Huedo et al., 2015). Several other environmental factors modulate DSF synthesis in *rpf*-1 strains. For example, while rich media and 28°C seem to be the optimal culture conditions to achieve high amounts of DSF in the supernatant (Huedo et al., 2015), iron restriction has been found to induce DSF production through the Fur system in strain K279a (García et al., 2015).

Contrary to *rpf*-1 strains, DSF synthesis in strains harboring the *rpf*-2 allele seems to be permanently repressed under wild-type conditions. Nevertheless, the presence of exogenous DSF triggers DSF production in these strains (Huedo et al., 2015; **Figure 1**). These findings suggest that *rpf*-2 strains require a stoichiometric unbalance (RpfF-2>RpfC-2) for DSF production and that the 5-TMR sensor component of RpfC-2 is much more specific than RpfC-1, enabling free-active RpfF-2 only upon detection of DSF itself.

Biological Processes Regulated by DSF in *rpf*-1 and *rpf*-2 Strains

Deletion of *rpfF*-1 in the *S. maltophilia* clinical strain E77 resulted in altered biofilm formation, reduced bacterial motility and reduced virulence in the *Caenorhabditis elegans* and zebrafish models of infection (Huedo et al., 2014b). In the clinical model strain K279a (*rpfF*-1), interruption of the *rpfF* gene also resulted in decreased antibiotic resistance and protease secretion, and an altered lipopolysaccharide (LPS) (Fouhy et al., 2007). In the environmental strain WR-C, DSF-derivative signals stimulate flagella-independent motility (Huang and Lee Wong, 2007) and deletion of *rpfF* or *rpfB* decrease the expression of the ferric citrate receptor FecA (Huang and Wong, 2007). Recently, DSF produced by strain 44/33 has been shown to contribute to outer membrane vesicle (OMV) secretion (Devos et al., 2015; **Table 1**).

On the contrary, mutation of *rpfF*-2 does not significantly alter biofilm formation, bacterial motility or virulence in the clinical strain M30 (**Table 1**). This results are in line with the fact that the RpfF-2 variant seems to be permanently repressed (Huedo et al., 2014b). Nevertheless, when the *rpf*-1 and *rpf*-2 subpopulations cohabit, both DSF production and

TABLE 1 | *Stenotrophomonas maltophilia* strains in which the diffusible signal factor (DSF) quorum sensing (QS) system has been investigated.

Strain	Origin	RpfF variant	DSF molecules	Biological processes	References
K279a	Clinical (blood infection)	1	*cis*-11-Methyl-2-dodecenoic acid (DSF)	Motility; Protease production; Lipopolysaccharide synthesis; Antimicrobial resistance; OMV production; Virulence	Fouhy et al., 2007; Devos et al., 2015
WR-C	Environmental (septic tank)	NA*	*cis*-11-Methyl-2-dodecenoic acid (DSF); Δ2-tridecenoic acid; 11-methyl-dodecanoic acid; 10-methyl-dodeccanoic acid; Δ2-12-methyl-tridecenoic acid; Δ2-tetradecenoic acid; Δ2-12-methyl-tetradecenoic acid; Δ2-13-methyl-tetradecenoic acid	Motility	Huang and Lee Wong, 2007
E77	Clinical (sputum)	1	*cis*-11-Methyl-2-dodecenoic acid (DSF)	Motility; Biofilm; Virulence	Huedo et al., 2014b, 2015
M30	Clinical (decubitus ulcer)	2	*cis*-11-Methyl-2-dodecenoic acid (DSF)	Virulence	Huedo et al., 2014b, 2015
R551-3	Environmental (endophyte of *Populus trichocarpa*)	1	*cis*-11-Methyl-2-dodecenoic acid (DSF)	Promote seed germination and plant growth	Alavi et al., 2013

NA, Genomic data is not available.*

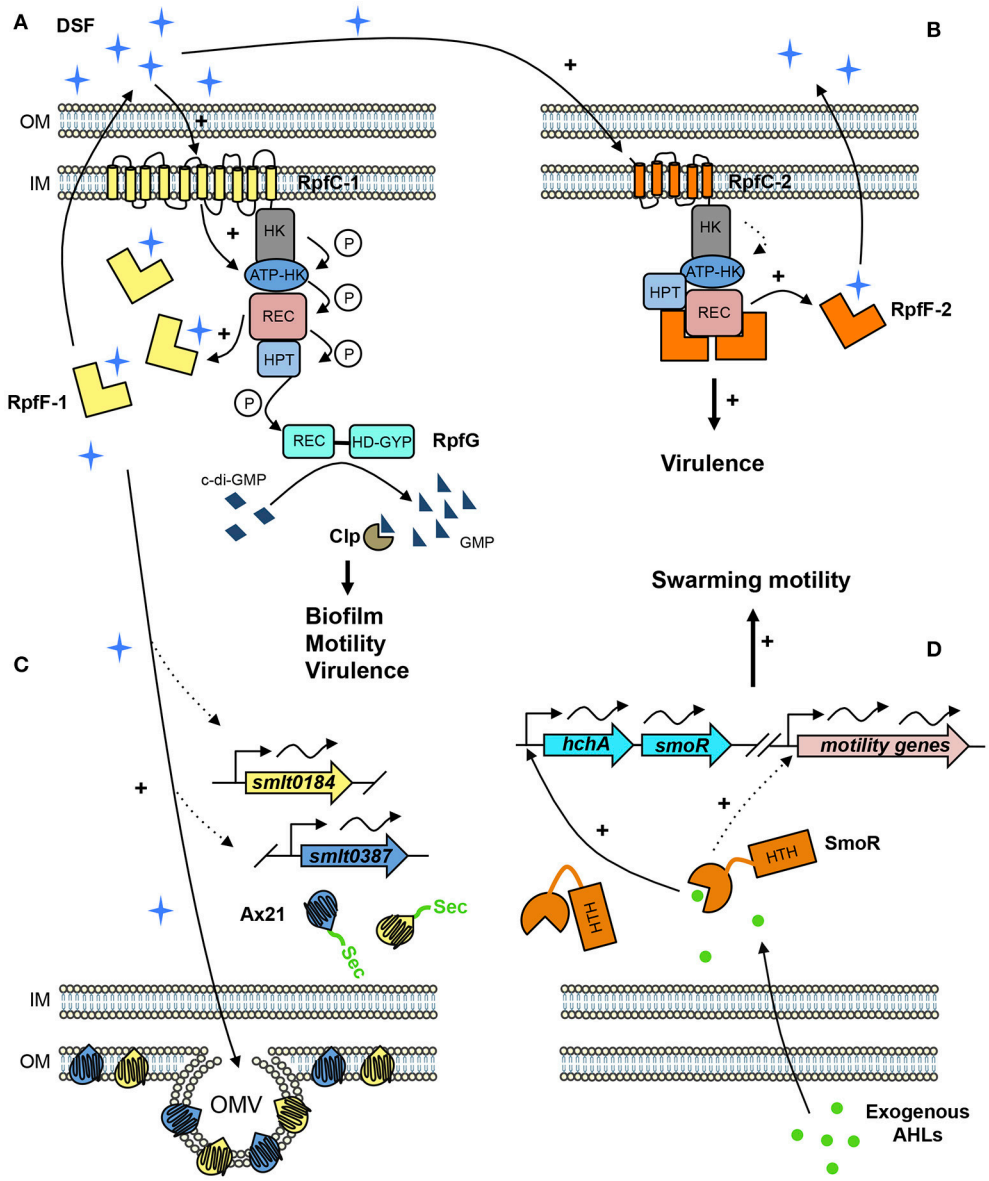

FIGURE 1 | Proposed QS signaling network in *S. maltophilia*. **(A)** In *rpf*-1 strains, RpfC-1 (including 10 TMR) stimulates RpfF-1 basal activity—that increases with cell density—and synthesizes DSF (cis-11-Methyl-2-dodecenoic acid) that accumulates in the extracellular environment. Once DSF concentration reaches a critical threshold, RpfC-1 senses DSF, and induces a phosphorylation cascade throughout its cytoplasmic domains ending in the response regulator RpfG, which degrades cyclic diguanylate monophosphate (c-di-GMP) to GMP activating the transcriptional regulator Clp that stimulates expression of genes involved in biofilm formation, motility, and virulence. **(B)** In *rpf*-2 strains, RpfC-2 (5 TMR) permanently represses RpfF-2, resulting in no DSF detection in axenic conditions. DSF produced by neighboring bacteria (e.g., *rpf*-1 strain) is sensed by RpfC-2 allowing free-active RpfF-2 and subsequent DSF synthesis. **(C)** DSF also stimulates the production of outer membrane vesicles (OMV) containing high amounts of the two Ax21 proteins (Smlt0184 and Smlt0387). Both Ax21 proteins present a signal peptide that is processed by the general secretory (Sec) system. **(D)** Exogenous AHL signals, specifically C8-HSL and oxo-C8-HSL, are sensed by the LuxR solo SmoR (Smlt1839), annotated as "LuxR chaperone HchA-associated," activating the transcription of its own operon and promoting swarming motility. Dotted lines represent predicted or supposed interactions on the basis of reported experimental evidences. Protein domains are abbreviated as follows. HK, Histidine kinase domain; REC, Receiver domain; HPT, Histidine phosphotransferase domain; HD-GYP, Phosphodiesterase domain containing an additional GYP motif; HTH, Helix-Turn-Helix domain.

virulence capacity of the whole population are enhanced (Huedo et al., 2015; **Figure 1**). This suggests that *rpf*-2 strains have evolved as a receptor group, in terms of DSF communication, displaying a lethargic DSF-deficient phenotype under axenic conditions until the presence of DSF-producing bacteria (e.g., *Xcc* or *S. maltophilia rpf*-1 variant) triggers reciprocal DSF communication. This behavior evokes to some extend the *P. aeruginosa* "social cheaters"—spontaneous *lasR* mutants that take advantage of the intact QS-regulation of their neighboring bacteria (Sandoz et al., 2007). Clearly, further research is required

to better understand the intriguing role of the DSF system in the *rpf*-2 *S. maltophilia* subpopulation, including the specific advantages and disadvantages of this particular behavior.

DSF-Mediated Communication of *S. maltophilia* With Distant Organisms

S. maltophilia has been shown to interact, via DSF production, with unrelated bacteria, yeast, and even plants. In particular, DSF produced by *S. maltophilia* K279a is detected by *P. aeruginosa* through the sensor kinase PA1396, modulating biofilm formation and antibiotic resistance (Ryan et al., 2008) as well as virulence and persistence in lungs of cystic fibrosis patients (Twomey et al., 2012). Likewise, synthesis of DSF by the strain K279a affects planktonic and biofilm growth of *Candida albicans* and inhibits its morphological transition (de Rossi et al., 2014). Finally, DSF produced by the environmental strain R551-3 causes a positive effect on plant germination and growth of rapeseed (Alavi et al., 2013) (**Table 1**).

AHL-BASED QUORUM SENSING

N-acyl homoserine lactone (AHL) QS is the most studied and widespread communication system in Gram-negative bacteria (Papenfort and Bassler, 2016). Typically, AHL signals are produced by LuxI-type synthases and sensed by LuxR-type transcriptional regulators (Ng and Bassler, 2009; LaSarre and Federle, 2013).

AHL Synthesis in *Stenotrophomonas* Species

It has been shown that *S. maltophilia* does not produce detectable levels of AHLs (Zhu et al., 2001; Veselova et al., 2003), reinforced by the lack of homologs to known AHL LuxI-family synthase genes in publicly available genomes. Nevertheless, AHL activity has been detected in some *Stenotrophomonas* sp. isolated from sediments of wastewater treatment systems (Valle et al., 2004; Hu et al., 2016) and activated sludge (Tan et al., 2014, 2015). Besides the *Stenotrophomonas* genus, AHL-activity has also been detected in other *Xanthomonadaceae* including *Thermomonas* (Ishizaki et al., 2017), *Lysobacter* (Tan et al., 2015) and *Xanthomonas* sp. (Veselova et al., 2003). Given the elevated genomic diversity of the genus *Stenotrophomonas*, future identification of more AHL-producing isolates or the existence of a novel LuxI-family synthase cannot be ruled out.

AHL Response in *S. maltophilia*

LuxR solos are typical AHL-regulators lacking its cognate LuxI and are widely spread throughout bacterial genomes, including *Xanthomonadaceae* species (Subramoni and Venturi, 2009; Hudaiberdiev et al., 2015). The genome of *S. maltophilia* strain K279 encodes for 15 putative LuxR solos from which only SmoR presents the typical N-terminal AHL-binding domain and the C-terminal helix-turn-helix (HTH) DNA-binding domain (Martínez et al., 2015). *In vitro* AHL-binding assays confirmed that SmoR from strain E77 binds to AHL signal oxo-C8-HSL, regulating swarming motility. The *S. maltophilia* E77 parental strain but not its derivative Δ*smoR* mutant strongly stimulates swarming motility in the presence of a *P. aeruginosa* supernatant (containing high levels of AHLs including oxo-C8-HSL), indicating that SmoR senses AHL signals produced by neighboring bacteria (Martínez et al., 2015) (**Figure 1**). The role of the other LuxR solos in *S. maltophilia* is yet to be elucidated.

THE PROPOSED QUORUM-SENSING FACTOR AX21

The small protein Ax21 (activator of XA21-mediated immunity in plants) was proposed to serve as a new QS mechanism in *Xanthomonadaceae* (Lee et al., 2009; Han et al., 2011; McCarthy et al., 2011; Ronald, 2011). However, after almost 10 years of research on the Ax21 protein, we are practically at the starting point, since the key studies proposing its function have been placed in doubt (Han et al., 2013; Lee et al., 2013; Bahar et al., 2014; McCarthy et al., 2017).

What appears to apply to *S. maltophilia,* based on two independent proteomic analyses, is that Ax21 is an outer membrane protein secreted in association with OMVs (Devos et al., 2015; Ferrer-Navarro et al., 2016). Interestingly, it has been found that the relative levels of the two Ax21 paralogs (K279a locus tags Smlt0184 and Smlt0387) in some *S. maltophilia* strains seem to correlate with their virulence potential (Ferrer-Navarro et al., 2013, 2016), and that the increase in OMV-associated secretion of Ax21 proteins is somehow regulated by the DSF-QS system (Devos et al., 2015) (**Figure 1**). Based on the evidences reported so far, we believe that Ax21 cannot be considered a QS system component itself. However, the link between DSF signaling, OMV production and Ax21 secretion, as well as the implication of this regulatory pathway on the virulence ability of *S. maltophilia,* should be further investigated.

QUORUM QUENCHING INVOLVING *S. MALTOPHILIA*

The most studied QQ mechanisms are those disrupting AHL signaling (Wang et al., 2004), although QQ has been described for almost all QS systems including DSF (Newman et al., 2008; Defoirdt, 2017). Despite quenching of DSF-QS in *S. maltophilia* has not yet been reported, this species exhibits an interesting behavior in terms of QQ. It has been shown that the FA *cis*-9-octadecenoic acid synthesized by *S. maltophilia* strain BJ01 displays QQ of AHL signals resulting in antibiofilm activity on *P. aeruginosa* (Singh et al., 2013). AHL-QQ activity against 3-oxo-C12-HSL has been also observed in several *Stenotrophomonas* sp. and *S. maltophilia* isolates from activated sludge samples (Tan et al., 2015). Another study on activated sludge samples reported that one isolate from the genus *Stenotrophomonas* was able to degrade the C10-HSL signal (Ochiai et al., 2013). Endophytic isolates of *S. maltophilia* have been also shown to degrade 3-hydroxy palmitic acid methyl ester (3OH-PAME), the main QS signal of *Ralstonia solanacearum* (Achari and Ramesh, 2015). On the other side, detection, and response to AHL signals by *S. maltophilia* can be disrupted by the lactonase AiiA from

Bacillus subtilis (Pan et al., 2008), resulting in non-swarming stimulation (Martínez et al., 2015).

Regarding the quenching of DSF-QS, *S. maltophilia* strain E77 grown in LB medium containing 5 μM of synthetic octadecanoic acid (18:0) reduces DSF production to undetectable levels (Huedo et al., 2015). Moreover, plant-associated bacterial species and particularly *Pseudomonas* spp. are able to rapidly degrade DSF molecules of *Xcc* (Newman et al., 2008), a mechanism that may apply against *S. maltophilia* DSF signals. Finally, DSF produced by *S. maltophilia* K279a inhibits the yeast-to-hyphal transition of *Candida albicans*, most probably by acting as antagonist of the *C. albicans* signal farnesoic acid, a DSF homolog (de Rossi et al., 2014).

In summary, *S. maltophilia* appears as a species with potential QQ applications. However, QQ mechanisms disrupting *S. maltophilia* signaling have never been reported.

CONCLUDING REMARKS AND FUTURE PERSPECTIVES

Research conducted during last years has significantly improved our understanding of cell-to-cell signaling processes in *S. maltophilia* but, at the same time, has aroused new questions and hypothesis.

The mechanistic processes of the DSF-QS system in the *rpf*-1 subpopulation seem highly similar to those reported for the DSF model organism *Xcc*. However, more efforts should be addressed to investigate the molecular basis of DSF-QS in the *rpf*-2 group (45% of isolates) in order to uncover the biological significance of this particular variant.

The sensing and quenching response of *S. maltophilia* to exogenous AHL signals suggests that this bacterium has evolved in close contact with AHL-producing bacteria. Given the high phenotypic and genotypic heterogeneity among isolates from the genus *Stenotrophomonas* and considering that AHL-producing isolates of *Stenotrophomonas* spp. have been already reported, the existence of *S. maltophilia* strains producing AHLs cannot be discarded and should be further investigated.

S. maltophilia clearly interacts with the organisms conforming its environment. Examples of cooperation via DSF are divers and include the stimulation of seed germination and growth of the rapeseed, but also an increment of biofilm formation and antibiotic resistance of *P. aeruginosa* in the lungs. However, in most known cases *S. maltophilia* appears to exert a negative effect on its competitors' QS systems. This is because *S. maltophilia* isolates possess an extraordinary array of QQ mechanisms including production of FAs with quenching activities as well as degradation of AHL and PAME signals.

Given the increasing incidence of multi-resistant isolates of *S. maltophilia* in clinical settings, new antimicrobial strategies should be explored. Exogenous mechanisms quenching DSF communication in *S. maltophilia* have not yet been investigated and may represent a promising approach to overcome bacterial multidrug resistance. With the knowledge on the DSF system increasing and particularly since the determination of the structure of the synthase RpfF and the sensor RpfC, designing and testing compounds with antagonist activity against these key QS components could provide further opportunities for the development of novel combination therapies with antibiotics.

Comprehensively, *S. maltophilia* appears to be extraordinarily well connected to its environment and to take part in inter-species communication by synthesizing sensing and degrading a wide range of signaling molecules, therefore actively participating in the decisions taken by the whole community.

AUTHOR CONTRIBUTIONS

PH, XC, and DY conceptually designed the article and authored the first draft. XD, IG, and DY provided academic input and expertise, and finished critical revision of the article. All authors have approved the final version.

ACKNOWLEDGMENTS

This work was supported by the Spanish MICINN (BIO2015-66674-R) and the Catalan AGAUR (2014-SGR-1280).

REFERENCES

Achari, G. A., and Ramesh, R. (2015). Characterization of bacteria degrading 3-hydroxy palmitic acid methyl ester (3OH-PAME), a quorum sensing molecule of *Ralstonia solanacearum*. *Lett. Appl. Microbiol.* 60, 447–455. doi: 10.1111/lam.12389

Adegoke, A. A., Stenström, T. A., and Okoh, A. I. (2017). *Stenotrophomonas maltophilia* as an emerging ubiquitous pathogen: looking beyond contemporary antibiotic therapy. *Front. Microbiol.* 8:2276. doi: 10.3389/fmicb.2017.02276

Alavi, P., Müller, H., Cardinale, M., Zachow, C., Sánchez, M. B., Martínez, J. L., et al. (2013). The DSF quorum sensing system controls the positive influence of *Stenotrophomonas maltophilia* on plants. *PLoS ONE* 8:e67103. doi: 10.1371/journal.pone.0067103

Amin, R., and Waters, V. (2014). Antibiotic treatment for *Stenotrophomonas maltophilia* in people with cystic fibrosis. *Cochrane Database Syst. Rev.* CD009249. doi: 10.1002/14651858.CD009249.pub4

Bahar, O., Pruitt, R., Luu, D. D., Schwessinger, B., Daudi, A., Liu, F., et al. (2014). The Xanthomonas Ax21 protein is processed by the general secretory system and is secreted in association with outer membrane vesicles. *PeerJ* 2:e242. doi: 10.7717/peerj.242

Bais, H. P., Weir, T. L., Perry, L. G., Gilroy, S., and Vivanco, J. M. (2006). The role of root exudates in rhizosphere interactions with plants and other organisms. *Annu. Rev. Plant Biol.* 57, 233–266. doi: 10.1146/annurev.arplant.57.032905.105159

Barber, C. E., Tang, J. L., Feng, J. X., Pan, M. Q., Wilson, T. J., Slater, H., et al. (1997). A novel regulatory system required for pathogenicity of *Xanthomonas campestris* is mediated by a small diffusible signal molecule. *Mol. Microbiol.* 24, 555–566. doi: 10.1046/j.1365-2958.1997.3721736.x

Berg, G., Eberl, L., and Hartmann, A. (2005). The rhizosphere as a reservoir for opportunistic human pathogenic bacteria. *Environ. Microbiol.* 7, 1673–1685. doi: 10.1111/j.1462-2920.2005.00891.x

Bi, H., Christensen, Q. H., Feng, Y., Wang, H., and Cronan, J. E. (2012). The *Burkholderia cenocepacia* BDSF quorum sensing fatty acid is synthesized by a bifunctional crotonase homologue having both dehydratase and thioesterase activities. *Mol. Microbiol.* 83, 840–855. doi: 10.1111/j.1365-2958.2012.07968.x

Brooke, J. S. (2012). *Stenotrophomonas maltophilia*: an emerging global opportunistic pathogen. *Clin. Microbiol. Rev.* 25, 2–41. doi: 10.1128/CMR.00019-11

Chatterjee, S., Wistrom, C., and Lindow, S. E. (2008). A cell–cell signaling sensor is required for virulence and insect transmission of *Xylella fastidiosa*. *Proc. Natl. Acad. Sci.U.S.A.* 105, 2670–2675. doi: 10.1073/pnas.0712236105

Defoirdt, T. (2017). Quorum-sensing systems as targets for antivirulence therapy. *Trends Microbiol.* 26, 313–328. doi: 10.1016/j.tim.2017.10.005

Deng, Y., Liu, X., Wu, J., Lee, J., Chen, S., Cheng, Y., et al. (2015). The host plant metabolite glucose is the precursor of diffusible signal factor (DSF) family signals in *Xanthomonas campestris*. *Appl. Environ. Microbiol.* 81, 2861–2868. doi: 10.1128/AEM.03813-14

Deng, Y., Wu, J., Tao, F., and Zhang, L. H. (2011). Listening to a new language: DSF-based quorum sensing in gram-negative bacteria. *Chem. Rev.* 111, 160–173. doi: 10.1021/cr100354f

Deng, Y., Wu, J., Yin, W., Li, P., Zhou, J., Chen, S., et al. (2016). Diffusible signal factor family signals provide a fitness advantage to *Xanthomonas campestris* pv. campestris in interspecies competition. *Environ. Microbiol.* 18, 1534–1545. doi: 10.1111/1462-2920.13244

de Rossi, B. P., García, C., Alcaraz, E., and Franco, M. (2014). *Stenotrophomonas maltophilia* interferes via the DSF-mediated quorum sensing system with *Candida albicans* filamentation and its planktonic and biofilm modes of growth. *Rev. Argent. Microbiol.* 46, 288–297. doi: 10.1016/S0325-7541(14)70084-7

Devos, S., Van Oudenhove, L., Stremersch, S., Van Putte, W., De Rycke, R., Van Driessche, G., et al. (2015). The effect of imipenem and diffusible signaling factors on the secretion of outer membrane vesicles and associated Ax21 proteins in *Stenotrophomonas maltophilia*. *Front. Microbiol.* 6:298. doi: 10.3389/fmicb.2015.00298

Dong, Y. H., Wang, L. H., and Zhang, L. H. (2007). Quorum-quenching microbial infections: mechanisms and implications. *Philos. Trans. R. Soc. B Biol. Sci.* 362, 1201–1211. doi: 10.1098/rstb.2007.2045

Ferrer-Navarro, M., Planell, R., Yero, D., Mongiardini, E., Torrent, G., Huedo, P., et al. (2013). Abundance of the quorum-sensing factor Ax21 in four strains of *Stenotrophomonas maltophilia* correlates with mortality rate in a new zebrafish model of infection. *PLoS ONE* 8:e67207. doi: 10.1371/journal.pone.0067207

Ferrer-Navarro, M., Torrent, G., Mongiardini, E., Conchillo-Solé, O., Gibert, I., and Daura, X. (2016). Proteomic analysis of outer membrane proteins and vesicles of a clinical isolate and a collection strain of *Stenotrophomonas maltophilia*. *J. Proteomics* 142, 122–129. doi: 10.1016/j.jprot.2016.05.001

Fouhy, Y., Scanlon, K., Schouest, K., Spillane, C., Crossman, L., Avison, M. B., et al. (2007). Diffusible signal factor-dependent cell-cell signaling and virulence in the nosocomial pathogen *Stenotrophomonas maltophilia*. *J. Bacteriol.* 189, 4964–4968. doi: 10.1128/JB.00310-07

García, C. A., Alcaraz, E. S., Franco, M. A., and Passerini de Rossi, B. N. (2015). Iron is a signal for *Stenotrophomonas maltophilia* biofilm formation, oxidative stress response, OMPs expression, and virulence. *Front. Microbiol.* 6:926. doi: 10.3389/fmicb.2015.00926

Han, S. W., Sriariyanun, M., Lee, S.-W., Sharma, M., Bahar, O., Bower, Z., et al. (2011). Small protein-mediated quorum sensing in a Gram-negative bacterium. *PLoS ONE* 6:e29192. doi: 10.1371/journal.pone.0029192

Han, S.-W., Sriariyanun, M., Lee, S.-W., Sharma, M., Bahar, O., Bower, Z., et al. (2013). Retraction: small protein-mediated quorum sensing in a gram-negative bacterium. *PLOS ONE* 6:e29192. doi: 10.1371/annotation/880a72e1-9cf3-45a9-bf1c-c74ccb73fd35

He, Y.-W., and Zhang, L.-H. (2008). Quorum sensing and virulence regulation in *Xanthomonas campestris*. *FEMS Microbiol. Rev.* 32, 842–857. doi: 10.1111/j.1574-6976.2008.00120.x

Heath, R. J., and Rock, C. O. (2002). The Claisen condensation in biology. *Nat. Prod. Rep.* 19, 581–596. doi: 10.1039/b110221b

Hu, H., He, J., Liu, J., Yu, H., Tang, J., and Zhang, J. (2016). Role of N-acyl-homoserine lactone (AHL) based quorum sensing on biofilm formation on packing media in wastewater treatment process. *RSC Adv.* 6, 11128–11139. doi: 10.1039/C5RA23466B

Huang, T.-P., and Lee Wong, A. C. (2007). Extracellular fatty acids facilitate flagella-independent translocation by *Stenotrophomonas maltophilia*. *Res. Microbiol.* 158, 702–711. doi: 10.1016/j.resmic.2007.09.002

Huang, T.-P., and Wong, A. C. L. (2007). A cyclic AMP receptor protein-regulated cell-cell communication system mediates expression of a FecA homologue in *Stenotrophomonas maltophilia*. *Appl. Environ. Microbiol.* 73, 5034–5040. doi: 10.1128/AEM.00366-07

Hudaiberdiev, S., Choudhary, K. S., Vera Alvarez, R., Gelencsér, Z., Ligeti, B., Lamba, D., et al. (2015). Census of solo LuxR genes in prokaryotic genomes. *Front. Cell. Infect. Microbiol.* 5:20. doi: 10.3389/fcimb.2015.00020

Huedo, P., Conchillo-Solé, Ó., Yero, D., Martínez-Servat, S., Daura, X., and Gibert, I. (2014a). Draft genome sequence of *Stenotrophomonas maltophilia* strain M30, isolated from a chronic pressure ulcer in an elderly patient. *Genome Announc.* 2:e00576-14. doi: 10.1128/genomeA.00576-14

Huedo, P., Yero, D., Martínez-Servat, S., Estibariz, I., Planell, R., Martínez, P., et al. (2014b). Two different rpf clusters distributed among a population of *Stenotrophomonas maltophilia* clinical strains display differential diffusible signal factor production and virulence regulation. *J. Bacteriol.* 196, 2431–2442. doi: 10.1128/JB.01540-14

Huedo, P., Yero, D., Martínez-Servat, S., Ruyra, À., Roher, N., Daura, X., et al. (2015). Decoding the genetic and functional diversity of the DSF quorum-sensing system in *Stenotrophomonas maltophilia*. *Front. Microbiol.* 6:761. doi: 10.3389/fmicb.2015.00761

Ishizaki, S., Sugiyama, R., and Okabe, S. (2017). Membrane fouling induced by AHL-mediated soluble microbial product (SMP) formation by fouling-causing bacteria co-cultured with fouling-enhancing bacteria. *Sci. Rep.* 7:8482. doi: 10.1038/s41598-017-09023-5

Kalia, V. C., and Purohit, H. J. (2011). Quenching the quorum sensing system: potential antibacterial drug targets. *Crit. Rev. Microbiol.* 37, 121–140. doi: 10.3109/1040841X.2010.532479

Kaur, A., Chaudhary, A., Kaur, A., Choudhary, R., and Kaushik, R. (2005). Phospholipid fatty acid: a bioindicator of environment monitoring and assessment in soil ecosystem. *Curr. Sci.* 89, 1103–1112.

Kim, H.-B., Srinivasan, S., Sathiyaraj, G., Quan, L.-H., Kim, S.-H., Bui, T. P. N., et al. (2010). *Stenotrophomonas ginsengisoli* sp. nov., isolated from a ginseng field. *Int. J. Syst. Evol. Microbiol.* 60, 1522–1526. doi: 10.1099/ijs.0.014662-0

Kleerebezem, M., Quadri, L. E., Kuipers, O. P., and de Vos, W. M. (1997). Quorum sensing by peptide pheromones and two-component signal-transduction systems in Gram-positive bacteria. *Mol. Microbiol.* 24, 895–904. doi: 10.1046/j.1365-2958.1997.4251782.x

LaSarre, B., and Federle, M. J. (2013). Exploiting quorum sensing to confuse bacterial pathogens. *Microbiol. Mol. Biol. Rev.* 77, 73–111. doi: 10.1128/MMBR.00046-12

Lee, S.-W., Han, S.-W., Sririyanum, M., Park, C.-J., Seo, Y.-S., and Ronald, P. C. (2009). A type I-secreted, sulfated peptide triggers XA21-mediated innate immunity. *Science* 326, 850–853. doi: 10.1126/science.1173438

Lee, S.-W., Han, S.-W., Sririyanum, M., Park, C.-J., Seo, Y.-S., and Ronald, P. C. (2013). Retraction. A type I-secreted, sulfated peptide triggers XA21-mediated innate immunity. *Science* 342:191. doi: 10.1126/science.342.6155.191-a

Lira, F., Berg, G., and Martínez, J. L. (2017). Double-face meets the bacterial world: the opportunistic pathogen *Stenotrophomonas maltophilia*. *Front. Microbiol.* 8:2190. doi: 10.3389/fmicb.2017.02190

Lowery, C. A., Dickerson, T. J., and Janda, K. D. (2008). Interspecies and interkingdom communication mediated by bacterial quorum sensing. *Chem. Soc. Rev.* 37, 1337–1346. doi: 10.1039/b702781h

Martínez, P., Huedo, P., Martinez-Servat, S., Planell, R., Ferrer-Navarro, M., Daura, X., et al. (2015). *Stenotrophomonas maltophilia* responds to exogenous AHL signals through the LuxR solo SmoR (Smlt1839). *Front. Cell. Infect. Microbiol.* 5:41. doi: 10.3389/fcimb.2015.00041

McCarthy, Y., Dow, J. M., and Ryan, R. P. (2011). The Ax21 protein is a cell-cell signal that regulates virulence in the nosocomial pathogen *Stenotrophomonas maltophilia*. *J. Bacteriol.* 193, 6375–6378. doi: 10.1128/JB.05949-11

McCarthy, Y., Dow, J. M., and Ryan, R. P. (2017). Retraction for McCarthy et al., "The Ax21 protein is a cell-cell signal that regulates virulence in the nosocomial pathogen *Stenotrophomonas maltophilia*." *J. Bacteriol.* 199:e00156-17. doi: 10.1128/JB.00156-17

Newman, K. L., Chatterjee, S., Ho, K. A., and Lindow, S. E. (2008). Virulence of plant pathogenic bacteria attenuated by degradation of fatty acid cell-to-cell signaling factors. *Mol. Plant Microbe Interact.* 21, 326–334. doi: 10.1094/MPMI-21-3-0326

Ng, W.-L., and Bassler, B. L. (2009). Bacterial quorum-sensing network architectures. *Annu. Rev. Genet.* 43, 197–222. doi: 10.1146/annurev-genet-102108-134304

Ochiai, S., Morohoshi, T., Kurabeishi, A., Shinozaki, M., Fujita, H., Sawada, I., et al. (2013). Production and degradation of N-acylhomoserine lactone quorum sensing signal molecules in bacteria isolated from activated sludge. *Biosci. Biotechnol. Biochem.* 77, 2436–2440. doi: 10.1271/bbb.130553

Pan, J., Huang, T., Yao, F., Huang, Z., Powell, C. A., Qiu, S., et al. (2008). Expression and characterization of aiiA gene from Bacillus subtilis BS-1. *Microbiol. Res.* 163, 711–716. doi: 10.1016/j.micres.2007.12.002

Papenfort, K., and Bassler, B. L. (2016). Quorum sensing signal–response systems in Gram-negative bacteria. *Nat. Rev. Microbiol.* 14:576. doi: 10.1038/nrmicro.2016.89

Pompilio, A., Pomponio, S., Crocetta, V., Gherardi, G., Verginelli, F., Fiscarelli, E., et al. (2011). Phenotypic and genotypic characterization of *Stenotrophomonas maltophilia* isolates from patients with cystic fibrosis: Genome diversity, biofilm formation, and virulence. *BMC Microbiol.* 11:159. doi: 10.1186/1471-2180-11-159

Ronald, P. C. (2011). Small protein-mediated quorum sensing in a gram-negative bacterium: novel targets for control of infectious disease. *Discov. Med.* 12, 461–470.

Rutherford, S. T., and Bassler, B. L. (2012). Bacterial quorum sensing: its role in virulence and possibilities for its control. *Cold Spring Harb. Perspect. Med.* 2:a012427. doi: 10.1101/cshperspect.a012427

Ryan, R. P., An, S., Allan, J. H., McCarthy, Y., and Dow, J. M. (2015). The DSF family of cell–cell signals: an expanding class of bacterial virulence regulators. *PLoS Pathog.* 11:e1004986. doi: 10.1371/journal.ppat.1004986

Ryan, R. P., Fouhy, Y., Garcia, B. F., Watt, S. A., Niehaus, K., Yang, L., et al. (2008). Interspecies signalling via the *Stenotrophomonas maltophilia* diffusible signal factor influences biofilm formation and polymyxin tolerance in *Pseudomonas aeruginosa*. *Mol. Microbiol.* 68, 75–86. doi: 10.1111/j.1365-2958.2008.06132.x

Ryan, R. P., Monchy, S., Cardinale, M., Taghavi, S., Crossman, L., Avison, M. B., et al. (2009). The versatility and adaptation of bacteria from the genus *Stenotrophomonas*. *Nat. Rev. Microbiol.* 7:514. doi: 10.1038/nrmicro2163

Sandoz, K. M., Mitzimberg, S. M., and Schuster, M. (2007). Social cheating in *Pseudomonas aeruginosa* quorum sensing. *Proc. Natl. Acad. Sci. U.S.A.* 104, 15876–15881. doi: 10.1073/pnas.0705653104

Singh, V. K., Kavita, K., Prabhakaran, R., and Jha, B. (2013). Cis-9-octadecenoic acid from the rhizospheric bacterium *Stenotrophomonas maltophilia* BJ01 shows quorum quenching and anti-biofilm activities. *Biofouling* 29, 855–867. doi: 10.1080/08927014.2013.807914

Slater, H., Alvarez-Morales, A., Barber, C. E., Daniels, M. J., and Dow, J. M. (2000). A two-component system involving an HD-GYP domain protein links cell–cell signalling to pathogenicity gene expression in *Xanthomonas campestris*. *Mol. Microbiol.* 38, 986–1003. doi: 10.1046/j.1365-2958.2000.02196.x

Subramoni, S., and Venturi, V. (2009). LuxR-family "solos": bachelor sensors/regulators of signalling molecules. *Microbiol. Read. Engl.* 155, 1377–1385. doi: 10.1099/mic.0.026849-0

Tan, C. H., Koh, K. S., Xie, C., Tay, M., Zhou, Y., Williams, R., et al. (2014). The role of quorum sensing signalling in EPS production and the assembly of a sludge community into aerobic granules. *ISME J.* 8, 1186–1197. doi: 10.1038/ismej.2013.240

Tan, C. H., Koh, K. S., Xie, C., Zhang, J., Tan, X. H., Lee, G. P., et al. (2015). Community quorum sensing signalling and quenching: microbial granular biofilm assembly. *Npj Biofilms Microbiomes* 1:15006. doi: 10.1038/npjbiofilms.2015.6

Twomey, K. B., O'Connell, O. J., McCarthy, Y., Dow, J. M., O'Toole, G. A., Plant, B. J., et al. (2012). Bacterial cis-2-unsaturated fatty acids found in the cystic fibrosis airway modulate virulence and persistence of *Pseudomonas aeruginosa*. *ISME J.* 6, 939–950. doi: 10.1038/ismej.2011.167

Valle, A., Bailey, M. J., Whiteley, A. S., and Manefield, M. (2004). N-acyl-l-homoserine lactones (AHLs) affect microbial community composition and function in activated sludge. *Environ. Microbiol.* 6, 424–433. doi: 10.1111/j.1462-2920.2004.00581.x

Vauterin, L., Yang, P., and Swings, J. (1996). Utilization of fatty acid methyl esters for the differentiation of new xanthomonas species. *Int. J. Syst. Bacteriol.* 46, 298–304. doi: 10.1099/00207713-46-1-298

Veselova, M., Kholmeckaya, M., Klein, S., Voronina, E., Lipasova, V., Metlitskaya, A., et al. (2003). Production of N-acylhomoserine lactone signal molecules by gram-negative soil-borne and plant-associated bacteria. *Folia Microbiol.* 48, 794–798. doi: 10.1007/BF02931516

Wang, L.-H., Weng, L.-X., Dong, Y.-H., and Zhang, L.-H. (2004). Specificity and enzyme kinetics of the quorum-quenching N-Acyl homoserine lactone lactonase (AHL-lactonase). *J. Biol. Chem.* 279, 13645–13651. doi: 10.1074/jbc.M311194200

Waters, C. M., and Bassler, B. L. (2005). Quorum sensing: cell-to-cell communication in bacteria. *Annu. Rev. Cell Dev. Biol.* 21, 319–346. doi: 10.1146/annurev.cellbio.21.012704.131001

Zhou, L., Yu, Y., Chen, X., Diab, A. A., Ruan, L., He, J., et al. (2015). The multiple DSF-family QS signals are synthesized from carbohydrate and branched-chain amino acids via the FAS elongation cycle. *Sci. Rep.* 5:13294. doi: 10.1038/srep13294

Zhou, L., Zhang, L.-H., Cámara, M., and He, Y.-W. (2017). The DSF family of quorum sensing signals: diversity, biosynthesis, and turnover. *Trends Microbiol.* 25, 293–303. doi: 10.1016/j.tim.2016.11.013

Zhu, H., Thuruthyil, S. J., and Willcox, M. D. (2001). Production of N-acyl homoserine lactones by Gram-negative bacteria isolated from contact lens wearers. *Clin. Experiment. Ophthalmol.* 29, 150–152. doi: 10.1046/j.1442-9071.2001.00397.x

Zhuo, C., Zhao, Q., and Xiao, S. (2014). The Impact of spgM, rpfF, rmlA gene distribution on biofilm formation in *Stenotrophomonas maltophilia*. *PLoS ONE* 9:e108409. doi: 10.1371/journal.pone.0108409

Conflict of Interest Statement: The authors declare that the research was conducted in the absence of any commercial or financial relationships that could be construed as a potential conflict of interest.

Advantages of publishing in Frontiers

OPEN ACCESS
Articles are free to read for greatest visibility and readership

FAST PUBLICATION
Around 90 days from submission to decision

HIGH QUALITY PEER-REVIEW
Rigorous, collaborative, and constructive peer-review

TRANSPARENT PEER-REVIEW
Editors and reviewers acknowledged by name on published articles

Frontiers
Avenue du Tribunal-Fédéral 34
1005 Lausanne | Switzerland

Visit us: www.frontiersin.org
Contact us: info@frontiersin.org | +41 21 510 17 00

REPRODUCIBILITY OF RESEARCH
Support open data and methods to enhance research reproducibility

DIGITAL PUBLISHING
Articles designed for optimal readership across devices

FOLLOW US
@frontiersin

IMPACT METRICS
Advanced article metrics track visibility across digital media

EXTENSIVE PROMOTION
Marketing and promotion of impactful research

LOOP RESEARCH NETWORK
Our network increases your article's readership